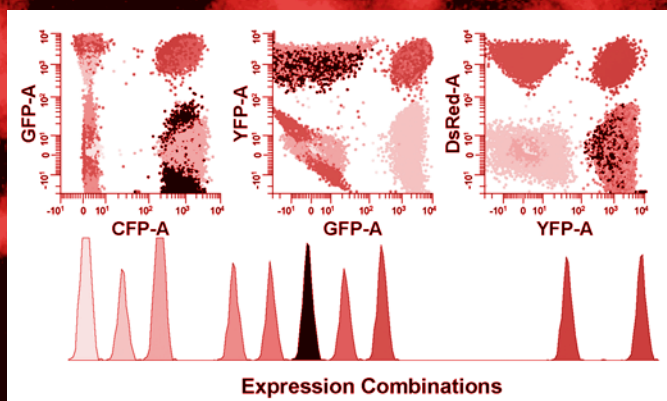


Flow Cytometry Protocols

SECOND EDITION

Edited by

Teresa S. Hawley
Robert G. Hawley



HUMANA PRESS

1

Flow Cytometry

An Introduction

Alice L. Givan

Summary

A flow cytometer is an instrument that illuminates cells (or other particles) as they flow individually in front of a light source and then detects and correlates the signals from those cells that result from the illumination. In this chapter, each of the aspects of that definition will be described: the characteristics of cells suitable for flow cytometry, methods to illuminate cells, the use of fluidics to guide the cells individually past the illuminating beam, the types of signals emitted by the cells and the detection of those signals, the conversion of light signals to digital data, and the use of computers to correlate and analyze the data after they are stored in a data file. The final section of the chapter will discuss the use of a flow cytometer to sort cells. This chapter can be read as a brief, self-contained survey. It can also be read as a gateway with signposts into the field. Other chapters in this book will provide more details, more references, and even some controversy about specific topics.

Key Words

Flow cytometry, fluidics, fluorescence, laser.

1. Introduction

An introductory chapter on flow cytometry must first confront the difficulty of defining a flow cytometer. The instrument described by Andrew Moldavan in 1934 (*1*) is generally acknowledged to be an early prototype. Although it may never have been built, in design it looked like a microscope but provided a capillary tube on the stage so that cells could be individually illuminated as they flowed in single file in front of the light emitted through the objective. The signals coming from the cells could then be analyzed by a photodetector attached in the position of the microscope eyepiece. Following work by Coul-

From: *Methods in Molecular Biology: Flow Cytometry Protocols*, 2nd ed.
Edited by: T. S. Hawley and R. G. Hawley © Humana Press Inc., Totowa, NJ

ter and others in the next decades to develop instruments to count particles in suspension (*see refs. 2–5*), a design was implemented by Kamensky and Melamed in 1965 and 1967 (*6,7*) to produce a microscope-based flow cytometer for detecting light signals distinguishing the abnormal cells in a cervical sample. In the years after publication of the Kamensky papers, work by Fulwyler, Dittrich and Göhde, Van Dilla, and Herzenberg (*see refs. 8–11*) led to significant changes in overall design, resulting in a cytometer that was largely similar to today's cytometers. Like today's cytometers, a flow cytometer in 1969 did not resemble a microscope in any way but was still based on Moldavan's prototype and on the Kamensky instrument in that it illuminated cells as they progressed in single file in front of a beam of light and it used photodetectors to detect the signals that came from the cells (*see Shapiro [12] and Melamed [13,14] for more complete discussions of this historical development*). Even today, our definition of a flow cytometer involves an instrument that illuminates cells as they flow individually in front of a light source and then detects and correlates the signals from those cells that result from the illumination.

In this chapter, each of the aspects in that definition are described: the cells, methods to illuminate the cells, the use of fluidics to make sure that the cells flow individually past the illuminating beam, the use of detectors to measure the signals coming from the cells, and the use of computers to correlate the signals after they are stored in data files. As an introduction, this chapter can be read as a brief survey; it can also be read as a gateway with signposts into the field. Other chapters in this book (and in other books [*e.g., refs. 12,15–24*]) provide more details, more references, and even some controversy concerning specific topics.

2. Cells (or Particles or Events)

Before discussing “cells,” we need to qualify even that basic word. “Cytometer” is derived from two Greek words, “κντοζ”, meaning container, receptacle, or body (taken in modern formations to mean cell), and “μετρον”, meaning measure. Cytometers today, however, often measure things other than cells. “Particle” can be used as a more general term for any of the objects flowing through a flow cytometer. “Event” is a term that is used to indicate anything that has been interpreted by the instrument, correctly or incorrectly, to be a single particle. There are subtleties here; for example, if the cytometer is not quick enough, two particles close together may actually be detected as one event. Because most of the particles sent through cytometers and detected as events are, in fact, single cells, those words are used here somewhat interchangeably.

Because flow cytometry is a technique for the analysis of individual particles, a flow cytometrist must begin by obtaining a suspension of particles. Historically, the particles analyzed by flow cytometry were often cells from the

blood; these are ideally suited for this technique because they exist as single cells and require no manipulation before cytometric analysis. Cultured cells or cell lines have also been suitable, although adherent cells require some treatment to remove them from the surface on which they are grown. More recently, bacteria (25,26), sperm (27,28), and plankton (29) have been analyzed. Flow techniques have also been used to analyze individual particles that are not cells at all (e.g., viruses [30], nuclei [31], chromosomes [32], DNA fragments [33], and latex beads [34]). In addition, cells that do not occur as single particles can be made suitable for flow cytometric analysis by the use of mechanical disruption or enzymatic digestion; tissues can be disaggregated into individual cells and these can be run through a flow cytometer. The advantage of a method that analyzes single cells is that cells can be scanned at a rapid rate (500 to >5000 per second) and the individual characteristics of a large number of cells can be enumerated, correlated, and summarized. The disadvantage of a single-cell technique is that cells that do not occur as individual particles will need to be disaggregated; when tissues are disaggregated for analysis, some of the characteristics of the individual cells can be altered and all information about tissue architecture and cell distribution is lost.

In flow cytometry, because particles flow in a narrow stream in front of a narrow beam of light, there are size restrictions. In general, cells or particles must fall between approx 1 μm and approx 30 μm in diameter. Special cytometers may have the increased sensitivity to handle smaller particles (such as DNA fragments [33] or small bacteria [35]) or may have the generous fluidics to handle larger particles (such as plant cells [36]). But ordinary cytometers will, on the one hand, not be sensitive enough to detect signals from very small particles and will, on the other hand, become obstructed with very large particles.

Particles for flow cytometry should be suspended in buffer at a concentration of about 5×10^5 to $5 \times 10^6/\text{mL}$. In this suspension, they will flow through the cytometer mostly one by one. The light emitted from each particle will be detected and stored in a data file for subsequent analysis. In terms of the emitted light, particles will scatter light and this scattered light can be detected. Some of the emitted light is not scattered light, but is fluorescence. Many particles (notably phytoplankton) have natural background (auto-) fluorescence and this can be detected by the cytometer. In most cases, particles without intrinsically interesting autofluorescence will have been stained with fluorescent dyes during preparation to make nonfluorescent compounds “visible” to the cytometer. A fluorescent dye is one that absorbs light of certain specific colors and then emits light of a different color (usually of a longer wavelength). The fluorescent dyes may be conjugated to antibodies and, in this case, the fluorescence of a cell will be a readout for the amount of protein/antigen (on the cell surface or in the cytoplasm or nucleus) to which the antibody has bound.

Some fluorochrome-conjugated molecules can be used to indicate apoptosis (37). Alternatively, the dye itself may fluoresce when it is bound to a cellular component. Staining with DNA-sensitive fluorochromes can be used, for example, to look at multiploidy in mixtures of malignant and normal cells (31); in conjunction with mathematical algorithms, to study the proportion of cells in different stages of the cell cycle (38); and in restriction-enzyme-digested material, to type bacteria according to the size of their fragmented DNA (39). There are other fluorochromes that fluoresce differently in relation to the concentration of calcium ions (40) or protons (41,42) in the cytoplasm or to the potential gradient across a cell or organelle membrane (43). In these cases, the fluorescence of the cell may indicate the response of that cell to stimulation. Other dyes can be used to stain cells in such a way that the dye is partitioned between daughter cells on cell division; the fluorescence intensity of the cells will reveal the number of divisions that have occurred (44). Chapters in this book provide detailed information about fluorochromes and their use. In addition, the Molecular Probes (Eugene, OR) handbook by Richard Haugland is an excellent, if occasionally overwhelming, source of information about fluorescent molecules.

The important thing to know about the use of fluorescent dyes for staining cells is that the dyes themselves need to be appropriate to the cytometer. This requires knowledge of the wavelength of the illuminating light, knowledge of the wavelength specificities of the filters in front of the instrument's photodetectors, and knowledge of the absorption and emission characteristics of the dyes themselves. The fluorochromes used to stain cells must be able to absorb the particular wavelength of the illuminating light and the detectors must have appropriate filters to detect the fluorescence emitted. For the purposes of this introductory chapter, we now assume that we have particles that are individually suspended in medium at a concentration of about 1 million/mL and that they have been stained with (or naturally contain) fluorescent molecules with appropriate wavelength characteristics.

3. Illumination

In most flow cytometers, fluorescent cells are illuminated with the light from a laser. Lasers are useful because they provide intense light in a narrow beam. Particles in a stream of fluid can move through this light beam rapidly; under ideal circumstances, only one particle will be illuminated at a time, and the illumination is bright enough to produce scattered light or fluorescence of detectable intensity.

Lasers in today's cytometers are either gas lasers (e.g., argon ion lasers or helium-neon lasers) or solid-state lasers (e.g., red or green diode lasers or the relatively new blue and violet lasers). In all cases, light of specific wavelengths

Table 1
Common Types of Lasers in Current Use

Laser	Emission Wavelength(s) (nm)
Argon ion	Usually 488, 514, UV(351/364)
Red helium–neon (He–Ne)	633
Green helium neon (He–Ne)	543
Krypton ion	Usually 568, 647
Violet diode	408
Blue solid state	488
Red diode	635

is generated (*see Table 1*). The wavelengths of the light from a given laser are defined and inflexible, based on the characteristics of the lasing medium. The most common laser found on the optical benches of flow cytometers today is an argon ion laser; it was chosen for early flow cytometers because it provides turquoise light (488 nm) that is absorbed efficiently by fluorescein, a fluorochrome that had long been used for fluorescence microscopy. Argon ion lasers can also produce green light (at 514 nm), ultraviolet light (at 351 and 364 nm), and a few other colors of light at low intensity. Some cytometers will use only 488-nm light from an argon ion laser; other cytometers may permit selection of several of these argon ion wavelengths from the laser.

Whereas the early flow cytometers used a single argon ion laser at 488 nm to excite the fluorescence from fluorescein (and later to include, among many possible dyes, phycoerythrin, propidium iodide, peridinin chlorophyll protein [PerCP], and various tandem transfer dyes—all of which absorb 488-nm light), there was an increasing demand for fluorochromes with different emission spectra so that cells could be stained for many characteristics at once and the fluorescence from the different fluorochromes distinguished by color. This led to the requirement for illumination light of different wavelengths and therefore for an increasing number of lasers on the optical bench. Current research flow cytometers may include, for example, two or three lasers from those listed in **Table 1**.

Flow cytometers with more than one laser focus the beam from each laser at a different spot along the stream of flowing cells (**Fig. 1**). Each cell passes through each laser beam in turn. In this way, the scatter and fluorescence signals elicited from the cells by each of the different lasers will arrive at the photodetectors in a spatially or temporally defined sequence. Thus, the signals from the cells can be associated with a particular excitation wavelength.

All the information that a flow cytometer reveals about a cell comes from the period of time that the cell is within the laser beam. That period begins at the

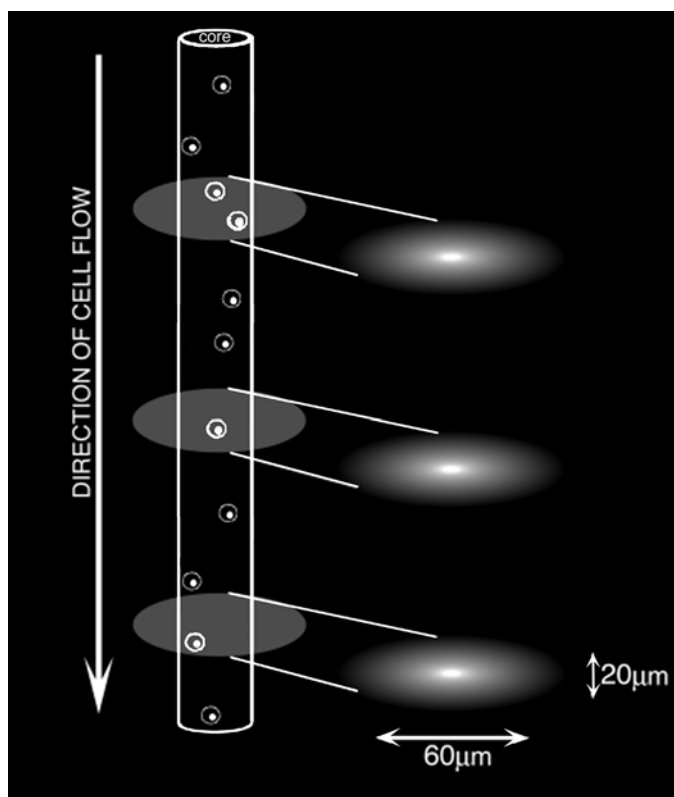


Fig. 1. Cells flowing past laser beam analysis points (in a three-laser cytometer). Beams with elliptical cross-sectional profiles allow cells to pass into and out of the beam quickly, mainly avoiding the coincidence of two cells in the laser beam at one time (but see the coincidence event in the first analysis point). In addition, an elliptical laser beam provides more uniform illumination if cells stray from the bright center of the beam.

time that the leading edge of the cell enters the laser beam and continues until the time that the trailing edge of the cell leaves the laser beam. The place where the laser beam intersects the stream of flowing cells is called the “interrogation point,” the “analysis point,” or the “observation point.” If there is more than one laser, there will be several analysis points. In a standard flow cytometer, the laser beam(s) will have an elliptical cross-sectional area, brightest in the center and measuring approx $10\text{--}20 \times 60 \mu\text{m}$ to the edges. The height of the laser beam ($10\text{--}20 \mu\text{m}$) marks the height of the analysis point and the dimension through which each cell will pass. In commercial and research cytometers, cells will flow through each analysis point at a velocity of $5\text{--}50 \text{ m/s}$. They will,

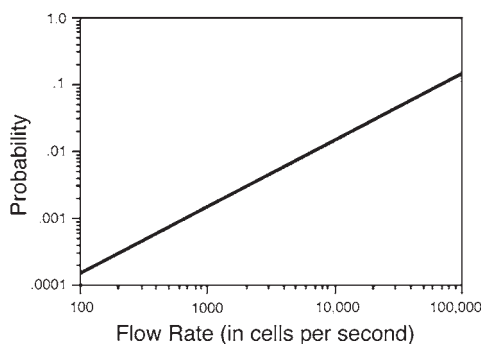


Fig. 2. The probability of a flow cytometric “event” actually resulting from more than one cell coinciding in the analysis point. For this model, the laser beam was considered to be 30 μm high and the stream flowing at 10 meters per second. (Reprinted with permission of John Wiley & Sons. Copyright 2001 from Givan, A. L. [2001] *Flow Cytometry: First Principles*, 2nd edit. Wiley-Liss, New York.)

therefore, spend approx 0.2–4 μs in the laser beam. Because fluorochromes typically absorb light and then emit that light in a time frame of several nanoseconds, a fluorochrome on a cell will absorb and then emit light approximately a thousand times while the cell is within each analysis point.

4. Fluidics: Cells Through the Laser Beam(s)

In flow cytometry, as opposed to traditional microscopy, particles flow. In other words, the particles need to be suspended in fluid and each particle is then analyzed over the brief and defined period of time that it is being illuminated as it passes through the analysis point. This means that many cells can be analyzed and statistical information about large populations of cells can be obtained in a short period of time. The downside of this flow of single cells, as mentioned previously, is that the particles need to be separate and in suspension. But even nominal single-cell suspensions contain cells in clumps if the cells tend to aggregate; or there may be cells in “pseudo-clumps” if they are in a concentrated suspension and, with some probability, coincide with other cells in the analysis point of the cytometer. Even in suspensions of low cell concentration, there is always some probability that coincidence events will occur (Fig. 2). The fluidics in a cytometer are designed to decrease the probability that multiple cells will coincide in the analysis point; in addition, the fluidics must facilitate similar illumination of each cell, must be constructed so as to avoid obstruction of the flow tubing, and must do all of this with cells flowing in and out of the analysis point as rapidly as possible (consistent with the production of sufficiently intense scattered and fluorescent light for sensitive detection).

One way to confine cells to a narrow path through the uniformly bright center of a laser beam would be to use an optically clear chamber with a very narrow diameter or, alternatively, to force the cells through the beam from a nozzle with a very narrow orifice. The problem with pushing cells from a narrow orifice or through a narrow chamber is that the cells, if large or aggregated, tend to clog the pathway. The hydrodynamics required to bring about focussed flow without clogging is based on principles that date back to work by Crosland-Taylor in 1953 (45). He noted that “attempts to count small particles suspended in fluid flowing through a tube have not hitherto been very successful. With particles such as red blood cells the experimenter must choose between a wide tube that allows particles to pass two or more abreast across a particular section, or a narrow tube that makes microscopical observation of the contents of the tube difficult due to the different refractive indices of the tube and the suspending fluid. In addition, narrow tubes tend to block easily.” Crosland-Taylor’s strategy for confining cells in a focussed, narrow flow stream but preventing blockage through a narrow chamber or orifice involved injecting the cell suspension into the center of a wide, rapidly flowing stream (the sheath stream), where, according to hydrodynamic principles, the cells will remain confined to a narrow core at the center of the wider stream (46). This so-called hydrodynamic focussing results in coaxial flow (a narrow stream of cells flowing in a core within a wider sheath stream); it was first applied to cytometry by Crosland-Taylor, who realized that this was a way to confine cells to a precise position without requiring a narrow stream that was susceptible to obstruction.

The “flow cell” is the site in the cytometer where the sample stream is injected into the sheath stream (Figs. 3 and 4). After joining the sheath stream, the velocity of the cell suspension (in meters per second) either increases or decreases so that it becomes equal to the velocity of the sheath stream. The result is that the cross-sectional diameter of the core stream containing the cells will either increase or decrease to bring about this change in the velocity of flow while maintaining the same sample volume flow rate (in milliliters per second). The injection rate of the cell suspension will therefore directly affect the width of the core stream and the stringency by which cells are confined to the center of the illumination beam.

After use of hydrodynamic focusing to align the flow of the cells within a wide sheath stream so that blockage is infrequent, there is still a requirement for rapid analysis, for better confining of the flow of cells to the very bright center of the laser beam, and for the avoidance of coincidence of multiple cells in the analysis point. These characteristics are provided by the design of the flow cell (cf. 47). Some cytometers illuminate the stream of cells within an optically clear region of the flow cell (as in a cuvet). Other systems use flow cells where the light beam intersects the fluid stream after it emerges from the

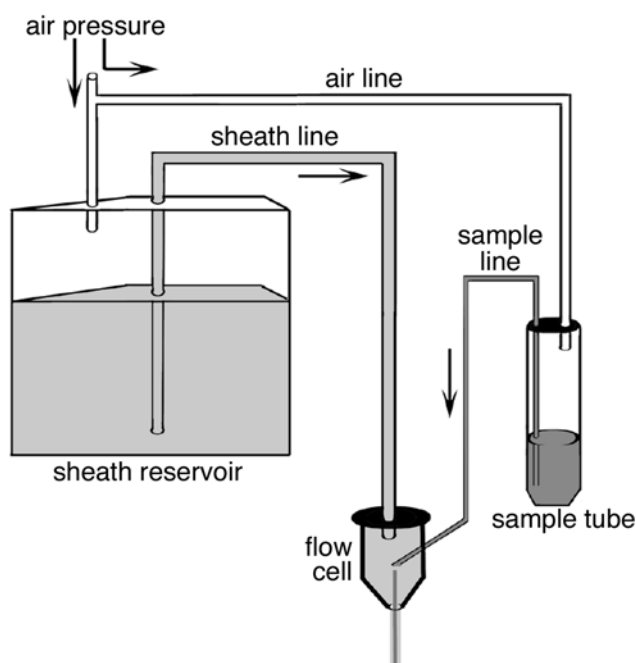


Fig. 3. The fluidics system of a flow cytometer, with air pressure pushing both the sample with suspended cells and the sheath fluid into the flow cell. (Reprinted with permission of John Wiley & Sons. Copyright 2001 from Givan, A. L. [2001] *Flow Cytometry: First Principles*, 2nd edit. Wiley-Liss, New York; and also from Givan, A. L. [2001] Principles of flow cytometry: an overview, in *Cytometry*, 3rd edit. [Darzynkiewicz, Z., et al., eds.], Academic Press, San Diego, CA, pp. 415–444.)

flow cell through an orifice (“jet-in-air”). In all cases, the flow cell increases the velocity of the stream by having an exit orifice diameter that is narrower than the diameter at the entrance. The differences in diameter are usually between 10- and 40-fold, bringing about an increase in velocity equal to 100- to 1600-fold (47). As the entire stream (with the cell suspension in the core of the sheath stream) progresses toward the exit of the flow cell, it narrows in diameter and increases in velocity. With this narrowing of diameter and increasing of velocity, the path of the cells becomes tightly confined to the center of the laser beam so that all cells are illuminated similarly and the cells move through the laser beam rapidly. In addition, cells are spread out at greater distances from each other in the now very narrow stream and are therefore less likely to coincide in the analysis point.

In summary, with regard to the fluidics of the flow cytometer, the hydrodynamic focussing of a core stream of cells within a wider sheath stream facili-

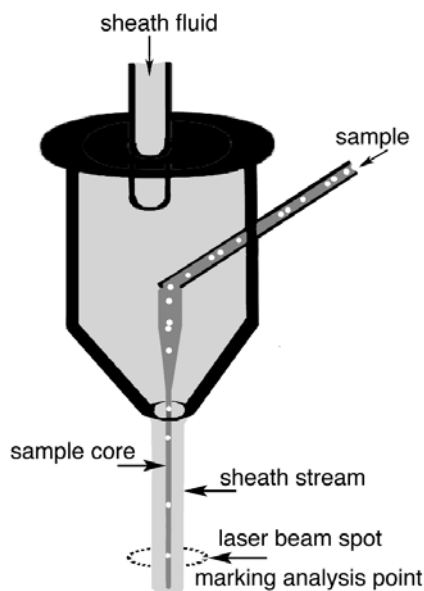


Fig. 4. A flow cell, with the sample suspension injected into the sheath fluid and forming a central core in the sheath stream. The small diameter of the flow cell at its exit orifice causes the sheath stream and sample core to narrow so that cells flow rapidly and are separated from each other and less likely to coincide in the analysis point.

tates the alignment of cells in the center of the laser beam without the clogging problems associated with narrow tubing and orifices. In addition, the flow cell itself increases the velocity of the stream; as well as increasing the rate at which cells are analyzed, this increased velocity also narrows the core stream to align it more precisely in the uniformly bright center of the laser beam and, at the same time, increases the distance between cells in the stream so that coincidence events in the analysis point are less frequent.

5. Signals From Cells

Lenses around the analysis point collect the light coming from cells as a result of their illumination by the laser(s). Typically there are two lenses, one in the forward direction along the path of the laser beam and one at right angles (orthogonal) to this direction (**Fig. 5**). These lenses collect the light (the signals) given off by each cell as it passes through the analysis point. The lens in the forward direction focusses light onto a photodiode. Across the front of this forward lens is a blocker (or “obscuration”) bar, approx 1 mm wide, positioned so as to block the laser beam itself as it passes through the stream. Only light

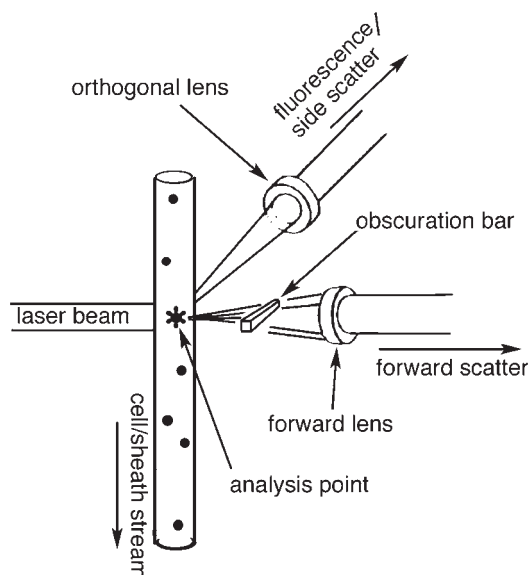


Fig. 5. The analysis point of a flow cytometer, with the laser beam, the sheath stream, and the lenses for collection of forward scatter and side scatter/fluorescence all at orthogonal angles to each other.

from the laser that has been refracted or scattered as it goes through a particle in the stream will be diverted enough from its original direction to avoid the obscuration bar and strike the forward-positioned lens and the photodiode behind it. Light striking this forward scatter photodetector is therefore light that has been bent to small angles by the cell: the three-dimensional range of angles collected by this photodiode falls between those obscured by the bar and those lost at the limits of the outer diameter of the lens. The light striking this photodetector is called forward scatter light (“fsc”) or forward angle light scatter (“fals”). Although precisely defined in terms of the optics of light collection for any given cytometer, forward scatter light is not well defined in terms of the biology or chemistry of the cell that generates this light. A cell with a large cross-sectional area will refract a large amount of light onto the photodetector. But a large cell with a refractive index quite close to that of the medium (e.g., a dead cell with a permeable outer membrane) will refract light less than a similarly large cell with a refractive index quite different from that of the medium. Because of the rough relationship between the amount of light refracted past the bar and the size of the particle, the forward scattered light signal is sometimes (misleadingly) referred to as a “volume” signal. This term belies its complexity (48).

The lens at right angles to the direction of the laser beam collects light that has been scattered to wide angles from the original direction. Light collected by this lens is defined by the diameter of the lens and its distance from the analysis point and is called side scatter light (“ssc”) or 90° light scatter. Laser light is scattered to these angles primarily by irregularities or texture in the surface or cytoplasm of the cell. Granulocytes with irregular nuclei scatter more light to the side than do lymphocytes with spherical nuclei. Similarly, more side scatter light is produced by fibroblasts than by monocytes.

The signals that have been described so far (forward scatter and side scatter) are signals of the same color as the laser beam striking the cell. In a single laser system, this is usually 488-nm light from an argon ion laser; in a system with two or more lasers, the scattered light is also usually 488 nm, because it is collected from the primary laser beam. As we have described, this scattered light provides information about the physical characteristics of the cell. In addition to this scattered light, the cell may also give off fluorescent light: fluorescent light is defined as light of a relatively long wavelength that is emitted when a molecule absorbs high energy light and then emits the energy from that light as photons of somewhat lower energy. Fluorescein absorbs 488-nm light and emits light of approx 530 nm. Phycoerythrin absorbs 488-nm light and emits light of approx 580 nm. Therefore, if a cell has been stained with antibodies of a particular specificity conjugated to fluorescein and with antibodies of different specificity conjugated to phycoerythrin and then the cell passes through a 488-nm laser beam, it will emit light of 530 nm and 580 nm. Some cells may also contain endogenous fluorescent molecules (such as chlorophyll or pyridine or flavin nucleotides). In addition, cells can be stained with other probes that fluoresce more or less depending on the DNA content of the cell or the calcium ion content of the cell, for example. In all these cases, the intensity of the fluorescent light coming from the cell is, to an arguable extent, related to the abundance of the antigen or the DNA or the endogenous molecule or the calcium ion concentration of the cell. Measuring the intensity of the fluorescent light will give, then, some indication of the phenotype or function of the cells flowing through the laser beam(s).

Detecting fluorescent light is similar to detecting side-scatter light, but with the addition of wavelength-specific mirrors and filters (*see ref. 49*). These mirrors and filters are designed so that they transmit and reflect light of well-defined wavelengths. The light emitted to the side from an analysis point is focussed by the lens onto a series of dichroic mirrors and bandpass filters that partition this multicolor light, according to its color, onto a series of separate photomultiplier tubes (*see Figs. 6 and 7*). In a simple example, side scatter light (488 nm) is directed toward one photomultiplier tube (PMT); light of 530 nm is directed toward another PMT; light of 580 nm is directed toward

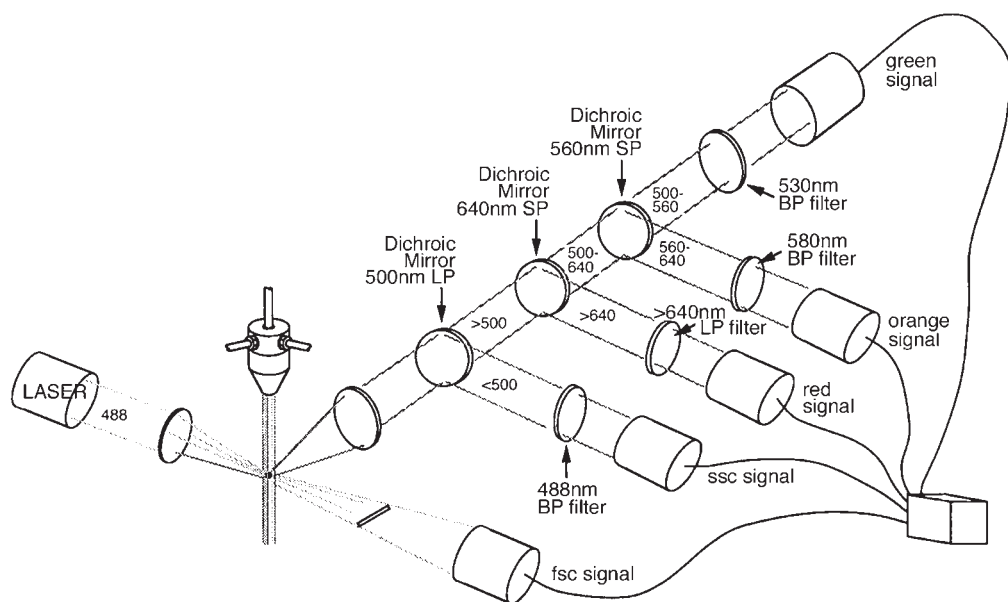


Fig. 6. The use of wavelength-specific bandpass and longpass filters and dichroic mirrors to partition the light signal from cells to different photodetectors according to its color. In the system depicted here, there are five photodetectors; they detect forward scatter light, side scatter light, and fluorescence light in the green, orange, and red wavelength ranges. (Reprinted with permission of John Wiley & Sons, Inc. Copyright 2001 from Givan, A. L. [2001] *Flow Cytometry: First Principles*, 2nd edition. Wiley-Liss, New York.)

another PMT; and light >640 nm is directed toward another PMT (**Fig. 6**). In this example, the system will have four PMTs at the side, individually specific for turquoise, green, orange, or red light. Adding in the additional photodetector for forward scatter light, this instrument would be called a five-parameter flow cytometer. Flow cytometers today have, typically, anywhere from 3 to 15 photodetectors and thus are capable of detecting and recording the intensity of forward scatter light, side scatter light, and fluorescent light of 1–13 different colors. Because multiple excitation wavelengths are required to excite a large range of fluorochromes (distinguishable by their fluorescence emission wavelengths), high-parameter cytometers normally will have several lasers. The cells will pass, in turn, through each of the laser beams and the photodetectors will be arranged spatially so that some of the detectors will measure light excited by the first laser, some will measure light excited by the second laser, and so forth.

The signals emitted by a cell as it passes through each laser beam are light pulses that occur over time, with a beginning, an end, a height, and an inte-

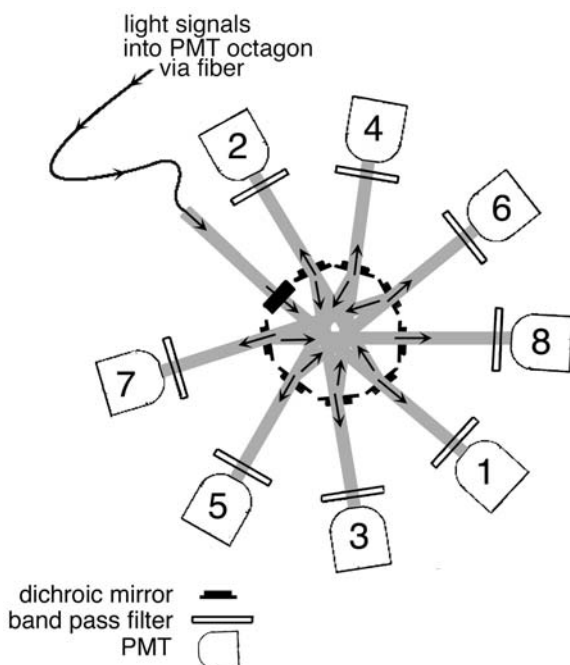


Fig. 7. Arrangement of eight PMTs with their dichroic mirrors and bandpass filters to partition light from the analysis point. Light enters the octagon via a fiber and progresses toward PMT 1; at the dichroic mirror in front of PMT 1, light of some colors is transmitted and reaches PMT 1, but light of other colors is partitioned and reflected toward PMT 2. At the dichroic mirror in front of PMT 2, light of some colors is transmitted toward PMT 2, but light of other colors is reflected toward PMT 3. In this way, light progresses through the octagon, with specific colors directed toward specific photodetectors. This octagon system has been developed by Becton Dickinson (BD Biosciences, San Jose, CA); this figure is a modification of graphics from that company.

grated area. On traditional cytometers, the signal is “summarized” either by the height of the signal (related to the maximum amount of light given off by the cell at any time as it passes through the laser beam) or by the integrated area of the signal (related to the total light given off by the cell as it passes through the laser beam). Some newer cytometers analyze the signal repeatedly (10 million times per second) during the passage of the cell through the beam and those multiple numbers are then processed to give a peak height or integrated area readout or can be used to describe the pattern of light as it is related to the structure of the cell along its longitudinal axis. With these options, there will be one or more values that are derived from each photodetector for each cell. In a simple case, for example, only the integrated (area) fluorescence

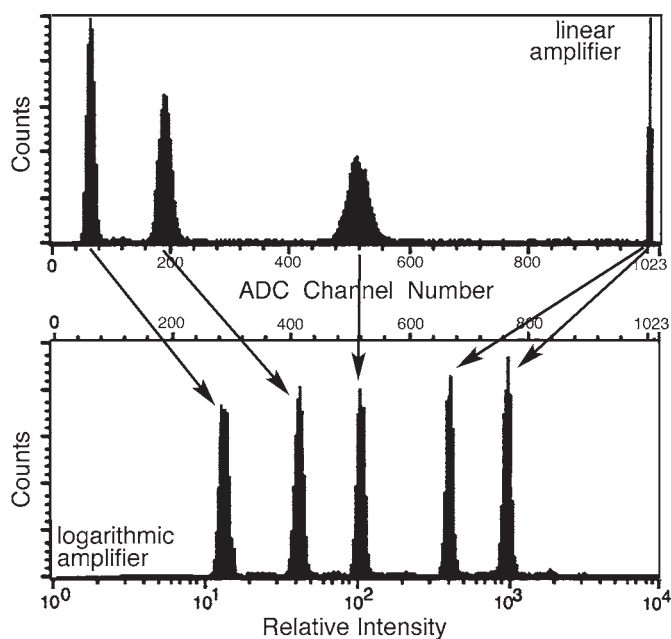


Fig. 8. The graphing of flow cytometric signals from fluorescent beads of five different intensities. The signals in the **upper graph** were acquired on an analog cytometer with linear amplification; the intensity values reported by an analog-to-digital converter with 1024 channels have been plotted directly on the histogram axis. The two brightest beads are off scale (at the right-hand edge of the graph). The signals in the **lower graph** were acquired on an analog cytometer with logarithmic amplification; intensity values reported by the 1024-channel ADC can be plotted according to channel number, but are conventionally plotted according to the derived value of “relative intensity.” With logarithmic amplification, beads of all five intensities are “on scale.” (Reprinted from Givan, A. L. [2001] *Principles of flow cytometry: an overview*, in *Cytometry*, 3rd edition [Darzynkiewicz, Z., et al., eds.], Academic Press, San Diego, CA, pp. 415–444.)

detected by each photodetector will be used; the values stored for these integrated intensities from, for example, a five-photodetector system, will form the five-number flow cytometric description of each cell. A fifteen parameter system will have, in this simple example, a 15-number flow description for each cell.

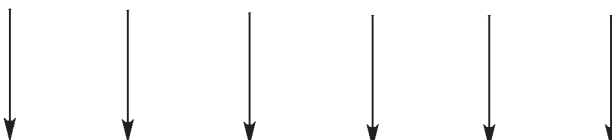
6. From Signals to Data

In a so-called “analog” or traditional cytometer, the current from each photodetector will be converted to a voltage, will be amplified, may be processed

for ratio calculations or spectral cross-talk correction, and then, finally, will be digitized by an analog-to-digital converter (ADC) so that the final output numbers will have involved binning of the analog (continuous) amplified and processed values into (digital) channels. The amplification can be linear or logarithmic. If linear amplification is used, the intensity value is usually digitized and reported on a 10-bit or 1024-channel scale and is displayed on axes with linear values; the numbers on the axis scale are proportional to the light intensity (**Fig. 8**, upper graph). By contrast, if logarithmic amplifiers are used, the output voltage from the amplifier is proportional to the logarithm of the original light intensity; it will be digitized, again usually on a 1024-channel scale, and the digitized final number will be proportional to the log of the original light intensity. In this case, the usual display involves the conversion of the values to “relative intensity units” and the display of these on axes with a logarithmic scale (**Fig. 8**, bottom axis of lower graph). When logarithmic amplifiers are used, they divide the full scale into a certain number of decades: that is, the full scale will encompass three or four or more 10-fold increases; a four decade scale is common (that is, something at the top end of the scale will be 10^4 times brighter than something at the bottom end of the scale). It is important here to understand the reasons for choice of linear or logarithmic amplification. Linear amplification displays a limited range of intensities; logarithmic amplification, by contrast, will display a larger range of intensities (compare upper and lower graphs in **Fig. 8**). For this reason, linear amplifiers are conventionally used for measurements of DNA content—where the cells with the most DNA in a given analysis will generally have about twice the DNA content of the cells with the lowest DNA content. By contrast, cells that express proteins may have, after staining, 100 or 1000 times the brightness of cells that do not express those proteins; logarithmic amplification allows the display of both the positive and negative cells on the same graph.

Although the terminology is confusing (because all cytometers report, in the end, digitized channel numbers), some newer flow systems are referred to as “digital systems” because the current from the photodetectors is converted to a voltage and then digitized immediately without prior amplification and processing. There are advantages to this early digitization that relate to time and to the elimination of some less than perfect electronic components (*see refs. 12,50*). By using high-resolution analog-to-digital converters, the intensity values from the signal (possibly sampled at 10 MHz) can be reported on a 14-bit or 16,384-channel scale. The reported digitized numbers can then be processed to describe the integrated area, the height, or the width of the signal, where the integrated area, in particular, is usually most closely proportional to the intensity of the original light signal. Because the numbers are reported to high resolution, they can then be plotted on either linear or logarithmic axes. These

CELL#	fsc	ssc	integrated area of signal		
			green fl.	orange fl.	red fl.
1	784	1233	10344	476	300
2	700	1145	11657	334	435
3	698	1289	13228	476	436
4	877	990	10453	335	478
5	789	1119	12897	501	512
6	690	998	14987	375	423
7	777	1309	14376	349	584
8	689	1401	13765	360	474
9	2089	3022	543	299	14099
10	786	1322	10367	474	499
11	688	1034	11438	356	375
12	1998	3400	464	487	15833
13	2134	3289	502	503	14998
14	745	1008	13245	499	416
15	300	432	321	321	431
16	876	1204	11498	509	485
17	775	1023	11749	464	458
18	2109	3356	387	375	15684
19	799	1039	12149	399	396



et cetera

Fig. 9. A flow cytometric data file is a list of cells in the order in which they passed through the analysis point. In this five-parameter file, each cell is described by five numbers for the signals from the forward scatter (fsc), side scatter (ssc), green fluorescence (fl.), orange fluorescence, and red fluorescence photodetectors.

high resolution ADCs obviate the need for logarithmic amplifiers, avoiding some of the problems that derive from their nonlinearity (*see refs. 51–53*).

What we now have described is a system that detects light given off by a particle in the laser beam; the light is detected according to which laser has excited the fluorescence or scatter, according to the direction the light is emitted (forward or to the side), and according to its color. The intensity of the light striking each photodetector may be analyzed according to its peak height intensity, its integrated area (total) intensity, or according to the many numbers that describe the signal over time. The numbers derived from each photodetector can be recorded digitally or can be amplified either linearly or logarithmically before digitization. Each cell will then have a series of numbers describing it, and the data file contains the collection of numbers describing each cell that has been run through the cytometer during the acquisition of a

particular sample (**Fig. 9**). If 10,000 cells have been run through the cytometer and it is a five-detector cytometer, there will be five numbers describing each cell (or ten, if, e.g., signal width and signal height are both recorded). If five parameters have been recorded for each cell, the data file will consist of a list of 50,000 numbers, describing in turn all the cells in the order in which they have passed through the laser beam. The data file structure will conform more or less to a published flow cytometry standard (FCS) format (**54**).

7. From Data to Information

After the data about a group of cells are stored into a data file, all the remaining processes of flow cytometry are computing. Instrument vendors write software for the analysis of data acquired on their instruments; independent programmers write software for the analysis of data acquired on any instrument. Software packages vary in price, elegance, and sophistication, but they all perform some of the same functions: they all allow a display of the distribution of any one parameter value for the cells in the data file (in a histogram); they all allow a display of correlated data between any two parameters' values (in a dot plot or contour plot or density plot); and they all allow the restriction of the display of information to certain cells in the data file ("gating").

A histogram (**Fig. 10**) is used to display the distribution of one parameter over the cells in the data file. With the data from a five-parameter flow cytometer, there will be five numbers describing each cell (e.g., the intensities of forward scatter, side scatter, green fluorescence, orange fluorescence, and red fluorescence). A histogram (really a bar graph, with fine resolution between categories so that the bars are not visible) can display the distribution of each of those five parameters (in five separate histograms), so that we can see whether the distribution for each parameter is unimodal or bimodal; what the average relative intensities are of the cells in the unimodal cluster or in the two bimodal clusters; what proportion of the cells have intensities brighter or duller than a certain value. Numbers can be derived from these histogram distributions; by using "markers" or "cursors" to delineate ranges of intensity, software can report the proportion of cells with intensities in each of the ranges.

Because a flow data file provides several numbers (in the case of a five-parameter flow cytometer, five numbers) describing each cell, plotting all the data on five separate histograms does not take advantage of the ability we have to reveal information about the correlation between parameters on a single-cell basis. For example, do the cells that fluoresce bright green also fluoresce orange or do they not fluoresce orange? For the display of correlated data, flow software provides the ability to plot dot plots or contour plots or density plots. Although these alternative two-dimensional plots have different advantages in

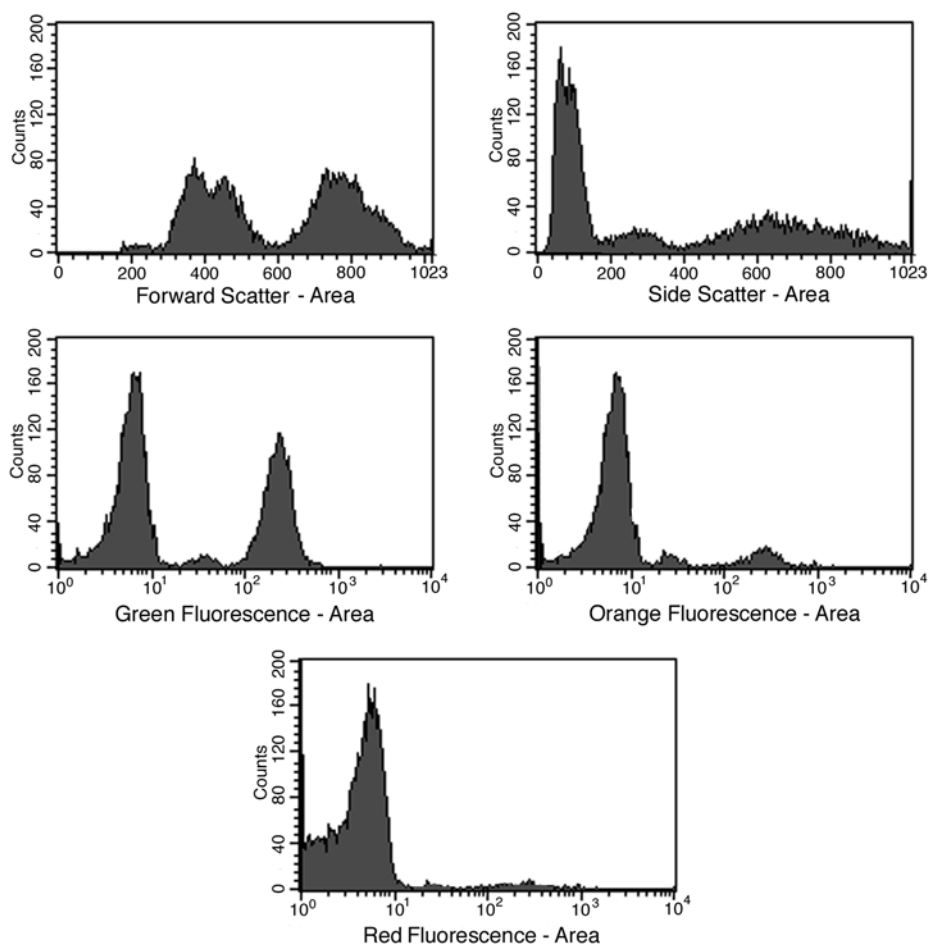


Fig. 10. The five histograms derived from a five-parameter flow cytometric data file. The scatter and fluorescence distributions are plotted individually for all the cells in the file. Forward and side scatter were acquired with linear amplification and the integrated intensity values ("area") are plotted according to the ADC channel number. The fluorescence signals were acquired with logarithmic amplification and their integrated intensity values are plotted according to the derived value of relative intensity.

terms of visual impact and graphical authenticity to the hard data, they all display two parameters at once and report the same quantitative analysis (**Fig. 11**). By using a two-dimensional plot, a scientist can see whether the cells that fluoresce green also fluoresce orange. Further, this information can be reported quantitatively, using markers to delineate intensity regions in two dimensions. These two-dimensional markers are called quadrants if they have been used to

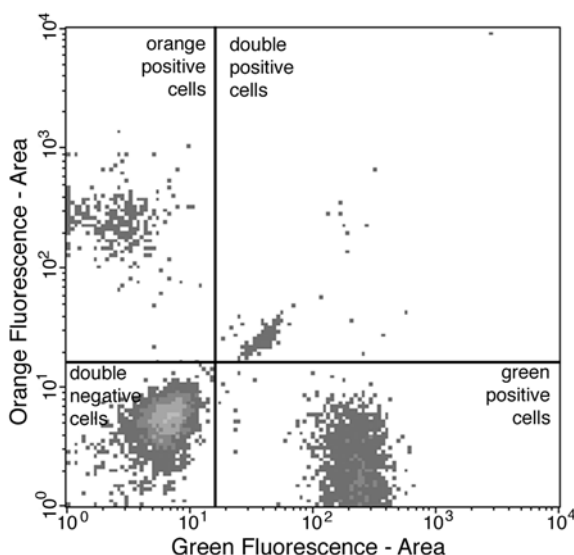


Fig. 11. A two-dimensional density plot, indicating the correlation of green and orange fluorescence for the cells in a data file. Quadrants divide the intensity distributions into regions for unstained (“double-negative”) cells, cells that are stained both green and orange (“double-positive cells”), and cells stained for each of the colors singly. In this example, it can be seen that most of the green-positive cells are not also orange-positive (that is, they are not double positive).

delineate so-called double-negative, single-positive (for one color), single-positive (for the second color), and double-positive cells (**Fig. 11**).

One of the unique aspects of flow cytometry is the possibility of “gating.” Gating is the term used for the designation of cells of interest within a data file for further analysis. It permits the analysis of subsets of cells from within a mixed population. It also provides a way to analyze cells in high levels of multiparameter space (55,56). **Figure 12** shows an example of a mixed population of white blood cells that have been stained with fluorescent antibodies. Because the white blood cells of different types can be distinguished from each other by the separate clusters they form in a plot of forward scatter vs side scatter light, the fluorescence of the monocytes can be analyzed without interference from the fluorescence of the lymphocytes or neutrophils in the data file. Similarly, the neutrophils and lymphocytes can also be analyzed independently of the other populations of cells. The procedure for doing this involves drawing a “region” around the cluster of, for example, monocytes in the fsc vs ssc plot. That region defines a group of cells with particular characteristics in

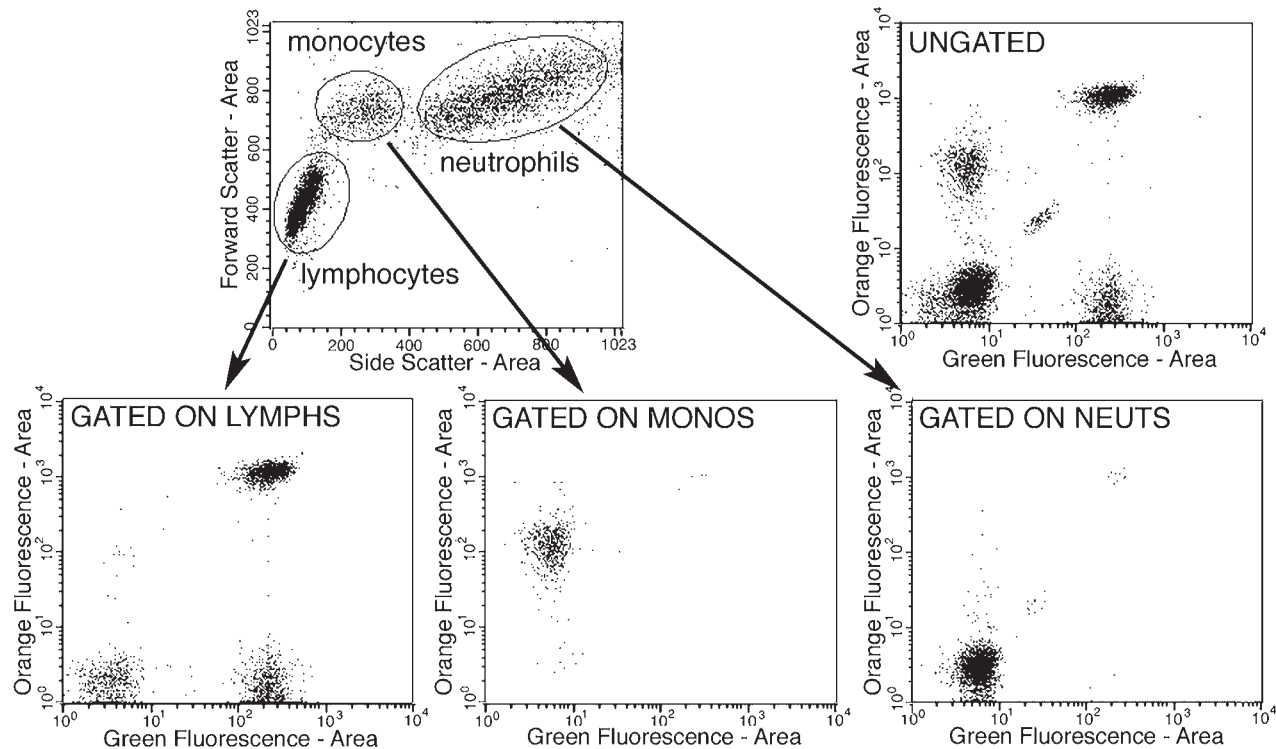


Fig. 12. A plot of forward vs side scatter for leukocytes from the peripheral blood indicates that regions can be drawn around cells with different scatter characteristics, marking lymphocytes, monocytes, and neutrophils. These regions can be used to define gates. The four plots of green vs orange fluorescence are either ungated displaying the fluorescence intensities of all the cells (*upper right*); or are gated on each of the three leukocyte populations, revealing that the three types of leukocytes stain differently with the orange and green antibodies.

the way they scatter light. The region can then be used as a gate for subsequent analysis of the fluorescence of cells. A gated dot plot of, for example, green fluorescence vs orange fluorescence can display the fluorescence data from only the cells that fall into the “monocyte” region. Gates can be simple in this way. Or they can be more complex, facilitating the analysis of cells that have been stained with many reagents in different colors: for example, a gate could be a combination of many regions, defining cells with certain forward and side scatter characteristics, certain green fluorescence intensities, and certain orange fluorescence intensities. The final step in analysis could use a gate that combines all these regions and could then ask how the cells with bright forward scatter, medium side scatter, bright green intensity, and little or no orange intensity are distributed with regard to red fluorescence.

8. Sorting

It might seem that flow cytometers would have developed first with the ability to detect many colors of fluorescence from particles or cells and that it then might have occurred to someone that it would be useful to separate cells with different fluorescent or scatter properties into separate test tubes for further culture, for RNA or DNA isolation, or for physiological analysis. The actual history, however, followed the opposite course. Early flow cytometers were developed to separate cells from each other (7,8,11). A cytometer was developed in 1965 by Mack Fulwyler at the Los Alamos National Laboratory to separate red blood cells with different scatter signals from each other to see if there were actually two separate classes of erythrocytes or, alternatively, if the scatter differences were artifactual based on the flattened disc shape of the cells. The latter turned out to be true—and the same instrument was then used to separate mouse from human erythrocytes and a large component from a population of mouse lymphoma cells (8). For several years, flow cytometers were thought of as instruments for separating cells (the acronym FACS stands for “fluorescence-activated cell *sorter*”). It was only slowly that these instruments began to be used primarily for the assaying of cells without separation. Modern cytometers most often do not even possess the capability of separating cells.

Although many methods are available for separating/isolating subpopulations of cells from a mixed population (e.g., adherence to plastic, centrifugation, magnetic bead binding, complement depletion) and these methods are usually significantly more rapid than flow sorting, flow sorting may be the best separation technique available when cells differ from each other by the way they scatter light, by slight differences in antigen intensity, or by multiparameter criteria. Cells sorted by flow cytometry are routinely used for functional assays, for polymerase chain reaction (PCR) replication of cell-type specific DNA sequences, for artificial insemination by sperm bearing X or Y chromo-

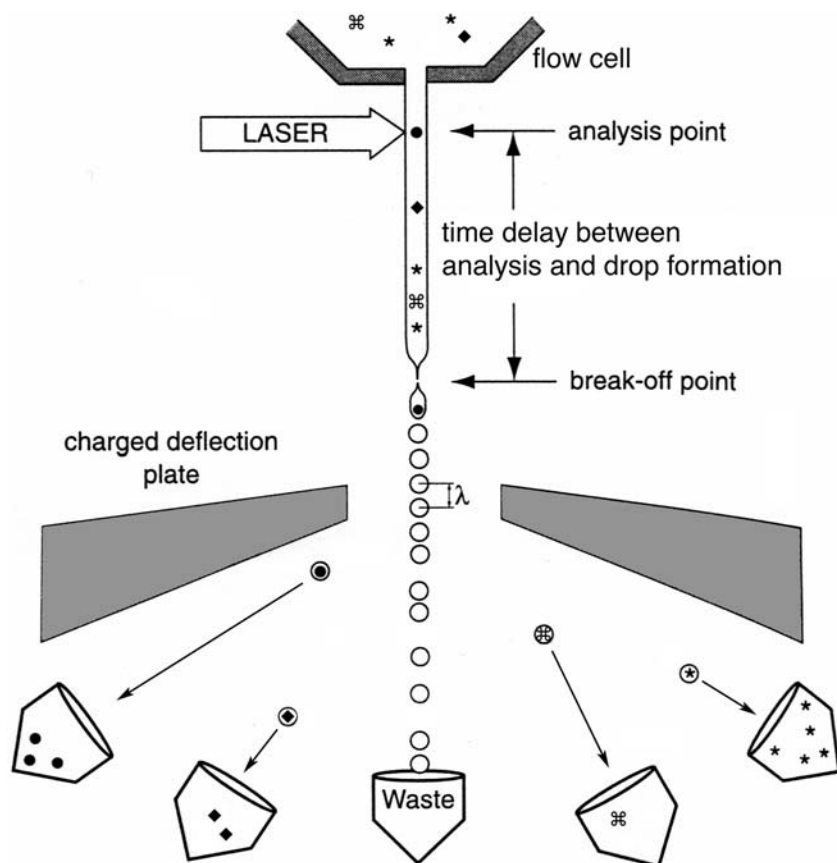


Fig. 13. Droplet formation for sorting. A vibrating flow cell causes the sheath stream to break up into drops at the breakoff point. Cells flowing in the stream are enclosed in drops and, in the example shown here, drops can be charged strongly or less strongly positive or negative, so that four different types of cells (as detected at the analysis point) can be sorted into four receiving containers.

somes, and for cloning of high-expressing transfected cells. In addition, sorted chromosomes are used for the generation of DNA libraries.

The strategy for electronic flow sorting involves the modification of a non-sorting cytometer in three ways: the sheath stream is vibrated so that it breaks up into drops; the stream (now in drops) flows past two charged (high-voltage) plates; and the electronics of the instrument are modified so that the drops can be charged or not according to the characteristics of any contained cell, as detected at the analysis point (**Fig. 13**). In a sorting cytometer, cells flow through the analysis point where they are illuminated and their scatter and fluorescence sig-

nals detected as in a nonsorting instrument. They then continue to flow downstream where, as the stream breaks up into drops, they become enclosed in individual drops. If the cells are far enough apart from each other in the stream, there will be very few cases in which there is more than one cell in each drop; there will be, by operator choice, cells in, on average, only every third or fifth or tenth drop—and there will be empty drops between the drops containing cells. The number of cells per drop (and the number of empty drops) will be determined by the number of cells flowing per second, by the vibration frequency that is creating the drops, and by the impact of the mathematics of a Poisson distribution, whereby cells are never perfectly distributed along the stream but can cluster with some probability (the Fifth Avenue bus phenomenon).

A vibrating stream breaks up into drops according to the following equation

$$v = f\lambda$$

which defines the fixed relationship between the velocity of the stream (v), the frequency of the drop generation vibration (f), and the distance between the drops (λ). Drop formation is stable when the distance between drops equals 4.5 times the diameter of the stream, so a given stream diameter (flow cell exit orifice) will determine the λ value. Rapid drop formation (high f) is desirable because rapid drop formation allows rapid cell flow rate (without multiple cells in a drop). Therefore this condition is facilitated by using a high stream velocity and also a narrow stream diameter (but being aware that a narrow flow cell orifice gets clogged easily). Common conditions for sorting, with a 70- μm flow cell orifice, involve stream velocities of about 10 m/s and drop drive frequencies of about 32 kHz (meaning that cells flowing at 10,000 cells per second will be, on average, in every third drop). Conditions for so-called high speed sorting involve stream velocities of about 30 m/s and drop drive frequencies of 95 kHz (cells flowing at 30,000 cells/s will be, on average, in every third drop).

Because drops break off from the vibrating stream at a distance from the fixed point of vibration, the stream of cells can be illuminated and the signals from the cells collected with little perturbation as long as the analysis point is relatively close to the point of vibration and far away from the point of drop formation. In a sorting cytometer, cells are illuminated close to the flow cell (or within an optically clear flow cell); their signals are collected, amplified, and digitized in ways similar to those in nonsorting cytometers. A sorting cytometer differs from a nonsorting cytometer because cells become enclosed in drops after they move down the stream. At points below the drop breakoff point, the stream will consist of a series of drops, all separate from each other, with some drops containing cells. The flow operator will have drawn sort regions around cells “of interest” according to their flow parameters. If a cell in the analysis point has been determined to be a cell of interest according to the sort regions,

the drop containing that cell will be charged positively or negatively so that it will be deflected either to the left or right as it passes the positive and negative deflection plates. Modern cytometers have the ability to charge drops in four ways (strongly or weakly positive and strongly or weakly negative), so that four sort regions can be designated and four subpopulations of cells can be isolated from the original population. Collecting tubes are placed in position, one or two more or less at the left and one or two more or less at the right, and the deflected drops, containing the cells of interest, will be collected in the tubes. Uninteresting cells will be in uncharged drops; they will not be deflected out of the main stream and they will pass down the center and into the waste container.

Sorted cells will be pure when only those drops containing the cells of interest are charged. This happens because the sort operator determines the length of time required for a cell to move from the analysis point to the position of its enclosure in a drop (at the drop “breakoff point” downstream); the stream is charged for a short period of time at exactly this time delay after a cell of interest has been detected. This drop delay time can be determined empirically, by testing different drop delay times on a test sort with beads. Alternatively, it can be measured using drop separation units (knowing the drop generation frequency, the reciprocal is equal to the number of seconds per drop; therefore, the distance between drops [which can be measured] has an equivalence in time units). Given the time that it takes between analysis of a cell in the laser beam and the enclosure of that cell into its own self-contained drop, the flow cytometer can be programmed to apply a charge to the stream for a short interval, starting at the time just before the cell of interest is about to detach from the main stream into the drop. If the charge is applied for a short interval, only one drop will be charged. If it is charged for a longer interval, then drops on either side of the selected drop can be charged (for security, in case the cell moves faster or slower than predicted). The charge on the stream can be positive or negative (or weakly or strongly positive or negative) and therefore the drops containing two or four mutually exclusive subsets of cells can be deflected into separate collection vessels.

Cell sorting is validated by three characteristics: the efficiency of the sorting of the cells of interest from the original mixed population; the purity of those cells according to the selection criteria; and the time it has taken to obtain a given number of sorted cells (57). In most cytometers, purity is protected because drop charging is aborted when cells of the wrong phenotype are enclosed with cells of interest in a single drop. In this way, high cell flow rates will compromise the sorting efficiency but will not compromise purity until the cell flow rate is so fast that there is significant coincidence of multiple cells in the laser beam. As the cell flow rate increases (using cells at higher concen-

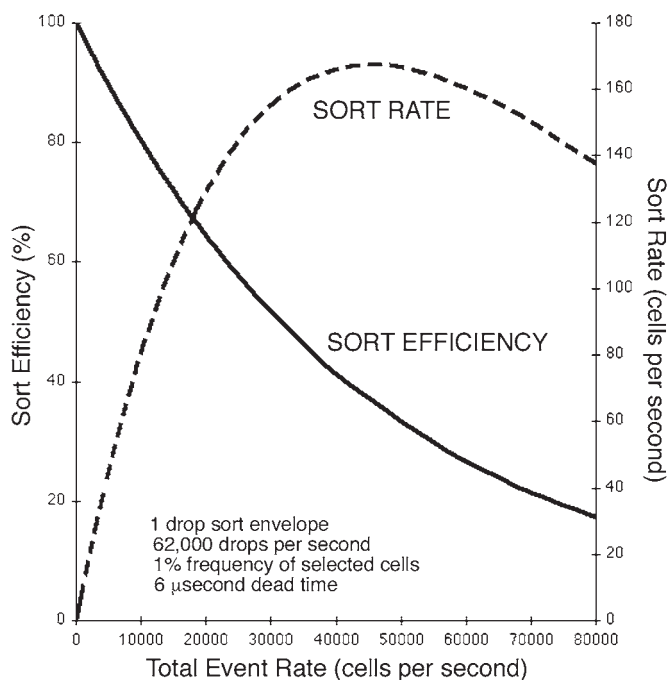


Fig. 14. The efficiency and speed of sorting are affected by the flow rate of cells through the analysis point. Sorting at a high flow rate decreases the efficiency but increases the speed at which sorted cells are collected (until so many sorts are aborted as a result of multiple cells in drops that the sort rate begins to decline). The model from which these graphs were derived is from Robert Hoffman.

trations), the speed of sorting will increase until the number of aborted sorts gets so high that the actual speed of sorting of the desired cells starts to drop off (**Fig. 14**). Some sorting protocols will be designed to obtain rare cells: these sorts will be done at relatively low speed but with resulting high efficiency. Other protocols will start with buckets of cells and will be concerned most with getting cells in a short period of time, without regard to the efficiency of the sort; these sorts can be done at high speed where the efficiency is low but the speed of sorting is high. The bottom line is that speed and efficiency interact and both cannot be optimized at the same time.

9. Conclusions

Flow cytometry has, arguably, remained a relatively constant technology since its entry in 1969 (**10,11**) into the modern era. The main technological changes that have occurred over the past 34 yr have been quantitative rather than qualitative. More parameters can now be analyzed simultaneously, more

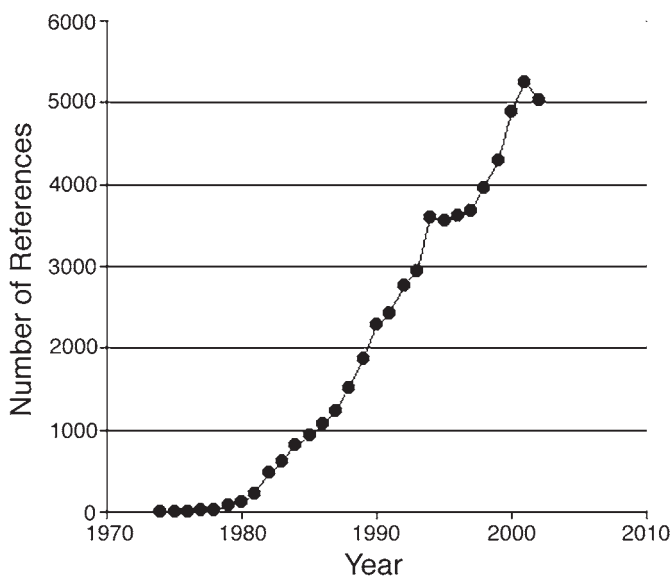


Fig. 15. Increasing reference to “flow cytometry” in the Medline-indexed literature over the past three decades. The actual use of flow cytometers predates the use of the term itself.

cells can be analyzed or sorted per second, and more sensitivity is available to detect fewer fluorescent molecules; in addition, flow cytometers are both smaller and less expensive than they were. However, a flow cytometer still involves particles flowing one by one past a laser beam, with photodetectors nestled around the analysis point to detect fluorescent or scattered light coming from the particles.

By contrast with the less than radical changes in flow instrument technology, the increasing diversity of applications has been striking. For a start, the use of flow cytometry has increased remarkably; **Fig. 15** indicates that references to “flow cytometry” in the Medline data base were zero in 1970, 113 in 1980, 2286 in 1990, and 4893 in the year 2000. But more important than the number of references is the range of applications that are now being addressed by flow cytometry. In the 1970s, leukocytes and cultured cells were the main particles analyzed by flow cytometry; now plankton, bacteria, disaggregated tissues, plant cells, viruses, chromosomes, latex beads, and DNA fragments are all, more or less, taken for granted. In addition, early flow cytometry looked at fluorescence emanating primarily from the stained proteins on the surface of cells or from stained DNA in their nuclei. Now plankton are examined for their auto-fluorescence, animal and plant cells are assayed for fluorescence that reflects their proliferative or metabolic function, sperm are sorted based on their X or

Y genotype, many aspects of protein or DNA synthesis are assayed to indicate stage of cell cycle or of apoptosis, and bacteria are typed according to the size of their DNA fragments after restriction enzyme digestion. Indeed, flow cytometry has also been applied to beads, which are used to capture soluble analytes from the blood or culture medium; the beads, not the cells, are analyzed by flow cytometry to see how much of the analyte has been bound to their surface and, by comparison with standard curves, to indicate the concentration of analyte in the medium (34).

Through its history, flow cytometry has sparked the collaboration of mathematicians, engineers, chemists, biologists, and physicians, working together to provide instrumentation that now probes not just our bodies and our culture flasks, but also the depths of the ocean (see ref. 58) and, potentially, life in space (or, at least, life in spaceships [59,60]). If nothing else, the example of flow cytometry should inspire us toward collaboration and to an open mind.

Acknowledgments

Howard Shapiro and Ben Verwer have provided me with advice on some of the electronic and illumination aspects of flow cytometry. I thank them for their help; all mistakes are very much my own.

References

1. Moldavan, A. (1934) Photo-electric technique for the counting of microscopical cells. *Science* **80**, 188–189.
2. Gucker Jr., F. T., O'Konski, C. T., Pickard, H. B., and Pitts Jr., J. N. (1947) A photoelectronic counter for colloidal particles. *J. Am. Chem. Soc.* **69**, 2422–2431.
3. Cornwall, J. B. and Davison, R. M. (1950) Rapid counter for small particles in suspension. *J. Sci. Instrum.* **37**, 414–417.
4. Coulter, W. H. (1956) High speed automatic blood cell counter and analyzer. *Proc. Natl. Electronics Conf.* **12**, 1034–1040.
5. Bierne, T. and Hutcheon, J. M. (1957) A photoelectric particle counter for use in the sieve range. *J. Sci. Instrum.* **34**, 196–200.
6. Kametsky, L. A. and Melamed, M. R. (1965) Spectrophotometer: new instrument for ultrarapid cell analysis. *Science* **150**, 630–631.
7. Kametsky, L. A. and Melamed, M. R. (1967) Spectrophotometric cell sorter. *Science* **156**, 1364–1365.
8. Fulwyler, M. J. (1965) Electronic separation of biological cells by volume. *Science* **150**, 910–911.
9. Dittrich, W. and Göhde, W. (1969) Impulsfluorometrie der einzelnzellen in suspensionen. *Z. Naturforsch.* **24b**, 360–361.
10. Van Dilla, M. A., Trujillo, T. T., Mullaney, P. F., and Coulter, J. R. (1969) Cell microfluorimetry: a method for rapid fluorescence measurement. *Science* **163**, 1213–1214.

11. Hulett, H. R., Bonner, W. A., Barrett, J., and Herzenberg, L. A. (1969) Cell sorting: automated separation of mammalian cells as a function of intracellular fluorescence. *Science* **166**, 747–749.
12. Shapiro, H. M. (2003) *Practical Flow Cytometry*, 4th edit. Wiley-Liss, New York.
13. Melamed, M. R., Mullaney, P. F., and Shapiro, H. M. (1990) An historical review of the development of flow cytometers and sorters, in *Flow Cytometry and Sorting*, 2nd edit. (Melamed, M. R., Lindmo, T., and Mendelsohn, M. L., eds.), Wiley-Liss, New York, pp. 1–8.
14. Melamed, M. R. (2001) A brief history of flow cytometry and sorting. *Methods Cell Biol.* **63(pt A)**, 3–17.
15. Van Dilla, M. A., Dean, P. N., Laerum, O. D., and Melamed, M. R., eds. (1985) *Flow Cytometry: Instrumentation and Data Analysis*. Academic Press, London.
16. Melamed, M. R., Lindmo, T., and Mendelsohn, M. L., eds. (1990) *Flow Cytometry and Sorting*, 2nd edit. Wiley-Liss, New York.
17. Watson, J. V. (1991) *Introduction to Flow Cytometry*. Cambridge University Press, Cambridge.
18. Watson, J. V. (1992) *Flow Cytometry Data Analysis: Basic Concepts and Statistics*. Cambridge University Press, Cambridge.
19. Robinson, J. P., Darzynkiewicz, Z., Dean, P. N., et al., eds. (1997) *Current Protocols in Cytometry*. John Wiley & Sons, New York.
20. Diamond, R. A. and DeMaggio, S., eds. (2000) in *Living Color: Protocols in Flow Cytometry and Cell Sorting*. Springer-Verlag, Berlin.
21. Durack, G. and Robinson, J. P., eds. (2000) *Emerging Tools for Single-Cell Analysis*, Wiley-Liss, New York.
22. Ormerod, M. G., ed. (2000) *Flow Cytometry: A Practical Approach*, 3rd edit. Oxford University Press, Oxford.
23. Darzynkiewicz, Z., Crissman, H. A., and Robinson, J. P., eds. (2001) *Cytometry: Methods in Cell Biology*, 3rd edit., Vol. 63. Academic Press, San Diego.
24. Givan, A. L. (2001) *Flow Cytometry: First Principles*, 2nd edit. Wiley-Liss, New York.
25. Lloyd, D. (1993) *Flow Cytometry in Microbiology*. Springer-Verlag, London.
26. Alberghina, L., Porro, D., Shapiro, H., Srienc, F., and Steen, H., eds. (2000) *Analysis of Microbial Cells at the Single Cell Level*, *J. Microbiol. Methods*, Vol. 42.
27. Fugger, E. F., Black, S. H., Keyvanfar, K., and Schulman, J. D. (1998) Births of normal daughters after MicroSort sperm separation and intrauterine insemination, in-vitro fertilization, or intracytoplasmic sperm injection. *Hum. Reprod.* **13**, 2367–2370.
28. Gledhill, B. L., Evenson, D. P., and Pinkel, D. (1990) Flow cytometry and sorting of sperm and male germ cells, in *Flow Cytometry and Sorting*, 2nd edit. (Melamed, M. R., Lindmo, T., and Mendelsohn, M. L., eds.), Wiley-Liss, New York, pp. 531–551.
29. Reckerman, M. and Collin, F., eds. (2000) *Aquatic Flow Cytometry: Achievements and Prospects*, *Scientia Marina*, Vol. 64.

30. Marie, D., Brussard, C. P. D., Thyraug, R., Bratbak, G., and Vaultot, D. (1999) Enumeration of marine viruses in culture and natural samples by flow cytometry. *Appl. Environ. Microbiol.* **59**, 905–911.
31. Hedley, D. W. (1989) Flow cytometry using paraffin-embedded tissue: five years on. *Cytometry* **10**, 229–241.
32. Gray, J. W. and Cram, L. S. (1990) Flow karyotyping and chromosome sorting, in *Flow Cytometry and Sorting*, 2nd edit. (Melamed, M. R., Lindmo, T., and Mendelsohn, M. L., eds.), Wiley-Liss, New York.
33. Habbersett, R. C., Jett, J. H., and Keller, R. A. (2000) Single DNA fragment detection by flow cytometry, in *Emerging Tools for Single-Cell Analysis* (Durack, G. and Robinson, J. P., eds.), Wiley-Liss, New York, pp. 115–138.
34. Carson, R. T. and Vignali, D. A. A. (1999) Simultaneous quantitation of 15 cytokines using a multiplexed flow cytometric assay. *J. Immunol. Methods* **227**, 41–52.
35. Steen, H. B. (2000) Flow cytometry of bacteria: glimpses from the past with a view to the future. *J. Microbiol. Methods* **42**, 65–74.
36. Harkins, K. R. and Galbraith, D. W. (1987) Factors governing the flow cytometric analysis and sorting of large biological particles. *Cytometry* **8**, 60–70.
37. Darzynkiewicz, Z., Juan, G., Li, X., Gorczyca, W., Murakami, T., and Traganos, F. (1997) Cytometry in cell necrobiology: Analysis of apoptosis and accidental cell death (necrosis). *Cytometry* **27**, 1–20.
38. Gray, J. W., Dolbeare, F., and Pallavicini, M. G. (1990) Quantitative cell-cycle analysis, in *Flow Cytometry and Sorting*, 2nd edit. (Melamed, M. R., Lindmo, T., and Mendelsohn, M. L., eds.), Wiley-Liss, New York, pp. 445–467.
39. Kim, Y., Jett, J. H., Larson, E. J., Penttila, J. R., Marrone, B. L., and Keller, R. A. (1999) Bacterial fingerprinting by flow cytometry: bacterial species discrimination. *Cytometry* **36**, 324–332.
40. June, C. H., Abe, R., and Rabinovitch, P. S. (1997) Measurement of intracellular calcium ions by flow cytometry, in *Current Protocols in Cytometry* (Robinson, J. P., Darzynkiewicz, Z., Dean, P. N., et al., eds.), John Wiley & Sons, New York, pp. 9.8.1–9.8.19.
41. Li, J. and Eastman, A. (1995) Apoptosis in an interleukin-2-dependent cytotoxic T lymphocyte cell line is associated with intracellular acidification. *J. Biol. Chem.* **270**, 3203–3211.
42. Chow, S. and Hedley, D. (1997) Flow cytometric measurement of intracellular pH, in *Current Protocols in Cytometry* (Robinson, J. P., Darzynkiewicz, Z., Dean, P. N., et al., eds.), John Wiley & Sons, New York, pp. 9.3.1–9.3.10.
43. Shapiro, H. M. (1997) Estimation of membrane potential by flow cytometry, in *Current Protocols in Cytometry* (Robinson, J. P., Darzynkiewicz, Z., Dean, P. N., et al., eds.), John Wiley & Sons, New York, pp. 9.6.1–9.6.10.
44. Lyons, A. B. (1999) Divided we stand: tracking cell proliferation with carboxy-fluorescein diacetate succinimidyl ester. *Immunol. Cell Biol.* **77**, 509–515.
45. Crosland-Taylor, P. J. (1953) A device for counting small particles suspended in a fluid through a tube. *Nature* **171**, 37–38.

46. Kachel, V., Fellner-Feldegg, H., and Menke, E. (1990) Hydrodynamic properties of flow cytometry instruments, in *Flow Cytometry and Sorting*, 2nd edit. (Melamed, M. R., Lindmo, T., and Mendelsohn, M. L., eds.), Wiley-Liss, New York, pp. 27–44.
47. Pinkel, D. and Stovel, R. (1985) Flow chambers and sample handling, in *Flow Cytometry: Instrumentation and Data Analysis* (Van Dilla, M. A., Dean, P. N., Laerum, O. D., and Melamed, M. R., eds.), Academic Press, London, pp. 77–128.
48. Salzman, G. C., Singham, S. B., Johnston, R. G., and Bohren, C. F. (1990) Light scattering and cytometry, in *Flow Cytometry and Sorting*, 2nd edit. (Melamed, M. R., Lindmo, T., and Mendelsohn, M. L., eds.), Wiley-Liss, New York, pp. 81–107.
49. Waggoner, A. (1997) Optical filter sets for multiparameter flow cytometry, in *Current Protocols in Cytometry* (Robinson, J. P., Darzynkiewicz, Z., Dean, P. N., et al. eds.), John Wiley & Sons, New York, pp. 1.5.1–1.5.8.
50. Verwer, B. (2002) BD FACSDiVa Option, BD Biosciences.
51. Bagwell, C. B., Baker, D., Whetstone, S., et al. (1989) A simple and rapid method of determining the linearity of a flow cytometer amplification system. *Cytometry* **10**, 689–694.
52. Muirhead, K. A., Schmitt, T. C., and Muirhead, A. R. (1983) Determination of linear fluorescence intensities from flow cytometric data accumulated with logarithmic amplifiers. *Cytometry* **3**, 251–256.
53. Wood, J. C. S. (1997) Establishing and maintaining system linearity, in *Current Protocols in Cytometry* (Robinson, J. P., Darzynkiewicz, Z., Dean, P. N., et al., eds.), John Wiley & Sons, New York, pp. 1.4.1–1.4.12.
54. Seamer, L. (2000) Flow cytometry standard (FCS) data file format, in *In Living Color: Protocols in Flow Cytometry and Cell Sorting* (Diamond, R. A. and DeMaggio, S., eds.), Springer-Verlag, Berlin.
55. Loken, M. R. (1997) Multidimensional data analysis in immunophenotyping, in *Current Protocols in Cytometry* (Robinson, J. P., Darzynkiewicz, Z., Dean, P. N., et al., eds.), John Wiley & Sons, New York, pp. 10.4.1–10.4.7.
56. Roederer, M., De Rosa, S., Gerstein, R., et al. (1997) 8 color, 10-parameter flow cytometry to elucidate complex leukocyte heterogeneity. *Cytometry* **29**, 328–339.
57. Hoffman, R. A. and Houck, D. W. (1998) High speed sorting efficiency and recovery: Theory and experiment. *Cytometry Suppl.* **9**, 142.
58. Dubelaar, G. B., Gerritzen, P. L., Beeker, A. E., Jonker, R. R., and Tangen, K. (1999) Design and first results of CytoBuoy: a wireless flow cytometer for in situ analysis of marine and fresh waters. *Cytometry* **37**, 247–254.
59. Sams, C. F., Crucian, B. E., Clift, V. L., and Meinelt, E. M. (1999) Development of a whole blood staining device for use during space shuttle flights. *Cytometry* **37**, 74–80.
60. Crucian, B. E. and Sams, C. F. (1999) The use of a spaceflight-compatible device to perform WBC surface marker staining and whole-blood mitogenic activation for cytokine detection by flow cytometry. *J. Gravit. Physiol.* **6**, 33–34.

2

Multiparameter Flow Cytometry of Bacteria

Howard M. Shapiro and Gerhard Nebe-von-Caron

Summary

The small size of bacteria makes some microbial constituents undetectable or measurable with only limited precision by flow cytometry. Bacteria may also behave differently from eukaryotes in terms of their interaction with dyes, drugs, and other reagents. It is therefore difficult to design multiparameter staining protocols that work, unmodified, across a wide range of bacterial species. This chapter describes reliable flow cytometric methods for assessment of the physiologic states of Gram-negative organisms, on the one hand, and Gram-positive organisms, on the other, based on measurement of membrane potential and membrane permeability. These techniques are useful in the assessment of effects of environmental conditions and antimicrobial agents on microorganisms.

Key Words

Bacteria, cyanine dyes, flow cytometry, membrane permeability, membrane potential.

1. Introduction

Although microscopy made us aware of the existence of the microbial world in the 17th century, it was not until the advent of cytometry in the late 20th century that it became possible to carry out detailed studies of microorganisms at the single-cell level.

In principle, one can use a flow cytometer to measure the same parameters in bacteria or even viruses as are commonly measured in eukaryotic cells. However, the size, mass, nucleic acid, and protein content, and so forth of bacteria are approx 1/1000 the magnitude of the same parameters in mammalian cells, and this affects measurement quality. Low-intensity measurements typically exhibit large variances as a result of photoelectron statistics; some microbial constituents may thus be undetectable or measurable with only limited precision.

From: *Methods in Molecular Biology: Flow Cytometry Protocols*, 2nd ed.
Edited by: T. S. Hawley and R. G. Hawley © Humana Press Inc., Totowa, NJ

Bacteria also tend to behave differently from eukaryotes in terms of their interaction with reagents used in cytometry. Uptake and efflux of dyes, drugs, and other reagents by and from bacteria are affected by the structure of the cell wall, and by the presence of pores and pumps that may or may not be analogous to those found in eukaryotes. Moreover, the outer membrane of Gram-negative bacteria excludes most lipophilic or hydrophobic molecules, including reagents such as cyanine dyes. Although chemicals such as ethylenediaminetetraacetic acid (EDTA) may be used to permeabilize the outer membrane to lipophilic compounds with at least transient retention of some metabolic function, the characteristics of the permeabilized bacteria are distinct from those of organisms in the native state. Gram-positive organisms may take up a somewhat wider range of reagents without additional chemical treatment, but are no more predictable; for example, Walberg et al. (1) found substantial variability in patterns of uptake of different nucleic acid binding dyes by Gram-positive species.

As one might guess from reading the preceding paragraph, it is, difficult, if not impossible, to design multiparameter staining protocols that will work, unmodified, across a wide range of bacterial genera and species. Both authors of this chapter have provided more general discussions of multiparameter flow cytometry of microorganisms elsewhere (2–4); here we concentrate on reliable methods developed in each of our laboratories for assessment of the physiologic states of Gram-negative organisms, on the one hand, and Gram-positive organisms, on the other.

1.1. Defining Bacterial “Viability”: Membrane Permeability vs Metabolic Activity

Both microbiologists and cytometrists would like to be able to characterize microorganisms as viable or nonviable at the single-cell level; this is essential in determining effects of antimicrobial agents or adverse environmental conditions. A number of criteria for “viability” have been suggested; impermeability of the membrane to nucleic acid dyes such as propidium is one, and the presence of metabolic activity, as indicated by the production and retention of fluorescent product from a nonfluorescent enzyme substrate or by maintenance of a membrane potential, is another. However, until recently, relatively few investigators had reported making flow cytometric measurements of more than one of these characteristics in the same cells at the same time.

Propidium (usually available as the iodide [PI]) and ethidium (usually available as the bromide [EB]) are structurally similar nucleic acid dyes; both contain a phenanthridinium ring, and both bind, with fluorescence enhancement, to double-stranded nucleic acids. However, ethidium has only a single positive charge; its *N*-alkyl group is an ethyl group. Ethidium and other dyes with a

single delocalized positive charge are membrane permeant; that is, they cross intact prokaryotic and eukaryotic cytoplasmic membranes, although the dyes may be pumped out by efflux pumps. Propidium bears a double positive charge because its *N*-alkyl group is an isopropyl group with a quaternary ammonium substituent. Like a number of other dyes that also bear quaternary ammonium groups and more than one positive charge (e.g., TO-PRO-1, TO-PRO-3, and Sytox Green, all from Molecular Probes) propidium is generally believed to be membrane impermeant; that is, such dyes are excluded by prokaryotic and eukaryotic cells with intact cytoplasmic membranes. Cells that take up propidium and other multiply charged dyes are usually considered to be nonviable, although transient permeability to these dyes can be induced by certain chemical and physical treatments, for example, electroporation, with subsequent recovery of membrane integrity and viability. Thus, staining (or the lack thereof) with propidium is the basis of a so-called dye exclusion test of viability. Acid dyes, such as trypan blue and eosin, are also membrane impermeant and are used in dye exclusion tests.

A variation on the dye exclusion test employs a nonfluorescent, membrane-permeant substrate for an intracellular enzyme, which crosses intact or damaged cell membranes and which is then enzymatically cleaved to form a fluorescent, impermeant (or slowly permeant) product. The product is retained in cells with intact membranes, and quickly lost from putatively nonviable cells with damaged membranes. One commonly used substrate is diacetylfluorescein, also called fluorescein diacetate (FDA), which yields the slowly permeant fluorescein; nonfluorescent esters of some other fluorescein derivatives are better for dye exclusion tests because their products are less permeant (5). Another substrate is 5-cyano-2,3-ditolyl tetrazolium chloride (CTC) (6); this is reduced by intracellular dehydrogenases to a fluorescent formazan, and provides an indication of respiratory activity as well as of membrane integrity.

Bacteria normally maintain an electrical potential gradient (membrane potential, $\Delta\Psi$) of >100 mV across the cytoplasmic membrane, with the interior side negative. Charged dyes that are sufficiently lipophilic to pass readily through the lipid bilayer portion of the membrane partition across the membrane in response to the potential gradient. Positively charged lipophilic dyes, such as cyanines, are concentrated inside cells that maintain $\Delta\Psi$, while negatively charged lipophilic dyes, such as oxonols, are excluded. Thus, if two cells of the same volume, one with a transmembrane potential gradient and one without, were equilibrated with a cyanine dye, the cell with the gradient would contain more dye than the one without; if the cells were equilibrated with an oxonol dye, the cell without the gradient would contain more dye. However, cells with different volumes may contain different amounts of dye, irrespective of their $\Delta\Psi$ s, because it is the concentration of dye, rather than the amount of dye, in

the cell that reflects $\Delta\Psi$. The flow cytometer measures the amount, not the concentration.

When the cyanine dye 3,3'-diethyloxacarbocyanine iodide ($\text{DiOC}_2[3]$) is added to cells at much higher concentrations than are normally used for flow cytometric estimation of $\Delta\Psi$, it is possible to detect red (~610 nm) fluorescence in addition to the green (~525 nm) fluorescence normally emitted by this dye (7); the red fluorescence is likely due to the formation of dye aggregates. At high dye concentrations, the green fluorescence is dependent on cell size, but independent of $\Delta\Psi$, whereas the red fluorescence is both size and potential dependent. The ratio of red and green fluorescence, which is largely independent of size, provides a more accurate and precise measurement of bacterial $\Delta\Psi$ than can be obtained from simple fluorescence measurements.

In theory, oxonol dyes should produce little or no staining of cells with normal $\Delta\Psi$ and brighter staining of cells in which the potential gradient no longer exists. However, it is likely that the increased oxonol fluorescence seen in the heat-killed and alcohol-fixed bacteria often used as zero-potential controls reflects changes in size and in lipid and protein chemistry resulting from these treatments, as well as changes in $\Delta\Psi$. Decreases in $\Delta\Psi$ of the Gram-positive *S. aureus* produced by less drastic treatments, for example, nutrient deprivation, were detected by the ratiometric method using $\text{DiOC}_2(3)$ but produced no change in oxonol fluorescence (7). However, oxonol fluorescence does appear to increase with decreasing $\Delta\Psi$ in *Escherichia coli* and other Gram-negative organisms (2).

1.2. Flow Cytometric Methods for Assessment of the Physiologic States of Gram-Negative and Gram-Positive Organisms

The protocol described here for work with *E. coli* and other Gram-negative organisms (2,8,9) combines the oxonol dye *bis*-(1,3-dibutyl-barbituric acid) trimethine oxonol ($\text{DiBAC}_4[3]$), which is used as an indicator of $\Delta\Psi$, with EB, which is retained by cells with intact membranes in which the efflux pump becomes inactive, as happens when energy metabolism is impaired. PI is used to demonstrate membrane permeability; once PI enters cells, it displaces EB from nucleic acids, presumably because PI has a higher binding affinity owing to its double positive charge. All three dyes are excited at 488 nm; $\text{DiBAC}_4(3)$ fluorescence is measured in a green (~525 nm) fluorescence channel, while EB and PI are, respectively, measured at ~575 nm and >630 nm.

The protocol described here for work with *S. aureus* and other Gram-positive organisms uses the ratio of red (~610 nm) and green (~525 nm) fluorescence of $\text{DiOC}_2(3)$, excited at 488 nm, as an indicator of $\Delta\Psi$ (7), and the far red (>695 nm) fluorescence of TO-PRO-3, excited by a red He-Ne (633 nm) or

diode (635–640 nm) laser, to demonstrate membrane permeability. Dividing the TO-PRO-3 fluorescence signal by the green DiOC₂(3) fluorescence signal produces a normalized indicator of permeability that provides better discrimination between cells with impermeable and permeable membranes than can be obtained from TO-PRO-3 fluorescence alone (10).

2. Materials

Note: All aqueous solutions should be made with deionized distilled water (dH₂O) and filtered through a filter with a pore size no larger than 0.22 μ m. Dye solutions should be stored in the dark.

2.1. For DiBAC₄(3)/EB/PI Staining

1. DiBAC₄(3) (Molecular Probes, Eugene, OR) (FW 516.64): Oxonols may require addition of a base to be soluble.
 - a. Stock solution: 10 mg/mL in dimethyl sulfoxide (DMSO), store at –20°C.
 - b. Working solution: 10 or 100 μ g/mL in dH₂O, 0.5% Tween; store at 4°C.
 - c. Final concentration: 10 μ g/mL.
2. EB (Sigma-Aldrich, St. Louis, MO) (FW 394.3):
 - a. Stock solution: 10 mg/mL in dH₂O, store at –20°C.
 - b. Working solution: 500 μ g/mL in dH₂O, store at 4°C.
 - c. Final concentration: 10 μ g/mL.
3. PI (Sigma-Aldrich) (FW 668.4):
 - a. Stock solution: 2 mg/mL in dH₂O; store at 4°C.
 - b. Working solution: 500 μ g/mL in dH₂O; store at 4°C.
 - c. Final concentration: 5 μ g/mL.
4. Dulbecco's buffered saline (DBS+), pH 7.2, with 0.1% peptone, 0.1% sodium succinate, 0.2% glucose, and 4 mM EDTA added.

2.2. For DiOC₂(3)/TO-PRO-3 Staining

1. DiOC₂(3) (Molecular Probes) (FW 460.31):
 - a. Stock and working solution: 3 mM in DMSO; store at 4°C.
 - b. Final concentration: 30 μ M.
2. TO-PRO[®]-3 iodide (Molecular Probes) (FW 671.42):
 - a. Stock and working solution: 1 mM in DMSO (supplied in this form); store at 4°C.
 - b. Final concentration: 100 nM.
3. Carbonyl cyanide *m*-chlorophenylhydrazone (CCCP) (Sigma-Aldrich) (FW 204.6):
 - a. Stock and working solution: 2 mM in DMSO, store at 4°C.
 - b. Final concentration: 15 μ M.
4. Nisin (Sigma-Aldrich) (FW 3354): The preparation sold by Sigma-Aldrich contains 2.5% nisin, with the rest NaCl and dissolved milk solids; the filtered aqueous suspension must be diluted to achieve a final concentration of 25 μ g/mL.

5. Valinomycin (Sigma-Aldrich) (FW 1111):
 - a. Stock and working solution: 2 mM in DMSO; store at 4°C.
 - b. Final concentration: 5 μ M.
6. Mueller–Hinton broth (Gibco™ Invitrogen Corporation, Carlsbad, CA) with 50 mg/L of Ca^{2+} (MHBc).

3. Methods

3.1. Functional Assessment of *E. coli* and Gram-Negatives Using DiBAC₄(3)/EB/PI Staining (see Note 1)

3.1.1. Sample Preparation; Disaggregation of Bacteria by Ultrasound and Staining Procedure

1. For samples in liquid media, dilute 10 μ L of sample in 200 μ L of DBS+. Resuspend samples from solid media in DBS+ and then dilute further.
2. Optimize the fraction of single organisms in samples by gentle sonication in a Sanyo MSE Soniprep 150 apparatus (Sanyo, Chatsworth, CA) operating at 23 kHz. Place a 3-mm exponential probe, with its tip 5 mm below the liquid surface of a 2-mL sample, in a disposable polystyrene 7-mL flat-bottom container. Sonicate the sample for 2 min at 2 μ m amplitude.
3. Add dyes: 10 μ g/mL of DiBAC₄(3), 10 μ g/mL of EB, and 5 μ g/mL of PI.
4. Keep the samples at 25°C for 30 min before running on the flow cytometer.

3.1.2. Flow Cytometry

1. Use 488 nm as the excitation wavelength.
2. Use forward and/or side scatter signals for triggering. A software gate excluding low-level scatter signals may be set to remove events due to noise and particulate contaminants in samples.
3. Set up detector filters so that PI fluorescence is measured above 630 nm, EB fluorescence at 575 nm, and DiBAC₄(3) fluorescence at 525 nm.
4. Adjust hardware or software compensation to minimize fluorescence of each dye in channels used primarily for measurement of other dyes.
5. For viability determination, single cells may be sorted directly onto nutrient agar plates.

3.1.3. Results

Figure 1 shows the results of a sorting experiment in which *Salmonella typhimurium* stored for 25 d on nutrient agar at 4°C was resuspended in DBS, sonicated to break up aggregates, and stained with DiBAC₄(3), EB, and PI.

The dye combination delineates cells in different functional stages. Active pumping cells do not stain significantly with any of the dyes. Deenergized cells take up ethidium, but not DiBAC₄(3) or propidium. Depolarized cells take up ethidium and DiBAC₄(3), but not propidium, and permeabilized cells and “ghosts,” that is, cells with damaged membranes, take up both DiBAC₄(3) and

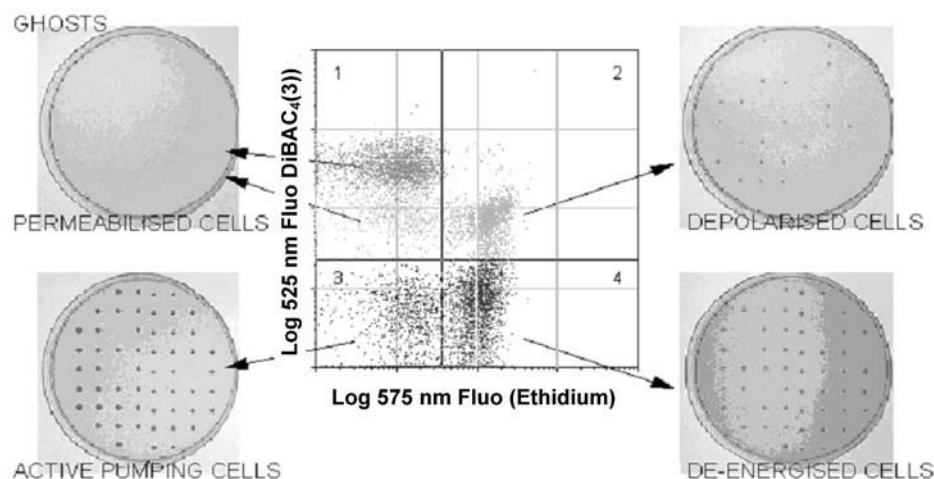


Fig. 1. DiBAC₄(3)/EB/PI staining delineates different functional stages of *Salmonella typhimurium* (stored for 25 d on nutrient agar at 4°C). Cells corresponding to the different functional stages were sorted onto nutrient agar plates to monitor recovery.

propidium. In most cases, all but the permeabilized cells are capable of recovery. In the experiment shown in the figure, approx one third of the electrically depolarized cells grew on agar plates; depolarization therefore indicates a decline in cell functionality, but certainly not cell death. Recovery of actively pumping and deenergized cells typically approaches 100%; deenergized cells lose pump activity but maintain $\Delta\Psi$ at least briefly. Fewer than 1% of events sorted from the regions containing permeabilized cells and ghosts will form colonies on agar.

3.2. Measurement of $\Delta\Psi$ and Permeability Using DiOC₂(3) and TO-PRO-3 (see Note 2)

3.2.1. Sample Preparation

1. Dilute samples in MHBc to a target concentration of 10^6 – 10^7 cells/mL.
2. Add dyes: 30 μ M DiOC₂(3) and 100 nM TO-PRO-3.
3. Keep the samples at room temperature (~25°C) for 5 min before running on the flow cytometer.

3.2.2. Flow Cytometry and Data Analysis

1. Use an instrument with 488 nm (argon-ion or solid-state laser) and red (633 nm from a He-Ne laser or approx 635 nm from a diode laser) excitation beams.
2. Use forward or side scatter as the trigger signal. A software gate may be set to exclude low-level scatter signals produced by noise and debris.

3. DiOC₂(3) is excited at 488 nm; its green fluorescence is detected through a 525- to 530-nm bandpass filter with approx 20 nm bandwidth and its red fluorescence is detected through a 610-nm bandpass filter with approx 20 nm bandwidth.
4. TO-PRO-3TM is excited by the red laser, and its far red fluorescence is detected through one or two 695-nm longpass color glass filters.

In instruments in which data are collected using logarithmic amplifiers, a quantity proportional to the ratio of [DiOC₂(3) red fluorescence]/[DiOC₂(3) green fluorescence] is calculated by adding a constant to the red fluorescence channel value and subtracting the green fluorescence channel value (7). The addition of a constant value is necessary to keep values of the calculated parameter on the same scale as is used for the raw fluorescence measurements. For a 256-channel logarithmic scale, with 64 channels per decade, a constant value of 96 is convenient; the calculated parameter, which serves as a measure of $\Delta\Psi$, then represents the log of ($10^{3/2} \times [\text{red fluorescence/green fluorescence}]$). A normalized permeability value, based on the ratio of [TO-PRO-3 fluorescence]/[DiOC₂(3) green fluorescence], is derived in the same manner. If high-resolution linear data are available, ratios may be calculated directly by division and multiplied by appropriate scaling constants.

Different mechanisms for perturbing $\Delta\Psi$ and permeability are incorporated into control samples. After 5–15 min of incubation, CCCP (15 μM) reduces $\Delta\Psi$ to zero, but does not affect permeability; nisin (25 $\mu\text{g/mL}$) reduces $\Delta\Psi$ to zero, and also renders organisms permeable to TO-PRO-3.

Measurements of $\Delta\Psi$ using DiOC₂(3) may be calibrated by controlled application of valinomycin in the presence of different external potassium ion concentrations (7). The red/green fluorescence ratio is measured for cells in a range of buffers containing 5 μM valinomycin and various concentrations of potassium; the concentration of sodium ion is adjusted to keep the combined molarity of potassium and sodium at 300 mM.

Figure 2 plots the membrane potential of amoxicillin-treated *S. aureus* against normalized permeability. The strain of *S. aureus* used was amoxicillin sensitive; aliquots were exposed to concentrations of amoxicillin above (1 $\mu\text{g/mL}$) and below (0.5 $\mu\text{g/mL}$) the minimal inhibitory concentration (MIC). In cultures treated with either dose, at time zero, most cells show low values of permeability and relatively high values of $\Delta\Psi$, appearing in the lower right quadrant of the display. After 2 h at an amoxicillin concentration above MIC (top strip), many cells have lost $\Delta\Psi$ completely, and most have lost $\Delta\Psi$ to some extent (lower and upper left quadrants); over 58% of the total have become permeable (upper left quadrant). By 4 h, some regrowth has occurred; about 17% of the events measured show normal $\Delta\Psi$ and no permeability. The situation is quite different at a sub-MIC amoxicillin concentration (bottom strip). At 2, 3, and even 4 h, a substantial fraction of events (as high as 28%) are in the

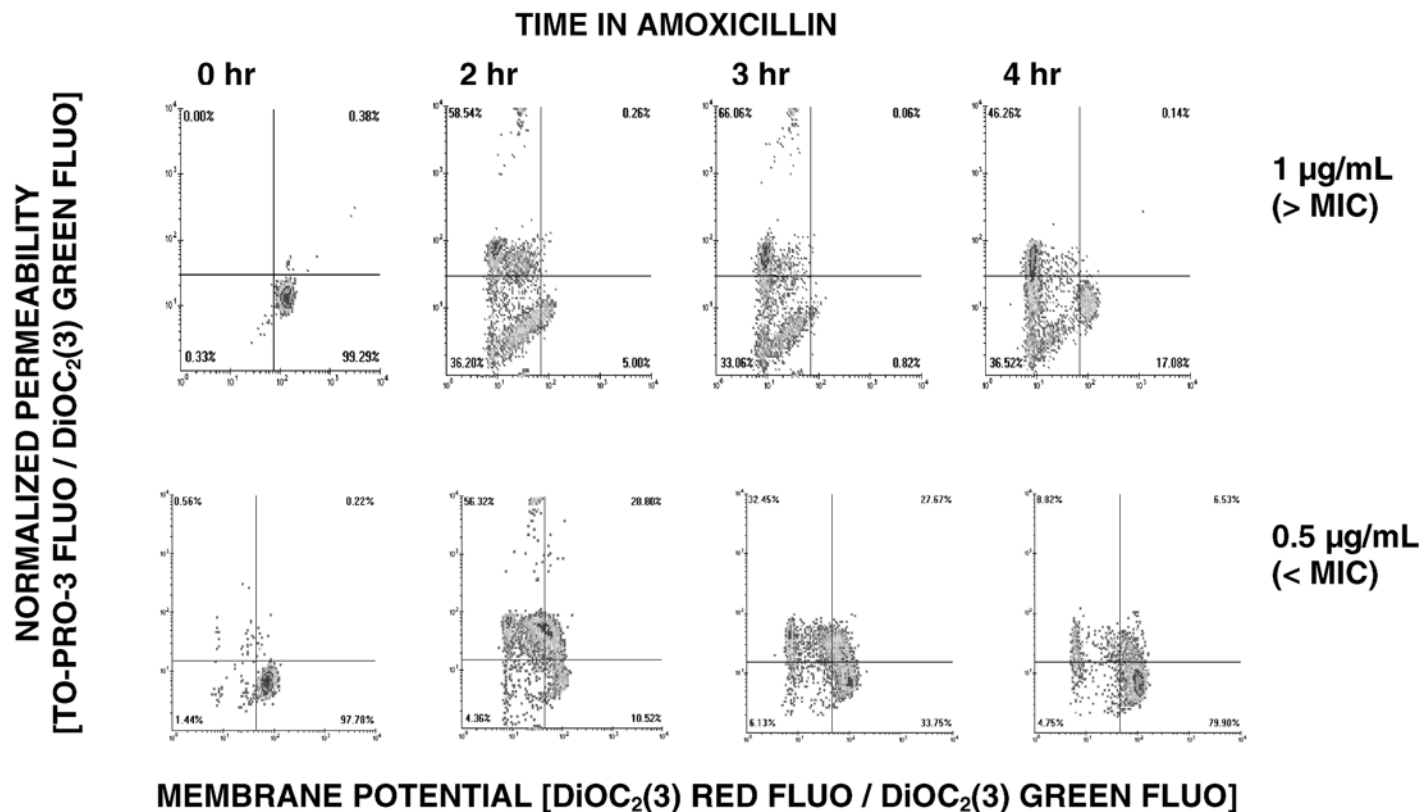


Fig. 2. DiOC₂(3)/TO-PRO-3 staining reveals the response of *S. aureus* exposed to different concentrations of amoxicillin for different lengths of time. Membrane potential (the ratio of DiOC₂(3) red to DiOC₂(3) green fluorescence, log scale, x-axis) is plotted against normalized permeability (the ratio of TO-PRO-3 far red to DiOC₂(3) green fluorescence, log scale, y-axis).

upper right quadrant, indicating a $\Delta\Psi$ greater than zero with permeability to TO-PRO-3. By 4 h, most cells (>79%) have regained normal $\Delta\Psi$ and lost permeability. Bacterial counts over this time period rule out the accumulation of a high- $\Delta\Psi$, impermeable population by expansion of the small population of such cells present after 2 h. Although some intermediate- $\Delta\Psi$, permeable events may represent aggregates of high- $\Delta\Psi$, impermeable viable cells and permeable, low- $\Delta\Psi$ dead cells, many of these events appear to be accounted for by TO-PRO-3 uptake into viable cells. This, parenthetically, suggests a novel approach to antimicrobial therapy (3,4,11).

4. Notes

1. DiBAC₄(3)/EB/PI staining: This methodology has been shown to work in some Gram-positive species, for example, *Micrococcus lysodeikticus*, and in yeasts (9). Some adjustment of DiBAC₄(3) concentration may be needed depending on the concentration of organisms and lipophilic components in samples; concentrations as low as 0.1 $\mu\text{g/mL}$ have been used with samples containing small numbers of cells.
2. DiOC₂(3)/TO-PRO-3 staining: This method has been used in instruments with 488 nm and red illuminating beams separated in space; it is not known whether it will work in instruments with collinear 488 nm and red beams. Both DiOC₂(3) and TO-PRO-3 adhere to the tubing used in most flow cytometers, and the high concentration of cyanine dye used in this protocol may necessitate replacement of some tubing if repeated cleaning with dilute chlorine bleach, ethanol, detergents, and so forth still leaves dye in the system. Some bacterial types (e.g., *S. aureus*) may be grown in culture following exposure to 30 μM DiOC₂(3). The method has been used with some Gram-negative species, for example, *E. coli*, with 5 mM EDTA added to staining solutions, and delineates cells with various apparent values of $\Delta\Psi$ as well as discriminating those that do and do not take up TO-PRO-3. However, Gram-negative bacteria appear to be damaged by the calibration buffers used with Gram-positive organisms, and it has not been possible to derive calibration curves for the former.

Acknowledgments

The authors thank Chris Hewitt, Dave Novo, Nancy Perlmutter, and Jared Silverman, who have played vital roles in the development and application of the methods described here.

References

1. Walberg, M., Gaustad, P., and Steen, H. B. (1999) Uptake kinetics of nucleic acid targeting dyes in *S. aureus*, *E. faecalis* and *B. cereus*: a flow cytometric study. *J. Microbiol. Methods* **35**, 167–176.
2. Nebe-von-Caron, G., Stephens, P. J., Hewitt, C. J., Powell, J. R., and Badley, R. A. (2000) Analysis of bacterial function by multi-colour fluorescence flow cytometry and single cell sorting. *J. Microbiol. Methods* **42**, 97–114.

3. Shapiro, H. M. (2000) Microbial analysis at the single-cell level: tasks and techniques. *J. Microbiol. Methods* **42**, 3–16.
4. Shapiro, H. M. (2003). *Practical Flow Cytometry*, 4th edit. Wiley-Liss, Hoboken, NJ.
5. Haugland, R. P. (2002) *Handbook of Fluorescent Probes and Research Products*, 9th edit., Molecular Probes, Eugene, OR. (online at www.probes.com)
6. Davey, H. M. and Kell, D. B. (1996) Flow cytometry and cell sorting of heterogeneous microbial populations-the importance of single-cell analyses. *Microbiol. Revs.* **60**, 641–696.
7. Novo, D., Perlmutter, N. G., Hunt, R. H., and Shapiro, H. M. (1999) Accurate flow cytometric membrane potential measurement in bacteria using diethylox-acarbocyanine and a ratiometric technique. *Cytometry* **35**, 55–63.
8. Hewitt, C. J., Nebe-von Caron, G., Nienow, A. W., and McFarlane, C. M. (1999) Use of multi-staining flow cytometry to characterise the physiological state of *Escherichia coli* W3110 in high cell density fed-batch cultures. *Biotechnol. Bioeng.* **63**, 705–711.
9. Hewitt, C. J. and Nebe-Von-Caron, G. (2004) The application of multi-parameter flow cytometry to monitor individual microbial cell physiological state, in *Physiological Stress Responses in Bioprocesses: Advances in Biochemical Engineering/Biotechnology* (Enfors, S.-V., ed.), Springer-Verlag, Heidelberg, Germany.
10. Novo, D. J., Perlmutter, N. G., Hunt, R. H., and Shapiro, H. M. (2000) Multi-parameter flow cytometric analysis of antibiotic effects on membrane potential, membrane permeability, and bacterial counts of *Staphylococcus aureus* and *Micrococcus luteus*. *Antimicrob. Agents Chemother.* **44**, 827–834.
11. Shapiro, H. M. (2001) Multiparameter flow cytometry of bacteria: implications for diagnostics and therapeutics. *Cytometry* **43**, 223–226.

3

Multiparameter Data Acquisition and Analysis of Leukocytes

Carleton C. Stewart and Sigrid J. Stewart

Summary

For data acquisition, each supplier provides the software necessary and unique to its instrument. For data analysis, the same software may be used. In addition, several second party vendors provide software often with more capabilities than that provided by the instrument companies. Because of the increase in multiparameter data acquisition, we describe one method for validating instrument performance prior to data acquisition. The fundamentals of data analysis leading to a generic strategy for analysis of any number of parameters are described. This generic approach is designed to simplify the increasing complexity of multiparameter data analysis.

Key Words

Bivariate histograms, color gating, gating, instrument performance, phenogram, univariate.

1. Introduction

Several software packages are currently available for the analysis of flow cytometry data. While each of them is unique in the way they process the data, the general strategies are similar. Because the complexity of analysis increases with the number of measured parameters, we focus on both the classical approaches as well as introduce a generic approach that can be utilized for any number of parameters. A parameter describes what is measured. A channel describes the value of the measurement. There are three kinds of parameters: forward scatter (FSC), side scatter (SSC), and fluorescence. FSC is measured between 2° and 22° from the laser beam (depending on instrument manufacturer), and it is proportional to the cross-sectional area of the particle. Because there are other factors that affect the measurement, it is only an estimate of size. SSC is also called orthogonal or 90° scatter because it is measured at 90°

From: *Methods in Molecular Biology: Flow Cytometry Protocols*, 2nd ed.
Edited by: T. S. Hawley and R. G. Hawley © Humana Press Inc., Totowa, NJ

to the laser beam, and it is sensitive to cell granularity provided the granules' index of refraction is different from that of the cytosol. The intensity of fluorescence is also measured orthogonal to the cell stream and it provides quantitative measurements from any number of resolvable colored fluorochromes used in the cell staining process. We do not cover sample preparation in this chapter (1,2).

The most commonly used fluorochromes that are conjugated to the primary antibody, secondary antibodies, or avidin can be excited at 488 nm or approx 633 nm. Those excited at 488 nm are fluorescein isothiocyanate (FITC), phycoerythrin (PE), a phycoerythrin-Texas red tandem complex (PE-TR), a phycoerythrin-cyanine 5 tandem complex (PE-CY5), peridinin chlorophyll protein (PerCP), a phycoerythrin-cyanine 7 tandem complex (PE-CY7), and several Alexa dyes from Molecular Probes (Eugene, OR). Their fluorescence emission wavelengths are: FITC = 530 nm, PE = 575 nm, PE-TR = 613 nm, PE-CY5 or PerCP = 670 nm, and PE-CY7 >700 nm. Other fluorochromes can be excited at 633 nm with a He-Ne laser or 635 nm with a red diode laser. Their fluorescence emission wavelengths are: CY5, APC, or Alexa 648 = 675 nm, and APC-CY7 >700 nm. Note that the tandem dyes consist of a donor fluorochrome, often phycoerythrin, and an acceptor molecule such as TR, CY5, or CY7, covalently linked to create a fluorochrome with a greater difference between its excitation and emission.

Antibodies can be conjugated with different fluorochromes of different excitation and/or emission properties (colors) so they can each be resolved. To accomplish color separation, spectral filters and dichroic mirrors are used that reflect or transmit specific wavelengths. Because the fluorochrome's emission wavelengths can be very broad, it is also necessary to remove unwanted overlapping fluorescence by appropriately adjusting the instrument's compensation circuits or by using software compensation. To perform this task it is necessary to use compensation standards. For more information on compensation additional reading is recommended (3-5).

All flow cytometers collect data in the same way using a process called LIST MODE. A standard list mode file includes a header containing information about the sample and instrument followed by a list of data in the order collected (6). The values that are stored in a list mode file are the voltages from the detectors for each parameter (P_1 , P_2 , P_3 , . . . P_n) after they have been electronically processed. As shown in **Table 1**, the data in a list mode file consists of the channel number corresponding to the value for each parameter for cell 1, followed by cell 2, and so forth until the last cell, n , is measured. If six parameters are measured for 10,000 cells, the file will contain 60,000 numbers in the order they are acquired.

Table 1
Correlated List Mode File: Values for Each Parameter

Cell	P1	P2	P3	P _n
C1	122	84	20	440
C2	424	92	20	460
C3	86	83	562	22
C4	101	98	487	33
C _n	330	79	30	452

2. Materials

1. A flow cytometer cell sorter and associated computer/software.
2. Beads for alignment.
3. A source of leukocytes.
4. Fluorescently conjugated antibodies to desired cell populations.
5. Solutions and reagents needed for cell staining.

3. Methods

The methods described below include instrument performance validation, data displays, and gating strategies.

3.1. Evaluating Instrument Performance

1. Before acquiring data, it is most important to assess instrument performance. To accomplish this, a process is established that can be easily applied for comparing the present day's performance with that of the previous day. Usually good quality microspheres are evaluated, and their median fluorescence intensity and coefficient of variation measured.
2. A threshold is established for each functioning parameter, and when the values are outside the threshold, corrective action must be taken. **Figure 1** illustrates the performance of a FACSCalibur operating every day for 1 yr. To ensure stability of performance, a preventative maintenance program should be established and maintained.
3. Because flow cytometers are used to measure cells, the final verification of performance needs to be cell based. A cell system is chosen that is relevant to the activity for which the instrument will be used.
4. As illustrated in **Fig. 2** for immunophenotyping, cells are stained with an antibody of each fluorochrome and their fluorescence intensity measured. Regions for the target population are drawn to produce a template that is used daily. All cells must appear in their respective regions for the instrument to pass the verification.

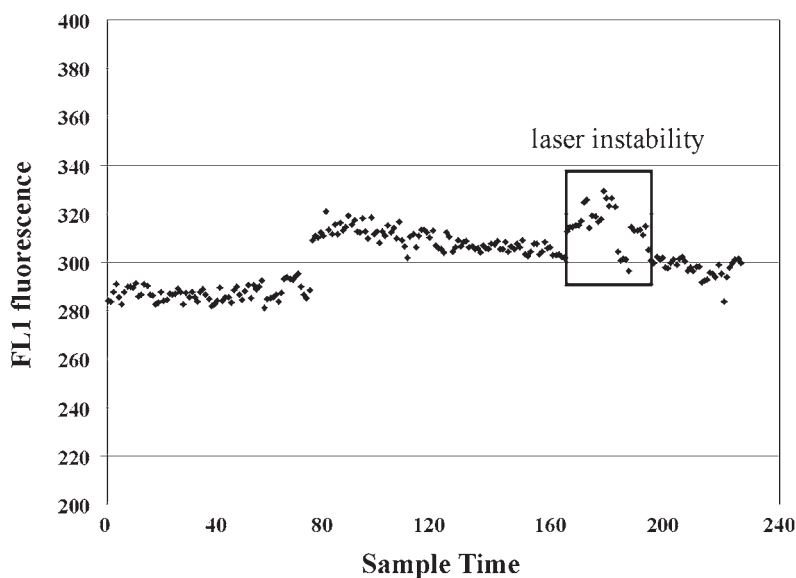


Fig. 1. Daily performance of a FACSCalibur. A Levi-Jennings plot of the peak fluorescence intensity of FL1 measured daily for 1 yr is shown. The FACSCalibur appears to be more stable than the microspheres used as the peak changes to new values when differing lots of microspheres are used. The coefficient of variation (not shown) must be $<3\%$ for the instrument to pass. An unstable argon laser caused the one period of high variation. Once replaced, stability was restored.

These simple tests verify instrument performance on a daily basis and assure that acquired data will be consistently good whenever it is obtained.

3.2. Displaying the Data

3.2.1. Univariate Histograms

1. The univariate histogram shown in **Fig. 3** is the simplest of all ways to display data. It is a frequency distribution where the number of events is plotted on the y-axis or ordinate as a function of the measured values (as channels) on the x-axis or abscissa. Generally, immunofluorescence is measured in logarithmic space. This is because the events can cover a range of three or four orders of magnitude in brightness. The instrument detectors must be adjusted so that unstained cells are in the lowest decade (represented by channels 1–10 in **Fig. 3A**).
2. Establish a marker position above which cells stained with immunophenotyping antibodies will be deemed positive. An isotype control immunoglobulin (Ig) is customarily used for this purpose. This is an IgG that has no known binding specificity for the cells and would therefore be a surrogate for any nonspecific IgG binding providing it is used at the same concentration as the antibodies. Unfortu-

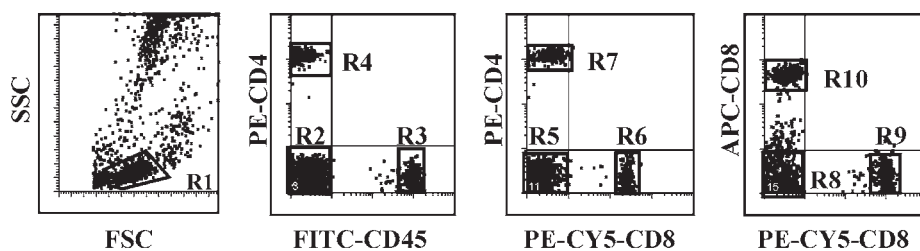


Fig. 2. Target regions. Using cells stained with a single antibody and then mixing them together, the instrument's performance can be determined every day. In this example, human blood was stained with each antibody in separate tubes, washed, fixed, and mixed together. A template is created containing regions to show the proper position of each cell population. Cells, gated on R1, stained with each color must fall within its appropriate region. By sampling both the newly prepared standard and the previous day's standard each day, it can be verified that both the instrument and the new standard are functioning properly because cells from both are in their correct regions. If the new standard contains one or more cell populations that fall outside their region, but the old one does not, the standard has been improperly made. If, however, both standards fall outside their respective regions then the instrument requires service. Changes in instrument settings to correct the position of a cell population are not recommended because that process is likely to cover up the problem.

nately, this latter requirement is rarely performed because of the erroneous belief that the supplier has properly configured the isotype control. As shown in **Fig. 3B**, the cells may be somewhat brighter than the autofluorescence control because of nonspecific and/or Fc receptor binding. Blocking of cells with an appropriate amount of IgG can reduce Fc but not nonspecific binding. The marker position is set to distinguish positive from negative cells so that between 0.5% and 2% of cells above the marker are positive. Strategies for rare event analysis cannot be adequately performed using univariate histograms.

3. The consensus report (7) and the NCCLS document (8) on immunophenotyping recommend using the negative population of the specific antibody as its own isotype control. We also recommend and support this practice because every antibody used for immunophenotyping will have its unique affinity constant which determines both the concentration to use and its specificity. Because both specific and nonspecific binding are functions of IgG concentration, it is its own isotype control. A more complete discussion of this aspect of immunophenotyping can be found in Chapter 1 of **ref. 9**.

3.2.2. Gating the Data

Gating is an analysis process of evaluating a restricted part of the file, for example, a specific cell population. Regions define the cells of interest. These

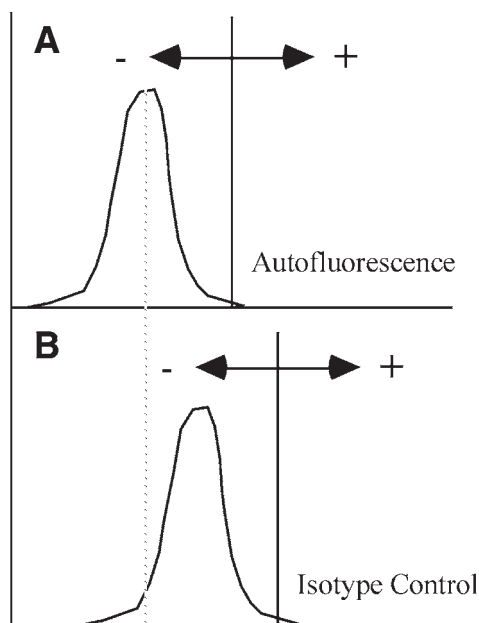


Fig. 3. Setting markers in a univariate histogram. In (A), the high voltage is adjusted using unstained cells so they are within the first decade (autofluorescence). The isotype control cells should not be used for this purpose. A marker is placed just after this negative cell population above which all cells are deemed positive for the antibody. For a properly titrated antibody and concentration matched isotype control (B), the position of the negative cells is the same as the autofluorescent cells.

regions are markers with upper and lower boundaries. The most common gating strategy is to use the FSC and SSC characteristics shown in **Fig. 4**. Considered in more detail later, this strategy is flawed by the belief that all the desired cells are within the selected region (*see Subheading 3.2.3., steps 4 and 5*).

1. Using the univariate histogram, shown in **Fig. 4**, list mode data can be analyzed to gate the cells. In **Fig. 4A**, two regions, R1 for small cells and R2 for large cells, in the FSC histogram can be used to determine the percentage of cells that are positive in R1 and in R2 by integrating the FSC values in the list between the selected boundaries of the regions. The fluorescence histograms for all cells (**Fig. 4B**), cells in R1 (**Fig. 4C**) or cells in R2 (**Fig. 4D**) can also be displayed. This process is called *gating* because the values of interest are restricted to a region of interest (small or large cells). Only cells that meet the region's *criteria* are displayed.
2. As shown in **Fig. 4C**, which was derived by gating on R1, there are two distinct frequency distributions similar in position to the negative cells and all the bright cells displayed in **Fig. 4B**. The ones on the left of the marker exhibit low fluo-

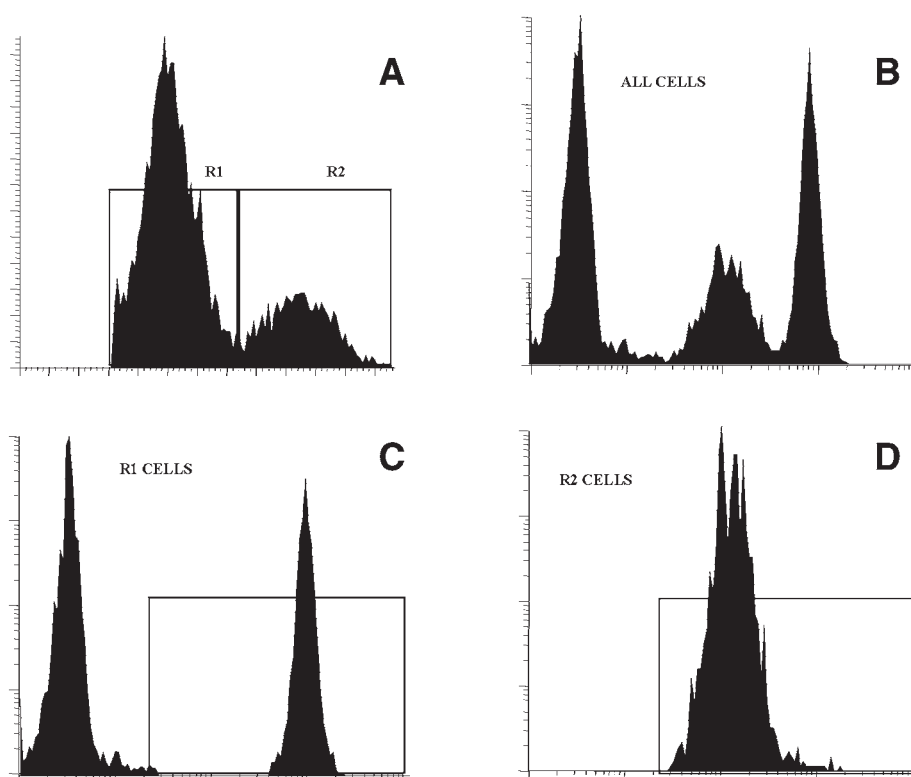


Fig. 4. Gating univariate histograms. Using human blood cells stained with PE-CD4, the histogram in (A) shows a small (R1) and large (R2) population of cells. In (B), three populations of cells are found: those on the left are negative, those in the middle are less positive than those on the right. When R1 cells are gated, histogram (C) shows they are all in either the negative or the brightly stained population. Gating on R2 in (D) shows that these cells are the less brightly stained population.

rescence while the ones on the right exhibit high or bright fluorescence, so it is easy to tell the cells that are positive from those that are negative. In **Fig. 4D**, which was derived by gating on R2, only one population is found; it corresponds to the dimmer positive population displayed in **Fig. 4B**.

3.2.3. Bivariate Distributions

When two parameters are collected to produce a bivariate histogram all possible combinations are displayed, as shown in **Fig. 5**. Quadrants are then assigned markers so that all binary combinations of positive (+) and negative (–) cells can be displayed. For this type of analysis a distinction between dim

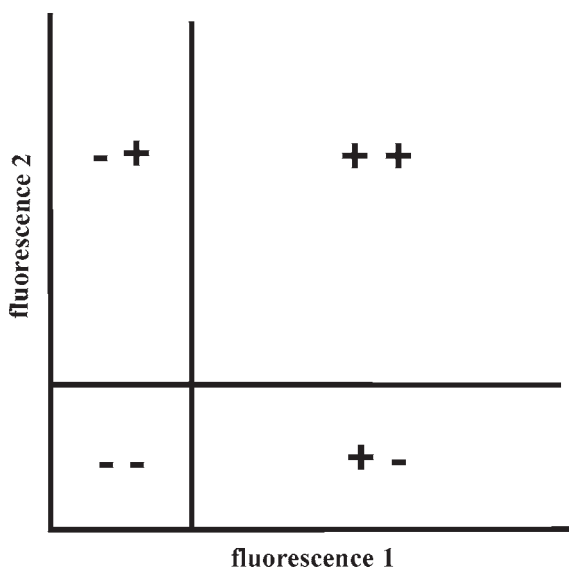


Fig. 5. Bivariate histograms. A bivariate histogram can be divided into four quadrants based on the position of the markers along the x - and y -axes. Those cells above the marker parallel to the x -axis and to its left are positive for the antibody in FL2 and negative for the one in FL1. Those cells to the right of the marker parallel to the y -axis and to its right are positive for FL1 and negative for FL2. Those in the middle are positive for both. Those in the box created by the two markers are negative for both antibodies.

and bright for a single color is not made. For two antibodies, there are four possible binary combinations, $+-$, $++$, $-+$ and $--$, and only one bivariate histogram is required to display them all, as shown in **Fig. 5**.

1. When one univariate histogram is plotted on the x -axis and a second univariate histogram is plotted on the y -axis, as shown in **Fig. 6**, a bivariate histogram results.
2. If the two univariate histograms are each projected into the central area of this two parameter display, the values in common produce clusters of the cells shown by the dots. Each dot represents a cell and there are many overlapping dots for cells sharing common properties that produce a cluster. These clusters can be of any size and shape, depending on the relationship between the two properties that were measured by the antibodies. This is possible because all the data in the list mode file are correlated.
3. In addition, more insight into the meaning of the data can be obtained. Now the CD4 bright cells are also CD3⁺, but the CD4 dim population is not. The CD4⁻ cells can be CD3⁺ or CD3⁻. Thus, the three clearly resolved populations when

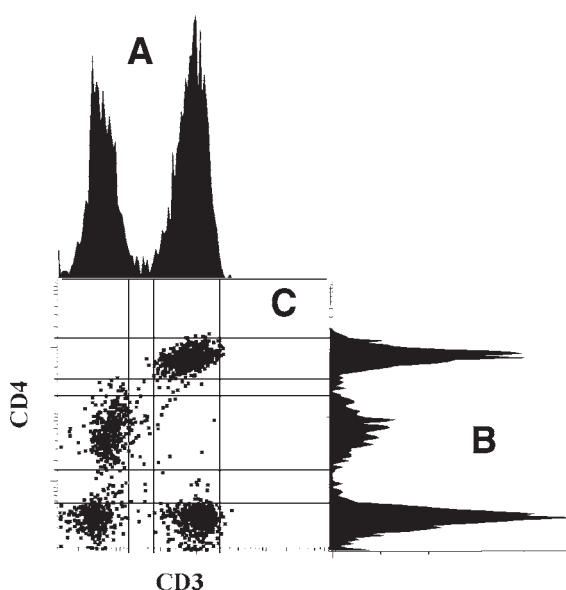
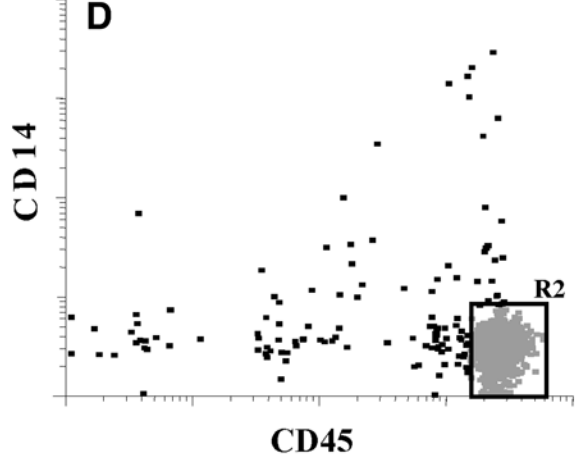
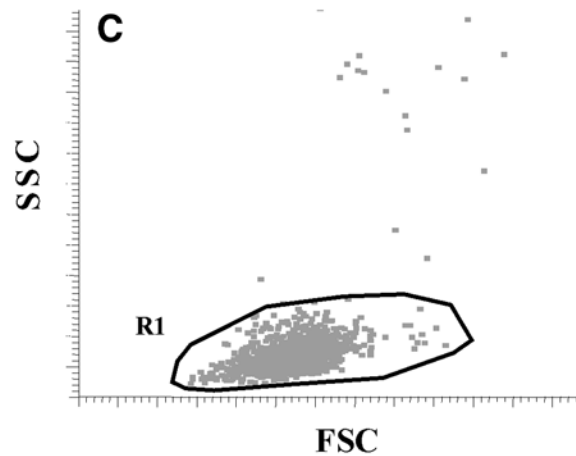
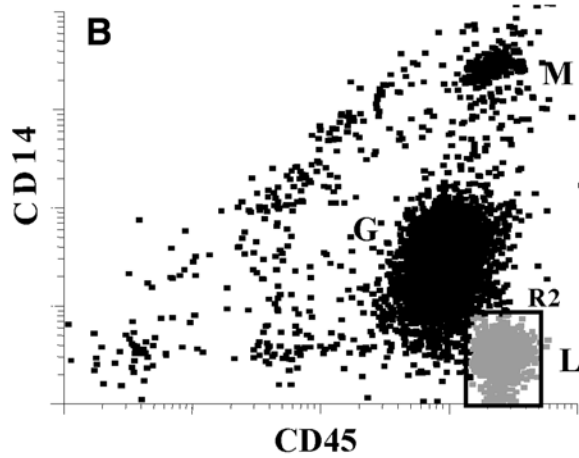
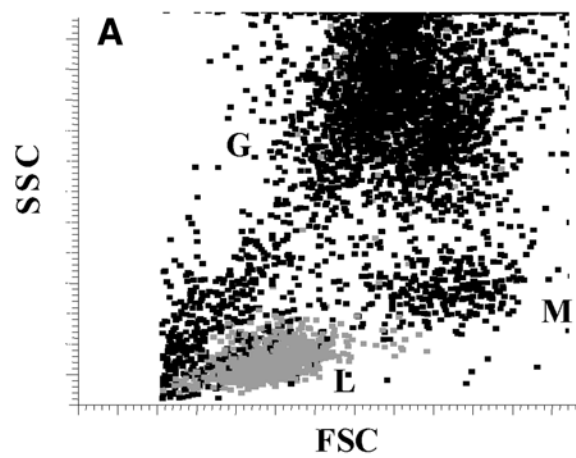


Fig. 6. Bivariate histograms of cells. Human peripheral blood was stained with FITC-CD3 and PE-CD4. The univariate histogram on the top (A) shows CD3-stained cells and the univariate histogram on the right side (B) shows CD4-stained cells. The bivariate plot (C) of the two univariate histograms show clusters of dots with each dot representing one cell. Because this is correlated list mode data, the bright CD4⁺ cells in (B) correspond to the cells that are CD3⁺ in (A). The intermediate CD4⁺ cells in (B) correspond to CD3⁻ cells in (A). Finally the CD4⁻ cells in (B) correspond to some CD3⁺ and some CD3⁻ cells in (C).

displayed as a univariate distribution can be resolved into four populations when displayed in bivariate space.

4. It has been customary to gate data using the FSC and SSC bivariate plot, and drawing a region around the cluster of lymphocytes. The assumption made is that all the cells in this cluster are lymphocytes and all the lymphocytes are in the cluster. As shown in **Fig. 7**, this is not true. For any region used for gating, the purity of the desired cell population can be evaluated. As shown in **Fig. 7A**, three fairly distinct clusters can be seen labeled L for lymphocytes, M for monocytes, and G for granulocytes. The bivariate plot of cells, stained with CD45 and CD14 are shown in **Fig. 7B**.
5. A region R2 containing all pure viable lymphocytes is drawn around the CD45 bright CD14⁻ cluster of cells. This region is applied as a gate to the FSC vs SSC view (**Fig. 7C**) and the location of all lymphocytes is found in the display. A second region, R1, is drawn around the lymphocytes and their CD45 vs CD14



characteristics are viewed in **Fig. 7D**. Cells inside R1, but falling outside R2 are events that are not lymphocytes. If R1 is drawn too large, it will contain more undesired cells so lymphocyte purity is reduced. As shown in **Fig. 7D**, the contaminating cells represent 7.5% of (R) gated cells. If the purity of the lymphocytes is low, for example, <90%, it may be improved by reducing the size of R1, but this may cause a loss of lymphocytes at the expense of improving purity. As long as the loss of only a small proportion of lymphocytes occurs concomitantly with a significant improvement in purity, the procedure may be acceptable and used to optimize the gate for lymphocytes, often called a lymphogate. This gate, in the FSC vs SSC view, once established, is then applied to the analysis of all subsequent samples. This same strategy can be applied to the monocyte and granulocyte clusters (**Fig. 7A**). But why go through this exercise in the first place? Had CD45 been used as the gate, the lymphocyte cluster represents them all whatever their scatter characteristics are.

3.2.4. Color Gating

When a third color is introduced, the analysis complexity increases because there are three bivariate views for displaying all the fluorescence data, shown in **Fig. 8**. In generic terms they are AB1-FITC (FL1) vs AB2-PE (FL2), AB1-FITC (FL1) vs AB3-PC (FL3), and AB2-PE (FL2) vs AB3-PC (FL3). Because there are three plots, we need to be able to visualize the position of a cell cluster found in one bivariate view with the same cell cluster found in another bivariate view. This can be accomplished by using color, called **color gating**, because a color is assigned to each gate.

1. A population of cells in FL1 vs FL2 has been colored black in **Fig. 8A**. These cells could be anywhere along the projection of FL2 onto the FL3 axis (**Fig. 8B**) or FL1 on to the FL3 axis (**Fig. 8C**).
2. As shown in **Fig. 8A**, a single population is seen, but in **Fig. 8B**, two distinct populations, one that is AB3-PC negative and one that is AB3-PC positive, are found. Because we colored the cells black, both populations resolved in **Fig. 8B** would also appear black, even though one of them is AB2-PE⁺AB3-PC⁻ and the other is AB2-PE⁺AB3-PC⁺. This situation can be corrected by coloring the AB2-PE⁺AB3-PC⁻ population gray.

Fig. 7. (see opposite page) (A) Setting a gate. Human peripheral blood was stained with FITC-CD45 and PE-CD14 to resolve lymphocytes (L), monocytes (M), and granulocytes (G). Because lymphocytes are CD45 bright and CD14⁻ a region (R2) in (B) can be drawn and used as a gate, shown in (C). These cells can be distinguished from all others by assigning them the color gray. In (C), a region R1 is drawn that contains most all the lymphocytes, but some are scattered outside this region. When R1 is used as the gate, shown in (D), cells (black events outside R2) that are not lymphocytes contaminate it.

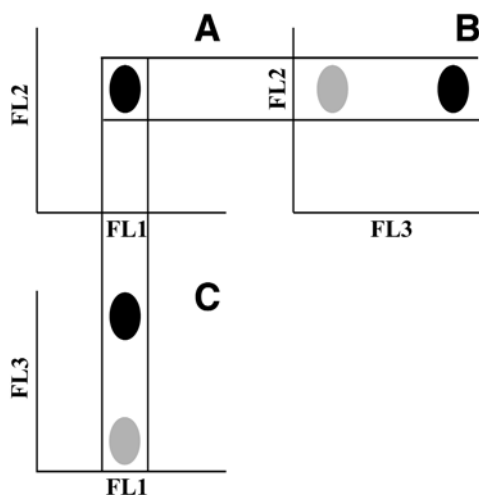


Fig. 8. Displaying three parameters and color gating. A single homogeneous population of cells is shown in the bivariate plot of FL1 vs FL2 (A). When a bivariate plot of FL3 vs FL2 is displayed (B), two populations (black and gray) are found because AB3 stains some but not all of the cells found in (A). When the bivariate plot of FL1 vs FL3 is displayed (C), both populations (black and gray) are positive for the FL1 fluorescent antibody.

3. In **Fig. 8C**, we are able to see that both populations are also AB1-FITC⁺, but the AB3-PC⁻ population is colored gray. Thus, this population is AB1-FITC⁺ AB2-PE⁺ and AB3-PC⁻ while the black one is AB1-FITC⁺ AB2-PE⁺ AB3-PC⁺. For the automatic analysis of large numbers of parameters (three or more colors), the method of color gating is a more streamlined strategy for data analysis.
4. **Figure 9** is an example of color gating using three different antibodies requiring two bivariate displays. Each quadrant is assigned a region, R1-R8. Only two of the three bivariate displays need to have quadrants because that will produce all the possible binary combinations for the three fluorescent antibodies. Any two can be used; in this example, CD3-FITC vs CD4-PE, and CD8-PC vs CD4-PE were chosen. Based on whether any given cell is positive or negative for any given antibody, there are eight possible binary combinations, shown in **Table 2**.
5. Cells with any given phenotype can therefore be explicitly defined by combining the regions using boolean algebra. Cells that are not stained can be found only in R3 and R7. We cannot use R3 alone because the cells could also be found in either R7 or R8. Similarly, R7 alone cannot be used because the cells could also be found in either R3 or R4. Thus, the boolean equation, R3 and R7 explicitly defines the only location cells negative for all three antibodies can be found. This same logic is used for all the other seven possible binary combinations.

Table 2
Binary Combinations of Quadrant Markers

Region	AB1-FITC	AB2-PE	AB3-TC	Boolean	Color
1	—	—	—	R3 and R7	Black
2	+	—	—	R4 and R7	Yellow
3	—	+	—	R1 and R5	Cyan
4	+	+	—	R2 and R5	Green
5	—	—	+	R3 and R8	Brown
6	+	—	+	R4 and R8	Blue
7	—	+	+	R1 and R6	Violet
8	+	+	+	R2 and R6	Red

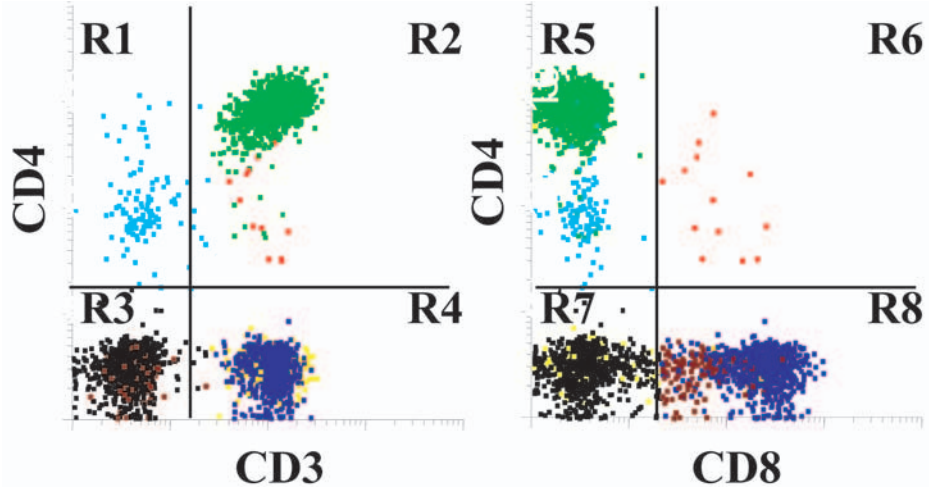


Fig. 9. Normal lymphocytes using three-color immunophenotyping. Blood was stained with the antibody combination FITC-CD3, PE-CD4, and PECY5-CD8. After acquiring data, the sample was analyzed using a lymphogate and the color gating shown in Table 2. Note that small monocytes (cyan, R1, and R5) contaminate the lymphogate.

6. Note also how the information in this table is arranged. The first column has the sequence $-+-+$ and so forth, the second column $---++--++$ and so forth, the third column $----++++----++++$ and so forth. When another parameter is added, we simply extend this sequence, doubling the number of populations that can be resolved so that the number of binary combinations $= 2^n$, where n is the number of antibodies (or parameters). Eight parameter data could yield 256 cell populations. Each combination of different antibodies will produce its own unique colored pattern as shown in the last column of Table 2 for the panel FITC-CD3, PE-CD4, and PC-CD8 in Fig. 9.

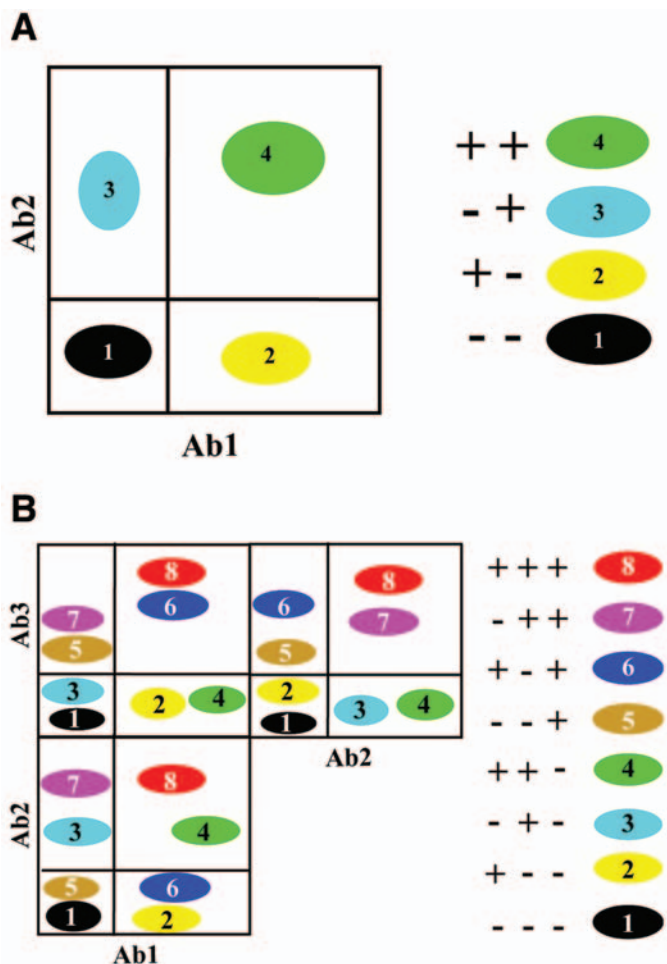


Fig. 10. Color gating. (A) When two antibodies conjugated with two different fluorochromes are combined, four populations of cells can be resolved. $Ab1^+Ab2^-$ cells are yellow, $Ab1^+Ab2^+$ are green, $Ab1^-Ab2^+$ cells are cyan, and $Ab1^-Ab2^-$ cells are black. (B) When three antibodies conjugated with different fluorochromes are combined, eight populations of cells can be resolved. Three bivariate histograms are required and each population is assigned a different color so it can be visualized in each plot. $Ab1^-Ab2^-Ab3^-$ cells are black, $Ab1^+Ab2^-Ab3^-$ are yellow, $Ab1^-Ab2^+Ab3^-$ cells are cyan, $Ab1^+Ab2^+Ab3^-$ cells are green, $Ab1^-Ab2^-Ab3^+$ cells are brown, $Ab1^+Ab2^-Ab3^+$ cells are blue, $Ab1^-Ab2^+Ab3^+$ cells are violet, and $Ab1^+Ab2^+Ab3^+$ cells are red. (C) When four antibodies conjugated with different fluorochromes are combined, 16 populations of cells can be resolved. Six bivariate histograms are required and each population is assigned a different color so it can be visualized in each plot.

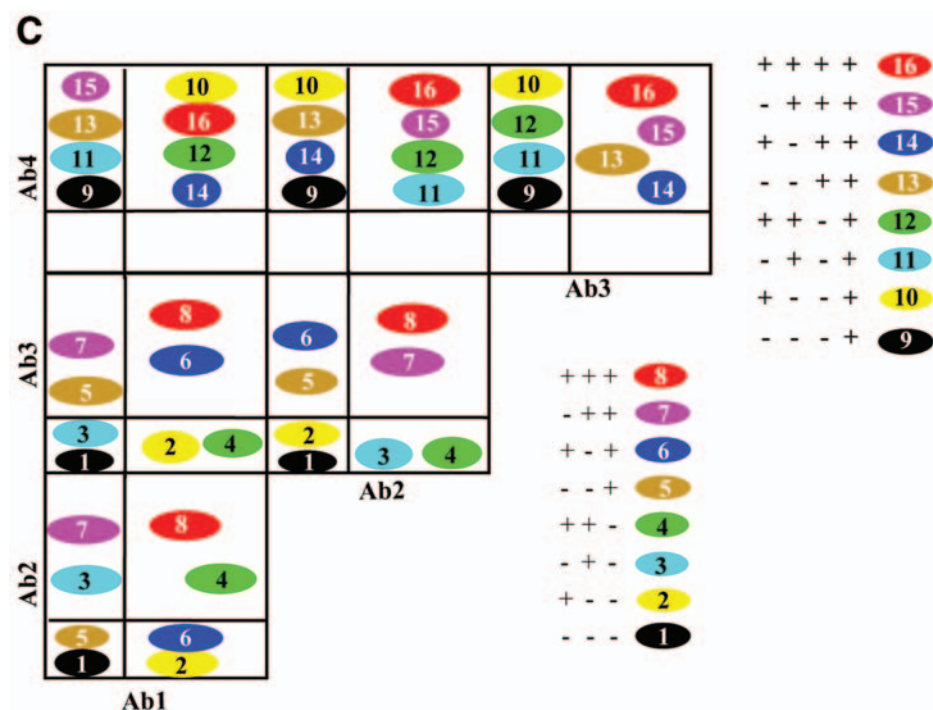


Fig. 10. (continued)

3.3. How to Make a Phenogram

The customary approach to data analysis is the marker method. For a bivariate histogram four quadrants are created from which negative, single-positive, and double-positive cells for each antibody can be readily determined. When more than two colors of fluorescence are used, multiple bivariate plots are required. These are summarized in **Fig. 10** for up to four antibodies. Note how each new parameter increases the number of bivariate plots needed to display and the complexity of the data.

It has been customary to first plot FSC vs SSC, then form a gate around the desired cluster, such as lymphocytes and then gate the fluorescence histogram on them. We have already discussed the problem with this approach, all the desired cells may not be included in the gate and undesired cells may be included. This has led to the realization that a process called “cell gating” may be a much better approach.

Basically one or more antibodies are used to define the cells of interest and used as a gate. For example, CD45 for all leukocytes (**10**), CD3 for T-cells (**11**), CD19 for B-cells, CD56 AND NOT CD3 for NK cells (**12**), CD14 for mono-

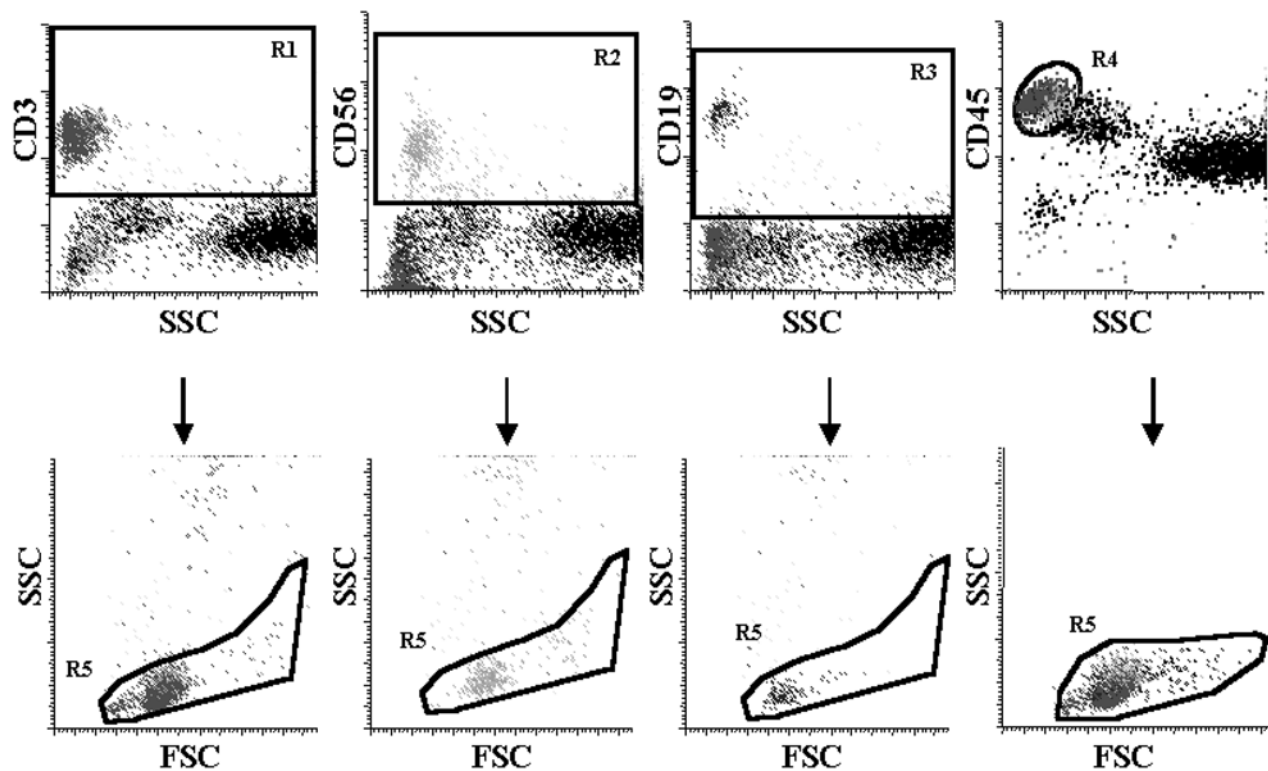
cytes, and CD34 for progenitor cells (**13**) are a few examples. In this approach, SSC (in linear or log) vs the fluorescent antibody is used to identify the desired cells. A region can be drawn around positive cells and that is then applied to other displays of the scatter or fluorescence parameters as a gate. The advantage of using this approach is that only one region for each antibody is required and any one of them or a boolean combination of them can be used to define a cell gate.

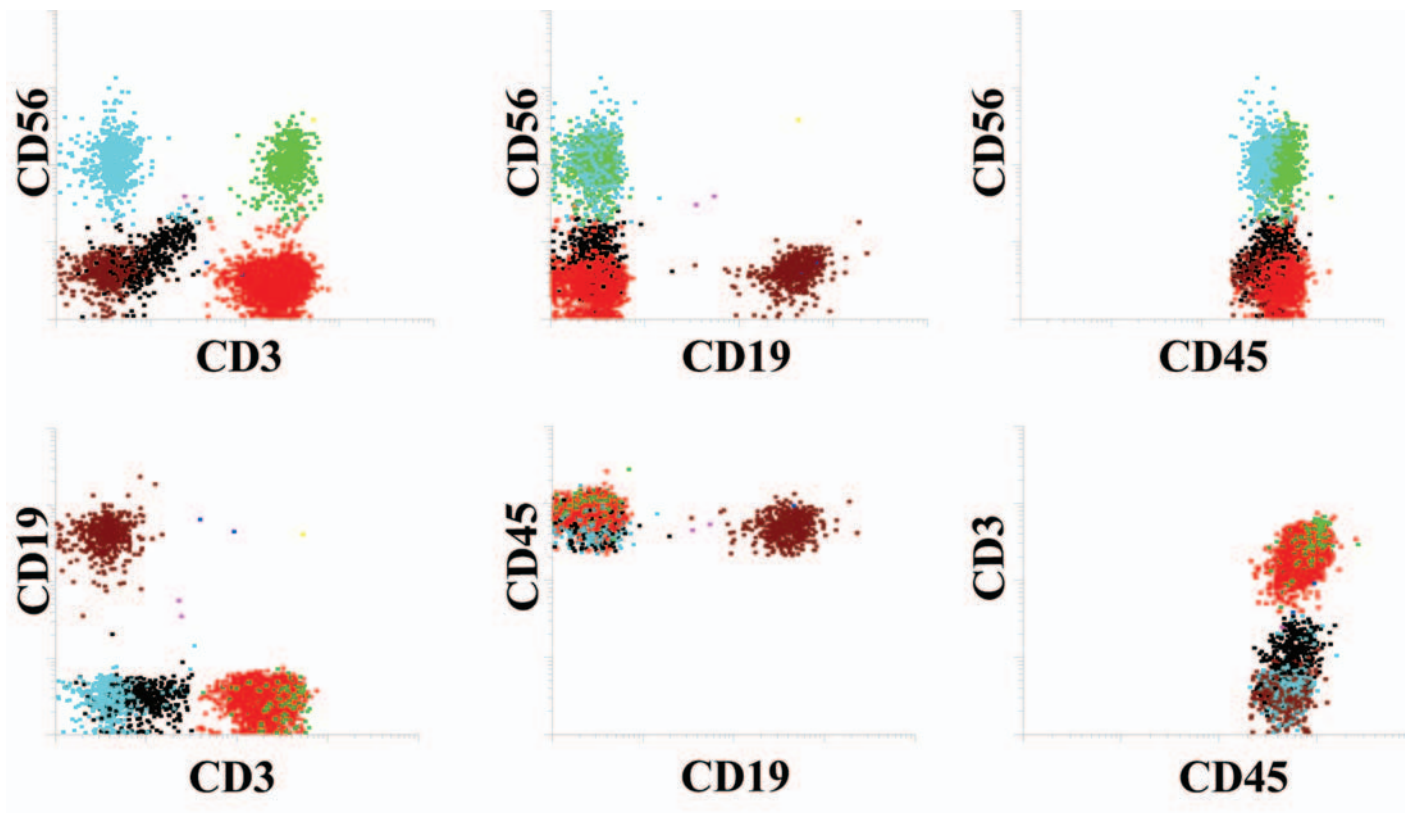
This feature has incorporated a generic approach to data analysis, which can easily be applied to any number of fluorescence parameters. This approach becomes increasingly easier as the number of analysis parameters increases, as shown in **Fig. 11** for a combination used to determine the lymphocyte subsets, T cells, NK cells, and B cells in human blood.

3.3.1. The Generic Phenogram

1. Display SSC vs the fluorescence parameter for each fluorescence parameter measured and draw a region around positive events or the desired cluster of cells, as shown in **Fig. 11** for four-color data. Negative cells (the best control, as shown here), an isotype control or autofluorescence control could be used to define negative events.
2. Next the FSC vs SSC display for the cells of interest is obtained by gating on the positive events in each SSC vs antibody view (R1–R4). This would provide the scatter characteristics of the positive cells, if desired, which might actually provide for the resolution of previously unknown populations. Another region, R5, can be applied to enumerate a specific population in this view creating the gate R5 and R_i ($i = 1, 2, 3$, or 4 in this example).
3. Display all fluorescence combinations, as shown in **Fig. 12**. These bivariate displays can be gated on any desired combination of fluorescence and scatter parameters. In this example, we have used CD45⁺ cells (region R4 in **Fig. 11**), exhibiting the scatter characteristics of mononuclear cells (region R5 in **Fig. 11**), as the gate (R4 and R5). Clearly, any region could be drawn in the fluorescence or scatter display for gating providing unlimited flexibility for data analysis.
4. To visualize each of the subsets of cells in all the bivariate combinations, color gating is used by assigning a color to each binary combination. Our strategy is to

Fig. 11. (*see facing page*) Multiparameter data analysis. To illustrate the strategy for evaluating multiparameter data analysis, human blood was stained with the antibody combination FITC–CD3, PE–CD56, PECY5–CD19, and APC–CD45. A bivariate plot of SSC vs each fluorescence parameter is displayed in the **top row**. A region (R1–R4) is drawn on the desired population of positive cells or to all events above negative cells for the antibody, as shown. Next the FSC vs SSC for each selected cluster is displayed by gating them on each of the regions. Another region, R5, can be drawn to further define the desired population, **bottom row**.





assign the color to the binary combination representing all possible phenotypes. Therefore, in the three-color combination +++, red is assigned. Thus, all cells stained with all three antibodies (whatever they might be) will be colored red in the bivariate histograms.

3.3.2. Color Gating for Four or More Parameters

Color gating, however, is not useful for four or more parameters because most individuals cannot distinguish more than 11 or 12 colors (e.g., red, yellow, orange, green, blue, violet, brown, gold, cyan, magenta, gray, and black). Although shades can be made between any two pairs, they too are not readily perceived in a colored figure. Thus, a five-color experiment that would generate 32 binary combinations using 32 different colors would be visually useless.

1. To solve this visualization problem we repeat the same colors in increments of up to eight as shown in **Fig. 10**. For example, four-color data would be represented by eight colors in one analysis and the same eight colors in a second analysis.
2. Five-color would require up to four analyses using the same eight colors in each. Thus, selecting one or more of the fluorescence parameters as a sequential gate is used to perform n separate analyses. Insight into the purpose of the antibody combinations is required to choose the proper color gating antibodies, their boolean combination and the cell gating strategy (see **Notes 1** and **2**).

Although there is no minimization of the increasing complexity of multiparameter data analysis produced by correlated list mode data, this strategy provides for a simple generic approach for its analysis and visualization no matter how many parameters are acquired. Thus, data becomes increasingly complex, but the analysis remains simple. We call this process cell gating because only the cells that meet the criteria selected can pass through the gate for display and numerical evaluation.

4. Notes

Strategies for combining antibodies. There are two major considerations for deciding what antibodies should be combined: technical and scientific.

Fig. 12. (see facing page) Four-color immunophenotyping. Human blood was stained with the antibody combination FITC-CD3, PE-CD56, PECY5-CD19, and APC-CD45. The bivariate plots of each antibody combination are displayed. For four-color data, there are six bivariate combinations. The frequency and color of each cluster of events defined by a boolean expression for the 16 binary combinations are then determined. In this example, the gate R4 and R5 (**Fig. 11**) that defines CD45⁺ mononuclear cells was used. There are no CD45⁻ events defined by the gate used. For clarity, red has been used instead of yellow for cells that are + - - +.

1. Technical considerations:
 - a. The technical consideration is the antibody's ability to provide the correct result. Antibodies to different epitopes on the same antigen may coblock, or incorrect compensation may provide an erroneous interpretation of the result.
 - b. Antigen density and fluorochrome brightness must also be considered. The general rule is to use the brightest fluorochromes such as PE or the tandems for low antigen expression, and dimmer fluorochromes such as FITC or PerCP for high antigen expression. APC is actually a relatively dim fluorochrome, but because there is little cellular autofluorescence at its excitation wavelength, the signal-to-noise ratio is high and resolution of dimly stained cells is good. One must realize that using increasing numbers of colors demands stringent compensation approaches that will negate the use of quadrant markers, and the approach described above is still valid using curvilinear instead of orthogonal regions (5).
2. Scientific considerations:
 - a. The scientific consideration is to define explicitly the question to be answered by the immunophenotyping experiment and to combine those antibodies that will provide the answer. This leads to the use of lineage specific antibodies that are then combined with the antibodies to the antigens of interest. For example, what chemokine receptors do T cells express? CD3 is used to identify the T cells and it is combined with the chemokine receptor antibodies of interest.
 - b. Cells of interest that may be in low frequency may require a "dump" combination of antibodies to remove cells of no interest and their associated backgrounds. For example, dendritic cells in blood are in low frequency. Since they do not express CD3, CD14, CD19 or CD56, these antibodies are combined using the same fluorochrome, for example, FITC. Because dendritic cells do express CD123-PE, HLADr-PerCP, and CD11c-APC, the four-color combination used to define them explicitly would be CD123 positive, HLADr positive, CD11c positive AND NOT (CD3 or CD14 or CD19 or CD56) positive.

References

1. Stewart, C. C. and Stewart, S. J. (1997) Immunophenotyping, in *Current Protocols in Cytometry* (Robinson, J. P., Darzynkiewicz, Z., Dean, P., et al., eds.), John Wiley & Sons, New York, pp. 6.2.1–6.2.15.
2. Stewart, C. C. and Stewart, S. J. (2001) Cell preparation for the identification of leukocytes, in *Methods of Cell Biology*, Vol. 64 (Darzynkiewicz, Z., Crissman, H., and Robinson, J. P., eds.), Academic Press, New York, pp. 218–270.
3. Stewart, C. C. and Stewart, S. J. (1999) Four color compensation. *Commun. Clin. Cytom.* **38**, 161–175.
4. Stewart, C. C. and Stewart, S. J. (2003) A software method for color compensation, in *Current Protocols in Cytometry* (Robinson, J. P., Darzynkiewicz, Z., Dean, P., et al., eds.), John Wiley & Sons, New York, 10.15.1–10.15.12.

5. Roederer, M. (2001) Spectral compensation for flow cytometry: visualization artifacts, limitations, and caveats. *Cytometry* **45**, 194–205.
6. Seamer, L. C., Bagwell, C. B., Barden, L., et al. (1997) Proposed new data file standard for flow cytometry, version FCS 3.0. *Cytometry* **28**, 118–122.
7. Stelzer, G. T., Marti, G., Hurley, A., McCoy, P. Jr., Lovett, E. J., and Schwartz, A. (1997) U.S.–Canadian Consensus recommendations on the immunophenotypic analysis of hematologic neoplasia by flow cytometry: standardization and validation of laboratory procedures. *Cytometry* **30**, 214–230.
8. Borowitz, M. (1993) Clinical applications of flow cytometry: immunophenotyping of leukemic cells. *NCCLS* **13**, 1–107.
9. Stewart, C. C. and Mayers, G. L. (2000) Kinetics of antibody binding to cells, in *Immunophenotyping* (Stewart, C. C. and Nicholson, J., eds.), John Wiley & Sons, New York, pp. 1–21.
10. Stelzer, G. T., Shults, K. E., and Loken, M. R. (1993) CD45 gating for routine flow cytometric analysis of human bone marrow specimens, in *Clinical Flow Cytometry* (Landay, A., Ault, K., Bauer, K., and Rabinovitch, P., eds.), The New York Academy of Sciences, New York, NY, pp. 265–280.
11. Mandy, F. F., Bergeron, M., Recktenwald, D., and Izaguime, C. A. (1992) A simultaneous three color T cell subsets analysis with single laser flow cytometers using T cell gating protocol. *J. Immunol. Methods* **156**, 151–162.
12. Center for Disease Control and Prevention (CDC). (1997) Revised guidelines for performing CD4+ T cell determinations in persons infected with human immunodeficiency virus (HIV). *MMWR* **46**, 1–29.
13. Sutherland, D. R., Anderson, L. M., Keeney, M., Nayar, R., and Chin-Yee, I. (1996) The ISHAGE guidelines for CD34+ cell determination by flow cytometry. *J. Hematother.* **5**, 213–226.

4

Flow Cytometric Analysis of Kinase Signaling Cascades

Omar D. Perez, Peter O. Krutzik, and Garry P. Nolan

Summary

Flow cytometry offers the capability to assess the heterogeneity of cellular subsets that exist in complex populations, such as peripheral blood, based on immunophenotypes. We describe methodologies to measure phospho-epitopes in single cells as determinants of intracellular kinase activity. Multiparametric staining, using both surface and intracellular stains, allows for the study of discrete biochemical events in readily discernible lymphocyte subsets. As such, the usage of multiparameter flow cytometry to obtain proteomic information provides several major advantages: (1) the ability to perform multiparametric experiments to identify distinct signaling profiles in defined lymphocyte populations, (2) simultaneous correlation of multiple active kinases involved in signaling cascades, (3) profiling of active kinase states to identify signaling signatures of interest rapidly, and (4) biochemical access to rare cell subsets such as those from clinically derived samples or populations that comprise too few in numbers for conventional biochemical analysis.

Key Words

Flow cytometry, kinase activation, phospho-proteins, proteomics, single-cell.

1. Introduction

Flow cytometry is routinely used for the identification of cellular populations based on a surface phenotype and also used for cellular based assays such as cytotoxicity, viability, and apoptosis, among others. It is well understood that flow cytometry offers the capability to assess the heterogeneity of cellular subsets that exist in complex populations such as peripheral blood. Current proteomic approaches, such as two-dimensional sodium dodecyl sulfate-polyacrylamide gel

From: *Methods in Molecular Biology: Flow Cytometry Protocols*, 2nd ed.
Edited by: T. S. Hawley and R. G. Hawley © Humana Press Inc., Totowa, NJ

electrophoresis (SDS-PAGE) and mass spectroscopy of protein posttranslational modifications, are extremely powerful and have provided valuable insights into many intracellular activation processes. However, as the cells are lysed, it is obvious that the readout of these experiments is an average for protein activation states across the cell population(s). Significant biology could be masked by such averaging, as there is no provision for the collection of information on the distribution of protein activation in individual cells within a population nor is there the ability to identify retroactively the cellular populations that corresponded to the detectable levels of active proteins. Therefore significant information on human and mouse immune cell population variations that exist in both defined cellular populations and across different cell subtypes is missed and cannot be addressed by methodologies that require cell lysis for protein analysis. Ultimately, protein activation signaling cascades must be measured in its most biological context to be both relevant and free of artifact.

Thus, development of methodologies for intracellular biochemical events, such as intracellular kinase activity measurements and others in single cells, will allow for a multiparametric approach to studying discrete biochemical events of particular lymphocyte subsets existing in complex heterogeneous populations. Multiparameter flow cytometric analysis allows for small subpopulations—representing different cellular subsets, differentiation, or activation states—to be discerned using cell surface markers. As such, the usage of single cell techniques to characterize signaling events provides two major advantages: (1) the ability to perform multiparametric experiments to identify the distinct signaling junctures of particular molecules in defined lymphocyte populations and (2) a way to obtain a global understanding of the extent of signaling networks by correlating several active kinases involved in signaling cascades simultaneously, at the single-cell level (*1*).

1.1. Principle

At present, the detection of active kinases is achieved by using phospho-specific antibodies that differentiate between the phospho and nonphospho version of a given protein. The generation of these highly specific antibodies (both monoclonal and polyclonal) requires thorough testing to ensure not only phospho-specificity but also specificity against closely related proteins with similar phosphorylation residues. Phospho-specific antibodies are conjugated directly to fluorophores, evaluated for optimal fluorophore-to-protein (FTP) ratios, titrated for optimal concentrations, and tested under predefined stimulating conditions. Occasionally, commercially available pharmacological inhibitors exist that block specific signaling cascades and thereby provide a confirmation of phospho-induction (*1,2*). However, for the majority of phospho-

proteins, these reagents do not exist and we provide alternative methods for determining phospho-specificity (*see* the following subheadings).

The technique for detecting intracellular phospho-proteins with the greatest differential between induced and uninduced, treated or untreated samples is a balance of several variables that include culture conditions, cellular manipulation, specificity of phospho-detecting reagent (antibody clone and fluorochrome ratio), cell fixation, and cell permeabilization. In our laboratory, several protocols have evolved that are designed to include protocols for phospho-detection alone, phospho-detection plus surface markers, and phospho-detection plus surface markers and other indicators of cellular function (i.e., apoptosis, cytokines). In general, they differ in the sequence of events and in the methods of fixation and permeabilization. Detergent-based permeabilization methods such as saponin are routinely used for intracellular cytokine detection. For instance, with phospho-protein analysis, we found that for saponin-based permeabilization, it was necessary to add combinations of phosphatase inhibitors to arrest phosphatases activity prior to intracellular staining as fixation methods did not abrogate all phosphatase activity within the cell or in *in vitro* phosphatase activity assays (O. D. P. and G. P. N., *unpublished results*). The saponin-based permeabilization technique also maintained the integrity of surface antigens, allowing us to discern readily between bright and low expression as well as other parameters such as annexin V staining (1,3). Alternatively, methanol permeabilization not only inhibits all cellular activity within the cell, but it also denatures all protein content, fully exposing intracellular epitopes for detection (cell shapes are still intact because of the prior fixation step). Methanol also has the benefit of allowing samples to be stored over time, a consideration for clinical samples or samples in which analysis is not immediately possible. However, methanol permeabilization does compromise detection of some surface antigens and makes population subgating more difficult. Both techniques have their advantages and disadvantages. We describe these in order of complexity and illustrate examples of each method. It is not obvious *a priori* which technique is suited for particular kinases and staining combinations. Therefore, the various protocols need to be evaluated by the investigator and determined as appropriate for a particular analysis setting.

Before carrying out the systems detailed in the subheadings that follow, the novice reader is directed to a series of treatises on flow cytometry. First, basic elements of flow cytometry is covered in various chapters throughout this methods series. Second, antibody conjugation and titration protocols are available at <http://herzenberg.stanford.edu/Protocols/default.htm>. Third, multicolor considerations, including cross-channel compensation for multiparameter analysis, are explained in **refs. 4-6**. Once the reader is comfortable in these different

arenas it is possible to undertake some of the more advanced subheadings below.

1.2. Cell System and Reagents—General Overview

Even with individuals experienced in flow cytometric staining it is advisable to start with a simple single staining experiment before attempting multiple-active kinase staining or phospho-proteins plus surface/other markers. Phospho-antibody specificities often do not always exist premade for flow cytometry for every circumstance that could be warranted. To overcome this, commercially available kits for most fluorophore dyes have simplified the conjugation protocols for creating antibody conjugates.

There are many considerations during the conjugation of antibodies for intracellular flow cytometry. For instance, we find that an acceptable range for FTP ratios is more restricted for intracellular phospho-flow then for other antibody conjugations. For example, in **Fig. 1A**, increasing the FTP ratio from 2.7 to 5.9 significantly degraded the detection capability of a phospho-p44/42 antibody conjugated to Alexa647, although this range is known to be acceptable for surface labeling. Each fluorochrome therefore needs to be evaluated for optimal FTP ratios. Overconjugation can result in interfering with the antigen recognizing capability of the antibody and/or can result in intramolecular quenching by the fluorophores. Therefore, antibody clones, concentrations, and FTP ratios need to be evaluated for in-house conjugated phospho-antibody production.

For setting up staining for phospho-epitopes it is best to start with an inexpensive and controllable resource. For this purpose cell lines are an acceptable place to start. We have had experience with Jurkat, CH27, HL60, U937, K562, and NIH3T3, and Web published reports have indicated that staining for PC12, A431, MOLT-3, and human endothelial cells are also possible. As most cell line systems need to be optimized for maximal induction conditions starting out with predefined conditions for phospho-induction is recommended. We have observed that kinases and phosphorylations as measured by flow cytometry allow for sensitive observations of activity given variations in stimulation and kinetics of phosphorylation. It is necessary, for instance, to titer stimulation conditions for a known amount of cells as cell density can affect the response seen to even potent stimulators such as phorbol myristate acetate (PMA) and ionomycin (IO) (**Fig. 1B**). In addition, **Fig. 1C** displays effects of temperature differences in the preparatory steps prior to phospho-staining. The protocols outlined in this chapter require a complete fixation and permeabilization of the cells for adequate detection of signaling response. Time delays prior to a complete fixation can affect the signaling responses observed (**Fig. 1C**). **Figure 2** shows examples of the differential between induced and uninduced states for several phospho-specificities in U937 cells under optimally defined conditions. (See **Note 1** for cell line considerations.)

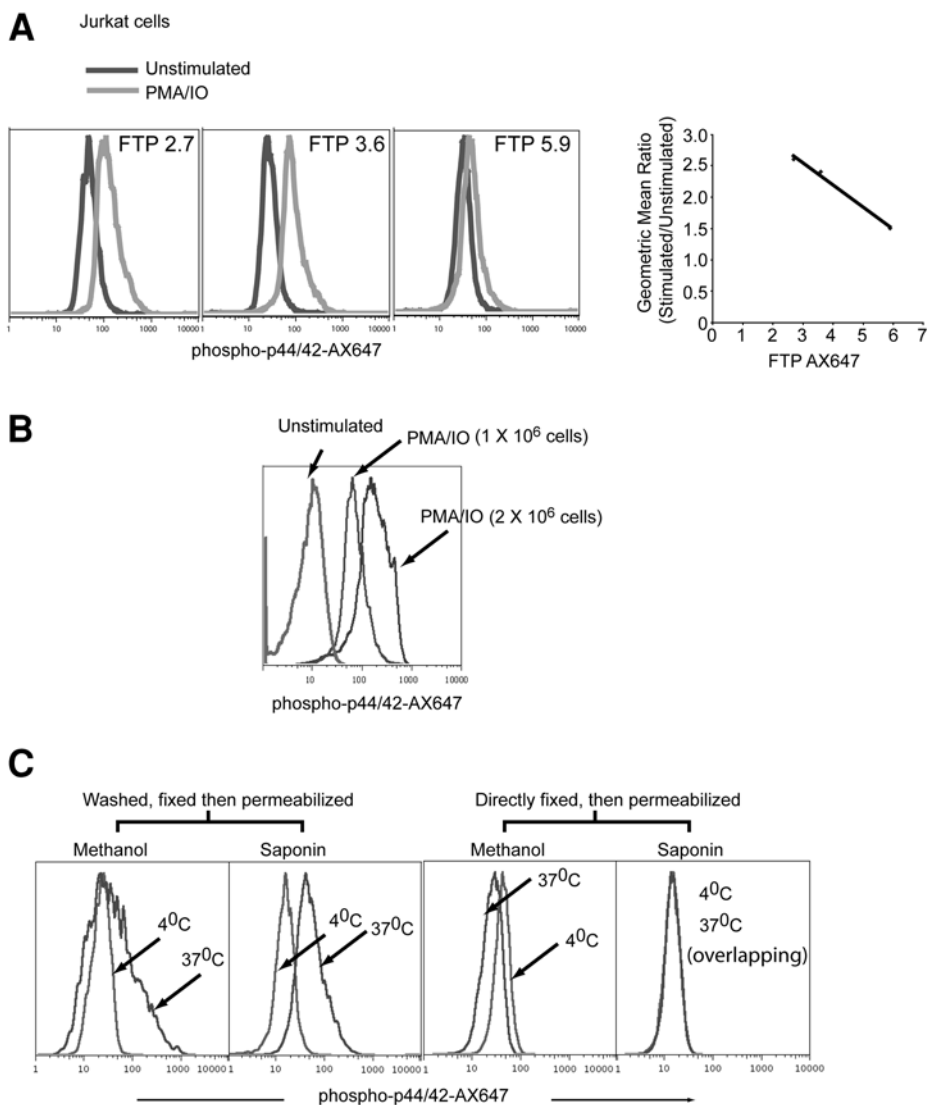


Fig. 1. Effect of FTP ratio, cell density, and time of fixation on signaling detected by flow cytometry. (A) 1×10^6 serum-starved (12 h) Jurkat cells were stimulated with PMA-IO (500 ng/mL, 15 min). Cells were fixed, permeabilized, and stained (*see Subheading 3.1.*) with antiphospho-p44/42(T202/Y204) (clone 20a) conjugated to varying ratios of Alexa-647 (AX647) as indicated; 0.125 μ g of antibody was used for all stains. Geometric mean values were computed as a ratio of stimulated to unstimulated, and plotted as a function of FTP ratio in graph. (B) Jurkat cells were stimulated with PMA-IO (500 ng/mL, 15 min) at indicated densities and prepared as described above. (C) Unstimulated Jurkat cells were either fixed after washing or directly fixed prior to washing. Cells were washed at 37°C or 4°C (including temperatures of buffers and centrifugation step) and permeabilized using either methanol or saponin based protocols. Phospho-p44/42-AX647 (clone 20a) was used as antibody stain.

U937 cells

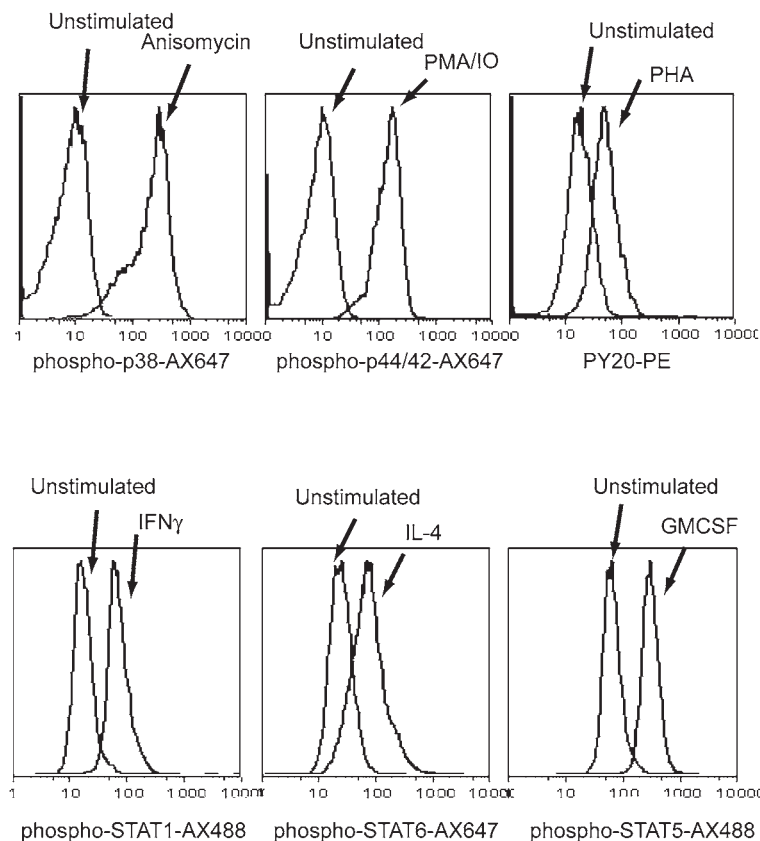


Fig. 2. Display of several phospho-specificities. 1×10^6 serum starved (12 h) U937 cells were stimulated with either 10 μM anisomycin, 500 ng/mL of PMA/IO, 50 $\mu\text{g/mL}$ of PHA, 200 ng/mL of IFN- γ , 200 ng/mL of IL-4, or 200 ng/mL of GMCSF for 15 min. Cells were fixed, permeabilized, and stained (*see Subheading 3.1.*) with phospho-p38(T180/Y182)-AX647 (clone 36), phospho-p44/42(T202/Y204)-AX647 (clone 20a), PY20-PE, phospho-STAT1(Y701)-AX488 (clone 14), phospho-STAT6(Y641)-AX647 (clone 18), and phospho-STAT5(Y694)-AX488 (clone 47). Antibodies were used at 0.125 μg .

2. Materials

2.1. Single Phospho-Staining

- 1X PBS (phosphate-buffered saline): Dissolve 1.44 g of Na_2HPO_4 , 0.24 g of KH_2PO_4 , 8 g of NaCl, and 0.2 g of KCl in 850 mL of distilled water. Adjust the pH to 7.4 with HCl and volume to 1 L. Store at room temperature.

2. Fetal calf serum (standard cell culture FCS). Store at 4°C.
3. Formaldehyde: Paraformaldehyde stocks of 4–36% can be made or bought (we use 16% paraformaldehyde stocks, cat. no. 15710 from Electron Microscopy Sciences, Washington, PA). See **Note 2** for preparation. Store at room temperature.
4. Methanol.
5. Staining media: 1X PBS, 4% FCS, and 1 mM sodium azide. Store at 4°C. (See **Note 3**).
6. EDTA: Make a 5 M stock solution and use in preparation of the PBS–EDTA buffer. EDTA is used to avoid cell clumps during flow cytometer acquisition. Store at room temperature.
7. PBS–EDTA: PBS and 1 mM EDTA. Store at room temperature.

2.2. Surface + Intracellular Staining (Methanol Rehydration Protocol)

1. All of the reagents described in **Subheading 2.1**.

2.3. Surface + Intracellular Staining (Saponin Protocol)

1. All of the reagents described in **Subheading 2.1**. (except methanol).
2. Saponin: Make a 10% saponin stock solution by mixing 10 g of saponin (containing $\geq 25\%$ saponigen content, from Sigma, St. Louis, MO) with 100 mL of PBS. Place at 37°C until saponin has dissolved with mild stirring. Sterile filter (0.22 μ L) and store at 4°C (see **Note 4**).
3. Phospho wash buffer: PBS, 1 mM β -glycerol phosphate, 1 mM sodium ortho-vanadate, 1 μ g/mL of microcystin (500- μ g vials can be purchased through Calbiochem, now EMD Biosciences, Inc., San Diego, CA), and 1 mM azide. This is the base buffer for all subsequent buffer formulations. Store at 4°C.
4. Saponin permeabilization buffer: Phospho wash buffer, 0.2% saponin, 4% FCS, and 1 mM azide. Store at 4°C. Final saponin concentration for permeabilization should be no less than 0.1% per sample. A 0.2% solution is made to account for residual volume in wells left after wash (see **Note 5**). Store at 4°C.
5. Saponin staining buffer: Same as saponin permeabilization buffer.

2.4. Combining Intracellular Phospho-Protein and Cytokine Staining, and Surface Markers

1. Phospho wash buffer as described in **Subheading 2.3**. This is the base buffer for all subsequent buffer formulations.
2. Extracellular staining buffer: Phospho wash buffer, 4% FCS, and protease inhibitor cocktail tablet (Boehringer Mannheim, now Roche Applied Science, Indianapolis, IN). Store at 4°C.
3. Fixation buffer: 1% Paraformaldehyde made in phospho wash buffer. Store at 4°C.
4. Permeabilization buffer: Phospho wash buffer, 0.2% saponin, and 4% FCS. This is also used for preparing the intracellular stain cocktail. Store at 4°C.

3. Methods

Here we provide optimized protocols for the detection of phospho-proteins and cytoplasmic proteins within intact cells. The advantages of these protocols allow for the detection of signaling intermediaries such as active kinases and intracellular proteins by flow cytometry. The flow cytometric platform allows for a multiparametric assessment of active kinases within immunophenotyped cells, among other parameters of interest. The staining principles are based on modified surface and intracellular staining procedures that were optimized for detection of phospho-proteins. The procedures are best used for suspension cells, although some success has been achieved with adherent fibroblasts. Direct fluorophore conjugated antibodies are used in combinations as they are best suited for multi-parameter analyses, although indirect staining is possible for one or two parameters. The procedures have been tested in a variety of cell lines, primary mouse splenocytes, and primary human peripheral blood mononuclear cells (PBMCs). Several protocols are described and are suited for different applications.

3.1. Single Phospho-Staining

3.1.1. Cell Preparation

1. For cell cultures, plate 1×10^6 cells/mL in standard tissue culture plates (6-, 12-, or 24-well plates). Cell lines typically must often be serum starved for up to 12 h (times may vary). For example, Jurkat cells, although useful as a model for T-cell studies, have genetic defects in the PTEN and SHIP-1 phosphatases (7,8), consequences of which allow for sustained signaling through the AKT and PI3-kinase effector pathways. Such genetic mutations enable Jurkat cells to proliferate in culture in comparison to naïve T-cells, which require exogenous stimulation to proliferate. Often, cells grown in high concentrations of a non-native serum component such as calf serum require high concentrations of growth factors to supply needed stimulants that the cells no longer obtain from their native milieu. Thus, they are “adapted” for growth in a non-native environment in which they are often hyperstimulated. Many signaling systems are not, under such conditions, at a basal state and their background activation is readily apparent. During the initial titration of antibodies, 1×10^6 cells are used. It is important to understand that titration of antibodies per cell number is a critical prerequisite to obtaining optimal signal-to-noise ratio. The reason is that the best antibody concentration and effectiveness at binding to targets within the cell is a function of the number of target phospho-epitopes to be bound per cell, the number of cells, appropriate concentration of nonspecific binding blocking agents, and the background binding events that can occur. Once optimal conditions have been determined the cell number and antibody amounts can be scaled accordingly. If multiple different stains are to be undertaken from the same sample, it is necessary to scale up the cell number so that after the fixation/permeabilization the sample can be split up into several assay tubes for individualized staining and treatment.

2. Add cell stimulation at the desired concentration. Make provisions for control stains in addition to unstimulated/stimulated samples (i.e., isotype control if available, or secondary alone stain if performing indirect stains). See **Note 6** for additional controls. Return to 37°C for 15 min.

3.1.2. Fixation and Permeabilization

1. Add concentrated formaldehyde solution to cell cultures directly so that final concentration of formaldehyde is 1–2% (i.e., if using 16% formaldehyde, add 100 μ L/mL of sample). Swirl the plate to homogeneously distribute fixative and return to 37°C for 15 min.
2. Transfer samples to fluorescence-activated cell sorter (FACS) (12 \times 75 mm) tubes by pipetting up and down to ensure complete cell removal and place samples on ice. Activated cells will tend to stick to the plastic, as will some others owing to the presence of the fixative. Pipetting up and down dislodges the majority of these cells. Calculations of cell loss can be performed by counting cells before and after. Check by microscope to determine that cells have been completely removed as this is a frequent place where novices have experienced significant cell loss.
3. Centrifuge the cells (500g, 4°C, 5 min).
4. Permeabilize cells by adding 1 mL of ice-cold methanol to the cell tube while it is being vortex-mixed (at medium speed). Addition of methanol is done at a reasonable rate (i.e., 2–3 s for 1 mL) (see **Note 7**). Allow to stand on ice for 15 min. (See **Note 8** for storage considerations.)
5. Wash cells three times with 2–4 mL of PBS to ensure removal of methanol. Washing with staining media may result in FCS protein precipitates if methanol is still present and is therefore to be avoided.

3.1.3. Staining

1. Stimulated cells may be redistributed to test several antibody stains originating from the same stimulated cell population. Resuspend cells in staining media and aliquot 25–100 μ L of cell sample. Cell number for antibody staining should be titered so that 0.5–1 $\times 10^6$ cells can be allotted for each stain in the 25- to 100- μ L sample. The fewer the number of cells per stain, the longer it can take for flow cytometry acquisition, so it is important to adjust accordingly (see **Note 9**).
2. Add the primary antibody to the cell mixture and incubate for 30 min (some reagents benefit from longer incubations such as 60 min). Typically, we make one uniform antibody staining cocktail for all samples. That is, if antibody is titered to 0.1 μ L/sample and we have 10 samples, we make up $N + 1$ samples in a final volume of 50 μ L so that all the sample are stained with uniform amounts of the reagent:

Reagent	Amount	\times	Samples	Total
Antibody (concentration titered to 1 $\times 10^6$ cells)	0.1 μ L		11	1.1 μ L
Staining media:	49.9 μ L		11	548.9 μ L
		Total:		550 μ L = 50 μ L/sample

3. Wash cells two times with 1 mL of PBS and resuspend in 100 μ L of PBS–EDTA. If the primary antibody was conjugated to a fluorophore, you may now proceed to analyze the sample(s) on the flow cytometer. If using indirect staining (i.e., secondary antibody), continue on to **step 4**.
4. Use fluorochrome-conjugated secondary at a predetermined dilution for 15 min (either the manufacturer's recommendation or 1:500–1000 is a starting point). You want to achieve a low level of background staining using the secondary alone control sample. This staining should be similar to a directly conjugated isotope control. It is often required to titer the secondary for achieving a maximal signal differential.
5. Wash cells two times in PBS, resuspend in 100 μ L of PBS–EDTA, and analyze by flow cytometry.
6. Set voltages on the flow cytometer to visualize the isotype control or the secondary control at the lowest possible range (i.e., below 10^1 log fluorescence). Uninduced treated sample is then collected, and induced sample is made relative to uninduced. Sometimes culture conditions artifactually activate signaling systems (thus the requirement for most cell lines to be serum starved). This, as noted earlier, raises the levels of some kinases in the “uninduced” cell to a higher state of basal activation. (See **Note 6** for additional staining controls.)

3.1.4. Staining for Multiple Kinases Simultaneously

The ability to discern multiple activation states of proteins simultaneously within the cell opens many opportunities to study signaling cascades, signaling crosstalk, and the ability to monitor activation states over time. We have used such approaches to gain insight in correlative biosignatures and kinetics of stimuli in time-referenced samples (9). In addition, the ability to screen rapidly multiple targets simultaneously would be advantageous in high-throughput drug screening, as these methods would offer detection of kinase activities intracellularly (ensuring that pharmaceutical regulators of key signaling component traversed cell membranes or acted according to expectation) and target validation (verifying specificity to desired protein and not other signaling molecules that may tap into the same pathway).

To assess multiple phospho-proteins simultaneously in the absence of surface markers or other flow cytometric markers (i.e., apoptosis, DNA, etc.), the above mentioned protocol is adequate. The second detecting antibody will be added to the antibody cocktail (calculated appropriately as with the first example) and the cocktail is applied to all samples. Increasing the number of intracellular phospho-proteins detected will require the usage of directly conjugated antibodies because using monoclonal or polyclonal antiphospho antibodies can complicate staining considerations. The commercial availability of directly conjugated antiphospho specific antibodies is expected to meet the need of most consumers; however, certain reagents may still need in-house laboratory generation.

Figure 3A demonstrates staining for kinases in two and three dimensions in human PBMCs, using interleukin-4 (IL-4) or IL-12 as stimulation. **Figure 3B** demonstrates the activation of several MAPK pathways in primary cells that are cultured. This is an example of (1) the effects of culture conditions and background of phosphorylation levels and (2) profiling of 3 MAPKs simultaneously.

3.1.5. Surface Marker and Intracellular Phospho-Staining

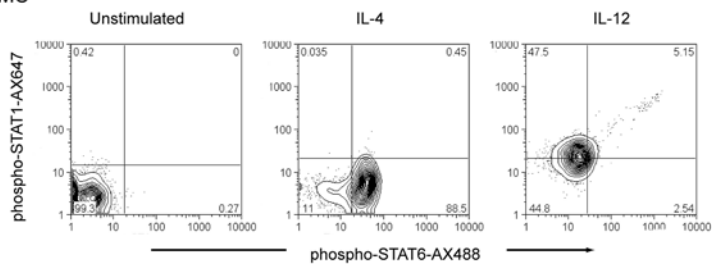
In complex cell populations, it would be desirable to distinguish cell subsets by surface markers, and then undertake intracellular phospho-protein staining in one step using either the saponin or methanol permeabilization techniques (see **Note 10**). To do this requires an initial evaluation of surface markers pre- and post-fixation, and permeabilization steps to assess maintenance of surface antigen detection. We have used the saponin-based technique (see **Subheading 3.3.**) in a two-step staining procedure to correlate phospho-profiles in immunologically defined cellular subsets as complex as 11 parameters (**I**). However, this procedure requires particular attention to detail and requires the arresting of phosphatase activity by a combination of phosphatase inhibitors and ice-cold buffers. If the methanol permeabilization is performed, we have observed in some circumstances that staining for surface antigens needs to be evaluated. We have observed that while the epitopes on some surface proteins are detectable only after extensive rehydration, others remain compromised after methanol fixation. Some epitopes are removed by methanol fixation as they are maintained on the cells loosely and can be stripped from the surface. As before, it is necessary to titrate the antibodies to surface epitopes.

In general, for two-step staining procedures involving sequential intracellular and extracellular staining, surface staining followed by fixation and permeabilization is best for saponin-based protocols. For one-step staining procedures, both intracellular and extracellular antibodies are combined and best applied post-fixation and post-permeabilization, for both saponin and methanol based procedures. Prior to attempting subset specific signaling, staining differences for surface markers need to be evaluated (depending on the protocol applied) and assessed if staining post-permeabilization increases the staining background.

We performed a series of sequential surface staining experiments, in which 200+ surface antibodies on all colors were profiled for the ability to stain in paraformaldehyde, saponin, and methanol pre-fixation, post-fixation, pre-permeabilization, post-permeabilization, as well as determining the effects of paraformaldehyde, saponin, and methanol on fluorochrome intensity to a panel of protein and inorganic dyes. In our experience, it was not predictable which antibody (clone or antigen) or fluorochrome would work the best (O. D. P. and G. P. N., *data not shown*). The majority of the dyes were not affected by

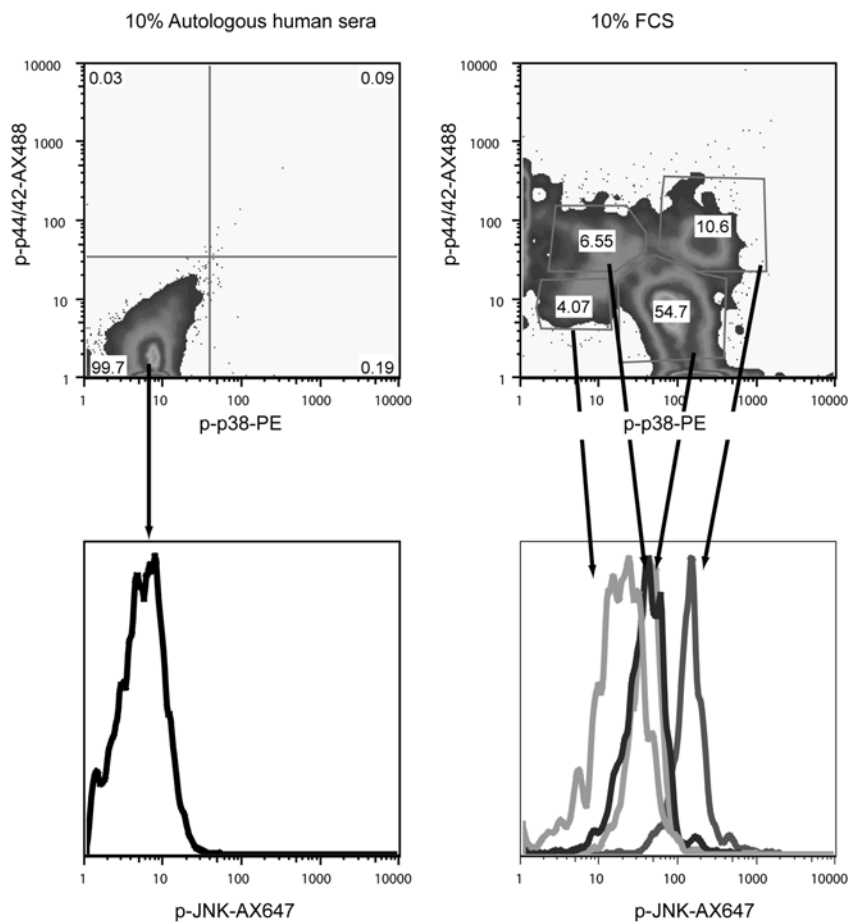
A

Human PBMC



B

Human PBMC: Testing 3 MAPK kinase signaling responses simultaneously



paraformaldehyde and/or saponin treatments, but a majority of the antibody reagents were compromised by the methanol treatment. For example, **Fig. 4** displays surface detection of typical T-cell markers—CD4, CD3, CD62L, and CD8—under various pre- and post-fixation and permeabilization conditions. These antibodies survived both the fixation and saponin permeabilization conditions. Staining post-fixation and saponin permeabilization resulted in reduced forward scatter (size). The additional population contained within the lymphocyte gating was reflected in the intermediate populations showing up in the fluorescent parameters that would typically be excluded (*column IV*). Methanol permeabilization, in this example, increased CD3 staining background and abrogated CD8 surface staining (*column V*). Therefore, for these specific monoclonal antibodies the permeabilization/staining conditions that work best are found in *column III*.

Fig. 3. (*see opposite page*) Phospho-staining in two and three dimensions. **(A)** 1×10^6 CD4⁺ naïve T cells (purified by negative isolation) were treated with IL-4 or IL-12 (200 ng/mL) for 12 h. Cells were fixed, permeabilized, and stained (*see Subheading 3.1.*) and stained with phospho-STAT6(Y641)-AX488 (clone 18) and phospho-STAT1(Y701)-AX647 (clone 4a). Antibodies were used at 0.25 μ g. **(B)** Three MAPK kinase signaling responses simultaneously. Human PBMC depleted for adherent cells were cultured in either 10% autologous human sera or 10% FCS (Hyclone, Logan, UT). Cells were stained for phospho-p44/42(T202/Y204)-AX488 (clone 20a), phospho-p38(T180/Y182)-PE (clone 36), and phospho-JNK(T183/Y185)-AX647 (clone 41) (*see Subheading 3.1.*). Antibodies were used at 0.125 μ g (p-p44/42) and 0.25 μ g (p-p38 and p-JNK).

Fig. 4. (*see next page*) Sequential staining of surface antigens upon fixative and permeabilization treatments. 1×10^6 PBMCs were either surface stained (*column I*), surface stained, then fixed in 1% paraformaldehyde (*column II*), surface stained, fixed in 1% paraformaldehyde, then permeabilized by 0.2% saponin (*column III*), fixed, permeabilized by 0.2% saponin, then surface stained (*column IV*), or fixed, permeabilized by methanol, then surface stained (*column V*). Cells were stained with CD62L-FITC (clone DREG 56), CD4-PE (clone RPA-T4), CD8-PerCP-Cy5.5 (clone SK1), and CD3-APC (clone UCHT1). **Top row** displays forward (FSC) and side scatter (SSC) profiles, and lymphocyte gate used for display of subsequent rows. Figure displays consequences of antigen staining toward fixation and permeabilization conditions for intracellular staining. Postpermeabilization often leads to a reduction in the forward scatter, and the appearance of these populations is illustrated by the intermediate populations appearing in the surface marker staining that are typically excluded by lymphocyte gating alone. *Column VI* displays the ungated surface stains alone.

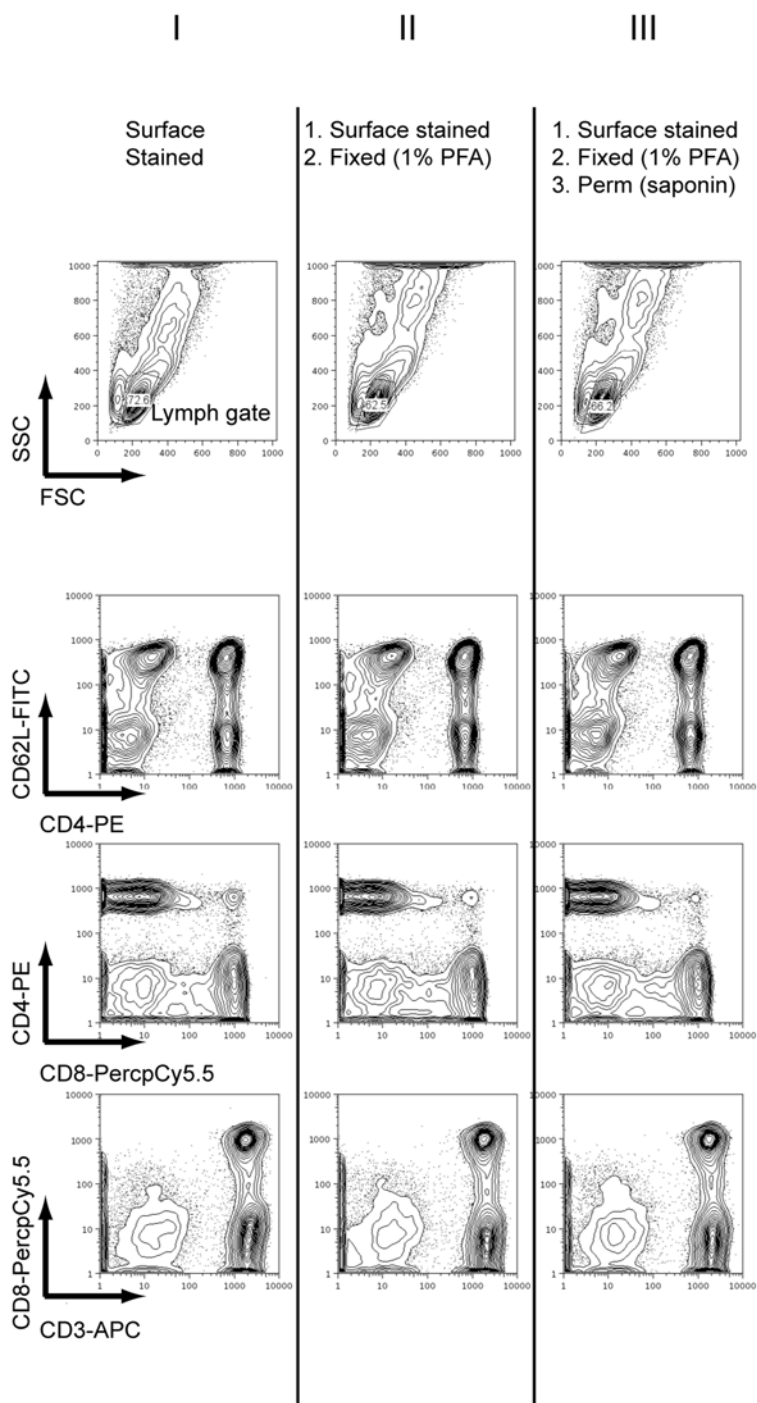


Fig. 4.

IV

V

VI

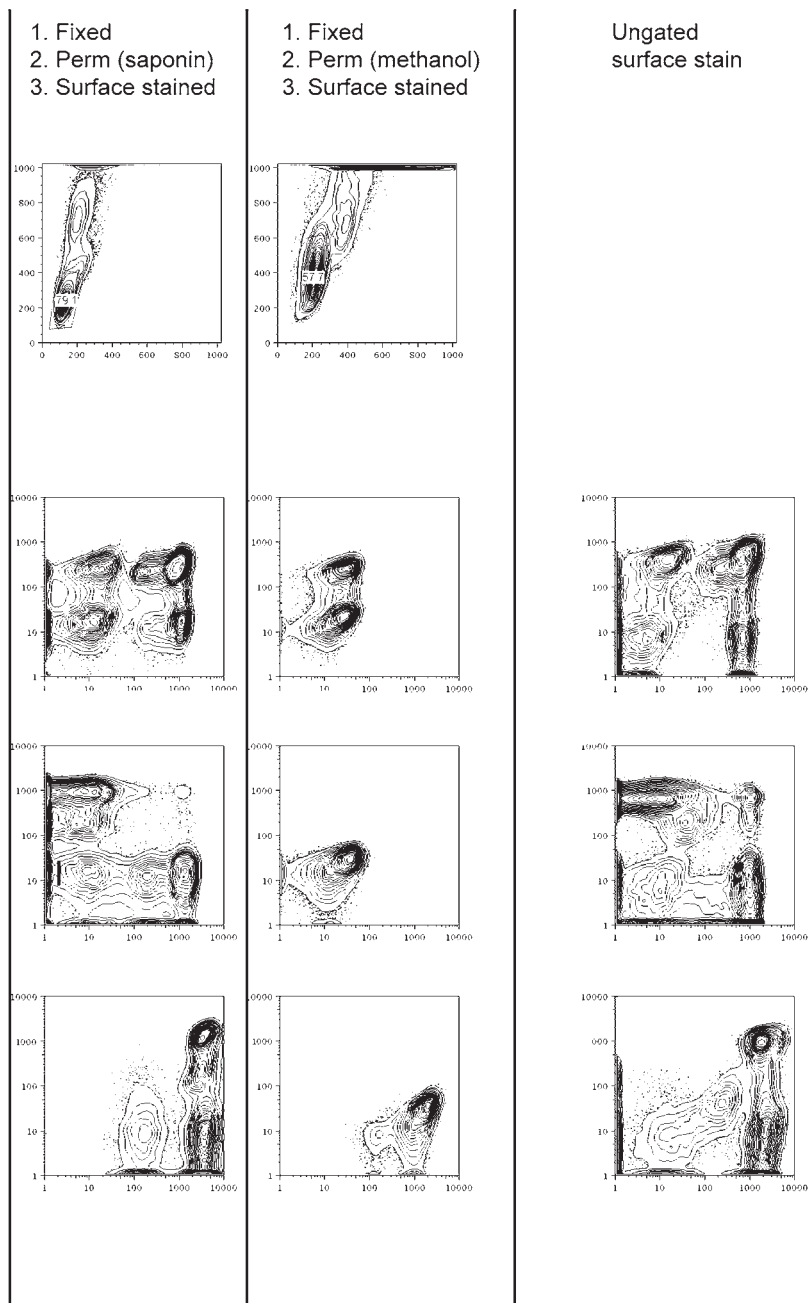


Fig. 4. (continued)

3.2. Surface + Intracellular Staining (Methanol Rehydration Protocol)

An example of this protocol's staining is shown in **Fig. 5B**, where human PBMCs were treated with various cytokines, stained for both surface (CD56 and CD11b, markers for natural killer (NK) cells and MAC-1 expression, respectively) and intracellular markers (phospho-STAT6) simultaneously, and then gated for lymphocyte subset signaling differences. The results show that CD56⁺ populations phosphorylated STAT6 on stimulation with IL-4 and IL-12. CD56⁺ populations with higher levels of CD11b in general had elevated levels of phospho-STAT6. CD56-CD11b^{high} populations did not display changes in phospho-STAT6 to stimulations tested.

3.2.1. Cell Preparation and Cell Fixation/Permeabilization

These procedures are the same as those outlined in **Subheading 3.1**. On completion of **step 5** in **Subheading 3.1.2.**, resuspend the cells in 500 μ L of staining media (4% FCS in PBS) for 1 h. The extensive washing and rehydration step increases detection of many epitopes for human surface antigens. For reasons we do not understand, at present, we do not observe as many difficulties with murine surface epitopes.

3.2.2. Staining

1. Make up antibody cocktails in staining media as exemplified in **Subheading 3.1.3**. Multicolor work requires staining with individual antibody-fluorophore conjugates to be used as compensation controls (**10**). In the antibody cocktails, one fifth of the final volume of the antibody cocktail should be staining media (containing 4% FCS). If higher amounts of diluted antibodies are used, the final volume of the antibody cocktail can be increased to 100 μ L with staining media. An example of a four-color setup is provided below.
2. Antibodies used for either surface or intracellular staining can be used in cocktails once an optimal concentration has been determined. A typical example of an antibody cocktail protocol is presented below:

$$\text{Total volume} = 50 \mu\text{L}/1 \times 10^6 \text{ cells}$$

For X amount of samples, make up sufficient reagents for X + 1.

Reagent	Volume per sample	No. of samples	Total volume required
Ab-FITC	5 μ L	5	25 μ L
Ab-PE	6 μ L	5	30 μ L
Ab-PerCP	10 μ L	5	50 μ L
Ab-APC	2 μ L	5	10 μ L
Staining media	27 μ L	5	135 μ L
Total	50 μ L		250 μ L

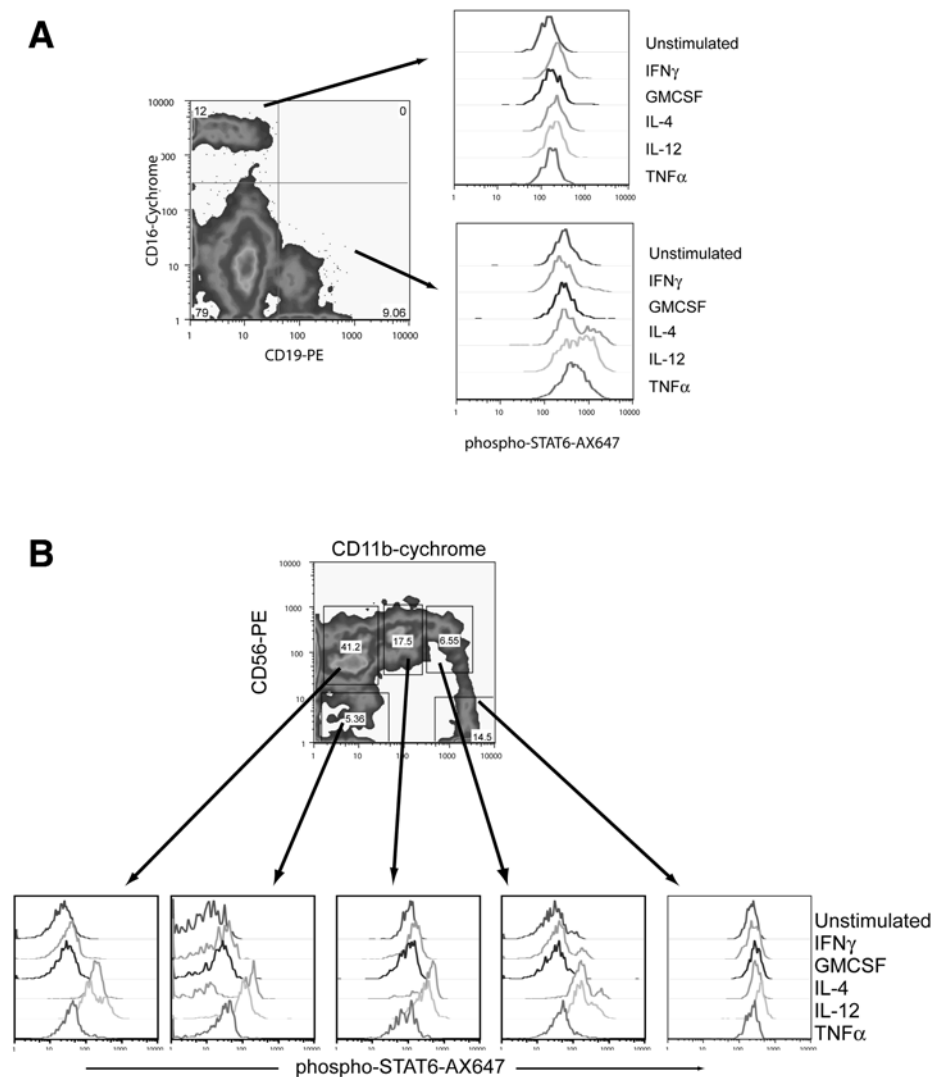


Fig. 5. Multiparameter staining: surface + intracellular staining. (A) 1×10^6 PBMCs (nondepleted) were treated with indicated cytokine (200 ng/mL, 15 min) and stained for CD16-cychrome (clone 3G8), CD19-PE (clone HIB19), and phospho-STAT6(Y641)-AX647 (clone 18) (as described in **Subheading 3.3.**). Cells were gated for either CD16 or CD19 and displayed for phospho-STAT6. (B) Cells were prepared as described above and stained with CD56-PE (clone B159), CD11b-cychrome (clone ICRF44) and phospho-STAT6(Y641)-AX647 (clone 18) (see **Subheading 3.2.**).

Because the final volume per sample is 50 μL , it is adjusted using staining media. A minimum of 10–15 μL of staining media is needed to ensure blocking agents are included in the stain; thus if diluted antibodies are used, it might be necessary to scale up to a 100- μL staining volume.

3. Perform antibody staining for 1 h at 4°C on ice (covered to protect from light).
4. Wash cells three times in PBS, resuspend in 100 μL of PBS–EDTA, and analyze by flow cytometry.

3.2.3. Single-Step Surface Marker Staining for Antigens Requiring Discrimination Between Bright/Dim or Med/High

As noted with methanol permeabilization, there can be a loss of staining for certain surface epitopes (such as with CD8 populations) as well as a loss of distinctive levels of expression (such as with CD11a, CD45RA, CD62L); the levels of expression between medium and high tend to collapse or strongly overlap. In addition, the side scatter (SSC) and forward scatter (FSC) properties are not always maintained with methanol or saponin permeabilization (**Fig. 4**, columns IV and V) in one-step staining procedures. Because scatter properties are used to differentiate different cell populations in PBMCs (such as monocytes and lymphocytes), this can cause difficulties during analysis. Owing to such considerations we have applied saponin based techniques for fine cellular subset characterization (*see Note 9*).

3.3. Surface + Intracellular Staining (Saponin Protocol)

An example of this protocol is shown in **Fig. 5A** where human PBMCs were treated with various cytokines, stained for both surface (CD16 and CD19) and intracellular markers (phospho-STAT6) simultaneously, and displayed for lymphocyte subset signaling differences. The results show that CD19⁺ cells phosphorylated STAT-6 on stimulation of IL-4 and IL-12. Stimulation with tumor necrosis factor- α (TNF- α) slightly induced phosphorylation in some CD19⁺ cells, whereas interferon- γ (IFN- γ) and granulocyte-macrophage colony-stimulating factor (GM-CSF) did not induce phosphorylation of STAT6. CD16⁺ cells did not display significant changes to STAT-6 phosphorylation on stimulations tested. Aspects of these findings are further supported by various studies (*11,12*).

3.3.1. Cell Preparation

Prepare cells as described in **Subheading 3.1.1**.

3.3.2. Fixation and Permeabilization

1. Fix cells as described in **Subheading 3.1.2**.
2. Permeabilize the cells in 200 μL of saponin permeabilization buffer for 15 min on ice. Pellet the cells (500g, 4°C, 5 min). (*See Note 5* for alternative permeabilization considerations.)

3.3.3. Staining

1. Stain cells in antibody cocktails as described in **Subheading 3.2.2.**, except that the staining media used is the saponin staining buffer. It is **very important** that the saponin-based buffer is used for the antibody cocktail, as saponin permeabilization is reversible and, if using the standard staining media, the antibodies for intracellular staining will not gain access to the appropriate compartments.
2. Stain cells for 1 h at 4°C, protected from light.
3. Wash cells three times in PBS, resuspend in 100 μ L of PBS-EDTA, and analyze by flow cytometry.

3.3.4. Surface Marker, Intracellular Phospho-Staining, and Staining for Other Intracellular Proteins or Flow Parameters (i.e., Cytokines, Annexin V, Nonphospho Proteins)

With the advent of instrumentation that is capable of processing up to 15 simultaneous parameters and with an appreciable desire to undertake biochemical analyses in rare cell subsets that require many surface markers to identify, the application of this methodology can provide correlative information on cellular subsets that are not possible to analyze by conventional biochemical approaches. It is also important to obtain as much information from a given sample if such a sample might be limited in its availability (i.e., diseased patient samples). In addition, combining phospho-profiling with detection of other parameters such as intracellular cytokine production and cellular states (such as cell cycle or apoptosis) can provide correlative information of surface phenotype, signal transduction, and effector function in a single experiment (3,9).

At present, we have been successful in combining intracellular phospho and cytokine detection, as well as intracellular phospho and the annexin V apoptotic marker using the saponin-based buffers as outlined in **Subheading 3.4.** Alternatively, procedures described in this section can be used for these efforts, although our previous work has utilized procedures described in **Subheading 3.4.** We have not currently evaluated if the methanol protocols are adequate for intracellular cytokine detection or other markers such as annexin V.

3.4. Combining Intracellular Phospho-Protein and Cytokine Staining, and Surface Markers

These procedures are best used on freshly isolated PBMCs. Isolation of PBMC is done by Ficoll-Paque density centrifugation, PBMCs are either used directly or enriched for particular populations of interest by cell sorting (magnetic activated cell sorting or FACS). Cells are then stimulated and processed for staining. (See **Note 11** for attention to particular steps in this protocol. See **Note 12** for live/dead cell discrimination for intracellular staining.)

3.4.1. Cell Preparation

1. Dispense PBMCs (or purified cells) in 96-well U-bottom plates at $0.5\text{--}1 \times 10^6$ cells per well in 100 μL of media.
2. Stimulate cells with desired stimulus and length of time at 37°C .
3. Set aside controls: (1) single-color controls for all colors used (both positive and negative), (2) controls for phospho-proteins (i.e., stimulated vs nonstimulated), (3) unlabeled control for autofluorescence, and (4) intracellular isotype controls for background staining.
4. Harvest the cells by adding 100 μL of phospho wash buffer. Centrifuge (500g, 4°C , 5 min), flick plate, immediately resuspend in ice-cold extracellular staining buffer (50 μL for $1\text{--}2 \times 10^6$ cell), and place at 4°C .

3.4.2. Surface Staining

1. Incubate samples with surface stain cocktail (50 μL in extracellular staining buffer) for 15 min on ice in the dark.
2. Add 150 μL of phospho wash buffer and centrifuge (500g, 4°C). Wash once with 200 μL of phospho wash buffer. Pellet the cells.

3.4.3. Fixation and Permeabilization

1. Fix cells with 100 μL of fixation buffer on ice for 30 min, in the dark. The final concentration should be between 1% and 2% if using a stock solution.
2. Add 100 μL of phospho wash buffer and pellet the cells. Wash once with 200 μL of phospho wash buffer. Pellet the cells.
3. Permeabilize with 200 μL of permeabilization buffer, and pipet up and down four or five times. Incubate for 15 min at 4°C in the dark.
4. Add 100 μL of phospho wash buffer, centrifuge the cells, and flick the plate.

3.4.4. Intracellular Staining

1. Resuspend in 50 μL of intracellular stain cocktail (made up in permeabilization buffer), at least 30 min, on ice, in the dark (usually sufficient). Incubating for a longer period (1 h) at room temperature can increase some staining. Add 150 μL of permeabilization buffer and centrifuge.
2. Wash one or two times in 200 μL of permeabilization buffer (two washes are usually sufficient, but more washes may decrease background).
3. Resuspend in PBS-EDTA (100–200 μL) and transfer to a FACS tube.
4. Analyze by flow cytometry.

3.5. Summary

We describe here several protocols to assess signaling in cells by intracellular staining of phospho-epitopes (*see Note 13* for specificity testing). The considerations for staining will inherently vary in the application desired (*see Note 14* for adherent cell considerations). Still, the ability to differentiate signaling responses

biochemically in lymphocyte subsets by multiparameter assessment will be a powerful and exciting opportunity to investigate samples in which conventional biochemical techniques are not suitable. This methodology is readily applicable to clinical samples or cells from diseased blood to monitor signaling changes on disease onset and hopefully allow correlations of intracellular signaling events with clinical parameters as a diagnostic indicator of disease progression. The development of analytical software capable of processing multivariate data to obtain both statistical and relevant information from flow cytometric data will greatly aid this effort. For example, in **Fig. 6**, FACS-based cluster analysis can identify populations of interest from multiparameter experiments, without prior subjectivity of gating, and is a step toward automation of data analysis. Furthermore, the assessment of multiple targets simultaneously offers advantages in both biochemical assessment of signaling networks and the potential for high-throughput FACS-based screens for specific modulatory agents.

4. Notes

1. Considerations for using cell lines. It is well understood that cell lines do not always functionally represent primary cells and that differences exist between mouse and human systems. It is also understood that model systems are dependent on the experimental conditions. For most cell lines adapted to culture, we have found it is often necessary to serum starve the cells for a period prior to subsequent stimulus and phospho-detection. This time period is variable as 6–12 h is typically required for most cells, and prolonged periods can result in stress-induced phosphorylation events. These conditions need to be determined prior to flow cytometric detection as serum starvation may not be suitable for all applications. Cell density and contamination (bacteria, yeast, and antibiotic salvaged cultures) will affect the signaling responses of the cells. For suspension cells, we recommend a cell density of $1\text{--}5 \times 10^5$ cells/mL. Too high of a cell density can change the signaling properties of most cells (in particular Jurkat [13]). Frozen cells have compromised signaling and should be allowed time to recover from freezing.
2. Paraformaldehyde preparation. Paraformaldehyde is toxic and volatile. Avoid breathing either fumes from dissolved paraformaldehyde or powder. Use a fume hood as necessary. Mix a required amount of paraformaldehyde (e.g., 4% is 4 g/100 mL [w/v]) to two thirds final volume in distilled water. Heat to 60°C while stirring in a fume hood (monitor temperature with thermometer and avoid boiling because it can volatilize and pose a serious hazard for respiratory and mucus membranes and is therefore especially hazardous for contact lens wearers). Add 50–100 μ L of 2 N NaOH to clear the solution required for appropriate solubilization. Remove the flask from the heat and add one-third volume of 3X PBS. Let cool and adjust to pH 7.2 with HCl. Filter and store at room temperature.
3. Blocking agents: Staining media contains fetal calf serum as a blocking agent. FCS is generally a good blocking agent for most specificities. However, detection

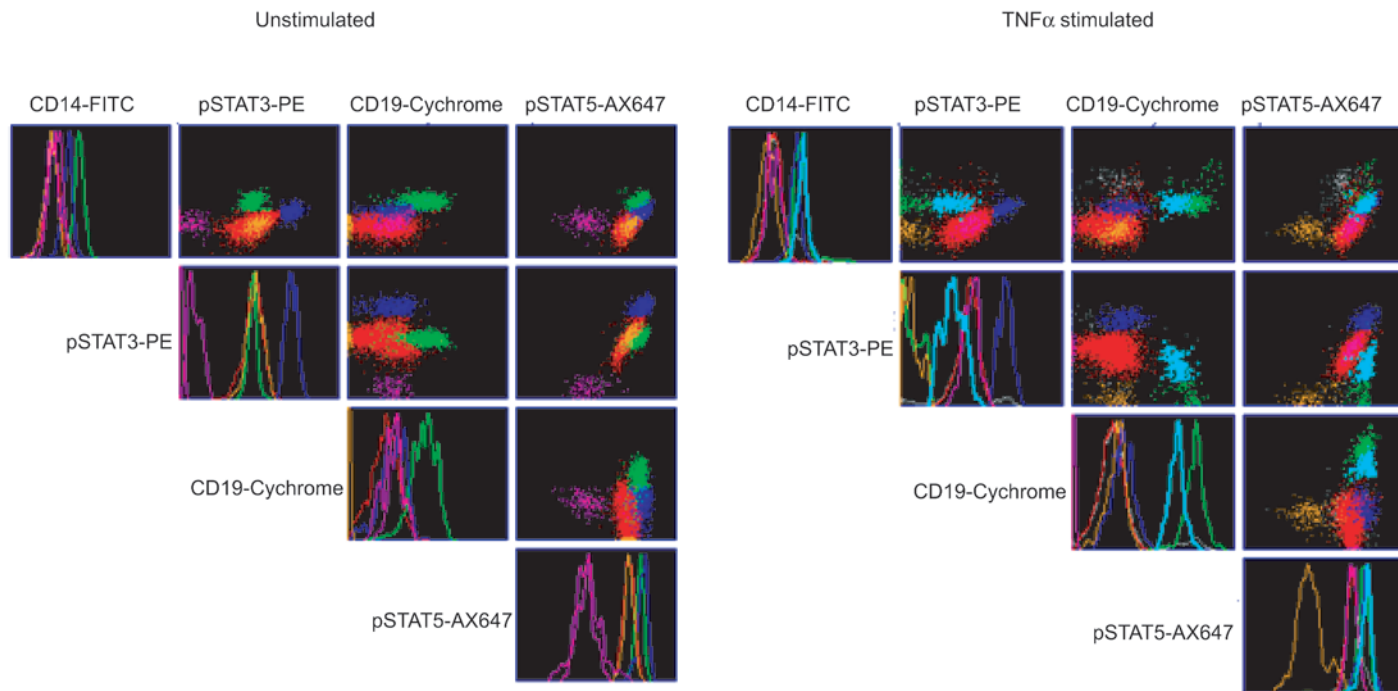


Fig. 6. Multivariate analysis of complex populations. 1×10^6 PBMCs (nondepleted) were left untreated or treated with indicated TNF- α (200 ng/mL, 15 min) and stained for CD14-FITC (clone M ϕ P9), CD19-cychrome (clone HIB19), phospho-STAT3(Y705)-PE (clone 4), and phospho-STAT5(Y694)-AX647 (clone 47) (as described in **Subheading 3.4.**). Multivariate analysis was performed using clustering algorithms developed by Dr. Mario Roederer in FlowJo 4.2 (Tree Star, San Carlos, CA).

of some specificities may be enhanced by using bovine serum albumin instead as it is typically used in phospho-Western blotting. Milk is not recommended, as it contains phospho-proteins that can result in higher background.

4. Saponin composition. Saponin is a glycoside derived from plants such as the Quillaja bark or produced synthetically. Saponins are natural surfactants and comprise of several different, but related molecules, triterpenoid structures that consist of aglycone (saponigen) structure with glycosyl moieties. The purity and chemical composition of commercially sold preparations will vary. We have observed that the final concentrations of the saponin content based buffers (w/v) are best using saponin containing $\geq 25\%$ saponigen content. The saponin buffer is yellow in color, and is to be stored sterile at 4°C .
5. Considerations for saponin-based permeabilization: Saponin concentrations for efficient permeabilization range from 0.1% to 0.5%. Too high concentrations of saponin start to destroy membranes and result in compromised stains. Final saponin concentration for permeabilization should be no less than 0.1% per sample. Often a 0.2% solution is made to account for residual volume in wells left after wash. The final staining concentration range is 0.1–0.5%. Saponin permeabilizes membranes by solvating sterol molecules (i.e., cholesterol molecules). The permeabilization is reversible, and therefore antibody cocktails need to be made in the saponin based buffers for entry into the cell. Saponin permeabilization is sufficient for various nuclear, mitochondrial, endoplasmic reticulum, and granule located proteins as we have confirmed staining patterns by confocal microscopy. Saponin permeabilization may not be suited for all phospho-epitopes. This is believed to be due to the inaccessibility of some epitopes in protein–protein interactions. For these reasons, comparing the same induction conditions using the methanol procedures may be necessary. Alternatively, Triton X-100 at 0.5% can be used to permeabilize cells (5 min, then washed out prior to antibody cocktail stains) as a way to permeabilize cells and retain surface antigen integrity. Also, Cytofix/cytoperm buffer from BD Biosciences Pharmingen (San Diego, CA) works well in this protocol, provided that the subsequent staining step is done in the permeabilization buffer (using plain staining media was not as effective). The combination fixation/permeabilization buffers greatly benefited from a second permeabilization step.
6. FC receptor blocking. When staining in PBMCs, often FC receptor bearing cells bind some antibody isotopes and therefore one must add blocking agents such as nonspecific mouse IgG or corresponding to the isotype recognized by the FC. This is of particular importance if using secondary staining techniques, where directly conjugated Fab fragments might be considered.
7. Efficient permeabilization using methanol: Adding the entire 1 mL of methanol rapidly to the cells prior to their resuspension by vortex-mixing can result in (1) inefficient permeabilization in some cell types and/or (2) cells sticking to the plastic and resultant cell loss.
8. Storage of fixed and permeabilized samples. Cells can be stored at -20°C in methanol or be processed directly afterwards. Samples in our hands have been stored for a short term (several days to 2–3 wk). We are currently evaluating longer term storage conditions.

9. Antibody titrations: Appropriate titration of antibodies is critical for optimal detection of phospho-epitopes, in addition to cost savings in antibody usage. We typically titer all our surface and intracellular antibodies to a standard of 1×10^6 cells. For intracellular phospho-stains, we use defined stimulation conditions and obtain the concentrations that allow for the maximum differential to be detected using the background of isotype controls or unstimulated controls as a measure against non-specific staining events. We also used a fixed number of cells to titer stimulations to obtain fixed concentrations of stimulating agent (i.e., cytokines). Cell density affects both the efficiency of antibody detection, stimulation conditions, as well as reproducibility in these protocols. Note that direct comparison of methanol and saponin methods present differences in the induction levels detected and the titration of the intracellular antibodies required. Often, titers of intracellular antibodies for saponin methods are higher than those for methanol permeabilization. Typically, we observe that intracellular phospho-antibodies stain at approx $0.25\text{--}1 \mu\text{g}/1 \times 10^6$ cells for saponin-based protocols, and $0.05\text{--}0.25 \mu\text{g}/1 \times 10^6$ cells for methanol protocols.
10. Considerations for one-step staining protocols: This also requires a thorough washing of the cells, as some surface antibodies may react nonspecifically with intracellular epitopes, as well as detect intracellular agents that are contained in vesicles waiting to be surface expressed on stimulation.
11. Inhibition of intracellular phosphatase activity. Phosphatase inhibitors were critical for the two-step saponin-based procedure as was ice-chilled buffers and refrigerated centrifuge spins. The fixing/permeabilization techniques did not completely abolish all phosphatases activity, and for these reasons using the phosphatase inhibitors, and keeping all samples on ice or at 4°C , is essential. The phosphatase inhibitors we have chosen were selected on the basis that they inhibit the majority of known or abundant phosphatases. There are essentially four classes of phosphatases: alkaline phosphatases, acid phosphatases, protein tyrosine phosphatases, and serine/threonine phosphatases (these categorizations are not exhaustive). Depending on the kinase being detected it is advisable to choose the phosphatase cocktail best suited for the application. Combine them if detecting different kinds of phosphorylation and take into consideration any special properties of a kinase of choice (i.e., kinetics of activation, rate of dephosphorylation, etc). We also added protease inhibitors to our buffers, 1 mM azide if the buffer is to be stored for some time (2–4 wk). EDTA is not recommended in the subsequent buffers, as divalent ions are needed for some antibody detection (and other agents such as annexin V). Buffers are stored at 4°C and are stable for 1 wk. Protease cocktail tablets, commercially available from Roche Applied Science (formerly Boehringer-Mannheim), were added to buffers on a per usage basis.

Protocols described in **Subheadings 3.3.** and **3.4.** utilize phosphatase inhibitors to aid in the detection. β -Glycerol phosphate, sodium orthovanadate, and microcystin constitute the minimum combination of phosphatases inhibitors needed to inhibit the majority of tyrosine and serine/threonine phosphatases. There are other reagents that inhibit phosphatases that may be considered for enhanced detection

(i.e., calyculin A, okadaic acid, sodium fluoride). These inhibitors are not as necessary with the methanol permeabilization, as methanol permeabilization abrogates the majority of phosphatase and enzymatic activity.

12. Live/dead cell discrimination. When performing intracellular stains, it is important to distinguish between live and dead cells by methods other than forward and side scatter gating, as these parameters can and do change on the fixation/permeabilization conditions (*see Fig. 4*). Dead cells often bind a large number of antibodies nonspecifically. Cell viability is routinely performed by membrane exclusion dyes such as propidium iodide (PI). When cells' membranes are compromised, they stain with PI and are so labeled "dead." PI is often read in the 670-nm channel of a 488-nm laser excitation. PI is useful as a live/dead discriminator when one is only undertaking surface staining alone, but is not adequate for intracellular staining where the permeabilization conditions will inadvertently label all cells as dead. For this reason, it is critical to use the compound such as ethidium monoazide (EMA). EMA is an ethidium bromide analog that is excluded by intact cellular membranes, but can enter dead cells and, in the presence of light, forms a covalent adduct with DNA. Therefore, cells in which the membranes have been compromised prior to permeabilization or fixation are permanently labeled as "dead" with EMA. Subsequent permeabilization does not affect this compound, making it a superior discriminator of live/dead cells when intracellular staining is performed. It is absolutely critical when working with cell populations that comprise <1–5% of the total cell population (i.e., lymphocyte subsets within PBMCs) as dead cells bind antibodies nonspecifically (*14*). EMA is equivalent in fluorescence to PI and is commercially available through Molecular Probes (Eugene, OR). If using EMA, the final concentration is 5 $\mu\text{g/mL}$ (make as stock of 5 mg/mL , 1000X). Typically 10 μL of stock diluted with 490 μL of media, then use 5 μL per 100 μL of final stain volume; minimize exposure to light until this step. EMA is either added in the first wash or with surface antibody cocktail. Cells are stained and maintained in the dark. After surface stains are washed, the tubes are pulsed with light (or held up a fluorescence light bulb for 30 s), then the rest of the staining procedure can be carried out as outlined.
13. Testing for phospho-specificity in the absence of specific pharmacological agents. It is necessary to confirm that the increased staining for phospho-epitopes observed is due to the biochemical reality of the cognate phosphorylation event. Pharmacological agents that will inhibit the phosphorylation of the protein of interest are not always available to allow such verification. In such examples, it is often necessary to use one of four alternatives: (1) out-compete phospho-antibody with phospho-peptide, (2) out-compete phospho-antibody binding with phenylphosphate solution, (3) test for phospho-specificity on phosphatase treatment of cellular samples after an activation condition has been established, or (4) obtain or generate kinase deficient, site-directed mutagenized kinase expressing cells (i.e., tyrosine sites mutagenized to phenylalanine), or knockout cells to test detection of phospho-

specificity First, conditions need to be established that will render phosphorylation of the protein of interest above unstimulated controls, and verified by traditional immunoblot analysis. Second, these same conditions must be tested on a flow platform, and be above the background of the unstimulated cells. Post activation, a sample of cells can be fixed, permeabilized, and treated with (1) 1 μ g of phospho-peptide, (2) resuspended in 10 mM phenylphosphate solution, or (3) phosphatases, such as λ phosphatase (1–5 U, 30 min, 37°C) in the same intracellular staining conditions established. Subsequent washing and intracellular staining with the phospho-specific antibody should be significantly decreased compared to activated and stained cells. Titration experiments can readily be applied with both the phenyl phosphate and phospho-peptide. Alternatively, incubating permeabilized cellular samples with phospho-tyrosine, phospho-serine, and phospho-threonine solutions (both free chemicals and conjugated to bovine serum albumin) can be used to raise the background to ensure titrations are appropriate as these treatments would increase the overall background. We are currently determining if other approaches, such as RNA interference (RNAi), can be more broadly applied to verify target staining observed is real and not artifactual.

14. Adherent cells and tissue samples: We have optimized the protocols for suspension cells, although have had success with adherent fibroblast such as NIH3T3 for intracellular phospho-staining. We have utilized two approaches for adherent cells, and at present have not extensively compared the methods directly. Adherent cells can be removed from the plate using a PBS–EDTA solution, and not trypsinized or scraped off (to do so may destroy cell integrity). For NIH3T3 cells, cell-permeable phosphatase inhibitors in the PBS–EDTA buffer greatly enhanced phospho-detection. We note that washing and centrifugation steps can affect signaling systems within cells and should be determined on an experimental basis if considered a concern. Adherent cells can also be fixed first and then “gently” scraped off into FACS tubes for permeabilization; however, a significant proportion of the cells will be fixed onto the plastic or can be destroyed in the scraping. This is a concern because most activated cells, the cells of interest, are the ones that adhere more strongly.

The potential to analyze phospho-signatures from tissues and biopsy sections is a promising application of this methodology. We have not optimized these protocols for cell samples taken from tissues because considerable cell manipulation is required to extract single-cell suspensions. Although tissues taken from mice have been demonstrated to be amenable to these procedures (15–17), we hope that in the future we will adapt these techniques to be able to profile phospho-signatures of cells derived from human tissue sections or tumor masses.

Acknowledgments

We acknowledge support and helpful discussion from BD Biosciences Pharmingen and the resources of the Stanford FACS facility. We are indebted to Leonard and Leonore Herzenberg for their consistent support in pursuit of

these endeavors. We thank the members of the Nolan laboratory for many helpful discussions, including Jonathan Irish, Matt Hale, and Peter Krutzik. O. D. P. was supported as a Bristol-Meyer Squibb—Irvington-Institute Fellow and the National Heart, Lung, and Blood Institute contract N01-HV-28183I. G. P. N. was supported by NIH grants P01-AI39646, AR44565, AI35304, N01-AR-6-2227, A1/GF41520-01, NHLBI contract N01-HV-28183, and the Juvenile Diabetes Foundation.

References

1. Perez, O. D. and Nolan, G. P. (2002) Simultaneous measurement of multiple active kinase states using polychromatic flow cytometry. *Nat. Biotechnol.* **20**, 155–162.
2. Chow, S., Patel, H., and Hedley, D. W. (2001) Measurement of MAP kinase activation by flow cytometry using phospho-specific antibodies to MEK and ERK: potential for pharmacodynamic monitoring of signal transduction inhibitors. *Cytometry* **46**, 72–78.
3. Perez, O. D., Kinoshita, S., Hitoshi, Y., et al. (2002) Activation of the PKB/AKT pathway by ICAM-2. *Immunity* **16**, 51–65.
4. Roederer, M., De Rosa, S., Gerstein, R., et al. (1997) 8 color, 10-parameter flow cytometry to elucidate complex leukocyte heterogeneity. *Cytometry* **29**, 328–339.
5. Baumgarth, N. and Roederer, M. (2000) A practical approach to multicolor flow cytometry for immunophenotyping. *J. Immunol. Methods* **243**, 77–97.
6. De Rosa, S. C., Herzenberg, L. A., and Roederer, M. (2001) 11-color, 13-parameter flow cytometry: identification of human naive T cells by phenotype, function, and T-cell receptor diversity. *Nat. Med.* **7**, 245–248.
7. Shan, X., Czar, M. J., Bunnell, S. C., et al. (2000) Deficiency of PTEN in Jurkat T cells causes constitutive localization of Itk to the plasma membrane and hyper-responsiveness to CD3 stimulation. *Mol. Cell Biol.* **20**, 6945–6957.
8. Freeburn, R. W., Wright, K. L., Burgess, S. J., Astoul, E., Cantrell, D. A., and Ward, S. G. (2002) Evidence that SHIP-1 contributes to phosphatidylinositol 3,4,5-trisphosphate metabolism in T lymphocytes and can regulate novel phosphoinositide 3-kinase effectors. *J. Immunol.* **169**, 5441–5450.
9. Perez, O. D., Mitchell, D., Jager, G. C., et al. (2003) Leukocyte functional antigen 1 lowers T cell activation thresholds and signaling through cytohesin-1 and Jun-activating binding protein 1. *Nat. Immunol.* **4**, 1083–1092.
10. Roederer, M. (2001) Spectral compensation for flow cytometry: visualization artifacts, limitations, and caveats. *Cytometry* **45**, 194–205.
11. Rudge, E. U., Cutler, A. J., Pritchard, N. R., and Smith, K. G. (2002) Interleukin 4 reduces expression of inhibitory receptors on B cells and abolishes CD22 and Fc gamma RII-mediated B cell suppression. *J. Exp. Med.* **195**, 1079–1085.
12. Morris, S. C., Dragula, N. L., and Finkelman, F. D. (2002) IL-4 promotes Stat6-dependent survival of autoreactive B cells in vivo without inducing autoantibody production. *J. Immunol.* **169**, 1696–1704.

13. Fiering, S., Northrop, J. P., Nolan, G. P., Mattila, P. S., Crabtree, G. R., and Herzenberg, L. A. (1990) Single cell assay of a transcription factor reveals a threshold in transcription activated by signals emanating from the T-cell antigen receptor. *Genes Dev.* **4**, 1823–1834.
14. Herzenberg, L. A., Parks, D., Sahaf, B., Perez, O., and Roederer, M. (2002) The history and future of the fluorescence activated cell sorter and flow cytometry: a view from Stanford. *Clin. Chem.* **48**, 1819–1827.
15. Zell, T., Khoruts, A., Ingulli, E., Bonnevier, J. L., Mueller, D. L., and Jenkins, M. K. (2001) Single-cell analysis of signal transduction in CD4 T cells stimulated by antigen in vivo. *Proc. Natl. Acad. Sci. USA* **98**, 10,805–10,810.
16. Zell, T. and Jenkins, M. K. (2002) Flow cytometric analysis of T cell receptor signal transduction. *Science's STKE*, <http://stke.sciencemag.org/cgi/content/full/OCsigtrans;2002/128/p15>.
17. Kaech, S. M., Hemby, S., Kersh, E., and Ahmed, R. (2002) Molecular and functional profiling of memory CD8 T cell differentiation. *Cell* **111**, 837–851.

5

Cytokine Flow Cytometry

Holden T. Maecker

Summary

Cytokine flow cytometry (CFC) is a general term that applies to flow cytometric analysis of cells using anticytokine antibodies as markers of activation. The most common version of this technique is the intracellular staining of cytokines in cells that have been fixed and permeabilized after short-term in vitro activation. When used with specific antigens, this technique allows for the quantitation of rare populations of antigen-specific T cells. In this chapter, specific methodology for such intracellular staining is elaborated, with emphasis on the effects of variables such as sample type, antigens, activation conditions, sample processing, and data acquisition and analysis.

Key Words

Antigen-specific, cytokines, flow cytometry, intracellular, T cells.

1. Introduction

1.1. Historical Background

Permeabilization of cells to stain for intracellular antigens has a relatively long history in flow cytometry, but the use of intracellular staining for secreted molecules such as cytokines is more recent. Jung et al. (1) and Prussin and Metcalfe (2) demonstrated that cytokines could be detected in activated cells with the aid of secretion inhibitors such as monensin or brefeldin A (3). These drugs prevent the export of newly synthesized proteins by disrupting transport between the endoplasmic reticulum and the Golgi apparatus (4). Intracellular cytokine staining was later refined to detect rare populations of antigen-specific T cells in peripheral blood mononuclear cells (PBMCs) (5) as well as whole blood (6). The technique has since been applied in murine, human, and other systems, using a wide variety of viral, bacterial, autoimmune, and tumor-associated antigens, as well as mitogens (reviewed in refs. 7 and 8).

From: *Methods in Molecular Biology: Flow Cytometry Protocols*, 2nd ed.
Edited by: T. S. Hawley and R. G. Hawley © Humana Press Inc., Totowa, NJ

Alternative methods of cytokine flow cytometry (CFC) that do not require cell permeabilization have also been developed. One of these methods relies on highly sensitive staining techniques to detect low levels of certain cytokines that are present on the cell surface, including interferon- γ (IFN- γ) and interleukin-10 (IL-10) (9). Another method uses a cell-surface antibody matrix to coat cells, allowing them to capture secreted cytokine on their surface for fluorescent staining (10). These techniques allow live cytokine-producing cells to be sorted and thus subjected to further analyses. However, the methods involved in these applications are sufficiently unique that they are not covered in this chapter.

1.2. Overview of Method and Applications

The basic CFC methodology involves short-term in vitro activation (often 6 h) with protein or peptide antigens or mitogens, in the presence of a secretion inhibitor such as brefeldin A. For peptides or mitogens, which do not require processing by host antigen-presenting cells, the secretion inhibitor can be present during the entire incubation period without detriment (11). For protein antigens, an initial period (often 2 h) of incubation is performed with antigen alone, to allow for antigen presentation, which could otherwise be compromised by the presence of brefeldin A or monensin (5,6). The entire incubation period is deliberately short in order to capture accurately the frequency of responsive cells in the blood or PBMC sample, prior to cell division or apoptosis, which would compromise the quantitative nature of the result.

After stimulation, cells are generally treated with EDTA to arrest activation and to remove adherent cells, then fixed (usually with a formaldehyde-based buffer), permeabilized (usually with a detergent-based buffer), and stained with fluorescent-labeled antibodies. For multiparameter staining of cell-surface and intracellular determinants, a surface staining step is often added prior to cell fixation. However, some antibodies to cell-surface determinants do recognize fixed and permeabilized epitopes. With these systems, all of the staining is done after fixation and permeabilization.

Finally, data are acquired by flow cytometry, and files are analyzed by gating on the cell population of interest (e.g., CD3⁺CD8⁺ lymphocytes). Often, CD69, an early activation marker, is used in combination with anticytokine antibody to identify more definitively activated cytokine-producing cells (5,6,11–33). When analyzing antigen-specific responses, the frequency of positive cells can be low ($\leq 0.1\%$ of CD4⁺ or CD8⁺ T cells), such that collecting sufficient cells per sample and proper gating techniques become critical to success (34).

The protocol presented here is based on the use of 96-well plates for stimulation, processing, and acquisition of samples (*see also* ref. 35). This improves the assay throughput considerably over tube-based methods, which

have also been recently reviewed (34). The use of a single plate throughout the entire assay also avoids cell transfers that can be time consuming and contribute to loss of cells.

Many variations in reagents for CFC processing and staining are in use by different laboratories. For simplicity, a protocol based on commercially available kits is reported here.

2. Materials

2.1. Reagents

Note: Reagents 4–9 are available in commercial kits (FastImmune,TM BD Biosciences, San Jose, CA).

1. Heparinized whole blood or PBMCs.
2. For PBMC assays: RPMI-1640 medium, 20 mM *N*- α -hydroxyethylpiperazine-*N'*-(α -ethanesulfonic acid) (HEPES), 10% fetal bovine serum, and antibiotic/antimycotic solution (cRPMI-10, all components from Sigma Chemical Co., St. Louis, MO).
3. Activation antigens (*see Table 1*).
4. (Optional) Costimulatory antibodies: CD28 and CD49d, 0.1 mg/mL of each in sterile phosphate-buffered saline (PBS).
5. Brefeldin A: Make up a stock solution of 5 mg/mL in dimethyl sulfoxide (DMSO).
6. 20 mM EDTA in PBS, pH 7.4.
7. Erythrocyte lysis and cell fixation buffer (e.g., BD FACS Lysing SolutionTM).
8. Cell permeabilization reagent (e.g., BD FACS Permeabilizing Solution 2TM).
9. Fluorescence-labeled antibodies (e.g., anti-IFN- γ fluorescein isothiocyanate [FITC]/CD69 PE/CD8 PerCP-Cy5.5/CD3 APC).
10. Wash buffer: PBS, 0.5% bovine serum albumin, and 0.1% NaN₃.
11. Fixation buffer: 1% Paraformaldehyde in PBS. Dilute 10% paraformaldehyde (EM Science, Gibbstown, NJ) 1:10 with PBS.

2.2. Equipment

1. 96-Well conical bottom deep-well polypropylene plates and lids (BD Discovery Labware, Bedford, MA) (for whole blood).
2. 96-Well round-bottom standard polystyrene tissue culture plates with lids (for PBMCs).
3. 12-Channel aspiration manifold (35 mm for whole blood, 7 mm for PBMCs) (V&P Scientific, San Diego, CA).
4. Plate holders, deep-well plate compatible, for tabletop centrifuge (e.g., Sorvall Instruments, Newtown, CT).
5. Flow cytometer with at least four fluorescence channels.
6. (Optional) 96-Well plate loader for cytometer.

Table 1
Activation Antigens

Activation agent	Suggested source	Stock solution	Use in assay
Staphylococcal enterotoxin B (SEB)	Sigma cat. no. S-4881	Add 2 mL of sterile PBS directly to a 1-mg vial of SEB. Cap and shake to dissolve. Dilute to 20 mL with PBS (50 µg/mL). Store at 4°C.	Use 4 µL of stock solution per 200 µL blood or PBMCs (final concentration 1 µg/mL).
CMV lysate	Advanced Biotechnologies cat. no. 10-144-000	Dilute a 1-mg vial to 20 mL with sterile PBS (50 µg/mL); freeze in small aliquots at -80°C.	Use 4 µL of stock solution per 200 µL blood or PBMCs (final concentration 1 µg/mL).
CMV pp65 protein	Austral Biotechnologies cat. no. CMA-1420-4	Dilute 50 µg vial with 2 mL of sterile PBS (25 µg/mL); freeze in small aliquots at -80°C.	Use 4 µL of stock solution per 200 µL blood or PBMCs (final concentration 0.5 µg/mL).
CMV pp65 peptide mix	BD Biosciences cat no. 551969	Provided as 0.7 mg/mL/peptide in DMSO; store at -80°C.	Dilute 1:10 with sterile PBS, use 5 µL per 200 µL blood or PBMCs (final concentration 1.7 µg/mL/peptide).
HIV p55 gag peptide mix	BD Biosciences cat. no. 551940	Provided as 0.7 mg/mL/peptide in DMSO; store at -80°C.	Dilute 1:10 with sterile PBS, use 5 µL per 200 µL blood or PBMCs (final concentration 1.7 µg/mL/peptide).
Single peptides	Custom peptide synthesis, various vendors	Dissolve at 5 mg/mL in DMSO; store in small aliquots at -80°C.	Dilute 1:10 with sterile PBS, use 4 µL per 200 µL blood or PBMCs (final concentration 10 µg/mL).

3. Methods

3.1. Sample Collection

1. Samples for assays.
 - a. For whole blood assays: Collect whole blood in sodium heparin and store at room temperature for not more than 8 h prior to use (*see Note 1*).
 - b. For fresh PBMC assays: Prepare PBMCs from whole blood by Ficoll gradient separation or other commercially available method (e.g., CPT™ tubes, BD Vacutainer, Franklin Lakes, NJ). Resuspend PBMCs at 2.5×10^6 to 1×10^7 viable lymphocytes/mL (*see Notes 2 and 3*).
 - c. For cryopreserved PBMC assays: Thaw PBMCs briefly in a 37°C water bath, then slowly dilute up to 10 mL with warm cRPMI-10 medium and centrifuge for approx 7 min at 250g. Resuspend in a small volume of warm cRPMI-10, perform a viable cell count using Trypan blue, and dilute to a final concentration of 2.5×10^6 to 1×10^7 viable lymphocytes/mL (*see Note 4*).
2. Add 200 μ L of whole blood or PBMCs per well to a 96-well plate. For whole blood and fresh PBMC assays, proceed directly to **Subheading 3.2**. For cryopreserved PBMC assays, incubate at 37°C overnight (12–18 h) prior to stimulation (*see Note 5*).

3.2. Activation of Cells

1. Thaw aliquots of peptides or other antigens and brefeldin A. Using PBS, make 1:10 dilutions of peptide stocks (**Table 1**) and of 5 mg/mL of brefeldin A stock.
2. Prepare a “master mix” of stimulation reagents for each activation antigen used (*see Table 2 and Note 6*). Always prepare a slight excess of each master mix (e.g., if 18 wells are to be stimulated, prepare enough master mix for 20 wells).
3. Pipet 20 μ L of the appropriate master mix into each well containing cells plated as described in **Subheading 3.1**. Mix by gentle pipetting.
4. Incubate covered plate for 6 h at 37°C (*see Notes 7 and 8*).

3.3. Sample Processing

3.3.1. Whole Blood (Deep Well Plates) (*see Note 9*)

1. After activation, add 20 μ L of 20 mM EDTA in PBS to each well, mixing by pipetting.
2. Incubate 15 min at room temperature, then mix again by vigorous pipetting.
3. Add 1.5 mL of room temperature 1X BD FACS Lysing Solution to each well. Incubate at room temperature for 10 min (*see Note 10*).
4. Centrifuge plate at 500g for 5 min (*see Note 11*). Aspirate the supernatant with a 35-mm vacuum manifold, and resuspend the pellet by pipetting up and down in the residual volume (*see Note 12*).
5. Add 1 mL of room temperature 1X BD FACS Permeabilizing Solution 2 per well. Incubate at room temperature for 10 min (*see Note 10*).
6. Add 0.5 mL of wash buffer to each well, and centrifuge the plate at 500g for 5 min. Aspirate the supernatant with a 35-mm vacuum manifold.

Table 2
Stimulus “Master Mix” Preparation

Amount to use per stimulated well:					
Condition	Antigen	Costimulatory antibodies CD28 + CD49d (optional)	Brefeldin A	PBS	Total
No stimulus	4–5 μ L of PBS or PBS + 10% DMSO, depending on buffer used for antigen(s)	2 μ L of 0.1 mg/mL stock	4 μ L of 0.5 mg/mL	9–12 μ L depending on antigen and use of costimulatory antibodies	20 μ L
Antigen or SEB	4–5 μ L of working stock (<i>see Table 1</i>)	2 μ L of 0.1 mg/mL stock	4 μ L of 0.5 mg/mL	9–12 μ L depending on antigen and use of costimulatory antibodies	20 μ L

7. Add 1.5 mL of wash buffer to each well, centrifuge, and aspirate the supernatant as above.
8. Resuspend the pellet with the appropriate titer of staining antibody mixture (e.g., anti-IFN- γ FITC/CD69 PE/CD8 PerCP-Cy5.5/CD3 APC) (*see Note 13*). Incubate in the dark at room temperature for 60 min, mixing by pipetting every 15–20 min.
9. Add 1.5 mL of wash buffer to each well, and centrifuge plate at 500g for 5 min. Aspirate supernatant with a 35-mm vacuum manifold.
10. Resuspend pellets with 150 μ L of 1% paraformaldehyde in PBS. Store at 4°C in the dark until ready for data acquisition, which should be performed within 24 h.

3.3.2. PBMC (Standard Plates) (*see Note 9*)

1. Add 20 μ L of 20 mM EDTA in PBS to each well, mixing by pipetting.
2. Incubate 15 min at room temperature, then mix again by vigorous pipetting.
3. Centrifuge the plate at 250g for 5 min. Aspirate supernatant with a 7-mm vacuum manifold.
4. Resuspend pellets with 100 μ L of 1X BD FACS Lysing Solution per well. Incubate at room temperature for 10 min (*see Note 10*).
5. Add 100 μ L of wash buffer to each well, then centrifuge plate at 500g for 5 min (*see Note 11*). Aspirate supernatant with a 7-mm vacuum manifold (*see Note 12*).
6. Resuspend pellets with 200 μ L of 1X BD FACS Permeabilizing Solution 2 per well. Incubate at room temperature for 10 min (*see Note 10*).
7. Centrifuge plate at 500g for 5 min. Aspirate supernatant with a 7-mm vacuum manifold.

8. Add 200 μ L of wash buffer to each well, and centrifuge the plate at 500g for 5 min. Aspirate supernatant with a 7-mm vacuum manifold.
9. Again add 200 μ L of wash buffer to each well, centrifuge, and aspirate supernatant as in **step 8** (multiple washes are necessary to remove permeabilizing solution effectively prior to antibody addition).
10. Resuspend pellet with appropriate titer of staining antibody mixture (e.g., anti-IFN- γ FITC/CD69 PE/CD8 PerCP-Cy5.5/CD3 APC) (*see Note 13*). Incubate in the dark at room temperature for 60 min, mixing by pipetting every 15–20 min.
11. Add 200 μ L of wash buffer to each well, and centrifuge plate at 500g for 5 min. Aspirate the supernatant with a 7-mm vacuum manifold.
12. Again add 200 μ L of wash buffer to each well, centrifuge, and aspirate supernatant as in **step 11**.
13. Resuspend pellets with 150 μ L of 1% paraformaldehyde in PBS. Store at 4°C in the dark until ready for data acquisition, which should be performed within 24 h.

3.4. Data Acquisition and Analysis (*see Note 14*)

1. Calibrate a flow cytometer either manually or using beads and calibration software:
 - a. For manual calibration: Use a sample stained with an isotype control cocktail to set each photomultiplier tube (PMT) value, and samples stained individually with each fluorochrome to set compensation values.
 - b. For bead-based calibration: Follow supplier recommendations for setup (e.g., select Lyse No Wash settings using BD FACSComp™ software and BD Calibrite™ beads).
2. Set an appropriate threshold on forward scatter to eliminate debris while still retaining the lymphocyte population. If desired, set a secondary threshold on CD3⁺ cells to eliminate non-T cells and thereby reduce file sizes.
3. Set collection criteria so as to collect 40,000 relevant events per file (e.g., CD4⁺ or CD8⁺ T cells) (*see Note 15*). When running from an automated plate loader, set the secondary collection criteria on time, so that samples are not run dry. For example, set a maximum time of 180 s for 200- μ L samples run on “high” on a BD FACS Calibur™.
4. Save the acquisition template and instrument settings after running some cells from the current experiment to verify the settings and gates.
5. Enter all appropriate information into the automated plate loader software, if applicable.
6. Acquire data from samples.
7. Analyze data by defining a small lymphocyte region in forward vs side scatter, and a region on the relevant cell population(s) using appropriate gating reagents (e.g., CD3⁺CD8⁺ cells). These regions can be defined by automated gating algorithms (e.g., “Snap-To” gates, CellQuest Pro v5.1, BD Biosciences). Be sure to size these regions appropriately to include cells that may have down-modulated CD3 and CD8 (or CD4) as a result of activation (*see Fig. 1*).
8. Create a dot plot gated on both of the regions defined in **step 7**, displaying cytokine vs CD69 staining.

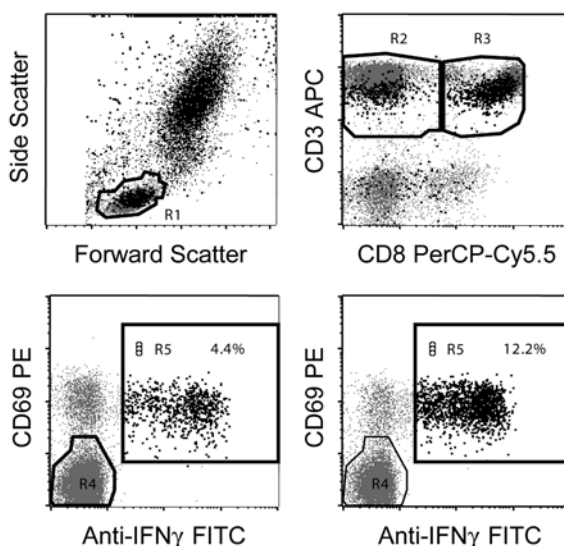


Fig. 1. Automated gating of CFC results. “Snap-To” regions are created for forward vs side scatter (R1, small lymphocytes), and CD8 vs CD3 (R2, CD3⁺CD8⁻ and R3, CD3⁺CD8⁺ cells). R2 and R3 are maximally sized so as to include activated cells (bold dots) that down-modulate CD3 and CD8 expression. Next, dot plots of anti-IFN- γ vs CD69 are displayed, gated either on R1 and R2 (**lower left** plot) or R1 and R3 (**lower right** plot). A snap-to region is created on the double-negative population (R4) and tethered to a static region (R5) that defines the double-positive “response region.” The percent of gated events in R5 is reported.

9. Using a positive control sample (e.g., SEB-stimulated), draw a “response region” that includes all events double-positive for CD69 and cytokine. If using automated gating algorithms, the response region can be a conventional region tethered to the double-negative population (as defined by an automated gate) (*see* **Fig. 1** and **Note 16**).
10. Report the percent positive in the response region for each sample. Subtract the percent positive in an unstimulated (negative control) sample from each of the stimulated samples to obtain the net antigen-specific response.
11. If desired, the percent response can be converted to an absolute number of responsive cells per milliliter of blood by multiplying by the count of CD4 or CD8 cells per milliliter for that donor.

4. Notes

1. Anticoagulant: Whole blood must be collected in sodium heparin to preserve functional responses. Blood collected for PBMC isolation can be collected in any anticoagulant, provided the PBMCs are washed after isolation and resuspended in calcium-containing medium such as cRPMI-10.

2. Shipping fresh samples: Whole blood should ideally be stimulated within 8 h of collection. Stimulation of 24-h shipped blood can result in variable losses depending on the donor and type of stimulus, with peptide antigen stimulation being affected the least (**11**). Performing CFC assays on whole blood that is significantly more than 24 h old is not recommended owing to sample degradation. A convenient way to ship PBMCs is in centrifuged cell preparation tubes (CPTs) (BD Vacutainer, Franklin Lakes, NJ), which provide increased stability compared to shipping of whole blood (**36**).
3. Larger blood volumes: Whole blood CFC assays in diseases such as HIV AIDS can sometimes require larger blood volumes per sample because of lower CD4 T-cell counts. This can be accommodated by use of deep-well 24-well plates (Qiagen, Hilden, Germany). For details, *see* **ref. 35**.
4. Cryopreservation: If PBMCs or whole blood samples cannot be processed within 24 h of blood draw, PBMCs should be cryopreserved by a validated protocol (**35**). Cryopreservation of PBMCs from healthy donors should result in recoveries of >60% and viabilities of >80%. If values significantly less than these are obtained, functional responses might be compromised.
5. Resting of cryopreserved cells: Overnight resting of thawed PBMCs can result in a significant increase in cytokine mean fluorescence intensity (**35**). Some increase in cytokine fluorescence intensity may also be seen with fresh PBMCs after resting overnight; but it is recommended that thawed cells always be rested prior to stimulation.
6. Use of costimulatory antibodies: Antibodies to CD28 and CD49d have been shown to costimulate effectively the activation of antigen-specific CFC responses (**12**). However, in occasional donors, they can contribute to spontaneous cytokine production in the absence of antigen. The effect of costimulation is less dramatic with optimal peptide stimulation (*unpublished data*), and thus may not be warranted with peptide antigens.
7. Length of stimulation: Six-hour stimulation is adequate for induction of IFN- γ , tumor necrosis factor- α (TNF- α), IL-2, and IL-4 (**15**). Incubation for longer periods (in the presence of brefeldin A) may increase the cytokine fluorescence intensity, but will eventually lead to toxicity (>12 h). Incubating with antigen prior to addition of brefeldin A is recommended only for whole protein antigens (which require processing by antigen-presenting cells). An incubation period of 2 h in antigen alone is optimal for CD4 responses to protein antigens (**15**). CD8 responses to whole protein antigens can sometimes be induced with longer incubation in antigen alone, but not in all donors (**19**).
8. Automated activation/stopping point: Activation can be terminated by cooling cells to 18°C prior to processing (end of **Subheading 3.2.**). This process can be automated using a programmable heat block or water bath.
9. Batching of samples: Samples can be frozen at -80°C at the end of **step 4**, **Subheading 3.3.1.** (or **3.3.2.** for PBMC). Because they are fixed, they need not be moved into a special freezing medium, but can be frozen directly in cell fixation buffer (**15,36**). In this fashion, samples can be accumulated for shipping to another

laboratory, or for later batch analysis. Stability of frozen activated samples has been tested for up to 6 mo without loss of signal (unpublished data).

10. Temperature of lysing and permeabilizing solutions: Fixation and permeabilization of cells are temperature dependent. Solutions for these steps should be stored and used at controlled room temperature. If ambient temperatures vary significantly above or below 22–25°C, a temperature-controlled incubation should be done.
11. Centrifugation speed: Fixation and permeabilization cause increased cell buoyancy. All centrifugation steps after fixation should therefore be carried out at 500g to avoid excessive cell loss.
12. Importance of washing: Because of the small wash volumes in 96-well plates, effective washing (without significant cell loss) is essential. Sufficient washing prior to addition of staining antibodies is at least as important as washing after intracellular staining. Use of appropriate-length vacuum manifolds is critical to achieving consistent washing without undue cell loss. Vacuum manifolds should be frequently cleaned with bleach to prevent clogging.
13. Surface vs intracellular staining of surface antigens: The protocols outlined here use a single intracellular staining step for all antibodies, which is possible using the antibodies provided in commercial kits (FastImmune, BD Biosciences). Staining CD3, CD4, and/or CD8 intracellularly reduces the signal-to-noise ratio relative to surface staining (prior to fixation), but decreases the down-modulation of these antigens seen with activation.
14. Automation of acquisition and analysis: In addition to the higher throughput realized by processing samples in 96-well plates, automated acquisition with a plate loader and automated batch analysis using gating algorithms (**Fig. 1**) can greatly reduce sample analysis time. Furthermore, the results compare favorably to results obtained in tubes and using manual gating schemes (**35**).
15. Number of events to collect: Detection of small populations of antigen-specific cells requires collection of a large number of relevant events. This protocol suggests collecting 40,000 CD4 or CD8 T cells, which is sufficient to distinguish a 0.1% response from a background of 0.02% with reasonable statistical significance. A standard power calculation for determining sample size can be used to assess whether the difference between two proportions is statistically significant, based on the number of events collected (**37**).
16. Importance of gating: Improper gating is a frequent source of quantitative variation in results. It is particularly important to include cells with lower levels of CD3, CD4, and/or CD8, as these antigens are down-modulated on activation. Also, “response regions” should be set with reference to positive control samples, to include all relevant cells, as well as with reference to negative control samples, to exclude nonspecifically stained cells.

Acknowledgments

The author thanks Maria Suni and Holli Dunn for providing data and protocol development and Laurel Nomura and Vernon Maino for critical review of the manuscript.

References

1. Jung, T., Schauer, U., Heusser, C., Neumann, C., and Rieger, C. (1993) Detection of intracellular cytokines by flow cytometry. *J. Immunol. Methods* **159**, 197–207.
2. Prussin, C. and Metcalfe, D. D. (1995) Detection of intracytoplasmic cytokine using flow cytometry and directly conjugated anti-cytokine antibodies. *J. Immunol. Methods* **188**, 117–128.
3. Picker, L. J., Singh, M. K., Zdraveski, Z., et al. (1995) Direct demonstration of cytokine synthesis heterogeneity among human memory/effector T cells by flow cytometry. *Blood* **86**, 1408–1419.
4. Nylander, S. and Kalies, I. (1999) Brefeldin A, but not monensin, completely blocks CD69 expression on mouse lymphocytes: efficacy of inhibitors of protein secretion in protocols for intracellular cytokine staining by flow cytometry. *J. Immunol. Methods* **224**, 69–76.
5. Waldrop, S. L., Pitcher, C. J., Peterson, D. M., Maino, V. C., and Picker, L. J. (1997) Determination of antigen-specific memory/effector CD4⁺ T cell frequencies by flow cytometry: evidence for a novel, antigen-specific homeostatic mechanism in HIV-associated immunodeficiency. *J. Clin. Invest.* **99**, 1739–1750.
6. Suni, M. A., Picker, L. J., and Maino, V. C. (1998) Detection of antigen-specific T cell cytokine expression in whole blood by flow cytometry. *J. Immunol. Methods* **212**, 89–98.
7. Maecker, H. T., Maino, V. C., and Picker, L. J. (2000) Immunofluorescence analysis of T-cell responses in health and disease. *J. Clin. Immunol.* **20**, 391–399.
8. Ghanekar, S. A. and Maecker, H. T. (2003) Cytokine flow cytometry: multiparametric approach to immune function analysis. *Cytotherapy* **5**, 1–6.
9. Scheffold, A., Assenmacher, M., Reiners-Schramm, L., Lauster, R., and Radbruch, A. (2000) High-sensitivity immunofluorescence for detection of the pro- and anti-inflammatory cytokines gamma interferon and interleukin-10 on the surface of cytokine-secreting cells. *Nat. Med.* **6**, 107–110.
10. Brosterhus, H., Brings, S., Leyendeckers, H., et al. (1999) Enrichment and detection of live antigen-specific CD4(+) and CD8(+) T cells based on cytokine secretion. *Eur. J. Immunol.* **29**, 4053–4059.
11. Maecker, H. T., Dunn, H. S., Suni, M. A., et al. (2001) Use of overlapping peptide mixtures as antigens for cytokine flow cytometry. *J. Immunol. Methods* **255**, 27–40.
12. Waldrop, S. L., Davis, K. A., Maino, V. C., and Picker, L. J. (1998) Normal human CD4⁺ memory T cells display broad heterogeneity in their activation threshold for cytokine synthesis. *J. Immunol.* **161**, 5284–5295.
13. Pitcher, C. J., Quittner, C., Peterson, D. M., et al. (1999) HIV-1-specific CD4⁺ T cells are detectable in most individuals with active HIV-1 infection, but decline with prolonged viral suppression. *Nat. Med.* **5**, 518–525.
14. Suni, M. A., Ghanekar, S. A., Houck, D. W., et al. (2001) CD4(+)CD8(dim) T lymphocytes exhibit enhanced cytokine expression, proliferation and cytotoxic activity in response to HCMV and HIV-1 antigens. *Eur. J. Immunol.* **31**, 2512–2520.

15. Nomura, L. E., Walker, J. M., and Maecker, H. T. (2000) Optimization of whole blood antigen-specific cytokine assays for CD4(+) T cells. *Cytometry* **40**, 60–68.
16. Ghanekar, S. A., Nomura, L. E., Suni, M. A., Picker, L. J., Maecker, H. T., and Maino, V. C. (2001) Gamma interferon expression in CD8(+) T cells is a marker for circulating cytotoxic T lymphocytes that recognize an HLA A2-restricted epitope of human cytomegalovirus phosphoprotein pp65. *Clin. Diagn. Lab Immunol.* **8**, 628–631.
17. Maino, V. C., Suni, M. A., Wormsley, S. B., Carlo, D. J., Wallace, M. R., and Moss, R. B. (2000) Enhancement of HIV type 1 antigen-specific CD4+ T cell memory in subjects with chronic HIV type 1 infection receiving an HIV type 1 immunogen. *AIDS Res. Hum. Retroviruses* **16**, 539–547.
18. Maecker, H. T., Auffermann-Gretzinger, S., Nomura, L. E., Liso, A., Czerwinski, D. K., and Levy, R. (2001) Detection of CD4 T-cell responses to a tumor vaccine by cytokine flow cytometry. *Clin. Cancer Res.* **7**, 902s–908s.
19. Maecker, H. T., Ghanekar, S. A., Suni, M. A., He, X. S., Picker, L. J., and Maino, V. C. (2001) Factors affecting the efficiency of CD8+ T cell cross-priming with exogenous antigens. *J. Immunol.* **166**, 7268–7275.
20. Asanuma, H., Sharp, M., Maecker, H. T., Maino, V. C., and Arvin, A. M. (2000) Frequencies of memory T cells specific for varicella-zoster virus, herpes simplex virus, and cytomegalovirus by intracellular detection of cytokine expression. *J. Infect. Dis.* **181**, 859–866.
21. Bitmansour, A. D., Douek, D. C., Maino, V. C., and Picker, L. J. (2002) Direct ex vivo analysis of human CD4(+) memory T cell activation requirements at the single clonotype level. *J. Immunol.* **169**, 1207–1218.
22. Bitmansour, A. D., Waldrop, S. L., Pitcher, C. J., et al. (2001) Clonotypic structure of the human CD4(+) memory T cell response to cytomegalovirus. *J. Immunol.* **167**, 1151–1163.
23. Dunn, H. S., Haney, D. J., Ghanekar, S. A., Stepick-Biek, P., Lewis, D. B., and Maecker, H. T. (2002) Dynamics of CD4 and CD8 T cell responses to cytomegalovirus in healthy human donors. *J. Infect. Dis.* **186**, 15–22.
24. He, X. S., Rehmann, B., Lopez-Labrador, F. X., et al. (1999) Quantitative analysis of hepatitis C virus-specific CD8(+) T cells in peripheral blood and liver using peptide-MHC tetramers. *Proc. Natl. Acad. Sci. USA* **96**, 5692–5697.
25. Jacobson, M. A., Schrier, R., McCune, J. M., et al. (2001) Cytomegalovirus (CMV)-specific CD4+ T lymphocyte immune function in long-term survivors of AIDS-related CMV end-organ disease who are receiving potent antiretroviral therapy. *J. Infect. Dis.* **183**, 1399–1404.
26. Karanikas, V., Lodding, J., Maino, V. C., and McKenzie, I. F. (2000) Flow cytometric measurement of intracellular cytokines detects immune responses in MUC1 immunotherapy. *Clin. Cancer Res.* **6**, 829–837.
27. Kern, F., Faulhaber, N., Frommel, C., et al. (2000) Analysis of CD8 T cell reactivity to cytomegalovirus using protein-spanning pools of overlapping pentadecapeptides. *Eur. J. Immunol.* **30**, 1676–1682.

28. Kern, F., Surel, I. P., Brock, C., et al. (1998) T-cell epitope mapping by flow cytometry. *Nat. Med.* **4**, 975–978.
29. Kern, F., Surel, I. P., Faulhaber, N., et al. (1999) Target structures of the CD8(+)-T-cell response to human cytomegalovirus: the 72-kilodalton major immediate-early protein revisited. *J. Virol.* **73**, 8179–8184.
30. Komanduri, K. V., Donahoe, S. M., Moretto, W. J., et al. (2001) Direct measurement of CD4+ and CD8+ T-cell responses to CMV in HIV-1- infected subjects. *Virology* **279**, 459–470.
31. Komanduri, K. V., Feinberg, J., Hutchins, R. K., et al. (2001) Loss of cytomegalovirus-specific CD4+ T cell responses in human immunodeficiency virus type 1-infected patients with high CD4+ T cell counts and recurrent retinitis. *J. Infect. Dis.* **183**, 1285–1289.
32. Komanduri, K. V., Viswanathan, M. N., Wieder, E. D., et al. (1998) Restoration of cytomegalovirus-specific CD4+ T-lymphocyte responses after ganciclovir and highly active antiretroviral therapy in individuals infected with HIV-1. *Nat. Med.* **4**, 953–956.
33. Mosca, P. J., Hobeika, A. C., Clay, T. M., Morse, M. A., and Lyster, H. K. (2001) Direct detection of cellular immune responses to cancer vaccines. *Surgery* **129**, 248–254.
34. Maecker, H. T. and Maino, V. C. (2002) Flow cytometric analysis of cytokines, in *Manual of Clinical Laboratory Immunology*, 6th edit. (Hooks, J., ed.), ASM Press, Washington, DC.
35. Suni, M. A., Dunn, H. S., Orr, P. L., et al. (2003) Optimization of plate-based cytokine flow cytometry assays. *BMC Immunol.* **4**, 9.
36. Nomura, L. E., deHaro, E. D., Martin, L. N., and Maecker, H. T. (2003) Optimal preparation of rhesus macaque blood for cytokine flow cytometry analysis. Cytometry in press.
37. Motulsky, H. (1995) *Intuitive Biostatistics*. Oxford University Press, Oxford.

6

Use of Cell-Tracking Dyes to Determine Proliferation Precursor Frequencies of Antigen-Specific T Cells

Alice L. Givan, Jan L. Fisher, Mary G. Waugh,
Nadège Bercovici, and Paul K. Wallace

Summary

The T-cell receptor provides T cells with specificity for antigens of particular molecular structure (the “epitope”); the T-cell pool in an individual responds to the presence of many different antigenic epitopes, but any particular T cell will respond preferentially to one defined epitope. After stimulation of a T cell by the binding of its receptor to its cognate antigen in the context of a major histocompatibility complex (MHC) molecule on an antigen-presenting cell, the T cell will begin to proliferate and synthesize cytokines. Tetramer binding and the enzyme-linked immunospot (ELISPOT) method have been used to determine what proportion of cells in the T-cell pool can bind to a defined antigenic peptide or will secrete cytokines in response to a particular antigenic stimulation. The method described here uses tracking dyes to determine what proportion of T cells will proliferate in response to stimulation. As a flow cytometric “single-cell” method, it can be combined with tetramer and cytokine staining to determine the precursor frequencies of cells in the T-cell pool able to bind tetramer, to synthesize cytokines, and to proliferate in response to antigen.

Key Words

Antigen specificity, carboxyfluorescein diacetate succinimidyl ester, cytokine synthesis, PKH, precursor frequency, proliferation, T cell, tetramers, tracking dye.

1. Introduction

Receptors on T cells bind to peptides presented in the context of major histocompatibility complex (MHC) class I or class II molecules on antigen-presenting cells. The T-cell receptor, by its structure, conveys antigen specificity to a T cell: any particular T cell will interact with and respond to presented peptide with a

From: *Methods in Molecular Biology: Flow Cytometry Protocols*, 2nd ed.
Edited by: T. S. Hawley and R. G. Hawley © Humana Press Inc., Totowa, NJ

defined epitope (that is, a 9- to 14-amino-acid peptide fragment that is an antigenic determinant). The entire T-cell pool in an individual contains cells that are specific to a wide variety of antigenic epitopes, but any particular T cell will respond preferentially to a particular or very closely related epitope. In the naïve state, T cells of particular specificity exist as a low percentage of the T-cell pool. After binding to presented antigen of the cognate specificity, T cells respond in various ways toward the goal of acquiring effector and memory functions, including cytokine synthesis and cytolytic activity as well as proliferation and long-term survival. During the period immediately after stimulation, T cells of particular specificity will exist in high numbers, that is, as a high proportion of the T-cell pool. At some period of time after stimulation, these T cells will decrease in number but will remain in higher numbers than before stimulation (that is, while in the naïve state). Because the proportion of T cells with any particular specificity changes in response to the history of past stimulation, determining this proportion is informative with regard to assessing past contact with antigens and also with regard to assessing the readiness of T cells to react to future stimulation (e.g., to reinfection or to transplantation or to malignancy).

While determining the number of T cells with particular antigen specificity is important, methods for making this determination are problematic. The difficulty results, in part, from the low frequency of T cells specific for a defined epitope; a relevant methodology needs to be able to detect rare cells. In addition, there is no “gold standard” for the definition of an antigen-specific cell. The “classical” responses of a T cell to antigen involve, first, binding to the antigen via the antigen receptor, then secretion of cytokines and proliferation, and finally the acquisition of effector function. Therefore, valid methods used, in the past, for determination of the number of T cells with a particular antigen receptor have involved assaying the ability of T cells to bind to peptides (by using fluorochrome-conjugated tetramers [1]); assaying the proportion of cells that synthesize cytokine in response to antigen (with flow cytometry [2] or with the enzyme-linked immunospot [ELISPOT] method [3]); and assaying the number of cells proliferating in response to antigen (traditionally by looking at tritiated thymidine incorporation by the limiting dilution assay [LDA] [4]).

During proliferation of a few cells with rare specificity, that small number of cells will expand and continually increase its representation in the pool of mainly nondividing cells (**Fig. 1**). It is, therefore, important to calculate the *precursor frequency* of proliferating cells in order to know the antigen-specific proliferative potential of the cells in the initial resting population (before stimulation). The flow cytometric method described here (5–8) uses cell tracking dyes as a simple replacement for the LDA method to determine the proportion of cells that will proliferate in response to antigen (*see Note 1*). Cells are stained with a tracking dye before culture. During cell division, the tracking dye is par-

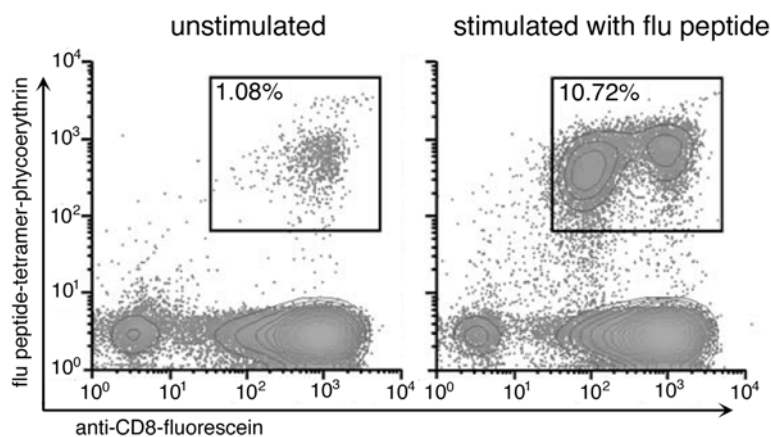


Fig. 1. Expansion of flu-peptide-tetramer-positive/CD8-positive T cells after 6 d of culture with flu peptide stimulation. The percentages indicate the tetramer-positive/CD8⁺ cells among live lymphocytes.

tioned between daughter cells, so that each division brings about a halving of fluorescence intensity; the intensity of a cell, by comparison with the intensity of resting cells, provides an indication of how many divisions the cell has undergone since stimulation (**Fig. 2**). Analysis of the staining levels of cells in the flow cytometric data file acquired after several days of culture provides the ability to calculate back to the precursor frequency (PF) of cells in the resting population that will respond to antigen stimulation by proliferation (*see Fig. 3 and Note 2*). This flow cytometric dye dilution method can be combined with tetramer staining and with intracellular cytokine detection in order to provide a description of T cells, on a single-cell basis, with regard to their ability to bind tetramer, synthesize cytokines, and proliferate. Results (**Fig. 4**) indicate that not all responding T cells do all three of these functions (5).

2. Materials

2.1. Staining of Cells With Tracking Dye for Cell Culture

1. Peripheral blood mononuclear cells (PBMCs), including lymphocytes and monocytes, prepared by Ficoll-Hypaque (Amersham Pharmacia Biotech, Piscataway, NJ) density gradient centrifugation.
2. Appropriate culture medium for the lymphocytes in question (e.g., AIM V medium [Gibco™ Invitrogen Corporation, Carlsbad, CA] with serum for human cells).
3. Protein or peptide for antigen stimulation.
4. Concanavalin A (Calbiochem brand, EMD Biosciences, San Diego, CA) or phytohemagglutinin (PHA [Sigma, St. Louis, MO]) for positive proliferation control:

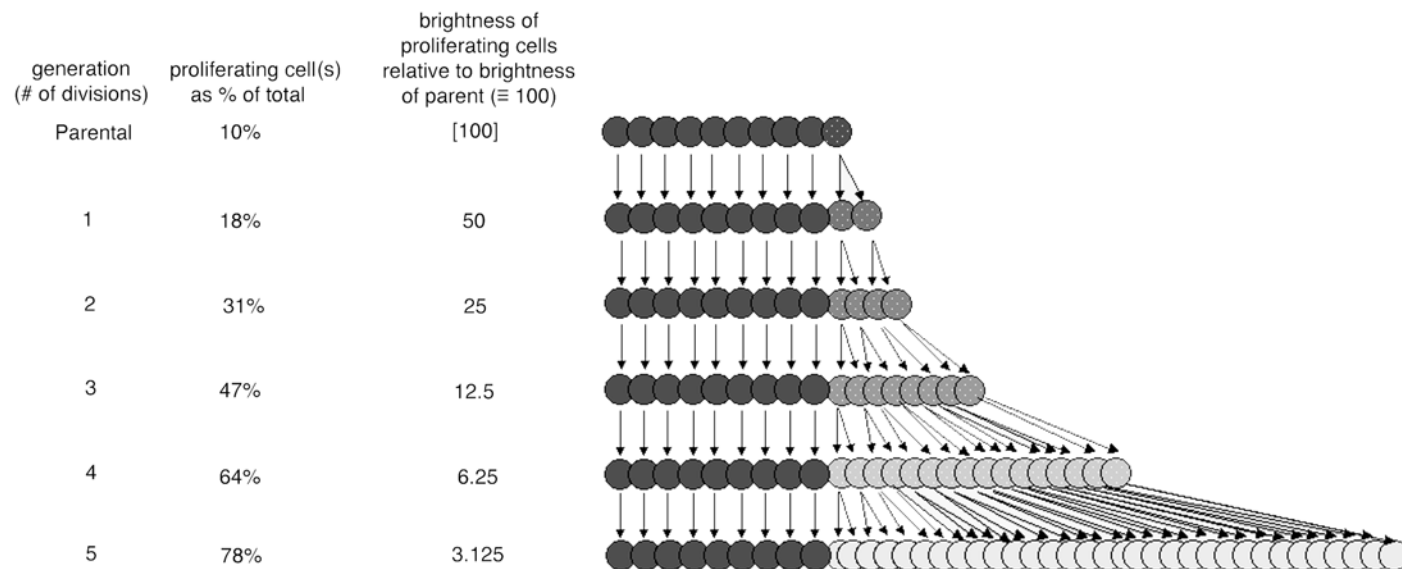


Fig. 2. A cartoon illustrating that dye intensity indicates the number of divisions that have occurred as a “specific” cell expands within a mainly resting population.

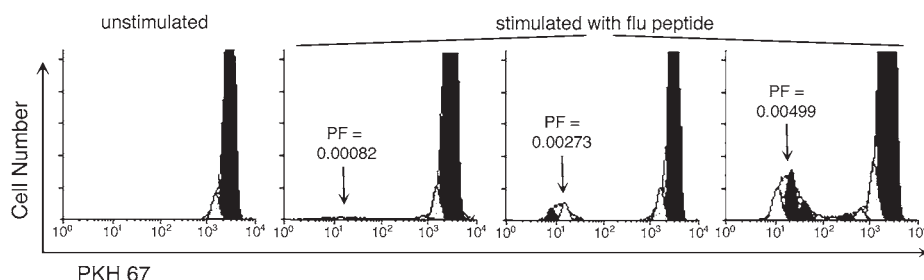


Fig. 3. PKH 67 histograms indicating a range of PBMC responses to flu peptide after 6 d in culture. Gaussian curves modeling each generation are drawn by ModFit software. Calculated precursor frequencies (PF) for proliferation are shown. Unstimulated cells are in the histogram on the **left**.

Prepare a stock solution of 2 mg/mL concanavalin A (Con A) in phosphate-buffered saline (PBS) and use at 5 μ g/mL final concentration; prepare a stock solution of 1 mg/mL PHA in PBS and use at 2 μ g/mL final concentration.

- Tracking dye: PKH 26 or PKH 67 (Cell Census Plus or Cell Linker kits [Sigma]), or carboxyfluorescein diacetate succinimidyl ester (CFSE [Molecular Probes, Eugene, OR] prepared as 10 mM stock concentration in dimethyl sulfoxide [DMSO]).
- Fetal bovine serum (Sigma or other suppliers) or human AB serum (Nabi, Boca Raton, FL) used in stopping PKH incorporation.
- 12- or 24-well culture plates.
- 15- or 50-mL conical centrifuge tubes.

2.2. Optional Treatment on the Last Day of Culture to Retain Cytokines Intracellularly

- Brefeldin A (Sigma): Prepare a stock solution of 1 mg/mL in ethanol and use at a final concentration of 1 μ g/mL.
- Phorbol myristic acid (PMA) and ionomycin (both from Sigma) for positive cytokine control: Prepare PMA stock solution at 1 mg/mL and use at a final concentration of 10 ng/mL; prepare ionomycin stock solution at 1 mg/mL in ethanol and use at a final concentration of 500 ng/mL.

2.3. Optional Staining After Culture Before Flow Cytometry

2.3.1. Staining for Surface Phenotype and/or Tetramer

- Antibody against CD8 or other phenotyping marker, conjugated to fluorochrome. The fluorochromes for phenotyping and tetramer need to be spectrally compatible with the tracking dye selected.

2. Tetramer of HLA-peptide complex conjugated to fluorochrome.
3. Washing buffer: PBS plus 1% bovine serum albumin and 0.1% sodium azide.
4. Human globulin Cohn fractions II and III (Sigma) to reduce antibody binding to Fc receptors: Prepare a stock solution of 6 mg/mL.
5. 96-Well plate.

2.3.2. Staining for Intracellular Cytokine

1. Washing buffer with 1 μ g/mL of brefeldin A.
2. Washing buffer with 4% formaldehyde (Ultrapure EM Grade from Polysciences, Warrington, PA).
3. Washing buffer with 0.1% saponin (Sigma).
4. Antibody conjugated to fluorochrome for cytokine of interest and equivalent isotype control. The cytokine fluorochrome needs to be spectrally compatible with the tracking dye and with any phenotyping and tetramer-conjugated fluorochromes.
5. 96-Well plate.

2.3.3. Washing, Fixing, and Centrifugation

1. Washing buffer.
2. Washing buffer with 1% formaldehyde (Ultrapure EM Grade from Polysciences).
3. Centrifuge for washing and pelleting cells in 96-well plates.

2.4. Flow Cytometry

1. Flow cytometer capable of detecting fluorochromes in use.
2. Rainbow Beads (RCP-30-5 from Spherotech, Libertyville, IL).

2.5. Data Analysis

1. The “proliferation wizard” module in ModFit software (Verity Software House, Topsham, ME) on a PC or Mac computer is used to analyze files acquired on the flow cytometer.

3. Methods

3.1. Staining of Cells With Tracking Dye for Cell Culture

Lymphocytes with monocytes (PBMCs) need to be isolated by Ficoll-Hypaque density gradient centrifugation from peripheral blood (*see* **Notes 3** and **4**). Cell preparation needs to be under sterile conditions. The final number of required PBMCs is 3×10^6 per culture well, but a recommended starting number of $5\text{--}6 \times 10^6$ is suggested anticipating a cell loss during the labeling and washing steps with either tracking dye. After isolation but before culture, the PBMCs are stained with the cell-tracking dye (PKH or CFSE). PKH 26 (551 nm abs/567 nm em) or PKH 67 (490 nm abs/504 nm em) can be chosen based on spectral compatibility with other fluorochromes used. For the choice between the PKH dyes or CFSE, *see* **Note 5**. At the end of the culture period,

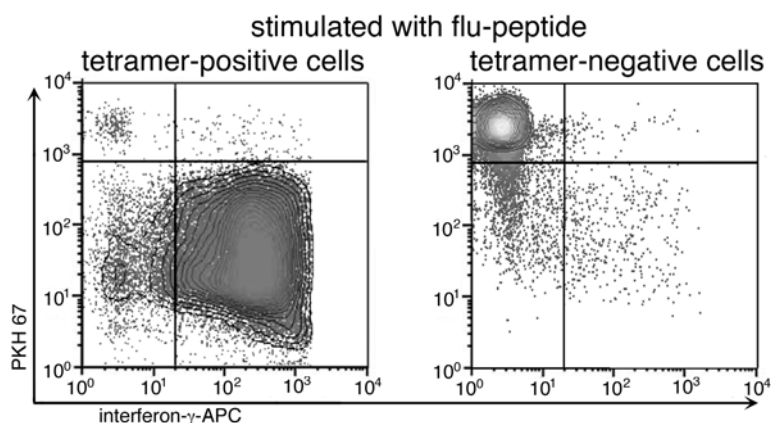


Fig. 4. Multiparameter density plots indicating PKH dye dilution and interferon- γ synthesis for tetramer-positive and tetramer-negative cells after 6 d in culture stimulated by flu peptide. On d 5, the cell suspensions were restimulated with peptide. The plots indicate that both tetramer-positive and tetramer-negative cells respond to antigen stimulation and that some cells proliferate and synthesize cytokine, some cells do neither, and some cells do one or the other.

the cells can be optionally stained for phenotype, for tetramer binding, and, internally, for cytokine. If the cells will be stained for cytokine, they need to have been restimulated with antigen for the last 16 h of culture.

3.1.1. Staining Procedure With PKH Dyes (see **Notes 6 and 7**)

1. Wash cells twice in serum-free medium and count with a hemocytometer. Following the second wash, aspirate the supernatant, leaving a cell pellet and 25–50 μ L of serum-free medium. Resuspend the cells gently in this residual medium.
2. In a separate conical tube, dilute the PKH dye stock in “diluent C” from the Sigma Cell Census Plus kit to twice the final staining concentration (e.g., 8 μ M if the final staining concentration is 4 μ M). After dilution, the dye should be used *immediately*; any unused dye should be discarded. The concentration of dye stock should be tested in advance to maximize both the brightness and the viability of the stained cells and also to ensure that high brightness does not make spectral compensation difficult with other fluorochromes used. For human lymphocytes, the final dye concentration will be approx 4 μ M.
3. Dilute the resuspended cell pellet in “diluent C” to give a final cell concentration of 2×10^7 cells/mL. A conical centrifuge tube equal in volume to more than six times the volume of the cell suspension should be used. The diluent is designed to produce even dispersal of the lipophilic dye but can be harsh on the cells. Therefore, for maximum yields, cells should not be left in this diluent any longer than necessary.

4. Add an equal volume of the PKH dye solution to the cell suspension. Incubate the cells with the dye for 3 min at room temperature. Cell labeling is rapid, with 80% occurring within the first 15 s. For homogeneous labeling, it is important that the cells and dye be rapidly combined and gently mixed.
5. After 3 min, add an equal volume of human AB serum or fetal bovine serum (FBS) to the cell suspension to stop the integration of the dye.
6. Wash the cells three times in culture medium, count, and resuspend to 1.5×10^6 cells/mL in medium.

3.1.2. Alternate Staining Procedure With CFSE

(adapted from **ref. 10**; see **Notes 6 and 7**)

1. Immediately prior to cell labeling, dilute the 10 mM stock solution of CFSE (in DMSO) to 1 mM in PBS.
2. Wash the cells twice in serum-free medium, count with a hemocytometer, and resuspend in 37°C medium at a final concentration of 5×10^7 cells/mL. Use a tube that is more than six times the volume of cells.
3. Add 2 μ L of CFSE/mL of cell suspension (giving a final CFSE concentration of 2 μ M). This concentration should be tested and modified to bring about bright staining with high cell viability (if the staining is too bright, spectral compensation with other fluorochromes may be difficult).
4. Incubate the cells with the dye for 15 min at 37°C with occasional mixing.
5. After 15 min, quench the stain by the addition of five volumes of ice-cold medium with 10% FBS.
6. Let stand at room temperature for 5–10 min.
7. Wash the cells three times in medium and resuspend in medium to a concentration of 1.5×10^6 cells/mL.

3.1.3. Cell Culture (see **Note 8**)

1. After staining with the tracking dye, count the cells and check for viability with Trypan blue.
2. Put the cells into culture with 3×10^6 cells/well in a 24-well tissue culture plate or 5×10^6 cells per well in a 12-well tissue culture plate. The final cell concentration in either case is 1.5×10^6 cells/mL.
3. Add antigenic peptides or proteins to appropriate wells at the beginning of the culture period at a concentration known to produce proliferation. This concentration should be titrated in advance with tritiated thymidine uptake or with the dye dilution assay.
4. As a positive proliferation control, add Con A at 5 μ g/mL final concentration or PHA at 2 μ g/mL final concentration for the last 4–5 d of the culture period to wells that have not received antigen stimulation.
5. As a negative control, use wells that contain medium without mitogen or antigen.
6. Incubate the culture plates at 37°C in 5% CO₂ for 6–10 d depending on the strength of the proliferative response (see **Note 9**). Check cultures regularly and feed with fresh culture medium as required.

7. If subsequent staining for intracellular cytokines, for phenotypic markers, or for tetramer binding will not be performed, centrifuge the cells down from culture, resuspend in 0.2–0.4 mL of washing buffer, and analyze directly by flow cytometry after the culture period. Alternatively, after washing the cells, resuspend them in washing buffer with 1% formaldehyde (0.2–0.4 mL). After overnight fixation at 4°C, analyze the fixed cells by flow cytometry.

3.2. Optional Treatment on the Last Day of Culture to Retain Cytokines Intracellularly

If the cells are to be stained for cytokine synthesis, they need to be restimulated with antigen and treated with brefeldin A during the last day of culture so that newly synthesized cytokine will remain in the cytoplasm for detection.

1. Sixteen hours before the end of the culture period, restimulate the cells with a second addition of antigen (or nothing for the control well).
2. At the same time, add brefeldin A (1 µg/mL, final concentration) to all wells.
3. Positive control wells for cytokine synthesis receive PMA (10 ng/mL final concentration) and ionomycin (500 ng/mL final concentration).

3.3. Optional Staining After Culture Before Flow Cytometry

After the culture period, the cells can be stained for tetramer binding and/or for phenotype and can then be fixed, permeabilized, and stained for cytokine synthesis, if desired (*see Note 10*).

3.3.1. Staining for Surface Phenotype and/or Tetramer

1. At the end of the culture period, harvest cells from the wells and pellet by centrifugation.
2. Resuspend the cells in washing buffer (or in washing buffer plus 1 µg/mL brefeldin A if the cells will be stained for cytokine). The concentration of cells after resuspension should be $3\text{--}8 \times 10^5$ cells/0.03 mL.
3. Mix the cells with an equal volume of human globulin (Cohn fractions II and III; stock solution 6 mg/mL) to block nonspecific binding to Fc receptors.
4. Add cells ($3\text{--}8 \times 10^5$ cells in 0.06 mL) to individual wells of a 96-well plate and stain them at saturating concentration with tetramer (2–10 µL) for 20 min at 37°C.
5. Add phenotyping antibodies at saturating concentration (5–20 µL) for an additional 20-min incubation at 4°C (*see Note 11*).
6. If no cytokine staining is to follow, wash the cells three times in cold washing buffer (200 µL/well for each wash) and fix overnight at 4°C in washing buffer with 1% formaldehyde (0.2–0.4 mL). Analyze by flow cytometry the next day.

3.3.2. Staining for Intracellular Cytokine

1. If staining for intracellular cytokines is to be performed, wash the cells three times in washing buffer with brefeldin (200 µL/well for each wash) and then fix them in washing buffer with 4% formaldehyde for 20 min at room temperature.

2. After the 20-min fixation, wash the cells three times in washing buffer containing 0.1% saponin for permeabilization.
3. Resuspend the cells in 0.1 mL of washing buffer plus 0.1% saponin; add 10 μ L of Cohn globulins (6 mg/mL).
4. Add fluorochrome-conjugated anticytokine antibody or isotype-matched control antibody to the well (5–20 μ L to a saturating concentration). Incubate the plate for 60 min at 4°C.
5. Wash the cells two times in washing buffer with 0.1% saponin and a final time in simple washing buffer.
6. Resuspend the cells in 0.2–0.4 mL of washing buffer with 1% formaldehyde, store overnight at 4°C, and assay on the flow cytometer the following day.

3.4. Flow Cytometry (see Note 12)

1. Laser excitation and the photomultiplier tube (PMT) bandpass filters on the flow cytometer need to be compatible with the fluorochromes selected. PKH 67 and CFSE have excitation and emission characteristics that are similar to fluorescein. PKH 26 is similar to phycoerythrin. All three dyes can be excited by a 488-nm laser.
2. Fluorescence parameters, including those for the tracking dye, are all acquired with logarithmic amplification. The PMT voltages for the tetramer, phenotyping, and cytokine parameters should be set so that the negative cells are in the bottom decade on a four-decade scale. The PMT voltage for the tracking dye parameter should be set so that the unproliferated cells are in the top decade (preferably at approx 5000 on a 1–10,000 [four-decade] relative intensity scale).
3. Forward scatter and side scatter are conventionally acquired with linear amplification. The voltage/amplification on the scatter parameters should be set so that gating can be used to exclude dead cells and debris with low forward scatter, but to include proliferating cells with high forward and side scatter (see Note 13).
4. When the assay involves multiparameter analysis, spectral compensation is important but can be difficult if the PKH or CFSE staining is very bright. Lowering the concentration of tracking dye used can make compensation easier.
5. Enough cells need to be acquired into the data file so that the least frequent cells of interest are present in high enough numbers for accurate data analysis. For example, a region could be drawn around the tetramer-positive cells or the PKH/CFSE dim cells or the cytokine-positive cells and enough cells acquired into the data file to give at least 500 cells in this gate (see Note 14). Data from all cells are stored in the list mode file.
6. Data from a mixture of Rainbow Beads of different intensities are acquired into a data file at the same voltage/amplification fluorescence settings (but with forward and side scatter settings altered so that the beads are above the forward scatter threshold).

3.5. Data Analysis

Before precursor analysis, cells from the data file can be gated on phenotype and/or on cytokine and tetramer fluorescence, if appropriate. For proliferation

and precursor frequency analysis, the “proliferation wizard” module of ModFit software is used to analyze PKH or CFSE fluorescence (*see* **Note 15**). In ModFit version 3.1 or later, the software will calculate the precursor frequencies. If earlier versions of the software are being used, then the precursor frequencies can be calculated with the following equation (*see* **Note 16**):

$$PF = \left[\sum_{k=2}^{k=10} A/2^k \right] / \left[\sum_{k=0}^{k=10} A/2^k \right]$$

where PF is the precursor frequency of the gated proliferating cells, k is the number of the generation ($k = 0$ for the parental generation), and A is the proportion of cells in each generation.

For the gated or ungated cells, the software examines the PKH or CFSE fluorescence intensity distribution, derives Gaussian curves centered on halving intensity values from the original parental intensity, and uses the above equation to calculate how many cells at the beginning of the culture period (the precursor cells) were required to account for the distribution of proliferating cells at the time of the assay (**6–8**).

For the calculation to be accurate, the number of channels that represent a halving of fluorescence intensity needs to be known. Although, on most cytometers, the full scale of 1024 channels represents a nominal range of 4 log decades of intensity, the fluorescence scale needs to be calibrated more accurately. This can be done using beads that have been standardized according to their intensities (e.g., Rainbow Beads from SpheroTech). These beads are of varying intensities and have been calibrated in terms of mean equivalents of soluble fluorochrome (MESF). After acquiring a data file for the mixture of beads with the same fluorescence settings used to acquire the cell data, use a spread sheet program to plot, on the x -axis, the channel number (on a 0–1023 scale) of the median intensity for each bead type and, on the y -axis, the log of the bead’s MESF value. The slope of this line will represent how many logs of intensity are encompassed by one fluorescence channel. Multiply the slope by 1024 to give how many logs of intensity are encompassed by the full 1024 channel scale. On standard cytometers where the full logarithmic scale represents 4 log decades, this number should be approx 4. The exact number should be entered into the “proliferation wizard” module of the ModFit software.

The software can determine precursor frequencies of the proliferating and nonproliferating cells in all individually gated populations (e.g., if cytokine and tetramer staining have been used, there will be four gated populations: double negative, cytokine positive, tetramer positive, and double positive) (**Fig. 5**). To bring all these numbers together to describe the response potential of the resting population, further calculations are necessary. The proportion of nonprolif-

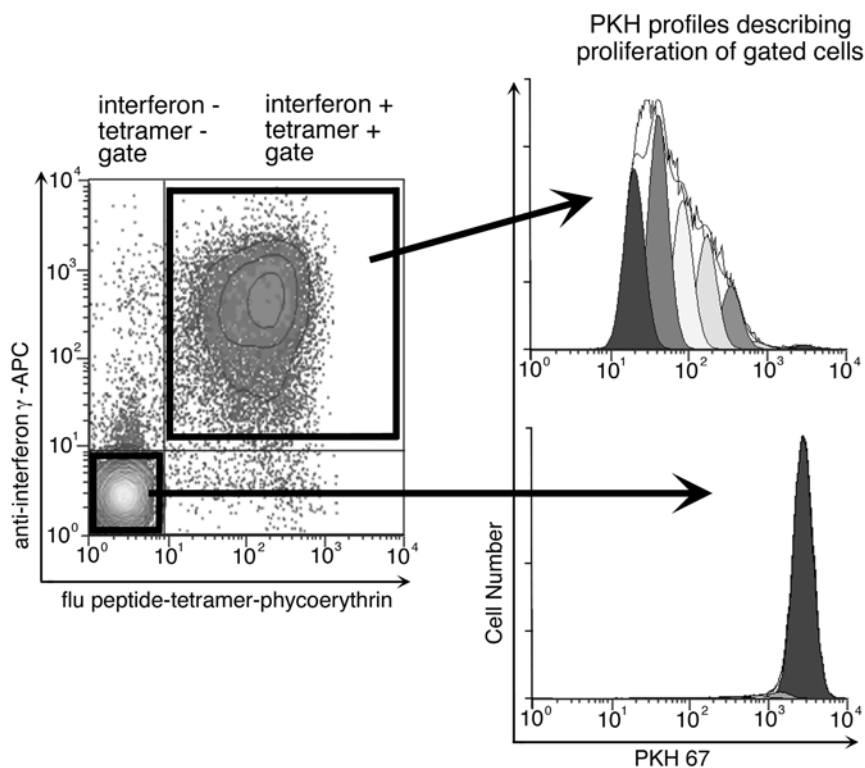


Fig. 5. Cells can be gated on tetramer-binding and cytokine synthesis before analysis of PKH staining on the gated cells. In this example, the tetramer-positive/cytokine-positive cells are mainly proliferating and outgrowing the nonproliferating cells left behind (small peak at ~3000); the tetramer-negative/cytokine-negative cells are mainly not proliferating (large peak at ~3000).

erating cells in each of the gated populations is applied to the number of gated cells in the data file to give the number of gated cells before culture that will not proliferate. Knowing the number of gated cells that will not divide and also knowing the precursor frequency of the proliferating cells in that gate, the number of cells before culture destined to divide can be calculated.

The following equations represent these calculations as performed for the results from each gated population (the example here is given for a culture that is harvested at d 6):

$$\begin{aligned} \text{number}_{\text{nonprolif cells (d 0)}} &= [(\text{proportion}_{\text{parental generation (d 6)}}) \\ &+ (0.5 * \text{proportion}_{\text{generation 2 (d 6)}})] * [\text{number}_{\text{gated cells in data file}}]. \\ \text{number cells}_{\text{(d 0) destined to proliferate}} &= [(\text{PF}_{\text{cells (d 0) destined to proliferate}}) \\ &* (\text{number}_{\text{nonprolif cells (d 0)}})] / [1 - \text{PF}_{\text{cells (d 0) destined to proliferate}}]. \end{aligned}$$

Table 1

Example of Precursor Frequencies (as Percentages) of CD8⁺ Human T Cells, With Regard to Their Ability to Respond to Flu-Peptide Stimulation by Proliferation and/or Interferon- γ Synthesis

Will proliferate	Will secrete IFN- γ	Flu-stimulated cells		Control cells	
		TET POS	TET NEG	TET POS	TET NEG
–	–	0.52	98.23	1.27	98.60
–	+	0.11	0.08	0.00	0.00
+	–	0.09	0.36	0.01	0.12
+	+	0.60	0.01	0.00	0.00
		100%		100%	

The percentages describe all the cells in the resting (d 0) population and add up to 100% for each culture condition.

This same set of calculations is applied to all the gated populations of cells individually (according to their tetramer binding and cytokine production, for example), resulting in a description of the proliferative potential of the time zero population with regard to each of the gated characteristics. The number of cells in the subpopulations are then summed so that all precursor results can be expressed as a percent of the total original, resting population (5) (*see Table 1*).

4. Notes

1. Tritiated thymidine uptake (either in bulk culture or in conjunction with LDA) is a common method to determine proliferative responses. The tritiated thymidine bulk method does not provide the ability to analyze precursor frequencies (a few cells dividing many times will give the same result as many cells dividing once or twice). The LDA method, although well documented (4), is cumbersome. Neither tritiated thymidine method is compatible with phenotyping of the responding cells. In addition, it has been shown, in direct comparison, that precursor frequency calculations using the LDA methodology give results that are 100-fold lower than results obtained by dye dilution methodology (6). Conventional LDA assays may underestimate precursor cells because of the possibility that the low density of factors, known and unknown, may limit proliferation of the cells of interest (9).
2. Simultaneous comparison of the dye dilution method with the ELISPOT method for cytokine synthesis and with uniparameter tetramer staining before culture indicates that all three methods give similar results for the frequency of antigen-specific cells (5) and that the dye dilution assay, therefore, reflects true antigen-specific T-cell proliferative capacity.

3. The methods in this chapter have been developed for human lymphocytes. With minor adaptations, they should be applicable to cells from other species.
4. A purified population of CD8 or CD4 cells, combined with antigen presenting cells, can be used instead of PBMCs to increase the frequency of antigen-specific cells in wells and thus to increase the number of positive events acquired for data analysis.
5. Choice of PKH or CFSE dye: CFSE stains the proteins of cells—after penetrating into the cytoplasm of a cell it becomes conjugated to the amine-containing residues on proteins. PKH, on the other hand, is a lipophilic dye that inserts into the lipid bilayer of the outer membrane. Both dyes have the potential for killing cells or inhibiting certain cell functions. It might be argued that CFSE is potentially more toxic as it binds directly to proteins. In our hands, we have found it easier to get bright staining without loss of viability using the PKH dyes. We have also found that CFSE, even at moderate concentrations, can inhibit some cell reactions (such as the proliferative response to antigen) without losing other responses (such as response to Con A). Finally, CFSE tends to stain cells very brightly and then is lost from cells rapidly for about 24 h as unstable proteins are broken down; therefore the level of staining is not immediately stable. There are, on the other hand, two serious problems with the PKH dyes. First, they are much more expensive than CFSE. Second, they do not form separate histogram peaks defining different proliferative generations (which, under optimal conditions, are seen with CFSE staining). Therefore, with the PKH dyes, there is more dependence on using curve-fitting algorithms for data analysis (but curve-fitting is easier because the algorithm does not have to match separate peaks for each generation).
6. Concentration of the cell tracking dye for staining: The dyes need to be titrated so that cells are stained brightly but with little immediate cell death. If the cells are too bright, spectral compensation with other fluorochromes will be difficult. An ideal staining level will put the nondividing cells in the fourth decade of a four-decade log scale, with unstained cells in the first decade. In addition, tritiated thymidine uptake should be checked with both stained and unstained cells—to confirm that staining does not inhibit proliferative capacity.
7. It is important to stain the cells with the tracking dye as uniformly as possible. Cells should be resuspended well before staining to avoid aggregates and should be mixed gently during staining.
8. By comparing the stained cells, before proliferation, with the autofluorescence level of those cells, one can determine the number of generations that can be tracked.
9. A longer culture period gives more sensitivity for detection of rare precursors as they expand during proliferation. It is necessary, however, to stop the culture before the dye on the dividing cells is diluted down to the level of autofluorescence. Therefore, longer culture periods are possible when the cells are stained brightly before culture. We have found 6–8 d to be a good culture period with antigen/peptide stimulation; however, with CFSE, where bright staining without toxicity is difficult, 8 d of culture may take the cells down to the autofluores-

cence level. When using polyclonal stimulation (such as ConA), 4–6 d of culture is sufficient.

10. With enough photodetectors on a cytometer, an unlimited number of parameters can be used for gating in this assay. For example, the method could be extended to include T-cell functional markers (e.g., multiple cytokines, chemokines, perforin/granzyme), activation markers (e.g., CD25, CD69), and markers of differentiation or migration (e.g., CD27, CD28, CD62L, CCR7). Many of these markers could be combined into a description of the complex response potential of a T-cell population.
11. If cells are stained for tetramer without staining for internal cytokine, it is recommended that a viability stain (such as propidium iodide or ToPro3) be used to gate dead cells out of the analysis; this will increase sensitivity for detection of tetramer-positive cells by lowering the background fluorescence from dead cells. Viability staining can be done only if flow cytometry is performed on unfixed cells (it is therefore not compatible with staining for intracellular cytokines). If flow cytometry is performed on fixed cells, then dead cells can be somewhat less successfully gated out of the analysis by the use of a gate based on forward and side scatter.
12. The sensitivity of the flow cytometric dye dilution method for proliferation precursor frequency detection is limited by three factors: the intensity of the parental generation stained with tracking dye relative to its autofluorescence, the range of intensities displayed by the logarithmic amplifier, and the ability of the flow cytometer to detect rare cells. With PKH dyes, it is usually possible to stain cells so that they are approx 1000-fold brighter than the autofluorescent level. Using a four-decade log amplifier, cells could therefore remain on scale after nine divisions (e.g., cells starting at a relative intensity of 6000 would fall to 12 after nine divisions; this would still be above the background level of 6). If we conservatively assume that a flow cytometer can detect cells that are 1% of the population, those cells that are, at the time of analysis, nine divisions away from the parental cell and are 1% of the population, were, at the time they were exposed to the stimulus, $2/10^5$ of the original population. This method should, therefore, be able to detect precursor cells of that frequency. Less conservative opinion (*11*) estimates that flow cytometry can detect cells of a frequency of $1/10^6$.
13. For analysis, cells are gated so as to exclude dead cells with low forward scatter but to include both resting and activated lymphocytes (with high forward scatter) for further analysis.
14. It is important to have enough cells in the data file to provide accurate precursor frequency analysis. Proliferating or cytokine-producing or tetramer-binding cells should be at least 500 in number; the data analysis will be more robust if more cells can be collected into the file. If, for example, the tetramer-binding cells are, at the end of culture, only 1% of the total number of cells, then the list mode data file needs to contain 50,000 cells to provide 500 tetramer-binding cells for analysis. Similarly, it needs to contain 200,000 cells to provide 2000 tetramer-binding cells for analysis.

15. Data analysis: Using deconvolution algorithms is somewhat more difficult with CFSE than with PKH staining because individual histogram peaks are often visible with CFSE and the Gaussian distributions need to fit well. With PKH dyes, separate histogram peaks are usually not visible; therefore it is impossible to know whether the algorithm is exactly right (but the algorithms provide rough justice).
16. Cells having undergone two or more divisions are included in the proliferative fraction. Cell having undergone only one division are considered to be either slow growing “nonspecific” or bystander cells or, alternatively, simply a low intensity shoulder on the parental peak.

References

1. Altman, J. D., Moss, P. A., Goulder, P. J., et al. (1996) Phenotypic analysis of antigen-specific T lymphocytes. *Science* **274**, 94–96.
2. Babcock, G. F. and Frede, S. F. (1998) Intracellular cytokines, in *Current Protocols in Cytometry* (Robinson, J. P., Darzynkiewicz, Z., Dean, P. N., et al., eds.), John Wiley & Sons, New York, pp. 9.9.1–9.9.10.
3. Herr, W., Schneider, J., Lohse, A. W., Meyer zum Buschenfelde, K. H., and Wolfel, T. (1996) Detection and quantification of blood-derived CD8+ T lymphocytes secreting tumor necrosis factor alpha in response to HLA-A2.1-binding melanoma and viral peptide antigens. *J. Immunol. Methods* **191**, 131–142.
4. Lefkovits, I. and Waldmann, H. (1999) *Limiting Dilution Analysis of Cells in the Immune System*. Cambridge University Press, Cambridge.
5. Bercovici, N., Givan, A. L., Waugh, M. G., et al. (2003) Multiparameter precursor analysis of T-cell responses to antigen. *J. Immunol. Methods* **276**, 5–17.
6. Givan, A. L., Fisher, J. L., Waugh, M., Ernstoff, M. S., and Wallace, P. K. (1999) A flow cytometric method to estimate the precursor frequencies of cells proliferating in response to specific antigens. *J. Immunol. Methods* **230**, 99–112.
7. Song, H. K., Noorchashm, H., Lieu, Y. K., et al. (1999) Cutting edge: alloimmune responses against major and minor histocompatibility antigens: distinct division kinetics and requirement for CD28 costimulation. *J. Immunol.* **162**, 2467–2471.
8. Wells, A. D., Gudmundsdottir, H., and Turka, L. A. (1997) Following the fate of individual T cells throughout activation and clonal expansion. Signals from T cell receptor and CD28 differentially regulate the induction and duration of a proliferative response. *J. Clin. Invest.* **100**, 3173–3183.
9. Tough, L. C. and Sprent, J. (1998) Anti-viral immunity: spotting virus-specific T cells. *Curr. Biol.* **8**, R498.
10. Lyons, A. B. and Doherty, K. V. (1998) Flow cytometric analysis of cell division by dye dilution, in *Current Protocols in Cytometry* (Robinson, J. P., Darzynkiewicz, Z., Dean, P. N., eds.), John Wiley & Sons, New York, pp. 9.11.1–9.11.9.
11. Gross, H. J., Verwer, B., Houck, D., and Recktenwald, D. (1993) Detection of rare cells at a frequency of one per million by flow cytometry. *Cytometry* **14**, 519–526.

Assessment of Lymphocyte-Mediated Cytotoxicity Using Flow Cytometry

Luzheng Liu, Beverly Z. Packard, Martin J. Brown,
Akira Komoriya, and Mark B. Feinberg

Summary

Cytotoxic lymphocytes, including cytotoxic T lymphocytes (CTLs) and natural killer (NK) cells, kill target cells by releasing granules containing perforin and granzymes, and/or via Fas–Fas ligand interactions. Both pathways lead to prompt activation within target cells of caspase cascades responsible for apoptosis induction and cell death. We have utilized cell-permeable fluorogenic caspase substrates and multiparameter flow cytometry to detect caspase activation in target cells, and applied these tools to quantify and visualize cytotoxic lymphocyte activities. This novel assay, referred to as the flow cytometric cytotoxicity (FCC) assay, is a nonradioactive single-cell-based assay that provides a more rapid, biologically informative, and sensitive approach to measure cytotoxic lymphocyte activity when compared to other assays such as the ^{51}Cr release assay. In addition, the FCC assay can be used to study CTL-mediated killing of primary target cells of different cell lineages that are frequently not amenable to study by the ^{51}Cr release assay. Furthermore, the FCC assay enables evaluation of the phenotype and fate of both target and effector cells, and as such, provides a useful new approach to illuminate the biology of cytotoxic lymphocytes.

Key Words

Apoptosis, caspase, caspase substrate, cytotoxic T lymphocyte, cytotoxicity, flow cytometry, flow cytometric cytotoxicity.

1. Introduction

1.1. Target Cell Killing Mediated by Cytotoxic Lymphocytes

Cytotoxic T lymphocyte (CTL) activity is triggered by T-cell receptor recognition of an antigenic peptide/major histocompatibility complex (MHC), while natural killer (NK) cell-mediated killing is based on inhibitory or stimulatory receptor recognition of specific ligands on target cells (1,2). Although

From: *Methods in Molecular Biology: Flow Cytometry Protocols*, 2nd ed.
Edited by: T. S. Hawley and R. G. Hawley © Humana Press Inc., Totowa, NJ

they recognize target cells through different mechanisms, both CTL and NK cells induce target cell apoptosis through either the directed exocytosis of perforin and granzymes or via ligation of “death receptors” in the Fas–Fas ligand (FasL) pathway. Both pathways of cellular cytotoxicity are mediated through the interaction of specific proteins that result in the activation of a cascade of proteases; the latter are characterized by a cysteine residue in the active site and a specificity for cleavage at an aspartic acid in the P₁ position (caspases) (1). Caspases exist within nonapoptotic target cells in inactive forms. Once activated, they cleave a large variety of substrates that are responsible for the subsequent morphological (cytoskeletal, nuclear, and plasma membrane breakdown) and biochemical (DNA laddering) changes associated with apoptosis. These events ultimately lead to target cell lysis, the end point of the cytotoxic killing process.

1.2. Limitations of the Conventional CTL Assay—⁵¹Chromium (⁵¹Cr) Release Assay

Over the past three decades, the ⁵¹Cr release assay has been widely used to quantitate cytotoxic lymphocyte activity (3). In this assay, target cells labeled with radioactive ⁵¹Cr are incubated with immune effector cells for 4–6 h. Target cell lysis is then measured by detecting radioactivity released into the culture supernatant.

Although the ⁵¹Cr release assay has been widely and productively employed in numerous studies of cellular cytotoxicity, its utility is limited by a number of disadvantages (4,5). First, ⁵¹Cr release assay measures bulk CTL activity using “lytic unit” calculations that do not quantitate target cell death at the single-cell level. Within the context of bulk cell populations used in the ⁵¹Cr release assay, variations in the phenotype and function of effector and target cells cannot be assessed directly. Second, CTL killing of primary host target cells often cannot be studied directly, as only certain types of cells, mostly immortalized cell lines, can be efficiently labeled with ⁵¹Cr (6,7). Third, the sensitivity of the ⁵¹Cr release assay is further limited by the fact that it measures only end point target cell death. Fourth, measurement of ⁵¹Cr release does not permit monitoring the physiology or fate of effector cells as they initiate and execute the killing process. Finally, radioactive materials require special licensing, handling, storage, and disposal, the combination of which substantially increases the total cost of the assay. In the hope of overcoming the limitations of available CTL assays, we sought to take advantage of the power of multiparameter flow cytometry and the advent of fluorogenic caspase substrates to develop a simple, more facile, and more informative strategy to quantify the levels and study the mechanisms of cell-mediated cytotoxicity. This chapter describes the materials and methods employed in the flow cytometric cytotoxicity (FCC) assay resulting from these efforts.

1.3. Recent Development of Flow Cytometry-Based Assays Study Cell-Mediated Immune Response

Recently developed immunologic methods including major histocompatibility complex (MHC) tetramers, intracellular cytokine detection, and enzyme-linked immunospot (ELISPOT) assays have greatly improved sensitivity to enumerate antigen-specific T cells; however, they do not assess the cytolytic function of antigen-specific CTLs (8–10). Given emerging data indicating that antigen-specific CD8⁺ T cells may be present in certain chronic infections (e.g., human immunodeficiency virus [HIV]) or malignancies (such as melanoma), but blocked in their ability to produce cytokines or to lyse target cells, assays that measure the complete spectrum of immune effector cell functions at the single-cell level are needed (11–14). Such assays will be essential for the development of new strategies to maximize immune responses to vaccine antigens, and to manipulate favorably host immune responses in a number of important diseases.

The advantages of utilizing flow cytometric approaches to characterize and quantitate CTL killing has also been apparent to others. Toward this end, other groups have developed flow cytometry-based CTL assays wherein target cell death is assessed based on the amount of fluorochrome released from or retained in the prelabeled target cells (15), or by detection of the late stages of target cell death using intercalative DNA dyes (16). However, although these assays provide information that cannot be gleaned from standard ⁵¹Cr release assays, none of them reveals the fundamental processes responsible for the initiation and execution of target cell killing. Furthermore, none of these alternative flow cytometric CTL assays has yet been tested and compared with the ⁵¹Cr release assay for their ability to quantitate sensitively and accurately CTL responses generated in the course of an in vivo exposure to a defined antigen.

1.4. Fluorogenic Caspase Substrates Detect Cytotoxic Lymphocyte-Induced Target Cell Apoptosis

This chapter describes a flow cytometry assay that detects effector cell-induced caspase activation within individual target cells using a novel and unique class of cell-permeable fluorogenic caspase substrates (17–19). These reagents (developed by OncoImmunin, Inc., Gaithersburg, MD) are composed of two fluorophores covalently linked to 18-amino-acid peptides containing the proteolytic cleavage sites for individual caspases. In the uncleaved substrates, fluorescence is quenched owing to the formation of intramolecular excitonic dimers. On cleavage of the peptides by specific caspases, the fluorophore–fluorophore interaction is abolished, leading to an increase in fluorescence that can be detected by flow cytometry. In the FCC assay, first target cells are fluorescently labeled (to distinguish them from effector cells [see Subheading 3.1.]) and then coincubated with cyto-

toxic effector cells. At the desired time point, medium is removed from samples and replaced with a solution containing a fluorogenic caspase substrate; the latter has spectroscopic properties complementary to those of the target cell label. Following incubation and washing, samples may be analyzed by flow cytometry or fluorescence microscopy. Cleavage of the substrate results in increased fluorescence in dying cells. This chapter uses the following model systems to illustrate the basic principles of the FCC assay: viral antigen-specific mouse CTL killing of target cells and human NK killing of both suspension and adherent human tumor cells. (Additional applications and further characterization of these probes as flow cytometry reagents can be found in Chapter 8 by Telford et al., this volume.)

1.5. Advantages of the FCC Assay Compared to the Conventional ^{51}Cr Release Assay

This assay has been shown to provide a single-cell-based, rapid, quantitative, and sensitive assay to detect lymphocyte-mediated target cell killing in various animal models (17). Unlike conventional chromium release assays, the FCC assay enables monitoring of cellular immune responses in real time and at the single-cell level using diverse fluorescence detection methods such as flow cytometry and fluorescence and confocal microscopy. Importantly, the assay can be used to study CTL-mediated killing of primary host target cells, and enables assessment of important biological details of the killing process, as well as the fate of immune effector cells during the killing process. These features should enable direct determination of whether specific subpopulations of cells can resist CTL-mediated lysis (e.g., tumor cells or certain virus-infected cells) (20,21) or alternatively, induce apoptotic deletion of the CTL effectors themselves (e.g., through expression of FasL on specific tumors or immunologically privileged tissues, or as an immune evasion strategy employed by immunodeficiency viruses) (22,23). Although developed using the murine lymphocytic choriomeningitis virus (LCMV) infection model, this novel approach is readily applicable to other models such as HIV, SIV, Epstein–Barr virus (EBV) and cytomegalovirus (CMV) infections (data not shown). In all, the favorable attributes of the FCC assay may permit new insights into the pathogenesis of important infectious, malignant, and immunologic diseases that have been experimentally unapproachable previously, and provide a practical and useful method to quantitate CTL activity in basic and applied studies of cellular immune responses.

2. Materials

2.1. Preparation of Target Cells

1. Target cells: Either tumor cell lines or primary cells such as mouse splenocytes can be used to prepare a single-cell suspension. For example, EL4 cells (American Type

Culture Collection [ATCC], Manassas, VA, cat. no. TIB-39) or A20 cells (ATCC, cat. no. TIB-208) can be used in mouse models with H-2^b haplotype or H-2^d haplotype, respectively. Other examples include Jurkat cells and MDA-MB-468 (ATCC, cat. no. HTB-132).

2. Complete media (*see Note 1*):
 - a. RPMI 1640 medium (Invitrogen, Carlsbad, CA) supplemented with 10% fetal bovine serum ([FBS], HyClone, Logan, VT), 100 U of penicillin G, 100 µg/mL of streptomycin sulfate, and 2 mM L-glutamine (100X stock, all from Mediatech, Herndon, VA). EL4, A20 and Jurkat cells can be maintained in this medium.
 - b. Dulbecco's modified Eagle medium (DMEM) supplemented with 10% FBS. Most adherent cell lines such as MDA-MB-468 can be maintained in this medium.
3. Trypan blue (Mediatech).
4. Target cell labeling reagents can be used to label target cells prior to introduction of effectors (two examples are listed below):
 - a. Celltracker™ orange CMTMR ([CTO], Molecular Probes, Eugene, OR). $\lambda_{\text{ex}} = 540 \text{ nm}$ and $\lambda_{\text{em}} = 566 \text{ nm}$. It is light sensitive. On receipt, it should be stored desiccated at -20°C until use. Avoid repeated freezing and thawing. Dissolve the lyophilized product in high-quality, anhydrous dimethyl sulfoxide ([DMSO], Sigma Chemical Co., St. Louis, MO) to a final concentration of 10 mM. Store small aliquots frozen at -20°C , desiccated, and protected from light. Avoid repeated freezing and thawing. When stored properly, both the solids and the stock solutions are stable for at least 6 mo.
 - b. TFL2 (OncoImmunin, Inc.). On receipt, it should be stored desiccated at -20°C until use.
5. For viral antigen-specific mouse CTL killing, synthetic peptides containing the viral CTL epitope of interest are used. An irrelevant peptide should also be employed as a negative control. High-purity peptides can be ordered from American Peptide Company, Inc. (Sunnyvale, CA).
6. Staurosporine *Streptomyces* sp. (Sigma Chemical Co.). Store at 4°C .
7. 15-mL Falcon polypropylene conical tubes with screw caps (BD Biosciences Discovery Labware, Bedford, MA).

2.2. Preparation of Effector Cells

1. Effector cells: Lymphocytes from the spleen or lymph nodes of mice acutely infected with viruses (d 5–8 postinfection) (17), the NK92 cell line (ATCC, cat. no. CRL-2407), or a CTL cell line.
2. Red blood cell (RBC) lysing buffer (Sigma Chemical Co.).
3. 50-mL Falcon polypropylene conical tubes with screw caps, 70-µm Falcon cell strainer, and 3-mL syringe (all from BD Biosciences).

2.3. Detection of Target Cell Apoptosis by Caspase Substrates

1. PhiPhiLux-G₁D₂ ([caspase 3-like substrate], OncoImmunin Inc.). $\lambda_{\text{ex}} = 505 \text{ nm}$ and $\lambda_{\text{em}} = 530 \text{ nm}$. It is light sensitive, but is stable in the dark at 4°C for up to 2 mo. Freeze at -20°C for longer-term storage. Keep the reagent sterile. *See Note 2*.

2. Washing buffer: Dulbecco's phosphate-buffered saline ([PBS], Invitrogen) supplemented with 2% FBS.
3. 96-well U- or V-bottom tissue culture plate with lid, and 5-mL Falcon polypropylene round-bottom tubes (fluorescence-activated cell sorter [FACS] tubes, both from BD Biosciences).

2.4. Flow Cytometry (see Note 3)

1. A flow cytometer such as the FACSCalibur (BD Biosciences Immunocytometry Systems, San Jose, CA) or Epics® XL (Beckman Coulter, Miami, FL).

2.5. Determine Cytotoxic Activity

1. FACS data analysis software such as CellQuest (BD Biosciences), FlowJo (Tree Star, San Carlos, CA), or WinMDI (Dr. Joseph Trotter, Scripps Institute, La Jolla, CA, and BD Biosciences).

3. Methods

3.1. Preparation of Target Cells (see Note 4)

1. Suspend target cells in complete RPMI 1640 medium in a 15-mL conical tube.
2. Count viable cells with the Trypan blue exclusion method. Adjust cell concentration to $2 \times 10^6/\text{mL}$.
3. Add a 0.5-mL aliquot of target cells into a FACS tube: tube A. Leave tube A on ice until sample acquisition by flow cytometer. (This will serve as the unlabeled target cell control for instrument setting of the flow cytometer.)
4. Add a 0.5-mL aliquot of target cells into a new 15-mL conical tube: tube B. Induce apoptosis by adding an apoptogen such as staurosporine at a final concentration of $1 \mu\text{M}$. Incubate in a 37°C 5% CO_2 incubator until **Subheading 3.3., step 5**. Conditions for apoptosis induction will vary with target cell type and apoptogen, but a good starting point is staurosporine at $1 \mu\text{M}$ for 3–5 h. (Tube B will serve as FL1 channel control for flow cytometer setting.)
5. Divide the rest of target cell suspension equally into two 15-mL conical tubes (tubes *a* and *b*). Add CTO/TFL2 into the tubes at a final concentration of $3/2 \mu\text{M}$. Antigenic peptide is added into tube *a* at final concentration of $1 \mu\text{M}$, irrelevant control peptide is added into tube *b*.
6. Incubate tubes *a* and *b* at 37°C 5% CO_2 for 1 h with caps loosened. During this time, prepare effector cells (see **Subheading 3.2.**).
7. After the 1-h incubation, wash target cells at least once in at least 10-fold volume of complete RPMI 1640.
8. Resuspend cells at $2 \times 10^6/\text{mL}$ in complete RPMI 1640. Leave the cells on ice until effector cells are ready.
9. Take a 0.5-mL aliquot from each of tube *a* and *b* into two FACS tubes (tubes C and D). Leave tube C on ice until sample acquisition. (This tube will serve as FL2 channel control for flow cytometer setting.) Leave tube D on ice until **Subheading 3.3., step 3**. (This tube will be used to measure base line target cell apoptosis.)

3.2. Preparation of Effector Cells From Spleen or Lymph Nodes (see Notes 4 and 5)

1. Harvest spleen or/and lymph nodes on d 5–8 post-viral infection.
2. Place a 70- μ m Falcon cell strainer on top of a 50-mL Falcon tube. Place freshly removed organs into the cell strainer.
3. Press the organs against bottom of the cell strainer with plunger of a 3-mL syringe until mostly fibrous tissue remains.
4. Rinse cells through the cell strainer with 20 mL of complete RPMI 1640 medium. Discard the cell strainer.
5. Centrifuge at 250g for 10 min and discard supernatant.
6. Remove RBC in spleen samples by resuspending spleen cell pellet in RBC lysing buffer (5 mL/spleen). Incubate at room temperature for 5 min. Add RPMI 1640 to fill the tube, centrifuge at 250g for 10 min. Discard the supernatant.
7. Resuspend the cell pellet in the appropriate volume of complete RPMI 1640. Count cells by trypan blue exclusion.
8. Adjust the cell concentration to 5×10^7 /mL (if maximal E/T ratio is 25:1).

3.3. Detection of Target Cell Apoptosis by Caspase Substrates

1. Prepare serial dilutions of effector cells in 96-well U-bottomed plate for the desired E/T ratios. For example, to obtain E/T ratios as 25:1, 12.5:1, and 6.25:1, 100 μ L/well complete RPMI 1640 is added into wells of rows B and C of the plate. Add 200 μ L/well of effector cells (5×10^7 /mL) into row A of the plate. Use a multichannel pipet to transfer 100 μ L/well of cell suspension from row A into the corresponding wells in row B, mix by pipetting three to five times. Change tips, then transfer 100 μ L/well cell suspension from row B into the corresponding wells in row C, mix well, and discard 100 μ L/well cell suspension from row C.
2. Add 100 μ L/well (2×10^5 cell/well) of target cell suspension into wells of the 96-well plate. Mix target cells and effector cells well by pipetting.
3. Add 200 μ L of target cells in tube D (see **Subheading 3.1., step 9**) into one well of the 96-well plate.
4. Incubate the plate in a 37°C 5% CO₂ incubator for 1–3 h (see **Note 6**).
5. Pellet cells by centrifuging the plate and tube B (see **Subheading 3.1., step 4**) at 250g. Discard the supernatant by flicking the plate and vacuum aspiration from the tube, respectively.
6. Add 75 μ L/sample of caspase substrate PhiPhiLux-G₁D₂ and mix by gentle pipetting. From this point on, do not vortex-mix samples, as apoptotic cells can be “fragile.”
7. Incubate cells in a 37°C 5% CO₂ incubator for 30 min (see **Note 7**).
8. Wash cells twice by adding 200 μ L/sample of ice-cold washing buffer.
9. After the final wash, resuspend the cell pellets into 300 μ L/sample of washing buffer.

10. Transfer cells into FACS tubes. Label the tube containing staurosporine-treated target cells as tube B.

3.4. Flow Cytometry

1. Use tube A (unlabeled target cells) to set FL1 and FL2 channels initially, so that the fluorescence intensities of the majority of the events are between 10^0 and 10^1 on each axis.
2. Use tube B (PhiPhiLux-G₁D₂-labeled apoptotic target cells) to set up FL2 channel compensation.
3. Use tube C (CTO/TFL2-labeled target cells) to set up FL1 channel compensation.
4. Run the remaining samples.

3.5. Determine Cytotoxic Activity

Data are analyzed by CellQuest, FlowJo, or WinMDI software to obtain quadrant statistics of distinct cell populations. The total target cell apoptosis is calculated as $\{(\% \text{ CTO/TFL2}^+ \text{ caspase}^+ \text{ cells})/[(\% \text{ CTO/TFL2}^+ \text{ caspase}^+ \text{ cells}) + (\% \text{ CTO/TFL2}^+ \text{ caspase}^- \text{ cells})]\} \times 100\%$. The following are a panel of representative experiments highlighting the broad applications and advantages of the FCC assay.

Typical FCC data measuring antigen-specific CTL activity are shown in **Fig. 1A,B (17)**. Spleen cells from C57BL/6 mice acutely infected with LCMV were used as effectors, and target EL4 cells were either loaded with the dominant LCMV H-2^b-restricted CTL epitope NP_{396–404} (**Fig. 1A**) or an irrelevant control peptide (**Fig. 1B**). Significant target cell apoptosis was detected with the FCC assay only when target EL4 cells were pulsed with the LCMV epitope NP_{396–404}, but not with the control epitope. The numbers at the upper right corners are the calculated percentages of target cell apoptosis. **Figure 1C,D** shows the direct comparison of the FCC assay with the ⁵¹Cr release assay. CTL activities against a panel of LCMV peptides were measured using the two methods in parallel. D 8 splenocytes were incubated with EL4 target cells pulsed with different peptides at various E/T ratios for 3 h (FCC assay) or 5 h (⁵¹Cr release assay). The two methods detected an identical pattern of dominance hierarchy of the CTL activities specific for different peptides. Importantly, the FCC assay was more sensitive than the ⁵¹Cr release assay in detecting the CTL response specific for the subdominant epitope NP_{205–212}. Similarly, the FCC assay can be used to detect human CTL activity against viral antigens. In **Fig. 2**, a human CTL line was used as effector cells in the FCC assay. Strong killing of BLCL targets pulsed with the HIV A2-restricted epitope QR9 but not the control peptide was detected at an E/T ratio of 5:1.

The FCC assay also provides a rapid and sensitive measurement for NK cell-mediated cytotoxicity. Jurkat cell death induced by the NK cell line NK92

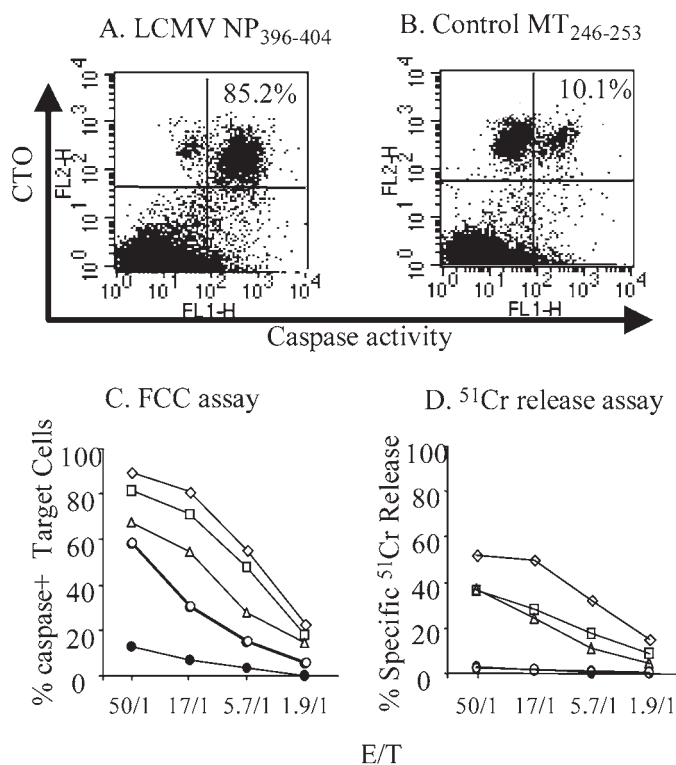


Fig. 1. Detection of LCMV antigen-specific CTL activity (17) using the FCC assay. (A,B) Spleen cells from d 8 LCMV-infected C57BL/6 were cocultured for 3 h with EL4 cells that were loaded with either the dominant LCMV CTL epitope NP₃₉₆₋₄₀₄ (A) or an irrelevant control peptide (B). The E/T ratio was 50:1. Subsequent incubation with PhiPhiLux detected strong caspase activity in target cells pulsed with the LCMV epitope NP₃₉₆₋₄₀₄, but not with the control peptide. The numbers at the upper right corners are the percentage of target cell apoptosis. (C,D) Comparison of CTL activities specific for a panel of LCMV epitopes measured by FCC and ⁵¹Cr release assays. CTO or ⁵¹Cr-labeled EL4 cells were pulsed with LCMV peptides NP₃₉₆₋₄₀₄ (◇), GP₃₃₋₄₂ (□), GP₂₇₆₋₂₈₆ (△), NP₂₀₅₋₂₁₂ (○), or irrelevant peptide MT₂₄₆₋₂₅₃ (●) and then cocultured with the same effectors as in (A) and (B) for 3 h (FCC assay) or 5 h (⁵¹Cr release assay). Target cell death was then assessed by either cleavage of the PhiPhiLux (C) or ⁵¹Cr release (D). Note that the curves representing CTL response specific for NP₂₀₅₋₂₁₂ and MT₂₄₆₋₂₅₃ overlapped in D.

was kinetically measured with a modified “rapid” protocol where the coincubation of targets and effectors was carried out in the caspase substrate solution. This modified protocol allows the detection of the onset of target cell death at considerably earlier time points. As shown in Fig. 3, significant target

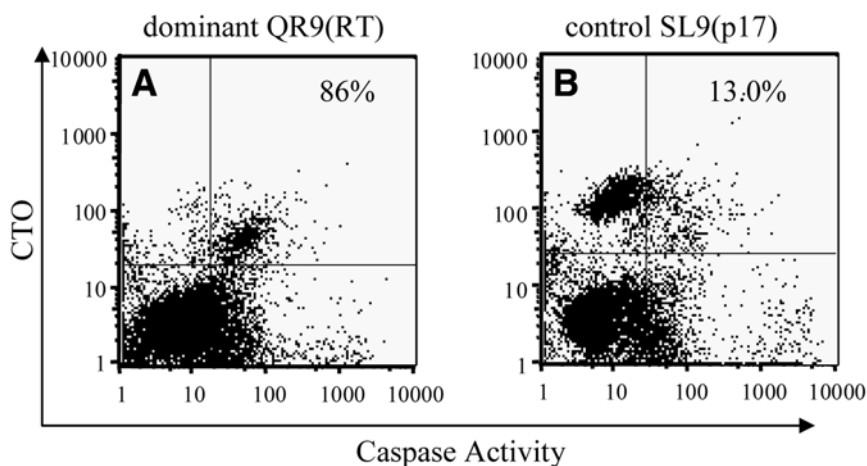


Fig. 2. Strong anti-HIV CTL activity was detected with the FCC assay. An HIV-specific T cell line was generated by stimulating PBMCs from an HLA A2⁺ HIV⁺ donor in vitro with the HIV peptide QR9. These T-cells were then coincubated with a CTO-labeled A2⁺ B-cell line bearing either the same peptide QR9 (A) or a control HIV peptide SL9 (B) at 5:1 ratios. Strong QR9-specific CTL activity was detected by the FCC assay.

cell death (50%) was detected as early as 20 min after the coincubation of effectors and targets at a 5:1 E/T ratio. At the end of a 2-h coincubation, 90% of the target cells were shown to be apoptotic.

In addition, the FCC assay is readily convertible to a fluorescence microscopic assay to visualize the lymphocyte-mediated cytotoxic action (8). **Figure 4** demonstrates the detection of NK92-mediated killing of breast carcinoma target cell line MDA-MB-468 cells using both flow cytometry (**Fig. 4A,B**) and confocal microscopy (**Fig. 4C,D**; nonapoptotic target cells are red; apoptotic target cells have both red and green fluorescence signals and therefore appear yellow). Thus, the FCC assay enables monitoring of cellular immune responses in real time and at the single-cell level using diverse fluorescence detection methods.

4. Notes

1. The character of the FBS used in cell culture can be a critical element in obtaining good results with the FCC assay protocol. It may be necessary to screen multiple lots of FBS to obtain an optimal lot that supports high effector cell activity and low target cell spontaneous apoptosis.
2. An alternative caspase substrate (for caspase 6) is used in the CyToxiLux cytotoxicity assay kit (OncoImmune Inc.) to detect target cell apoptosis (<http://www.phiphilux.com/cytotox.htm>). Similar results can be obtained using the CyToxiLux kit and the protocol described in this chapter.

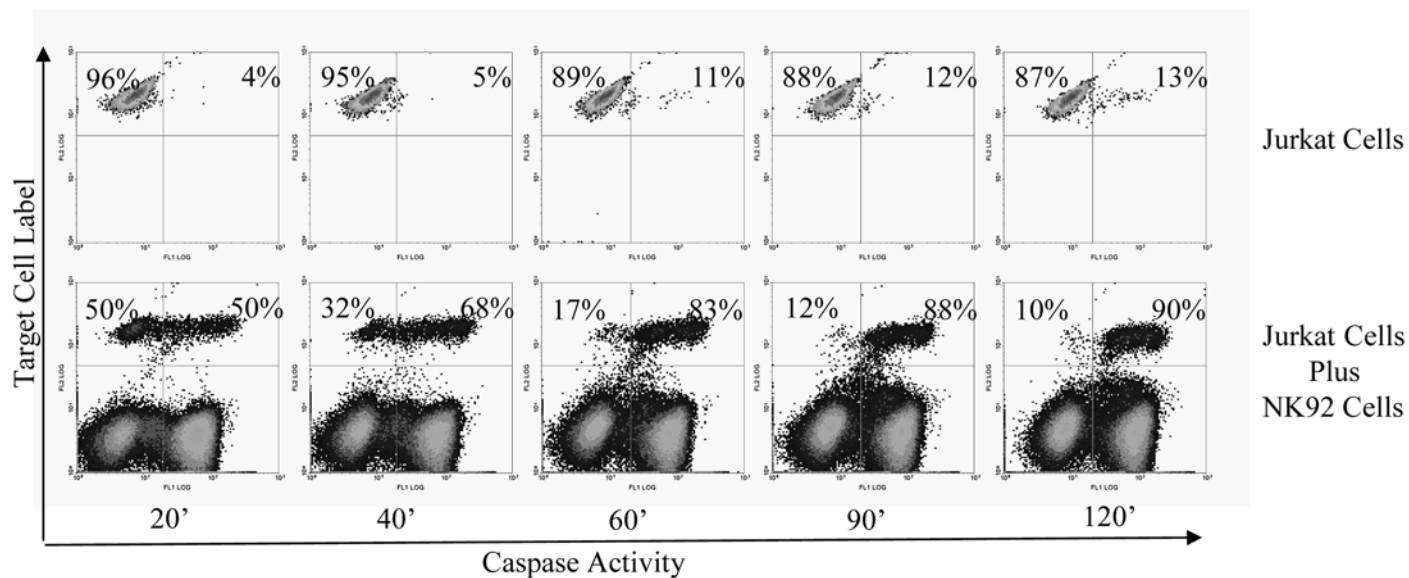


Fig. 3. The FCC assay provides rapid and sensitive detection of NK cell cytotoxicity. TFL2-labeled Jurkat cells were incubated with the NK cell line NK92 at an E/T ratio of 5:1 for the time indicated in the presence of the caspase 6 substrate. Significant cytotoxicity (50%) was detected as early as 20 min.

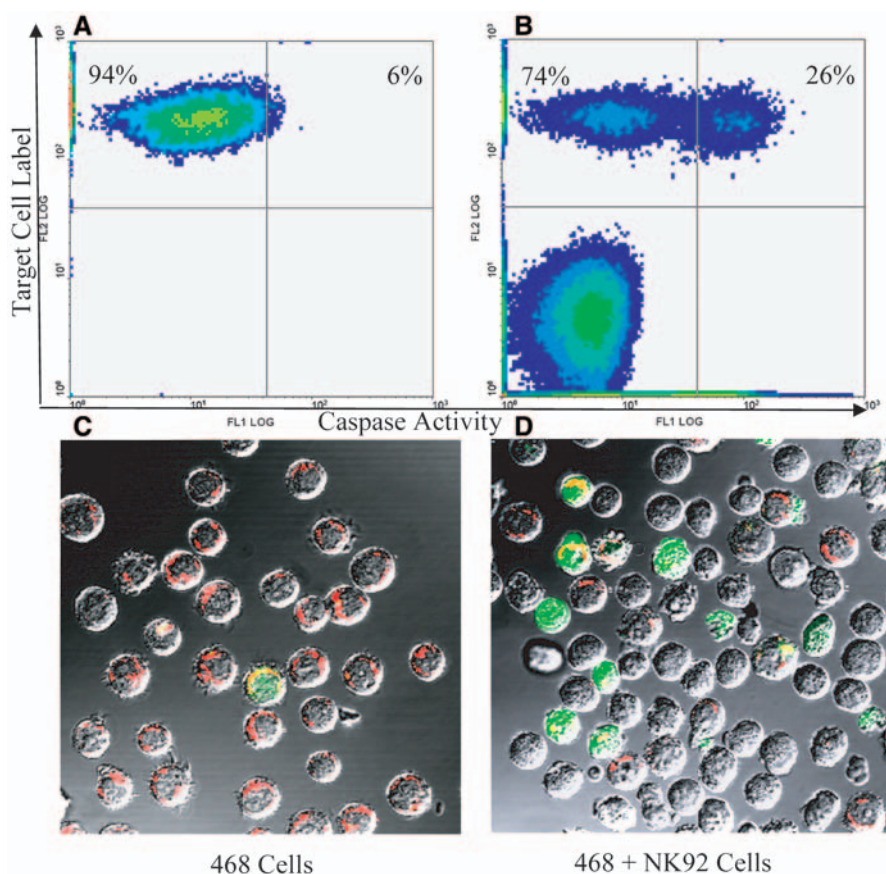


Fig. 4. The detection of NK92-mediated killing of breast carcinoma target cell line MDA-MB-468 cells using both flow cytometry (A,B) and confocal microscopy (C,D). Target cells were labeled with TFL2 and incubated without (A,C) or with (B,D) NK92 cells for 2 h in the presence of caspase 6 substrate at an E/T ratio of 5:1. Nonapoptotic target cells are red; apoptotic target cells have both red and green fluorescence signals and therefore appear yellow.

- Instrument settings of flow cytometry-based assays are critical for quantitation accuracy. Because the fluorescence emissions from PhiPhiLux-G₁D₂ and CTO/TFL2 overlap to some extent, compensation is necessary. A significant amount of orange fluorescence is present in the PhiPhiLux-G₁D₂ emission, and compensation for the FL2 channel may require subtraction of 80% or more from FL1 (FL2 minus $\geq 80\%$ FL1). A new version of the FCC which uses the same principles described herein but does not require compensation is now available from OncoImmunin, Inc. The only additional requirement is a flow cytometer equipped with both 488-nm and 633/635-nm laser lines.

4. Viability of both target cells and effector cells prior to coincubation is critical for the sensitivity of the assay. Target cells should be maintained in complete medium at optimal concentration, so that baseline cell apoptosis is <15%. For primary cell targets, they should be cocultured with effector cells within 2 h after harvesting to prevent increased spontaneous apoptosis *ex vivo*. Increased baseline target cell death reduces sensitivity of the assay. Cells should be left on ice whenever applicable. If necessary, nonviable cells can be removed by Ficoll-Paque density gradient centrifugation.
5. In vitro stimulated CTL precursors (CTLp) from previously primed animals can be used as effector cells in the FCC assay. A detailed protocol for CTLp stimulation *in vitro* is beyond the scope of this chapter and has been described elsewhere (13). In brief, stimulator cells are prepared by irradiating naïve spleen cells (γ -irradiation using 2000 rad) and pulse them with 1–10 μ M antigenic peptide. The stimulator cell suspension is adjusted to $1\text{--}6 \times 10^6/\text{mL}$. The concentration of the responder cells should be $2\text{--}10 \times 10^6/\text{mL}$. Optimal concentrations of stimulator and responder cells may vary with the nature of the antigenic differences. Titration of both cell types may be required to identify optimal concentrations. Add 1 mL each of responder and stimulator cells to the wells of a 24-well tissue culture plate (BD Biosciences). Set up at least six wells for each concentration of responder and stimulator cells. Culture cells for 5 d in a 37°C 5% CO₂ incubator. Harvest effector cells into a 15-mL conical tube, centrifuge at 250g for 5 min, and resuspend the pellet in complete RPMI 1640 at the desired concentration. Process with the FCC protocol described in **Subheading 3.3**.
6. If coincubation of effector cells and target cells is longer than 3 h, some apoptotic target cells may be lysed and become “invisible” by flow cytometry. Thus, the percentage of CTO/TFL2-positive cells in the total cell population at the end of the assay would be significantly less than at the beginning of the assay. For example, if the E/T ratio is 25:1, target cells (CTO/TFL2-positive) account for only 3.8% of total cells; by the end of the assay, only 1% of CTO⁺ cells may remain. This target cell loss has been shown to be antigen specific and effector cell dependent, and therefore, the portion of lost target cells should be considered in the calculation of total target cell death to avoid underestimation of cytotoxic activity.
7. Additional surface marker staining of target and/or effector cells can be done following caspase substrate incubation. Do not fix or permeabilize cells that have been incubated with the caspase substrate for antibody labeling. Fixation will cause caspase labeling to be lost. Samples can be stored at 4°C overnight without significant loss of fluorescence signals.

Acknowledgments

We wish to thank Ann Chahroudi, Guido Silvestri, and John Altman for their very helpful intellectual and practical contributions to the development of the FCC assay, and Marcus Altfeld, William Rodriguez, and Bruce Walker for their generous provision of HIV-specific CTL clones and advice concerning their

propagation and use. Development of the FCC assay was facilitated by support to Mark Feinberg from the National Institutes of Health (R21 AI49089).

References

1. Meier, P., Finch, A., and Evan, G. (2000) Apoptosis in development. *Nature* **407**, 796–801.
2. Raulet, D. H., Vance, R. E., and McMahon, C. W. (2001) Regulation of the natural killer cell receptor repertoire. *Annu. Rev. Immunol.* **19**, 291–330.
3. Brunner, K. T., Mauel, J., Cerottini, J. C., and Chapuis, B. (1968) Quantitative assay of the lytic action of immune lymphoid cells on 51-Cr-labelled allogeneic target cells in vitro; inhibition by isoantibody and by drugs. *Immunology* **14**, 181–196.
4. McElrath, M. J., Siliciano, R. F., and Weinhold, K. J. (1997) HIV type 1 vaccine-induced cytotoxic T cell responses in phase I clinical trials: detection, characterization, and quantitation. *AIDS Res. Hum. Retroviruses* **13**, 211–216.
5. Doherty, P. C. and Christensen, J. P. (2000) Accessing complexity: the dynamics of virus-specific T cell responses. *Annu. Rev. Immunol.* **18**, 561–592.
6. Nociari, M. M., Shalev, A., Benias, P., and Russo, C. (1998) A novel one-step, highly sensitive fluorometric assay to evaluate cell-mediated cytotoxicity. *J. Immunol. Methods* **213**, 157–167.
7. Radosevic, K., Garritsen, H. S., Van Graft, M., De Grooth, B. G., and Greve, J. (1990) A simple and sensitive flow cytometric assay for the determination of the cytotoxic activity of human natural killer cells. *J. Immunol. Methods* **135**, 81–89.
8. Altman, J. D., Moss, P. A. H., Goulder, P. J. R., et al. (1996) Phenotypic analysis of antigen-specific T lymphocytes [published erratum appears in *Science* **280**, 1821 (1998)]. *Science* **274**, 94–96.
9. Butz, E. A. and Bevan, M. J. (1998) Massive expansion of antigen-specific CD8+ T cells during an acute virus infection. *Immunity* **8**, 167–175.
10. Maino, V. C. and Picker, L. J. (1998) Identification of functional subsets by flow cytometry: intracellular detection of cytokine expression. *Cytometry* **34**, 207–215.
11. Appay, V., Nixon, D. F., Donahoe, S. M., et al. (2000) HIV-specific CD8(+) T cells produce antiviral cytokines but are impaired in cytolytic function. *J. Exp. Med.* **192**, 63–75.
12. Lee, P. P., Yee, C., Savage, P. A., et al. (1999) Characterization of circulating T cells specific for tumor-associated antigens in melanoma patients. *Nat. Med.* **5**, 677–685.
13. Zajac, A. J., Blattman, J. N., Murali-Krishna, K., et al. (1998) Viral immune evasion due to persistence of activated T cells without effector function [see comments]. *J. Exp. Med.* **188**, 2205–2213.
14. Packard, B. Z. and Komoriya, A. (1998) Tumor cell recognition by lymphocytes: is the MHC always essential? *Crit. Rev. Immunol.* **18**, 139–144.
15. Sheehy, M. E., McDermott, A. B., Furlan, S. N., Klenerman, P., and Nixon, D. F. (2001) A novel technique for the fluorometric assessment of T lymphocyte antigen specific lysis [erratum appears in *J. Immunol. Methods* **252**, 219–220 (2001)]. *J. Immunol. Methods* **249**, 99–110.

16. Lecoœur, H., Fevrier, M., Garcia, S., Riviere, Y., and Gougeon, M. L. (2001) A novel flow cytometric assay for quantitation and multiparametric characterization of cell-mediated cytotoxicity. *J. Immunol. Methods* **253**, 177–187.
17. Liu, L., Chahroudi, A., Silvestri, G., et al. (2002) Visualization and quantification of T cell-mediated cytotoxicity using cell-permeable fluorogenic caspase substrates. *Nat. Med.* **8**, 185–189.
18. Packard, B. Z., Toptygin, D. D., Komoriya, A., and Brand, L. (1996) Profluorescent protease substrates: intramolecular dimers described by the exciton model. *Proc. Natl. Acad. Sci. USA* **93**, 11,640–11,645.
19. Komoriya, A., Packard, B. Z., Brown, M. J., Wu, M. L., and Henkart, P. A. (2000) Assessment of caspase activities in intact apoptotic thymocytes using cell-permeable fluorogenic caspase substrates. *J. Exp. Med.* **191**, 1819–1828.
20. Ploegh, H. L. (1998) Viral strategies of immune evasion. *Science* **280**, 248–253.
21. Xu, X. N., Screaton, G. R., Gotch, F. M., et al. (1997) Evasion of cytotoxic T lymphocyte (CTL) responses by nef-dependent induction of Fas ligand (CD95L) expression on simian immunodeficiency virus-infected cells. *J. Exp. Med.* **186**, 7–16.
22. Restifo, N. P. (2000) Not so Fas: Re-evaluating the mechanisms of immune privilege and tumor escape. *Nat. Med.* **6**, 493–495.
23. Collins, K. L., Chen, B. K., Kalams, S. A., Walker, B. D., and Baltimore, D. (1998) HIV-1 Nef protein protects infected primary cells against killing by cytotoxic T lymphocytes. *Nature* **391**, 397–401.

8

Multiparametric Analysis of Apoptosis by Flow and Image Cytometry

William G. Telford, Akira Komoriya, and Beverly Z. Packard

Summary

Flow cytometric assays for apoptosis are now in widespread use. The multiparametric nature of flow cytometry allows multiple assays for several apoptotic characteristics to be combined in a single sample, providing a powerful tool for elucidating the complex progression of apoptotic death in a variety of cell types. This chapter describes one such assay, allowing simultaneous analysis of caspase activation, annexin V binding to “flipped” phosphatidylserine residues and membrane permeability to DNA binding dyes. This multidimensional approach to analyzing apoptosis provides far more information than single-parameter assays that provide only an ambiguous “percent apoptotic” result, given that multiple early, intermediate, and late apoptotic stages can be visualized simultaneously. This multiparametric approach is also amenable to a variety of flow cytometric instrumentation, both old and new.

Key Words

7-Aminoactinomycin D, annexin V, apoptosis, caspase, flow cytometry, propidium iodide.

1. Introduction

The importance of apoptosis in the regulation of cellular homeostasis has mandated the development of accurate assays capable of measuring this process. Apoptosis assays based on flow cytometry have proven particularly useful; they are rapid, quantitative, and provide a individual cell-based mode of analysis (rather than a bulk population) (*1*). The multiparametric nature of flow cytometry also allows the detection of more than one cell death characteristic to be combined in a single assay. For example, apoptosis assays that utilize DNA dyes as plasma membrane permeability indicators (such as propidium iodide [PI]) can be combined with assays that assess different cellular responses associated with cell death, including mitochondrial membrane potential and

From: *Methods in Molecular Biology: Flow Cytometry Protocols*, 2nd ed.
Edited by: T. S. Hawley and R. G. Hawley © Humana Press Inc., Totowa, NJ

annexin V binding to “flipped” phosphatidylserine (PS) (2–4). Combining measurements for cell death into a single assay has a number of important advantages; it provides simultaneous multiple confirmation of apoptotic activity (important in a process that has proven highly pleiotrophic in phenotype). It also provides a much more comprehensive and multidimensional picture of the entire cell death program.

Recognition of the pivotal role of caspases in the death process has led to the recent development of assays that can measure these important enzymes *in situ*. Caspase activation represents one of the earliest measurable markers of apoptosis (5). In most cases, caspase activation precedes degradation in cell permeability, DNA fragmentation, cytoskeletal collapse, and PS “flipping,” and is likely important in triggering these later manifestations of cell death. Combining fluorogenic assays for caspase activity with fluorescence-based assays for later manifestations of cell death (such as membrane alterations and loss of membrane permeability) can provide a very information-intensive view of cell death, particularly in its early stages (when most of the relevant biochemical signaling activities occur and are likely to still be intact prior to complete cell structural collapse) (6–10).

Several fluorogenic assays for caspase activity have been described in the literature, including the OncoImmunin PhiPhiLux system and the FLICA substrates (11–16). In this chapter, we describe the integration of the PhiPhiLux caspase substrate system with two simultaneous assays for later manifestations of cell death, namely annexin V binding to “flipped” PS residues and cell membrane permeability to a DNA binding dye (16). The PhiPhiLux caspase substrates have several notable characteristics; they are cell permeable, demonstrate relatively good caspase specificity, possess high signal-to-noise ratios between their uncleaved and cleaved forms, and have fluorescence spectral properties that are compatible with other fluorescent probes (14–16). The ability to measure three apoptotic phenotypes in a single assay provides a powerful and comprehensive view of the apoptotic process, applicable to both suspension cells by traditional flow cytometry, and adherent cells using laser scanning cytometry (16). This assay can be adapted to both current and older flow cytometers.

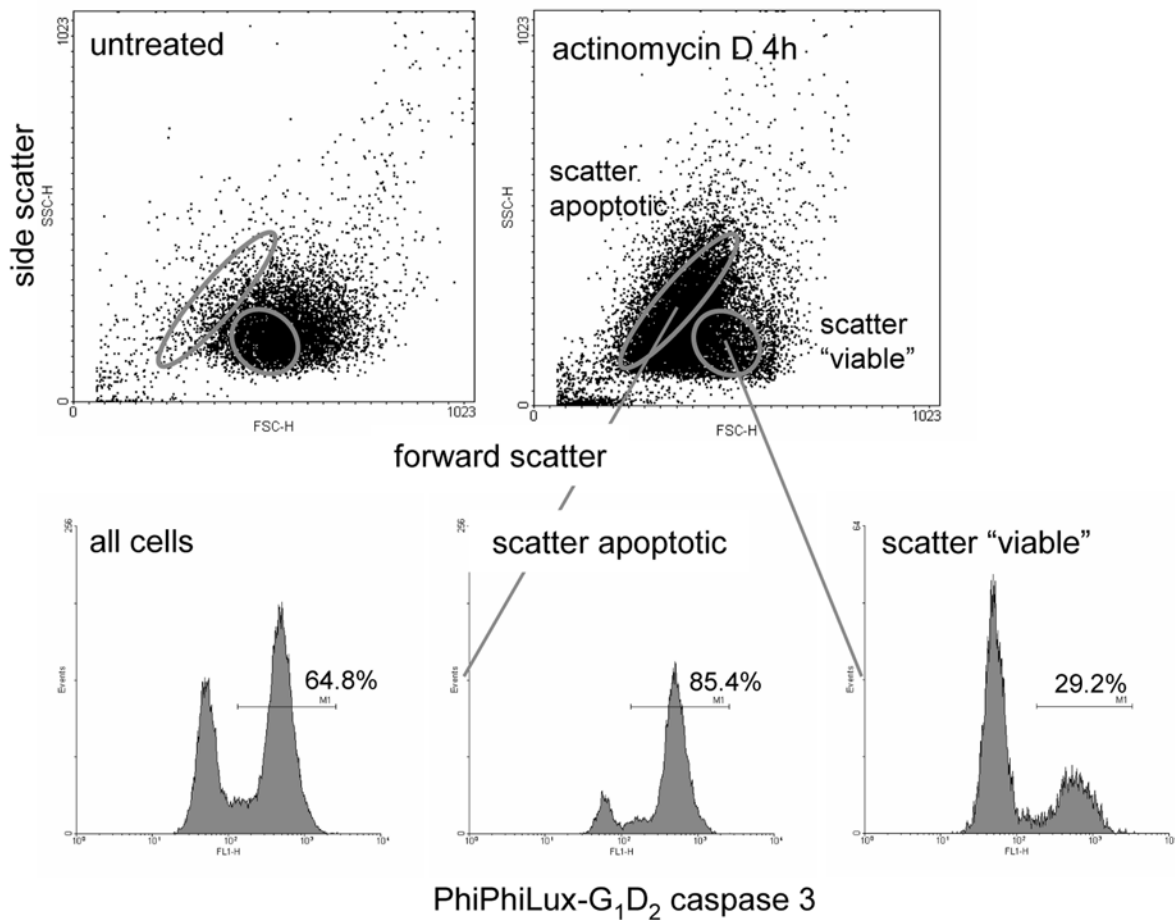
2. Materials

1. PhiPhiLux- G_1D_2 fluorogenic caspase 3 substrate (OncoImmunin, Inc., Gaithersburg, MD): OncoImmunin makes a wide variety of fluorogenic enzyme substrates that become fluorescent upon cleavage. The fluorogenic caspase 3/7 substrate (termed PhiPhiLux- G_1D_2) consists of an 18-amino-acid peptide constituting the recognition and cleavage sequence from poly(ADP-ribose) polymerase (PARP), a physiological target for caspase 3 (17). The substrate is homodoubly labeled with fluorophores (in this case, one similar in properties to fluorescein) on opposite

sides of the molecule; in this conformation, the fluorochrome molecules are in close physical proximity ($<15 \text{ \AA}$), and the fluorescence of the resulting complex is largely quenched (**15,18**). After the substrate enters a cell by passive diffusion and is cleaved by caspase 3 (or 7), the unquenched fluorescent fragments will be retained on the side of the membrane where the cleavage took place. This is attributable to the fact that these singly labeled peptides have very low membrane permeability as compared with the intact substrate, allowing the cleaved fragments to remain in the cell for several hours (**15,18**).

- a. PhiPhiLux- G_1D_2 can be excited with a standard 488-nm laser found on most flow cytometers, and is spectrally compatible with PI or 7-aminoactinomycin D (7-AAD) (which will be subsequently used for measuring apoptotic cell permeability) and either phycoerythrin (PE)- or allophycocyanin (APC)-conjugated annexin V (for detection of PS “flipping” during apoptotic death).
 - b. The PhiPhiLux reagents are largely nonfluorescent in the uncleaved state and is extremely bright on caspase activation. The expected signal-to-noise ratio between unlabeled and substrate-loaded viable and apoptotic cells is shown in **Fig. 1**, where actinomycin D-treated EL-4 thymoma cells were labeled with PhiPhiLux G_1D_2 and analyzed by flow cytometry; the apoptotic cells possess one to three orders of magnitude higher fluorescence than the presumably viable cell population. It should be noted that primary cell cultures may show somewhat lower levels of caspase activation than cell lines, with subsequent lower levels of substrate fluorescence (*see Note 1*).
 - c. The PhiPhiLux reagents are also available with other fluorescent tags, including a rhodamine-like fluorochrome (requiring a green excitation source, not commonly available on commercial flow cytometer systems), and a proprietary Cy5-like fluorochrome that can be excited with a red laser. While the rhodamine-conjugated caspase substrates are not commonly used for flow cytometry because of their excitation requirements, the Cy5-like substrate can be used on flow cytometers equipped with a red laser source. They can also be combined with the fluorescein-like PhiPhiLux- G_1D_2 substrate for detection of multiple caspases in a single assay, as shown in **Fig. 4**.
 - d. The PhiPhiLux reagents are commercially provided at concentrations of 5–10 μM in sealed aliquots and can be stored at 4°C prior to opening; once the ampule is opened, any remaining substrate should be stored at -20°C . Avoid repeated freezing and thawing.
2. PE- or APC-conjugated annexin V (e.g., Caltag Laboratories, Burlingame, CA): Annexin V is available conjugated to a variety of fluorochromes, and binds tightly to apoptotic cells with “flipped” PS residues on their extracellular membrane leaflet. It should be noted that damaged or necrotic cells with a high degree of membrane permeability will also bind annexin V to their intracellular membrane leaflet, despite their questionable apoptotic nature; therefore, a DNA binding dye as a cell permeability indicator should always be incorporated into annexin V binding assays.
 3. PI: PI is an intercalating DNA binding dye available from a wide variety of sources. It excites at 488 nm and emits in the 570–630 nm range. It should be

144



dissolved in deionized water at 1 mg/mL and stored in the dark at 4°C for up to 3 mo.

4. 7-aminoactinomycin D (Sigma Chemical Co., St. Louis, MO or Molecular Probes, Eugene, OR): 7-AAD is a DNA binding dye that excites at 488 nm and emits in the far red, with an emission peak at approx 670 nm. 7-AAD can be used as an alternative to PI where a longer wavelength cell permeability probe is desired. 7-AAD should be dissolved in 95% ethanol at 1 mg/mL and stored at -20°C. Solubilized stocks are good for three months. Diluted stocks should be used within 24 h. *See Note 2.*
5. Wash buffer: Dulbecco's phosphate-buffered saline (PBS) (containing calcium and magnesium) supplemented with 2% fetal bovine serum. This is used for cell washing prior to DNA dye addition.
6. Complete medium: RPMI-1640 and 10% fetal bovine serum.

3. Methods

3.1. Combinations of Fluorochromes

This assay introduces fluorescent labels for three characteristics of cell apoptosis: caspase activation, PS “flipping,” and cell permeability. There is some flexibility of fluorochrome selection for the investigator depending on the flow cytometric instrumentation available. Two possible combinations are described below, one for analysis on instruments equipped with a single 488-nm argon-ion laser, and the second on instruments equipped with dual 488 nm/red diode or red helium–neon (He–Ne) lasers.

1. Single 488-nm laser instruments: Examples of these include the Becton-Dickinson FACSscan (or single laser FACSort or FACSCalibur) (BD Biosciences, San Jose, CA), and the Beckman Coulter XL (Beckman Coulter, Miami, FL) flow cytometers. The following combination should be used when analysis is limited to this instrument type:
 - a. PhiPhiLux-G₁D₂ (similar to fluorescein): This fluorochrome will occupy the fluorescein isothiocyanate (FITC) detector channel on most commercial instruments.
 - b. PE-conjugated annexin V: This fluorochrome will be detected in the phycoerythrin channel of most instruments. Some fluorescent compensation will be required to separate the PE signal from PhiPhiLux-G₁D₂ and 7-AAD.

Fig. 1. (*see facing page*) Caspase activation in apoptotic cells. EL-4 cells were incubated with no treatment or with actinomycin D at 5 µg/mL for 4 h, followed by labeling with PhiPhiLux-G₁D₂. **Top** dot plots show forward vs side scatter profiles for both untreated and drug-treated cells. **Lower** histograms show caspase activation distributions for all actinomycin D-treated cells (**left**), scatter apoptotic cells only (**middle**), and scatter “viable” cells (**right**).

- c. 7-AAD: This far-red emitting DNA binding dye can be detected in the far red (or PE-Cy5) detector of most commercial instruments.
2. Dual 488-nm/red laser-equipped instruments: Several more recent benchtop flow cytometers are equipped with more than one laser, most commonly a red source (such as a 635-nm red diode or 633-nm red He-Ne laser). The Becton-Dickinson FACSsort, FACSCalibur, LSR and LSR II fall into this category, as does the Beckman Coulter FC500. A red laser allows several red-excited fluorochromes to be incorporated into flow cytometry assays, including APC. Another group of PhiPhiLux caspase substrates incorporating a proprietary red-excited fluorochrome analogous to Cy5 can also be used on these instruments. The following combination is suggested for dual-laser instrumentation:
 - a. PhiPhiLux- G_1D_2 (similar to fluorescein): This fluorochrome will occupy the FITC detector channel on most commercial instruments.
 - b. APC-conjugated annexin V: This fluorochrome can be excited with either red diode or He-Ne lasers and emits in the far red range. It requires little fluorescent color compensation to separate its signal from PhiPhiLux- G_1D_2 or the DNA binding dyes described in **step2**.
 - c. PI or 7-AAD: Both of these DNA binding dyes can be incorporated into a cell death assay with PhiPhiLux- G_1D_2 and APC-annexin V. Both are detected through the far red detector channel (usually with a mid-600-nm bandpass or longpass filter) on most flow cytometers.
3. Other fluorochrome combinations: Multilaser flow cytometers with unusual wavelength laser sources are becoming more common in flow cytometry. Similarly, the number of fluorochromes available for flow cytometry is increasing exponentially. Other fluorochrome combinations for the above assays are certainly possible and can be considered by the experienced investigator, particularly if additional fluorescence-based apoptotic assays are to be incorporated into the assay described in **Subheading 3.6**.

3.2. Preparation of Cells

1. Harvest suspension cell lines or cultured primary cells; transfer to 12×75 mm cell culture tubes.
2. Centrifuge cells at 400g for 5 min and decant supernatant. Nearly complete removal of the supernatant is critical for the steps that follow; the amount of remaining supernatant should be as low as possible. Although cells can be washed prior to labeling, performing the assay in the remaining complete media supernatant will reduce the amount of cell death occurring during the assay. If cells are obtained from clinical or other in vivo sources, they should be centrifuged and resuspended in complete medium prior to use, then centrifuged and decanted as described above.
3. Label $0.5\text{--}2 \times 10^6$ cells per sample; increasing this number will reduce caspase and annexin V labeling efficiency. Adherent cells pose special challenges for apoptotic analysis due to the trauma associated with cell dissociation; analysis in the

adherent state by laser scanning cytometry is preferable to suspension flow cytometry under these circumstances (see **Note 3**).

4. EL-4 cells treated with actinomycin D at 5 $\mu\text{g}/\text{mL}$ for 4 h were used to illustrate this assay in **Figs. 1–4**. This cell system also can make a useful positive control for more general use. See **Note 1**.

3.3. Fluorogenic Caspase Substrate Labeling

Cells are initially loaded with the PhiPhiLux caspase substrate. Substrate concentration and incubation time are critical factors in cell-permeable substrate labeling.

1. Tap each tube to resuspend the cell pellet in the remaining supernatant. The supernatant in the tubes will be approx 50 μL in volume.
2. Add 50 μL of the PhiPhiLux reagent to each tube and shake gently. The PhiPhiLux reagent should be diluted as little as possible for maximum detection, hence the need for minimal sample supernatant. For an initial PhiPhiLux reagent solution concentration of 10 μM , this will give a final concentration between 3 and 5 μM . For optimal labeling, the PhiPhiLux reagent can be titrated between 0.5 and 5 μM , although this should be done with caution (see **Note 4**).
3. Incubate the tubes for 45 min at 37°C.

3.4. Annexin V Labeling

Cells are now labeled with fluorochrome-conjugated annexin V. Since centrifuge washings are minimized in this method to reduce assay-associated cell death, the cells are not washed following caspase substrate loading but are labeled immediately with fluorochrome-conjugated annexin V. Because most cell culture media and serum supplements contain calcium and magnesium, it is assumed that cation concentrations are sufficient to allow annexin V binding to “flipped” PS residues. Subsequent cell washing is done in wash buffer (containing calcium and magnesium) to maintain annexin V binding. See **Note 5**.

1. Remove the above tubes after 45 min of incubation and add the appropriate fluorochrome-conjugated annexin V (in this case, either PE or APC). Annexin V is generally available in suspension at concentrations ranging from 0.1 to 1 mg/mL . Cell labeling should be carried out at approx 0.5–5 μg annexin V per sample. Therefore, 0.5–5 μL of a 1 mg/mL annexin V solution would be added to the above tubes (now at approx 100–150 μL total volume). Again, fluorochrome-conjugated annexin V labeling should be titrated in advance of actual use.
2. Incubate at room temperature for 15 min.
3. Add 3 mL of the wash buffer to each tube. Centrifuge at 400g for 5 min, and decant the supernatant.

3.5. DNA Binding Dye Labeling

Depending on the instrumentation available, cells can be subsequently labeled with either PI or 7-AAD for assessment of cell permeability in the later stages of apoptosis (6). PI should be used with dual laser instruments, as it is spectrally compatible with both the PhiPhiLux-G₁D₂ substrate and APC; while it can be used with PE, the significant spectral overlap between the two fluorescent molecules makes this inadvisable. The DNA binding dye 7-AAD can be used with either single- or dual-laser instrument configurations, as it is spectrally compatible with all of the above fluorochromes. (See **Note 2**.)

1. Prepare a solution of either PI at 2 µg/mL or 7-AAD at 5 µg/mL in complete medium.
2. Once the above tubes are decanted, add 0.5 mL of either the PI or 7-AAD solution. Samples should then be maintained at room temperature and *analyzed within 60 min*. See **Note 6**.

3.6. Flow Cytometric Analysis

Cells should be analyzed as quickly as possible to minimize post-assay apoptotic death. The instrument should be set up and ready for sample acquisition immediately on completion of the assay. The choice of fluorescent reagents for both single- and dual-laser flow cytometers is described above; fluorescent detector assignments and analysis issues are described here.

1. PhiPhiLux-G₁D₂: This fluorescein-like caspase substrate is analyzed through the fluorescein or FITC channel on most flow cytometers (often with the arbitrary designation of “FL1”), usually equipped with a 530/30 nm or similar narrow bandpass filter. The spectral properties of the PhiPhiLux-G₁D₂ fluorochrome is similar to fluorescein, requiring some color compensation when used simultaneously with PE or PI (and to a lesser extent with 7-AAD).
2. PE-conjugated annexin V: Like most PE-conjugated reagents, this reagent is detected through the PE channel on most cytometers (frequently with the designation “FL2”), usually equipped with a 575/26-nm or similar bandpass filter. PE requires color compensation when used with PhiPhiLux-G₁D₂ and 7-AAD.
3. APC-conjugated annexin V: APC is excited with a red laser source and detected through the APC channel on many flow cytometers (sometimes with an “FL4” designation) using a 660/20-nm or similar bandpass filter. An advantage of APC in multicolor assays is its minimal need for color compensation; there is no significant spectral overlap between PhiPhiLux-G₁D₂, PI, or 7-AAD.
4. PI: This DNA binding dye is extremely bright even at low concentrations, and has a broad emission range, necessitating compensation when used with PhiPhiLux-G₁D₂. It can be detected in either the PE or far red detection channel (with either the PE 575/26-nm filter or a longer red optic), with the latter choice being preferable to reduce spillover into the fluorescein detector.

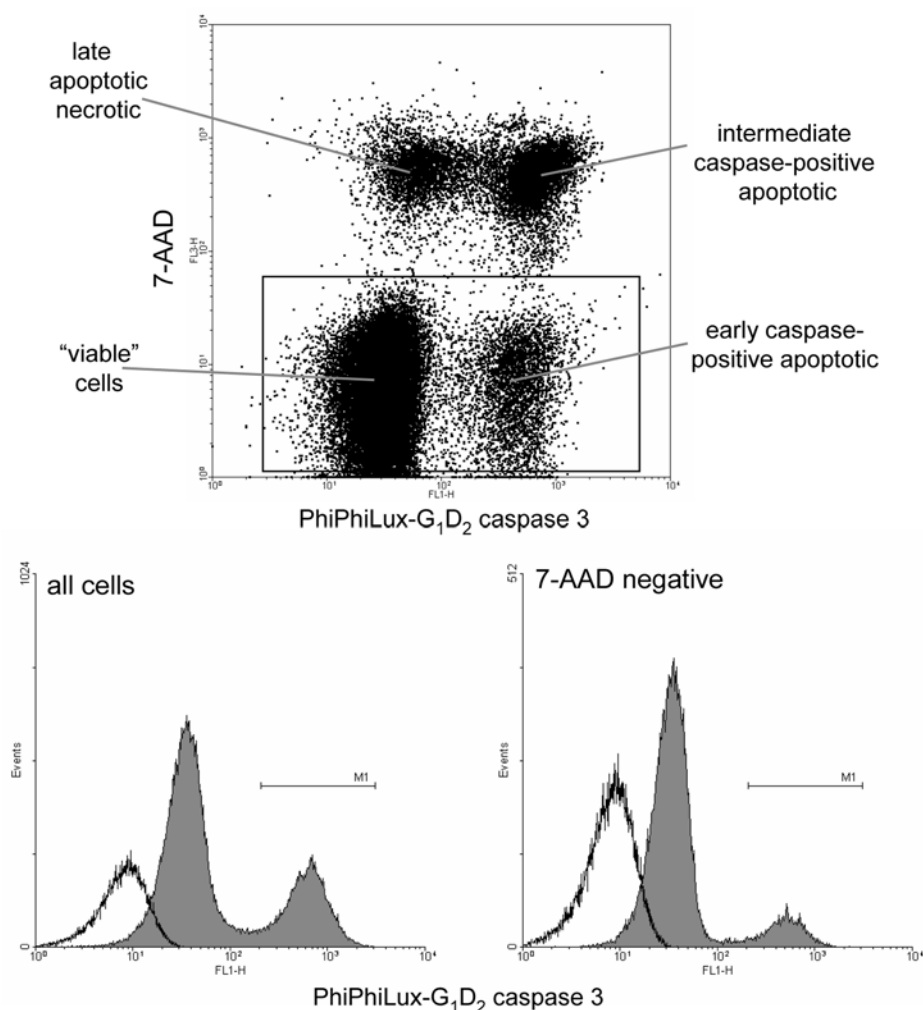


Fig. 2. Caspase activation and 7-AAD permeability in apoptotic cells. EL-4 cells were incubated with actinomycin D at 5 $\mu\text{g}/\text{mL}$ for 4 h, followed by labeling with PhiPhiLux-G₁D₂ and 7-AAD at 5 $\mu\text{g}/\text{mL}$. **Top** dot-plot shows caspase activation vs 7-AAD permeability protocols, with the four major populations of “viable” and apoptotic cells identified. **Lower** histograms show caspase activation distributions for all cells (**left**) and 7-AAD-negative cells, derived from the indicated cytogram gate (**right**). Cell controls with no PhiPhiLux-G₁D₂ loading are shown in the open histogram peaks.

5. 7-AAD: This DNA binding dye is dimmer than PI and emits in the far red, allowing its detection in the far red channel on most flow cytometers (often designated “FL3”) with a 675/20-nm bandpass or 650-nm longpass dichroic or similar filter. Compensation will be required when used with PhiPhiLux G₁D₂ and PE. 7-AAD

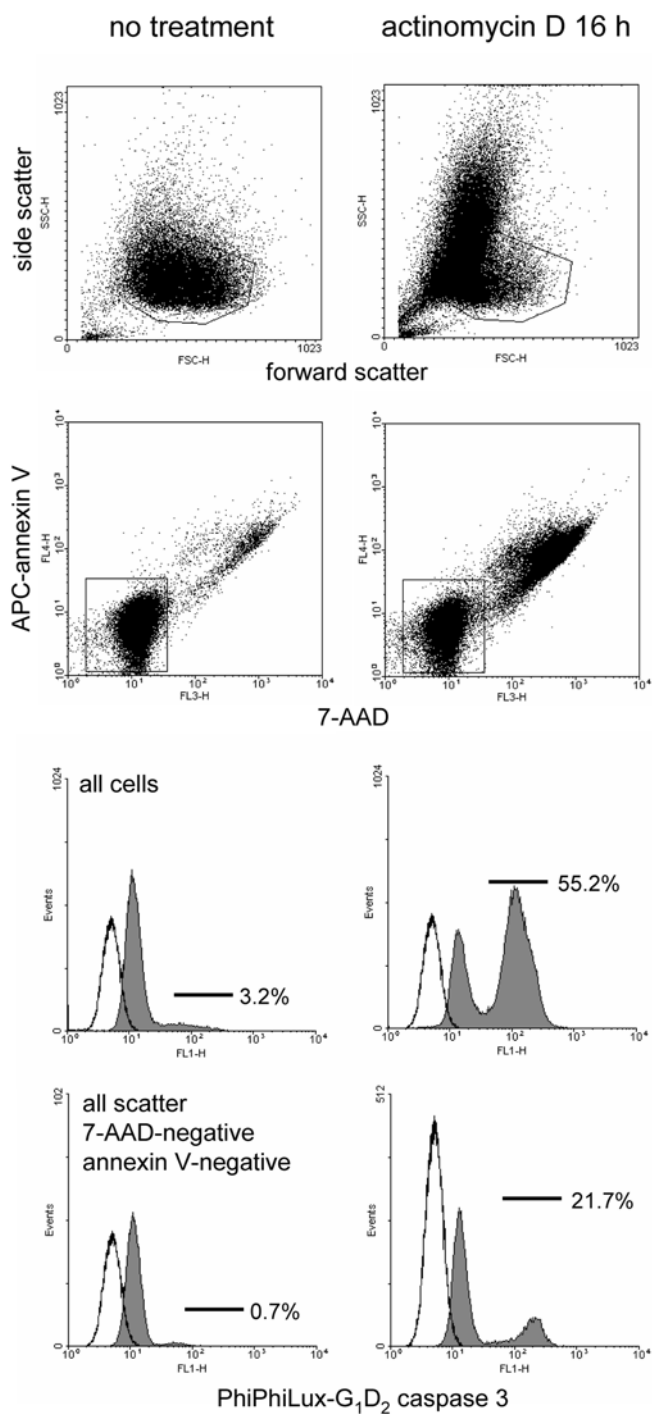
has an unexplained ability to slightly quench PE fluorescence in some multicolor assay systems, so this should be taken into account during instrument setup.

3.7. Gating for Flow Cytometry

Gating at several levels is critical for meaningful analysis of apoptosis. A typical gating scheme is illustrated in **Fig. 3** and is described in more detail in **Subheading 3.9**. Some general guidelines are listed here.

1. Scatter gating: Many cell lines and some primary cells show a dramatic alteration in forward and side scatter measurements (rough indicators of cell size and optical density, respectively) late in the onset of apoptosis. It is therefore tempting to draw a gate around the scatter “viable” population, and look at caspase activation, annexin V binding and DNA dye uptake in these cells alone as measures of early cell death. However, there is considerable evidence that the scatter apoptotic population (shown in **Fig. 1**) may in fact contain some viable cells that have undergone a transient shift in cell volume well prior to other “early” markers of cell death such as caspase activation. It is therefore advisable to gate the entire scatter population (excluding obvious debris) for the most accurate analysis of cell death. Subsequent gating of the “viable” population (which may in fact contain early apoptotic cells) can be done at the level of annexin V binding and DNA dye incorporation.
2. Annexin V binding and DNA binding dye exclusion: These markers usually occur after caspase activation and are considered “later” markers of apoptosis. Therefore, annexin V and DNA binding dye positive and negative subpopulations can be gated for discrimination of “early” and “late” apoptotic cells. Subsequent analysis of caspase activation in these subsets can further delineate the early stages of cell death, as illustrated in **Fig. 3**.
3. PI vs 7-AAD: As pointed out in **Note 2**, PI and 7-AAD are not completely interchangeable with regard to exclusion by apoptotic cells; 7-AAD is somewhat more cell permeable than PI and will label an earlier subset of apoptotic cells. If 7-AAD-positive cells are excluded from the analysis (in an attempt to quantify very early apoptotic events), this greater cell permeability will result in a lower

Fig. 3. (*see facing page*) Caspase activation, annexin V binding, and 7-AAD permeability in apoptotic cells. EL-4 cells were incubated with no treatment or with actinomycin D at 5 $\mu\text{g}/\text{mL}$ for 4 h, followed by labeling with PhiPhiLux- G_1D_2 , APC-conjugated annexin V, and 7-AAD at 5 $\mu\text{g}/\text{mL}$. The **top two** dot plots show forward vs side scatter profiles for both untreated and drug-treated cells; the **next two** dot plots show APC-annexin V vs 7-AAD permeability profiles for the same cells. The **third row** of histograms show caspase activation distributions for all cells, not gated for any other parameters; the **fourth row** for 7-AAD-negative annexin V-negative cells, with no gating for scatter characteristics. Percentage caspase-positive cells are shown. Cell controls with no PhiPhiLux- G_1D_2 loading are shown in the open histogram peaks.



apparent number of caspase-positive cells that are DNA dye-negative. This exclusion should be kept in mind when analyzing these early apoptotic subsets.

3.8. Simultaneous Immunophenotyping

The protocol in **Subheading 3.7.** is very compatible with simultaneous antibody immunophenotyping of the “viable” subpopulation. For example, PE-conjugated antibodies against a marker of interest could be combined with PhiPhiLux-G₁D₂, 7-AAD and APC-annexin V labeling as a very stringent “filter” for the removal of dead cells from the phenotyping analysis. While a natural extension of this method would appear to be the immunophenotyping of early apoptotic cells (such as caspase-positive/7-AAD negative/annexin V-negative), this should be approached with caution (*see Note 7*).

3.9. Sample Results

Sample results for fluorogenic caspase substrate labeling are shown below. In all of the illustrated results, apoptosis was induced in EL-4 murine thymoma cells by treatment with the transcriptional inhibitor actinomycin D for 4 h. This cell cycle blocker rapidly induced apoptosis via the caspase 3 pathway in many rapidly dividing cell lines. **Figures 1–4** both illustrate the expected results for the individual components of the multiparametric cell death assay described above, and demonstrate how the simultaneous analysis of multiple cell death characteristics in a single assay gives a multidimensional picture of the total apoptotic process.

1. Fluorescence distribution of PhiPhiLux-G₁D₂ labeling: **Figure 1** illustrates the typical signal-to-noise ratio between “viable” and apoptotic EL-4 cells labeled with the PhiPhiLux-G₁D₂ substrate (here without subsequent annexin V and DNA binding dye labeling). Drug-treated EL-4 cells were analyzed for forward vs side scatter, where easily distinguishable populations of “viable” and “apoptotic” cells were distinguishable based on cell size and optical density. The total population, the scatter “viable,” and scatter apoptotic populations were then gated for PhiPhiLux-G₁D₂ fluorescence. The caspase substrate was readily detectable in the fluorescein channel by flow cytometry, in this case on a Becton-Dickinson FACSCalibur. The substrate is largely nonfluorescent in the uncleaved state; signal-to-noise ratios of 1–3 log orders of magnitude are normally seen between “viable” and apoptotic cells loaded with PhiPhiLux-G₁D₂, making the discrimination of apoptotic cells unambiguous.

Interestingly, the “viable” and apoptotic distribution based on scatter measurements does not strictly correlate with caspase activation. The scatter “viable” cells in fact have a significant percentage of caspase-positive cells, indicating that cells activate caspases prior to gross changes in scatter morphology. Even more interesting, the scatter apoptotic population has some caspase-negative cells. While

some of these cells may be advanced apoptotic or necrotic cells with diminished or degraded caspase activity, there may also be viable cells in this population. Previous studies have demonstrated that cells may undergo transient volume fluctuations as a very early apoptotic marker, well prior to caspase activation. These results indicate the importance of not gate-excluding cells from subsequent apoptotic analysis based on their apparently apoptotic scatter characteristics; this population may contain some of the earliest detectable apoptotic cells.

2. PhiPhiLux-G₁D₂ and 7-AAD labeling. **Figure 2** shows the addition of 7-AAD labeling to the PhiPhiLux-G₁D₂ assay. The cytogram at the top of the figure shows 7-AAD labeling versus caspase activation for drug-treated EL-4 cells. Even with only two probes for apoptosis, four distinct subpopulations are apparent: a “viable” population at lower left, a caspase-positive population that has not progressed to 7-AAD permeability (lower right), and a caspase-positive population that is permeable to 7-AAD (upper right). Interestingly, a fourth population is also apparent that is permeable to 7-AAD but has little caspase activity. These cells are probably necrotic or advanced apoptotics, where caspases have leaked out of the cells, or have been proteolytically digested. Another potential source of this population is cells that have undergone apoptosis in the incubation period following PhiPhiLux labeling but prior to flow analysis. Cells in this region demonstrate the importance of analyzing cells promptly at the completion of the assay, as apoptosis is still occurring.

Although we included all cells based on scatter in this analysis, 7-AAD labeling can now be used to exclude the more advanced apoptotics for specific measurement of the earlier dying cells. The left-most histogram shows caspase activation for all cells, while the histogram on the right is gated for 7-AAD-negative cells. Caspase activation is therefore clearly occurring prior to 7-AAD permeability.

3. PhiPhiLux-G₁D₂, 7-AAD and APC-annexin V labeling. **Figure 3** shows simultaneous analysis of all three cell death phenotypes in a single assay. The top two cytograms show the scatter characteristics of untreated and drug-treated EL-4 cells. The next two cytograms shown APC-annexin V binding vs 7-AAD permeability, ungated for scatter. These two characteristics appear to occur at approximately the same time for this cell type, with almost no single-positive cells for either phenotype. The histograms below were then gated for either the entire population, or APC-annexin V and 7-AAD-negative fluorescence. As above, these “early” apoptotics negative for PS “flipping” and loss of membrane permeability have a significant component of caspase-positive cells.
4. Detection of multiple caspases by flow cytometry. As was described in **Subheading 3.6.**, the PhiPhiLux system can incorporate a number of both consensus peptides for different caspase specificities, and fluorochromes for flow cytometric detection. It is therefore possible to load cells with more than one PhiPhiLux reagent, if they possess specificity for different caspases, and if they can be spectrally distinguished from one another by flow cytometry. In **Fig. 4**, apoptotic EL-4 cells have been loaded with PhiPhiLux-L₁D₂, which incorporates a caspase 8 consensus peptide instead of caspase 3/7 (**19**), and PhiPhiLux-

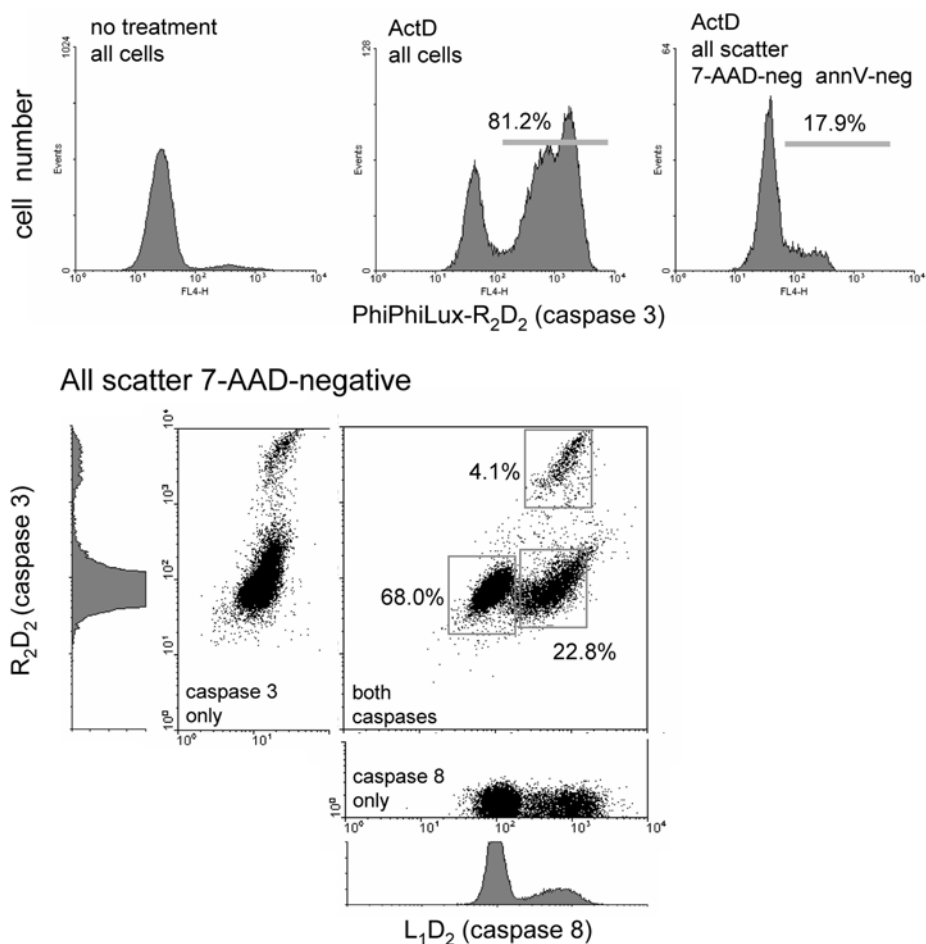


Fig. 4. Multiple caspase activation and 7-AAD permeability in apoptotic cells. EL-4 cells were incubated with no treatment or with actinomycin D at 5 μ g/mL for 4 h, followed by labeling with PhiPhiLux-L₁D₂ (specific for caspase 8) and PhiPhiLux 3-R₂D₂ (specific for caspase 3), PE-conjugated annexin V and 7-AAD at 5 μ g/mL. The **top row** of histograms shows caspase 3 activation distributions using the red-excited PhiPhiLux-3-R₂D₂ substrate for all untreated cells (**left**), all drug-treated cells (**middle**), and annexin V-negative 7-AAD-negative drug-treated cells (**right**). The dot-plot **below** shows PhiPhiLux-L₁D₂ (caspase 8) vs PhiPhiLux-3-R₂D₂ (caspase 3) distributions for 7-AAD-negative cells (no scatter gate). Histograms of **plot fragments** on the **left** and **below** show single caspase substrate labeling controls. Percentages for caspase-positive populations are shown.

3-R₂D₂, which possesses the PARP consensus peptide and incorporates a proprietary Cy5-like red-excited fluorochrome. The cells were subsequently labeled with PE-conjugated annexin V and 7-AAD and analyzed on a dual-laser Becton-Dickinson FACSCalibur flow cytometer. The three histograms at the top of the figure show the caspase 3 activation profiles for untreated, all drug-treated, and annexin V-negative/7-AAD-negative drug-treated cells using this novel red-excited substrate; the profiles are similar to the PhiPhiLux-G₁D₂ reagent illustrated above. The dual caspase labeling experiment is shown in accompanying cytogram, gated for 7-AAD-negative cells. A caspase 8-positive caspase 3-negative population is clearly visible, consistent with previous biochemical observations that show caspase 8 activation to be necessary for caspase 3 activation. No caspase 3-positive caspase 8-negative population is present. This modification to the multiparametric cell death assay allows an even earlier stage of cell death to be distinguished and identified.

These collective results are consistent with many immune cell types and established cell lines; however, wider variations in apoptotic phenotype between different cell types should be expected (*see Note 8*).

4. Notes

1. Controls: Both “viable” and apoptotic controls are important for a meaningful analysis of apoptosis, and should be incorporated into any assay. If possible, an untreated negative control and an independent positive control should be included, the latter being induced by an agent other than that under study (such as a cytotoxic drug). Samples with both the absence and presence of the PhiPhiLux reagents are particularly important to include as controls, since the substrate does possess some low but detectable intrinsic fluorescence in the uncleaved state that can be erroneously interpreted as apoptosis without the appropriate control samples.
2. DNA binding dyes: Although PI and 7-AAD can be chosen based on their spectral characteristics, they are not completely interchangeable with regard to their permeability characteristics. 7-AAD is somewhat more cell permeable than PI; hence, it will give a greater percentage of apoptotic cells when compared directly to PI. This difference should be kept in mind while designing cell death assays, and may dictate the use of 7-AAD when this property is desired.
3. Multiparametric analysis of apoptosis in adherent cells: Flow cytometric analysis of apoptosis in adherent cell lines poses special challenges, as the removal of cells from their growth substrate may itself induce apoptosis. In addition, cell removal methods (such as trypsinization) can trigger false apoptotic indicators, such as aberrant annexin V binding in the absence of true cell death. By far the best solution to this problem is to utilize a laser scanning cytometer (LSC) for the analysis of apoptosis in these cell types; this specialized flow cytometer can perform “flow” analysis of cells on a flat surface, allowing minimal disruption during cell preparation (20). Several apoptosis assays, some utilizing caspase substrates have been described (16,21). The cell labeling protocol is similar to that for suspension

cells as described above, using cells cultured on tissue culture microslides as described previously (16). An example is shown in **Fig. 5**, where adherent L929 mouse fibroblasts were incubated with tumor necrosis factor- α (TNF- α) and cycloheximide, and labeled with PhiPhiLux-G₁D₂ and 7-AAD while still attached to their growth substrate. Analysis on a Compucyte laser scanning cytometer allowed easy discrimination of 7-AAD permeability and caspase activation, indicating that this assay is applicable to an adherent cell format as well.

4. Caspase substrate specificity and background. While the PhiPhiLux substrates seem reasonably specific for their target caspases, no synthetic substrate is exclusively specific for any particular enzyme. This should be kept in mind for any assay involving specific proteolytic activity. In general, a considerable excess of substrate will encourage low levels of nonspecific cleavage, increasing the non-caspase background of the assay. Titration of the substrate to the lowest concentration able to distinguish activity may be necessary when the specificity of the assay is in doubt.
5. Annexin V: The presence of calcium and magnesium is critical for annexin V binding; even removal of divalent cations after the binding reaction will result in rapid dissociation from PS residues. The cells must therefore remain in a calcium/magnesium buffer up to analysis.
6. Incubation periods: All incubation periods and conditions are critical parameters for this assay, as is prompt analysis of samples following the labeling procedure. Insufficient incubation time for the PhiPhiLux substrates will result in poor labeling; prolonged incubation periods will increase the level of nonspecific substrate binding and cleavage, resulting in high background fluorescence and decreased signal-to-noise ratios. In addition, prolonged storage of cells following removal of the surrounding PhiPhiLux substrate will eventually result in leakage of the cleaved substrate from the cell, despite its reduced cell permeability in the cleaved state. Overly long annexin V incubation periods will also increase the amount of nonspecific binding to cells, making discrimination of "viable" and apoptotic cells more difficult. Although PI (and to a lesser extent 7-AAD) are relatively impermeant to viable cells, prolonged incubation will cause uptake even in healthy cells. If laboratory conditions do not allow prompt analysis of sample, cell death assays involving fixed cells (such as TUNEL assays or immunolabeling of active caspases) should be considered as alternatives.
7. Simultaneous immunophenotyping of "viable" and early apoptotic cells: This method is readily amenable to the incorporation of antibody immunophenotyping along with the cell death markers, resulting in a very sophisticated "screening out" of dead cells for measurement of receptor expression in "viable cells." A potentially exciting extension of this method would appear to be the phenotyping of early apoptotic cells, positive for caspase expression but negative for later markers. This method should be approached with care; from a cellular standpoint, caspase activation is probably not an "early" event in cell death, and many alterations in the plasma membrane may have occurred by this timepoint, resulting in aberrant antibody binding to cells as is observed in later cell death. Any cell sur-

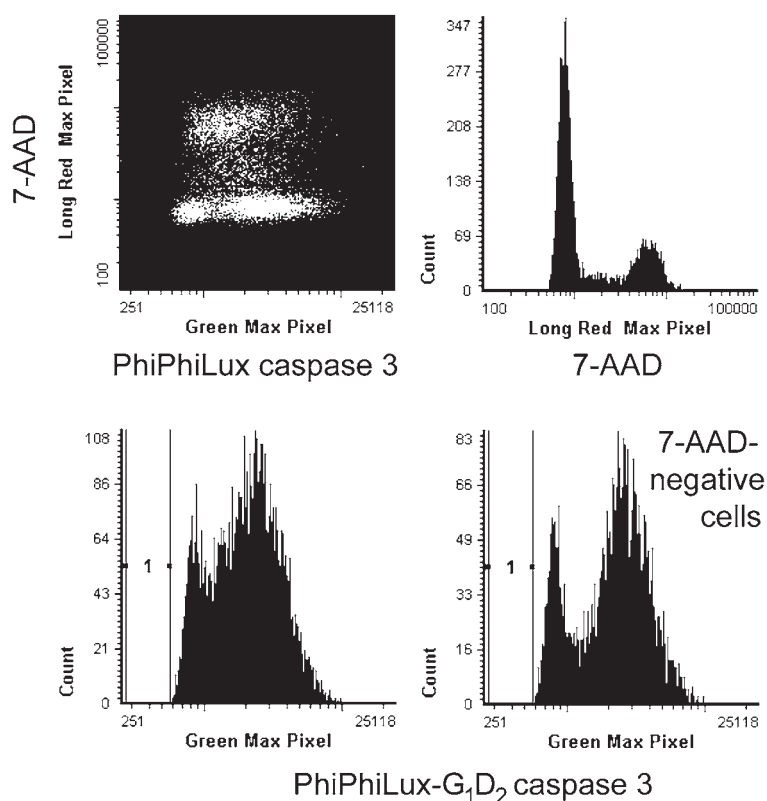


Fig. 5. Caspase activation and 7-AAD permeability in L929 fibroblasts by laser scanning cytometry. L929 cells were cultured on Nunc tissue culture microslides and incubated with TNF- α at 10 ng/mL and cycloheximide at 20 μ g/mL for 8 h, followed by labeling with PhiPhiLux-G₁D₂ and 7-AAD at 5 μ g/mL. Cells were then analyzed on a Compucyte laser scanning cytometer (Cambridge, MA) equipped with a 488-nm argon-ion laser. **Top left** dot-plot shows caspase 3 vs 7-AAD permeability, **top right** histogram shows 7-AAD permeability. The **lower** histograms show caspase activation distributions for all cells (**left**) and 7-AAD-negative cells (**right**).

face marker expression results obtained by such methodology should be therefore be interpreted with caution.

8. Pleiotrophy in apoptosis: Apoptosis is a highly pleiotrophic process involving a variety of biochemical pathways; therefore, there are no universal morphological or physiological characteristics that are common to apoptosis in all cells. Cell death in different cell types (even in physiologically or morphologically similar ones) may present very different phenotypes, and may not necessarily be detectable by the same assays. Multiparametric assays for apoptosis are very amenable to this feature of apoptosis as the investigator is not limiting themselves

to one characteristic of cell death. However, the picture of cell death illustrated here may differ significantly in other tissues; this fact should be kept in mind.

Acknowledgments

The authors wish to acknowledge Veena Kapoor of the National Cancer Institute for excellent technical assistance, and Dr. Z. Darzynkiewicz of the New York Medical College for helpful discussion.

References

1. Telford, W. G., King, L. E., and Fraker, P. J. (1994) Rapid quantitation of apoptosis in pure and heterogeneous cell populations using flow cytometry. *J. Immunol.* **172**, 1–16.
2. Darzynkiewicz, Z., Juan, G., Li, X., Gorczyca, W., Murakami, T., and Traganos, F. (1997) Cytometry in cell necrobiology: analysis of apoptosis and accidental cell death (necrosis). *Cytometry* **27**, 1–20.
3. Del Bino, G., Darzynkiewicz, Z., Degraef, C., Mosselmans, R., and Galand, P. (1999) Comparison of methods based on annexin V binding, DNA content or TUNEL for evaluating cell death in HL-60 and adherent MCF-7 cells. *Cell Prolif.* **32**, 25–37.
4. Vermes, I., Haanen, C., and Reutelingsperger, C. (2000) Flow cytometry of apoptotic cell death. *J. Immunol. Methods* **243**, 167–190.
5. Henkart, P. A. (1996) ICE family proteases: mediators of all cell death? *Immunity* **14**, 195–201.
6. Ormerod, M. G., Sun, X.-M., Snowden, R. T., Davies, R., Fearhead, H., and Cohen, G. M. (1993) Increased membrane permeability in apoptotic thymocytes: a flow cytometric study. *Cytometry* **14**, 595–602.
7. Castedo, M., Hirsch, T., Susin, S. A., et al. (1996) Sequential acquisition of mitochondrial and plasma membrane alterations during early lymphocyte apoptosis. *J. Immunol.* **157**, 512–521.
8. Green, D. R. and Reed, J. C. (1998) Mitochondria and apoptosis. *Science* **281**, 1309–1312.
9. Overbeek, R., Yildirim, M., Reutelingsperger, C., and Haanen, C. (1998) Early features of apoptosis detected by four different flow cytometry assays. *Apoptosis* **3**, 115–120.
10. Earnshaw, W. C., Martins, L. M., and Kaufmann, S. H. (1999) Mammalian caspases: structure, activation, substrates and functions during apoptosis. *Annu. Rev. Biochem.* **68**, 383–424.
11. Koester, S. K. and Bolton, W. E. (2001) Cytometry of caspases. *Methods Cell Biol.* **63**, 487–504.
12. Gorman, A. M., Hirt, U. A., Zhivotovsky, B., Orrenius, S., and Ceccatelli, S. (1999) Application of a fluorimetric assay to detect caspase activity in thymus tissue undergoing apoptosis in vivo. *J. Immunol. Meth.* **226**, 43–48.
13. Belloc, F., Belaund-Rotureau, M. A., Lavignolle, V., et al. (2000) Flow cytometry of caspase-3 activation in preapoptotic leukemic cells. *Cytometry* **40**, 151–160.

14. Bedner, E., Smolewski, P., Amstad, P., and Darzynkiewicz, Z. (2000) Activation of caspases measured in situ by binding of fluorochrome-labeled inhibitors of caspases (FLICA); correlation with DNA fragmentation. *Exp. Cell Res.* **260**, 308–313.
15. Komoriya, A., Packard, B. Z., Brown, M. J., Wu, M. L., and Henkart, P. A. (2000) Assessment of caspase activities in intact apoptotic thymocytes using cell-permeable fluorogenic caspase substrates. *J. Exp. Med.* **191**, 1819–1828.
16. Telford, W. G., Komoriya, A., and Packard, B. Z. (2002) Detection of localized caspase activity in early apoptotic cells by laser scanning cytometry. *Cytometry* **47**, 81–88.
17. Lazebnik, Y., Kaufmann, S. H., Desnoyers, S., Poirier, G. G., and Earnshaw, W. C. (1994) Cleavage of poly(ADP-ribose) polymerase by proteinase with properties like ICE. *Nature* **371**, 346–347.
18. Packard, B. Z., Topygin, D. D., Komoriya, A., and Brand L. (1996) Profluorescent protease substrates: intramolecular dimers described by the exciton model. *Proc. Natl. Acad. Sci. USA* **93**, 11,640–11,645.
19. Packard, B. Z., Komoriya, A., Brotz, T. M., and Henkart, P. A. (2001) Caspase 8 activity in membrane blebs after anti-Fas ligation. *J. Immunol.* **167**, 5061–5066.
20. Kametsky, L. A., Burger, D. E., Gershman, R. J., Kametsky, L. D., and Luther, E. (1997) Slide-based laser scanning cytometry. *Acta Cytol.* **41**, 123–143.
21. Smolewski, P., Bedner, E., Du, L., et al. (2001) Detection of caspases activation by fluorochrome-labeled inhibitors: multiparameter analysis by laser scanning cytometry. *Cytometry* **44**, 73–82.

9

Detection and Enrichment of Hematopoietic Stem Cells by Side Population Phenotype

Shannon S. Eaker, Teresa S. Hawley, Ali Ramezani,
and Robert G. Hawley

Summary

A flow cytometric procedure has recently been described to isolate hematopoietic stem cells from mouse bone marrow based on the efflux properties of the vital dye Hoechst 33342. The assay defines a subset of cells—termed the “side population” (SP)—by simultaneously measuring fluorescence of the dye at two wavelengths (~450 nm and >670 nm). In this chapter, SP protocols are provided to detect candidate hematopoietic stem cells in mouse bone marrow and human cord blood. In the standard method, SP profiles are readily observed on a stream-in-air cell sorter using 30 mW of 351–356 nm ultraviolet excitation from a krypton-ion laser. Alternatively, SP profiles can be resolved on an analytical flow cytometer with cuvette flow cell using 8 mW of 325-nm ultraviolet excitation from a helium–cadmium laser. The ability to perform the SP assay on an analytical instrument facilitates optimization of staining conditions to identify hematopoietic and other stem cells in a variety of tissues. It is also demonstrated that SP profiles of slightly lower resolution can be obtained on a stream-in-air cell sorter using 100 mW of 407-nm violet excitation from a krypton-ion laser, raising the possibility that with appropriate validation the SP assay could be performed on flow cytometers that are not equipped with ultraviolet lasers.

Key Words

Bone marrow, cord blood, hematopoietic stem cells, Hoechst 33342, side population, ultraviolet excitation, violet laser.

1. Introduction

Somatic stem cells are being increasingly characterized in a variety of tissues by a number of techniques (**1**). Within the hematopoietic system, stem cells can be identified by flow cytometric procedures on the basis of their cell-surface phenotype, but the question of which cell-surface antigens are optimal for identifi-

From: *Methods in Molecular Biology: Flow Cytometry Protocols*, 2nd ed.
Edited by: T. S. Hawley and R. G. Hawley © Humana Press Inc., Totowa, NJ

cation is still a matter of some debate (2). Other strategies that have been employed to detect and purify hematopoietic stem cells (HSCs) using flow cytometry are based on the staining patterns of fluorescent dyes (3–8). Decreased staining with the vital fluorescent dyes Hoechst 33342 (a *bis*-benzimidazole that binds to adenine–thymine-rich regions of the minor groove of DNA) and rhodamine 123 (which preferentially accumulates in active mitochondria) has long been used in flow cytometry experiments to enrich for HSCs (3–6). Until recently, it had been generally assumed that the weak HSC staining obtained with both of these dyes was a reflection of a kinetically and metabolically quiescent cell that had condensed chromatin and very few or inactive mitochondria (9–11) (see also Chapter 10 by Bertoncello and Williams, *this volume*). However, it is now appreciated that dim staining of HSCs with Hoechst 33342 and rhodamine 123 is in large part the result of efflux mediated by at least two members of the ATP-binding cassette (ABC) family of transporters, ABCG2 (also referred to as BCRP, MXR, or ABCP) and P-glycoprotein (also referred to as MDR1 or ABCB1) (12–16).

In 1996, Goodell et al. reported a novel method to identify HSCs in mouse bone marrow that depends on dual-wavelength flow cytometric analysis of cells stained with Hoechst 33342 alone (17). By simultaneously monitoring fluorescence emission of Hoechst 33342 at approx 450 nm (“Hoechst Blue” fluorescence) and at >675 nm (“Hoechst Red” fluorescence) following ultraviolet (UV) excitation, a rare subset of mouse bone marrow cells (<0.1%) was observed that displayed low blue and red fluorescence. The investigators showed that these so-called “side population” (SP) cells, which expressed the Sca-1 HSC antigen but were not stained by a cocktail of antibodies directed against a number of lineage markers found on mature hematopoietic cells, contained the vast majority of long-term hematopoietic repopulating activity in mouse bone marrow. Because the SP profile was selectively eliminated when Hoechst 33342 staining was performed in the presence of verapamil, a potent inhibitor of P-glycoprotein, the low level of staining was concluded to be caused by P-glycoprotein-like-mediated efflux of the dye from the cells. In accord with these findings, ectopic expression of the human *MDR1* gene (which encodes P-glycoprotein) in mouse bone marrow cells was shown to result in an increase in SP cell numbers (18). Examination of mice with targeted disruptions of the *Mdr1a* and *Mdr1b* genes (the mouse orthologs of human *MDR1*) indicated, however, that *Mdr1*-type gene products are not necessary for the bone marrow SP phenotype (19). The ABC transporter expressed in mouse bone marrow cells, which is the major determinant of the SP profile, has been identified as *Bcrp1* (the mouse ortholog of human ABCG2) (16,19,20).

SP cells have also been detected in human hematopoietic tissues (21–25). Interestingly, unlike mouse bone marrow SP cells, human hematopoietic SP

cells constitute a phenotypically and functionally heterogeneous population (22,23,25). This finding needs to be borne in mind if quantitative analyses of cell function and fate are contemplated with human hematopoietic SP cells (26,27). HSCs are operationally defined as having the capacity to self renew and the ability to regenerate all of the different types of blood cells following transplantation into an appropriate host (28,29). With the exception of human gene transfer trials, there are no experimental systems available to characterize human HSCs (30). Multilineage engraftment in nonobese diabetic/severe combined immunodeficient (NOD/SCID) mice is therefore widely used as a surrogate assay to evaluate human hematopoietic precursors for *in vivo* repopulating potential, and the cells exhibiting this property have been termed SCID-repopulating cells (SRCs) (31,32). Using the NOD/SCID xenograft model, Uchida et al. demonstrated that SRC activity in second-trimester human fetal liver was contained within the CD34⁺CD38⁻ subset of SP cells (23). At time of writing, SRC activity of SP cells isolated from other human hematopoietic tissue sources, such as cord blood, had not been documented.

This chapter provides protocols for the flow cytometric detection and characterization of SP cells in mouse bone marrow and human cord blood. Procedures for sample processing and Hoechst 33342 staining are described in detail, and different flow cytometer configurations that can be used to resolve SP profiles are presented. Also included are approaches to determine whether the SP cells exhibit phenotypic or functional characteristics of HSCs.

2. Materials

2.1. Supplies and Equipment

1. Sterile surgical instruments for isolating mouse bone marrow cells: fine scissors, bone-cutting scissors, syringes, needles, forceps, and 80- μ m filters/mesh.
2. Sterile tissue culture supplies: pipets, polypropylene tubes, tissue culture dishes, and Petri dishes.
3. Hemacytometer (or other devices for counting cells).
4. Water bath set at 37°C.
5. Refrigerated centrifuge.
6. Flow cytometer equipped with:
 - a. Excitation wavelength: UV (325 nm or 351–364 nm) (*see Note 1*).
 - b. Detection filters: 450/20-nm bandpass (BP) filter, 675-nm longpass (LP) filter, and 610-nm shortpass dichroic mirror.

2.2. Reagents and Solutions

1. 70% Ethanol.
2. Buffer: Phosphate-buffered saline (PBS) or Hank's balanced salt solution (HBSS), and 2% (v/v) fetal bovine serum (FBS).

3. Medium: Dulbecco's modified Eagle medium (DMEM) with high glucose, 2% (v/v) FBS, and 10 mM *N*-(2-hydroxyethyl)piperazine-*N'*-(2-ethanesulfonic acid) (HEPES).
4. Solutions for isolating mononuclear cells from human cord blood: anticoagulant (such as anticoagulant citrate dextrose solution A [ACD-A], sodium citrate, citrate-dextrose, citrate-phosphate-dextrose, or ethylenediaminetetraacetic acid [EDTA]) and Ficoll-Paque (Amersham Pharmacia Biotech, Piscataway, NJ).
5. Erythrocyte lysing solution: 154 mM ammonium chloride, 10 mM sodium or potassium bicarbonate, and 0.082 mM tetrasodium EDTA. Commercial lysing solutions are also available.
6. (Optional) VarioMACS CD34 progenitor cell isolation kit (Miltenyi Biotec, Auburn, CA).
7. Hoechst 33342 (Sigma, St. Louis, MO): Prepare a stock solution of 1 mg/mL in distilled water. Store in 0.1-mL aliquots at -20°C . Refrain from refreezing and discard unused portion.
8. Verapamil (Sigma): Prepare a stock solution of 5 mM in distilled water. Store at 4°C .
9. Fumitremorgin C (FTC) (kindly provided by R. Robey and S. Bates, Medicine Branch, National Cancer Institute, National Institutes of Health, Bethesda, MD): Prepare a stock solution of 10 mM in dimethyl sulfoxide (DMSO). Store at -20°C .
10. Propidium iodide (PI): Prepare a stock solution of 1 mg/mL in distilled water. Store in the dark at 4°C .
11. Calibration-grade beads for aligning the laser providing UV excitation.

2.3. Cells

1. Cord blood cells: Obtain human cord blood after informed consent in conformity with a human subjects protocol approved by an Institutional Review Board, or purchase from a commercial source.
2. A549 cells: A human lung carcinoma cell line (American Type Culture Collection, Manassas, VA, cat. no. CCL-185).

2.4. Mice

1. C57BL/6J mice (The Jackson Laboratory, Bar Harbor, ME, stock no. 000664).
2. NOD/SCID mice: NOD.CB17-*Prkdc*^{scid}/J mice homozygous for the severe combined immune deficiency spontaneous mutation (*Prkdc*^{scid}, commonly referred to as *scid*) on the NOD/LtSz background (nonobese diabetic mice deficient in macrophage function and having inherently low natural killer cell activity) (The Jackson Laboratory, stock no. 001303). The mice are housed in sterile microisolator cages on laminar flow racks to minimize adventitious infections.

All procedures involving mice must follow the guidelines set forth in the National Institutes of Health *Guide for the Care and Use of Laboratory Animals* and be approved by an Institutional Animal Care and Use Committee.

3. Methods

3.1. Isolation and Preparation of Mouse Bone Marrow and Human Cord Blood Cells

Because Hoechst 33342 staining conditions for C57BL/6 mouse bone marrow cells have been well established, we recommend using these cells to set up and validate the SP assay.

3.1.1. Isolation of Mouse Bone Marrow Cells

1. Euthanize a mouse according to an institutionally approved protocol.
2. Disinfect the mouse with 70% ethanol and place it on a cutting board.
3. Using sterile surgical instruments, make a transverse cut in the middle of the abdominal area. Remove the skin from the hindquarters and the hind limbs.
4. Remove the hind limbs from the body at the hip joint. Cut off the feet and place the hind limbs in a Petri dish containing buffer.
5. Trim all muscle tissue from the femurs and tibias, and transfer them to a fresh Petri dish containing buffer.
6. Separate the femurs and tibias, and cut off the ends of the bones.
7. Transfer the femurs and tibias to a fresh Petri dish containing buffer. Gently flush out the bone marrow with 4 mL of buffer. Flush from both ends (*see Note 2*).
8. Pipet cell suspension into a 10-mL tube, rinsing the Petri dish to ensure that all cells are recovered. The cell suspension can be filtered using an 80- μ m filter to remove any cell clumps (*see Notes 3 and 4*).

3.1.2. Isolation of Human Cord Blood Mononuclear Cells

This section provides a protocol for the isolation of human cord blood mononuclear cells using a Ficoll-Paque gradient separation technique. Other published protocols and commercial isolation kits can also be used.

1. Dilute anticoagulated cord blood 1:3 with sterile room-temperature PBS containing 0.6% ACD-A or 2 mM EDTA.
2. Slowly layer 35 mL of diluted cord blood over 12 mL of Ficoll-Paque in a 50-mL polypropylene tube.
3. Centrifuge at 20°C at 375g for 30 min in a swinging bucket rotor.
4. Aspirate off the top clear layer down to the mononuclear layer (termed the buffy coat, a thin white layer at the interface).
5. Using a 10-mL pipet, remove the buffy coat and place in a separate 50-mL tube (filling each tube to 20 mL).
6. Bring each tube up to 50 mL with room-temperature PBS containing 0.6% ACD-A or 2 mM EDTA, and centrifuge at 20°C at 375g for 15 min.
7. Resuspend cells in 10 mL of erythrocyte lysing solution (mixing well), then bring the volume up to 50 mL with erythrocyte lysing solution.

8. Let sit for 10 min at room temperature, then centrifuge at 20°C at 375g for 15 min.
9. Wash cells in 20 mL of room-temperature PBS, centrifuge at 375g for 15 min, then resuspend in prewarmed medium (*see* **Notes 3 and 4**).
10. (Optional) Enrich for CD34⁺ mononuclear cells by super paramagnetic microbead selection using the VarioMACS CD34 progenitor cell isolation kit, according to the manufacturer's instructions (*see* **Note 5**).

3.2. Staining of Cells With Hoechst 33342

The Hoechst 33342 SP fluorescence pattern is highly dependent on the following variables: cell concentration, dye concentration, staining temperature, and staining time. The procedures described below have been successfully used to stain mouse bone marrow and human cord blood cells resuspended at 1×10^6 cells/mL (*see* **Note 6**). It is important to keep the sample protected from light throughout the staining procedure and during analysis (*see* **Note 7**).

1. Designate a water bath set at 37°C (*see* **Note 8**). Prewarm medium at 37°C.
2. Count nucleated cells, and resuspend at 1×10^6 cells/mL in medium (*see* **Notes 9–11**).
3. To the cell suspension, add the Hoechst 33342 stock solution to obtain a final concentration of 5 µg/mL.
4. Transfer the cell/dye suspension to a tube suitable for submersion in the water bath. For a volume of 1–3 mL, use a 5-mL tube. For a volume of 4–10 mL, use a 15-mL tube. For larger volumes, use 50-mL tubes. Make certain that the top level of the cell suspension is totally submerged under water in the bath. This will ensure that the 37°C temperature will be maintained throughout the sample (*see* **Note 8**).
5. Allow the sample to remain in the water bath for 90 min. Gently invert the tube every 20 min to discourage cell settling and clumping.
6. After the 90-min incubation, centrifuge the cells at 375g for 6 min at 4°C (in a pre-cooled rotor), and resuspend in an appropriate volume of cold buffer. **Important:** To inhibit further dye efflux, the cells must remain at 4°C for the remainder of the experiment.
7. (Optional) If the SP assay is combined with staining for cell surface antigens, the cells can now be processed for antibody staining (*see* **Note 12**). The cell suspension should be maintained at 4°C at all times.
8. If desired, add PI to a final concentration of 2 µg/mL for dead cell discrimination immediately prior to flow cytometry.

3.3. Flow Cytometric Detection of SP Cells

The excitation maximum of Hoechst 33342 is 346 nm. Therefore, the flow cytometer should be equipped with a laser that provides excitation in the UV range for optimal sensitivity of the SP assay. When the assay is combined with antibody staining, other excitation wavelengths are also required (*see* **Note 13**).

1. Install the 450/20 BP filter for Hoechst Blue detection, the 675 LP filter for Hoechst Red detection, and the 610 shortpass dichroic mirror for separation of Blue and Red signals (*see* **Notes 14** and **15**).
2. PI fluorescence generated from UV excitation will be captured by the 675 LP filter as well. However, the high fluorescence intensity signals produced by PI-positive dead cells can be easily discriminated from Hoechst Red-positive signals produced by live cells.
3. Create the following two-parameter plots (x-axis vs y-axis) with all of the parameters in linear scale:
 - a. Forward scatter (FSC) vs side scatter (SSC).
 - b. Hoechst Red vs Hoechst Blue.
4. Keep the sample cold and protected from light during analysis (*see* **Note 7**).
5. Run sample while viewing the FSC vs SSC plot. Adjust voltages of both parameters until all of the cells are captured on the dot-plot.
6. Adjust voltages of Hoechst Red and Hoechst Blue parameters until the cells stained brightly for Hoechst 33342 are visible on the dot-plot. Continue to increase voltages until the cells stained weakly for Hoechst 33342 are visible on the lower left side of the plot.
7. Acquire 100,000–500,000 events (*see* **Note 16**).
8. Use a nonrectilinear marker to delineate the SP population on the Hoechst Red vs. Hoechst Blue plot. SP cells constitute a discrete population on the left side of the plot, indicating low fluorescence intensity at both emission wavelengths (**Fig. 1**).

3.4. Immunophenotypic and Functional Characterization of SP Cells

3.4.1. Expression of HSC Surface Antigens on SP Cells Derived From Mouse Bone Marrow Cells

In vivo studies have shown that the fraction of mouse bone marrow cells that reconstitute the hematopoietic system of lethally irradiated recipients express c-Kit and Sca-1, but lack expression of lineage-specific cell surface antigens (**26,27**). Demonstrating that c-Kit⁺Lin⁻Sca-1⁺ (KLS) cells were highly enriched in the SP region confirmed the utility of the SP assay in enriching for HSCs in mouse bone marrow (**16,17,21**) (**Fig. 2**).

Recently, violet laser diodes providing 15–30 mW of 405/407/408 nm excitation (exact wavelength depends on the manufacturer of the laser) have become commercially available (*see* Chapter 23 on small lasers by Telford, *this volume*). They can be purchased as options on some models of new flow cytometers, or retrofitted onto existing flow cytometers. For some applications, they promise to be attractive alternatives to cumbersome lasers providing UV excitation (**41**). To determine the feasibility of performing the SP assay with violet excitation, we compared UV (8 mW of 325 nm provided by a helium–cadmium (He–Cd) laser on an analyzer with cuvette flow cell) and violet (100 mW of 407 nm pro-

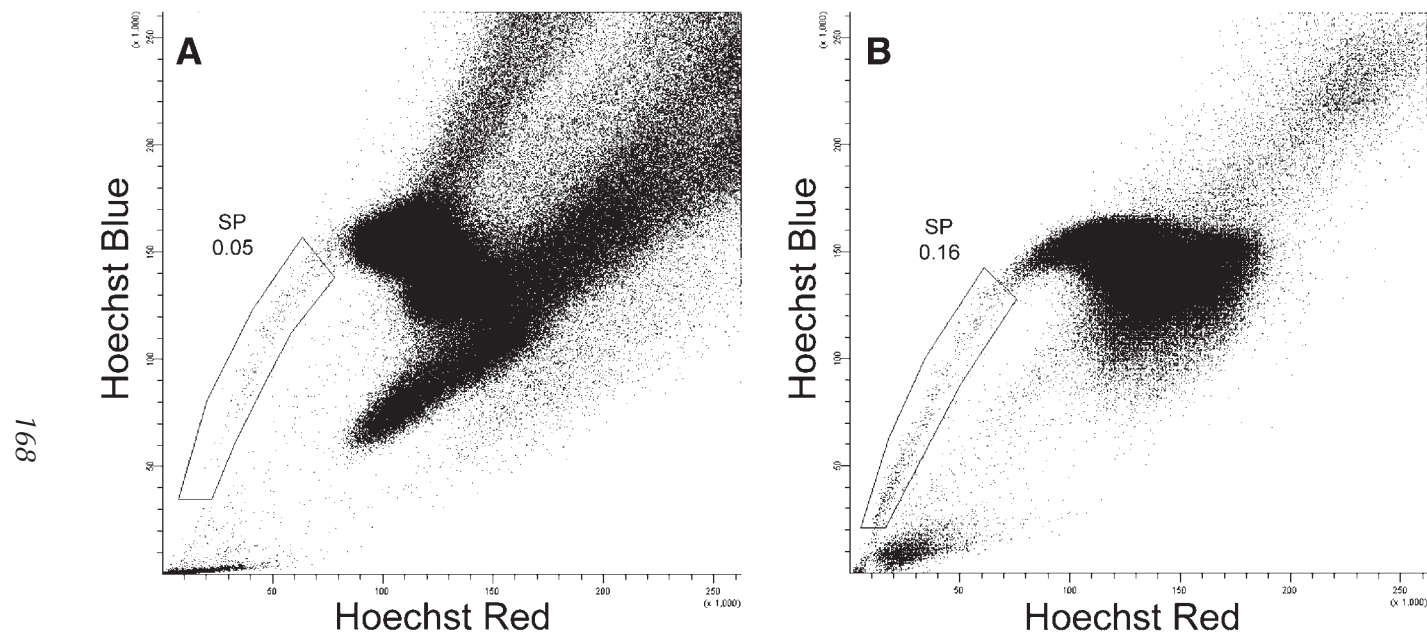


Fig. 1. Flow cytometric identification of SP cells in mouse bone marrow (A) and human cord blood enriched for CD34⁺ cells (B). Cells were stained with 5 $\mu\text{g}/\text{mL}$ of Hoechst 33342 at 37°C for 90 min. Samples were analyzed on a FACSVantage SE/FACSDiVa (BD Biosciences) equipped with an Innova 302C krypton-ion laser (Coherent Inc., Santa Clara, CA) providing 30 mW of UV (351–356 nm) excitation. Five hundred thousand events were collected. Observation of Hoechst 33342 fluorescence at its blue emission wavelength (with a 450/20 BP filter) and red emission wavelength (with a 675 LP filter) simultaneously on a Hoechst Blue (y-axis) vs Hoechst Red (x-axis) dot-plot revealed a discrete population of cells on the lower left side of the plot. SP cells were identified by low fluorescence at both wavelengths.

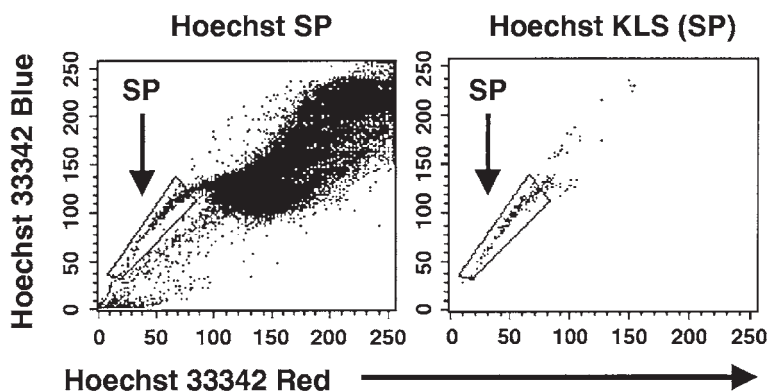
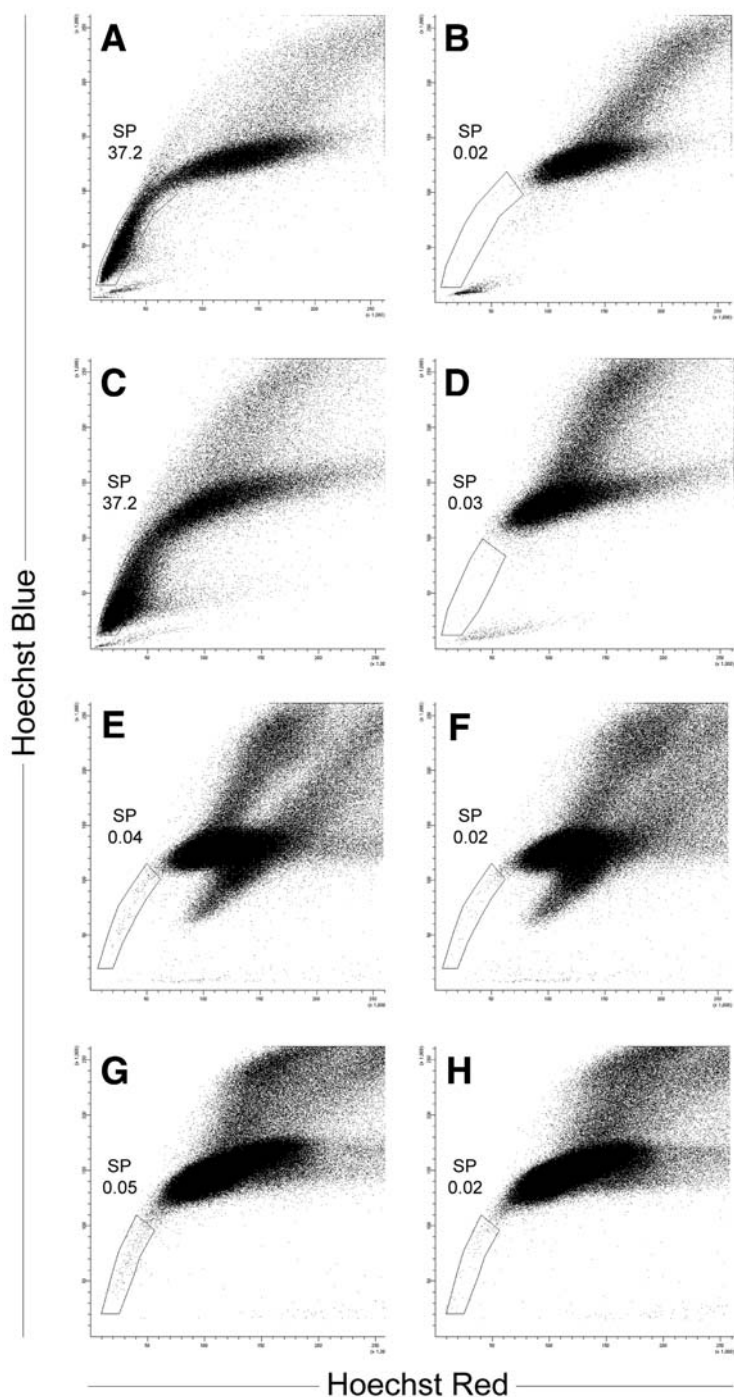


Fig. 2. Correlation of the SP phenotype with expression of HSC surface antigens in mouse bone marrow cells using UV excitation. Cells were stained with Hoechst 33342 alone (**left**), or in combination with antibodies against c-Kit, a cocktail of lineage-specific markers and Sca-1 (**right**). Samples were analyzed on a FACS Vantage SE equipped with an Enterprise IIC laser (Coherent Inc.) providing 30 mW of 351–364 nm excitation. Five hundred thousand events were collected. KLS (c-Kit⁺Lin⁺Sca-1⁺) cells were highly enriched in the SP region. (Reproduced by permission of AlphaMed Press from **ref. 16**.)

vided by a krypton-ion laser on a stream-in-air cell sorter) excitation of C57BL/6 bone marrow cells stained with Hoechst 33342 (*see Fig. 3E,G*, respectively). To confirm the identity of cells falling into the SP region as candidate HSCs, fluorochrome-conjugated antibodies to c-Kit and Sca-1 were combined with the assay. As shown in **Fig. 4**, the majority of the SP cells identified by violet excitation coexpressed c-Kit and Sca-1. Even though it is feasible to perform the SP assay with violet excitation, relatively high laser power is required to produce discernible SP profiles of slightly lower resolution than those generated by the standard method (compare **Fig. 3G** to **Fig. 1A**). Violet laser diodes providing 15–30 mW power output in a stream-in-air system will not be able to achieve resolution of the SP profile. However, a cuvet flow cell coupled with sensitive detection optics may bode well for the violet laser diode on that platform.

3.4.2. Engraftment of Human Cord Blood SP Cells in NOD/SCID Mice

We isolated human cord blood-derived CD34⁺ SP cells by fluorescence-activated cell sorting and injected them intravenously into sublethally irradiated NOD/SCID mice at 10^3 – 10^4 or 10^4 – 10^5 cells per mouse. Twelve weeks after transplantation, the mice were euthanized and the bone marrow cells col-



lected for flow cytometric analysis. Human cells could be consistently detected in the mouse bone marrow for cell doses above 10^4 (**Fig. 5**), demonstrating the presence of SRC in the CD34⁺ SP population.

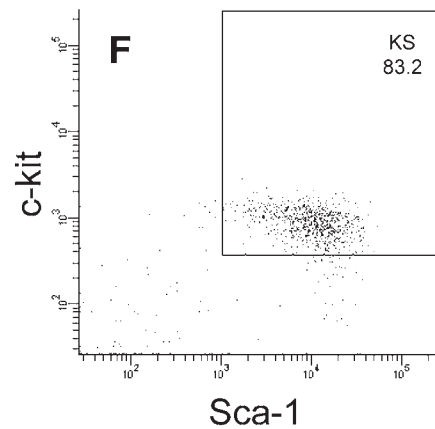
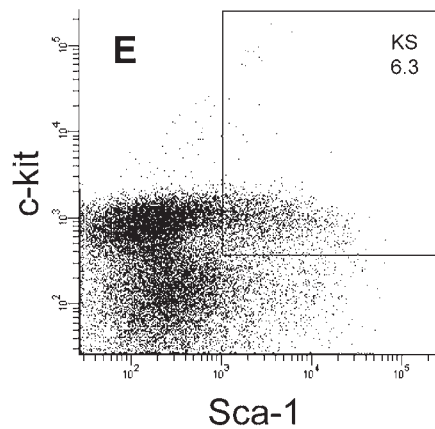
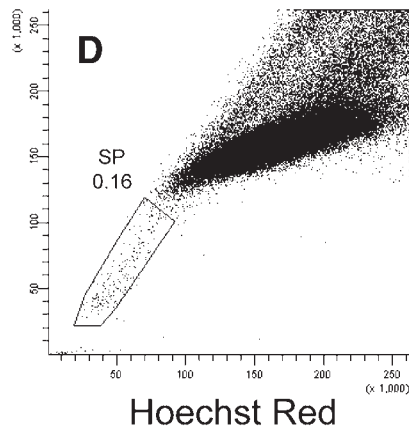
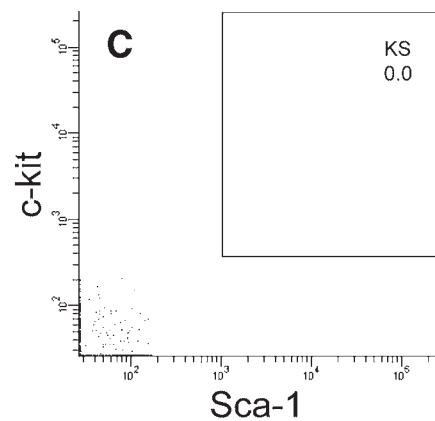
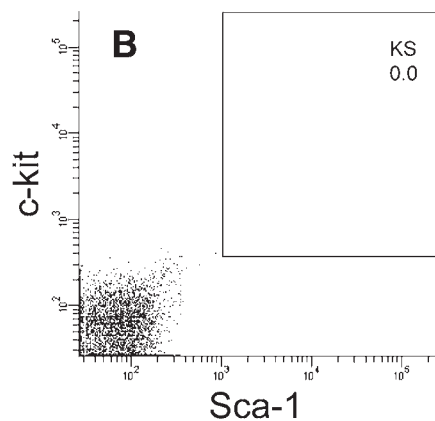
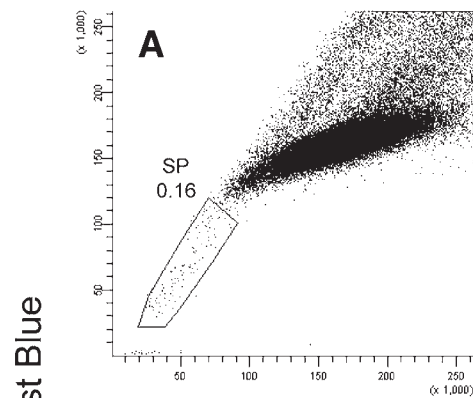
3.4.3. Hoechst 33342 Efflux by SP Cells

Suppression of the SP phenotype can be achieved by disruption of ABC transporter function. It can be accomplished by depletion of ATP with 2-deoxyglucose and sodium azide, or addition of specific transporter inhibitors. Verapamil, an inhibitor of P-glycoprotein/Mdr1, appears to be effective in diminishing the SP phenotype in mouse bone marrow cells (**Fig. 6B** and *see Note 17*). FTC, an inhibitor of ABCG2/Bcrp1 (but not P-glycoprotein), is also effective in mouse bone marrow cells (**Fig. 6C**), and demonstrates suppression of the SP phenotype in A549 human lung carcinoma cells which express a high level of ABCG2 (**24**) (**Fig. 3B**). Reserpine, which is a functional inhibitor of several ABC transporters, including P-glycoprotein and ABCG2, can also be used. Examples of effective inhibitor concentrations are listed in **Note 18**, but may need to be altered depending on cell type. The inhibitors can be used 15 min prior to Hoechst 33342 addition to the sample (preinhibition) or concomitant with Hoechst 33342 (coinhibition). Published protocols vary with respect to this step; however, we have obtained good results with coinhibition.

4. Notes

1. The original publication on SP cells employed 50–100 mW of UV at 350 nm for the excitation of Hoechst 33342. It was performed on a stream-in-air cell sorter using a water-cooled argon-ion laser. We have determined that if the detection system is sensitive, SP profiles can be resolved even at low laser power and suboptimal excitation wavelength. Detection in a cuvet flow cell using 8 mW of UV excitation at 325 nm from an air-cooled Kimmon IK Series He–Cd laser on a BD LSR analyzer

Fig. 3. (*see facing page*) Direct correlation of ABCG2 activity and the SP phenotype. A549 human lung carcinoma cells, expressing high levels of ABCG2, were stained with 5 $\mu\text{g/mL}$ of Hoechst 33342 at 37°C for 90 min, in the absence (**A,C**) or presence (**B,D**) of 1 μM FTC. Samples were analyzed on a BD LSR with 8 mW of UV excitation (**A,B**), and on a FACSVantage SE/FACSDiVa with 50 mW of violet excitation (**C,D**). One hundred thousand events were collected. As previously reported by Scharenberg et al. (**24**), FTC reduced the number of cells within the SP region by inhibiting ABCG2 efflux activity. C57BL/6 mouse bone marrow cells were stained with Hoechst 33342 in the absence (**E,G**) or presence (**F,H**) of 1 μM FTC. Samples were analyzed on a BD LSR with 8 mW of UV excitation (**E,F**), and on a FACSVantage SE/FACSDiVa with 100 mW of violet excitation (**G,H**). Four hundred thousand live (PI-negative) cells were analyzed. FTC reduced the number of the cells within the SP region.



(BD Biosciences, San Jose, CA) successfully generates SP profiles, even though excitation of Hoechst 33342 at this wavelength is approx 56% of that intensity expected from equivalent power at 350 nm. In addition to the He–Cd laser, the BD LSR is equipped with a Spectra-Physics 163 argon-ion laser providing 488-nm excitation at 20 mW. Excitation with 488 nm produces FSC signal, SSC signal, and four fluorescence signals. The detectors for the four fluorescence signals are designated as FL1, FL2, FL3, and FL6. Fluorescence signals generated by UV excitation are normally collected in FL4 and FL5. For SP analysis, the BD LSR optical bench is reconfigured to collect Hoechst Red fluorescence emission in FL3 with a modified pinhole assembly that permits detection of the signal generated by UV excitation. The standard 670-nm LP filter is left in front of the FL3 detector. Hoechst Blue fluorescence emission is collected in FL5 with the 424/44-nm BP filter. The standard steering optics mounted on the BD LSR are left in place. Linear signals from both blue and red fluorescence channels are used to produce typical histograms for identification of SP cells. We also have evidence indicating that at 407 nm excitation (using 100 mW of laser power on a stream-in-air cell sorter), Hoechst Blue and Red fluorescence can still be detected (*see Subheading 3.4.1.*). High laser power is necessary, however, to compensate for the diminished excitation of Hoechst 33342 at 405–408 nm (2–3% of maximum).

2. When flushing the femur, use a 21-gage needle and a 5-mL syringe. A smaller needle (e.g., 27-gage) may sometimes be required when flushing the tibia. Repeat if desired, but use fresh buffer each time. Avoid passing the cell suspension repeatedly through the needle (this may cause cell shearing). Processing both the tibias and femurs from a single mouse will yield $2\text{--}8 \times 10^7$ cells. This number will vary from strain to strain.
3. Same-day staining is recommended. However, if cells are to be stained the next day, they can be stored in medium at 4°C. Following overnight incubation, PI should be included in the assay to evaluate cell viability.
4. Although an advantage of the SP assay is that it is independent of cell surface characteristics, in some instances it may be desirable to include a preenrichment

Fig. 4. (*see facing page*) Correlation of the SP phenotype with expression of HSC surface antigens in mouse bone marrow cells using violet excitation. Cells were stained with Hoechst 33342 alone (**A–C**), or in combination with c-Kit-PE-Cy5 and Sca-1-PE (**D–F**). Samples were analyzed on a FACSVantage SE/FACSDiVa equipped with an Innova 302C krypton-ion laser providing 100 mW of 407 nm excitation. Optical filter configuration was the same as described in **Fig. 1** (*see also Notes 1, 12, and 13*). Five hundred thousand events were collected. For the Hoechst 33342/c-Kit/Sca-1 sample, the Hoechst 33342 staining profile is shown in (**D**), and the cell surface antigen staining profile is displayed as c-Kit (y-axis) vs Sca-1 (x-axis), with the region KS defining coexpression of both antigens (**E**). When cells within the SP region were displayed on a c-Kit vs Sca-1 plot, the majority showed coexpression of both c-Kit and Sca-1 (**F**). The sample stained with Hoechst 33342 alone served as a control (**A–C**).

5. In the experiments presented in **Fig. 5**, the cord blood mononuclear cells were enriched for cells expressing the CD34 surface antigen prior to Hoechst 33342 staining and SP cell sorting (*see Subheading 3.4.2.*).
6. Staining conditions that have been used to detect hematopoietic SP cells in:
 - a. Mouse bone marrow: 5 $\mu\text{g/mL}$ of Hoechst 33342 at 37°C for 90 min at 1×10^6 cells/mL (**17**).
 - b. Human fetal liver: 5 $\mu\text{g/mL}$ of Hoechst 33342 at 37°C for 90 min at 1×10^6 cells/mL (**23**).
 - c. Human cord blood: 2.5 $\mu\text{g/mL}$ of Hoechst 33342 at 37°C for 90 min at 1×10^6 cells/mL (**22**); in our laboratory, however, 5 $\mu\text{g/mL}$ gave slightly better resolution.
 - d. Human bone marrow: 5 $\mu\text{g/mL}$ of Hoechst 33342 at 37°C for 120 min at 1×10^6 cells/mL (**21**).
 - e. Human peripheral blood (Lin⁻ CD34⁻ cell population): 5 $\mu\text{g/mL}$ of Hoechst 33342 at 37°C for 120 min (**25**).
 - f. A549 human lung carcinoma cell line (positive control): 5 $\mu\text{g/mL}$ of Hoechst 33342 at 37°C for 45 min at $0.5\text{--}1 \times 10^6$ cells/mL; cells were washed and then

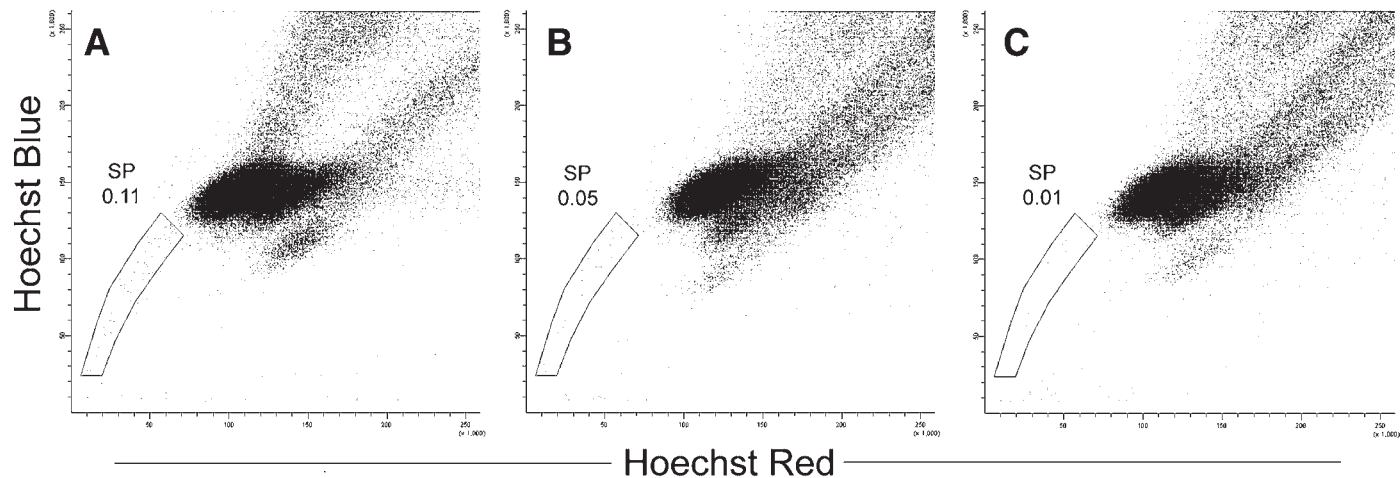


Fig. 6. Reduction of SP cells by inhibitors of ABC transporter activity. Mouse bone marrow cells were stained with Hoechst 33342 alone (A) and in the presence of 50 μ M verapamil (B) or 1 μ M FTC (C). Dead cells were identified by the uptake of PI and excluded from analyses. Samples were analyzed on a BD LSR equipped with a He-Cd laser providing 8 mW of UV (325 nm) excitation. Hoechst 33342 fluorescence was monitored simultaneously with a 424/44 BP filter and a 670 LP filter. One hundred thousand live cells were analyzed. The number of SP cells was reduced in the presence of verapamil (an inhibitor of P-glycoprotein/Mdr1 activity) or FTC (an inhibitor of ABCG2/Bcrp1 activity).

incubated an additional 45 min in the absence of Hoechst 33342 (poststaining efflux period) (24).

7. Although Hoechst 33342 is a vital dye, it is not without cytotoxic effects, especially in proliferating cells. It induces DNA single-strand breaks, which increase significantly following exposure to UV light (33–35). Caution is therefore warranted when performing functional studies with sorted non-SP cells that still retain the dye. As a preventative measure, the water bath should be covered (e.g., with a cardboard box) to minimize exposure of the cells to light while the staining is in progress, and the stained samples kept in the dark prior to analysis.
8. It is important that the temperature of the water bath is maintained at 37°C. Therefore, to prevent temperature fluctuations, use a dedicated water bath and avoid the addition of other items during the staining procedure.
9. Lysing erythrocytes will aid in the accurate determination of nucleated cell number. If erythrocyte lysis has not been performed during sample preparation, take a small aliquot of the sample, resuspend in erythrocyte-lysing solution and allow to stand at room temperature for 10 min. Count nucleated cells.
10. Volumes less than 1 mL (1×10^6 cells) are difficult to process. If a smaller volume is required, process positive controls in parallel.
11. If freshly thawed cells are used, incubate the thawed cells in medium for 30 min before adding the dye. This will allow the cells to equilibrate with the media prior to staining.
12. (Optional) In the case of mouse bone marrow cells, the SP phenotype correlates with the KLS (c-Kit⁺Lin⁻Sca-1⁺) phenotype. An example of antibody combinations for KLS cell detection is: lineage cocktail-FITC, Sca-1-PE, and c-Kit-PE-Cy5.
13. (Optional) If the fluorochrome-conjugated antibodies suggested in **Note 12** are used in combination with the SP assay, the flow cytometer should also be equipped with: excitation wavelength at 488 nm; detection filters including 488/10 BP filters for FSC and SSC detection, 530/30 BP filter for FITC detection, 575/26 BP filter for PE detection, and 675/20 BP filter for PE-Cy5 detection.
14. The peak emission wavelength of Hoechst 33342 is 460 nm. Red-shifted fluorescence of Hoechst 33342 and related *bis*-benzimidazole dyes is thought to be due to different types of dye-binding interactions with DNA (36–40). Some standard filters that are supplied with commercial flow cytometers have been successfully used for the SP assay: 424/44 BP filter for Hoechst Blue detection and 670 LP filter for Hoechst Red detection. Dichroic mirrors that have been successfully used include 570 LP, 640 LP, and 670 LP.
15. If the UV laser is not the primary laser, triggering may be achieved with the laser providing the primary excitation wavelength (such as 488 nm). In this case, band-pass filters of the excitation wavelength (such as 488/10 BP) will need to be installed in front of the FSC and SSC detectors.
16. When the percentage of SP cells is low, recording only events of interest with a live gate will aid in their detection. If PI is not included as a live/dead cell discriminator, a live gate can be drawn on the FSC vs SSC plot by excluding debris and most of the erythrocytes (if present). If PI is included, a live gate can be

drawn on the Hoechst Red vs Hoechst Blue plot by excluding erythrocytes (events at the lower left corner) and dead cells (events accumulated as a vertical line on the far right).

17. Many inhibitors are substrates for more than one ABC transporter as well as for other enzyme systems. Thus, a high concentration of an inhibitor, even in the absence of overt toxicity, may have unpredictable effects on cellular metabolism (42). This may explain why 50 μ M verapamil, a P-glycoprotein/Mdr1 inhibitor, is effective in diminishing the SP profile in mouse bone marrow cells even though ABCG2/Bcrp1 has been reported to be the major determinant of the SP phenotype (19).
18. Recommended concentrations of inhibitors of ABC transporters:
 - a. Verapamil, 50 μ M (5 mM stock solution in distilled water) (17).
 - b. FTC, 1–10 μ M (10 mM stock solution in DMSO) (24).
 - c. Reserpine, 5 μ M (5 mM stock solution in DMSO) (19).
 - d. 2-Deoxyglucose, 50 mM; sodium azide, 15 mM (19).

Acknowledgments

This work was supported in part by National Institutes of Health Grants R01 HL65519 and R01 HL66305 (to R. G. H.). We thank Rick Fishel (BD Biosciences) for assistance in reconfiguring the BD LSR, and Rob Robey and Susan Bates for funitremorgin C.

References

1. Ramos, C. A., Venezia, T. A., Camargo, F. A., and Goodell, M. A. (2003) Techniques for the study of adult stem cells. *Biotechniques* **34**, 572–591.
2. Guo, Y., Lubbert, M., and Engelhardt, M. (2003) CD34(–) hematopoietic stem cells: current concepts and controversies. *Stem Cells* **21**, 15–20.
3. Visser, J. W., Bol, S. J., and van den Engh, G. (1981) Characterization and enrichment of murine hemopoietic stem cells by fluorescence activated cell sorting. *Exp. Hematol.* **9**, 644–655.
4. Bertoncello, I., Hodgson, G. S., and Bradley, T. R. (1985) Multiparameter analysis of transplantable hemopoietic stem cells: I. The separation and enrichment of stem cells homing to marrow and spleen on the basis of rhodamine-123 fluorescence. *Exp. Hematol.* **13**, 999–1006.
5. Wolf, N. S., Kone, A., Priestley, G. V., and Bartelmez, S. H. (1993) In vivo and in vitro characterization of long-term repopulating primitive hematopoietic cells isolated by sequential Hoechst 33342-rhodamine 123 FACS selection. *Exp. Hematol.* **21**, 614–622.
6. Leemhuis, T., Yoder, M. C., Grigsby, S., Aguero, B., Eder, P., and Srour, E. F. (1996) Isolation of primitive human bone marrow hematopoietic progenitor cells using Hoechst 33342 and Rhodamine 123. *Exp. Hematol.* **24**, 1215–1224.
7. Jones, R. J., Barber, J. P., Vala, M. S., et al. (1995) Assessment of aldehyde dehydrogenase in viable cells. *Blood* **85**, 2742–2746.

8. Storms, R. W., Trujillo, A. P., Springer, J. B., et al. (1999) Isolation of primitive human hematopoietic progenitors on the basis of aldehyde dehydrogenase activity. *Proc. Natl. Acad. Sci. USA* **96**, 9118–9123.
9. Arndt-Jovin, D. J. and Jovin, T. M. (1977) Analysis and sorting of living cells according to deoxyribonucleic acid content. *J. Histochem. Cytochem.* **25**, 585–589.
10. Johnson, L. V., Walsh, M. L., and Chen, L. B. (1980) Localization of mitochondria in living cells with rhodamine 123. *Proc. Natl. Acad. Sci. USA* **77**, 990–994.
11. Darzynkiewicz, Z., Staiano-Coico, L., and Melamed, M. R. (1981) Increased mitochondrial uptake of rhodamine 123 during lymphocyte stimulation. *Proc. Natl. Acad. Sci. USA* **78**, 2383–2387.
12. Juliano, R. L. and Ling, V. (1976) A surface glycoprotein modulating drug permeability in Chinese hamster ovary cell mutants. *Biochim. Biophys. Acta* **455**, 152–162.
13. Lalande, M. E., Ling, V., and Miller, R. G. (1981) Hoechst 33342 dye uptake as a probe of membrane permeability changes in mammalian cells. *Proc. Natl. Acad. Sci. USA* **78**, 363–367.
14. Neyfakh, A. A. (1988) Use of fluorescent dyes as molecular probes for the study of multidrug resistance. *Exp. Cell Res.* **174**, 168–176.
15. Chaudhary, P. M. and Roninson, I. B. (1991) Expression and activity of P-glycoprotein, a multidrug efflux pump, in human hematopoietic stem cells. *Cell* **66**, 85–94.
16. Bunting, K. D. (2002) ABC transporters as phenotypic markers and functional regulators of stem cells. *Stem Cells* **20**, 11–20.
17. Goodell, M. A., Brose, K., Paradis, G., Conner, A. S., and Mulligan, R. C. (1996) Isolation and functional properties of murine hematopoietic stem cells that are replicating in vivo. *J. Exp. Med.* **183**, 1797–1806.
18. Bunting, K. D., Zhou, S., Lu, T., and Sorrentino, B. P. (2000) Enforced P-glycoprotein pump function in murine bone marrow cells results in expansion of side population stem cells in vitro and repopulating cells in vivo. *Blood* **96**, 902–909.
19. Zhou, S., Schuetz, J. D., Bunting, K. D., et al. (2001) The ABC transporter Bcrp1/ABCG2 is expressed in a wide variety of stem cells and is the molecular determinant of the side-population phenotype. *Nat. Med.* **7**, 1028–1034.
20. Zhou, S., Morris, J. J., Barnes, Y., Lan, L., Schuetz, J. D., and Sorrentino, B. P. (2002) Bcrp1 gene expression is required for normal numbers of side population stem cells in mice, and confers relative protection to mitoxantrone in hematopoietic cells in vivo. *Proc. Natl. Acad. Sci. USA* **99**, 12,339–12,344.
21. Goodell, M. A., Rosenzweig, M., Kim, H., et al. (1997) Dye efflux studies suggest that hematopoietic stem cells expressing low or undetectable levels of CD34 antigen exist in multiple species. *Nat. Med.* **3**, 1337–1345.
22. Storms, R. W., Goodell, M. A., Fisher, A., Mulligan, R. C., and Smith, C. (2000) Hoechst dye efflux reveals a novel CD7+CD34– lymphoid progenitor in human umbilical cord blood. *Blood* **96**, 2125–2133.

23. Uchida, N., Fujisaki, T., Eaves, A. C., and Eaves, C. J. (2001) Transplantable hematopoietic stem cells in human fetal liver have a CD34⁺ side population (SP) phenotype. *J. Clin. Invest.* **108**, 1071–1077.
24. Scharenberg, C. W., Harkey, M. A., and Torok-Storb, B. (2002) The ABCG2 transporter is an efficient Hoechst 33342 efflux pump and is preferentially expressed by immature human hematopoietic progenitors. *Blood* **99**, 507–512.
25. Preffer, F. I., Dombkowski, D., Sykes, M., Scadden, D., and Yang, Y.-G. (2002) Lineage-negative side-population (SP) cells with restricted hematopoietic capacity circulate in normal human adult blood: immunophenotype and functional characterization. *Stem Cells* **20**, 417–427.
26. Riz, I., Eaker, S., and Hawley, R. G. (2002) Genomic biology of hematopoietic stem cells: perspectives and promise for advanced therapeutics. *Appl. Genom. Proteom.* **1**, 95–108.
27. Bunting, K. D. and Hawley, R. G. (2002) The Tao of hematopoietic stem cells: toward a unified theory of tissue regeneration? *Sci. World J.* **2**, 983–995.
28. Abramson, S., Miller, R.G., and Phillips, R.A. (1977) The identification in adult bone marrow of pluripotent and restricted stem cells of the myeloid and lymphoid systems. *J. Exp. Med.* **145**, 1567–1579.
29. Capel, B., Hawley, R. G., and Mintz, B. (1990) Long- and short-lived murine hematopoietic stem cell clones individually identified with retroviral integration markers. *Blood* **75**, 2267–2270.
30. Stewart, A. K., Dubé, I. D., and Hawley, R. G. (1999) Gene marking and the biology of hematopoietic cell transfer in human clinical trials, in *Hematopoiesis and Gene Therapy, Blood Cell Biochemistry*, Vol. 8 (Fairbairn, L. J. and Testa, N., eds.), Kluwer Academic/Plenum Publishers, New York, pp. 243–268.
31. Bhatia, M., Wang, J. C. Y., Kapp, U., Bonnet, D., and Dick, J. E. (1997) Purification of primitive human hematopoietic cells capable of repopulating immune-deficient mice. *Proc. Natl. Acad. Sci. USA* **94**, 5320–5325.
32. Guenechea, G., Gan, O. I., Dorrell, C., and Dick, J. E. (2001) Distinct classes of human stem cells that differ in proliferative and self-renewal potential. *Nat. Immunol.* **2**, 75–82.
33. Van Zant, G. and Fry, C. G. (1983) Hoechst 33342 staining of mouse bone marrow: effects on colony-forming cells. *Cytometry* **4**, 40–46.
34. Siemann, D. W. and Keng, P. C. (1986) Cell cycle specific toxicity of the Hoechst 33342 stain in untreated or irradiated murine tumor cells. *Cancer Res.* **46**, 3556–3559.
35. Erba, E., Ubezio, P., Broggin, M., Ponti, M., and D’Incalci, M. (1988) DNA damage, cytotoxic effect and cell-cycle perturbation of Hoechst 33342 on L1210 cells in vitro. *Cytometry* **9**, 1–6.
36. Latt, S. A. and Stetten, G. (1976) Spectral studies on 33258 Hoechst and related bisbenzimidazole dyes useful for fluorescent detection of deoxyribonucleic acid synthesis. *J. Histochem. Cytochem.* **24**, 24–33.
37. Watson, J. V., Nakeff, A., Chambers, S. H., and Smith, P. J. (1985) Flow cytometric fluorescence emission spectrum analysis of Hoechst-33342-stained DNA in chicken thymocytes. *Cytometry* **6**, 310–315.

38. Ellwart, J. W. and Dormer, P. (1990) Vitality measurement using spectrum shift in Hoechst 33342 stained cells. *Cytometry* **11**, 239–243.
39. Belloc, F., Dumain, P., Boisseau, M. R., et al. (1994) A flow cytometric method using Hoechst 33342 and propidium iodide for simultaneous cell cycle analysis and apoptosis determination in unfixed cells. *Cytometry* **17**, 59–65.
40. Chiu, L., Cherwinski, H., Ransom, J., and Dunne, J. F. (1996) Flow cytometric ratio analysis of the Hoechst 33342 emission spectrum: multiparametric characterization of apoptotic lymphocytes. *J. Immunol. Methods* **189**, 157–171.
41. Telford, W. G., Hawley, T. S., and Hawley, R. G. (2003) Analysis of violet-excited fluorochromes by flow cytometry using a violet laser diode. *Cytometry* **54A**, 48–55.
42. Thomas, H. and Coley, H.M. (2003) Overcoming multidrug resistance in cancer: an update on the clinical strategy of inhibiting P-glycoprotein. *Cancer Control* **10**, 159–165.

10

Hematopoietic Stem Cell Characterization by Hoechst 33342 and Rhodamine 123 Staining

Ivan Bertoncello and Brenda Williams

Summary

A dual-dye efflux strategy utilizing the supravital dyes Hoechst 33342 (Ho) and rhodamine 123 (Rh123) is described and illustrated for the detection and analysis of hematopoietic stem cells in murine bone marrow. Mononuclear cells from bone marrow cell suspensions were incubated in a cocktail of Rh123 plus Ho, and both dyes were effluxed by two 15-min incubations in dye-free buffer prior to sorting. Compared to our original prototype method in which Rh123, but not Ho, was effluxed, this dual-dye efflux protocol more rapidly and efficiently resolves the most primitive $\text{Ho}^{\text{dull}}/\text{Rh}^{\text{dull}}$ hematopoietic stem cells. Moreover, under conditions of optimal dual-dye uptake and efflux, $\text{Ho}^{\text{dull}}/\text{Rh}^{\text{dull}}$ cells map to the subfraction of side population (SP) cells with the highest efflux of Ho, which were previously demonstrated to possess the highest hematopoietic stem cell activity.

Key Words

Dual-dye efflux, $\text{Ho}^{\text{dull}}/\text{Rh}^{\text{dull}}$ cells, Hoechst 33342, primitive hematopoietic stem cells, rhodamine 123.

1. Introduction

The supravital dyes rhodamine 123 (Rh123) and Hoechst 33342 (Ho) have proven to be remarkably powerful probes for the characterization, resolution, isolation, and purification of primitive hematopoietic stem cells (PHSCs). When used alone (*1–10*) or together (*11–17*), and in combination with antibodies specifying stem cell associated cell surface antigens (*18–22*), lectins (*23,24*), or other supravital dyes (*25,26*), Rh123 and Ho precisely dissect and order the murine PHSC compartment, discriminating between closely related stem cell cohorts differing in long-term transplantation potential (*11,13*), cell cycle kinetic status and turnover rate (*13*), rate of entry into cell cycle (*17*), cytokine

From: *Methods in Molecular Biology: Flow Cytometry Protocols*, 2nd ed.
Edited by: T. S. Hawley and R. G. Hawley © Humana Press Inc., Totowa, NJ

receptor repertoire and gene expression patterns, cytokine preferences and responsiveness (16 and 17), and in vitro clonogenic capacity (11–13,17).

The fidelity of Rh123 and Ho as stem cell probes resides in their individual and combined ability to hierarchically order the hematopoietic stem cells on the basis of their probability of cycling by probing individual traits that define the quiescent state (27–29), and by exploiting the overlapping activity of transmembrane efflux pumps belonging to the ABC transporter superfamily (30), including MDR-1 (31,32), MRP1 (33), and Bcrp1/ABCG2 (33–35), for which they are preferential substrates.

1.1. Rh123 and Ho As Stem Cell Probes

Rh123 was first characterized as a mitochondrial membrane specific dye that bound to mitochondria in proportion to their negative membrane potential (36,37). Rh123 is also a preferential substrate for the P-glycoprotein membrane efflux pump, encoded by the murine *mdr1a* and *mdr1b* homologs of human MDR1, which are highly expressed by PHSCs (31,32). Rh123 fluorescence intensity is an index of mitochondrial mass, number and activation state (38), and P-glycoprotein efflux pump activity. The Rh^{dull} phenotype distinguishes primitive, metabolically inactive, relatively quiescent PHSCs with long-term transplant potential from developmentally more mature transplantable cells capable only of short-term regeneration of the hematopoietic system of myeloablated mice (1,6,18,21,22).

Ho is a supravital DNA stain that stoichiometrically binds to the AT-rich regions of the minor groove of DNA (39–41). Ho fluorescence intensity is an index of DNA content, chromatin structure and conformation, and discriminates between cells in different phases of cell cycle (41). Second, although Ho is also a substrate for P-glycoprotein and MRP1 membrane pumps, it is predominantly effluxed by a recently described novel member of the ABC transporter superfamily, bcrp1/ABCG2, that is also highly expressed in PHSCs (33–35). Thus, the Ho^{dull} phenotype also characterizes relatively quiescent PHSCs with long-term transplant potential. PHSCs and primitive hematopoietic progenitor cells are preferentially enriched in the sub-G₁ region of the Ho fluorescence histogram (5), and this supravital dye has also been utilized for stem cell enrichment by many investigators over the last 20 yr (4,7,8). In recent years, the potency and utility of Ho as a stem cell probe has been greatly enhanced by exploitation of long recognized characteristics of Ho binding to DNA.

On binding to DNA, the Ho fluorescence emission undergoes a violet-to-red spectral shift (42–44) contingent on Ho affinity and binding energy, and on the ratio of Ho binding sites to intracellular dye concentration. In addition, Ho dye uptake can be resolved into a concentration-dependent–time-independent component that reaches a plateau minutes after incubation with Ho, and a

time-dependent component that reaches a plateau approx 90 min after incubation. Optimization of Ho dye incubation time to account for these differing binding dynamics, and display of Ho fluorescence as a bivariate Ho-blue vs Ho-red dot-plot to visualize the violet-to-red spectral shift in Ho fluorescence emission has led to further resolution of the sub-G₁ binding fraction to reveal a side population (SP cells) highly enriched in stem cell activity (9,10) (see also Chapter 9 by Eaker et al., *this volume*).

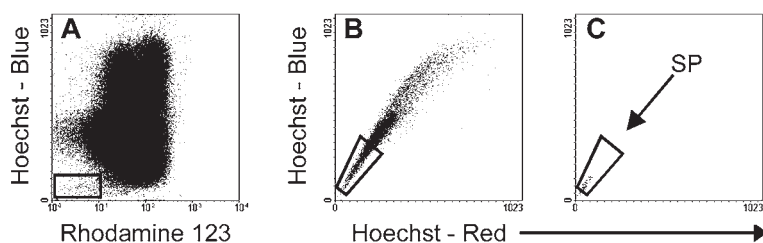
1.2. The Relationship of Ho^{dull}/Rh^{dull} Cells and Ho-SP Cells

On the other hand, the dual-dye cell separative strategy combining Rh123 and Ho dye uptake and efflux exploits the complementary properties of the two dyes and the overlapping roles of different ABC transporter superfamily members (30,33). The bivariate dot-plot display of Rh123 vs Ho fluorescence reveals a Ho^{dull}/Rh^{dull} cluster (Figs. 1A and 2D) that contains PHSCs able to clonally regenerate the hematopoietic system of lethally irradiated mice (11), and contribute to steady-state blood cell production long-term when transplanted in nonablated recipients (14). The dual-dye approach to stem cell sorting has also proven a powerful tool for kinetic analysis of PHSCs, and the analysis of gene expression patterns and cytokine receptor repertoire within the stem cell continuum in steady-state hematopoiesis *in situ* (13,16,17).

In essence, we believe that Rh123 effectively subsets and orders Hoechst-SP cells to define highly synchronous stem cell targets that are superior candidates for the definition of early events in the process of hematopoietic stem cell activation, proliferation, and commitment. However, the precise relationship between Ho^{dull}/Rh^{dull} and SP cells is uncertain as optimal detection of each target cell population utilizes incubation conditions that exploit different characteristics of Rh123 and Ho binding and efflux. For example, incubation conditions for identification of Ho^{dull}/Rh^{dull} cells do not fully exploit the time-dependent Ho efflux component required for optimal revelation of the SP region (Fig. 1A,B). And conversely, the extended efflux time required for optimal resolution of SP cells leads to some loss of definition of the Ho^{dull}/Rh^{dull} cell cluster (Fig. 1D,E). However, it is pertinent to note that in both cases Ho^{dull}/Rh^{dull} cells have an SP phenotype (Fig. 1C,F), and that murine Ho^{dull}/Rh^{dull} cells are predominantly CD34⁻ (*unpublished observation*).

The studies cited thus far describe the use of Rh123 and Ho to separate murine PHSC. Rh123 and Ho have also been used alone, and together to isolate and characterize primitive human hematopoietic stem and progenitor cells with similar outcomes (20,45,46). However, the fluorescence profile of primitive human Ho^{dull}/Rh^{dull} hematopoietic cells are not as clearly resolved and visualized in bivariate fluorescent dot-plots and histograms as the comparable profiles of murine hematopoietic cells. Whether this is related to the differential activity of

Optimal dual-dye uptake and efflux method:



Optimal Hoechst SP cell labeling method:

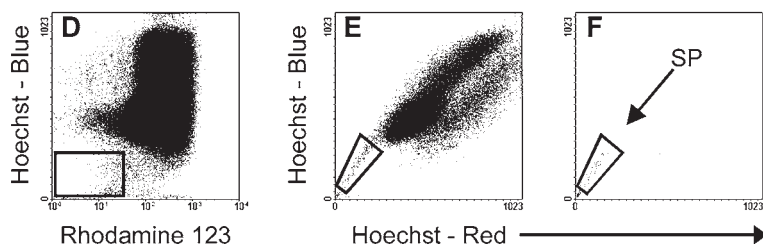


Fig. 1. The relationship between the $\text{Ho}^{\text{dull}}/\text{Rh}^{\text{dull}}$ phenotype and the Hoechst SP phenotype in Lin^- murine bone marrow cell suspensions. Cells were labeled with a cocktail of both fluorochromes using incubation conditions optimized for (A–C) the detection of $\text{Ho}^{\text{dull}}/\text{Rh}^{\text{dull}}$ PHSC (30 min dye uptake at 37°C followed by two 15-min incubation in dye-free medium) or (D–F) the resolution of SP cells (90-min dye uptake at 37°C followed by washing in ice-cold buffer). In each instance, gated $\text{Ho}^{\text{dull}}/\text{Rh}^{\text{dull}}$ cells (A,D) are identified as a subset of Hoechst SP cells (C,F) defined with reference to the Hoechst-blue vs Hoechst-red bivariate dot-plot of each Lin^- bone marrow cell suspension (B,E).

human and murine membrane efflux pumps or the less efficient preenrichment of human hematopoietic stem cell targets is unclear.

1.3. Caveats and Limitations in the Application of Dye-Based Cell Sorting

Despite the robustness of dye-based approaches to stem cell sorting, investigators using these methods must be aware of their limitations, and be vigilant in controlling the critical variables affecting the reproducibility of the technique.

Rh123 and Ho are “functional probes” that exploit the kinetic and metabolic inertia of PHSCs. They are most effective when applied in the steady state,

and less so following perturbation (47) when cell activation, the recruitment of stem cells into the cycle, and the modulation of membrane pump activity distort the relationship between cells of differing developmental potential and maturational age. Mouse strain differences have not been noted. However, it has been reported that the Rh^{dull} phenotype is predominantly attributed to inactive mitochondria in young mice, and to enhanced P-glycoprotein activity in old mice (21,22). Significantly, PHSCs continue to be resolved in the Rh^{dull} cell fraction at all ages.

The significant variables that determine the binding efficiency of Rh123 and Ho and the activity of membrane efflux pumps are: time of incubation and efflux, incubation temperature, dye concentration, density of cell suspensions, and the colligative properties of buffers (48) used for cell manipulation. All have the potential to influence the resolution and homogeneity of sorted stem cell targets. In this context it is interesting to note that the dual-dye staining protocols originally developed or adopted by ourselves (13) and others (11,14,15,25,46) have used different dye-loading and efflux incubation conditions that have exploited membrane pump activity to different degrees. These methods have either allowed for efflux of Rh123 but not Ho (13,25), or have followed a protocol (11,14,15,46) in which cells incubated with Rh123 and Ho were washed in ice-cold dye-free buffer without allowing for efflux of either dye.

The protocol we describe in this chapter is a recent modification (17). Target cells are incubated in a cocktail of Rh123 plus Ho, and both dyes are effluxed by two 15-min incubations in dye-free buffer prior to sorting. This method appears to resolve and discriminate Ho^{dull}/Rh^{dull} cells more rapidly and efficiently than our prototype method (13) in which Rh123, but not Ho, was effluxed.

2. Materials

1. Hoechst 33342 powder (Molecular Probes, Inc., Eugene, OR): Make up a 20 mM stock solution in sterile distilled water and store frozen at -20°C in 50- μL aliquots. Prepare a 1 mM working solution on the day of use by diluting 50 μL of stock solution in 950 μL of phosphate-buffered saline (PBS) (see Note 1). The working solution is protected from light and should be used within a few hours of preparation.
2. Rh123 powder (Molecular Probes, Inc.): Make up a 10 mg/mL stock solution in methanol and store frozen at -20°C in 100- μL aliquots. Make up an intermediate 1 mg/mL dilution by diluting 100 μL of the stock solution in 900 μL of PBS; store frozen in 10- μL aliquots. Prepare a working solution of 10 $\mu\text{g/mL}$ Rh123 on the day of use by diluting 10 μL of the intermediate stock solution in 990 μL of PBS. The working solution is protected from light and should be used within a few hours of preparation.
3. 7-Aminoactinomycin D (7-AAD) powder (Sigma-Aldrich Pty. Ltd., Sydney, Australia): Make up a 1 mg/mL solution in ethanol, followed by a 1:10 dilution

in PBS to give a 100 $\mu\text{g/mL}$ stock solution that is stored frozen at -20°C in 1-mL aliquots. This stock solution is added to cells suspended in PBS–2% heat-inactivated serum (HiSe) at a 1:50 dilution to give a final working concentration of 2 $\mu\text{g/mL}$ 7-AAD for the flow cytometric detection of nonviable cells.

4. Nycoprep™ 1.077A (265 mosM) (Axis-Shield PoC AS, Oslo, Norway) (*see Note 2*).
5. PBS (*see Note 3*): Prepare 1 L of PBS with 8 g of NaCl, 0.2 g of KCl, 1.15 g of Na_2HPO_4 , 0.2 g of K_2HPO_4 , and 0.2 g of glucose (*see Note 4*). Dissolve NaCl in approx 800 mL of distilled H_2O . Add the remaining salts and glucose sequentially, ensuring that each has fully dissolved before adding the next ingredient. Adjust the buffer to pH 7.4 using 1 N HCl or 1 N NaOH. Make up the volume to 1 L, check the osmolality by osmometer and adjust to 310 mosM by addition of the required volume of distilled H_2O . Sterile filter the buffer through a 0.2- μm filter and store refrigerated.
6. Heat-inactivated fetal or newborn bovine serum (HiSe): Heat-inactivate by incubation at 56°C for a minimum of 1 h, cool, and filter through coarse filter paper and filters of progressively smaller pore size. Sterile filter through a 0.2- μm filter, aliquot, and store frozen for use as required. HiSe is added to buffers used for bone marrow cell harvesting and cell manipulation (*see Note 5*).
7. Collagenase/dispase: Make up 3 mg/mL collagenase type 1 (Worthington Biochemical Corp., Lakeside, NJ) and 3 mg/mL of dispase II (neutral protease) from *Bacillus polymyxa*, grade II (Roche Applied Science, Indianapolis, IN) in PBS, separately. Pool the two enzyme solutions 1:1 (v/v) and store frozen for use as required.
8. Antibody reagents: The panel of hematopoietic lineage antibody reagents and isotype control antibodies used for lineage negative selection of PHSCs are listed in **Table 1**. Dilute these antibodies in PBS–2% HiSe containing 0.1% sodium azide (w/v), and pretiter to establish optimal working concentrations for flow cytometric analysis and immunomagnetic selection. Typically we have found that the optimal dilutions for these commercially sourced antibodies range between 1:80 and 1:640 (v/v).
9. Ceramic mortar (approx 10 cm diameter) and pestle.
10. Sterile 40- μm nylon cell strainers (Falcon brand, BD Biosciences Discovery Labware, Bedford, MA).
11. Reagents for immunomagnetic preenrichment using a magnetic activated cell sorter (MACS) (*see Note 6*):
 - a. Streptavidin microbeads (*see Note 7*).
 - b. Columns and MACS devices (Miltenyi Biotec Australia Pty. Ltd., North Ryde, NSW) suitable for this application are listed in **Table 2**.
 - c. Labeling buffer (PBS–2 mM EDTA, pH 7.2) and separation buffer (PBS–2 mM EDTA supplemented with 0.5% bovine serum albumin [BSA], pH 7.2) (*see Note 8*).
 - d. Streptavidin–phycoerythrin (Strep–PE) conjugated rat antimouse antibody.
12. Fluorescence-activated cell sorter (FACS): A dual-laser instrument fitted with appropriate detectors and filter sets (*see Table 3*), and equipped with a 200-mW

Table 1**Description and Source of Antibody Reagents for Negative Immunomagnetic Selection of Murine Hematopoietic Stem and Progenitor Cells**

Biotinylated antibodies ^a	Bone marrow specificity and alternate nomenclature	Clone	Supplier cat. no.	Isotype	Supplier ^b cat. no.
CD3e	T lymphocytes and NK-T cells	145-2C11	Pharmingen 553059	Hamster IgG1,κ	Pharmingen 553970
CD4	L ₃ T ₄ : T helper cells	GK1.5	Pharmingen 553728	Rat IgG2b,κ	Pharmingen 553987
CD5	Mature T lymphocytes and a subset of B lymphocytes	53-7.3	Pharmingen 553018	Rat IgG2a,κ	Pharmingen 553928
CD8a	Ly2: T-suppressor cells	53-6.7	Pharmingen 553028	Rat IgG2a,κ	Pharmingen 553928
B220	CD45R: Pro-B cells through to mature and activated B-cells, but not plasma cells	RA3.6B2	Pharmingen 553085	Rat IgG2a,κ	Pharmingen 553928
Gr-1	Ly6G: Neutrophils, and transiently by bone marrow cells of the monocyte lineage	RB6-8C5	Pharmingen 553124	Rat IgG2b,κ	Pharmingen 553987
Mac-1 (CD11b)	CD11b: Macrophages, granulocytes, dendritic cells, and NK cells	M1/70	Pharmingen 557395	Rat IgG2b,κ	Pharmingen 553987
Ter-119	Ly76: Erythroblasts through to mature erythrocytes, but not BFU-e and CFU-e	Ter-119	Pharmingen 553672	Rat IgG2b,κ	Pharmingen 553987

^aAll antibodies are rat antimouse, with the exception of anti-CD3 which is Armenian hamster antimouse.

^bThe supplier is BD Biosciences Pharmingen (San Diego, CA).

laser (such as an argon laser) capable of exciting at 488 nm, and an ultraviolet (UV) laser running at 50 mW power.

13. FACS collection tubes: Sterile 1.5-mL Eppendorf tubes or sterile 12 × 75 mm polypropylene tissue culture tubes.

3. Methods

3.1. Bone Marrow Cell Harvesting

1. Excise femurs, tibiae, and iliac crests. Scrape with a sterile surgical blade to remove adherent muscle and tissues. Place in cold PBS–2% HiSe.
2. Crush the bones using a sterile mortar and pestle, and filter the cell suspension through a 40-μm nylon cell strainer to remove bone debris (*see Note 9*).
3. Resuspend the bone fragments in a sterile 50-mL centrifuge tube in equal volumes of 3 mg/mL collagenase and 3 mg/mL dispase (*see Note 10*); incubate at 37°C for at least 5 min in an orbital shaker. Top up the tube with 25 mL of

Table 2

Maximum Capacity and Optimal Configuration of MACS Separation Columns Used for Negative Immunomagnetic Selection of Murine PHSCs

Column type	Magnetic separation device	Optimal flow resistor	Maximum column capacity (magnetically labeled cells)	Maximum column capacity (total cells)
LD	MidiMACS VarioMACS or SuperMACS with column adaptors		10^8	5×10^8
CS	VarioMACS SuperMACS	Three-way stopcock and 22G flow resistor	2×10^8	10^9
D	SuperMACS	Three-way stopcock and 21G flow resistor	10^9	5×10^9

PBS–2% HiSe, shake vigorously, and carefully decant the supernatant cells through a 40- μ m nylon cell strainer. Resuspend the bone fragments in 25 mL of PBS–2% HiSe a second time and decant supernatant cells as before.

4. Centrifuge the cell suspension at 400g for 5 min at 4°C. Resuspend the cell pellet in PBS–2% HiSe. Pool all bone marrow cells, centrifuge, and wash twice in excess PBS–2% HiSe prior to dilution to an approximate cell density of 10^7 cells/mL.

3.2. Preparation of Low-Density Cells

1. Carefully layer 20-mL aliquots of bone marrow cell suspension over 10 mL of Nycoprep 1.077A in 50-mL centrifuge tubes (*see Note 11*). Centrifuge in a refrigerated centrifuge (600g at 4°C for 20 min) with the brake off.
2. Collect low density mononuclear cells at the Nycoprep interface in excess PBS–2% HiSe, wash, centrifuge twice, and resuspend in PBS–2% HiSe. Determine the cell count.

3.3. Negative Immunomagnetic Selection

1. Pellet low-density bone marrow cells and resuspend at 10^8 cells/mL in an optimally pretitered cocktail of biotinylated antibodies directed against CD3, CD4, CD5, CD8, B220, Gr1, Mac-1, and TER119 antigens (*see Table 1*). Incubate for 30 min on ice.

Table 3

Instrument Settings and Optical Filter Selection for the Isolation of Ho^{dull}/Rh^{dull} PHSC

Fluorochrome/ conjugate	PMT parameter	Excitation wavelength (nm)	Emission wavelength (nm)	Optical filter set characteristics (nm)
Rhodamine 123	FL1	488	530	530/30
PE-conjugated antibodies	FL2	488	575	575/26
7-AAD	FL3	488	650	675/20
Hoechst 33342	FL4	350	450	424/44

- At the same time, set aside two small aliquots of low-density bone marrow cells to be used as reference samples for setting a Lin⁻ sort gate (*see Subheading 3.6., step 3*). Incubate one aliquot with Strep-PE alone, the other aliquot with Strep-PE and a cocktail of relevant isotype control antibodies made up at the same protein concentration as the lineage antibodies.
- Wash labeled cells in excess MACS labeling buffer and centrifuge (400g at 4°C for 5 min) to remove residual unbound antibody. Resuspend in MACS labeling buffer.
- Perform a cell count. Set aside a small aliquot of labeled cells ($\sim 2.5 \times 10^5$) for incubation with Strep-PE as a pre-MACS control sample to be used for: (a) flow cytometric evaluation of the efficacy of negative immunomagnetic selection, (b) adjustment of fluorescence compensation settings, and (c) setting a sort gate excluding contaminating lineage positive cells in the Ho^{dull}/Rh^{dull} cell separation strategy.
- Centrifuge the remainder of the cell suspension a second time (400g at 4°C for 5 min) and decant the supernatant, leaving a dry cell pellet.
- Resuspend the antibody labeled cell pellet in 90 μ L of labeling buffer plus 10 μ L of streptavidin microbeads per 10^7 cells according to the manufacturer's instructions (*see Note 12*). Mix well and incubate on ice for 15 min with periodic agitation.
- Following microbead incubation, wash labeled cells in 1–2 mL of MACS separation buffer per 10^7 cells (400g at 4°C for 5 min). Resuspend the cell pellet in MACS separation buffer at a cell density of 10^8 cells/500 μ L.
- During the antibody and microbead labeling steps described in the preceding, select an appropriate MACS column (*see Table 2*), prepare, assemble, and place in the magnetic separator following the instructions provided in the manufacturer's data sheets (*see Note 13*).
- In brief, apply the cell suspension to the washed column and allow the cells to penetrate the matrix by turning the stopcock to run position. Collect the nonmagnetic, hematopoietic lineage negative cells in the column effluent by washing the column with three to five column volumes of MACS separation buffer (*see Note 14*).

3.4. Rh123 and Ho Staining

1. Prepare working solutions of 10 $\mu\text{g/mL}$ of Rh123 and 1 mM Ho from frozen stock solutions immediately prior to use.
2. Following determination of lineage-negative cell yield, centrifuge the cell suspension (400g at 4°C for 5 min) and resuspend the cell pellet at a density of 1×10^6 cells/mL in PBS–5% HiSe in preparation for staining with Rh123 and Ho.
3. Add a 10- μL volume of each fluorochrome per milliliter of low-density, Lin^- , cell suspension to give a final concentration of 0.1 μg of Rh123 and 10 μM Hoechst. Gently agitate the cell suspension and incubate in a 37°C water bath for 30 min in the dark (*see* **Note 15**).
4. Follow Rh123 and Ho dye staining by two incubations at 37°C in dye-free buffer to exploit membrane efflux pump activity in the resolution of Ho^{dull} / Rh^{dull} cells.
 - a. Pellet the Rh123/Ho-stained cells by centrifugation at room temperature (400g for 5 min), resuspend at 1×10^6 cells/mL in prewarmed dye-free PBS–5% HiSe, and return to the 37°C water for 15 min in the dark.
 - b. Pellet the cells again by centrifugation and repeat the dye-efflux step a second time.
5. Following the second dye-efflux step, set aside an aliquot of Rh123/Ho-stained cells (2.5×10^5) on ice as a flow cytometry control.
6. Pellet the remainder of the cell suspension, resuspend in Strep–PE at 10^8 cells/mL, and incubate on ice for 30 min in the dark to detect residual contaminating hematopoietic lineage positive cells.
7. Add excess PBS–0.25% HiSe. Pellet the cell suspension by centrifugation (400g at 4°C for 5 min) and resuspend in PBS–0.25% HiSe at $5\text{--}10 \times 10^6$ cells/mL. Add 7-AAD stock solution (1:50 v/v) to give a final 7-AAD concentration of 2 $\mu\text{g/mL}$. Store the labeled cells on ice in preparation for flow cytometric analysis and sorting.

3.5. FACS Instrument Settings

Aliquots of the following cell samples are required for selection of instrument settings and fluorescence compensation.

1. Unfractionated bone marrow cells stained with 7-AAD for determining cell viability settings and for setting a lymphoblastoid light scatter gate.
2. Low-density bone marrow cells labeled with biotinylated isotype control antibody cocktail and Strep–PE to determine background fluorescence and quantify non-specific labeling.
3. Pre-MACS control cells labeled with biotinylated antibody cocktail followed by Strep–PE to be used in conjunction with low-density cells labeled with Strep–PE alone to set the Lin^- cell gate.
4. Rh/Ho-stained and effluxed nonmagnetic Lin^- cells to determine photomultiplier tube (PMT) settings for optimal detection and resolution of Ho^{dull} / Rh^{dull} cells.

Table 4

Flow Cytometric Gating Strategy for Flow Cytometric Analysis and Sorting of Murine Ho^{dull}/Rh^{dull} PHSC

Region	Display	PMT parameter and scaling
R1	7-AAD dye uptake	FL3 histogram (logarithmic)
R2	Cell size and structure	FSC vs SSC (linear vs linear)
R3	Lineage antibody expression	FL2 histogram (logarithmic)
R4	Rh123 vs. Hoechst dye uptake	FL1 vs FL4 (logarithmic vs linear)

Sequential gating strategy	Gate	Target cell description
R1	G1	Viable cells
R1 and R2	G2	Viable lymphoblastoid-like cells
R1 and R2 and R3	G3	Viable, Lin ⁻ , lymphoblastoid-like cells
R1 and R2 and R3 and R4	G4	Viable, Lin ⁻ , Ho ^{dull} /Rh ^{dull} lymphoblastoid-like cells

- Adjust fluorescence compensation settings using the above control cell samples to account for the overlapping spectral emissions of Rh123, PE, and 7-AAD excited by the argon laser.
 - Rh123 (FL1) vs PE (FL2): Rh/Ho-stained Lin⁻ cells.
 - PE (FL2) vs Rh123 (FL1): Biotinylated antibody/Strep-PE labeled pre-MACS control cells.
 - PE (FL2) vs 7-AAD (FL3): Biotinylated antibody/Strep-PE labeled pre-MACS control cells.
 - 7-AAD (FL3) vs PE (FL2): Unfractionated, 7-AAD stained bone marrow cells.
- Ho fluorescence is excited by the second (UV) laser and does not require compensation.

3.6. Sort Gating Strategy for Isolation of Ho^{dull}/Rh^{dull} Cells

The sequential gating strategy for the isolation of Ho^{dull}/Rh^{dull} PHSCs is described in **Table 4** and illustrated in **Fig. 2**.

- Set an appropriate gate on the 7-AAD histogram profile to exclude nonviable (7-AAD positive) cells.
- Select a forward scatter (FSC) vs side scatter (SSC) window defining viable lymphoblastoid cells, and excluding debris and cell doublets.

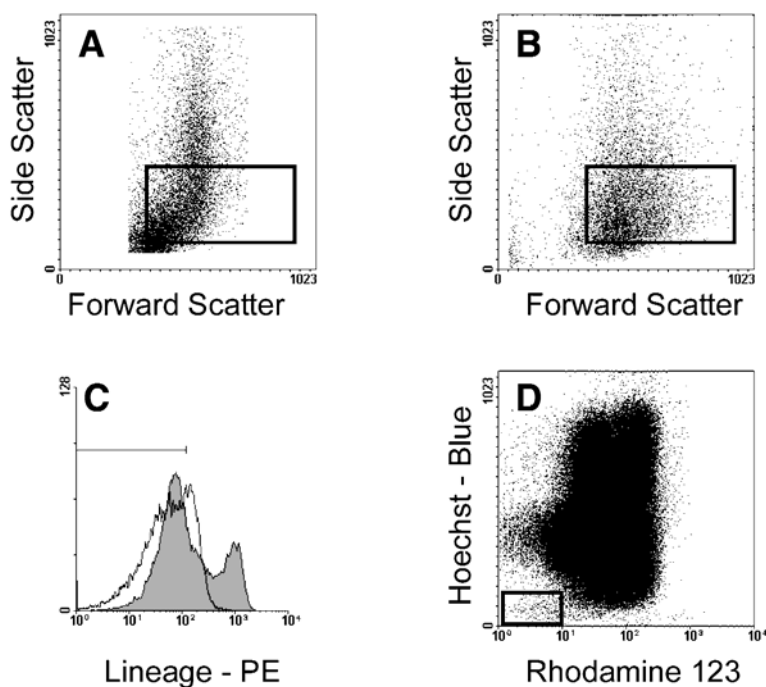


Fig. 2. The sequential gating strategy for the isolation of Lin⁻ Ho^{dull}/Rh^{dull} PHSC. Unseparated murine bone marrow (**A**) is used to define a FSC vs SSC lymphoblastoid gate that contains the majority of hematopoietic stem and progenitor cells (**I**). This gate is then imposed on the FSC vs SSC bivariate plot of viable low density Lin⁻ cells prepared by negative immunomagnetic selection using the MACS system (**B**). Residual Lin⁺ cells within the light scatter gate are excluded by setting a histogram region (**C**) with reference to the fluorescence profiles of an antibody labeled pre-MACS control sample (*shaded histogram*) and low-density cells labeled with a cocktail of relevant biotinylated isotype control antibodies and streptavidin-PE (*solid line*). A sort window defining the Ho^{dull}/Rh^{dull} phenotype (**D**) is then set with reference to the bivariate Rh123 vs Ho fluorescence dot-plot of cells within these conditional gates.

3. Within this light scatter window, exclude contaminating Lin⁺ cells in the Lin⁻ cell fraction (prepared by negative immunomagnetic selection) by setting a histogram gate with reference to the fluorescence histogram profile of low-density cells labeled with a cocktail of relevant biotinylated isotype control antibodies and Strept-PE.
4. Set a sort window defining the Ho^{dull}/Rh^{dull} phenotype within these conditional gates with reference to the bivariate Rh123 vs Ho fluorescence dot-plot in which Ho fluorescence is displayed on a linear scale, and Rh123 fluorescence is displayed on a logarithmic scale (*see Note 16*).

3.7. Sorting *Ho^{dull}/Rh^{dull} PHSC*

1. Selection of sort mode is instrument dependent. For the FACStar^{Plus} cell sorter (BD Biosciences, San Jose, CA), we sort cells in a two-droplet packet in “Normal R” mode. For the FACS Vantage SE (BD Biosciences), sort with a purity mask.
2. The *Ho^{dull}/Rh^{dull}* cell cluster typically comprises no more than 0.5% of listed events in the conditionally gated Rh123 vs Ho bivariate dot-plot. Consequently, it is recommended that the sort sample be run at low to medium differential pressures/flow rates to improve the definition and resolution of this subpopulation. For cell suspensions of 5×10^6 cells/mL we generally sort at rates of 2500–5000 events per second even when using a high-speed cell sorter.
3. The choice of collection vessel for sorted cells is determined by the expected cell recovery. Typically cells are sorted into sterile 1.5-mL Eppendorf tubes or 12 × 75 mm sterile polypropylene tissue culture tubes. The collection tubes are coated with a small volume of sterile HiSe or with PBS–5% HiSe into which the cells are collected.
4. Low-density Lin[−] *Ho^{dull}/Rh^{dull}* cells comprise approx 0.007% of cells in starting unfractionated murine bone marrow cell suspensions. Theoretical cell yields at each step of this cell separative protocol are given in the flowchart in **Fig. 3**. In practice, the actual number of sorted *Ho^{dull}/Rh^{dull}* cells recovered is generally lower. The yield is dependent on nonspecific cell losses during cell manipulation (which are proportionately more significant when processing small bone marrow harvests), day-to-day variation in cell sorting efficiency, and the precise setting of the Rh123 vs Ho sort window (*see Note 16*).

4. Notes

1. Hoechst 33342 can also be purchased from Molecular Probes Inc., as a 10 mg/mL solution dissolved in water. Some investigators have noted that Hoechst 33342 can precipitate in PBS at concentrations >30 μ M (**26**). We have occasionally noticed this when using serum-supplemented PBS. Precipitation is not instantaneous and can be avoided by making serial dilutions quickly. If precipitation is observed, the working solution should be discarded.
2. Murine mononuclear cells, like those of most mammalian species, are denser than human mononuclear cells. While commercial density gradient media for isolation of human mononuclear cells are generally formulated at osmolarities isotonic with human plasma, Nycoprep 1.077A is specifically formulated at a lower osmolarity (265 mosm) for optimal isolation of nonhuman mammalian mononuclear cells.
3. We routinely use PBS for all cell manipulations prior to cell culture. It is possible to use bicarbonate buffered balanced salt solutions, or more complex media, but these should be buffered using *N*-(2-hydroxyethyl)piperazine-*N*-(2-ethanesulfonic acid) (HEPES). It is preferable to avoid use of buffers containing phenol red, as this dye can be excited at 488 nm and can cause cells to autofluoresce. However, these fluorescent emissions can be compensated, and we have used these buffers in the past without adversely affecting the detection of *Ho^{dull}/Rh^{dull}* target cells.

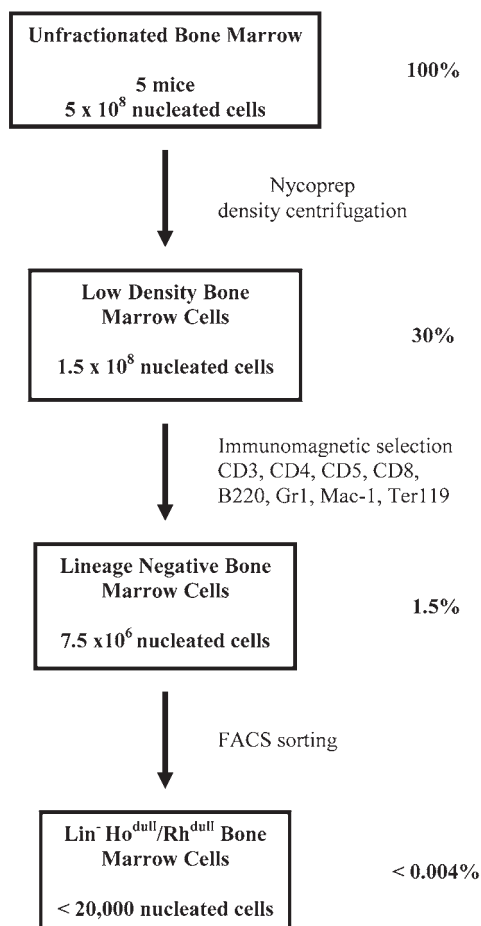


Fig. 3. Flowchart showing typical yields of nucleated cells at each step of the multiparameter cell separative strategy devised for the isolation of $\text{Ho}^{\text{dull}}/\text{Rh}^{\text{dull}}$ PHSC from normal murine bone marrow.

4. The weights of chemical reagents used for making up PBS are for the anhydrous form of buffer ingredients. If hydrated forms of these reagents are used the weights need to be adjusted accordingly.
5. Heat inactivation of serum for this application is adopted as a precautionary measure. Although is not strictly necessary when using highly purified antibody reagents, we do so because we have occasionally experienced significant nonspecific cell losses when using buffers supplemented with non-heat-inactivated serum especially when incubating bone marrow cells with unpurified or partially purified

antibody supernatants. Alternately, 0.5% BSA (fraction V, tissue culture grade) can be substituted for serum as a buffer constituent.

6. We use MACS systems as the immunomagnetic cell separation platform in our laboratory. It is equally valid to use Dynabeads for this purpose. Alternatively, cells can be labeled with a cocktail of PE-conjugated primary antibodies. In this case, hematopoietic lineage antigen positive cells can be excluded flow cytometrically in the sort gating strategy. We have often used this approach for flow cytometric analysis of Ho^{dull}/Rh^{dull} bone marrow cells. However, because lineage positive cells constitute up to 95% of the low density cell fraction this alternative significantly extends the amount of cell sorter time required to isolate Ho^{dull}/Rh^{dull} PHSC.
7. We have chosen to use biotinylated antibody reagents and streptavidin beads for immunomagnetic selection based on the versatility of the primary antibody reagents in other applications in our laboratory. It is equally valid to use purified primary rat antimouse antibodies and microbead-conjugated antirat IgGs. The choice of fluorochrome conjugates will also ultimately be guided by laser configuration and fluorescence emission detection capabilities of the cell sorter.
8. It is imperative that biotin-free buffer is used for labeling with biotinylated antibodies to prevent competition of free biotin with biotinylated antibody in the binding of the streptavidin microbeads. This buffer can be supplemented with certified biotin-free BSA, but not serum or BSA of unknown status. BSA-supplemented buffer is recommended for the immunomagnetic separation steps following antibody and immunomagnetic bead conjugation.
9. The collection of bone marrow cells by crushing bones using a mortar and pestle rather than solely by flushing the bone shafts from both ends with cold PBS–2% HiSe using a 1-mL syringe fitted with a 23-gage needle significantly reduces the number of donor mice. Lambert et al. (49) have shown that approx 5×10^8 cells can be recovered from the entire skeleton of single adult mouse using this method. We typically harvest approx 10^8 cells from the pooled femurs, tibiae, and iliac crest of a single adult mouse.
10. PHSC are intimately associated with endosteal marrow (50). Digestion of crushed bone fragments using collagenase/dispase also maximizes stem cell yield. Periodic agitation of the tube will aid dispersion of the cells if a 37°C water bath is used in place of a shaker.
11. We routinely use 50-mL tubes for density gradient centrifugation. If preferred, gradients can be prepared in 15-mL centrifuge tubes by overlaying 6 mL of cell suspension on a 5-mL Nycoprep cushion. On average, a single 50-mL gradient tube is required for the bone marrow harvested from two mice.
12. Although it is advisable to follow the manufacturer's advice, a lower bead/cell ratio can be used; but the likelihood of contamination of the nonmagnetic fraction with cells expressing low levels of hematopoietic lineage antigens is increased.
13. Typically, a CS column (capacity 2×10^8 magnetically labeled cells) is required for the bone marrow harvested from five or six mice. The manufacturer's data sheets specify a number of flow resistors that are suitable for use with various

MACS columns. We have found that optimal resolution of Lin⁻ cells is achieved using a 22G flow resistor with a CS column and a 21G flow resistor if using a D column.

14. There are a number of critical variables that must be controlled to ensure an optimal enrichment of lineage-negative cells using the MACS system. The separator must be chilled, and buffers and cell suspensions kept cold. Degassing of buffers used to prime and wash MACS columns is essential to prevent the formation of air bubbles in the column or flow resistor with consequent impairment of flow rate. Likewise, it is essential that the column not be allowed to run dry during the separation procedure.
15. Temperature is an important variable that must be precisely controlled for optimal performance of efflux pumps. It is essential that buffers and media used in dye loading and efflux steps be prewarmed; and that tubes be immersed in a 37°C water bath to at least the level of the meniscus of the cell suspension during this procedure.
16. In contrast to the gating strategy used by others to isolate Ho^{dull}/Rh^{dull} cells (**11**) in which this fraction is delimited by the lowest 15 percentiles of Rh123 fluorescence within the lowest 3 percentiles of Ho fluorescence, we have defined Ho^{dull}/Rh^{dull} cells with reference to the bivariate Rh123 vs Ho fluorescence dot-plot (**13**). In the first strategy placement of the Rh123 sort gate is contingent on the distribution of Ho fluorescent cells. Although our approach by-and-large defines a similar population (0–14th percentile of Rh123 fluorescence within the 0–5th percentile of Ho fluorescence), we believe that definition Ho^{dull}/Rh^{dull} cells with reference to the bivariate plot provides a more accurate and reproducible definition of the Ho^{dull}/Rh^{dull} phenotype. However, in those instances in which the Ho^{dull}/Rh^{dull} cell cluster is difficult to visualize in the bivariate dot-plot, we defer to the former method.

References

1. Bertoncello, I., Hodgson, G. S., and Bradley, T. R. (1985) Multiparameter analysis of transplantable hemopoietic stem cells. I. The separation and enrichment of stem cells homing to marrow and spleen on the basis of Rhodamine 123 fluorescence. *Exp. Hematol.* **13**, 999–1006.
2. Bertoncello, I., Hodgson, G. S., and Bradley, T. R. (1988) Multiparameter analysis of transplantable hemopoietic stem cells. II. Stem cells of long-term bone marrow reconstituted recipients. *Exp. Hematol.* **16**, 245–249.
3. Bertoncello, I., Bradley, T. R., Hodgson, G. S., and Dunlop, J. M. (1991) The resolution, enrichment, and organisation of normal bone marrow high proliferative potential colony-forming cell subsets on the basis of rhodamine 123 fluorescence. *Exp. Hematol.* **19**, 174–178.
4. Visser, J. W., Bol, S. J., and van den Engh, G. (1981) Characterization and enrichment of murine hemopoietic stem cells by fluorescence activated cell sorting. *Exp. Hematol.* **9**, 644–655.
5. Baines, P. and Visser, J. W. (1983) Analysis and separation of murine bone marrow stem cells by H33342 fluorescence-activated cell sorting. *Exp. Hematol.* **11**, 701–708.

6. Ploemacher, R. E. and Brons, N. H. (1988) Cells with marrow and spleen repopulating ability and forming spleen colonies on day 16, 12 and 8 are sequentially ordered on the basis of increasing rhodamine 123 retention. *J. Cell. Physiol.* **136**, 531–536.
7. Pallavicini, M. G., Summers, L. J., Dean, P. N., and Gray, J. W. (1985) Enrichment of murine hemopoietic clonogenic cells by multivariate analyses and sorting. *Exp. Hematol.* **13**, 1173–1181.
8. Neben, S., Redfearn, W. J., Parra, M., Brecher, G., and Pallavicini, M. (1991) Short- and long-term repopulation of lethally irradiated mice by bone marrow stem cells enriched on the basis of light scatter and Hoechst 33342 fluorescence. *Exp. Hematol.* **19**, 958–967.
9. Goodell, M. A., Brose, K., Paradis, G., Conner, A. S., and Mulligan, R. C. (1996) Isolation and functional properties of murine hematopoietic stem cells that are replicating in vivo. *J. Exp. Med.* **183**, 1797–1806.
10. Goodell, M. A., Rosenzweig, M., Kim, H., et al. (1997) Dye efflux studies suggest that hematopoietic stem cells expressing low or undetectable levels of CD34 antigen exist in multiple species. *Nat. Med.* **3**, 1337–1345.
11. Wolf, N. S., Kone, A., Priestley, G. V., and Bartelmez, S. H. (1993) In vivo and in vitro characterization of long-term repopulating primitive hematopoietic cells isolated by sequential Hoechst 33342-rhodamine 123 FACS selection. *Exp. Hematol.* **21**, 614–622.
12. Sitnicka, E., Ruscetti, F. W., Priestley, G. V., Wolf, N. S., and Bartelmez, S. H. (1996) Transforming growth factor beta 1 directly and reversibly inhibits the initial cell divisions of long-term repopulating hematopoietic stem cells. *Blood* **88**, 82–88.
13. Bradford, G. B., Williams, B., Rossi, R., and Bertoncello, I. (1997) Quiescence, cycling and turnover in the primitive hematopoietic stem cell compartment. *Exp. Hematol.* **25**, 445–453.
14. Nilsson, S., Dooner, M., Tiarks, C., Heinz-Ulrich, W., and Quesenberry, P. J. (1997) Potential and distribution of transplanted hematopoietic stem cells in a non-ablated mouse model. *Blood* **89**, 4013–4020.
15. Reddy, G. P., Tiarks, C. Y., Pang, L., Wu, J., Hsieh, C. C., and Quesenberry, P. J. (1997) Cell cycle analysis and synchronization of pluripotent hematopoietic progenitor stem cells. *Blood* **90**, 2293–2299.
16. Micallef, S., Ramsay, R., Williams, B., Rossi, R., Mucenski, M., and Bertoncello, I. (2000) The role of c-myc and BCL-2 in hematopoietic stem cell regulation. *Exp. Hematol.* **28**(Suppl. 1), **68**.
17. Reddy, G. P. V., McAuliffe, C. I., Pang, L., Quesenberry, P. J., and Bertoncello, I. (2002) Cytokine receptor repertoire and cytokine responsiveness of Ho^{dull}/Rh^{dull} stem cells with differing potentials for G₁/S phase progression. *Exp. Hematol.* **30**, 792–800.
18. Spangrude, G. J. and Johnson, G. R. (1990) Resting and activated subsets of mouse multipotent hematopoietic stem cells. *Proc. Natl. Acad. Sci. USA* **87**, 7433–7437.
19. Li, C. L. and Johnson, G. R. (1995) Murine hematopoietic stem and progenitor cells: I. Enrichment and biologic characterization. *Blood* **85**, 1472–1479.

20. Uchida, N., Combs, J., Chen, S., Zanjani, E., Hoffman, R., and Tsukamoto, A. (1996) Primitive human hematopoietic cells displaying differential efflux of the rhodamine 123 dye have distinct biological activities. *Blood* **88**, 1297–1305.
21. Kim, M., Cooper, D. D., Hayes, S. F., and Spangrude, G. J. (1998) Rhodamine-123 staining in hematopoietic stem cells of young mice indicates mitochondrial activation rather than dye efflux. *Blood* **91**, 4106–4117.
22. Kim, M., Moon, H. B., and Spangrude, G. J. (2003) Major age-related changes of mouse hematopoietic stem/progenitor cells. *Ann. NY Acad. Sci.* **996**, 195–208.
23. Zijlmans, J. M., Visser, J. W., Kleiverda, K., Kluin, P. M., Willemze, R., and Fibbe, W. E. (1995) Modification of rhodamine staining allows identification of hematopoietic stem cells with preferential short-term or long-term bone marrow-repopulating ability. *Proc. Natl. Acad. Sci. USA* **92**, 8901–8905.
24. Visser, J. W. and de Vries, P. (1988) Isolation of spleen-colony forming cells (CFU-s) using wheat germ agglutinin and rhodamine 123 labeling. *Blood Cells* **14**, 369–384.
25. Huttman, A., Liu, S. L., Boyd, A. W., and Li, C. L. (2001) Functional heterogeneity within rhodamine123(lo) Hoechst33342(lo/sp) primitive hemopoietic stem cells revealed by pyronin Y. *Exp. Hematol.* **29**, 1109–1116.
26. Srour, E. F. and Jordan, C. T. (2002) Isolation and characterization of primitive hematopoietic cells based on their position in the cell cycle, in *Hematopoietic Stem Cell Protocols* (Klug, C. A. and Jordan, C. T., eds.), Humana Press, Totowa, NJ, pp. 93–111.
27. Hellman, S., Botnick, L. E., Hannon, E. C., and Vigneulle, R. M. (1978) Proliferative capacity of murine hematopoietic stem cells. *Proc. Natl. Acad. Sci. USA* **75**, 490–494.
28. Lajtha, L. G. (1979) Stem cell concepts. *Differentiation* **14**, 23–34.
29. Hodgson, G. S., Bradley, T. R., and Radley, J. M. (1982) The organization of hemopoietic tissue as inferred from the effects of 5-fluorouracil. *Exp. Hematol.* **10**, 26–35.
30. Bunting, K. D. (2002) ABC transporters as phenotypic markers and functional regulators of stem cells. *Stem Cells* **20**, 11–20.
31. Schinkel, A. H., Smit, J. J., van Tellingen, O., et al. (1994) Disruption of the mouse *mdr1a* P-glycoprotein gene leads to a deficiency in the blood–brain barrier and to increased sensitivity to drugs. *Cell* **77**, 491–502.
32. Schinkel, A. H., Mayer, U., Wagenaar, E., et al. (1997) Normal viability and altered pharmacokinetics in mice lacking *mdr1*-type (drug-transporting) P-glycoproteins. *Proc. Natl. Acad. Sci. USA* **94**, 4028–4033.
33. Scharenberg, C. W., Harkey, M. A., and Torok-Storb, B. (2002) The ABCG2 transporter is an efficient Hoechst 33342 efflux pump and is preferentially expressed by immature human hematopoietic progenitors. *Blood* **99**, 507–512.
34. Zhou, S., Schuetz, J. D., Bunting, K. D., et al. (2001) The ABC transporter Bcrp1/ABCG2 is expressed in a wide variety of stem cells and is a molecular determinant of the side-population phenotype. *Nat. Med.* **7**, 1028–1034.

35. Zhou, S., Morris, J. J., Barnes, Y., Lan, L., Schuetz, J. D., and Sorrentino, B. P. (2002) Bcrp1 gene expression is required for normal numbers of side population stem cells in mice, and confers relative protection to mitoxantrone in hematopoietic cells in vivo. *Proc. Natl. Acad. Sci. USA* **99**, 12,339–12,344.
36. Johnson, L. V., Walsh, M. L., and Chen, L. B. (1980) Localization of mitochondria in living cells with rhodamine 123. *Proc. Natl. Acad. Sci. USA* **77**, 990–994.
37. Johnson, L. V., Walsh, M. L., Bockus, B. J., and Chen, L. B. (1981) Monitoring of relative mitochondrial membrane potential in living cells by fluorescence microscopy. *J. Cell Biol.* **88**, 526–535.
38. Darzynkiewicz, Z., Staiano-Coico, L., and Melamed, M. R. (1981) Increased mitochondrial uptake of rhodamine 123 during lymphocyte stimulation. *Proc. Natl. Acad. Sci. USA* **78**, 2383–2387.
39. Latt, S. A. and Stetten, G. (1976) Spectral studies on 33258 Hoechst and related bisbenzimidazole dyes useful for fluorescent detection of deoxyribonucleic acid synthesis. *J. Histochem. Cytochem.* **24**, 24–33.
40. Lalande, M. E. and Miller, R. G. (1979) Fluorescence flow analysis of lymphocyte activation using Hoechst 33342 dye. *J. Histochem. Cytochem.* **27**, 394–397.
41. Arndt-Jovin, D. J. and Jovin, T. M. (1977) Analysis and sorting of living cells according to deoxyribonucleic acid content. *J. Histochem. Cytochem.* **25**, 585–589.
42. Watson, J. V., Nakeff, A., Chambers, S. H., and Smith, P. J. (1985) Flow cytometric fluorescence emission spectrum analysis of Hoechst-33342-stained DNA in chicken thymocytes. *Cytometry* **6**, 310–315.
43. Smith, P. J., Nakeff, A., and Watson, J. V. (1985) Flow-cytometric detection of changes in the fluorescence emission spectrum of a vital DNA-specific dye in human tumour cells. *Exp. Cell Res.* **159**, 37–46.
44. Smith, P. J., Morgan, S. A., and Watson, J. V. (1991) Detection of multidrug resistance and quantification of responses of human tumour cells to cytotoxic agents using flow cytometric spectral shift analysis of Hoechst 33342-DNA fluorescence. *Cancer Chemother. Pharmacol.* **27**, 445–450.
45. Ratajczak, M. Z., Pletcher, C. H., Marlicz, W., et al. (1998) CD34⁺, kit⁺, rhodamine123(low) phenotype identifies a marrow cell population highly enriched for human hematopoietic stem cells. *Leukemia* **12**, 942–950.
46. Leemhuis, T., Yoder, M. C., Grigsby, S., Aguero, B., Eder, P., and Srouf, E. F. (1996) Isolation of primitive human bone marrow hematopoietic progenitor cells using Hoechst 33342 and Rhodamine 123. *Exp. Hematol.* **24**, 1215–1224.
47. Szilvassy, S. J. and Cory, S. (1993) Phenotypic and functional characterization of competitive long-term repopulating hematopoietic stem cells enriched from 5-fluorouracil-treated murine marrow. *Blood* **81**, 2310–2320.
48. Borth, N., Kral, G., and Katinger, H. (1993) Rhodamine 123 fluorescence of immortal hybridoma cell lines as a function of glucose concentration. *Cytometry* **14**, 70–73.

49. Lambert, J. F., Carlson, J. E., Colvin, G. A., and Quesenberry, P. J. (2000) Evaluation of mouse whole body bone marrow cellularity and distribution of hematopoietic progenitors. *Exp. Hematol.* **28**, 1493.
50. Nilsson, S. K., Johnston, H. M., and Coverdale, J. A. (2001) Spatial localization of transplanted hemopoietic stem cells: inferences for the localization of stem cell niches. *Blood* **97**, 2293–2299.

Phenotypic and Functional Analyses of CD34^{NEG} Hematopoietic Precursors From Mobilized Peripheral Blood

Douglas C. Dooley and Barbara K. Oppenlander

Summary

Methods are described for the characterization of CD34 antigen modulation and its relationship to cell proliferation in early human hematopoietic cells. Toward that end, quiescent primitive CD34⁺ and CD34^{NEG} cells are purified from mobilized peripheral blood (MoPB). Unlike CD34^{NEG} cells from other sources, those from MoPB grow readily in stroma-free culture, facilitating their analysis. Using a lineage-depleted, low-density mononuclear cell fraction, CD34^{NEG}CD38^{NEG}LIN^{NEG} and CD34⁺CD38^{NEG}LIN^{NEG} cells are purified by cell sorting. Cells are cultured in serum-free medium supplemented with early acting cytokines. Up- and down-modulation of CD34 antigen can be observed within 40 h of incubation. Samples are removed for analysis of expression of CD34, CD38 and lineage-commitment antigens as well as for cell proliferation as determined by expression of Ki67 antigen and uptake of pyronin Y. This approach permits an assessment of changes in CD34 and CD38 antigen expression by primitive LIN^{NEG} cells as they are activated for growth or remain in a quiescent state.

Key Words

CD34-negative, cell cycle, flow cytometry, hematopoiesis, stem cells.

1. Introduction

CD34 antigen has been considered a “pan” hematopoietic cell marker, present from the earliest stages of hematopoietic differentiation. The exact function of CD34, a sialomucin, is not known, though cytoadhesion and/or differentiation have been suggested (1,2). In the laboratory, CD34 antigen has become the standard by which human hematopoietic cells have been identified, quantitated and/or purified for laboratory and clinical studies (3–5). For example, it is widely used as a surrogate marker for stem cell mobilization. Thus, it was sur-

prising when Osawa et al. (6) demonstrated that murine CD34^{NEG}LIN^{NEG} cells could reconstitute the lymphohematopoietic system. Subsequent studies identified early hematopoietic precursors in the CD34^{NEG} fractions of human marrow, umbilical cord blood (UCB) and mobilized peripheral blood (MoPB) which possessed engrafting activity in fetal sheep and nonobese diabetic/severe combined immunodeficient (NOD/SCID) mice (7–13).

In vitro studies of human CD34^{NEG} cells in serum-free, stroma-free culture systems has proven difficult as cells from marrow and UCB grow poorly under such conditions (10,13–16). In contrast, CD34^{NEG} precursors from MoPB can be readily grown and offer an ideal system for studying proliferation and regulation of CD34 antigen in normal cells. Below, we describe a method for following CD34 antigen modulation and changes in proliferative status of primitive CD34^{NEG}CD38^{NEG}LIN^{NEG} cells and CD34⁺CD38^{NEG}LIN^{NEG} cells in serum-free culture. To distinguish cycling from noncycling cells, cells are stained with pyronin y (PY) (17,18) or analyzed for expression of Ki67 antigen (19). G₀ cells are both PY^{LOW} and Ki67^{NEG}. In contrast, proliferating cells are PY^{HIGH} and Ki67⁺. The method is particularly convenient for laboratories lacking access to a UV laser-equipped flow cytometer.

2. Materials

2.1. Reagents and Media

1. Iscove's modified Dulbecco's medium (IMDM) (Gibco™ Invitrogen Corporation, Carlsbad, CA, cat. no. 12440-053).
2. Serum-free expansion medium (SFEM) (StemCell Technologies, Vancouver, British Columbia, Canada, cat. no. 9650).
3. Heat-inactivated fetal bovine serum (HIFBS).
4. Cytokines: rhSCF, rhFlt3 Ligand (rhFL), rhIL-3, rhIL-6, and rh-TPO.
5. Sterile 10X phosphate-buffered saline (PBS), calcium, magnesium-free (Gibco™ Invitrogen Corporation, cat. no. 14200-075), diluted to 1X with sterile distilled water.
6. DNase (deoxyribonuclease I from bovine pancreas) (Sigma-Aldrich, St. Louis, MO, cat. no. 2025).
7. Ficoll-Paque (Amersham Biosciences, Piscataway, NJ).
8. Ammonium chloride-EDTA (StemCell Technologies, cat. no. 7850).
9. Nonfluorescent antibodies from StemCell Technologies for immunomagnetic separation: The lineage-depletion reagent (Human Progenitor Enrichment Cocktail, cat. no. 14056) is used for magnetic fractionation of cells. It consists of glycoporphin A (GlyA), CD2, CD3, CD14, CD16, CD19, CD24, CD56, and CD66b and includes the magnetic colloid. Also required is the CD41 tetrameric antibody complex (cat. no. 14050).
10. Fluorescent antibodies from BD Biosciences (San Jose, CA): The following fluorescein isothiocyanate (FITC)-labeled antibodies are needed: CD3, CD7, CD14,

CD16, CD19, CD20, CD42a, and CD56 (all but CD7 and CD42a come in their lineage cocktail, cat. no. 340546). In addition, CD38-APC, the Ki67-FITC Kit (BD Biosciences, #556026) and appropriate isotypic control antibodies are required.

11. Fluorescent antibodies from Beckman Coulter (Miami, FL): The following are required: GlyA-FITC, CD34-PE-CY5 (clone 581, class III), and isotypic control antibodies. The following phycoerythrin (PE)-labeled antibodies are needed: GlyA, CD4, CD14, CD16, CD19, CD20, CD41, and CD56. To make a single "LIN-PE" pool, combine 100 μ L of each and store in a dark bottle at 4°C. For cell analysis, use 25 μ L of the pool per tube. Appropriate isotypic control antibodies are also required.
12. Cytofix/Cytoperm Kit (BD Biosciences, cat. no. 554714).
13. Penicillin + streptomycin liquid, 10,000 U (Sigma-Aldrich, cat. no. 15140-122).
14. Low-density lipoproteins (LDLs) (Sigma-Aldrich, cat. no. L2139).
15. Immuno-Brite QC beads (Beckman Coulter, cat. no. 6603473).
16. Paraformaldehyde (PFA) (Sigma-Aldrich).
17. Pyronin Y (PY) (Sigma-Aldrich).
18. Hoechst 33342 (HO) (Sigma-Aldrich).

2.2. Working Solutions

1. Overnight storage medium (OSM): 10 mL of SFEM containing 100 μ L of penicillin/streptomycin, 20 μ L of LDL, 10 ng/mL of flt3 ligand (FL), and 10 ng/mL of stem cell factor (SCF).
2. DNase wash solution: 100 mL of sterile PBS containing 1 mg of DNase, 1% penicillin/streptomycin, and 2% HIFBS. Make fresh on the day of use.
3. Supplemented SFEM: SFEM containing 1% bovine serum albumin, 10 μ g/mL of insulin, 200 μ g/mL of human transferrin (iron saturated), 10⁻⁴ M 2-mercaptoethanol, and 2 mM L-glutamine in IMDM is supplemented with 50 ng/mL of rhSCF, 50 ng/mL of rhFL, 12.5 ng/mL of rhIL-3, 10 ng/mL of rhIL-6, 100 ng/mL of rh-thrombopoietin (TPO), and 1:200 LDL.
4. PFA: 4% solution in PBS diluted monthly to 1%. Dilute the latter two- to fivefold into cells for fixation.
5. PBSFB: 1X PBS containing 2% HIFBS and 1% penicillin + streptomycin.
6. N-(α -hydroxyethyl)piperazine-N'-(α -ethanesulfonic acid) (HEPES) buffer: 20 mM HEPES, pH 7.2, in Hank's balanced salt solution containing 1 g/L of glucose and 10% HIFBS. Store at 4°C.
7. HO: Stock solution is 1.6 mM. Filter-sterilize and store at 4°C, protected from light. *Day of use:* dilute stock solution 1:1000 to 1.6 μ M with HEPES buffer. Keep on ice, protected from light.
8. PY: Stock solution is 100 μ g/mL. Filter-sterilize and store at 4°C, protected from light. *Day of use:* dilute stock solution to 10 μ g/mL with HEPES buffer before use. Keep on ice, protected from light.

2.3. Supplies and Equipment

1. Green Magnet (StemCell Technologies, cat. no. 11055) and green magnet stand (StemCell Technologies, cat. no. 11056).

2. 0.5-Inch diameter column (StemCell Technologies, cat. no. 12052) or 0.6-inch diameter column (StemCell Technologies, cat. no. 12056).
3. Rainin Dynamax pump (RP-1 peristaltic pump, Rainin Instrument Co., Inc., Woburn, MA).
4. Fresh or cryopreserved MoPB cells. Sample should contain $\geq 4 \times 10^8$ MNC (a higher starting number facilitates later steps).
5. Flow cytometer must be equipped with two lasers capable of emitting at 488 nm (for FITC, PY, PE, and PE-CY5) and 633 nm (for allophycocyanin [APC]).

3. Methods

3.1. Overview

The methods describe: (1) preparation of thawed cells, (2) isolation of a red cell-depleted mononuclear cell (MNC) fraction, (3) depletion of lineage (LIN) committed cells, (4) purification of CD34^{NEG} and CD34⁺ fractions by sorting (*see Note 1*), (5) cell cultivation, and (6) analysis of proliferative status and phenotype. If the procedure starts with fresh MoPB cells, begin at **Subheading 3.2., step 3**.

3.2. Initial Preparation of Thawed Cells (*see Note 2*)

1. Thaw sample rapidly in a 37°C water. With continuous mixing, slowly dilute the preparation with an equal volume of cold IMDM containing 20% HIFBS. Centrifuge for 10 min at 300g at room temperature.
2. Discard supernatant and wash the cells in 30 mL of room-temperature DNase wash solution (*see Note 3*). Discard supernatant. Resuspend cells evenly in 10 mL of DNase wash solution.
3. Layer cells over 5 mL of Ficoll-Paque in a 15-mL tube. Centrifuge at 300g, for 25 min at room temperature (leave brake off). Collect the low density MNC band in a 50-mL tube and wash twice by centrifugation through DNase wash solution. Use 400g at room temperature for 15 min to minimize cell loss. (Use the same wash solutions for fresh and thawed cells).
4. Remove as much supernatant as possible. To hemolyze residual red cells, add 15 mL of ammonium chloride–EDTA to the pellet, mix and hold for 10 min at room temperature. Fill the tube with PBS and centrifuge for 10 min at 300g at room temperature. Wash with DNase wash solution. Before final wash, remove an aliquot for a cell count (required to determine final suspension volume).
5. Resuspend at a cell concentration of 6×10^7 /mL in DNase wash solution (the permissible concentration range is $2\text{--}8 \times 10^7$ cells/mL per StemCell Technology).

3.3. Depletion of LIN⁺ Cells by Immunomagnetic Separation

1. First incubation: Add 100 μ L of human progenitor enrichment cocktail for every 1.0 mL of cell suspension. Also add anti-CD41 at 10 μ L/mL of cell suspension. Incubate for 30 min on ice.
2. Second incubation: Without washing, add 60 μ L of magnetic colloid per 1.0 mL of cells. Continue incubation for an additional 30 min on ice. Do not wash the cells.

3. The separation system, which enriches LIN^{NEG} cells by depletion of LIN⁺ cells, consists of a magnet, column, stand, and optional pump. The “green magnet” can be used with gravity loading or pump loading. The other magnets are designed for gravity feed of smaller quantities of cells or for single or multiple pump separations. The manufacturer recommends that for 5×10^7 to 5×10^8 cells, a 0.5-inch column should be used. For 1×10^8 to 2×10^9 cells, use a 0.6-inch column. Cell purity suffers if too small a column is used whereas yield decreases with too large a column.
4. In a laminar flow hood, lower the column into the gap of the magnet (do not insert from the front). To prime the system, slowly pump sterile PBS up through the bottom of the column until the liquid completely immerses the matrix (pump setting 1.5 for a 0.5-inch column or 3.0 for a 0.6-inch column). Remove air bubbles by sharply tapping the side of the column. Run sterile PBS (15 mL for 0.5-inch column, 25 mL with 0.6-inch column) through the column from the top and collect the waste in a discard tube. Do not allow the PBS level to fall below the level of the matrix. Replace the discard tube with a sterile collection tube (50-mL centrifuge tube). Apply the cell-colloid suspension to the top of the column, using a pump speed of 5.0 for a 0.5-inch column (10.0 for a 0.6-inch column). LIN^{NEG} cells will emerge in the column eluate.
5. To capture all LIN^{NEG} cells, run three column volumes of DNase wash solution and collect eluate. Obtain a viable count from the pooled eluates.
6. Centrifuge pooled eluates for 10 min, 300g at room temperature. Remove supernatant and resuspend cells in 10 mL of OSM. Incubate overnight in a T25 culture flask (not treated to promote adherence) at 37°C in a humidified 5% CO₂ incubator. Under these conditions, cell viability can be maintained without stimulating the cells into proliferation.

3.4. Isolation of Primitive CD34^{NEG} and CD34⁺ Cells

1. After overnight incubation, obtain a viable count of the cell suspension in the flask ($\sim 10^7$ is average for an initial MoPB sample containing 4×10^8 cells).
2. Collect all but 2×10^5 cells from the T25 flask. To the flask, add 5 mL of fresh, supplemented SFEM to promote vigorous expansion of the LIN-depleted cells. These cells will be used for positive controls later in the experiment (*see Subheading 3.5.1.*).
3. Centrifuge the remainder of the LIN-depleted cells harvested from the T25 flask in sterile PBS in a 15-mL tube at 300g, at room temperature, 10 min.
4. Resuspend the cells in 0.5–1.0 mL of PBSFB. Aliquot the bulk of the suspension into one tube for antibody labeling. Utilize the residual cells to establish sort controls based on in-house practices. Add 2.0 mL of PBS to each tube and centrifuge them at 300g 10 min, 4°C. Discard all but 200 μ L of the supernatants and resuspend the pellets in their remaining supernatants.
5. In this step, cells intended for sorting will be labeled with antibodies against CD34, CD38 and LIN antigens. LIN antigens are tagged with a commercial lineage cocktail of FITC-labeled antibodies against CD3, CD14, CD16, CD19,

CD20, and CD56 supplemented with additional FITC-antibodies against CD42a, CD7, and GlyA. Thus, for every 1×10^6 cells, add 12 μL of the LIN-FITC cocktail and 15 μL each of GlyA-FITC, CD7-FITC, and CD-38-APC. Also add 10 μL of CD34-PE-CY5 and CD42a-FITC. Set up isotype controls as appropriate. Incubate for 30 min, on ice, protected from light. Wash cells twice with in PBSFB at 4°C. Resuspend the cells in PBSFB at a concentration appropriate for sorting. Keep cells cold and protected from light.

6. After completion of in-house quality control procedures for the flow cytometer, run isotype control samples. Run a small number of the labeled cells to establish sort gates for $\text{CD34}^{\text{NEG}}\text{CD38}^{\text{NEG}}\text{LIN}^{\text{NEG}}$ cells and $\text{CD34}^+\text{CD38}^{\text{NEG}}\text{LIN}^{\text{NEG}}$ cells (**Fig. 1**). To optimize purification of cells lacking CD34, CD38, and LIN antigens, set gates conservatively, that is, choose regions encompassing the dimmest one-third to one-half of antigen-negative populations. Less stringent gating increases yield but may reduce purity.
7. Sort the LIN-depleted cell suspension to obtain $\text{CD34}^{\text{NEG}}\text{CD38}^{\text{NEG}}\text{LIN}^{\text{NEG}}$ and $\text{CD34}^+\text{CD38}^{\text{NEG}}\text{LIN}^{\text{NEG}}$ fractions. Keep both the starting cell suspension and the two sorted fractions cold throughout the procedure.
8. Obtain a viability count on sorted fractions.
9. Set aside approx 1×10^4 cells from the CD34^+ and CD34^{NEG} fractions for **step 10**. Culture the remaining purified cells by transferring them to supplemented SFEM in 24-well trays in a 37°C humidified 5% CO_2 incubator. Initial cell concentration should be $<5 \times 10^4/\text{mL}$.
10. Analyze the freshly sorted fractions for uptake of PY or expression of Ki67 (*see Subheading 3.5.*). Because the freshly isolated cells are quiescent, the results identify the PY^{LOW} or Ki67^{NEG} populations. The sample can also be used for purity analysis by restaining for CD34, CD38, and LIN.
11. When sorting is complete, run a no. 2 or no. 3 Immuno-Brite bead sample without changing any voltage settings. This provides a reference brightness for analysis of Ki67 on later days (*see Subheading 3.5.2., step 9*).

3.5. Staining for Immunophenotype and Proliferative Status of Sorted Cells Before and After Cultivation

3.5.1. Introduction

Separate protocols are provided below for analysis of cultured cells for (1) CD34, CD38, LIN, and Ki67 and (2) CD34, CD38, LIN, and PY. The latter is based on the method of Ladd et al. (17). Separate protocols are required because of the fluorochromes used and the need for cell permeabilization for Ki67 staining. Note that the number of available cells in the CD34^+ and CD34^{NEG} cultures is often insufficient to run both test and control samples. To circumvent that limitation, *unsorted* LIN^{NEG} cells were also cultured (*see Subheading 3.4., step 2*) to provide material to assess autofluorescence and positive controls.

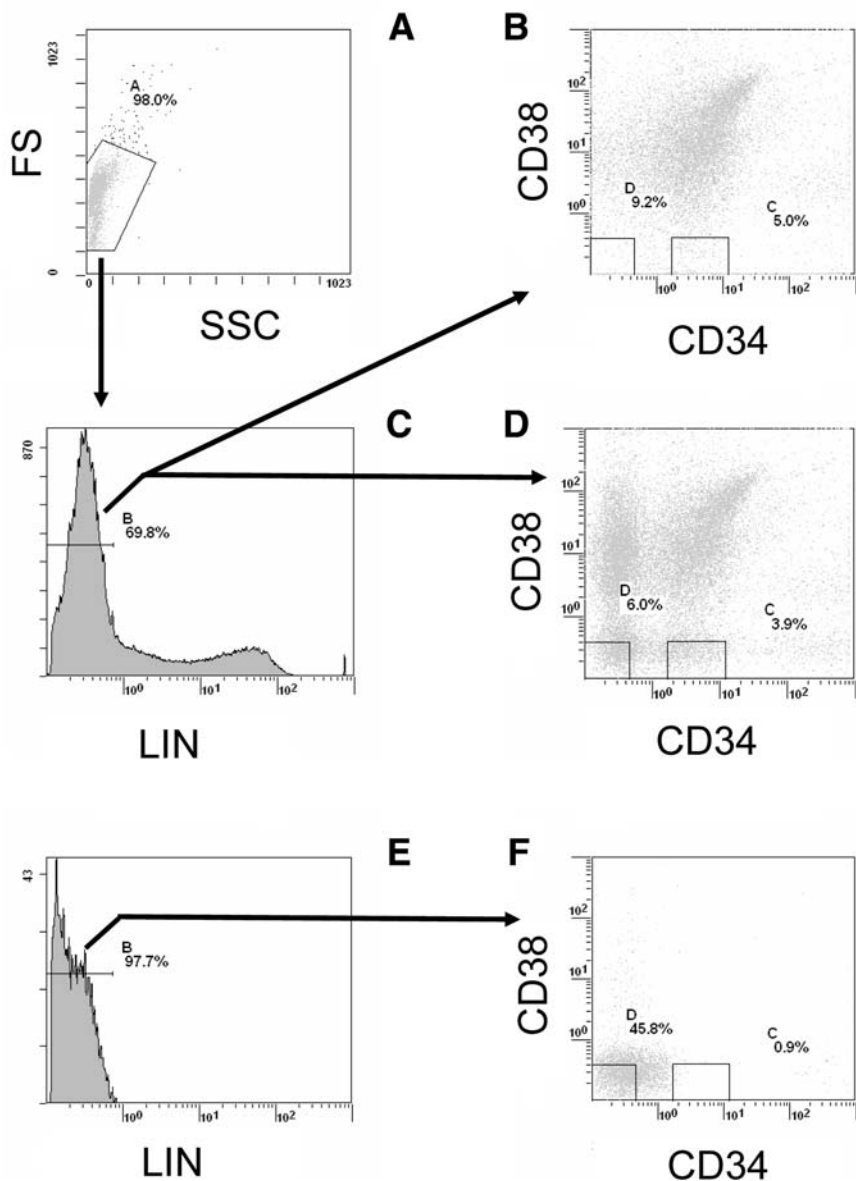


Fig. 1. Purification of primitive CD34^{NEG} and CD34⁺ cells. Thawed, MoPB cells were depleted of LIN⁺ cells and the enriched LIN^{NEG} population labeled for flow cytometric sorting. (A) Light scatter pattern of the LIN^{NEG} population. (C) Single-parameter histogram of LIN expression. (B) LIN^{NEG} cells were analyzed for expression of CD34 and CD38 and setting of sort gates to capture CD34^{NEG}CD38^{NEG}LIN^{NEG} and CD34⁺CD38^{NEG}LIN^{NEG} cells. In this display, events with very low CD34 and CD38 fluorescence rest on the axes and are not visible. (D) The Baseline Offset function was applied to the same data shown in (B) to enhance the display of low fluorescence events. This function randomizes low level signals in a Gaussian distribution across the first decade, thereby showing CD34^{NEG} CD38^{NEG} LIN^{NEG} and CD34⁺ CD38^{NEG} LIN^{NEG} cells more clearly. (E,F) Isotypic controls for LIN, and for CD34 and CD38 (baseline offset engaged).

3.5.2. Staining Cells for Expression of CD34, CD38, LIN, and Ki67

1. If cells have been cultured for 2 or more days, the number of available cells will be low and variable. If possible, remove $1-4 \times 10^4$ cells from the CD34^{NEG} culture, 2×10^5 from the CD34⁺ culture, and 4×10^5 from the cultured LIN-depleted fraction. Wash each aliquot in PBS and resuspend in PBS.
2. Label four tubes A–D for control cells from the LIN-depleted culture. Also label four tubes as E⁺, E^{NEG}, F⁺, and F^{NEG} (two for CD34⁺ cells and two for CD34^{NEG} cells), and one tube as G for Immuno-Brite beads. You now have nine tubes total:
 - A = Unstained cells for determination of autofluorescence.
 - B = Ki67-FITC alone (positive control).
 - C = Lin-PE alone (positive control).
 - D = 34-PE-CY5 alone (positive control).
 - E⁺ and E^{NEG} = Isotype-PE-CY5, Isotype-APC, Isotype-PE and Isotype-FITC (E⁺ for the CD34⁺ culture and E^{NEG} for the CD34^{NEG} culture).
 - F⁺ and F^{NEG} = Test antibodies Ki67-FITC, LIN-PE, 34-PE-CY5, 38-APC (F⁺ for the CD34⁺ culture and F^{NEG} for the CD34^{NEG} culture).
 - G = Immuno-Brite beads.
3. Into each of tubes A, B, C, and D, add 1×10^5 cells from the cultured LIN-depleted fraction. For E and F tubes, use the smallest possible number of cells consistent with in-house guidelines. For example, into E⁺ and E^{NEG} tubes, add $\geq 1 \times 10^4$ cells from the CD34^{NEG}CD38^{NEG}LIN^{NEG} culture and $\geq 1 \times 10^4$ cells from the CD34⁺CD38^{NEG}LIN^{NEG} culture. Repeat for F⁺ and F^{NEG} tubes.
4. For tubes A and B, wash and resuspend cells in 0.5–1.0 mL of PBSFB. Hold tubes A and B on ice in the dark.
5. For tubes C–F, stain with indicated monoclonal antibodies using standard in-house techniques for extracellular antigens. After last wash of tubes C and D, resuspend cells in 0.5–1.0 mL PBSFB and hold on ice. After last wash of tubes E and F (and B) proceed directly to **step 6**.
6. For fixation and permeabilization of tubes B, E⁺, E^{NEG}, F⁺, and F^{NEG} for Ki67 staining, proceed as follows:
 - a. Resuspend the washed cells in tubes B, E⁺, E^{NEG}, F⁺, and F^{NEG} in 250 μ L of Cytofix/Cytoperm solution. Incubate for 20 min at 4°C, protected from light. During the 20-min period, dilute the Perm/Wash buffer 1:10 in distilled H₂O.
 - b. Wash tubes B, E⁺, E^{NEG}, F⁺, and F^{NEG} twice in *diluted* perm/wash buffer, at 4°C. After the second centrifugation, remove all but 50 μ L of overlying perm/wash buffer and resuspend the cells.
7. To tube B and the two F tubes add: 20 μ L of Ki-67-FITC (test). To the two E tubes add: 10 μ L of isotype-FITC (control). Incubate for 30 min, on ice, in the dark.
8. Wash B, E⁺, E^{NEG}, F⁺, and F^{NEG} twice in diluted perm/wash buffer and resuspend in PBSFB for flow analysis. The manufacturer states that cells must be kept in the presence of saponin (perm/wash) during the intracellular staining.
9. Read within 24 h. Calibrate flow cytometer by first using tube G to set Immuno-Brite beads to the same peak channel as described in **Subheading 3.4., step 11**.

3.5.3. Staining Cells for Expression of CD34, CD38, LIN, and PY (see **Note 4**)

1. Day of use: Diluted HO/HEPES buffer: 10 μ L of stock HO into 10 mL of HEPES buffer. Diluted PY: 10 μ L of stock PY into 90 μ L of HEPES buffer.
2. This section describes the collection and distribution of cells. Because of significant procedural differences from the method presented in **Subheading 3.5.2.**, four aliquots are herein defined as samples 1–4. As stated above, the number of available cells will be low and variable.
3. After two or more days of cultivation, remove $1\text{--}4 \times 10^4$ cells from the CD34^{NEG} culture (termed “sample 1”), 2×10^5 from the CD34⁺ culture (termed “sample 2”), and 1×10^5 from the cultured LIN-depleted fraction (termed “sample 3”). Wash each in PBS and resuspend in 1.5 mL of diluted HO/HEPES buffer. Cover the three tubes loosely and immediately place in a 37°C humidified 5% CO₂ incubator for 45 min. This constitutes the first step in PY staining (the next step is **step 6** below).
4. Remove 3×10^5 cells from the cultured LIN-depleted fraction (termed “sample 4”), bring up volume to 2.0 mL with SFEM and hold on ice.
5. Label four tubes A–D for control cells from the LIN-depleted culture. Also label four tubes as E⁺ and E^{NEG} and F⁺ and F^{NEG} (two for CD34⁺ cells and two for CD34^{NEG} cells). You now have eight tubes total:
 - A = Unstained cells (for determination of autofluorescence).
 - B = PY alone (positive control; there is no “negative” control *per se* for PY).
 - C = Lin-FITC alone (positive control).
 - D = 34-PE-CY5 (positive control).
 - E⁺ and E^{NEG} = PY and Isotype-PE-CY5, Isotype-APC, and Isotype-FITC (E⁺ for the CD34⁺ culture and E^{NEG} for the CD34^{NEG} culture).
 - F⁺ and F^{NEG} = PY and test antibodies LIN-FITC, 34-PE-CY5, 38-APC (F⁺ for the CD34⁺ culture and F^{NEG} for the CD34^{NEG} culture).
6. After completion of the initial 45-min incubation of samples 1–3 at 37°C, add 15 μ L of diluted PY to each tube (final concentration 0.1 μ g/mL). Replace covers loosely on the three tubes and immediately return to the 37°C humidified 5% CO₂ incubator for an additional 45 min.
7. Remove samples 1–3 from the incubator. You now have four populations: three stained with PY (**steps 3 and 6**) and sample 4 held on ice (**step 4**). The four samples must now be distributed into eight tubes.
 - a. For sample 1, transfer one-third of the CD34^{NEG} cells into tube E^{NEG} and two-thirds into tube F^{NEG}. Wash cells twice in 1.5 mL of HEPES buffer. Resuspend in 200 μ L of PBS.
 - b. For sample 2, transfer one-half of the CD34⁺ cells into tube E⁺ and one-half into tube F⁺. Wash cells twice in 1.5 mL of HEPES buffer. Resuspend in 200 μ L of PBS.
 - c. For sample 3, wash cells twice in 1.5 mL of HEPES buffer. Resuspend in 1.0 mL of PBSFB. Hold on ice in the dark. This completes the steps for tube B.
 - d. For sample 4, divide cells equally among tubes A, C, and D. Wash A, C, and D twice with PBS. Resuspend A in 1.0 mL of PBSFB and hold on ice. Resus-

- pend C and D in 200 μ L of PBS. Cells in tubes C, D, E⁺, E^{NEG}, F⁺, and F^{NEG} are now ready for staining for extracellular antigens.
8. Stain tubes C, D, E⁺, E^{NEG}, F⁺, and F^{NEG} with indicated monoclonal antibodies for LIN-FITC, 34-PE-CY5, 38-APC, or the appropriate isotype controls using standard techniques for extracellular antigens.
 9. Analyze or add 1% PFA for later analysis.

3.6. Expected Results

3.6.1. Purification of CD34⁺ and CD34^{NEG} Fractions

Figure 1 illustrates the gating strategy used to isolate CD34^{NEG}CD38^{NEG} LIN^{NEG} cells and CD34⁺CD38^{NEG} LIN^{NEG} cells from LIN-depleted MoPB. After a single pass over the LIN depletion column, the proportion of LIN^{NEG} cells ranges from 30% to >70%. The resulting population is uniformly small and lacking in side scatter (**Fig. 1A**). Thus, establishing a light scatter gate is straightforward. Cells within the light scatter gate are sent to a single-parameter histogram of LIN (**Fig. 1C**). LIN^{NEG} cells are assessed for expression of CD34 and CD38. In some flow cytometers (such as the Coulter EPICS Elite ESP shown in **Fig. 1**), cells with low fluorescence hug the axes and are not readily visible even when the bulk of the cells are brought into the middle of the histogram (**Fig. 1B**). Nonetheless, conservative gates can be placed such that CD34^{NEG} cells and CD38^{NEG} cells are defined by regions having one-half (or less) the fluorescence of isotypic controls, as shown in **Fig. 1B**. To observe dim cells better, the “baseline offset” feature may be used to push cells off the axes, as shown in **Fig. 1D**. The position of the CD34 and CD38 gates relative to isotypic controls (baseline offset feature engaged) is shown in **Fig. 1F**.

3.6.2. Analysis of Cell Activation and Antigen Modulation

Cells should be harvested from the cultures when both cycling and quiescent cells are present. For MoPB cells, the initial sampling time should be approx 2 d. Autofluorescence is prominent in this system and must be minimized before listmode data can be analyzed. Spurious events are readily identified by their simultaneous presence in narrow 45° diagonal regions in two-parameter plots of Ki67 (or PY) vs CD34 and CD34 vs LIN. Any event that fluoresces in both of those diagonal regions (in all three photomultiplier tubes [PMTs]) is considered to be due to autofluorescence and is eliminated by boolean gating logic. This is shown in panels **B** and **C** of **Figs. 2–5**, where autofluorescent events (black points) are identified and subsequently removed from all other histograms shown. Note that for a cell to be counted as an autofluorescent event, it must appear in *both* of the regions shown in panels **B** and **C**.

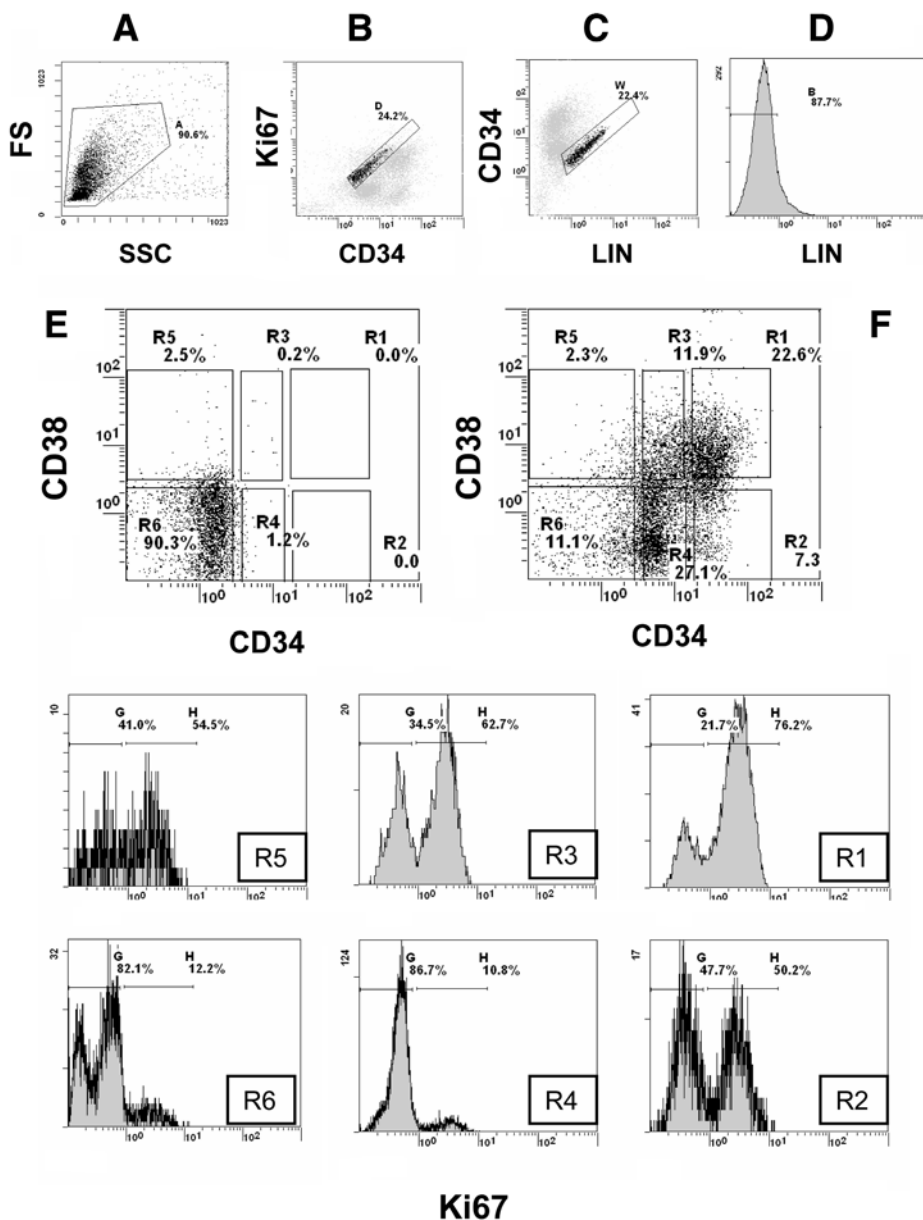


Fig. 2. Ki67 analysis of cell proliferation in a CD34⁺ culture. After 40 h of incubation, the CD34⁺CD38^{NEG}LIN^{NEG} culture was stained for expression of Ki67 and immunophenotype. (A) Light scatter histogram. Permeabilization of cells distorts original light scatter properties of cells (compare to Fig. 4A). (B,C) Identification of autofluorescent events removed from (D-F) and (R1-R6). (D) LIN profile. (E,F) CD34 and CD38 phenotypes of LIN^{NEG} cells examined after staining with isotypic antibodies (E) or antigen-specific antibodies (F). Regions R1-R6 established to identify populations modulating expression of CD34 and CD38. (R1-R6) Ki67 expression in populations R1-R6.

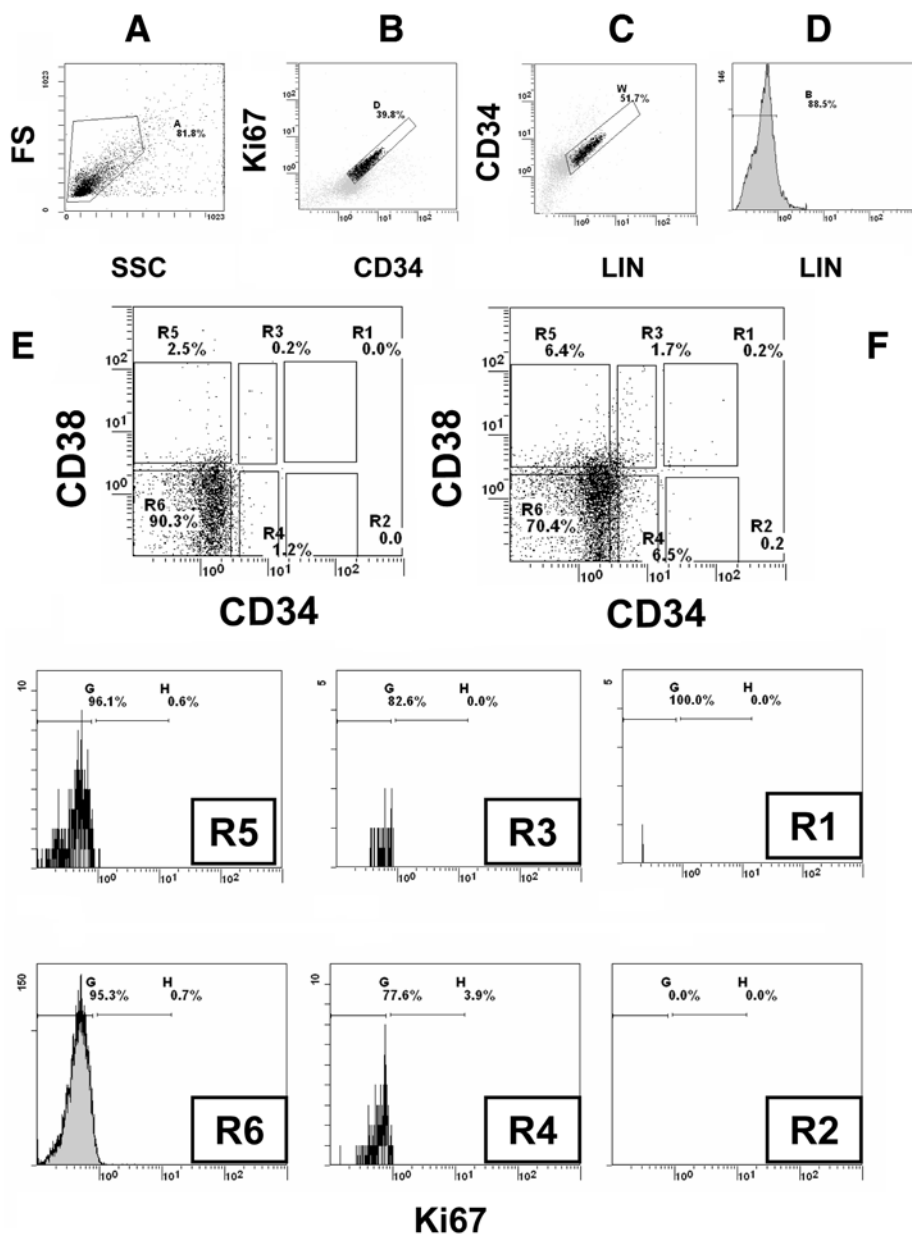


Fig. 3. Ki67 analysis of cell proliferation in the CD34^{NEG} culture. The CD34^{NEG}CD38^{NEG} LIN^{NEG} sister culture was stained for expression of Ki67 and immunophenotype. See Fig. 2 legend.

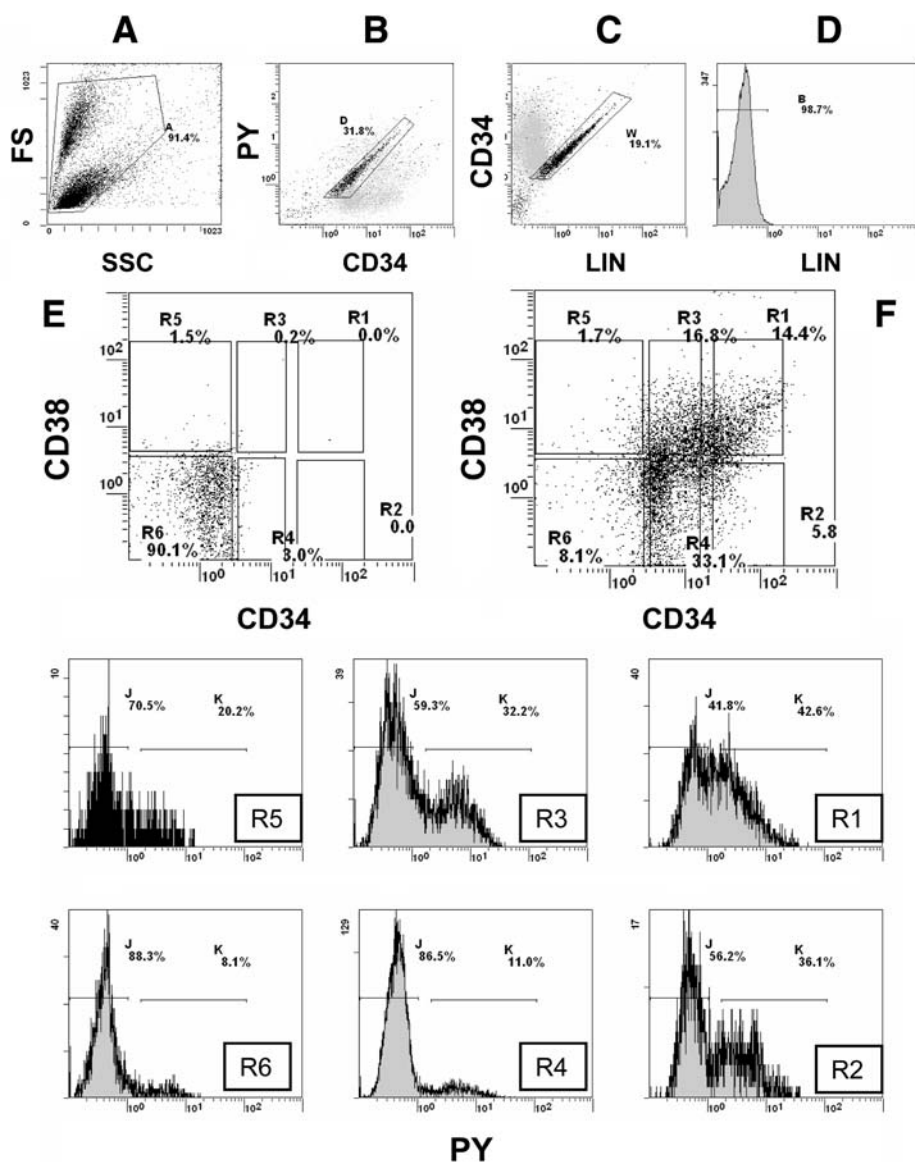


Fig. 4. PY analysis of cell proliferation in the CD34⁺ culture. The same CD34⁺CD38^{NEG} LIN^{NEG} culture shown in Fig. 2 was stained for uptake of PY and immunophenotype. (A) Light scatter histogram. (B,C) Identification of autofluorescent events removed from (D-F) and (R1-R6). (D) LIN profile. (E,F) CD34 and CD38 phenotypes of LIN^{NEG} cells examined after staining with isotypic antibodies (E) or antigen-specific antibodies (F). Regions R1-R6 established to identify populations modulating expression of CD34 and CD38. (R1-R6) PY uptake by populations R1-R6.

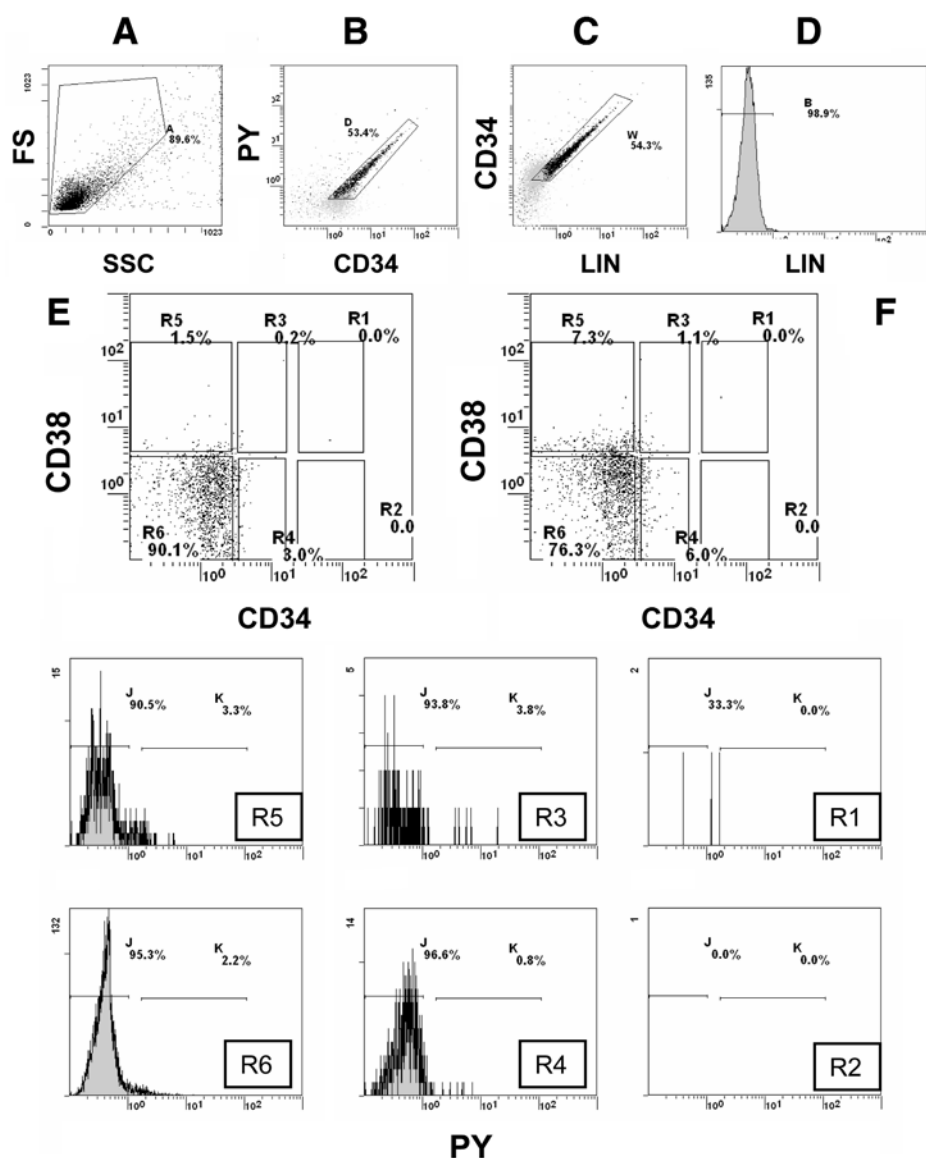


Fig. 5. PY analysis of cell proliferation in the CD34^{NEG} culture. The CD34^{NEG} CD38^{NEG} LIN^{NEG} culture shown in Fig. 3 was stained for uptake of PY and immunophenotype. See Fig. 4 legend.

Figure 2 shows the analysis of a CD34⁺ culture after 40 h of incubation. LIN^{NEG} cells (**D**) are sent to a histogram of CD38 vs CD34 (**F**) where events are divided into six regions (R1–R6). Most LIN^{NEG} cells expressing high levels of CD34 are CD38⁺ (R1). For LIN^{NEG} cells expressing CD34 at lower levels, more are CD38^{NEG} (R4) than CD38⁺ (R3). Interestingly, cells that have down-regulated CD34 completely are almost exclusively CD38^{NEG} (R6). Each of the six regions was analyzed for expression of the intracellular proliferation antigen Ki67. LIN^{NEG} cells in R1 and R3 (those that retained CD34 expression and had upmodulated CD38) were actively proliferating. In contrast, LIN^{NEG} cells in R4 and R6 (CD34^{LO-MID} to CD34^{NEG} cells that had remained CD38^{NEG}) were essentially quiescent. Thus, an association between CD34 and CD38 modulation and the onset of proliferation can be documented. **Figure 3** shows the sister CD34^{NEG} culture. Expression of CD34 antigen by LIN^{NEG} cells is observed (R3, R4) albeit at low levels (compare to isotypic controls in **E**). Almost none of the cells were proliferating, demonstrating that CD34 is upregulated quite early in activation.

The use of PY to analyze the same two cultures is shown in **Figs. 4** and **5**. With PY, permeabilization of the cells is not required and discrete populations are resolved by lightscatter in the CD34⁺ culture (**Fig. 4A**). In the CD34^{NEG} culture, where proliferation lagged, the cells remained small (**Fig. 5A**). Permeabilization did not affect CD34 versus CD38 histogram patterns (compare panel **F** in **Figs. 2** vs **4** and in **Figs. 3** vs **5**). Results obtained with PY agree well with and support those obtained with Ki67. With both probes, proliferation in CD34⁺ cultures was maximal in cells that had upregulated CD38 and continued to express CD34 while downregulation of CD34 was associated with continued quiescence (*see Note 5*). Furthermore, both Ki67 and PY showed that growth lagged in the CD34^{NEG} culture, even though CD34 antigen upregulation was beginning (*see Note 6*).

4. Notes

1. Cell preparation and sorting can be accomplished by one person in 2 d. However, overnight storage of the cells with low level cytokines is required. The procedure can be shortened to a single day (and overnight storage eliminated) if several people work together.
2. The methods described here should be modified for use with UCB. Slower removal of cryoprotectant is necessary with UCB. UCB contains more red blood cells (RBC) which are comparatively resistant to hemolysis. In the initial NH₄Cl hemolysis step, it is important not to remove too much of the supernatant to avoid loss of leukocytes. After several washes, a distinct cell layer appears, facilitating discrimination between cells and supernatant. To achieve a RBC/WBC ratio <20:1 prior to LIN depletion, two ammonium chloride–EDTA treatments can be used. However, this will lower leukocyte recovery.

3. When PBSC clumped after thawing, the aggregates were often not affected by DNase. However, cellular clumps appearing in thawed UCB could be redispersed as viable cells if the suspension was incubated at room temperature for 10–15 min in DNase.
4. An extensive discussion of PY staining of live and fixed cells was presented by Shapiro (20). There is evidence for PY staining of mitochondria in live cells. However, in human lymphoid cells, PY predominately stains RNA (most likely double-stranded RNA in polyribosomes). Several demonstrations of the RNase sensitivity of PY staining have been reported (17,20). Use of Hoechst 33342 has been recommended in PY staining of RNA to block possible binding to DNA, although its necessity is uncertain (20). The final concentration of PY used in these experiments is approx 10-fold lower than that recommended by Ladd et al. (17). However, with the very small number of cells available for analysis, the reduced concentration works well.
5. The methods presented here provide two techniques for gauging the proliferative status of cells. Analysis of Ki67 expression is easier than determination of PY staining. However, PY staining is not difficult and confirms results obtained with Ki67.
6. With both MoPB and UCB, the starting proportions (and final yields) of CD34⁺ and CD34^{NEG} hematopoietic cells vary considerably. Furthermore, a wide range of growth kinetics are observed. The investigator must be prepared to work with small numbers of cells.

References

1. Simmons, P. J., Levesque, J. P., and Haylock, D. N. (2001) Mucin-like molecules as modulators of the survival and proliferation of primitive hematopoietic cells. *Ann. NY Acad. Sci.* **938**, 196–206.
2. Civin, C. I., Strauss, L. C., Brovall, C., Fackler, M., Schwartz, J., and Shaper, J. (1984) Antigenic analysis of hematopoiesis II. Hematopoietic progenitor cell surface antigen defined by a monoclonal antibody raised against Kgl₁a cells. *J. Immunol.* **133**, 157–165.
3. Chang, H., Jensen, L., Quesenberry, P., and Bertoncello, I. (2000) Standardization of hematopoietic stem cell assays: a summary of workshops and working group meeting sponsored by National Heart Lung and Blood Institute held at the National Institutes of Health, Bethesda, MD, on September 8-9, 1998 and July 30, 1999. *Exp. Hematol.* **28**, 743–752.
4. Civin, C. I., Almeida-Porada, G., Lee, M.-J., Olweus, J., Terstappen, L. W. M. M., and Zanjani, E. D. (1996) Sustained, retransplantable multilineage engraftment of highly purified adult bone marrow stem cells in vivo. *Blood* **88**, 4102–4109.
5. Michallet, M., Philip, T., Philip, I., et al. (2000) Transplantation with selected autologous peripheral blood CD34⁺ Thy1⁺ hematopoietic stem cells (HSC) in multiple myeloma: impact of HSC dose on engraftment, safety and immune reconstitution. *Exp. Hematol.* **28**, 858–870.

6. Osawa, M., Hanada, K., Hamada, H., and Nakauchi, H. (1996) Long-term lymphohematopoietic reconstitution by a single CD34^{NEG} hematopoietic stem cell. *Science* **273**, 242–244.
7. Zanjani, E. D., Almeida-Porada, G., Livingstone, A., Flake, A., and Ogawa, M. (1998) Human bone marrow CD34[−] cells engraft in vivo and undergo multilineage expression that includes giving rise to CD34⁺ cells. *Exp. Hematol.* **26**, 353–360.
8. Verfaillie, C., Almeida-Porada, G., Wissink, S., and Zanjani, E. (2000) Kinetics of engraftment of CD34[−] and CD34⁺ cells from mobilized blood differs from that of CD34[−] and CD34⁺ cells from bone marrow. *Exp. Hematol.* **28**, 1071–1079.
9. Gallacher, L., Murdoch, B., Wu, D., Karanu, F., Fellows, F., and Bhatia, M. (2000) Identification of novel circulating human embryonic blood stem cells. *Blood* **96**, 1740–1747.
10. Bhatia, M., Bonnet, D., Murdoch, B., Gan, O., and Dick, J. E. (1998) A newly discovered class of human hematopoietic cells with SCID-repopulating activity. *Nat. Med.* **4**, 1038–1045.
11. Engelhardt, M., Lubbert, M., and Guo, Y. (2002) CD34⁺ or CD34^{NEG}: which is the more primitive? *Leukemia* **16**, 1603–1608.
12. Ando, K. (2002) Human CD34^{NEG} hematopoietic stem cells: basic features and clinical relevance. *Int. J. Hematol.* **75**, 370–375.
13. Bonnet, D. (2001) Normal and leukemic CD34^{NEG} human hematopoietic stem cells. *Rev. Clin. Exp. Hematol.* **5**, 42–61.
14. Kim, D. K., Fujiki, Y., Fukushima, T., Ema, H., Shibuya, A., and Nakauchi, H. (1999) Comparison of hematopoietic activities of human bone marrow and umbilical cord blood CD34 positive and negative cells. *Stem Cells* **17**, 286–294.
15. Nakamura, Y., Ando, K., Chargui, J., et al. (1999) Ex vivo generation of CD34⁺ cells from CD34[−] hematopoietic cells. *Blood* **94**, 4053–4059.
16. Gallacher, L., Murdoch, B., Wu, D., Karanu, F., Keeney, M., and Bhatia, M. (2000) Isolation and characterization of human CD34[−]Lin[−] and CD34⁺Lin[−] hematopoietic stem cells using cell surface markers AC133 and CD7. *Blood* **95**, 2813–2819.
17. Ladd, A., Pyatt, R., Gothot, A., et al. (1997) Orderly process of sequential cytokine stimulation is required for activation and maximal proliferation of primitive human bone marrow CD34⁺ hematopoietic progenitor cells residing in G₀. *Blood* **90**, 658–668.
18. Gothot, A., Pyatt, R., McMahon, J., Rice, S., and Srour, E. (1997) Functional heterogeneity of human CD34⁺ cells isolated in subcompartments of the G₀/G₁ phase of the cell cycle. *Blood* **90**, 4384–4393.
19. Gerdes, J., Lemke, H., Baisch, H., Wacker, H., Schwab, U., and Stein, H. (1984) Cell cycle analysis of a cell proliferation associated human nuclear antigen defined by the monoclonal antibody Ki-67. *J. Immunol.* **133**, 1710–1715.
20. Shapiro, H. (1995) *Practical Flow Cytometry*, 3rd edit. Wiley-Liss, New York.

Multiparameter Flow Cytometry of Fluorescent Protein Reporters

Teresa S. Hawley, Donald J. Herbert, Shannon S. Eaker,
and Robert G. Hawley

Summary

Reporters based on the green fluorescent protein (GFP) from the jellyfish *Aequorea victoria* and GFP-like proteins from other marine organisms provide valuable tools to monitor gene transfer and expression noninvasively in living cells. Stable cell lines were generated from the Sp2/0-Ag14 hybridoma that express up to three spectral enhanced versions of GFP, the enhanced cyan fluorescent protein (ECFP), the enhanced green fluorescent protein (EGFP), and the enhanced yellow fluorescent protein (EYFP), and/or a variant of the *Discosoma* coral red fluorescent protein (DsRed). The panel of lines was used to demonstrate a flow cytometric procedure for simultaneous analysis of all four fluorescent proteins that utilizes dual-laser excitation at 488 nm and 407 nm. Additional schemes for simultaneous detection of two, three or four of these fluorescent proteins are also presented.

Key Words

Discosoma coral red fluorescent protein (DsRed), enhanced cyan fluorescent protein (ECFP), enhanced green fluorescent protein (EGFP), enhanced yellow fluorescent protein (EYFP), gene transfer, multiparameter flow cytometry.

1. Introduction

Derivatives of the green fluorescent protein (GFP) from the bioluminescent jellyfish *Aequorea victoria* have been demonstrated to be convenient and sensitive vital markers of transgene expression in mammalian cells, including hematopoietic stem cells (1–9). A number of spectral variants of GFP have been developed in mutagenesis studies that are suitable for simultaneous use in multiparameter flow cytometric applications (1–3,8–16). The ability to detect multiple fluorescent proteins simultaneously by flow cytometry provides the

opportunity to differentiate noninvasively among various cell populations, or to assess gene function and monitor protein–protein interactions in individual cells (8,9,17–19) (see also Chapter 10 by Pruitt et al., Chapter 14 by Galbraith et al., and Chapter 15 by Chan and Holmes, *this volume*). In this regard, we and others have found the combination of enhanced GFP (EGFP) (3), a blue-shifted emission variant of GFP termed enhanced cyan fluorescent protein (ECFP) (10), and a red-shifted emission variant referred to as enhanced yellow fluorescent protein (EYFP) (14) to be useful for this purpose (9,15,16).

GFP orthologs have been isolated from other bioluminescent organisms, such as the Atlantic sea pansy *Renilla reniformis* (20), the Gulf of Mexico sea pansy *Renilla mulleri* (21), and the sea pen *Ptilosarcus gurneyi* (21). However, in no instance has it been possible to produce stable far-red fluorescent GFP derivatives. It was noteworthy, therefore, when a red fluorescent protein, drFP583 (commonly referred to as *Discosoma* coral red fluorescent protein [DsRed]), was identified among a group of GFP-like proteins discovered in nonbioluminescent Anthozoa reef corals (22). DsRed has an emission maximum that is shifted by more than 50 nm toward the red end of the spectrum in comparison with the most red-shifted GFP mutant (22). Approximately 30 GFP-like proteins have now been cloned and spectroscopically characterized (23,24). While additional red fluorescent proteins have been identified or generated by mutagenesis of non-fluorescent purple-blue chromoproteins (23,25–27), new versions of DsRed that exhibit improved folding and spectral properties make them well suited for simultaneous multicolor flow cytometric analyses with the ECFP, EGFP, and EYFP variants (28).

This chapter will describe the derivation of cell lines stably expressing ECFP, EGFP, EYFP, and/or DsRed. These cell lines are used to illustrate one particular flow cytometric detection strategy for simultaneous analysis of all four of these fluorescent proteins. Additional detection strategies for different combinations of these fluorescent proteins are discussed as well.

2. Materials

1. Sp2/0-Ag14 cells (American Type Culture Collection, Manassas, VA, cat. no. CRL-1581).
2. GP+E-86 supernatant containing retroviral vectors carrying the ECFP, EGFP, EYFP, or DsRed fluorescent protein gene plus the bacterial neomycin resistance (*neo*) gene (see **Note 1**).
3. 0.45- μ m Sterile filters.
4. Hexadimethrine bromide (polybrene): Make up a stock solution of 1 mg/mL in distilled water. Filter sterilize. Store at 4°C.
5. Geneticin (G418): Make up a stock solution of 40 mg/mL in distilled water. Filter sterilize. Aliquot and store at –20°C.

6. Growth medium for Sp2/0-Ag14: Dulbecco's modified Eagle medium (DMEM) with high glucose, and 5% (v/v) fetal bovine serum.
7. Growth medium for GP+E-86: DMEM with high glucose, and 10% (v/v) calf serum.
8. Analysis buffer: Phosphate-buffered saline (PBS) and 2% (v/v) fetal bovine serum.
9. Flow cytometer equipped with:
 - a. Excitation wavelengths: 488 nm as the primary beam and 407 nm (*see Note 2*) as the secondary or tertiary beam.
 - b. Detection optics: 488/10-nm bandpass (BP) filters, 470/20-nm BP filter, 510/20-nm BP filter, 550/30-nm BP filter, 610/20-nm BP filter, 525-nm short-pass (SP) dichroic mirror, and 610-nm SP dichroic mirror (BD Biosciences; Omega Optical Inc., Brattleboro, VT; *see Note 3*).
 - c. Intra- and inter-laser compensation capability (*see Note 4*).
10. Calibration-grade alignment beads (*see Note 5*).

3. Methods

The methods described below outline: (1) the derivation of cells stably expressing ECFP, EGFP, EYFP, and/or DsRed; (2) simultaneous detection of all four of these fluorescent proteins; and (3) additional schemes for simultaneous detection of two, three, or four of these fluorescent proteins.

3.1. Derivation of Cells Stably Expressing Individual or Multiple Fluorescent Proteins

Configuring the flow cytometer for simultaneous detection of multiple fluorescent proteins requires cells expressing the individual fluorescent protein genes (*see Note 6*). In addition, cells expressing multiple fluorescent protein genes can be used to confirm correct delineation of different populations.

3.1.1. Cells

Many cell types can be used to express stably the fluorescent protein genes. Sp2/0-Ag14 cells were chosen because of their ease of culture.

3.1.2. Introduction of the Fluorescent Protein Genes Into Cells

Retroviral vectors were used to introduce the fluorescent protein genes into Sp2/0-Ag14 cells. Construction of the retroviral vectors and generation of the producer cell lines have been previously described (**16**). Because of space limitations, they are not described here in detail. In brief, each retroviral vector was engineered by standard recombinant DNA methodology to coexpress the fluorescent protein gene and the bacterial *neo* gene. The latter confers resistance to the neomycin analog G418. The retroviral vectors were transfected into GP+E-86 ecotropic packaging cells (**32**). Supernatant from transfected GP+E-86 cells was

harvested and passed through 0.45- μ m sterile filters. Filtration removed any contaminating cells from the retroviral vector particles.

Sp2/0-Ag14 cells were incubated with supernatant containing ECFP, EGFP, EYFP, or DsRed retroviral vector particles for 4 h at 37°C, in the presence of 2 μ g/mL polybrene. The procedure was repeated with fresh vector supernatant. Two days later, cells expressing individual fluorescent protein genes were selected by the addition of 750 μ g/mL of G418. In addition, cells expressing four fluorescent protein genes were generated by incubation with mixtures of the retroviral vector supernatants using the same transduction protocol (*see Note 7*).

3.2. Simultaneous Detection of Four Fluorescent Proteins

Because of overlapping excitation spectra, multiple fluorescent proteins can be excited by a single excitation wavelength (**15**). As few as two laser lines are sufficient to excite ECFP, EGFP, EYFP, and DsRed, and we have previously described a protocol for simultaneous detection of these four fluorescent proteins on a flow cytometer equipped with tunable lasers (**16**). However, the two lasers were tuned to 458 nm and 568 nm, excitation wavelengths that are not widely available on current commercial flow cytometers. Many flow cytometers are equipped with lasers providing fixed excitation wavelengths, most commonly 488 nm and 633 nm. With the recent introduction of violet laser diodes, new flow cytometers can also provide 405/407/408-nm excitation (exact wavelength depends on the manufacturer of the laser). These small violet laser diodes can also be retrofitted onto existing flow cytometers. The protocol described here for the simultaneous detection of ECFP, EGFP, EYFP, and DsRed utilizes dual-laser excitation at 488 nm and 407 nm. It is applicable to many flow cytometers (*see also* Chapter 13 by Pruitt et al., *this volume*).

3.2.1. Configuring the Flow Cytometer (*see Note 8 and Fig. 1*)

1. Install the appropriate filters in front of detectors:
 - a. 488/10-nm BP filters for forward scatter (FSC) and side scatter (SSC).
 - b. 470/20-nm BP filter for the detection of ECFP.
 - c. 510/20-nm BP filter for the detection of EGFP.
 - d. 550/30-nm BP filter for the detection of EYFP.
 - e. 610/20-nm BP filter for the detection of DsRed.
 - f. 525-nm SP dichroic mirror between the 510/20-nm and 550/30-nm BP filters.
 - g. 610-nm SP dichroic mirror between the 510/20-nm and 610/20-nm BP filters.
2. Using calibration-grade microspheres, align both lasers to obtain maximum fluorescence intensity and minimum coefficient of variation (*see Note 9*).

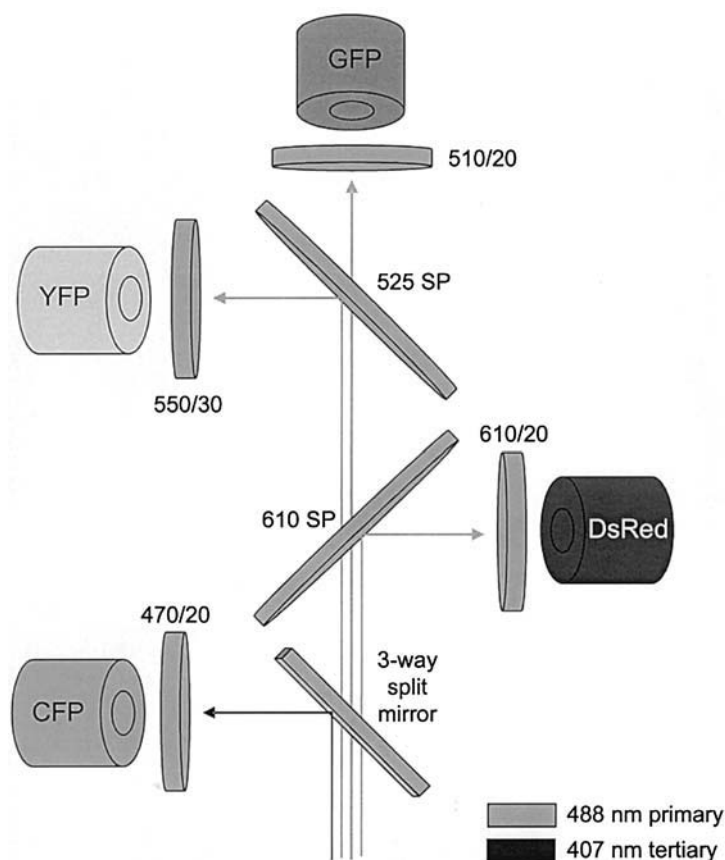


Fig. 1. Optical configuration for simultaneous detection of ECFP, EGFP, EYFP, and DsRed using dual-laser excitation at 488 nm and 407 nm on a FACSVantage SE/FACSDiVa equipped with Innova 70C-Spectrum argon-ion and Innova 302C krypton-ion lasers. The two beams were spatially separated. The three-way split mirror directed signals from the primary beam (488 nm) to the GFP, YFP, and DsRed detectors, and signals from the tertiary beam (407 nm) to the CFP detector. 488/10 BP filters were placed in front of the FSC and SSC detectors to enable triggering from the primary beam (not shown). 470/20, 510/20, 550/30, 610/20 BP filters were used to capture ECFP, EGFP, EYFP, and DsRed fluorescence, respectively. The 525 SP dichroic mirror was used to separate the GFP and YFP signals. The 610 SP dichroic mirror was used to separate the GFP/YFP and DsRed signals.

3.2.2. Instrument Settings on the FACSVantage SE/FACSDiVa (see **Note 10**)

1. Laser power: 70 mW of 488 nm (primary beam) and 50 mW of 407 nm (tertiary beam).
2. Voltages: CFP, 430 log; GFP, 450 log; YFP, 540 log; DsRed, 580 log.
3. Spectral overlap (%):

Colors/Channel	CFP	GFP	YFP	DsRed
CFP	100.0	2.72	1.81	0.90
GFP	0.52	100.00	43.96	11.52
YFP	0.04	58.75	100.00	33.65
DsRed	0.04	0.86	17.45	100.00

3.2.3. Data Acquisition and Analysis

1. Format a bivariate histogram correlating forward scatter (FSC) and side scatter (SSC) using linear scales. Draw a region to exclude debris (typically low FSC and SSC) and unhealthy cells (typically low FSC and intermediate-to-high SSC).
2. Format bivariate histograms (gated on cells of interest) encompassing all combinations of fluorescence parameters using logarithmic scales.
3. Suspend cells in analysis buffer. While running the “negative” cells (cells not expressing any fluorescent protein), adjust voltage for each fluorescence detector so that the cells are confined to the first decade of the log scale on each histogram. Acquire at least 5000 events.
4. Run the following “positive” cells sequentially: cells expressing ECFP, EGFP, EYFP, or DsRed. Acquire at least 5000 events of each sample.
5. Perform compensation among all parameters (see **Note 11**). A properly compensated sample should have equivalent median values of fluorescence intensities for negative and positive cells with respect to each parameter (**33–35**) (see **Note 12**).
6. Draw nonrectilinear markers to delineate different populations (see **Note 13** and **Fig. 2**).
7. Mix in equal proportions: Negative cells, ECFP-positive cells, EGFP-positive cells, EYFP-positive cells and DsRed-positive cells. Run the sample. Acquire 50,000 events (**Fig. 3A**). Apply compensation (**Fig. 3B**).
8. (Optional) Mix in equal proportions: Negative cells, cells expressing individual fluorescent proteins, and cells expressing all four fluorescent proteins. Acquire 50,000 events (**Fig. 3C**). Apply compensation (**Fig. 3D**).

3.2.4. Data Display

In cytometry, all measurements of signals are subject to at least two fundamental sources of variability: photon counting (counting error) and analog-to-digital conversion (digital error), both of which are intensity dependent and symmetric (see **Note 14**). Subtle but important problems result when data are compensated and presented in a log display. Because signal compensation is a

subtractive process, some of the events could have negative computed channel values after compensation. If the data could be visualized adequately in linear space, the measurement variability would manifest as an intensity-dependent symmetric increase in the breadth of a control population. When these compensated data are transformed back to a log display, negative and zero channel values are normally set to 1, as the log function is undefined at less than or equal to 0. This truncation of data has at least two undesirable consequences. First, the truncated data are plotted on the axis and are not easily visualized in the display. Second, the variability is no longer symmetric and, as a result, the data appear to be undercompensated (**Figs. 3D** and **4A**). The first problem can be circumvented by adding a small random number to the data (**Fig. 4B**, WinList v5.0 “log bias” feature). Although this feature allows the visualizaiton of events that are on the axis, it does not address the more important problem of the loss of symmetry and subsequent misinterpretation of the data. The second problem has been recently solved by two new types of transforms, biexponential and hyper-log, that have all the benefits of the log transform but are defined over the entire real domain, which includes 0 and negative numbers (*see* **Note 15** and cover illustration). The advantage of these transforms is that the symmetry of the measurement error is preserved, making it far easier to visualize properly compensated data.

3.3. Additional Schemes for Simultaneous Detection of Two, Three, or Four Fluorescent Proteins

Because of their broad excitation and emission spectra, detection of various combinations of ECFP, EGFP, EYFP, and DsRed can be achieved with different schemes. Some of the possibilities are described below.

3.3.1. Excitation and Emission Spectra of the Four Fluorescent Proteins (**39**)

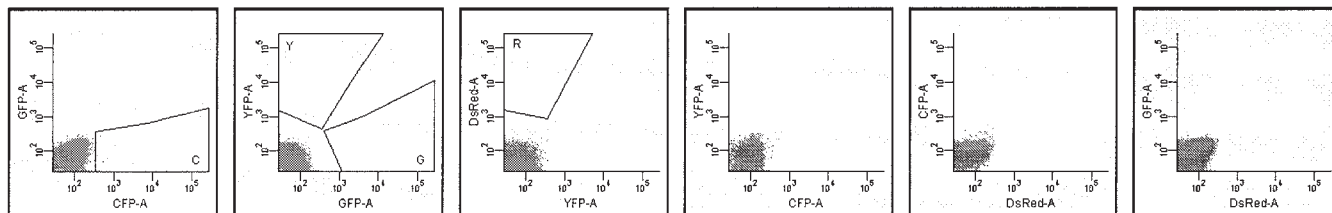
	<u>Excitation maximum (nm)</u>	<u>Emission maximum (nm)</u>
ECFP	434	477
EGFP	489	508
EYFP	514	527
DsRed	558	583

3.3.2. Feasible Excitation Wavelengths (nm) (*see* **Note 16**)

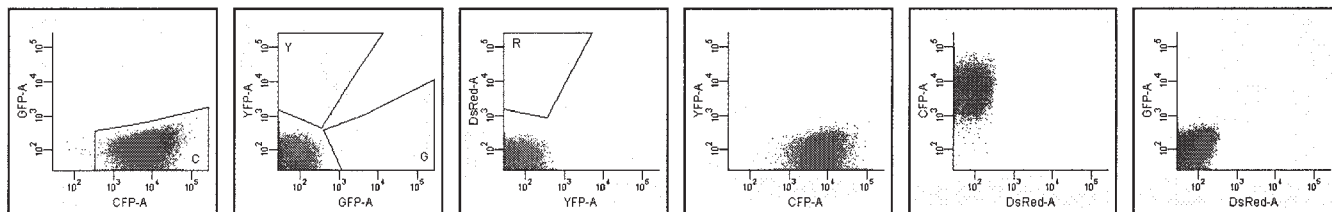
1. ECFP: 407, 413, or 458 (*see* **Note 17**).
2. EGFP: 458 or 488.
3. EYFP: 458, 488, or 514.
4. DsRed: 488, 514, 531, or 568.

226

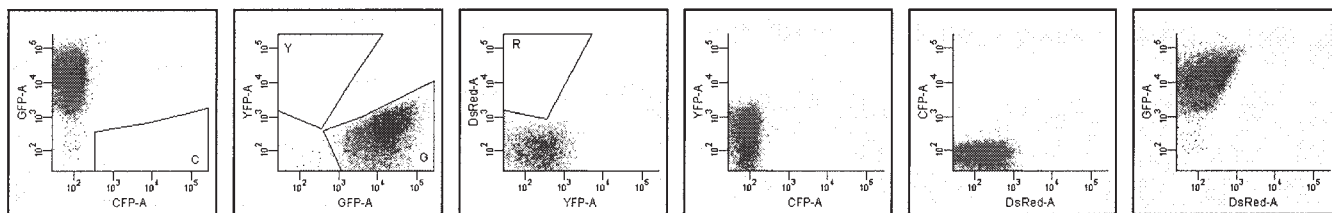
A



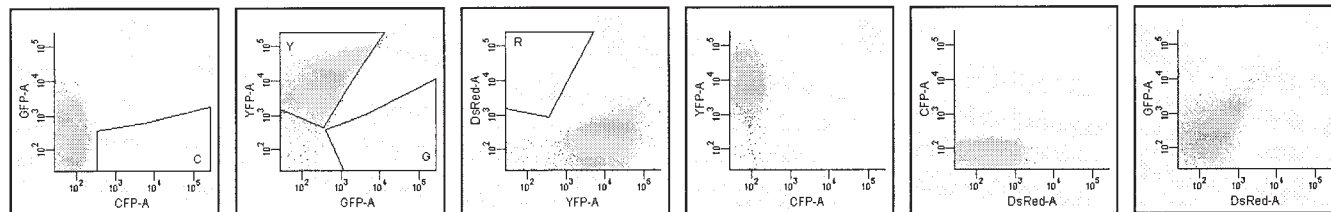
B



C



D



E

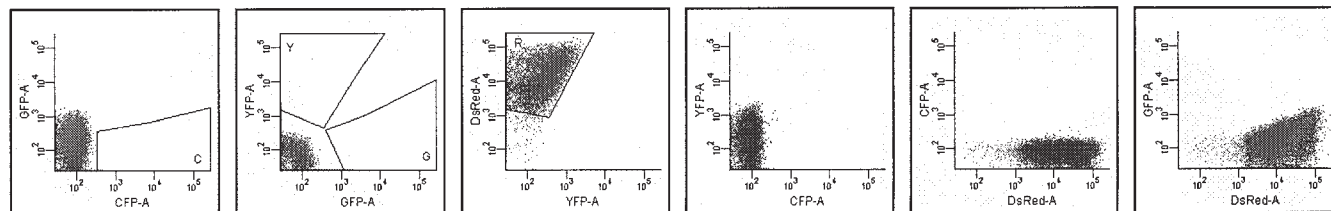
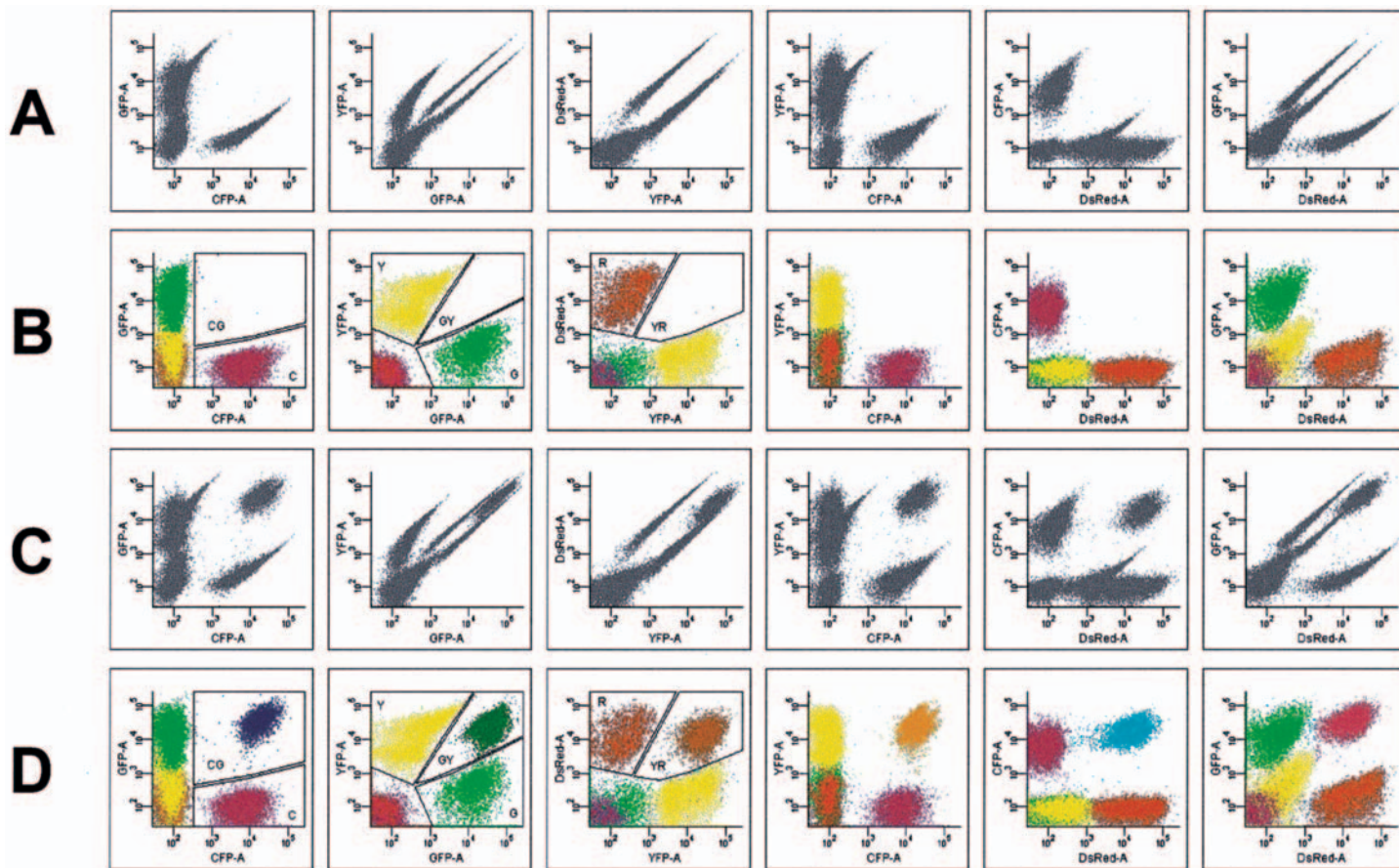


Fig. 2. Bivariate histograms depicting detection of parental Sp2/0-Ag14 cells (A), Sp2/0-Ag14 cells expressing ECFP (B), EGFP (C), EYFP (D), or DsRed (E) using 488-nm and 407-nm excitation as described in **Fig. 1**. The area of the pulse was used to measure fluorescence intensity. Data was acquired and analyzed using FACSDiVa software. The software calculated spectral overlap among all parameters and applied compensation post-acquisition. Nonrectilinear markers were used to delineate different populations in the first three plots (from **left to right**). “C,” “G,” “Y,” and “R” represent ECFP-positive, EGFP-positive, EYFP-positive, and DsRed-positive, respectively.



3.3.3. Feasible Detection Optics (nm) (see **Note 18**)

1. ECFP: 470/20- or 485/22-BP filter.
2. EGFP: 510/20- or 530/30-BP filter.
3. EYFP: 530/30-, 546/20-, or 550/30-BP.
4. DsRed: 585/42- or 610/20-BP filter.
5. Dichroic mirrors are used to separate the appropriate wavelengths: 500-longpass (LP), 525-SP, 560-SP, or 610-SP filters.
6. Filters for scatter parameters: BP filters capturing the (primary) excitation wavelength.
7. Laser line restriction band (RB) filters or notch filters, if necessary (see **Note 19**).

3.3.4. Feasible Detection Schemes (see **Note 20**)

<u>Combination</u>	<u>Excitation (nm)</u>	
EGFP/EYFP	488	(Fig. 5A)
EGFP/DsRed	488	(Fig. 5B)
EYFP/DsRed	488	(Fig. 5B)
ECFP/EGFP/EYFP	458	(Fig. 5C)
EGFP/EYFP/DsRed	488	(Fig. 5D)
ECFP/EYFP/DsRed	514 (primary) and 413 (tertiary)	(Fig. 5E)
ECFP/EGFP/EYFP/DsRed	458 (primary) and 568 (tertiary)	(Fig. 5F)

4. Notes

1. The pECFP, pEGFP-1, pEYFP-N1, and pDsRed-1 plasmids encoding ECFP, EGFP, EYFP, and DsRed, respectively, were obtained from BD Biosciences Clontech (Palo Alto, CA). DsRed.T1 and DsRed.T4 (developed by Benjamin Glick, University of Chicago, Chicago, IL) are improved versions of DsRed (28). DsRed.T1, known commercially as DsRed-Express, is available from BD Biosciences Clontech. BD Biosciences Clontech also sells other Anthozoa reef coral GFP-like proteins (26,29). Other commercially available GFP-like proteins that may serve as useful alternatives to the fluorescent proteins employed in this study include the

Fig. 3. (see opposite page) Bivariate histograms depicting simultaneous detection of ECFP, EGFP, EYFP, and DsRed using 488-nm and 407-nm excitation as described in **Fig. 1**. Data were acquired and analyzed using FACSDiVa software. A mixture of Sp2/0-Ag14 cells and cells expressing the individual fluorescent proteins is shown before (A) and after (B) spectral overlap compensation. A mixture of Sp2/0-Ag14 cells, cells expressing the individual fluorescent proteins and cells expressing all four fluorescent proteins is shown before (C) and after spectral overlap compensation (D). In addition to the markers shown in **Fig. 2**, nonrectilinear markers were drawn to delineate double-positive populations in the first three plots (from left to right). “CG,” “GY,” and “YR” represent ECFP/EGFP-positive, EGFP/EYFP-positive, and EYFP/DsRed-positive, respectively. Cells expressing all four fluorescent proteins appeared as a double-positive cluster in every histogram.

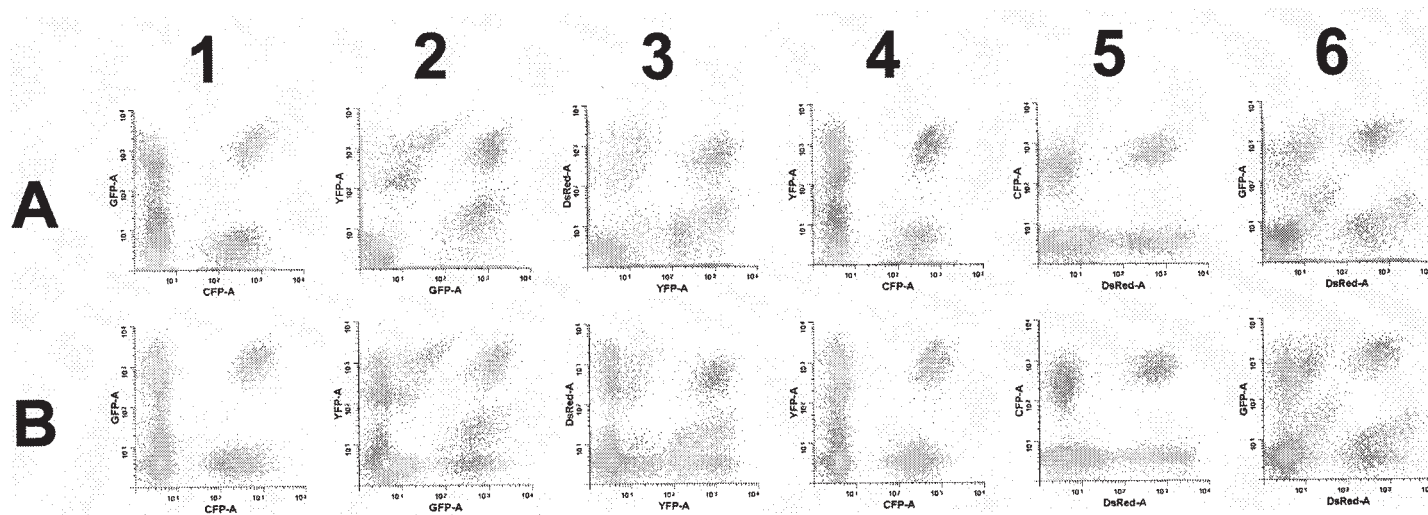
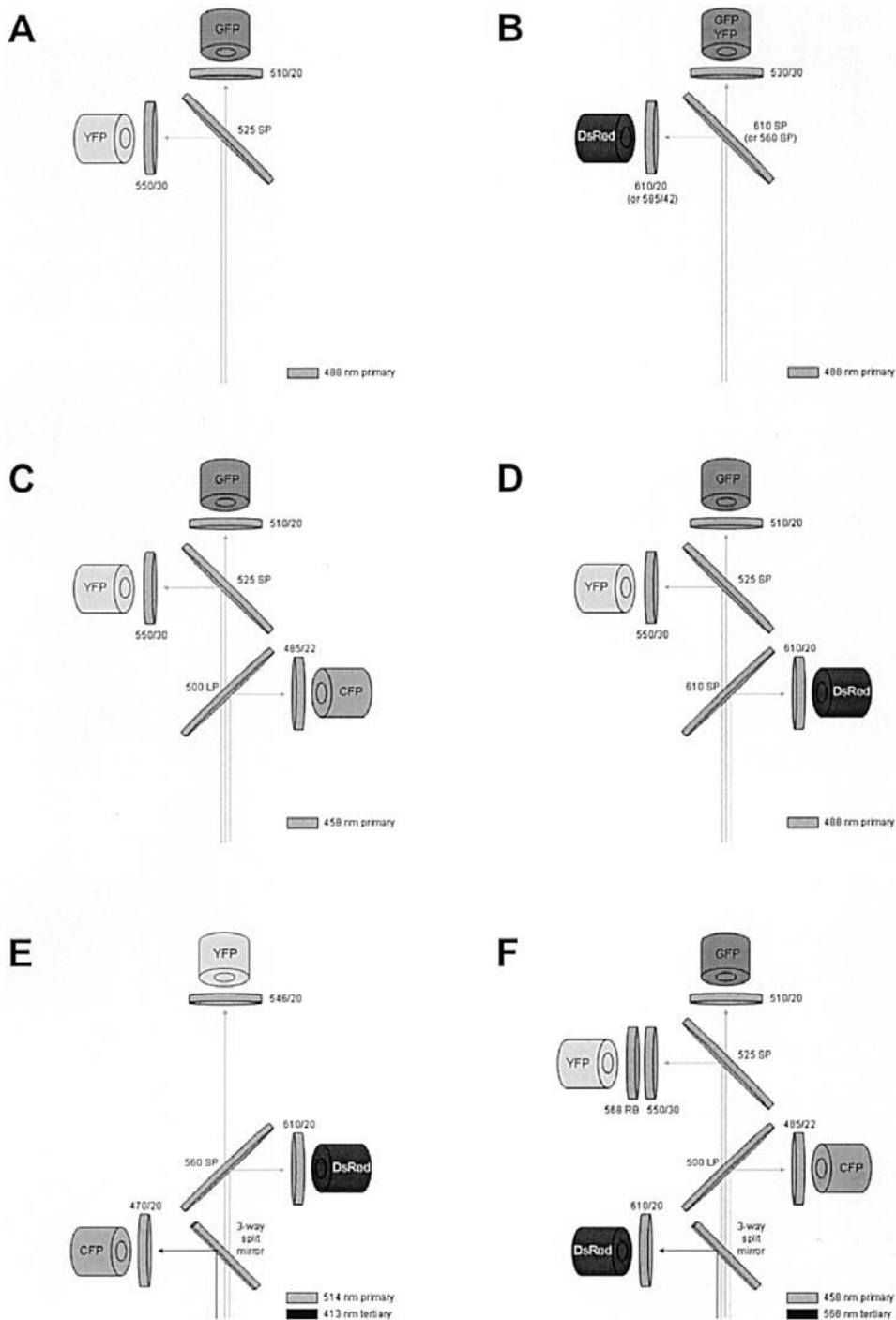


Fig. 4. Visual effect of log bias. These bivariate histograms were generated from high-resolution (262,144 channel) files (the same data files as described in **Fig. 3C**) using WinList's option to display in four decades. They were color compensated using WinList's n-color compensation system, displayed with log bias off (**A**) or log bias on (**B**). With log bias enabled, compensated values that have 0 intensity are assigned a random value between 0 and the log bias setting, 3 by default. This feature allows the visualization of events that are on the axes. This visual effect can be appreciated particularly well in (**B**), histograms 2, 3, and 6.

- Vitality[®] humanized *Renilla reniformis* GFP ($Ex_{\lambda_{max}} = 500$ nm; $Em_{\lambda_{max}} = 506$ nm) distributed by Stratagene (La Jolla, CA) (20), and the humanized CopGFP[™] ($Ex_{\lambda_{max}} = 482$ nm; $Em_{\lambda_{max}} = 502$ nm), *Aequorea coerulescens* AceGFP[™] ($Ex_{\lambda_{max}} = 480$ nm; $Em_{\lambda_{max}} = 505$ nm) (24), and PhiYFP[™] ($Ex_{\lambda_{max}} = 525$ nm; $Em_{\lambda_{max}} = 537$ nm) fluorescent proteins marketed by Evrogen (Moscow, Russia).
2. The tunable water-cooled krypton-ion laser can provide 407 nm. Violet laser diodes can provide 405, 407, or 408 nm (depending on the manufacturer), and can be retrofitted onto existing flow cytometers (30). At present, the following flow cytometers are equipped with (or can be upgraded as an option) air-cooled lasers that provide excitation wavelengths including 488 nm and 405/407 nm: LSR, LSR II, FACSARIA (all from BD Biosciences, San Jose, CA), CyAn (Dako-Cytomation, Fort Collins, CO), and CyFlow ML (Partec GmbH, Münster, Germany). The model of flow cytometer and the type of laser are not critical (31).
 3. Chroma Technology Corp. (Rockingham, VT) is another supplier of optical filters.
 4. Compensation for spectral overlap among all fluorescence parameters can be performed by utilizing hardware user-manipulated pairwise corrections during acquisition or software computer-aided calculations post-acquisition. For flow cytometers not equipped with inter-laser compensation electronic circuitry, software post-acquisition compensation is the only option. Available commercial software includes WinList (Verity Software House, Topsham, ME), FlowJo (Tree Star Inc., San Carlos, CA) and FCS Express (De Novo Software, Thornhill, Ontario, Canada). Some free software can perform compensation as well. A catalog of free cytometry software is available on the website managed by the Purdue University Cytometry Laboratories at <http://www.cyto.purdue.edu/flowcyt/software/catalog.htm>.
 5. Calibration-grade alignment beads are available from many suppliers including Molecular Probes (Eugene, OR), Polysciences Inc. (Warrington, PA), Spherotech Inc. (Libertyville, IL), Beckman Coulter (Miami, FL), BD Biosciences, and Bangs Laboratories Inc. (Fishers, IN).
 6. The authors welcome requests for Sp2/0-Ag14 cells expressing the various fluorescent protein genes.
 7. (Optional) Pure populations of cells expressing all four fluorescent proteins were isolated by fluorescence-activated cell sorting. Cell sorting was performed on a FACSVantage SE/FACSDiVa (BD Biosciences) equipped with two tunable lasers, an Innova 70C-Spectrum argon-ion laser and an Innova 302C krypton-ion laser (both from Coherent Inc., Santa Clara, CA), providing excitation wavelengths of 488 nm and 407 nm, respectively. A three-way split mirror allowed the 488-nm beam to be directed along the first laser pathway (primary position) and the 407-nm beam along the third laser pathway (tertiary position), maximizing their spatial separation and minimizing laser noise as well as crosstalk between the signals. Data were acquired and analyzed using FACSDiVa software.
 8. Cells were analyzed on the same flow cytometer as described in **Note 7**.
 9. AlignFlow Plus 6- μ m flow cytometry alignment beads (Molecular Probes) were used for 488-nm excitation. Fluoresbrite Calibration Grade 6- μ m YG microspheres (Polysciences Inc.) were used for 407-nm excitation.

232

Hawley et al.



10. The degree of spectral overlap correction depends on the voltages applied to the detectors. Depending on laser power and the orientation of dichroic mirrors (especially the 525 SP between the GFP and YFP detectors), comparable results can be achieved with different settings on different instruments.
11. The FACSVantage SE/FACSDiVa has digital electronics. Data are stored uncompensated in the linear domain. Compensation is performed by FACSDiVa software with matrix algebra. For flow cytometers equipped with analog circuitry and logarithmic amplifiers, compensation is performed by pulse subtraction. The percentages of compensation are adjusted by the user while viewing the data in a log display during acquisition. In this case, some negative cells should be added to each sample of positive cells so that the median values of fluorescence intensity for both populations can be compared. Alternatively, compensation can be applied using third-party software post-acquisition (*see Note 4*).
12. The photon counting statistics error is one of the errors intrinsic to the measurement process. It contributes to the spread of compensated data on a log scale. High degrees of spillover (as in the case of fluorescent proteins) and increased number of parameters exacerbate the error, especially for high fluorescence intensity populations. Consequently, visual adjustment of spectral overlap is prone to overcompensation. Computer-aided adjustment is highly recommended (**36**).
13. Owing to the spread of compensated data on a log scale, the use of quadrant markers will erroneously classify some single positives as double positives. Nonrectilinear markers should be used instead.
14. It is beyond the scope of this chapter to describe all of the potential errors associated with compensation. A discussion on software compensation can be found in the classic paper by Bagwell and Adams (**37**).
15. The biexponential transform (**38**) is a derivative of the hyperbolic sine and its inverse has many of the properties of the log distribution. The hyper-log transform developed by Verity Software House (Bruce Bagwell, personal communication) is a log-type transformation that smoothly moves from a log domain to a linear

Fig. 5. (*see opposite page*) Alternative optical configurations for simultaneous detection of different combinations of fluorescent proteins. Some of the optical filters shown here represent filters that are commonly used in other applications and are supplied with flow cytometers as standard filters. In some cases, resolution of the fluorescent proteins can be improved by custom-designed filters. (A) Detection of EGFP and EYFP using 488-nm excitation. (B) Detection of EGFP and DsRed, or EYFP and DsRed using 488-nm excitation. (C) Detection of ECFP, EGFP and EYFP using 458-nm excitation as described in **ref. 15**. (D) Detection of EGFP, EYFP, and DsRed using 488-nm excitation. (E) Detection of ECFP, EYFP, and DsRed using 514-nm and 413-nm excitation. (F) Detection of ECFP, EGFP, EYFP, and DsRed using 458-nm and 568-nm excitation as described in **ref. 16**.

domain around the first decade. In addition, the FCOM feature in WinList can be used to define properly all combinations of fluorescence (2^x , where x is the number of fluorescence parameters). This approach is readily scalable to as many parameters as required.

16. The required laser power for each wavelength depends on the detection sensitivity of the flow cytometer. In general, 15–35 mW is adequate for cuvet flow cell detection while 50–70 mW may be necessary for stream-in-air detection. Other factors also contribute to the efficiency of light collection. For example, lowering the stream velocity will increase the dwell time of the particle in the laser beam and enhance signal detection.
17. With the Innova 302C krypton-ion laser, the power output at 407 nm is half of that at 413 nm. However, at 50 mW of laser power, both wavelengths of excitation generate comparable data (data not shown).
18. The filter of choice for each fluorescence parameter is the one that allows the lowest spillover signals from other fluorescent proteins while capturing adequate signal from the primary fluorescent protein. It is not necessarily the filter that captures the maximal primary signal. Some of the optical filters suggested here represent filters that are commonly used in other applications (such as immunophenotyping) and are supplied with flow cytometers as standard filters. In some cases, resolution of the fluorescent proteins can be improved by using custom-designed filters.
19. It is critical to ensure that the detection optics do not capture the excitation wavelengths; under certain circumstances, notch filters that block out the excitation wavelengths should be included. For example, in the absence of a 514-nm notch filter, using 514 nm as the excitation wavelength precludes the detection of EGFP with a 510/20-BP filter. For simultaneous analysis of ECFP/EGFP/DsRed utilizing excitation wavelengths of 488 nm and 407 nm, a 488-nm notch filter is required for the detection of ECFP if a 485/22 BP filter is used (31). When the excitation wavelength is in close proximity to the wavelengths spanned by the detection filter, addition of a laser line restriction band filter to remove stray laser light may be required. As shown in **Fig. 5F**, the 568-nm RB filter ensures that detection of EYFP with a 550/30-BP filter is free of laser noise (16). When Beavis and Kalejta developed the detection scheme depicted in **Fig. 5C**, they installed 457-nm RB filters in front of all three fluorescence detectors (15).
20. Fluorescence resonance energy transfer studies utilizing CFP and YFP can be performed with excitation wavelengths of 413 nm and 514 nm (19) (see also Chapter 15 by Chan and Holmes, *this volume*). In addition, the detection schemes described here can be combined (depending on the availability of detectors and excitation wavelength) with red-shifted fluorochromes in other studies. Commonly used red-shifted fluorochromes excited by 488 nm include PerCP-Cy5.5 and tandem conjugates of phycoerythrin (PE); those excited by 633 nm include allophycocyanin (APC) and tandem conjugates of APC. Alexa Fluor dyes and their tandem conjugates (Molecular Probes) of the appropriate excitation and emission wavelengths can be used as well.

Acknowledgments

This work was supported in part by National Institutes of Health grants R01 HL65519 and R01 HL66305 (to R. G. H.). We thank Ali Ramezani for constructing the ECFP, EGFP, EYFP, and DsRed retroviral vectors, Bill Telford for fruitful collaborations, Dave Houck and Steven Merlin for their suggestions, and John Swanson for his support. Most of all, we are grateful to Bruce Bagwell and other members of the Verity Software House team (Ben Hunsberger, Christopher Bray, and Mark Munson), and to Joe Trotter at BD Biosciences for analyzing the data with the hyper-log transform and biexponential transform, respectively, prior to release.

References

1. Tien, R. Y. (1998) The green fluorescent protein. *Annu. Rev. Biochem.* **67**, 509–544.
2. Cormack, B. P., Valdivia, R. H., and Falkow, S. (1996) FACS-optimized mutants of the green fluorescent protein (GFP). *Gene* **173**, 33–38.
3. Yang, T. T., Cheng, L., and Kain, S. R. (1996) Optimized codon usage and chromophore mutations provide enhanced sensitivity with the green fluorescent protein. *Nucleic Acids Res.* **24**, 4592–4593.
4. Cheng, L., Fu, J., Tsukamoto, A., and Hawley, R. G. (1996) Use of green fluorescent protein (GFP) variants to monitor gene transfer and expression in mammalian cells. *Nat. Biotech.* **14**, 606–609.
5. Cheng, L., Du, C., Murray, D., et al. (1997) A GFP reporter system to assess gene transfer and expression in viable human hematopoietic progenitors. *Gene Ther.* **4**, 1013–1022.
6. Persons, D. A., Allay, J. A., Riberdy, J. M., et al. (1998) Use of the green fluorescent protein as a marker to identify and track genetically modified hematopoietic cells. *Nat. Med.* **4**, 1201–1205.
7. Dorrell, C., Gan, O. I., Pereira, D. S., Hawley, R. G., and Dick, J. E. (2000) Expansion of human cord blood CD34+CD38- cells in *ex vivo* culture during retroviral transduction without a corresponding increase in SCID repopulating cell (SRC) frequency: dissociation of SRC phenotype and function. *Blood* **95**, 102–110.
8. Horn, P. A., Topp, M. S., Morris, J. C., Riddell, S. R., and Kiem, H. P. (2002) Highly efficient gene transfer into baboon marrow repopulating cells using GALV-pseudotype oncoretroviral vectors produced by human packaging cells. *Blood* **100**, 3960–3967.
9. Hawley, T. S., Telford, W. G., and Hawley, R. G. (2001) “Rainbow” reporters for multispectral marking and lineage analysis of hematopoietic stem cells. *Stem Cells* **19**, 118–124.
10. Heim, R. and Tsien, R. Y. (1996) Engineering green fluorescent protein for improved brightness, longer wavelengths and fluorescence resonance energy transfer. *Curr. Biol.* **6**, 178–182.

11. Heikal, A. A., Hess, S. T., Baird, G. S., Tsien, R. Y., and Webb, W. W. (2000) Molecular spectroscopy and dynamics of intrinsically fluorescent proteins: coral red (dsRed) and yellow (Citrine). *Proc. Natl. Acad. Sci. USA* **97**, 11,996–12,001.
12. Nagai, T., Ibata, K., Park, E. S., Kubota, M., Mikoshiba, K., and Miyawaki, A. (2002) A variant of yellow fluorescent protein with fast and efficient maturation for cell-biological applications. *Nat. Biotechnol.* **20**, 87–90.
13. Anderson, M. T., Tjioe, I. M., Lorincz, M. C., Parks, D. R., Herzenberg, L. A., and Nolan, G. P. (1996) Simultaneous fluorescence-activated cell sorter analysis of two distinct transcriptional elements within a single cell using engineered green fluorescent proteins. *Proc. Natl. Acad. Sci. USA* **93**, 8508–8511.
14. Lybarger, L., Dempsey, D., Patterson, G. H., Piston, D. W., Kain, S. R., and Chervenak, R. (1998) Dual-color flow cytometric detection of fluorescent proteins using single-laser (488-nm) excitation. *Cytometry* **31**, 147–152.
15. Beavis, A. J. and Kalejta, R. F. (1999) Simultaneous analysis of the cyan, yellow and green fluorescent proteins by flow cytometry using single-laser excitation at 458 nm. *Cytometry* **37**, 68–73.
16. Hawley, T. S., Telford, W. G., Ramezani, A., and Hawley, R. G. (2001) Four-color flow cytometric detection of retrovirally expressed red, yellow, green and cyan fluorescent proteins. *BioTechniques* **30**, 1028–1034.
17. De Sepulveda, P., Okkenhaug, K., Rose, J. L., Hawley, R. G., Dubreuil, P., and Rotapel, R. (1999) Socs 1 binds to multiple signalling proteins and suppresses Steel factor-dependent proliferation. *EMBO J.* **18**, 904–915.
18. Leung, B. L., Haughn, L., Veillette, A., Hawley, R. G., Rottapel, R., and Julius, M. (1999) TcR $\alpha\beta$ independent CD28 signaling and costimulation require non-CD4-associated Lck. *J. Immunol.* **163**, 1334–1341.
19. Chan, F. K., Siegel, R. M., Zacharias, D., et al. (2001) Fluorescence resonance energy transfer analysis of cell surface receptor interactions and signaling using spectral variants of the green fluorescent protein. *Cytometry* **44**, 361–368.
20. Felts, K., Rogers, B., Chen, K., Ji, H., Sorge, J., and Vaillancourt, P. (2000) Recombinant *Renilla reniformis* GFP displays low toxicity. *STRATEGIES Newsletter* **13**, 85–87. http://www.stratagene.com/vol13_3/p85-87.htm.
21. Pelle, B., Gururaja, T. L., Payan, D. G., and Anderson, D. C. (2001) Characterization and use of green fluorescent proteins from *Renilla mulleri* and *Ptilosarcus guernei* for the human cell display of functional peptides. *J. Protein Chem.* **20**, 507–519.
22. Matz, M. V., Fradkov, A. F., Labas, Y. A., et al. (1999) Fluorescent proteins from nonbioluminescent Anthozoa species. *Nat. Biotechnol.* **17**, 969–973.
23. Labas, Y. A., Gurskaya, N. G., Yanushevich, Y. G., et al. (2002) Diversity and evolution of the green fluorescent protein family. *Proc. Natl. Acad. Sci. USA* **99**, 4256–4261.
24. Gurskaya, N. G., Fradkov, A. F., Pounkova, N. I., et al. (2003) A colourless green fluorescent protein homologue from the non-fluorescent hydromedusa *Aequorea coerulescens* and its fluorescent mutants. *Biochem. J.* **373**, 403–408.

25. Lukyanov, K. A., Fradkov, A. F., Gurskaya, N. G., et al. (2000) Natural animal coloration can be determined by a nonfluorescent green fluorescent protein homolog. *J. Biol. Chem.* **275**, 25,879–25,882.
26. Gurskaya, N. G., Fradkov, A. F., Tersikh, A., et al. (2001) GFP-like chromoproteins as a source of far-red fluorescent proteins. *FEBS Lett.* **507**, 16–20.
27. Wiedenmann, J., Schenk, A., Rocker, C., Girod, A., Spindler, K. D., and Nienhaus, G. U. (2002) A far-red fluorescent protein with fast maturation and reduced oligomerization tendency from *Entacmaea quadricolor* (Anthozoa, Actinaria). *Proc. Natl. Acad. Sci. USA* **99**, 11,646–11,651.
28. Bevis, B. J. and Glick, B. S. (2002) Rapidly maturing variants of the *Discosoma* red fluorescent protein (DsRed). *Nat. Biotechnol.* **20**, 83–87.
29. Richards, B., Zharkikh, L., Hsu, F., Dunn, C., Kamb, A., and Teng, D. H. (2002) Stable expression of Anthozoa fluorescent proteins in mammalian cells. *Cytometry* **48**, 106–112.
30. Telford, W. G. (2003) How to mount a violet laser diode on the FACSVantage/FACSDiVa. <http://home.ncicrf.gov/ccr/flowcore/index.htm>.
31. Telford, W. G., Hawley, T. S., and Hawley, R. G. (2003) Analysis of violet-excited fluorochromes by flow cytometry using a violet laser diode. *Cytometry* **54A**, 48–55.
32. Markowitz, D., Goff, S., and Bank, A. (1988) A safe packaging line for gene transfer: separating viral genes on two different plasmids. *J. Virol.* **62**, 1120–1124.
33. Roederer, M. (May 24, 2000) Compensation (an informal perspective). <http://www.drmm.com/compensation/index.html>.
34. Roederer, M. (2001) Spectral compensation for flow cytometry: visualization artifacts, limitations, and caveats. *Cytometry* **45**, 194–205.
35. Baumgarth, N. and Roederer, M. (2000) A practical approach to multicolor flow cytometry for immunophenotyping. *J. Immunol. Methods* **243**, 77–97.
36. Stewart, C. C. and Stewart, S. J. (2003) A software method for color compensation, in *Current Protocols in Cytometry* (Robinson, J. P., Darzynkiewicz, Z., Dean, P., et al., eds.), John Wiley & Sons, New York, pp. 10.15.1–10.15.12.
37. Bagwell, C. B. and Adams, E. G. (1993) Fluorescence spectral overlap compensation for any number of flow cytometry parameters. *Ann. NY Acad. Sci.* **677**, 167–184.
38. Shapiro, H. M. (2003) Afterword, in *Practical Flow Cytometry*, 4th edit., Wiley-Liss, New York, pp. 561–566.
39. BD Fluorescence Spectrum Viewer. <http://www.bdbiosciences.com/spectra>.

13

Analysis of Fluorescent Protein Expressing Cells by Flow Cytometry

Steven C. Pruitt, Lawrence M. Mielnicki, and Carleton C. Stewart

Summary

The process for transfection of cells with expression and gene-trap vectors expressing fluorescent reporter proteins is described. The measurement and sorting of discrete populations of transfected cells is also described and illustrated. Of particular importance, the maintenance of stability may be important and a simple strategy to monitor this has been developed. Finally, an effective method for improving the ability to measure low-level fluorescence from autofluorescence is described.

Key Words

DsRed, enhanced cyan fluorescent protein, enhanced green fluorescent protein, enhanced yellow fluorescent protein, fluorescence-activated cell sorter, fluorescent protein, HcRed.

1. Introduction

The availability of fluorescent proteins now allows real-time monitoring of gene expression and protein localization. Many applications for these proteins require the ability to analyze and sort expressing cells accurately and quantitatively using a fluorescence-activated cell sorter (FACS) (1–4). In particular we demonstrate the utilization of FACS to isolate populations of cells that express the enhanced green fluorescent protein (EGFP) from expression vectors and from endogenous gene promoters following gene trapping. Gene trapping with fluorescent reporter genes provides a sensitive means of calibrating the level of expression from trapped genes (5) and also allows the possibility of recovering cells in which the trapped genes are expressed within defined levels of expression. This protocol addresses: (1) the process of transfecting fluorescent vectors into cells, (2) configuring flow cytometers for analyzing expressed fluorescent proteins in cells, (3) sorting cells expressing fluorescent proteins, (4) the appar-

From: *Methods in Molecular Biology: Flow Cytometry Protocols*, 2nd ed.
Edited by: T. S. Hawley and R. G. Hawley © Humana Press Inc., Totowa, NJ

ent stability of EGFP expression following cell growth, and (5) a simple but effective method for improving the ability to discriminate low level EGFP fluorescence from autofluorescence.

2. Materials

1. Access to a FACS and an analyzer (optional).
2. Eukaryotic fluorescent protein expression vector system (e.g., Living Colors vectors, BD Biosciences Clontech, Palo Alto, CA) (6–8).
3. Restriction enzymes and buffers, *E. coli* host strain (e.g., HB101), growth media (e.g. LB), and ampicillin.
4. Cells: Jurkat, P19 embryonic carcinoma (EC), and HEK 293.
5. Media: RPMI 1600 for Jurkat; DMEM for P19 and HEK 293.
6. Electroporation apparatus and sample cuvetts (e.g., Bio-Rad Laboratories, Hercules, CA).
7. CaPO₄ transfection reagents: 250 mM CaCl₂, 2X HBS (280 mM NaCl, 50 mM *N*-(2-hydroxyethyl)piperazine-*N'*-2-ethanesulfonic acid (HEPES), 1.5 mM Na₂H₂PO₄, pH 7.1), and sterile H₂O.
8. Standard cell culture reagents and supplies.
9. Geneticin (G418) (Invitrogen, Carlsbad, CA).
10. Vital DNA stain (e.g., Hoechst 33342).
11. Incandescent light source (e.g., fiber optic lamp).
12. Fixative (e.g., paraformaldehyde).

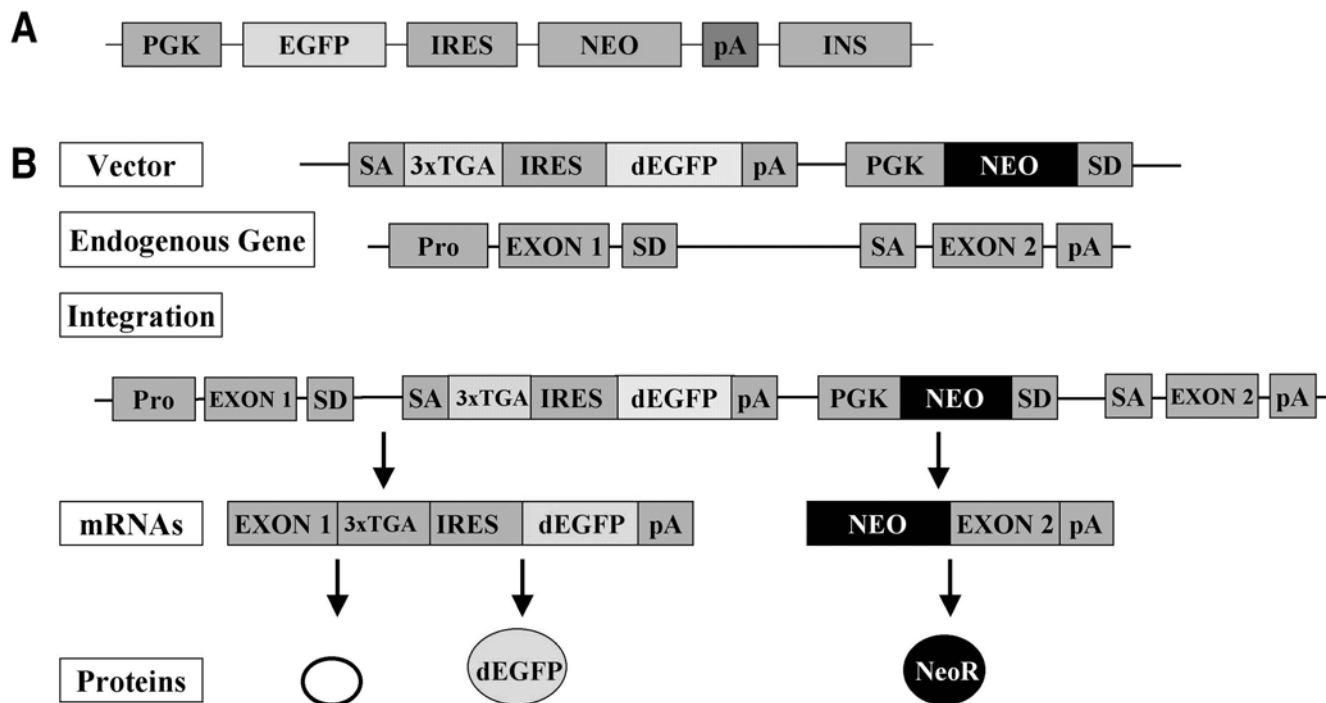
3. Methods

3.1. Introduction of Fluorescent Protein Expression Vectors Into Cells

Preparation of cells expressing enhanced cyan (ECFP), green (EGFP), yellow (EYFP), or red (DsRed2, HcRed) fluorescent proteins from plasmid vectors carrying the fluorescent protein encoding genes can be accomplished by any of the standard DNA introduction methodologies (e.g., calcium phosphate coprecipitation, lipofection) either transiently or as stably expressing clones. Experiments performed for this study employed both stable and transient introduction of fluorescent protein expression vectors.

1. The stable fluorescent protein expressing cells were constructed using Jurkat and P19 EC cells with the following vectors and methods. Jurkat cells were electroporated with the plasmid pIV (**Fig. 1A**, S. C. Pruitt, *unpublished*). P19 EC cells

Fig. 1. (*see facing page*) Fluorescent protein expression vectors structure and use. (**A**) pIV sequence elements. (**B**) Gene trap vector sequence elements and functions. P_{gk} is the P_{gk} promoter, IRES is the internal ribosome entry site, pA is a polyadenylation site, INS is an insulator sequence, *NeoR* is the neomycin resistance gene, SA is the splice acceptor, 3XTGA is the series of translational stop codons, an SD is the splice donor.



were electroporated with either pIV or the gene-trapping vector shown in **Fig. 1B** to create gene-trap libraries. Features of the gene trap vector include from 5' to 3': a splice acceptor, a triplet translational termination sequence that will terminate translation in all three reading frames from an endogenous protein, an internal ribosome entry site, the reporter gene (such as EGFP), a polyadenylation signal, an insulator sequence derived from the β -globin gene, the Pkg promoter, the neomycin resistance gene, and a splice donor.

2. The vectors were introduced as linear molecules by electroporation. Electroporation was performed using a Bio-Rad Gene Pulser II set to 200 V and 500 μ F. 1×10^7 cells were electroporated in a 1-mL volume containing between 40 and 60 μ g of DNA.
3. Cells were grown in the presence of G418 for a period of 10 d and surviving cells were pooled from approx 1500 colonies. Cells were amplified by trypsinization and passage to additional culture flasks, retaining all of the resulting cells, until approx 5×10^7 cells were obtained. This population was then prepared for FACS by trypsinizing and filtering using standard protocols.
4. We also utilized a transient transfection approach for generating fluorescent protein marked cells employing DsRed2, EGFP, EYFP, and ECFP (all from BD Biosciences Clontech) which were cloned into a parallel series of plasmids in which the fluorescent protein is expressed bicistronically 3' to a second cDNA (**Fig. 2**). These constructs were introduced individually into HEK 293 cells using calcium phosphate-mediated transfection techniques (9). For this set of experiments only, 2 d following transfection, cells were prepared for flow cytometric analysis by trypsinizing, fixing in 1.5% formalin (see **Note 1**) and filtering using standard protocols.

3.2. Simultaneous Detection of Multiple Fluorescent Proteins

The number of fluorescent proteins that can be detected will depend on the instrument and lasers available to the user. We provide some possible instrument setups based on the properties of fluorescent proteins (summarized in **Table 1**) and lasers that can be used to excite them.

Five different lasers can be used. The argon laser is the most versatile because it can be tuned to 350- to 360-nm lines in the UV, 458-nm line, or 488-nm line. An argon laser operating in the UV or 458 nm, a krypton laser operating at 407 nm or 413 nm, or a violet solid-state laser operating at 405–408 nm can be used for exciting ECFP (4). If the argon 488-nm line is used, EGFP, EYFP, and DsRed FP can be excited. With two argon lasers with spatially separated beams, one can be tuned to 458 nm to excite ECFP and EGFP, and the other to 488 nm to excite EYFP and DsRed FP. In this configuration, all four fluorescent proteins can be measured.

3.2.1. One- or Two-Laser Excitation

There are several ways to set up the flow cytometry for four-color vector analysis, and we have used the approach of Hawley et al. (4) (see **Note 2**). The

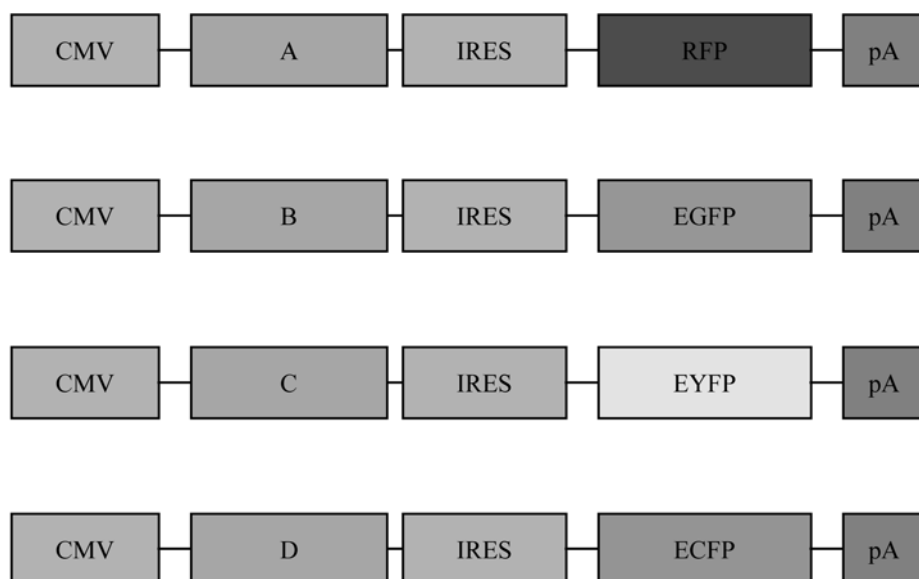


Fig. 2. Drawing of parallel color vector series. The parent vector for each construct was the pTRGS plasmid described in **ref. 11**. (A–D) represent different possible cDNAs that can be expressed.

selection of laser excitation will depend on what is available to the investigator. There is an ideal laser combination, and there are acceptable combinations; but the latter will not perform quite as well for some vectors.

1. For example, a solid-state violet laser operating at 405 nm will excite ECFP as well as an argon laser operating at 458 nm, but better than an argon laser operating in the UV (*see Note 3*). A second argon laser operating at 488 nm to excite EGFP and EYFP can be used. A 532-nm solid-state laser can be used to excite EYFP and DsRed FP (*see Table 1*).
2. The configuration shown in **Fig. 3** utilizes a flow cytometer with a 405-nm violet solid-state laser (Coherent, Santa Clara, CA) to excite ECFP, and an air-cooled argon laser operating at 488 nm to excite EGFP, EYFP, and DsRed FP. This configuration can be found on the LSR, FACSaria (both from BD Biosciences, San Jose, CA), or CyAn (DakoCytomation, Fort Collins, CO).
3. For single-laser measurements, laser 2 (violet laser) is not used. Results using 293 cells expressing each fluorescent protein with this configuration are shown in **Fig. 4**.

3.2.2. Three-Laser Configuration

For all five fluorescent proteins, spatial separation of three lasers will be necessary to provide optimal excitation of all fluorescent proteins including

Table 1**Some Fluorescent Protein Vectors and Their Fluorescent Properties**

FP	Lasers—nm	Ex Max	Em Max	Ext Coef	Qy
ECFP	Argon—UV	434	477	26,000	0.4
	Argon—458				
	Krypton—407				
	Krypton—413				
	Solid state—405				
EGFP	Argon—458	489	508	55,000	0.6
	Argon—488				
EYFP	Argon—458	514	527	84,000	0.6
	Argon—488				
	Argon—514				
	Solid state—532				
DsRed FP	Argon—488	558	583	22,500	0.7
	Argon—514				
	Solid state—532				
	Krypton—568				
HcRed FP	Tunable Dye—570	588	618	20,000	0.015
	Krypton—568				
	Tunable dye—570				

From refs. 6–8 and 10.

HcRed FP. The three spatially separated lasers shown in **Fig. 5** are a 405-nm solid state laser, a 488-nm argon laser, and dye laser operating at 570 nm (pumped by an argon laser). The 568-nm line on a krypton laser could be substituted for the dye laser. This configuration is available on cell sorters from Beckman Coulter (Miami, FL), BD Biosciences or DakoCytomation. This configuration is very similar to that used for one- or two-laser excitation with the addition of the third laser for exciting DsRed FP and HcRed FP.

3.3. Suppression of Heterogeneity in Fluorescent Protein Detection

Previous studies have allowed us to refine several important parameters for accurate windowing of EGFP fluorescing cells. In particular, we have observed a phenomenon we call fluorescence detection heterogeneity. In brief, in existing fluorescence activated cell sorters, the excitation source is at 90° to the detector optics. An assumption has been made that the excited fluorescence molecules are detected in an approximately equal manner as the cell passes through the detection volume. However, the detection volume is approx $\pi/6$ of

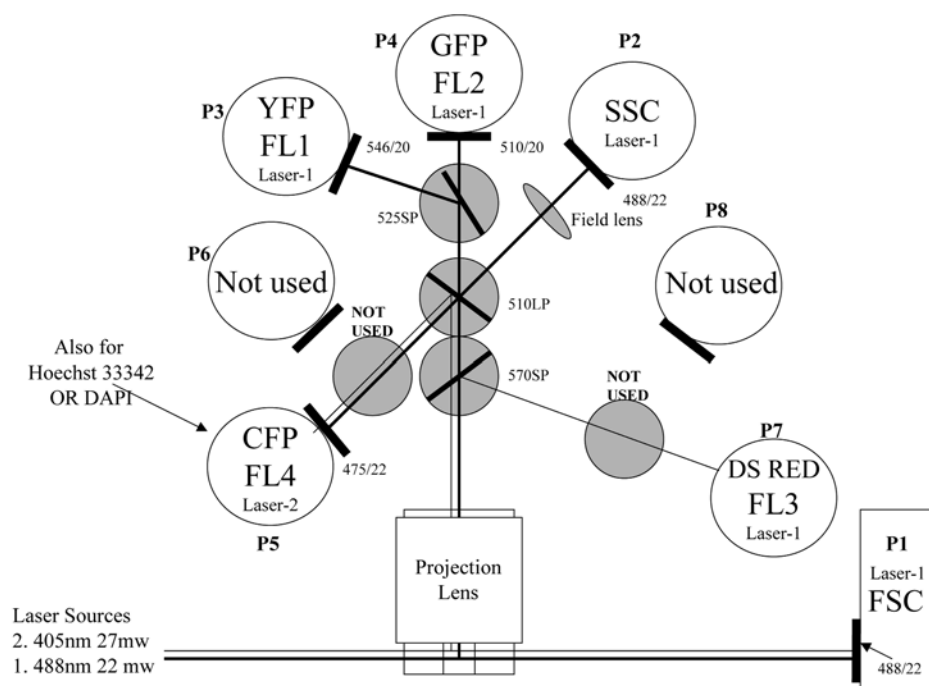


Fig. 3. One- or two-laser excitation. An LSR (BD Biosciences) eight-parameter flow cytometer was configured as shown. Laser 1 was an air-cooled argon laser operating at 488 nm. The pinholes in front of the PMTs P1–P4 and P7 were aligned to the interrogation point of this beam. No bandpass (BP) filter is used for DsRed as selectivity is sufficient from the 570-nm shortpass (SP) dichroic mirror. Laser 2 was a 405-nm solid-state laser and the pinhole in front of P5 was aligned to the interrogation point of this laser. PMTs P6 and P8 were not used. The 570 SP-dichroic mirror was used to direct DsRed FP to P7/FL3 and transmit the other colors to the 510 nm long pass (LP) dichroic mirror. This mirror reflects both the side scatter (SSC) and ECFP fluorescence to the 475/22 BP filter* which transmits ECFP fluorescence to P5/FL4 and reflects enough of the SSC fluorescence back through the 510-nm dichroic mirror into P2. (This is the configuration supplied by BD Biosciences.) The 510-LP dichroic mirror transmits EGFP and EYFP fluorescence to the 525-SP dichroic mirror, which reflects EYFP fluorescence to P3/FL1 and EGFP fluorescence to P4/FL2. (*Although not evaluated, a 450/20-BP filter could improve fluorescence detection of ECFP. This photomultiplier tube could also be used for Hoechst or DAPI measurements.)

the total volume and photons outside the detection volume are not detected. Our prior studies (Stewart et al., *unpublished observations*) have revealed that, the detection time may be too brief (e.g., high-speed sorting), and cells with equal total fluorescence can appear heterogeneous in their fluorescence con-

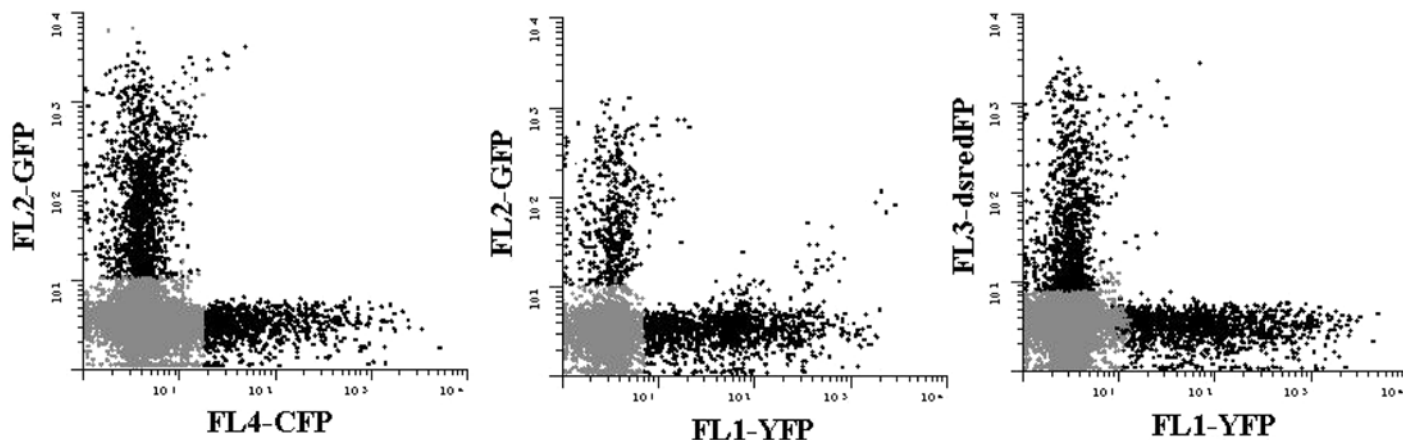


Fig. 4. Simultaneous detection of ECFP, EGFP, EYFP, and DsRed FP. HEK 293 cells were individually transfected with ECFP, EGFP, EYFP or DsRed FP and the individually transfected cells were pooled for analysis. Two days later the cells were harvested, fixed in paraformaldehyde, and data were acquired using the setup shown in **Fig. 3**. Data was acquired uncompensated using each individually unmixed transfected cells to establish the compensation matrix for software compensation (12).

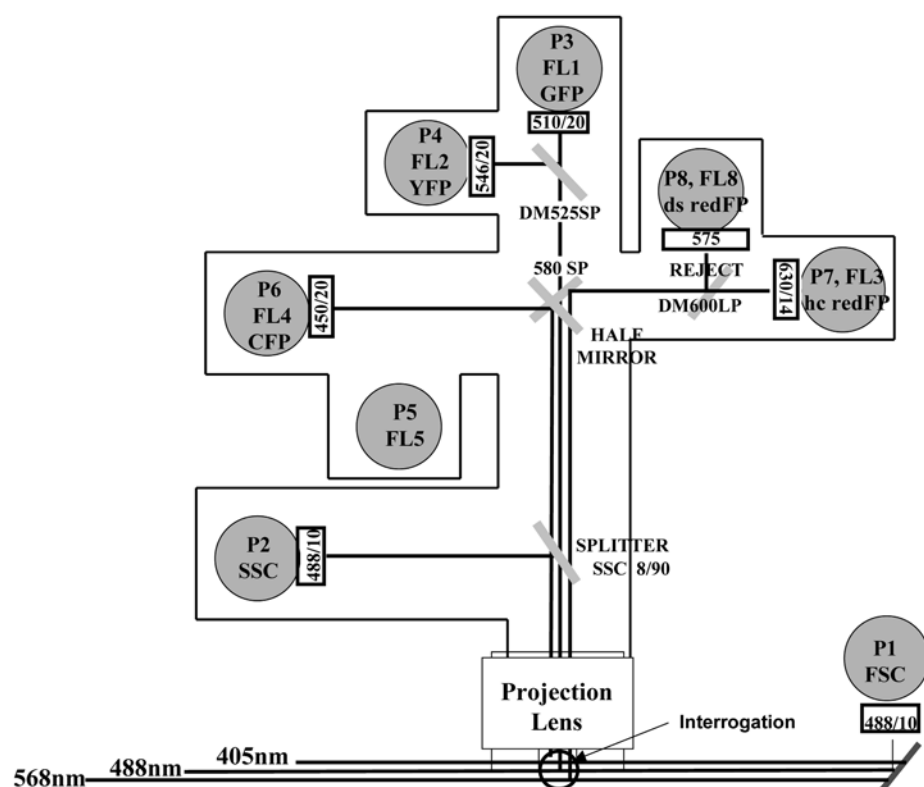


Fig. 5. Three-laser excitation of fluorescent proteins. A UV or 405-nm laser can be used to excite ECFP. Its fluorescence is reflected off the half mirror and detected by P6/FL4 after passing through a 450/20-BP filter. The second laser operating at 488 nm is used to detect forward scatter (FSC), SSC after reflection off an 8/92 splitter and passing through a 488/10 BP filter. The fluorescence from EGFP and EYFP pass over a half mirror. EGFP fluorescence is detected after passing through a 525-SP dichroic mirror and a 510/20-BP filter. EYFP fluorescence is reflected off the dichroic mirror and passes through a 546/20-BP filter. For excitation of HcRed and DsRed fluorescent proteins, a dye or krypton laser operating at 568 nm is used and their fluorescence is reflected off the 580-SP dichroic mirror. A 600-LP dichroic mirror is used to reflect DsRed FP through a 575-nm reject filter into P8 and transmit HcRed FP into P7.

tent. The degree to which this happens will depend on the nonuniformity of the fluorescent molecular distribution within the cells and the cells' orientation at the time of detection. This is caused by the scatter and absorption of emitted photons outside the detection volume. The effect is cells that appear bright after one pass (e.g., sorted) may appear dim on a second pass (e.g., reanalysis of

sort). Two immediate steps have been taken to minimize the effect of this phenomenon on our ability to discretely window fluorescent cell populations.

1. The first is to ensure that expression of EGFP from the gene trap vector utilized in these experiments does not lead to differential localization of the EGFP through the generation of fusion proteins. As shown in **Fig. 2**, the gene trap vector utilized incorporates technology to prevent the formation of such fusion proteins.
2. The second is to modify the flow sorting parameters. By reducing the flow rate within the detection tube, rotation of the cells during photon collection is allowed. This allows emissions from the cell to be collected as an average of the intensity from different perspectives, relative to the distribution of EGFP expression in the cell. These two modifications greatly enhance the accuracy with which pools of cells that fluoresce within a given window can be generated and evaluated. With these modifications, the current technology is sufficient to provide accurately fluorescent “windowed” populations of cells for multiplex screening.
3. The efficacy of these methods in allowing cells to be sorted into populations that fluoresce at well defined levels are shown in **Figs. 6–8** for Jurkat cells. Cells can be divided into as many as eight different levels (windows) of fluorescence (**Fig. 6**). Cells from each window can be isolated (**Fig. 7**) where subpopulations can be purified to the point that $<0.02\%$ of the cells fall outside of the defined fluorescence window (**Fig. 8**).

3.4. Compensation for the Effects of Cell Growth on Signal Strength

3.4.1. Stability of Fluorescence Signal As a Function of Time

A second issue that may influence the utility of cells for which fluorescence levels have been tightly defined is that the fluorescence signal from the cells is not stable as a function of time. **Figure 9** illustrates the problem.

1. The first panel labeled “starting” shows the fluorescence distribution of a pool of gene trap events.
2. On d 1 of the experiment the cells were enriched for a specific window of fluorescence as shown in the second panel labeled “enriched.”
3. Following growth for 1 wk the enriched population of cells was reassessed for fluorescence as shown in the third panel week 1 and “enriched” a second time as shown in the fourth panel.
4. Following growth for an addition week, the level of fluorescence was compared for the starting population (left panel) and the twice-enriched population (right panel). When the left and right panels are compared no significant tightening of the spectrum of fluorescence was achieved.
5. To address the underlying cause of the scatter in fluorescence levels of the cells with time, cells were assessed over a much shorter time frame of 20 h. A nearly identical drift in the fluorescence properties was seen after only 20 h to that seen following 1 wk (not shown), demonstrating that the underlying phenomena was unlikely to be genetic or epigenetic instability.

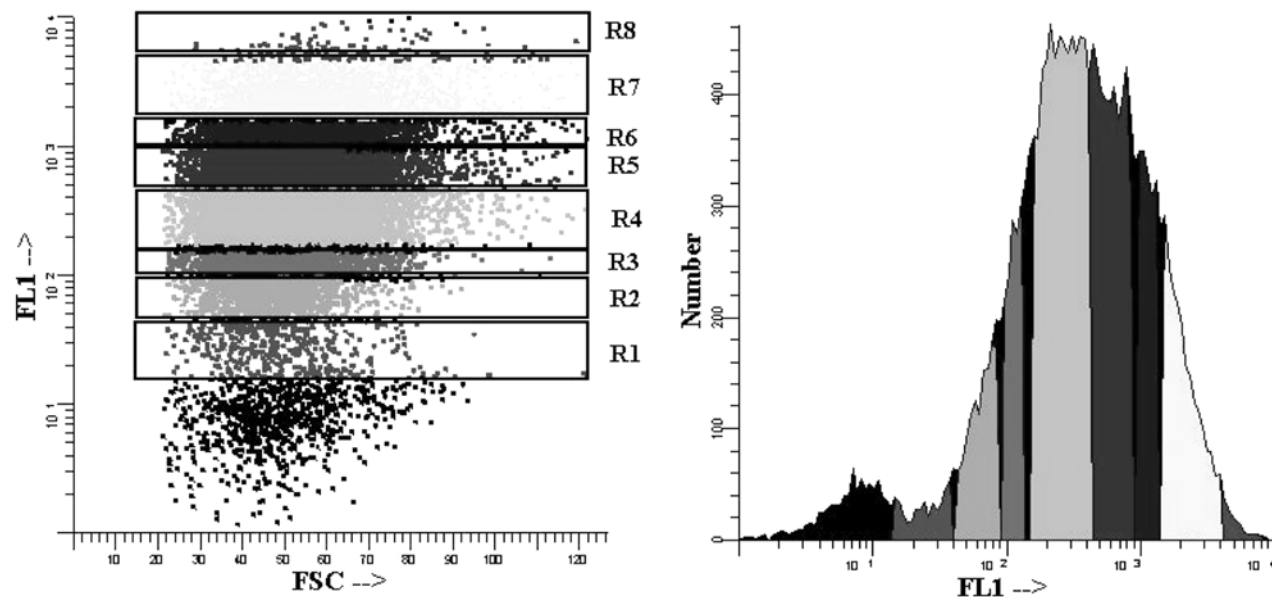


Fig. 6. EGFP cellular fluorescence distribution in Jurkat cells. Dot-plot (**left**) and histogram (**right**) obtained after FACS analysis of EGFP-expressing Jurkat cells derived following electroporation of the pIV vector as described in the text. FL1, fluorescence intensity; FSC, forward scatter, R1–8 represent the regions of fluorescence intensity derived from the dot-plot, shaded to the corresponding areas of the histogram.

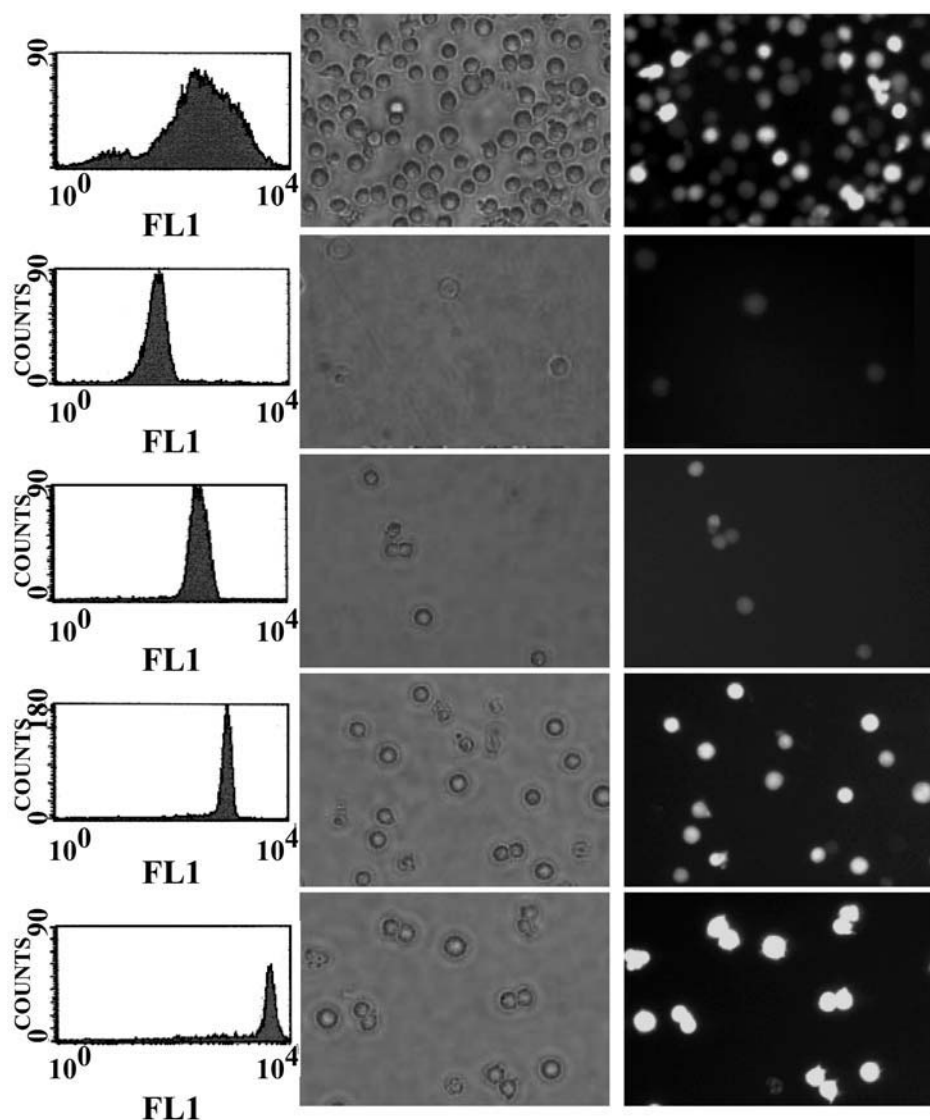


Fig. 7. EGFP cellular fluorescence after low-speed sorting. EGFP-expressing Jurkat cells were sorted using a cell stream velocity of approx 5 m/s in a detection height of 30 μ m. Reanalysis of sorted cells indicates a major improvement in purity of the desired cells. The initial cell population is the same as is shown in **Fig. 6**. In each case the **left** panel shows the distribution of fluorescence from individual cells plotted as a histogram and the **middle** and **right** panels show images obtained after phase-contrast and fluorescence microscopy, respectively. The **topmost** set is the total cell population before sorting. The remaining sets are, from **top** to **bottom**, post-sort analyses of the R2, R4, R6, and R8 regions defined in **Fig. 6**.

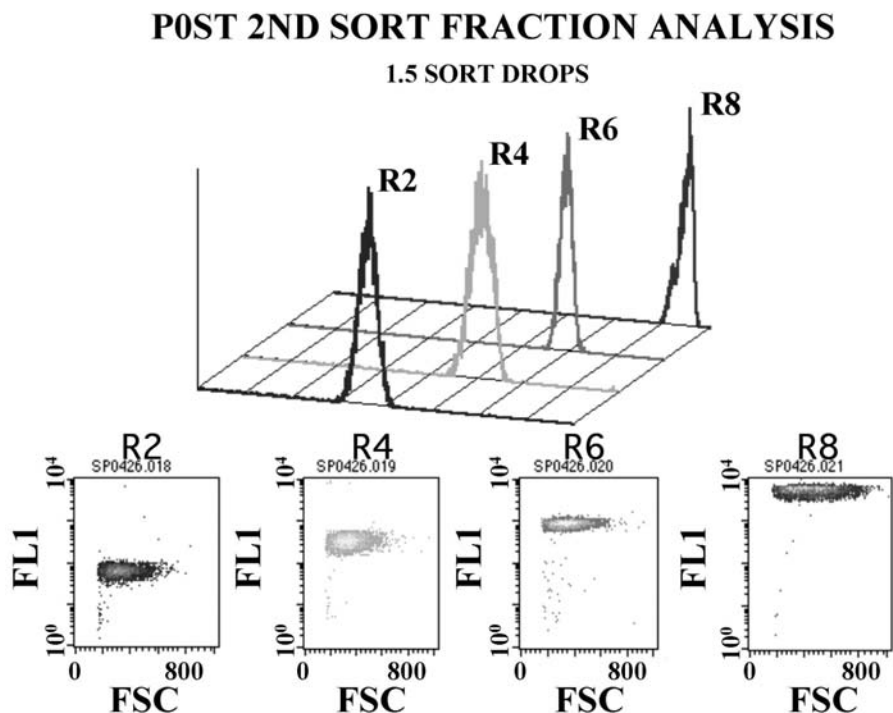


Fig. 8. Post-sort analysis of EGFP cellular fluorescence from “windowed” Jurkat cells. The sorting regions are a subset of those defined in **Fig. 6** (R2, R4, R6, and R8) where the **upper** portion of the figure shows the distribution of fluorescence from individual cells plotted as a histogram, and the **lower** panels show dot-plots of fluorescence as a function of forward scatter. The data are derived after three consecutive rounds of sorting. With few exceptions, the level of contamination of sorting windows separated from the initial sort window by two or more windows is <0.02%. Furthermore, in many of the exceptional cases the contaminants show a forward scatter value of less than 200, indicating that they are cellular debris, not whole cells.

3.4.2. Distribution of Fluorescence Intensity During the Cell Cycle

DNA content was determined by staining with the vital dye Hoechst 33342 (**Fig. 10**). The right panel in **Fig. 10** shows that dimmer cells are biased toward G1 and brighter cells toward G2. This relationship between signal intensity and cell cycle is also reflected by forward scattering, as illustrated in **Fig. 11** (based on the data obtained in **Fig. 10**). We call this phenomenon cell cycle dependent reporter heterogeneity (CDRH). The upper left panel shows the result of this relationship on the spread of signal intensity when standard sorting parameters are used. This relationship suggests a simple solution to maintaining signal stability: selection of a sorting window that accounts for the cell cycle

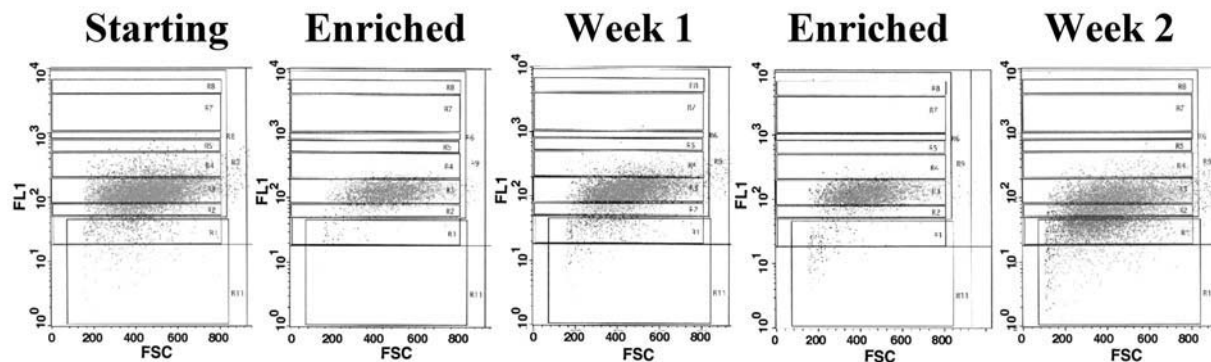


Fig. 9. FACS analysis illustrating the effects of cell growth on signal strength. Gene-trapped P19 EC cells expressing EGFP (starting) were sorted into a fluorescence window (R3) and reassessed for purity (enriched). Following 1 wk of growth, the sorted cells were reassessed for fluorescence intensity before (wk 1) and after (enriched) sorting to R3. The sorted wk 1 cells were grown for one additional week and reassessed for fluorescence (wk 2).

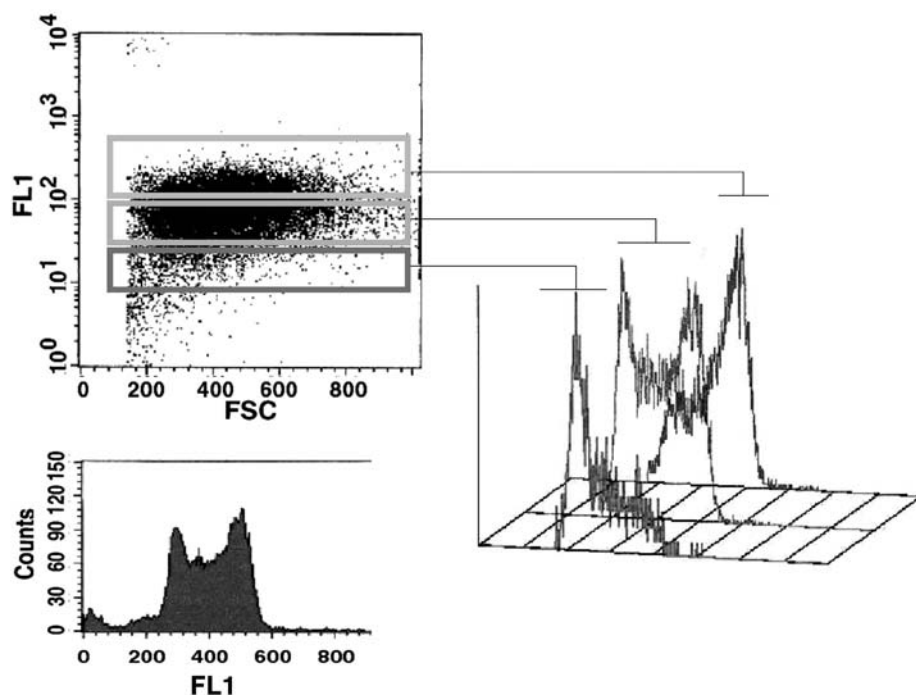


Fig. 10. Distribution of cellular EGFP fluorescence varies during the cell cycle. The dot-plot (**top left**) shows the fluorescence intensity distribution of EGFP-expressing P19 EC cells plotted vs forward scatter. The histogram (**bottom left**) shows a DNA content determination (by Hoechst 33342 staining) of the same cells. The three-dimensional plot on the **right** shows the DNA content histogram of the cell populations defined by the regions in the EGFP fluorescence dot-plot.

changes in fluorescence as suggested in the lower left and right panels. **Fig. 12** demonstrates that this change can compensate for CDRH.

1. In this experiment (**Fig. 12**), cells exhibiting a range of fluorescence values were sorted based on the use of a horizontal (upper left panel) or slanted (lower left panel) sorting window in the fluorescence \times forward scatter channels. The initial sorting window was selected such that approx 43% of the total starting population was present in either the horizontal or slanted windows. Cells were sorted one time in the absence of additional methods to improve the sort such that any effect could be attributed to the change in sorting windows.
2. Sorted cells were placed into culture for a period of approx 24 h and reevaluated for the proportion present in the original sorting window (upper right panel, horizontal window; lower right panel, slanted window). In the case of the horizontal window the percentage of cells actually decreased from 43% to 41%. In contrast

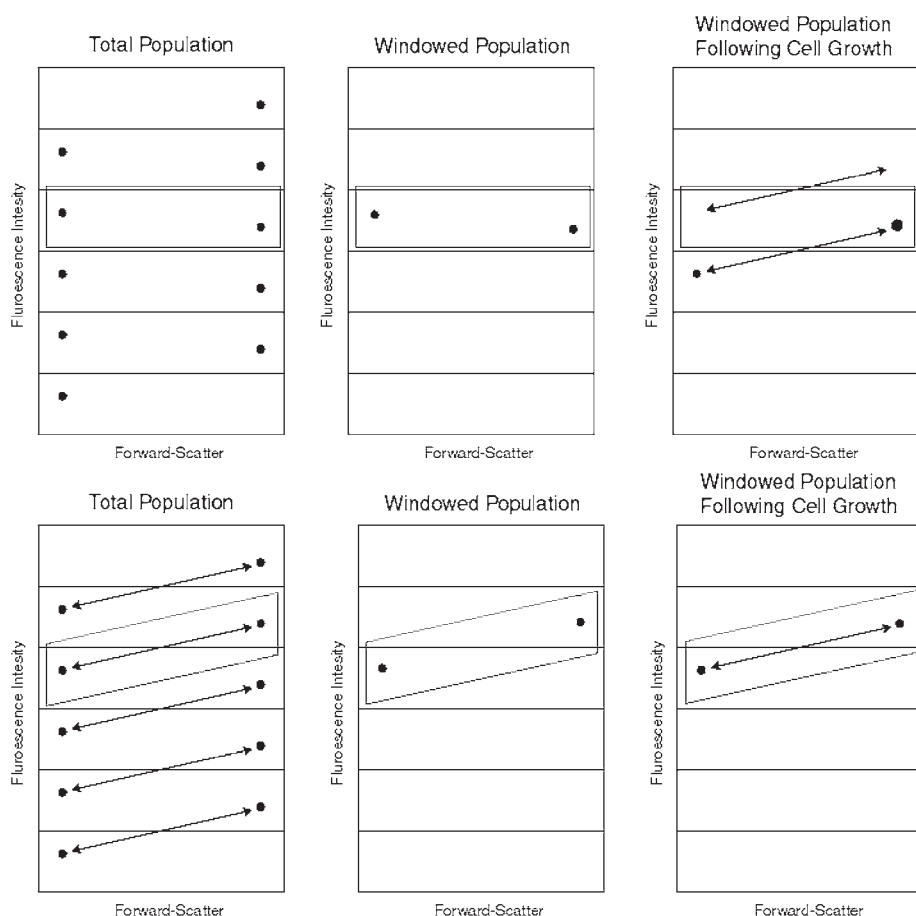


Fig. 11. CDRH compensation method. Diagram illustrating how a redefined sort window compensates for the cell cycle dependent changes in fluorescence signal intensity. The representation in the **upper** panels is derived from the data shown in **Fig. 10**. The representations in the bottom panels shows the redefinition of the sort windows based on the above derivation.

the percentage of cells recovered in the original slanted window increased from 43% to 54%. This initial experiment demonstrates the utility of cell cycle compensation, on a single-pass sort, in the absence of any additional techniques for improving sorting efficiency.

3.5. A Simple Method for Suppression of Autofluorescence

Under conditions where there are low levels of fluorescent signal from a fluorescent protein reporter, cellular autofluorescence can obscure the useful signal range. To address this problem we have identified a method by which

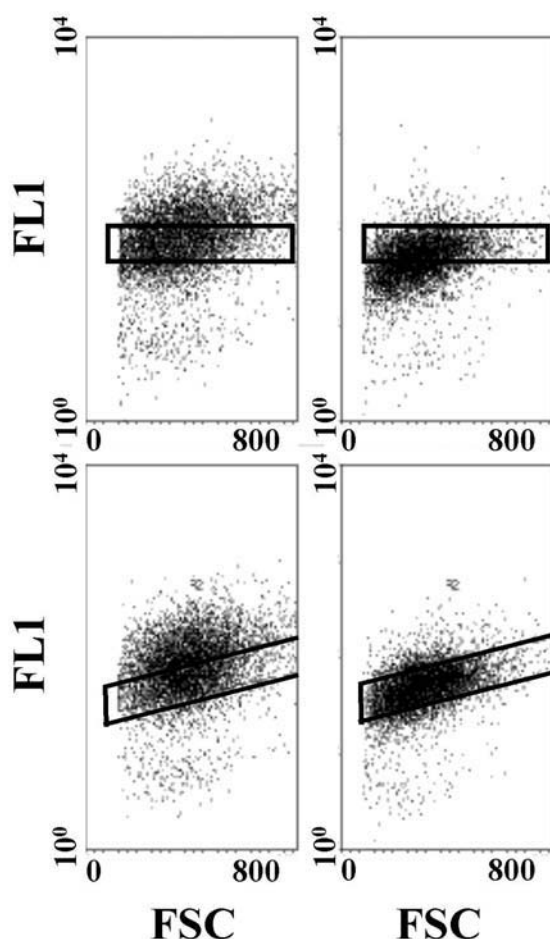


Fig. 12. Redefined sort window compensates for CDRH. Effect of compensating for CDRH in the forward scatter axis on the recovery of fluorescence windowed cells following cell growth. Cells exhibiting a range of fluorescence values were sorted based on the use of a horizontal (**upper left**) or slanted (**lower left**) sorting window in the fluorescence \times forward scatter channels. Cells were allowed to grow for approx 24 h and reassessed using the same windows (**upper right**, horizontal window; **lower right**, slanted window).

much of the cellular autofluorescence can be reduced without significantly affecting the level of fluorescence from the fluorescent protein. This can be applied to reduce autofluorescence relative to fluorescent protein expression for any purpose. The basis of the process is that cellular autofluorescence is rapidly quenched by broad-spectrum visible light while expression from fluorescent protein reporters is much less affected by such exposure.

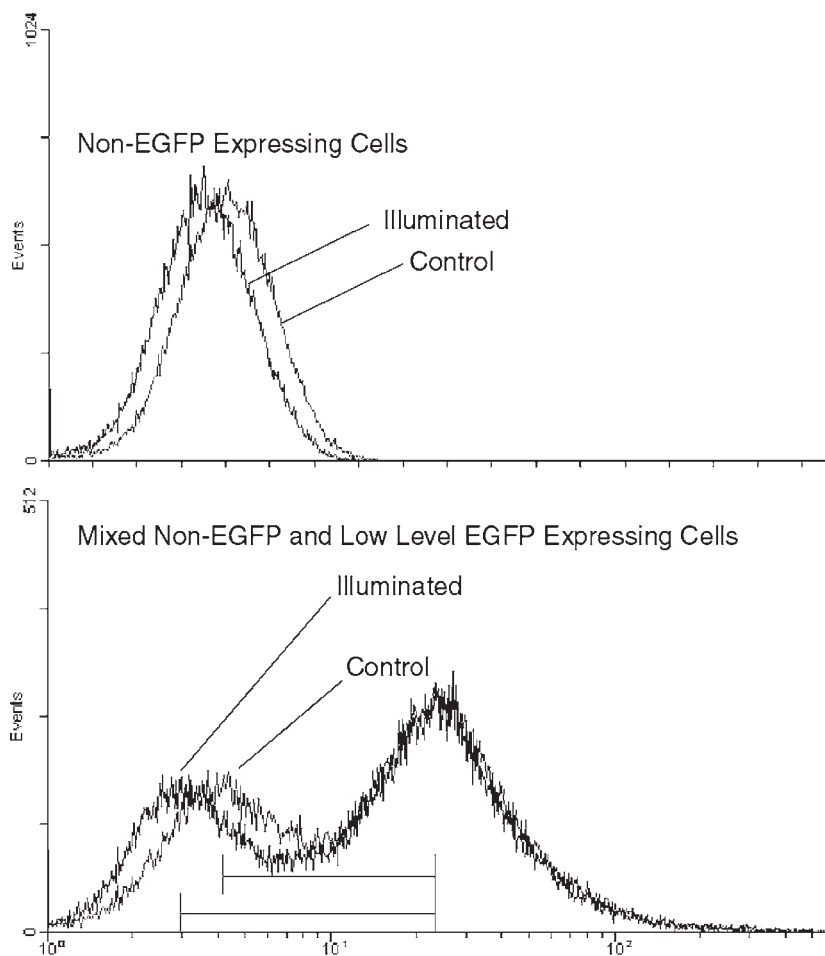


Fig. 13. Effect of broad-spectrum illumination on autofluorescence and EGFP-dependent fluorescence. The **upper** panel shows the effect of illumination on a population of control cells that do not express EGFP. All of the cells shift downwards in their fluorescence values. The **lower** panel shows the effect of illumination on a mixed population of cells consisting of those that do not express EGFP and those that express low levels of EGFP. In this case only the nonexpressing cells show a downward shift in their fluorescence values. The consequence of this shift is a greater separation between cells with EGFP-dependent fluorescence and those without, as indicated by the bars.

1. To apply this observation to FACS, cells are exposed immediately prior to FACS to a light source that preferentially quenches autofluorescence over fluorescence from the fluorescent protein reporter. This is accomplished by placing a high-intensity fiber optic incandescent light source in the fluidics stream of the FACS.

2. The effect of this technique on autofluorescence vs fluorescence from EGFP is shown in **Fig. 13** where two populations of cells were analyzed by FACS. One does not carry a fluorescent reporter protein (upper panel) and the other (lower panel) is a mixture of low-level EGFP expressing cells, resulting from gene trapping, which includes a subpopulation that does not express the reporter. In each case cells were assessed without light exposure and with light exposure, and histograms representing the distribution of fluorescence are overlaid.
3. In the case of cells that do not carry the fluorescent protein reporter (upper panel), the entire population of cells is shifted to a lower level of fluorescence, demonstrating a decrease in cellular autofluorescence. In contrast, in the population of cells containing both cells exhibiting low-level fluorescence from the fluorescent protein and non-expressing cells (lower panel), only the nonexpressing cells show a downward shift in fluorescence. Hence, use of this process effectively extends the lower limit over which the fluorescent reporter protein can be detected.

4. Notes

1. Fixation does not compromise detection of the fluorescent proteins inside the cells although autofluorescence will increase with time after fixation.
2. The preceding chapter by Hawley et al. provides additional protocols for detection and analysis of multiple fluorescent proteins.
3. 405 or 407 nm gives approx 60% of maximum excitation, 413 nm or 458 nm gives approx 70%.

Acknowledgments

The authors are grateful to Ed Podniesinski, David Sheedy, and Amy Bussman for excellent technical assistance. This work was supported by grants from the NIH (HD36416, DA14773, AG020946, and AG019863) and the Roswell Park Alliance. In addition, the Flow Cytometry core facility was supported in part by CCGS Grant CA16056 from the NCI.

References

1. Beavis, A. J. and Kalejta, R. F. (1999) Simultaneous analysis of the cyan, yellow and green fluorescent proteins by flow cytometry using single-laser excitation at 458 nm. *Cytometry* **37**, 68–73.
2. Lybarger, L., Dempsey, D., Patterson, G. H., Piston, D. W., Kain, S. R., and Chervenak, R. (1998) Dual-color flow cytometric detection of fluorescent proteins using single-laser (488-nm) excitation. *Cytometry* **31**, 147–152.
3. Zhu, J., Musco, M. L., and Grace, M. J. (1999) Three-color flow cytometry analysis of tricistronic expression of eBFP, eGFP and eYFP using EMCV-IRES linkages. *Cytometry* **37**, 51–59.
4. Hawley, T. S., Telford, W. G., Ramezani, A., and Hawley, R. G. (2001) Four-color flow cytometric detection of retrovirally expressed red, yellow, green and cyan fluorescent proteins. *Biotechniques* **30**, 1028–1033.

5. Medico, E., Gambarotta, G., Gentile, A., Comoglio, P. M., and Soriano, P. (2001) A gene trap vector system for identifying transcriptionally responsive genes. *Nat. Biotechnol.* **19**, 579–582.
6. Clontech Laboratories. (1999) Features of Living Colors™ vectors *CLONTECHniques*, <http://www.clontech.com/gfp/GFPTable.shtml>.
7. Clontech Laboratories. (2001) Living Colors™ DsRed2 red fluorescent protein. *CLONTECHniques*, http://www.clontech.com/archive/JUL01UPD/pdf/LC_DsRed2.pdf.
8. Clontech Laboratories. (2002) BD Living Colors™ HcRed red fluorescent protein. *CLONTECHniques*, <http://www.clontech.com/archive/APR02UPD/pdf/HcRed.pdf>.
9. Sambrook, J., Fritsch, E. F., and Maniatis, T. (1989) *Molecular Cloning: A Laboratory Manual*, 2nd edit. Cold Spring Harbor Laboratory Press, Cold Spring Harbor, NY.
10. Baird, G. S., Zacharias, D. A., and Tsien, R. Y. (2000) Biochemistry, mutagenesis, and oligomerization of DsRed, a red fluorescent protein from coral. *Proc. Natl. Acad. Sci. USA* **97**, 11984–11989.
11. Zolotukhin, S., Potter, M., Hauswirth, W. W., Guy, J., and Muzyczka, N. (1996) A “humanized” green fluorescent protein cDNA adapted for high-level expression in mammalian cells. *J. Virol.* **70**, 4646–4654.
12. Stewart, C. C. and Stewart, S. J. (2003) A Software Method For Color Compensation, in *Current Protocols in Cytometry* (Robinson, J. P., Darzynkiewicz, Z., Dean, P., eds.), John Wiley & Sons, New York, pp. 10.15.1–10.15.12.

Integrative Flow Cytometric and Microarray Approaches for Use in Transcriptional Profiling

David W. Galbraith, Rangasamy Elumalai, and Fang Cheng Gong

Summary

Flow cytometry and cell sorting provides unparalleled means for the identification and purification of specific cell types. It is a mature technology having been in existence commercially for the last 25 yr. High-throughput transcriptional profiling methods have emerged relatively recently. These provide the means to characterize efficiently the genome-wide contribution of individual genes to gene expression. A combination of these methods offers the opportunity to explore the relationship between gene expression and the ways in which different cell types are formed and maintained. This chapter provides a review of published methods for analysis of global gene expression within different cell types in complex tissues and organs, and provides practical details concerning microarray fabrication and use based on presynthesized 70-mer oligonucleotide array elements.

Key Words:

Cell sorting, functional genomics, gene expression, green fluorescent protein, microarrays.

1. Introduction

1.1. Integrating Flow Cytometric and Global Gene Expression Technologies

The twin technologies of flow cytometry and global gene expression share common features. Both technologies involve complex and sophisticated instrumentation. Both provide means for the analysis of cells that are unique, and that cannot be easily achieved. Both require extensive data analysis and archiving capabilities. However, they also differ in a specific and important conceptual way: flow cytometry (and the kindred technology of cell sorting) provides a means to reduce the complexity of mixtures of cells, which are analyzed based on their optical properties, and then sorting into homogeneous populations for

From: *Methods in Molecular Biology: Flow Cytometry Protocols*, 2nd ed.
Edited by: T. S. Hawley and R. G. Hawley © Humana Press Inc., Totowa, NJ

further studies. Methods of global gene expression, on the other hand, provide information about all genes within a specific biological sample, and therefore provide a harvest of information that is by its very nature complex, and which therefore has to be simplified by *post hoc* data reduction methods.

Combined, the potential power of these technologies is particularly attractive. In principle, it should be possible to determine the global gene expression patterns within any particular cell type, assuming specific methods of marking can be devised for the different cell types that are compatible with flow sorting, the tissues can be dissociated, and sufficient cells sorted for subsequent global analysis of gene expression. Below we consider these three topics by reference to published work. We then go on to outline a specific method of functional genomics, long oligonucleotide-based microarrays, for characterization of global gene expression patterns.

1.2. Applying Flow Cytometry and Cell Sorting to Complex Tissues

Flow sorting of living cells was originally popularized by the pioneering work of Herzenberg (1), which recognized the value of combining fluorescence labeling, antibodies recognizing cell surface epitopes, and the ability of flow sorters to examine the optical properties of single-cell populations and individually sort subsets of these based on these properties. Flow sorting techniques are ideally suited to the cells comprising the hematopoietic system, as they comprise natural cell suspensions. As many as 13 different parameters can now be employed for discrimination and analysis of specific cellular subtypes (2). By way of contrast, most cells of multicellular eukaryotic species are found in the form of tissues and organs, within which individual cells are structurally and functionally interconnected. Therefore to apply flow sorting techniques to cells within these tissues it is first necessary to dissociate these tissues to release the individual cells. For animal cells, this is done primarily using hydrolytic enzymes to dissolve protein and glycoprotein connections between cells. A recent example (3) shows how pancreatic islets of Langerhans can be isolated from mice, and converted into single-cell suspensions. This requires *in vivo* inflation of the pancreas via the pancreatic duct with collagenase solution, followed by surgical removal, incubation at 37°C, and vigorous shaking to disrupt the tissue. Differential gradient centrifugation is then used to separate islets from acinar tissue. Single-cell suspensions are prepared from isolated islets by a second period of incubation using trypsin. The resulting single-cell suspensions are washed, resuspended in buffer, and filtered through a 70- μ m mesh, prior to use (3). For plants, the approach is conceptually similar, dissolution of the cell wall requiring use of cellulases, hemicellulases, and pectinases (4), but the period of incubation is typically longer (3 h to overnight). An important difference is the requirement for an osmoticum, which serves to sta-

bilize the plant plasma membrane under slightly hypertonic conditions. Modification of intercellular connections is known to affect cellular physiology, as is, for plants, the incubation of tissues in hypertonic media. Caution must therefore be observed in recording gene expression data from the resultant single-cell suspensions, in that these data may be modified by the imposition of the procedures required for preparation of single cells.

1.3. Specifying Different Cell Types Within Complex Mixtures

A prerequisite to the use of flow sorting for purification of specific cell types is a method to tag these cells that provides a suitable fluorescent signal. As mentioned previously, this can be achieved using antibodies recognizing cell surface antigens, which are then in turn either directly or indirectly labeled with fluorescence. Of increasing popularity is the use of fluorescent expression tags, proteins whose biosynthesis *in vivo* leads to the production of a recognizable fluorescent signals. The green fluorescent protein (GFP) of *Aequorea victoria* is the founder member of this functional class of protein (5), which now includes a variety of different proteins isolated from marine organisms as well as a large number of sequence variants of GFP (6).

A feature of the fluorescent proteins (FPs) is that formation of the fluorescent chromophore does not require specific enzymes, cofactors, or prosthetic groups, but occurs via an intramolecular reaction between the side chains of specific amino acids. A large number of different FPs are now available that have been optimized in various ways, to improve protein yield and folding rates, to minimize aggregation and toxicity, and to provide a palette of different colors that can be employed for simultaneous flow analysis and sorting of different cell populations. Recent developments include destabilized FPs, which provide more precise temporal resolution concerning transcriptional activation and repression than do the nonmodified forms of the FPs, which are rather stable (for a recent review, *see* ref. 7).

In general, FP expression appears to be nontoxic within the recipient organism. Reports exist of an increasing number of species that transgenically express GFP without displaying obvious problems. It should be noted that overexpression of any protein can have adverse effects on cellular metabolism, and the use of highly sensitive methods for phenotypic analysis (e.g., microarrays) might uncover GFP-specific effects. FPs are highly amenable to subcellular targeting, via translational fusions to the N- and C-termini, and targeting to defined subcellular locations has been proposed as a means to reduce toxicity (8). Targeting to large subcellular organelles, for example, the nucleus (9–12), provides increased detection sensitivity (signal-to-noise ratio) when using image cytometry and microscopy, as background autofluorescence tends to be dispersed throughout the cytoplasm. This advantage in sensitivity evidently

does not generally translate to flow cytometry since the fluorescence of the entire cell is quantified. However, we have proposed (13) the analysis of gene expression within specific cell types by examining the RNA complements of nuclei labeled by nuclear targeting of FPs. FP-tagged nuclei can be recognized by flow cytometry (12) and transcripts can be extracted from sorted nuclei (14).

For use in flow cytometry and sorting, consideration must be made of the type of light sources that are available, including spectral quality and quantity. Most forms of green fluorescent protein (GFP) and yellow fluorescent protein (YFP) are efficiently excited at 488 nm, the workhorse wavelength for flow cytometry, and *Discosoma* coral red fluorescent protein (DsRed) and other red FPs can be excited using the krypton laser line at 568 nm. Cyan fluorescent protein (CFP) excitation is optimal at approx 425 nm, but it can be excited at 457 nm (using a tunable argon laser), or 407/413 nm (using a krypton laser), or at 405 nm using the new solid-state laser diodes. Blue fluorescent protein (BFP) and its derivatives have not been routinely employed as fluorescent reporters, owing to their low brightness.

Hawley et al. (15) have described vectors and infection protocols appropriate for mammalian cell cultures, and in further work (16) illustrate the use of flow cytometry for four-color discrimination of mixed cell populations expressing CFP, GFP, YFP, and DsRed. In this work, FP expression was achieved using a retroviral transduction vector within which was engineered the FP coding sequence under the control of the long terminal repeat (LTR) promoter, and a selectable marker under the control of an internal ribosome entry site (IRES). Recombinant retroviral vector particles were produced by GP+E-86 ecotropic helper-free packaging cells, and stable cell lines were generated expressing the individual FPs.

Hara et al. (3) employed standard transgenic strategies to produce mouse lines expressing GFP under the regulatory control of the mouse insulin I promoter. The pancreatic beta cells of these transgenic mice are highly fluorescent. Isolated pancreatic cells can also be infected with recombinant adenovirus leading to GFP expression within beta cells (17). In this case, the dissociated cells are cultured for 2 d following viral infection to allow GFP expression, and are treated after harvesting with trypsin-EDTA to obtain a single-cell suspension.

Similar strategies have been employed for infection of dissociated cells leading to expression of FPs in a cell type-specific manner. For example, Keyoung et al. (18) infected dissociated fetal human brain cells with adenoviruses containing recombinant genomes in which GFP was regulated by promoter/enhancer sequences from the nestin and muhashi1 genes. Expression of these genes, and of GFP under the control of these different promoter/enhancer sequences, defines overlapping domains within the developing ventricular zone of the fetal brain.

As an alternative to viral infection, DNA transfection can also be employed for identification of specific cell types. Roy et al. (19) describe liposome-mediated transfection of dissociated white matter cells using a construction in which GFP expression was regulated by the early (P2) promoter of the 2',3'-cyclic nucleotide 3'-phosphodiesterase gene. One potential disadvantage of this approach is that a rather prolonged period of culture is required after transfection (6–7 d) for observation of the greatest number and proportion of GFP-expressing cells.

For higher plants, a number of methods are available for defining cell types within complex mixtures. Mesophyll and epidermal cells within leaves can be defined based on the presence or absence of chlorophyll, and protoplasts can be isolated and sorted based on this parameter (20). Plant protoplasts can also be flow sorted based on the transgenic expression of GFP (21), as can nuclei (12). Cell type specificity of FP expression can be achieved by production of transgenic plants containing constructions in which the FP coding sequence is placed under the control of specific promoters (*see, e.g., ref. 9*). Alternatively, promoter/enhancer trap methodologies can be employed to provide transgenic plant lines within which selected subsets of cells are highlighted by FP expression (*see <http://www.arabidopsis.org/abrc/haseloff.htm> for details*). Work toward flow sorting of protoplasts and nuclei based on accumulation of FPs within specific cell types is ongoing (47; Galbraith *et al.*, *unpublished*). **Table 1** provides examples of recent publications employing combinations of FP labeling and flow cytometry for analysis and (sometimes) sorting of specific cell types from complex tissues.

1.4. Microarrays for Analysis of Gene Expression

Since their invention (28), DNA microarrays have emerged as one of the most popular platforms for the highly parallel analysis of gene expression (DNChips, formed photolithographically, and available commercially from Affymetrix, are not considered in this chapter, as methods for their use are essentially turnkey). Under most experimental circumstances, DNA microarrays are used to provide a measure of the abundances of the RNA molecules that are accumulated within the cells or tissues of interest. It should be noted, therefore, that they represent a rather particular aspect of the process of gene expression (13).

DNA microarrays are, in most cases, formed by deposition, using robotic equipment to place different DNA molecules on coated glass slides at the intersection points of arrays having microscopic spacing (~150–200 μm). The DNA array elements either comprise polymerase chain reaction (PCR) amplicons, produced in the overwhelming majority of cases from cDNA library inserts, or, increasingly, are presynthesized long (50–70 mer) oligonucleotides, designed

Table 1**Recent Examples of Methods for Tissue Dissociation and Cell Type Identification Within Complex Organs**

Organ system	Cell type	Dissociation method	Method of cell type identification	Reference
Mouse pancreas	Islet beta cells	Proteolysis/mechanical	Transgenic cell type-specific GFP labeling	3
Human brain (mature)	White matter progenitor cells	Dissection; proteolysis/mechanical	Cell type-specific GFP labeling following transfection, and antibody labeling of the A2B5 surface marker	22
Human brain (adult)	Neuronal progenitor cells	Dissection; proteolysis/mechanical	Cell type-specific GFP labeling following liposomal transfection	23
Human brain (fetal)	Neural stem cells	Dissection; proteolysis/mechanical	Cell type-specific GFP labeling following adenoviral infection	18
Human brain (mature)	Mitotic oligodendrocyte progenitor cells	Dissection; proteolysis/mechanical	Cell type-specific GFP labeling following liposomal transfection	19
Mouse brain (fetal)	Midbrain dopaminergic neurons	Dissection; proteolysis/mechanical	Transgenic cell type-specific GFP labeling	24
Mouse brain (embryonic)	Radial glial cells	Dissection; proteolysis/mechanical	Transgenic cell type-specific GFP labeling	25
Rainbow trout	Primordial germ cells	Dissection; proteolysis/mechanical	Transgenic cell type-specific GFP labeling	26
Mouse eye	Cone photoreceptors	Dissection; proteolysis/mechanical	Transgenic cell type-specific GFP labeling	27
Arabidopsis seedling	Phloem companion cells	Homogenization ^a	Transgenic cell type-specific labeling of nuclei with GFP	9
Arabidopsis aerial organs	Guard cells	Homogenization ^a	Transgenic cell type-specific labeling of nuclei with GFP	9
Arabidopsis root	Miscellaneous cell types	Protoplast preparation	Transgenic cell type-specific labeling of whole cells with GFP	47

^aHomogenization releases fluorescent nuclei which can then be sorted ([12]; Galbraith et al., unpublished).

according to sequence database information. The DNA molecules (termed “probes”) are covalently attached to the microarray surfaces either chemically or through UV crosslinking, and are then available for hybridization.

Hybridization to microarrays is done using fluorescent “targets” produced from the extracted cellular RNA most frequently by reverse transcription in the presence of fluorescent (Cy3- or Cy5-substituted) deoxyribonucleotide triphosphates. Under most circumstances, microarrays are hybridized with pairs of targets carrying complementary fluorescent labels, prepared from two different starting samples. During the process of hybridization, targets complementary to the array elements become immobilized to the slide surface. Following washing under stringent conditions, the amounts of fluorescence remaining attached to the array elements are determined using slide scanners, and the intensities are tabulated using spot-finding programs. Because as many as 30,000 different array elements can be easily printed as single microarrays, microarray hybridization enables parallel analysis of entire genomes. It should be noted in passing that the hybridization intensity value for a specific gene provides a sensitive and accurate measure of how the concentration of the cognate RNA may change as a function of the different cellular conditions under which the RNA was extracted; comparisons of RNA amount should not be made between genes, as the scaling factors linking intensity of hybridization to input RNA concentration are not generally the same.

The increasing popularity of microarrays based on long oligonucleotides over those produced from amplicons reflects their greater specificity and reproducibility. In terms of specificity, a problem of amplicon-based microarrays is the occurrence of sequence similarities between different array elements, resulting in target cross-hybridization. This is greatly diminished if array elements exhibit <70% overall sequence similarity, and lack regions of sequence identity longer than 20 bp (29). Design criteria for long oligonucleotides include these specifications, as well as specifications for a single, elevated T_m (which enables a higher degree of hybridization stringency than typically employed), the location of the oligonucleotide within 1000 bp of the 3'-end of the gene, and an absence of defined microsequence structures such as homomeric runs and stem-loops. For a minority of genes, these criteria cannot all be fulfilled, in which case one or more may be relaxed. In terms of reproducibility, it is likely that satisfying some of the aforementioned criteria is responsible for the increased reproducibility of oligo-based microarrays as compared to those made from amplicons (13). For example, competition will occur between target and the complementary ds DNA probe molecules during hybridization of amplicon-based microarrays, which will not be seen for oligo-based arrays. It appears likely that this might generate a series of local minima in the hybridization

free-energy landscape, which could result in unpredictable hybridization behavior for the different probe–target pairs.

A complete description of methods for the production of oligonucleotide-based microarrays and their hybridization using fluorescent targets is provided in this chapter.

1.5. RNA Amplification Methods for Use With Microarrays

Despite the fact that modern flow sorters can usefully operate at rates of approx 40,000 cells/s, the numbers of specific cells that can be recovered are restricted by the proportion of the cells within the target tissue, the degree of enrichment/purification specified for the sort operation, and the size of the cells. Cell sizes govern the sizes of flow tips that are required for sorting; for use of larger flow tips, the system pressure must be reduced, which in turn reduces the drive frequency for droplet production, and thereby reduces the upper sort rate (a complete discussion of large particle sorting can be found in **ref. 30**).

Individual eukaryotic cells contain of the order of 1–10 pg of total RNA, varying according to organism, species, tissue type, and developmental stage. Because approx 100 µg of total RNA or 2–5 µg of poly(A)⁺ RNA are generally required for microarray analyses, target amplification techniques are essential for studies integrating flow sorting with microarray analysis. For example, microarray hybridization using a single cell as the source of RNA requires amplification of the starting material by a factor of 10⁷–10⁸.

Most of the target amplification techniques are based around the work of Eberwine (**31**), which employed RNA transcription in vitro as a means to linearly increase the concentrations of RNA. RNA amplification is achieved through a series of enzymatic processing steps applied to the starting material (total RNA). The first cDNA strand is synthesized by an RNA-dependent reverse transcriptase, which initiates the reaction from a phage promoter (T7, T3, or SP6) linked oligo-dT primer binding to the poly(A)⁺ tail of mRNA. Second strand cDNA synthesis is usually performed with RNase H, *Escherichia coli* DNA polymerase I, and DNA ligase via strand replacement (**32**). The cDNA is then blunt-ended by treatment with T4 DNA polymerase. Antisense RNA (aRNA) is synthesized and amplified from the cDNA template by the cognate RNA polymerase corresponding to the specific promoter sequence (T7, T3, or SP6) that was previously incorporated into cDNA. The second round of RNA amplification is similar to the first round except for the following: (1) amplified aRNA is primed with random oligomer for the first strand synthesis of cDNA and (2) T7, T3, or SP6 promoter-linked oligonucleotide-dT primer is used for the second strand synthesis.

The optimized Eberwine RNA amplification method is capable of amplifying mRNA up to approx 10³-fold for one round of amplification, and up to approx 10⁵-fold for two rounds (**33–35**). Therefore two rounds of Eberwine

RNA amplification requires at least 10 ng of input total RNA for successful microarray hybridization (36). However, such a low amount of starting material comes with a price, in that the percentage of gene calls in the same sample drops by 15–20 % (from 55% to 35–40% [36]). The drop in the coverage of genome transcription (i.e., gene calls) is due partly to the loss of 5'-complexity during RNA amplification, and partly to insufficient starting materials from low-expressed genes for adequate amplification. To ensure good coverage of genome transcription, RNA amplification is routinely performed with total RNA amounts in the microgram and submicrogram range.

The major advantage of RNA amplification is attributed to its linear amplification characteristic, which should preserve even after amplification the original transcript abundances. However, the standard two rounds of RNA amplification requires long and tedious experimental manipulation, and in any case are insufficient for total RNA samples in the picogram range. One way to raise the amplification yield is to increase the number of cycles of amplification. Xiang et al. (37) reported that a linear relationship between transcript abundances was maintained after five cycles of RNA amplification. It is currently unclear as to whether the loss of 5'-complexity is a severe issue under their multiple cycles of RNA amplification. Another approach is to adapt PCR for RNA amplification. This has the potential both to achieve high yield and to simplify experimental procedures. Iscove et al. (38) have attempted to amplify mRNA exponentially from subpicogram quantities through reverse transcriptase-PCR (RT-PCR) for global gene profiling. To preserve the abundance relationships of transcripts, they limited the extent of reverse transcription to only a few hundred bases of extreme 3' sequence, so that they could be able to start PCR amplification with a more uniform individual mRNA transcripts and achieve a uniform cycle efficiency (38). Although they achieved the goal of exponential amplification as well as preservation of abundance relationship in the tested set of genes, their approach is applicable only to microarrays having probes located within a few hundred bases from 3'-end. A variety of similar attempts have been reported (39–44). Their suitability for routine microarray analyses needs to be assessed with consideration in the following areas: (1) the amplification yield, (2) the degree of fidelity afforded by the amplification procedure, (3) the degree of coverage of the microarrays (i.e., the proportion of elements providing detectable signals), and (4) the polarity of the probes (for oligonucleotide-based arrays, the sense strand of DNA is printed, in comparison to amplicon microarrays which contain ds DNA elements).

2. Materials

General information and precautions: Always wear a laboratory coat, disposable gloves, and protective eyewear. Clean the working areas with 70%

ethanol and RNaseZAP (Ambion, Inc., Austin, TX) before and after use. All chemicals are reagent grade, unless otherwise noted.

2.1. Microarray Fabrication

1. Microarray surfaces: SuperAmine SMM (TeleChem International, Inc., Sunnyvale, CA).
2. Microarray printing pins: SMP3 (TeleChem).
3. Microarray printer: An OmniGrid 100 (GeneMachines, San Carlos, CA) equipped with a Stealth print head SPH48 (TeleChem).
4. *Arabidopsis thaliana* whole genome 70-mer 5-amino modified oligonucleotides (Qiagen-Operon, Inc., Alameda, CA).
5. 384-Well plates (Genetix, New Milton, England, cat. no. X7001).

2.2. Microarray Hybridization and Analysis

1. Dynabeads® Oligo (dT)₂₅ (cat. no. 610.05) and the 1.7-mL Magnetic Particle Concentrator (MPC) (cat. no. 120.20) (both from Dynal, Oslo, Norway).
2. Nuclease-free 1.7-mL microfuge tubes (Life Science Products Inc., Denver, CO., cat. no. 7509-2002).
3. Binding buffer: 1 M LiCl, 2 mM EDTA, 20 mM Tris-HCl, pH 7.5, total volume 50 mL with RNase-free water. Store at 4°C; bring to room temperature before use. Also prepare 2X binding buffer.
4. Washing buffer: 0.15 mM LiCl, 10 mM Tris-HCl, pH 7.5, total volume 50 mL with RNase-free water. Store at 4°C; bring to room temperature before use.
5. Elution buffer: 10 mM Tris-HCl, pH 7.5, total volume 15 mL with RNase-free water. Store at 4°C; place on ice before use.
6. Reconditioning buffer: 0.1 M NaOH.
7. Storage buffer: 250 mM Tris-HCl, pH 7.5, 20 mM EDTA, 0.1% Tween-20, and 0.02% sodium azide.
8. Liquid block (Amersham Biosciences, Piscataway, NJ, cat. no. RPN3601).
9. Cy3- and Cy5-dUTP (Amersham Biosciences, cat. no. PA53022 and PA55022).
10. PowerScript reverse transcriptase (BD Biosciences Clontech, Palo Alto, CA, cat. no. 8460-1, 8460-2).
11. Trizol (Invitrogen, Carlsbad, CA, cat. no. 15596-026).
12. RNase inhibitor (Invitrogen, cat. no. 15518-0120).
13. Microcon columns (Millipore, Billerica, MA, cat. no. YM30).
14. Primers: Random 15-mer primer (Qiagen-Operon, cat. nos. SP180-1, SP180-2); random hexamer primer (Invitrogen, cat. no. 48190-011).
15. Coverslips: Hybri-Slips, 24 × 60 mm (Sigma, St. Louis, MO, cat. no. H-0784).

3. Methods

3.1. Printing of *Arabidopsis thaliana* Oligonucleotide Microarrays

3.1.1. Preparing Oligonucleotides for Printing

1. Add 15 µL of sterile distilled water (dH₂O) to each of the wells of the 384-well microplates containing 600 pmol of the oligonucleotides.

2. Centrifuge the plates briefly at 200g (1000 rpm, using a SH 3000 rotor) in a Sorvall 5B centrifuge (Kendro Laboratory Products, Asheville, NC) equipped with 384-well plate holders.
3. Transfer onto an orbital shaker (e.g., Belly Dancer from Stovall Life Science, Greensboro, NC) for 1 h at room temperature.
4. Using a 12-channel pipet, mix the solutions in the wells by resuspension several times, and transfer 7.5 μL to a new 384-well microplate.
5. Dry the plate at 50°C in a SpeedVac (Savant Instruments, Holbrook, NY).
6. Store one set of plates at -20°C. Use the first set for printing (approx 750 microarrays can be printed from the 300-pmol aliquot), then switch to the second set.

3.1.2. Rehydration and Printing of the Oligonucleotide Microarrays

(see **Note 1**)

1. Add 8 μL of 3X saline sodium citrate (SSC) to each well.
2. Transfer onto the orbital shaker for 1 h at room temperature. The oligonucleotides are now ready for printing.
3. The Arabidopsis oligonucleotide microarrays are printed on aminosilane-coated "SuperAmine" slides (TeleChem), using TeleChem type SMP3 printing pins.
4. The microarrays are printed in runs of 100 as single element arrays (no replicate spots), at 160 μm center-to-center spacing, using 48 pins in the print head, 31% relative humidity, with redipping after every 50 slides. The print head velocity is set to a maximum of 10 mm/s.
5. Bake slides for 1 h at 80°C. Store dry in darkness at room temperature.
6. After printing, dry the plates using the SpeedVac. For subsequent printing runs, we resuspend in $10 - (N/2)$ μL of deionized water (dH_2O), where N is the number of the print run.

3.1.3. Immobilization of the Oligonucleotide Array Elements (see **Note 2**)

1. Rehydrate the microarray slide over 50°C water for 5–10 s; immediately snap-dry on a 65°C heating block for 5 s. Repeat this step three or four times.
2. UV crosslink the slides by exposing them DNA-side-up to 65 mJ/cm^2 in a UV crosslinker (e.g. Stratalinker from Stratagene, La Jolla, CA). Crosslinking can be done using up to 130 mJ/cm^2 .
3. Wash the slides in 1% sodium dodecyl sulfate (SDS) for 5 min at room temperature.
4. Remove the SDS by dipping microarrays in 100% ethanol for 30 s, with gentle shaking.
5. Spin-dry the slides in the Sorvall centrifuge at 200g (1000 rpm, using the SH 3000 rotor) for 2 min.
6. Store the slides in a lightproof box under dry conditions at room temperature.

3.2. Hybridization of Arabidopsis thaliana Oligonucleotide Microarrays

3.2.1. Preparation of RNA (see **Note 3**)

Total or poly (A)⁺ RNA should be prepared as appropriate for the experimental organism and tissue. For *Arabidopsis thaliana*, our procedures involve

the most basic and simple method of RNA isolation using Trizol, followed by isolation of poly(A)⁺ RNA using magnetic beads. The Trizol reagent was developed from the single-step RNA isolation method described by Chomczynski and Sacchi (45). Trizol is a monophasic mixture of phenol and guanidine isothiocyanate, which during sample homogenization, maintains RNA integrity while solubilizing and precipitating other cellular components. In this method, Trizol is added to plant materials pulverized by grinding in liquid nitrogen. For smaller samples, homogenization can be done using a glass-in-glass homogenizer. Phase separation is induced by addition of chloroform, and the aqueous phase, containing the RNA, DNA, and polysaccharides, is recovered. The nucleic acids (and the polysaccharides) are then precipitated using isopropanol.

3.2.1.1. PREPARATION OF TOTAL RNA

1. Put gloves on! RNA is exceptionally labile, and contamination by ubiquitous RNases can occur easily. All aqueous solutions should be made using diethyl pyrocarbonate (DEPC)-treated deionized (di) water. Glassware should be autoclaved.
2. Chill mortar, containing pestle, by addition of approx 100 mL of liquid nitrogen. Add 200 mg of tissue after nitrogen has evaporated to one-half its original volume.
3. Grind the tissue with the pestle quickly, but carefully to avoid loss of sample. When liquid nitrogen has completely evaporated, increase the grinding speed to generate a fine talc-like powder.
4. Add 1 mL of Trizol per 100 mg of tissue and continue to mix using the pestle. If the liquid mixture freezes, wait to allow it to thaw slightly, and then continue.
5. When mixed thoroughly, allow slurry to liquefy (cover the mortar with foil while waiting), and transfer this in 1-mL aliquots to RNase-free 1.5-mL tubes using an Eppendorf pipet.
6. Incubate for 5 min at room temperature.
7. Add 0.2 mL of chloroform per 1-mL volume of Trizol, and vortex-mix for 15 s.
8. Incubate for 1 min at room temperature.
9. Centrifuge at 15,300g for 10 min at 4°C.
10. Transfer the (upper) aqueous phase to fresh RNase-free tubes and transfer immediately onto ice. During this transfer step, remove the aqueous phase by pipetting from the very top and side of tube, leaving a good buffer zone above the lower (organic) layer.
11. Precipitate by adding an equal volume of isopropanol. Mix by inverting tubes twice, and incubate for 15–30 min on ice.
12. Centrifuge at 15,000g for 10 min at 4°C. A small white pellet should be visible (this depends on the amounts of starting material, but for the 200 mg of tissue that we are using, the pellet should be obvious). Occasionally, the pellet may appear purple or brown depending on the type of starting tissues used or the conditions under which the plants are grown.

13. Discard supernatant by decanting. Centrifuge briefly (1 min) in the microfuge, and remove remaining supernatant using a 200- μ L Eppendorf pipet.
14. Wash pellet by addition of 1.0 mL of 75% ethanol made using RNase-free (DEPC-treated) water; be careful, as the pellet may be loose. Remove most of the ethanol using a pipettor.
15. Air-dry the pellet for 5 min at room temperature by inverting the tube onto a Kimwipe. (**Do not** let it dry for longer, as the pellet will become very difficult to resuspend.)
16. Add 25 μ L of RNase-free water. Resuspend by pipetting using a 200- μ L Eppendorf pipet (disrupting the pellet assists it to dissolve). Incubate on ice for at least 1 h with occasional resuspension using the pipettor. For quick RNA quality check, use a 1% agarose gel prepared in TBE (Tris–borate–EDTA) buffer (*see* **ref. 46** for details of this routine procedure).
17. Centrifuge the solubilized RNA at 20,000g for 15 min at 4°C.
18. Transfer supernatant to a fresh RNase-free tube. Note that you do not always get a clear distinction between the supernatant and the unwanted debris layer underneath. To avoid transferring debris, pipet slowly from the surface of the supernatant.
19. (Optional) Repeated precipitation is needed only for “difficult” tissues (for maize endosperm, precipitation is done three times; for root tissues, it is repeated once). Repeat precipitation by addition of a 10% volume 3 *M* sodium acetate and an equal volume of 100% isopropanol. Precipitate on ice for 1 h (or overnight at –80°C).
20. Centrifuge at 20,000g for 20 min at 4°C.
21. Dissolve in 25 μ L of RNase-free water for 1 h on ice, with resuspension.
22. Centrifuge at 20,000g for 20 min at 4°C.
23. Measure RNA concentration spectrophotometrically. Repeat isopropanol precipitation if concentration is <100 ng/ μ L.
24. Check RNA integrity by electrophoresis on a 1% agarose gel in 1X TBE.
25. Store remaining RNA at –80°C.

3.2.1.2. PREPARATION OF POLY (A)⁺ RNA FROM TOTAL RNA USING DYNABEADS[®]

1. Resuspend Dynabeads uniformly (they have a brown color) by shaking, and transfer 200 μ L (two times the volume of total RNA) of the suspension into a nuclease-free 1.7-mL tube.
2. Place the tube in the Dynal MPC magnet for 1 min. Check for clear separation of the beads and the solution, and remove the storage buffer from the tube by pipetting without disturbing the pellet.
3. Remove the tube from the MPC, and resuspend the beads in 200 μ L of binding buffer. Mix by pipetting.
4. Repeat wash **steps 2 and 3**. The Dynabeads are now ready for use.
5. Transfer 75 μ g total RNA to a nuclease-free 1.7-mL tube, bring to 100 μ L with DEPC-treated sterile water, and add 100 μ L of 2X binding buffer.
6. Incubate the RNA at 65°C for 2 min, then add to the binding buffer/Dynabead suspension.

7. Mix well by pipetting and anneal by gently inverting vial for 3–5 min at room temperature.
8. Place tube in the MPC for 30 s or until the suspension clears, then remove the supernatant using an Eppendorf pipet.
9. Remove the tube from the MPC, and wash the beads twice with 200 μ L of washing buffer using the MPC each time to concentrate the beads prior to removing the supernatant.
10. Elute mRNA from the Dynabeads by addition of 10 μ L of elution buffer and incubation at 80°C for 2 min. Immediately place tube in MPC and quickly transfer the supernatant to a sterile 1.5-mL tube without disturbing the pellet. If the eluted mRNA is not to be used immediately, store at –70°C.
11. Quantify RNA amounts spectrophotometrically at 260/280 nm using TE (Tris–EDTA) pH 8.0 as a buffer. An A_{260}/A_{280} ratio of 1.8–2.0 indicates a pure preparation of poly(A)⁺ RNA. The poly(A)⁺ yield should be approx 2–3% of the total RNA.
12. Dynabeads can be reused up to four times. Regenerate Dynabeads by adding 150 μ L of reconditioning buffer. Mix thoroughly with a pipet.
13. Incubate tube at 65°C for 2 min.
14. Transfer tube to the MPC, and remove liquid when clear.
15. Remove tube from the MPC, and add 200 μ L of reconditioning buffer. Mix thoroughly with pipet.
16. Replace tube in the MPC and completely remove all liquid.
17. Remove tube and add 200 μ L of storage buffer.
18. Replace tube in the MPC, and remove buffer when clear.
19. The Dynabeads are now ready for further use, starting at **step 5**.

3.2.2. Labeling the RNA for Oligonucleotide Microarray Hybridization

Target labeling is conventionally done in a single-step process by direct incorporation of Cy3- and Cy5-substituted deoxyribonucleotides using reverse transcriptase (RT). These reagents are expensive, and alternatives include the two-step approach of RT-based incorporation of aminoallyl-dNTPs followed by direct labeling of the terminal amino groups using reactive fluorochromes. The advantages of this second approach include: (1) the fluorochromes are considerably cheaper than the fluor-substituted dNTPs; (2) a wide variety of fluorochromes are available, allowing flexible selection of different combinations of fluor (including >2 fluor experiments); (3) historically, aminoallyl-dNTPs were found to be incorporated more readily than fluor-substituted dNTPs; and (4) dye-specific incorporation artifacts were eliminated. The primary disadvantage of the two-step approach is that it is less convenient than the single-step approach. Further, engineered improvements in RT performance have largely eliminated problems of incorporation and dye-bias.

3.2.2.1. PRODUCTION OF FLUORESCENT TARGETS FROM TOTAL RNA

1. Label two 0.5-mL tubes "Cy3" and "Cy5," respectively. Cover tubes with foil to protect them from light (dyes are light sensitive). Each hybridization is done using a pair of Cy3- and Cy5-labeled RNA targets, which are separately prepared, then mixed prior to hybridization. Keep RNA on ice at all times, unless otherwise indicated.
2. In each of the two 0.5-mL tubes, mix the following: 20–50 μg total RNA up to 20.0 μL , 2.0 μL dNTP (10 mM dATP, dCTP, dGTP, 2 mM dTTP), 2.0 μL Cy3- or Cy5-dUTP (1 mM), and 2.0 μL oligo-dT primer (0.5 $\mu\text{g}/\mu\text{L}$).
3. Incubate the mix in a 65°C water bath for 5 min.
4. To the heated mixture, add: 8.0 μL 5X first strand buffer, 4.0 μL 0.1 M DTT, 1.0 μL RNase inhibitor (10 U/ μL), and 1.0 μL PowerScript RT, to make 40.0 μL .
5. Incubate the tubes at 42°C for 2 h. This can be conveniently done by programming a PCR machine.
6. Add 5 μL of 0.5 M EDTA and 5 μL of 1 N NaOH. Incubate at 65°C for 10 min.
7. Add 25 μL of 1 M Tris-HCl, pH 8.0, and 100 μL of TE. Store on ice, or freeze in –20°C freezer overnight, until ready to purify. Be sure tubes are completely wrapped in foil.

3.2.2.2. PRODUCTION OF FLUORESCENT TARGETS FROM POLY(A)⁺ RNA

1. Label two 0.5-mL tubes "Cy3" and "Cy5" respectively. Cover tubes with foil to protect from light (dyes are light sensitive). Each hybridization is done using a pair of Cy3- and Cy5-labeled RNA targets, which are separately prepared, then mixed prior to hybridization. Keep RNA on ice at all times, unless otherwise indicated.
2. In each of the two 0.5-mL tubes, mix the following: 1–2 μg poly(A)⁺ RNA up to 20.0 μL , 2.0 μL dNTP (10 mM dATP, dCTP, dGTP, 2 mM dTTP), 2.0 μL 1 mM Cy3- or Cy5-dUTP, 1.0 μL 3 $\mu\text{g}/\mu\text{L}$ random hexamer primer.
3. Incubate the mix in a 65°C water bath for 5 min. Chill on ice for 5 min.
4. To the heated mixture, add: 8.0 μL 5X First strand buffer, 4.0 μL 0.1 M DTT, 1.0 μL 10 U/ μL RNase inhibitor, and 2.0 μL PowerScript RT to make 40.0 μL .
5. Incubate the tubes at room temperature for 20 min, then at 42°C for 2 h (use a PCR machine for this purpose).
6. Add 5 μL of 0.5 M EDTA and 5 μL of 1 N NaOH. Incubate in a 65°C water bath for 10 min.
7. Add 25 μL of 1 M Tris-HCl, pH 8.0, and 100 μL of TE. Store on ice, or freeze in –20°C freezer overnight, until ready to purify. Be sure tubes are completely wrapped in foil.

3.2.3. Target Purification (see **Note 4**)

Target purification is done based on size exclusion, using nitrocellulose filters contained in the Microcon YM30 columns. These filters retain single-

stranded DNA molecules that are larger than 55 bp and other molecules of mol wt > 30,000.

1. Write labels on both the column and tube pair corresponding to each labeled target that will be purified.
2. Using a 200- μ L Eppendorf pipet, transfer the labeled targets to the centrifuge column without touching the membrane.
3. Centrifuge at 11,700g for 15 min at 15°C (make sure no liquid is left in the column).
4. Add 100 μ L of TE to each column. Mix the solution by pipetting a few times, being careful not to damage the membrane. Save the column output solution, in case the membrane breaks.
5. Centrifuge the columns at 11,700g for 15 min at 15°C.
6. Repeat TE wash (**steps 4–6**) a total of four times.
7. After the fourth wash and final centrifugation add 40 μ L of TE to the column. Mix carefully with an Eppendorf pipet.
8. Leave for 2 min at room temperature.
9. Turn the column upside down into a fresh centrifuge tube. Centrifuge at 11,700g for 1 min at 15°C.
10. Use the labeled target immediately for hybridization, or store it at –20°C freezer covered with aluminum foil.

3.2.4. Microarray Hybridization

Hybridization is done with pairs of Cy3- and Cy5-labeled targets.

1. Mix the following reagents in a microfuge tube: 25.0 μ L 20X SSC, 16.0 μ L Liquid block, 10.0 μ L 2% SDS, X μ L Labeled targets, and diH₂O to 250 μ L.
2. Denature the labeled targets by placing the microfuge tube over boiling water for 2 min. Transfer the tube rapidly to ice.
3. Place the microarray slide (DNA-side-up) on a 65°C heating block, apply the labeled target, and cover it with the plastic 24 \times 60 mm Hybri-Slip, avoiding trapping any air bubbles. A raised coverslip configuration is recommended (*see* <http://ag.arizona.edu/microarray/Troubleshooting1.html> for details).
4. Incubate the slide at 65°C for 8–12 h within a humidity chamber. A simple humidity chamber can be constructed using disposable Petri dishes as described below:
 - a. Place the lower half of a square 100 \times 15 mm Petri dish (VWR International, Tempe, AZ, cat. no. 25378-047) upside down within a larger round 150 \times 15 mm petri dish (VWR International, cat. no. 25384-139).
 - b. Add 5 mL of distilled water into the round Petri dish.
 - c. Place the entire setup inside a 65°C oven to equilibrate for 1–2 h.
 - d. Place the microarray slide on the top of the square Petri dish, and cover with the lid for the round Petri dish. An example of this arrangement is given at www.ag.arizona.edu/microarray.

5. Wash the slide in 2X SSC + 0.5% SDS for 5 min at 55°C, 0.5X SSC for 5 min at room temperature, and 0.05X SSC for 5 min at room temperature.
6. Spin dry the slides at 200g (1000 rpm, in the Sorvall SH 3000 rotor) in a Sorvall centrifuge. Scan the slides immediately using a microarray scanner according to the manufacturer's recommendations.

4. Notes

1. Microarray printing: Overall microarray quality is greatly influenced by the quality of the printing process. We recommend the use of TeleChem SMP3 split pins for printing. The Z-velocity of the print head should be reduced to the minimal compatible with a reasonable overall speed of printing. An excessive Z-velocity will blunt the ends of the (expensive!) pins and make them useless for printing. The washing and drying steps between each sample are particularly critical, as they are required to avoid cross-contamination between samples. After extensive testing, we recommend washing the pins a minimum of six times, with 10 s of vacuum drying between each wash. The drying time can be reduced depending on the number of pins used for printing (fewer pins require a shorter drying time). Dry pins pick up an optimum amount of sample and produce even spots through all the slides in a print. Incompletely dried pins can dilute the sample in unpredictable ways, and thereby can introduce variation in microarray quality. Humidity and temperature are likewise important parameters that can influence microarray quality. We try to limit humidity fluctuations to 30–45% relative humidity, and temperature fluctuations to 23°C ± 3°C. Higher levels of humidity can result in array element merging; lower levels result in shorter print runs due to probe evaporation from the printing pins.
2. Microarray rehydration and crosslinking: The step of microarray rehydration helps to spread the probe evenly within the printed spot. However, care must be taken not to over rehydrate the slides by leaving them within the water vapor for longer than the recommended period. This has the effect of merging adjacent spots. It is recommended that the crosslinker be routinely checked for correct function and energy output levels, as this step is absolutely essential.
3. RNA isolation: We have found the described methods work very well for many different tissue types. They are also very flexible, in that they can be readily modified to accommodate the differing requirements of specific tissues. For example, if you are working with tissues that contain large quantities of starch or other polysaccharides, such as maize endosperm or root tips, the protocol should be modified to eliminate solubilization of polysaccharide which would interfere with target production. This can be simply achieved by dissolving the pellet containing the RNA in a larger volume than described in the protocol (increasing the resuspension volume from 0.1 to 0.5 mL), and incubating the solution on ice for a few hours. This precipitates most of the dissolved starch from the RNA solution, and the precipitate can be removed by centrifugation. If necessary this step can be

repeated once or twice more. It should be noted that total RNA can be employed for target production, although for reasons of specificity we prefer use of poly(A)⁺ RNA. If total RNA is to be used, we recommend nonphenolic methods using commercial kits (e.g., the RNeasy Plant Mini Kit from Qiagen-Operon or the RNA Extraction Kit from Amersham Biosciences), as target labeling is very sensitive to traces of contamination by phenol.

4. Target purification: Target purification is one of the most critical steps in hybridization. If you do not purify the targets sufficiently, you will end up with very high background on your slides. Unincorporated Cy dyes have a tendency to adhere to the coated slides. The high background would have adverse effects on the detection sensitivity for signals of expressed genes, mostly manifested with respect to background subtraction and the calculation of gene calls. Under the worst circumstances, high background noise results in negative hybridization images with the printed probes appearing as black holes on the slide surfaces.

Acknowledgments

This work was supported by Grants 9872657, 9813360, and 0211857 from the NSF Plant Genome program.

References

1. Loken, M. R. and Herzenberg, L. A. (1975) Analysis of cell-populations with a fluorescence-activated cell sorter. *Ann. NY Acad. Sci.* **254**, 163–171.
2. De Rosa, S. C., Herzenberg, L. A., Herzenberg, L. A., and Roederer, M. (2001) Eleven-color, thirteen-parameter flow cytometry: Identification of human naive T cells by phenotype, function, and T-cell receptor diversity. *Nat. Med.* **7**, 245–248.
3. Hara, M., Wang, X. Y., Kawamura, T., et al. (2003) Transgenic mice with green fluorescent protein-labeled pancreatic beta-cells. *Am. J. Physiol. Endocrinol. Metab.* **284**, E177–E183.
4. Galbraith, D. W., Bartos, J., and Dolezel, J. (2003) Flow cytometry and cell sorting in plant biotechnology, in *Flow Cytometry in Biotechnology* (Sklar, L., ed.), Oxford University Press, Oxford, UK.
5. Chalfie, M., Tu, Y., Euskirchen, G., Ward, W. W., and Prasher, D. C. (1994) Green fluorescent protein as a marker for gene expression. *Science* **263**, 802–805.
6. Tsien, R. (1998) The green fluorescent protein. *Annu. Rev. Biochem.* **67**, 509–544.
7. Lippincott-Schwartz, J. and Patterson, G. H. (2003) Development and use of fluorescent protein markers in living cells. *Science* **300**, 87–91.
8. Haseloff, J., Siemering, K. R., Prasher, D. C., and Hodge, S. (1997) Removal of a cryptic intron and subcellular localization of green fluorescent protein are required to mark transgenic Arabidopsis plants brightly. *Proc. Natl. Acad. Sci. USA* **94**, 2122–2127.
9. Chytilova, E., Macas, J., and Galbraith, D. W. (1999) Green fluorescent protein targeted to the nucleus, a transgenic phenotype useful for studies in plant biology. *Ann. Botany* **83**, 645–654.

10. Chytilova, E., Macas, J., Sliwinski, E., Rafelski, S., Lambert, G., and Galbraith, D. W. (2000) Nuclear dynamics in *Arabidopsis thaliana*. *Mol. Biol. Cell* **11**, 2733–2741.
11. Grebenok, R. J., Pierson, E. A., Lambert, G. M., et al. (1997) Green-fluorescent protein fusions for efficient characterization of nuclear localization signals. *Plant Journal* **11**, 573–586.
12. Grebenok, R. J., Lambert, G. M., and Galbraith, D. W. (1997) Characterization of the targeted nuclear accumulation of GFP within the cells of transgenic plants. *Plant J.* **12**, 685–696.
13. Galbraith, D. W. (2003) Global analysis of cell type-specific gene expression. *Comp. Funct. Genomics* **4**, 208–215.
14. Macas, J., Lambert, G. M., Dolezel, D., and Galbraith, D. W. (1998) NEST (Nuclear Expressed Sequence Tag) analysis: a novel means to study transcription through amplification of nuclear RNA. *Cytometry* **33**, 460–468.
15. Hawley, T. S., Telford, W. G., and Hawley, R. G. (2001) “Rainbow” reporters for multispectral marking and lineage analysis of hematopoietic stem cells. *Stem Cells* **19**, 118–124.
16. Hawley, T. S., Telford, W. G., Ramezani, A., and Hawley, R. G. (2001) Four-color flow cytometric detection of retrovirally expressed red, yellow, green and cyan fluorescent proteins. *BioTechniques* **30**, 1028–1034.
17. Meyer, K., Irminger, J.-C., Moss, L. G., et al. (1998) Sorting human β -cells consequent to targeted expression of green fluorescent protein. *Diabetes* **47**, 1974–1977.
18. Keyoung, H. M., Roy, N. S., Benraiss, A., et al. (2001) High-yield selection and extraction of two promoter-defined phenotypes of neural stem cells from the fetal human brain. *Nature Biotech.* **19**, 843–850.
19. Roy, N. S., Wang, S., Harrison-Restelli, C., et al. (1999) Identification, isolation, and promoter-defined separation of mitotic oligodendrocyte progenitor cells from the adult human subcortical white matter. *J. Neurosci.* **19**, 9986–9995.
20. Harkins, K. R., Jefferson, R. A., Kavanagh, T. A., Bevan, M. W., and Galbraith, D. W. (1990) Expression of photosynthesis-related gene fusions is restricted by cell-type in transgenic plants and in transfected protoplasts. *Proc. Natl. Acad. Sci. USA* **87**, 816–820.
21. Sheen, J., Hwang, S., Niwa, Y., Kobayashi, H., and Galbraith, D. W. (1995) Green Fluorescent Protein as a new vital marker in plant cells. *Plant J.* **8**, 777–784.
22. Nunes, M. C., Roy, N. S., Keyoung, H. M., et al. (2003) Identification and isolation of multipotential neural progenitor cells from the subcortical white matter of the adult human brain. *Nat. Med.* **9**, 439–447.
23. Roy, N. S., Wang, S., Jiang, L., et al. (2000) Promoter-selected selection and isolation of neural progenitor cells from the adult human ventricular zone. *J. Neurosci. Res.* **59**, 321–331.
24. Sawamoto, K., Nakao, N., Kobayashi, K., et al. (2001) Visualization, direct isolation, and transplantation of midbrain dopaminergic neurons. *Proc. Natl. Acad. Sci. USA* **98**, 6423–6428.

25. Malatesta, P., Hartfuss, E., and Gotz, M. (2000) Isolation of radial glial cells by fluorescent-activated cell sorting reveals a neuronal lineage. *Development* **127**, 5253–5263.
26. Takeuchi, Y., Yoshizaki, G., Kobayashi, T., and Takeuchi, T. (2002) Mass isolation of primordial germ cells from transgenic rainbow trout carrying the green fluorescent protein gene driven by the vasa gene promoter. *Biol. Reprod.* **67**, 1087–1092.
27. Fei, Y. J. and Hughes, T. E. (2001) Transgenic expression of the jellyfish green fluorescent protein in the cone photoreceptors of the mouse. *Visual Neurosci.* **18**, 615–623.
28. Schena, M., Shalon, D., Davis, R. W., and Brown, P. O. (1995) Quantitative monitoring of gene expression patterns with a complementary DNA microarray. *Science* **270**, 467–470.
29. Xu, W., Bak, S., Decker, A., Paquette, S. M., Feyereisen, R., and Galbraith D. W. (2001) Microarray-based analysis of gene expression in very large gene families: the Cytochrome P450 gene superfamily of *Arabidopsis thaliana*. *Gene* **272**, 61–74.
30. Galbraith, D. W. and Lucretti, S. (2000) Large particle sorting in *Flow Cytometry and Cell Sorting*, 2nd edit. (Radbruch, A., ed.), Springer-Verlag, Berlin, pp. 293–317.
31. Van Gelder, R. N., von Zastrow, M. E., Yool, A., Dement, W. C., Barchas, J. D., and Eberwine, J. H. (1990) Amplified RNA synthesized from limited quantities of heterogeneous cDNA. *Proc. Natl. Acad. Sci. USA* **87**, 1663–1667.
32. Gubler, U. and Hoffman, B. J. (1983) A simple and very efficient method for generating cDNA libraries. *Gene* **25**, 263–269.
33. Wang, E., Miller, L. D., Ohnmacht, G. A., Liu, E. T., and Marincola, F. M. (2000) High-fidelity mRNA amplification for gene profiling. *Nat. Biotechnol.* **18**, 457–459.
34. Baugh, L. R., Hill, A. A., Brown, E. L., and Hunter, C. P. (2001) Quantitative analysis of mRNA amplification by in vitro transcription. *Nucleic Acids Res.* **29**, E29.
35. Zhao, H., Hastie, T., Whitfield, M. L., Borresen-Dale, A. L., and Jeffrey, S. S. (2002) Optimization and evaluation of T7 based RNA linear amplification protocols for cDNA microarray analysis. *B.M.C. Genomics* **3**, 31.
36. Luzzi, V., Mahadevappa, M., Raja, R., Warrington, J. A., and Watson, M. A. (2003) Accurate and reproducible gene expression profiles from laser capture microdissection, transcript amplification, and high density oligonucleotide microarray analysis. *J. Mol. Diagn.* **5**, 9–14.
37. Xiang, C. C., Chen, M., Ma, L., et al. (2003) A new strategy to amplify degraded RNA from small tissue samples for microarray studies. *Nucleic Acids Res.* **31**, e53.
38. Iscove, N. N., Barbara, M., Gu, M., Gibson, M., Modi, C., and Winegarden, N. (2002) Representation is faithfully preserved in global cDNA amplified exponentially from sub-picogram quantities of mRNA. *Nat. Biotechnol.* **20**, 940–943.

39. Brandt, S., Kloska, S., Altmann, T., and Kehr, J. (2002) Using array hybridization to monitor gene expression at the single cell level. *J. Exp. Bot.* **53**, 2315–2323.
40. Ginsberg, S. D. and Che, S. (2002) RNA amplification in brain tissues. *Neurochem. Res.* **27**, 981–992.
41. Aoyagi, K., Tatsuta, T., Nishigaki, M., et al. (2003) A faithful method for PCR-mediated global mRNA amplification and its integration into microarray analysis on laser-captured cells. *Biochem. Biophys. Res. Commun.* **300**, 915–920.
42. Chiang, M. K. and Melton, D. A. (2003) Single-cell transcript analysis of pancreas development. *Dev. Cell* **4**, 383–393.
43. Seth, D., Gorrell, M. D., McGuinness, P. H., et al. (2003) SMART amplification maintains representation of relative gene expression: quantitative validation by real time PCR and application to studies of alcoholic liver disease in primates. *J. Biochem. Biophys. Methods* **55**, 53–66.
44. Smith, L., Underhill, P., Pritchard, C., et al. (2003) Single primer amplification (SPA) of cDNA for microarray expression analysis. *Nucleic Acids Res.* **31**, e9.
45. Chomczynski, P. and Sacchi, N. (1987) Single-step method of RNA isolation by acid guanidinium thiocyanate phenol chloroform extraction. *Anal. Biochem.* **162**, 156–159.
46. Sambrook, J. and Russel, D. W. (2001) *Molecular Cloning: A Laboratory Manual*. Cold Spring Harbor Laboratory Press, Cold Spring Harbor, NY.
47. Birnbaum, K., Shasha, D. E., Wang, J. Y., et al. (2003) A gene expression map of the *Arabidopsis* root. *Science* **302**, 1956–1960.

Flow Cytometric Analysis of Fluorescence Resonance Energy Transfer

*A Tool for High-Throughput Screening
of Molecular Interactions in Living Cells*

Francis Ka-Ming Chan and Kevin L. Holmes

Summary

The study of cellular processes has been facilitated by the use of methods to detect molecular associations both in vivo and in vitro. An invaluable tool to study molecular associations associated with dynamic processes in living cells utilizes the phenomenon of fluorescence resonance energy transfer (FRET), together with selected fluorophores that are attached to molecules of interest. Many reports have utilized fluorophores conjugated to antibodies for FRET pairs. However, these methods are restricted to extracellular molecules and dependent upon the availability of appropriate antibodies. The recent development of green fluorescent protein (GFP) variants suitable for FRET has expanded the utility of this methodology by permitting the study of intracellular as well as extracellular processes. Combining FRET with flow cytometric analysis results in a powerful high-throughput assay for molecular associations. This article details the use of green fluorescent protein (GFP) mutants cyan fluorescent protein (CFP) and yellow fluorescent protein (YFP) to measure the association of the signaling component TRAF2 with the TNFR-2 receptor to illustrate the versatility of this methodology.

Key Words

Energy transfer, flow cytometry, fluorescence resonance energy transfer, green fluorescent protein, molecular interactions, tumor necrosis factor receptor.

1. Introduction

The various biological functions of the cell are coordinated by the interaction of distinct molecular machineries. Numerous methods have been developed over the years to detect molecular associations both in vivo as well as in vitro.

From: *Methods in Molecular Biology: Flow Cytometry Protocols*, 2nd ed.
Edited by: T. S. Hawley and R. G. Hawley © Humana Press Inc., Totowa, NJ

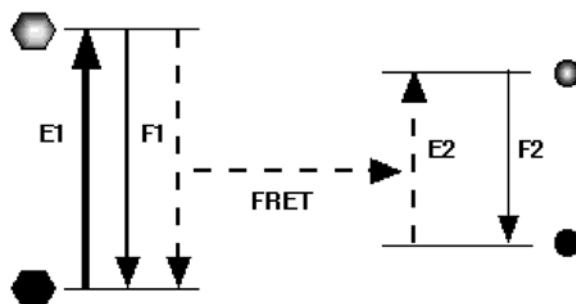


Fig. 1. Principles of FRET. The excitation of the first fluorophore (E1) results in the emission of energy (F1) at a longer wavelength as it returns to the ground state. Fluorescence emission from the first fluorophore (F1) can be “absorbed” by a nearby second fluorophore with an excitation wavelength (E2) that overlaps with the emission from the first fluorophore (F1) through dipole–dipole interactions. The net result is the transfer of energy in the form of fluorescence emission from the second fluorophore (F2 or FRET) and the “quenching” of fluorescence emission from the first fluorophore.

Many of these methods, however, do not allow the examination of dynamic processes in the living cells. The phenomenon of fluorescence resonance energy transfer (FRET) describes the transfer of energy from a fluorophore (donor) in an excited state to a neighboring fluorophore (acceptor) through dipole–dipole interaction (1,2) (**Fig. 1**). FRET can be a sensitive means to measure molecular distances within 100 Å (**Fig. 1**) (3,4). Many methods utilizing the concept of FRET have been used successfully for the measurement of biological interactions (5–8). For example, subunit associations of the interleukin-2 (IL-2) receptor and epidermal growth factor (EGF) receptor have been detected with FRET-compatible, fluorochrome-labeled antibodies using the flow cytometer (9,10). Furthermore, molecular interactions between the dimeric subunits of the transcription factor Pit-1 and the interaction between the apoptotic regulatory proteins Bcl-2 and Bax were determined using microscopic FRET measurement (11,12). These methods are superior to conventional biochemical methods in that they allow the investigators to monitor biological processes in living cells. However, their use was sometimes limited by the availability of the appropriate antibodies that allow FRET without disrupting the interaction under examination or the relatively small sample size of microscopic measurements.

Recently, several spectral variants of green fluorescent protein (GFP) (13) were developed that have compatible fluorescence excitation and emission properties for FRET analysis (**Table 1**). In particular, the excitation and emission spectra of the cyan (CFP) and yellow (YFP) versions of the GFP proteins allow them to be used in FRET analysis as donor and acceptor fluorophores,

Table 1
Spectral Properties of GFP Variants

Clone name	Mutations	Excitation peak (nm)	Emission peak (nm)
BFP (blue)	F64L, Y66H, Y145F	383	447
GFP (green)	F64L, S65T, H231L	488	507
CFP (cyan)	K26R, F64L, S65T, T66W, N146I, M153T, V163A, N164H, H231L	434 (452)	476 (505)
YFP (yellow)	S65G, S72A, T203Y, H231L	514	527

respectively. By creating fusion proteins to these GFP variants and introducing them into the appropriate cellular system, one can monitor the molecular associations of different biological machineries in living cells using flow cytometric methods. Combining FRET analysis with flow cytometry is advantageous as the investigator can screen a large number of cells within a short time. Unlike fluorescently labeled antibodies, the use of GFP fusion proteins permits the examination of extra- as well as intracellular associations. The versatility of flow cytometric FRET analysis is illustrated here using the interaction between p80 TNFR-2 and TRAF2 as an example. TRAF-2 is an important signal transduction component to many of the members of the tumor necrosis factor (TNF) receptor superfamily. On activation with TNF- α , TRAF2 is directly recruited to the preassembled TNFR-2 receptor (reviewed in **refs. 14** and **15**). This interaction will be monitored by the expression of fusion proteins of CFP and YFP to p80 TNFR-2 and TRAF2 in 293T cells.

2. Materials

1. Plasmids: pEF6-myc-HisB (Invitrogen, Carlsbad, CA), pECFP-N1, pEYFP-N1 (BD Biosciences Clontech, Palo Alto, CA).
2. cDNAs for p80 TNFR-2, TRAF2 and SODD (silencer of death domain).
3. Oligonucleotide primers for polymerase chain reaction (PCR).
4. Restriction enzymes, T4 DNA ligase.
5. QIAEX gel purification kit (Qiagen, Valencia, CA).
6. Competent *E. coli* cells for transformation (e.g., XL-1 blue from Stratagene, La Jolla, CA).
7. HEK 293T cells.
8. Complete Dulbecco's modified Eagle's medium (DMEM) (BioWhittaker, Walkersville, MD): DMEM without phenol red, 10% fetal calf serum (FCS), 100 units of penicillin and streptomycin, and 2 mM L-glutamine.

9. FuGENE 6 (Roche Applied Science, Indianapolis, IN).
10. Phosphate-buffered saline (PBS).
11. Nonidet P-40 (NP-40) lysis buffer: 10 mM Tris-HCl, pH 7.5, 150 mM NaCl, and 1% NP-40.
12. Bio-Rad protein assay reagent (Bio-Rad Laboratories, Hercules, CA).
13. 10% Bis-Tris NuPAGE protein gels (Invitrogen).
14. Rabbit polyclonal antiserum against TRAF2 (Santa Cruz Biotechnology, Santa Cruz, CA).
15. 6-mL fluorescent-activated cell sorter (FACS) tubes (Falcon brand).
16. 500 μ g/mL of propidium iodide (PI) solution.
17. FACS Vantage SE flow cytometer (BD Biosciences, San Jose, CA) (*see Subheading 3.3.3.*).
18. FlowJo analytical software (Tree Star, Inc., San Carlos, CA) or other flow cytometry analytical softwares.

3. Methods

3.1. Design of the Constructs (*see Note 1*)

The crystal structure of TRAF2 homotrimer bound to the TNFR-2 peptide reveals a “mushroomlike” conformation of TRAF2 with the C- and N-termini resembling the cap and the stalk of a mushroom, respectively (**16**). The p80 TNFR-2 polypeptide makes contact with TRAF2 at the edge of the mushroom cap. To maximize the potential for interaction and therefore FRET, CFP was cloned at the C-terminus of full-length p80 TNFR-2 and YFP was cloned at the N-terminus of the full length TRAF2 protein. The silencer of death domain (SODD) protein (**17**), which binds to only TNFR-1 but not TNFR-2, was used as a non-interacting negative control.

3.1.1. The Vectors and the Generation of the CFP and YFP Vectors (*see Note 2*)

1. Design PCR primers for CFP and YFP cDNA inserts.
2. Perform PCR using pECFP-N1 or pEYFP-N1 as templates.
3. Resolve PCR products on 1% agarose gel. Excise and purify the correct fragments using QIAEX.
4. Digest PCR fragments with:
 - a. *Bam*HI/*Eco*RV (YFP fragment)
 - b. *Eco*RV/*Xba*I (CFP and YFP fragments)
5. Digest vector pEF6-myc-HisB with:
 - a. *Bam*HI/*Eco*RV
 - b. *Eco*RV/*Xba*I
6. Ligate fragment from **step 4a** with vector from **step 5a**. Resulting plasmid is pEF6B-YFP-C. Ligate CFP or YFP fragment from **step 4b** with vector from **step 5b**. Resulting plasmids are pEF6B-CFP-N and pEF6B-YFP-N.

7. Transform into competent XL-1 blue cells.
8. Screen resulting clones for PCR inserts in minipreps.
9. Sequence miniprep DNAs to confirm sequence integrity.

3.1.2. Cloning of the cDNAs

1. PCR amplify cDNAs for p80 TNFR-2, TRAF2 and SODD.
2. Digest p80 PCR product with *Bam*HI/*Eco*RV. Digest TRAF2 and SODD PCR products with *Eco*RV/*Xba*I.
3. Digest pEF6B-YFP-C with *Eco*RV/*Xba*I. Ligate TRAF2 and SODD cDNA inserts from **step 2** to create pEF6B-YFP-TRAF2 and pEF6B-YFP-SODD.
4. Digest pEF6B-CFP-N and pEF6B-YFP-N with *Bam*HI/*Eco*RV. Ligate p80 fragment from **step 2** to create pEF6B-p80-CFP and pEF6B-p80-YFP.
5. Repeat **steps 7–9** as described in **Subheading 3.1.1**.

3.2. Examination of the Expression of the Constructs

The next step in this process involves the confirmation of protein expression from the FRET donor and acceptor plasmids. To determine the expression of the plasmids, they were introduced into the human kidney epithelial cell line HEK 293T cells.

3.2.1. Transfection in 293T Cells (see **Note 3**)

1. Seed 2.5×10^5 cells in each well of a 12-well plate in 1 mL of complete DMEM medium. Incubate at 37°C for 16–20 h.
2. Transfect 2 μ g of each plasmid into HEK 293T cells using 6 μ L of FuGENE 6 to give a DNA/FuGENE 6 ratio of 1:3.
3. Grow and incubate cells at 37°C for 24 to 48 h.
4. Harvest cells for subsequent analyses by Western blotting or flow cytometry.

3.2.2. Western Blotting Analysis

1. Aspirate medium from wells. Add 1 mL of PBS to each well. Gently resuspend cells in PBS and transfer cell suspension to microfuge tubes.
2. Centrifuge the cells for 5 min at 480g. Aspirate PBS.
3. Resuspend the cell pellet in 100 μ L of NP-40 lysis buffer and incubate for 15 min on ice.
4. Centrifuge at 17,900g at 4°C in a microfuge for 10 min.
5. Transfer the supernatant to a fresh microfuge tube. Measure lysate concentration using the Bio-Rad protein assay reagent.
6. Load 50 μ g of cell lysates on a 10% Bis-Tris NuPAGE gel and transfer onto nitrocellulose membrane.
7. Probe the membrane with antibody against TRAF2 and secondary HRP-conjugated antibody against rabbit IgG. **Figure 2** shows the expression of YFP-TRAF2 (lane 2) and untagged TRAF2 (lane 3) in HEK 293T cells (see **Note 4**).



Fig. 2. Expression of YFP-TRAF2 in HEK 293T cells. HEK 293T cells were transfected with (1) pEF6-myc-HisB, (2) pEF6B-YFP-TRAF2, and (3) pcDNA3-TRAF2. Twenty-four hours later, cells were harvested for whole cell lysates. Equal amounts (50 μ g) of lysates were loaded on a 10% Bis-Tris NuPAGE gel and resolved by electrophoresis. The expression of TRAF2 was examined in Western blotting using antibody against TRAF2. YFP-TRAF2 and TRAF2 were indicated.

3.2.3. Monitoring Fluorescence of the Expressed Proteins

As an alternative to Western blot analysis, expression of the transfected plasmids can be monitored by flow cytometry.

1. Wash cells twice in 1 mL of PBS supplemented with 2% FCS by centrifuging for 5 min at 4°C at 480g.
2. Resuspend cells in 1 mL of PBS supplemented with 2% FCS.
3. Add 2 μ L of PI solution (500 μ g/mL) to the cell suspension.
4. Acquire events on the flow cytometer.

3.3. Performing Flow Cytometric FRET Analysis

Once the expression of the FRET plasmids is confirmed, they can be tested in flow cytometric FRET analysis. Unlike the transfection procedure described in **Subheading 3.2.1.**, transfections with a combination of FRET donor and acceptor plasmids were performed here.

3.3.1. Transfections

The transfection procedure was similar to what was described in **Subheading 3.2.1.** using FuGENE 6 (*see Note 5*).

Sample number	Sample description
1	2 μ g of pEF6-myc-HisB
2	0.5 μ g of pEF6B-p80-CFP + 1.5 μ g of pEF6-myc-HisB
3	1.5 μ g of pEF6B-p80-YFP + 0.5 μ g of pEF6-myc-HisB

(continued)

4	1.5 μ g of pEF6B-YFP-TRAF2 + 0.5 μ g of pEF6-myc-HisB
5	1.5 μ g of pEF6B-YFP-SODD + 0.5 μ g of pEF6-myc-HisB
6	0.5 μ g of pEF6B-p80-CFP + 1.5 μ g of pEF6B-p80-YFP
7	0.5 μ g of pEF6B-p80-CFP + 1.5 μ g of pEF6B-YFP-TRAF2
8	0.5 μ g of pEF6B-p80-CFP + 1.5 μ g of pEF6B-YFP-SODD

3.3.2. Cell Harvesting

1. After 24–48 h, harvest cells by washing and centrifuging twice in PBS supplemented with 2% FCS in FACS tubes.
2. Resuspend cells in PBS supplemented with 2% FCS.
3. Pass cells through a nylon filter prior to analysis.
4. Keep cells at 4°C until they are ready for analysis. Alternatively, if further manipulations of the cell samples are required (such as ligand stimulation), they can be kept at room temperature.

3.3.3. Acquisition of Events on the Flow Cytometer

(see **Notes 6** and **7**)

Cells were analyzed on a FACSVantage SE flow cytometer. Two lasers were used on the FACSVantage SE; an ILT air-cooled argon laser and a krypton laser (Spectra-Physics model 2060, Spectra-Physics, Mountain View, CA) that is equipped with violet optics. The argon laser was tuned to 514 nm for direct excitation of YFP (**Fig. 3**, laser 1). The krypton laser was tuned to 413 nm for excitation of CFP (**Fig. 3**, laser 2). Forward (FSC) and side scatter (SSC) filters were replaced with 513/10-nm bandpass (BP) filters. CFP fluorescence was detected in FL5 (P6) using a 470/20-nm BP filter. A 505LP dichroic mirror (DM) was used for separating CFP fluorescence and FRET emission from laser 2. FRET signal was detected in FL4 (P5) using a 546/10-nm BP filter. Direct YFP fluorescence was detected using a 546/10-nm BP filter in the FL1 (P3) channel but was directed to the P7 channel to allow P5-P7 interlaser compensation using the Omnicomp option (see **Fig. 3** and **Note 8**). Samples were collected with fluidics pressure at 30 pound per square inch (psi). This was done to shorten the pulse timing between the argon laser and the krypton laser in order to allow interlaser compensation using the standard delay module with a maximum delay of 17.5 μ s. One microgram per milliliter of PI was added prior to the acquisition of events. Fifty thousand live cells were collected.

3.3.4. Analyzing the Data Using FlowJo

1. Draw live cells gate by plotting SSC against FSC (**Fig. 4A**) or PI (detected in P8) against FSC.
2. Construct a two-dimensional dot-plot of CFP fluorescence (FL5/P6) vs FRET (FL4/P5) using cells in the live cells gate (**Fig. 4B**).

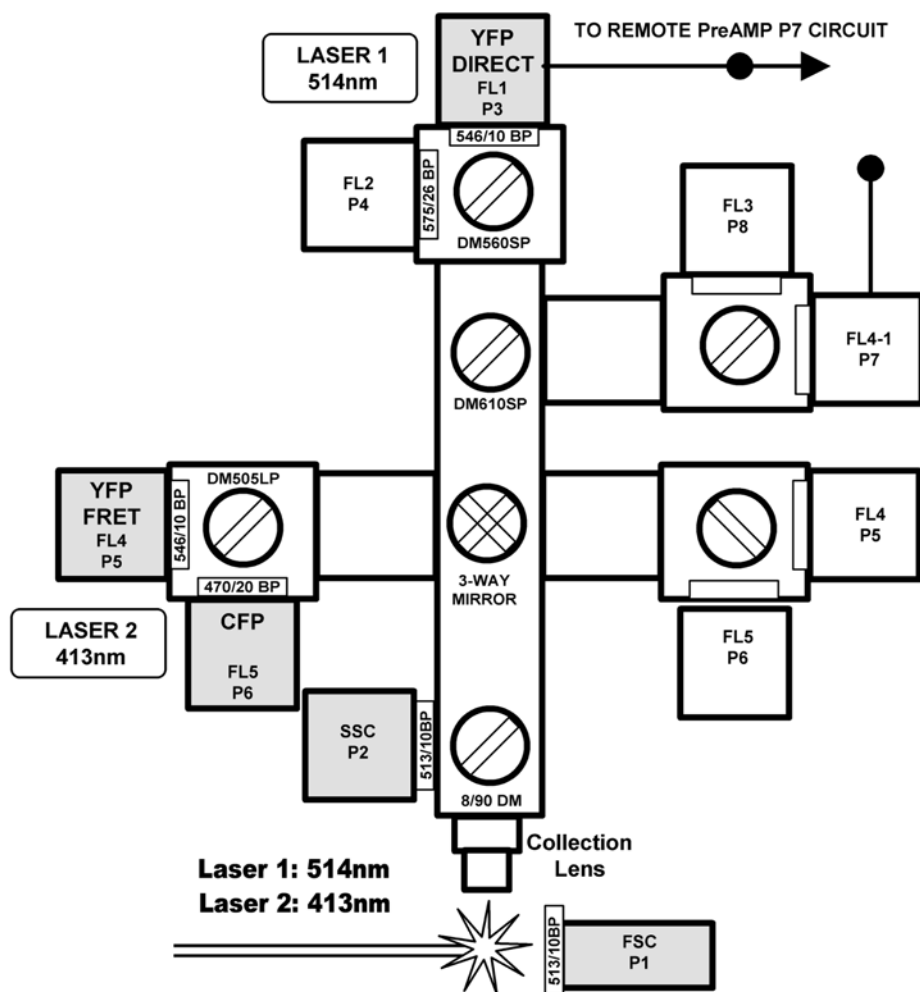


Fig. 3. Schematic setup of the FACS Vantage SE flow cytometer. Only the relevant filters and mirrors are labeled. The channels that were used for FRET analysis were colored gray. Other unused channels were shown for reference only.

3. Use vector-transfected sample (sample 1; *see Subheading 3.3.1.*) as the negative control to set the cutoff between CFP-positive and CFP-negative populations. Draw the CFP-positive gate accordingly.
4. Using cells in the CFP-positive gate, perform histogram analysis for FRET intensity (*see Note 9*) (**Fig. 4C**).
5. Perform FRET histograms overlay using p80-CFP (sample 2) as the negative control (**Fig. 4D**, dashed lines). Overlay histograms from samples 6, 7, or 8 on

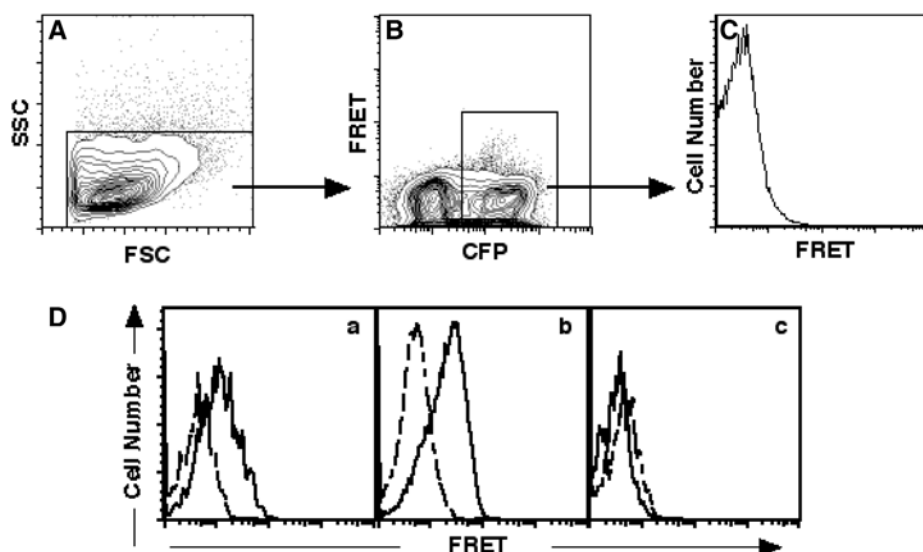


Fig. 4. Analysis of FRET data using FlowJo software. (A) Live cells (*box*) were determined by their forward and side scatter profile. (B) The cells that were in the live gate in (A) were analyzed for their CFP fluorescence and FRET signal on two dimensional dot-plot analysis. The transfected cells (CFP-positive cells in the *box*) were gated for histogram analysis of FRET. (C) Histogram analysis of FRET on CFP-positive cells from (B). (D) Histograms overlay showed that only cells coexpressing (a) p80-CFP and p80-YFP or (b) p80-CFP and YFP-TRAF2 exhibited significant level of FRET (*solid lines*). (c) Cells expressing p80-CFP and YFP-SODD did not exhibit any FRET (*solid line*). *Dashed lines*: baseline level of FRET in cells expressing only p80-CFP.

histogram from sample 2. Expression of p80-CFP and p80-YFP (sample 6) resulted in a strong FRET signal (**Fig. 4D**, panel a). Coexpression of p80-CFP and YFP-TRAF2 (sample 7) also resulted in strong FRET signal (**Fig. 4D**, panel b). However, the noninteracting control YFP-SODD failed to generate any significant FRET signal with p80-CFP (sample 8) when cotransfected with p80-CFP (**Fig. 4D**, panel c).

4. Notes

1. The success of FRET is most dependent on two criteria: (a) the physical distance between the fluorophores and (b) the relative orientation of the fluorophores (**18**). In using CFP and YFP as FRET donor and acceptor molecules, the investigator should also pay particular attention to the spacer length between the CFP (or YFP) moiety and the protein polypeptide itself. Owing to the size of CFP and YFP (~30 kDa), it is not uncommon that their fusion to another protein may affect

the protein function itself. In fact, fusion of CFP and YFP to the extracellular preassembly domain of TNFRs can severely hamper the ability of the receptor to bind ligand (19). However, this effect is ameliorated by increasing the spacer length between YFP and the receptor.

2. The vector pEF6-myc-HisB, which has an EF promotor, was chosen because of its ability to drive strong expression of the protein of interest in mammalian cells. The readers should note that the pECFP and pEYFP series of plasmids from BD Biosciences Clontech can be used directly for the introduction of the cDNA insert of interest. This will save time in the cloning steps.
3. HEK 293T cells are ideal for high protein expression because of the presence of the SV40 large T-antigen. However, other cell lines including Jurkat T cells have also been used successfully in FRET analysis. For 293T cells, FuGENE 6 is the transfection reagent of choice because of its consistency in yielding high protein expression. Cell culture conditions should be carefully monitored as they can significantly affect the transfection efficiency. Typically, seeding 2.5×10^5 cells on 12-well plates will yield a 70–80% confluent culture after 16–20 h of incubation, which generally results in >50% transfection efficiency.
4. To detect protein expression for the fusion proteins, monoclonal antibody against GFP can also be used. GFP-specific monoclonal antibody from Roche Applied Science can cross-recognize both CFP and YFP in Western blotting analysis (data not shown).
5. To optimize the FRET signal, it is necessary to have the acceptor molecule in slight excess relative to the donor molecule. To achieve that, a 1:3 ratio of CFP plasmids and YFP plasmids were used in the experiments described in this chapter. However, the investigators should empirically determine the optimal DNA ratio for each pair of FRET plasmids. Because the phenol red present in most tissue culture media can sometimes affect the autofluorescence level of the cells, phenol red-free medium is recommended for culturing cells for FRET analysis.
6. The more standard 488-nm laser found in most flow cytometers can sufficiently excite the YFP protein and therefore can replace the argon laser tuned to 514 nm. However, the 488-nm laser is not optimal for CFP excitation. Therefore, a separate laser tuned to ≤ 440 nm is needed (see **Subheading 3.3.3.**) for CFP excitation.
7. The LSR II model of flow cytometer from BD Biosciences has an optional fourth laser (405-nm wavelength) that can be used for CFP excitation and therefore will be compatible for FRET analysis as well. Other models of flow cytometer may also work provided that they have the proper lasers installed. The investigators should consult the individual vendor for more information.
8. The use of flow cytometers equipped with digital electronics (such as the FACSVantage SE with FACSDiVa option) will simplify the acquisition, particularly for interlaser compensation, since the output of P3 can be compensated against P7 without redirection of the signal output.
9. In the example given in this chapter, we used two-dimensional dot-plot of CFP vs FRET to define the CFP positive gate for subsequent FRET signal analysis.

However, other ways of defining the transfected populations such as plotting CFP fluorescence versus YFP fluorescence and gating on the double positive population are plausible alternatives for determining the transfected populations from which FRET is analyzed.

Acknowledgments

The authors would like to thank Michael Lenardo, Richard Siegel, and Ruth Swofford for discussion and technical help.

References

1. Forster, T. (1946) Energiewanderung und Fluoreszenz. *Naturwissenschaften* **6**, 166–175.
2. Forster, T. (1948) Zwischenmolekulare Energiewanderung und Fluoreszenz. *Ann. Phy. (Leipzig)* **2**, 55–75.
3. dos Remedios, C. G. and Moens, P. D. (1995) Fluorescence resonance energy transfer spectroscopy is a reliable “ruler” for measuring structural changes in proteins. Dispelling the problem of the unknown orientation factor. *J. Struct. Biol.* **115**, 175–185.
4. Hillisch, A., Lorenz, M., and Diekmann, S. (2001) Recent advances in FRET: distance determination in protein-DNA complexes. *Curr. Opin. Struct. Biol.* **11**, 201–207.
5. Tron, L., Szollosi, L., Damjanovich, S., Helliwell, S. H., Arndt-Jovin, D. J., and Jovin, T. M. (1984) Flow cytometric measurement of fluorescence resonance energy transfer on cell surfaces. Quantitative evaluation of the transfer efficiency on a cell-by-cell basis. *Biophys. J.* **45**, 939–946.
6. Tron, L., Szollosi, J., and Damjanovich, S. (1987) Proximity measurements of cell surface proteins by fluorescence energy transfer. *Immunol. Lett.* **16**, 1–9.
7. Szollosi, J., Matyus, L., Tron, L., et al. (1987) Flow cytometric measurements of fluorescence energy transfer using single laser excitation. *Cytometry* **8**, 120–128.
8. Szollosi, J., Damjanovich, S., and Matyus, L. (1998) Application of fluorescence resonance energy transfer in the clinical laboratory: routine and research. *Cytometry* **34**, 159–179.
9. Carraway, K. L. and Cerione, R. A. (1991) Comparison of epidermal growth factor (EGF) receptor-receptor interactions in intact A431 cells and isolated plasma membranes. Large scale receptor micro-aggregation is not detected during EGF-stimulated early events. *J. Biol. Chem.* **266**, 8899–8906.
10. Damjanovich, S., Bene, L., Matko, J., et al. (1997) Preassembly of interleukin 2 (IL-2) receptor subunits on resting Kit 225 K6 T cells and their modulation by IL-2, IL-7, and IL-15: a fluorescence resonance energy transfer study. *Proc. Natl. Acad. Sci. USA* **94**, 13,134–13,139.
11. Day, R. N. (1998) Visualization of Pit-1 transcription factor interactions in the living cell nucleus by fluorescence resonance energy transfer microscopy. *Mol. Endocrinol.* **12**, 1410–1419.

12. Mahajan, N. P., Linder, K., Berry, G., Gordon, G. W., Heim, R., and Herman, B. (1998) Bcl-2 and Bax interactions in mitochondria probed with green fluorescent protein and fluorescence resonance energy transfer. *Nat. Biotechnol.* **16**, 547–552.
13. Tsien, R. Y. (1998) The green fluorescence protein. *Annu. Rev. Biochem.* **67**, 509–544.
14. Wallach, D., Varfolomeev, E. E., Malinin, N. L., Goltsev, Y. V., Kovalenko, A. V., and Boldin, M. P. (1999) Tumor necrosis factor receptor and Fas signaling mechanisms. *Annu. Rev. Immunol.* **17**, 331–367.
15. Chan, F. K. M., Siegel, R. M., and Lenardo, M. J. (2000) Signaling by the TNF Receptor Superfamily and T Cell Homeostasis. *Immunity* **13**, 419–422.
16. Park, Y. C., Burkitt, V., Villa, A. R., Tong, L., and Wu, H. (1999) Structural basis for self-association and receptor recognition of human TRAF2. *Nature* **398**, 533–538.
17. Jiang, Y., Woronicz, J., Liu, W., and Goeddel, D. V. (1999) Prevention of constitutive TNF receptor 1 signaling by silencer of death domains. *Science* **283**, 543–546.
18. Miyawaki, A. and Tsien, R. Y. (2000) Monitoring protein conformations and interactions by fluorescence resonance energy transfer. *Methods Enzymol.* **327**, 472–500.
19. Chan, F. K. M., Siegel, R. M., Zacharias, D., et al. (2001) Fluorescence resonance energy transfer analysis of cell surface receptor interactions and signaling using spectral variants of the green fluorescent protein. *Cytometry* **44**, 361–368.

Design of a Fluorescence-Activated Cell Sorting-Based Mammalian Protein–Protein Interaction Trap

Sam Lievens, José Van der Heyden, Els Vertenten, Jean Plum, Joël Vandekerckhove, and Jan Tavernier

Summary

The mammalian protein–protein interaction trap (MAPPIT) is a two-hybrid assay based on insights in type I cytokine signal transduction. Bait and prey polypeptides are tethered to mutant cytokine receptor chimeras which are impaired in signaling. On bait–prey interaction and after ligand stimulation, the JAK-STAT signaling cascade is initiated leading to transcription of a reporter or marker gene under the control of the STAT3-responsive rPAP1 promoter. In addition to a physiologically relevant context for mammalian protein–protein interactions this method provides separation of interactor and effector zones, and can be applied for both analytical and screening purposes. In the protocol described here, a cytokine receptor derived surface tag is used as a selectable marker. After an initial presort step using magnetic-activated cell sorting (MACS), “positive” cells are selected by fluorescence-activated cell sorting (FACS).

Key Words

Cytokine, flow cytometry, fluorescence-activated cell sorting, JAK-STAT, magnetic-activated cell sorting, protein–protein interaction, receptor signal transduction, two-hybrid.

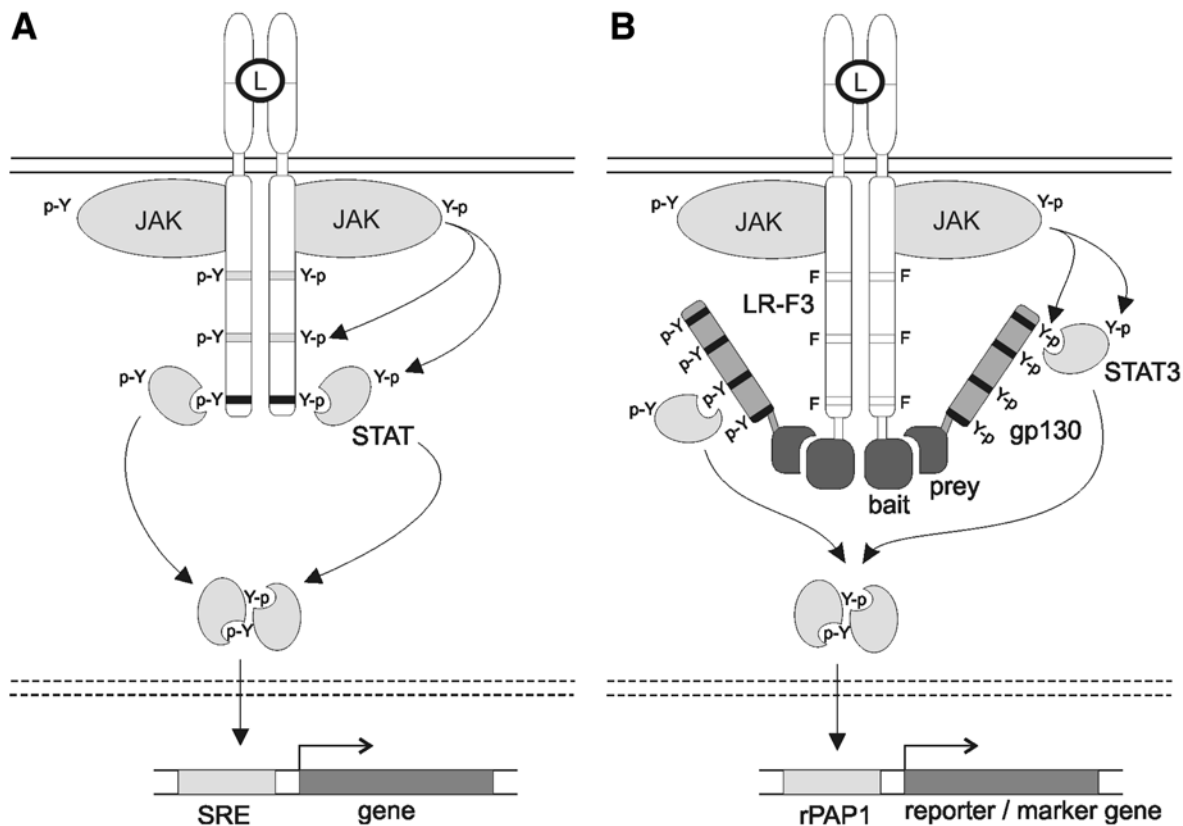
1. Introduction

To date, a variety of genetic and biochemical methods exist for studying protein–protein interactions in mammalian cells. Many of those are limited to analytical use, however. For a review we refer to Eyckerman and Tavernier (*1*). Recently, we developed a new tool that allows screening of complex cDNA libraries for new protein interaction partners. The mammalian protein–protein interaction trap (MAPPIT) is a two-hybrid strategy that is founded on the basic

principles of type I cytokine signaling (2). Ligand-induced cytokine receptor clustering results in cross-phosphorylation of receptor-associated Janus kinases (JAKs). Activated JAKs subsequently phosphorylate tyrosine residues in the receptor tails, thus creating recruitment sites for signal transducer and activator of transcription (STAT) molecules. On phosphorylation by JAKs, activated STATs dimerize and migrate to the nucleus where they induce transcription of specific gene sets (3) (*see Fig. 1A*). In MAPPIT, the bait protein is coupled to a mutant leptin receptor chimera from which STAT3 recruitment sites have been removed, and prey proteins are linked to a gp130 receptor fragment capable of binding STAT3. When bait and prey interact, phosphorylation of the prey chimeras leads to STAT3 recruitment, activation, dimerization, and migration, ultimately resulting in transcription of a reporter gene (for analytical purposes) or a selectable marker gene (for screening) under the control of the STAT3-responsive rPAP1 promoter (**Fig. 1B**).

Thus, whereas bait–prey interaction occurs in the cytosol, signal readout is initiated in the nucleus. This physical separation of interactor and effector zones avoids interference of the chimeric prey proteins with reporter activity, a common flaw in many (mammalian) two-hybrid methods. In addition, signals are ligand dependent, adding an additional level of control as variant bait chimeras that are activated by different ligands can be employed in the rapid discrimination of false positives. Taking further into consideration the near-optimal physiological context in which bait and prey interact, MAPPIT presents an attractive alternative for screening for new protein–protein interactions. Furthermore, some bait polypeptides containing target sites for JAK activity have been found to be phosphorylated on receptor activation, opening the door to screening for modification-dependent protein–protein interactions. In heteromeric MAPPIT, heteromeric receptor–bait complexes were used to demonstrate the serine phosphorylation-dependent interactions whereby a

Fig. 1. (*see facing page*) (A) Schematic drawing of the JAK-STAT pathway. See text for details. L, Ligand, SRE, STAT responsive element. (B) Principle of MAPPIT. A receptor chimera consisting of the extracellular domain of either the human erythropoietin receptor (EpoR) or the murine leptin receptor (LR) and the transmembrane and intracellular domains of a LR variant in which STAT3 recruitment sites and recruitment sites involved in negative feedback have been eliminated by tyrosine to phenylalanine mutations (LR-F3), is coupled to the prey polypeptide. The prey polypeptide is fused to a gp130 receptor fragment containing four functional STAT3 recruitment sites. If bait and prey interact, the receptor fragment is phosphorylated upon ligand-induced receptor activation, STAT3 is recruited, dimerizes, migrates to the nucleus, and leads to the transcription of a reporter or marker gene under the control of the STAT3-responsive rPAP1 promoter.



serine-threonine kinase and the bait substrate were linked to each one of the receptor chains (4).

The method described here is an adaptation of the basic MAPPIT protocol described previously (5). When using MAPPIT as a screening tool, we experienced that selection based on puromycin resistance did not fully reflect the analytical capabilities of the method. We reasoned that this might, at least in part, be due to the strong demands that have to be met by cells harboring a prey that interacts with the bait to survive: at each moment of the complete selection span (about 2–3 wk), high enough levels of puromycin resistance marker have to be maintained. A number of cellular mechanisms can, however, result in a transient suppression of rPAP1 promoter activation. These include condensation of the genome during cell division, and the reduced transcription rates associated with it, or receptor internalization. In particular in the case of weak or transient bait–prey interactions this might imply that the critical threshold level of resistance gene expression may not be maintained. As a consequence, such cells might die, resulting in the loss of prey detection.

In the alternative screening procedure described here, a membrane surface tag is used as a marker, enabling selection by flow cytometry. In brief, the method involves cloning of the bait construct in a vector for receptor–bait chimera expression. This vector is transfected into a host cell line containing a surface tag expression construct under the control of the STAT3-dependent rPAP1 promoter, and a pool of isogenic cells that express the receptor–bait chimera is selected. After confirmation of membrane expression of the chimera by fluorescence-activated cell sorting (FACS) analysis, the bait-expressing cells are infected with a retroviral prey cDNA library and subsequently stimulated with the receptor ligand. Given the low incidence of prey cDNAs that interact with the bait protein, the sample is first enriched for positive cells by magnetic cell sorting (MACS) before being sorted by FACS. A functional test can be performed to confirm the bait–prey interaction, and the identity of the prey is revealed by polymerase chain reaction (PCR) amplification and sequencing of the integrated prey sequences. During the MACS and FACS selection procedure, a cell sample that has been infected with a mock retroviral library is processed in parallel and serves as a background reference for setting the flow cytometer's sorting gate, which may vary from bait to bait. This specific adjustment of the selection threshold for each screen represents a main advantage of the FACS-based MAPPIT screening method, and better reflects the conditions of an analytical MAPPIT experiment (Fig. 2).

2. Materials

1. FLP-In T-REx System (Invitrogen, Carlsbad, CA) or T-Rex44 cell line.
2. Plat-E cell line (available from T. Kitamura, Division of Hematopoietic Factors, Institute of Medical Science, University of Tokyo, Tokyo 108-8639, Japan, kitamura@ims.u-tokyo.ac.jp).

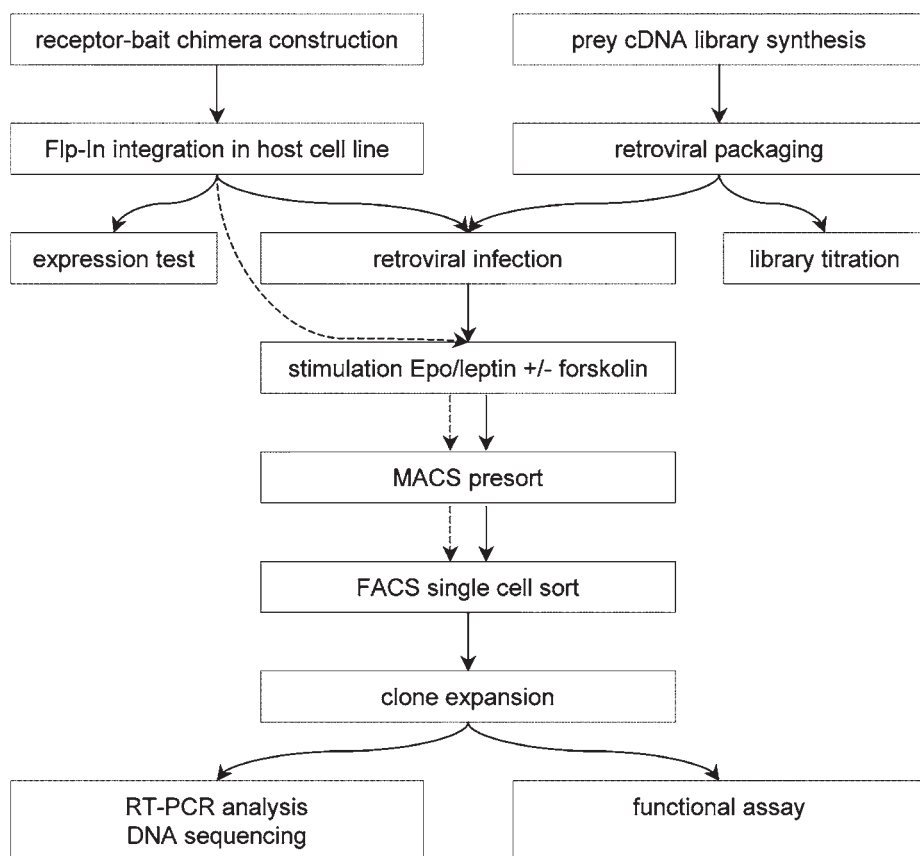


Fig. 2. Flowchart of the FACS-based MAPPIT screening procedure. *Full* and *dashed* arrows indicate the stages followed by the test sample and the negative control sample that serves as a reference for sorting (mock infected).

3. pXP2d2-rPAP1-hIL-5R α Δ cyt (pXP2d2 available from S. Nordeen, Colorado Health Sciences Center, Department of Pathology, Denver, CO, 80262, USA, steve.nordeen@uchsc.edu).
4. pCEL1f, pCLL1f (derived from pcDNA5/FRT vector; Flp-In System, Invitrogen) and pBG1 vectors (derived from pBABE available from G. Nolan, Department of Molecular Pharmacology, Stanford University, Stanford, CA, 94305, USA, gnolan@stanford.edu).
5. Growth medium: Dulbecco's modified Eagle's medium (DMEM) supplemented with 10% fetal calf serum.
6. Human leukemia inhibitory factor (LIF) (Sigma-Aldrich, St. Louis, MO), Human erythropoietin (Epo) (R&D Systems, Abingdon, Oxon, UK), and Mouse leptin (R&D Systems).

7. Forskolin (Sigma-Aldrich).
8. Cell dissociation agent (Invitrogen) and penicillin/streptomycin solution (Invitrogen).
9. Polybrene (Sigma-Aldrich).
10. Hygromycin B (Invitrogen) and Zeocin (Invitrogen).
11. Mouse monoclonal $\alpha 16$ antibody against the extracellular part of the human IL5R α receptor chain.
12. Antibody against the extracellular part of the human Epo receptor (e.g., goat polyclonal antibody, cat. no. AF-322-PB, R&D Systems) and the extracellular part of the mouse leptin receptor.
13. Fluorochrome-coupled secondary antibodies (e.g., AlexaFluor488-conjugated antibodies, Molecular Probes, Eugene, OR).
14. Magnetic cell sorting supplies (Miltenyi Biotec, Bergisch Gladbach, Germany): MidiMACS separation unit, LS columns, and Anti-biotin MACS MicroBeads.
15. FACS buffer: Ca²⁺- and Mg²⁺-free phosphate-buffered saline (PBS) containing 1% FCS, 0.5 mM EDTA, and 0.1% gentamycin. Pass through a 0.22- μ m filter, store at 4°C.
16. Propidium iodide. (**Caution:** this agent is mutagenic.)
17. FACS sorter (e.g., BD FACSVantage) with automated cell deposition unit, and FACS analyzer (e.g., BD FACSCalibur).

3. Methods

3.1. Generation of the Screening Tools

In the first part of this protocol, an overview is given of how the necessary “tools” for a MAPPIT screen are generated: the cell line, the receptor–bait expression vectors, and the prey cDNA libraries. Standard molecular biology methods are applied throughout this part of the method.

3.1.1. A Cell Line Adapted for FACS-Based cDNA Library Screening

Central to FACS-based MAPPIT screening is the generation of a cell line with three distinct properties. First, the cells should contain an integrated Flp recombination target (FRT) site which allows efficient integration of the receptor–bait chimera expression construct. Here, a host cell line is used that is derived from HEK 293 Flp-In T-REx cells (Flp-In T-REx system; *see Note 1*), which not only contains this FRT site but also a Tet repressor expression construct, enabling inducible expression of the receptor–bait chimera. Next, the cells should stably express the murine ecotropic retroviral receptor (EcoR), facilitating infection with Moloney murine leukemia virus-derived vectors containing the cDNA library and stable expression of the prey chimeras. Finally, the cell line should also contain a membrane tag expression construct controlled by a STAT3-responsive promoter to enable FACS-based selection. Basically any surface marker can be used that is readily selectable by MACS and FACS. In the

MAPPIT screening protocol described here, a fragment of the human IL-5 receptor α -subunit (hIL-5R α Δ cyt) is used, given the availability of a monoclonal antibody (α 16) with a very strong affinity for the extracellular domain of the human IL-5 receptor α -chain (6). This mutant receptor chain lacks the cytosolic domain (Δ cyt), which prevents it from interfering with components of the MAPPIT core mechanism, and which also avoids internalization of the receptor tag and the attenuation of the signal this might cause. An expression cassette was developed in which the hIL-5R α surface marker is put under the control of the STAT3-dependent rPAP1 promoter. After cotransfection of HEK 293 Flp-In T-Rex cells, clones were selected that had stably integrated the plasmids bearing this cassette and the EcoR expression construct. These clones were tested by FACS analysis for the level of hIL-5R α marker after stimulation with leukemia inhibitory factor (LIF), which also signals via STAT3 through endogenously expressed receptors. In these analyses, α 16 was used in combination with AlexaFluor488-labeled anti-mouse IgG as a secondary antibody. Two criteria were taken into consideration when evaluating the clones. On the one hand hIL-5R α membrane expression after activation of the STAT3 signal transduction pathway should be maximal, facilitating discrimination between positive and negative cells. On the other hand, in view of the MACS preselection, it is equally important that cells exhibit a basal hIL-5R α membrane expression that is as low as possible. Based on these considerations, clone T-Rex44 was selected as the host cell line for FACS-based MAPPIT screening (Fig. 3).

3.1.2. Expression Vectors for the Receptor–Bait Chimera

The pCEL1f and pCLL1f vectors for expression of the receptor–bait chimera are derived from the pcDNA5/FRT plasmid (Flp-In system) which contains an FRT site linked to the hygromycin resistance gene for Flp recombinase-assisted integration into the T-Rex44 host cell line containing an integrated FRT site and subsequent selection of a stable cell line. Chimeric receptor expression is under the control of the human cytomegalovirus (CMV) promoter. The pCEL1f and pCLL1f plasmids differ in the nature of the extracellular portion of the chimeric receptor which is either derived from the human erythropoietin receptor (EpoR) or the murine leptin receptor (LR) (see Note 2). Both chimeric receptors further consist of the transmembrane and intracellular parts of a LR variant in which tyrosine residues have been mutated to phenylalanine (LR-F3). Bait protein (fragments) can be cloned after a short hinge sequence using SacI and NotI restriction sites (Fig. 4A).

3.1.3. Prey cDNA Libraries

Prey cDNA libraries are generated in pBG1, derived from pBABE, a murine retroviral vector containing the Moloney leukemia virus long terminal repeat

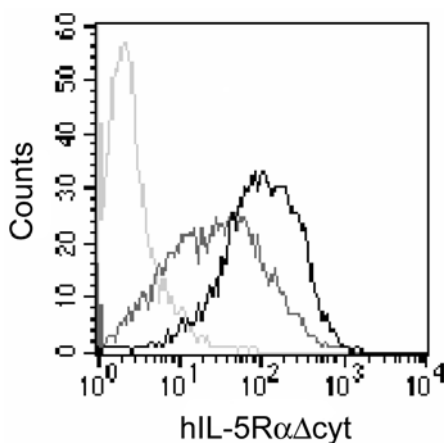
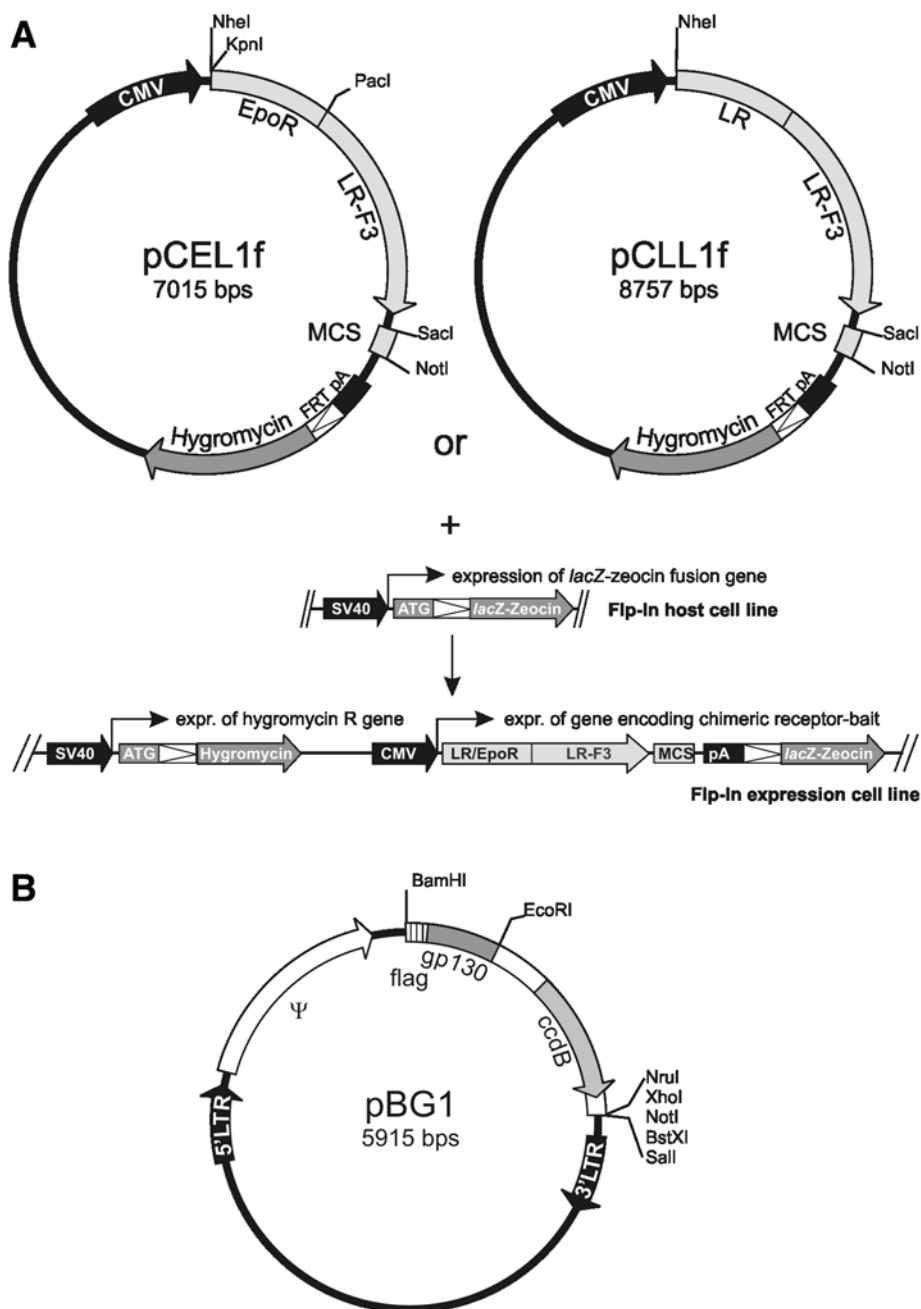


Fig. 3. FACS evaluation of hIL-5R $\alpha\Delta$ cyt marker expression in T-Rex44 cells. T-Rex44 cells left unstimulated (light gray) or stimulated with 1 ng/mL of LIF and measured before (dark gray) or after (black) MACS presort were first incubated with biotinylated α 16 antibody, and after MACS sort with AlexaFluor488-conjugated anti-mouse IgG secondary antibody.

(LTR) and ψ sequences. The pBG1 plasmid encodes a FLAG-tagged gp130 fragment with a glycine-glycine-serine (GGS) amino acid linker region that precedes the multiple cloning site in which the cDNAs are inserted by unidirectional cloning using *EcoRI* and *NotI* or *XhoI* restriction sites. Integration of prey sequences removes a stuffer encoding the bacterial “control of cell death B” (*ccdB*) protein in order to permit counter selection for self-ligated plasmids (**Fig. 4B**). Both oligo(dT)- or random-primed cDNA libraries, or a combination of both can be used for screening. Typically, at least 10^6 independent cDNA clones are obtained per library, starting from 5 μ g of poly(A)⁺ RNA. Virus particles containing the cDNA library are produced by transfection of Plat-E cells (7). The virus titer can be determined by cotransfection of a sample with a LacZ-

Fig. 4. (see facing page) (A) Schematic representation of the pCEL1f and pCLL1f bait vectors and reorganization of the FRT region on Flp-mediated recombination in the Flp-In host cell line. On cotransfection of the bait vector and the Flp recombinase expression plasmid pOG44 (Invitrogen), recombination occurs between FRT sites in the bait vector and in the genome of the host cell line resulting in a switch from zeocin to hygromycin resistance (by introducing a polyadenylation signal sequence [pA] before the lacZ-Zeocin fusion gene) and stable expression of the gene encoding the receptor-bait chimera. (B) Schematic drawing of the pBG1 prey vector. This vector contains the *E. coli ccdB* counterselection cassette to facilitate cDNA library generation.



or enhanced green fluorescent protein (EGFP)-encoding retroviral vector. Serial dilutions of this “contaminated” virus population should be used for infection of the host cells, and reporter expression in these cells can be measured by β -galactosidase staining for LacZ or FACS analysis for EGFP.

3.2. Preparing the Screen

3.2.1. Generation of an Isogenic Cell Pool

That Stably Expresses the Receptor–Bait Chimera

Expression constructs for the receptor-bait chimera are transfected into T-Rex44 cells and an isogenic cell pool stably expressing the chimera is selected according to the manufacturer’s directions (Flp-In system; *see also* **Fig. 4A** and **Note 3**). Membrane expression of the receptor–bait chimera can then be confirmed through FACS analysis (**Fig. 5**).

1. Plate 4×10^5 cells from the isogenic cell pool in 10-cm² tissue culture plates with 2 mL of growth medium (also include parental T-Rex44 cells as a negative control), and grow them overnight at 37°C, 8–10% CO₂.
2. Detach and dissociate the cells with 500 μ L of cell dissociation agent.
3. Remove the cell dissociation agent by adding 500 μ L of FACS buffer and pelleting the cells by centrifugation (2 min at 150g).
4. Resuspend the cells in 100 μ L of FACS buffer supplemented with an antibody directed against the extracellular part of the receptor-bait chimera (we use polyclonal goat antibody to human EpoR at a final concentration of 2 μ g/mL in the case of pCEL1f expression constructs, or “home made” rat monoclonal antibodies (4A9 or 1G2) against mouse LR at a final concentration of 3 μ g/mL when pCLL1f constructs are used), and incubate the cells for 2 h at 4°C with end-over-end rotation.
5. Wash the cells carefully: Add 900 μ L of FACS buffer, centrifuge for 2 min at 150g, add 500 μ L of FACS buffer, vortex-mix gently, and centrifuge again for 2 min at 150g.
6. Resuspend the cells in 100 μ L of FACS buffer supplemented with a suitable fluorochrome-coupled secondary antibody (we use AlexaFluor488-coupled antibodies), and incubate the cells for 45 min at 4°C with end-over-end rotation.
7. Wash the cells by adding 900 μ L of FACS buffer and centrifuging 2 min at 150g.
8. Resuspend the cells in 250 μ L of FACS buffer supplemented with 3 μ M propidium iodide (*see* **Note 4**).
9. Perform FACS analysis to estimate the expression of the receptor–bait chimera (*see* **Note 5**).

3.2.2. Determination of the Screening Conditions

To enable MACS presorting, cells that carry the hIL-5R α surface marker are first labeled with biotinylated α 16 antibody, and in a second step with antibiotin-antibody-coupled MACS MicroBeads. The cells are then separated on a column placed in a strong magnetic field, and the fraction that is eluted is

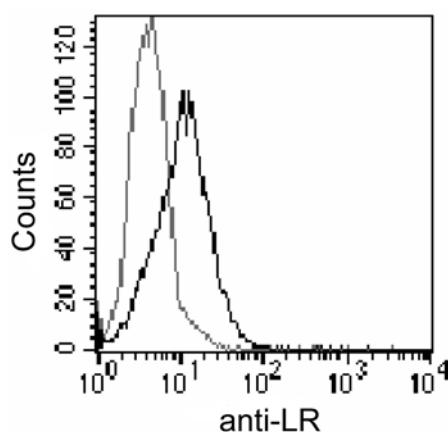


Fig. 5. FACS analysis of receptor-bait chimera membrane expression in T-Rex44 cells. Parental T-Rex44 cells (*gray*) and T-Rex44 cells which stably express a receptor-bait chimera containing the extracellular domain of the LR (*black*) were stained with a mixture of 4A9 and 1G2 anti-LR antibodies and subsequently labeled with a FITC-conjugated anti-rat IgG antibody.

strongly enriched for positive cells (**Fig. 3**). The advantage of this MACS pre-sort can be compromised to some extent by prey-independent hIL-5R α marker expression. As the amount of background may vary from bait to bait, screening conditions that result in an optimal signal-to-noise ratio should be determined for each bait individually (*see Note 6*).

1. For each screening condition to be tested (*see Note 7*) and for an additional negative and positive (*see Note 8*) control, plate 5×10^6 cells from the isogenic cell pool in 75-cm² tissue culture flasks with 20 mL of growth medium, and grow them overnight at 37°C, 8–10% CO₂.
2. Add Epo or leptin with or without forskolin according to the screening conditions to be tested, and incubate the cells another 24 h at 37°C, 8–10% CO₂.
3. Detach and dissociate the cells with cell dissociation agent, pool them, and pass them through a 70- μ m cell strainer.
4. Remove the cell dissociation agent by diluting the cell suspension with FACS buffer and pelleting the cells by centrifugation.
5. Resuspend the cells in a suitable volume (1 mL/10⁷ cells) of FACS buffer supplemented with biotinylated α 16 antibody at a final concentration of 1 μ g/mL, and incubate the cells for 2 h at 4°C with end-over-end rotation.
6. Wash the cells carefully: Add 10–20 times the volume of FACS buffer, centrifuge for 3 min at 500g, resuspend the cells again in FACS buffer, and centrifuge again for 3 min at 500g.

7. Resuspend the cells in 80 μL of FACS buffer per 10^7 cells, add 20 μL of anti-biotin MACS MicroBeads per 10^7 cells, vortex-mix gently, and incubate at 6–12°C for 15 min.
8. Wash the cells: Add 10–20X the volume of FACS buffer, centrifuge for 3 min at 500g, resuspend the cells again in FACS buffer, and centrifuge again for 3 min at 500g.
9. Resuspend the cells in 500 μL of degassed FACS buffer per 10^8 cells, for a minimum of 1 mL.
10. Proceed to the MACS (*see Note 9*) and follow the manufacturer's directions: place an LS column in the magnetic field of a MACS separator magnet and prepare the column by washing with 3 mL of degassed FACS buffer.
11. Apply the cell suspension (1–10 mL) onto the column while passing them through a 70- μm cell strainer, and collect the flow-through.
12. Wash the column three times with 3 mL of degassed FACS buffer, and pool the flow-through with that of the previous step (together these constitute the non-retained or “wash” fraction of the cell sample).
13. Remove the column from the separator, apply 5 mL of degassed FACS buffer, and, using the plunger, firmly flush out the cells into a collection tube (this is the “eluate” fraction of the sample).
14. Pellet the cells by centrifuging for 3 min at 500g and resuspend the cells in FACS buffer supplemented with a suitable fluorochrome-coupled secondary antibody (we use an AlexaFluor488-coupled antibody against mouse IgG at a final concentration of 1.3 $\mu\text{g}/\text{mL}$; use 1 mL/ 10^7 cells; *see Note 10*) and incubate the cells for 45 min at 4°C with end-over-end rotation.
15. Wash the cells by diluting the sample with 10–20 times the volume of FACS buffer and centrifuging 3 min at 500g.
16. Resuspend the cells in FACS buffer supplemented with 3 μM propidium iodide.
17. Perform FACS analysis to test the level of background expression of the hIL-5R α marker, and also record the number of cells present in “wash” and “eluate” fraction in order to evaluate the percentage of cells retained to the column under the different screening conditions (*see Note 11*).

3.3. The Screen

3.3.1. Retroviral Infection and Stimulation

1. Plate 10^7 cells from the isogenic cell pool in 175-cm² tissue culture flasks with 20 mL of growth medium (*see Note 12*), and grow the cells for 5 h at 37°C, 8–10% CO₂.
2. Add polybrene at a final concentration of 2.5 $\mu\text{g}/\text{mL}$ and add an appropriate dilution of the virus particles containing the cDNA library (*see Note 13*). In the screening experiment also include at least one flask in which the cells are mock infected, as a reference for FACS analysis.
3. Grow the cells overnight at 37°C, 8–10% CO₂.
4. Change the medium and add Epo or leptin with or without forskolin (*see Note 6*).
5. Grow the cells overnight at 37°C, 8–10% CO₂.

3.3.2. MACS Presort and FACS Single-Cell Sort

1. Prepare the cells for magnetic cell sorting by following **steps 3–10** from **Subheading 3.2.2**.
2. Place an LS column in the magnetic field of a MACS separator magnet and prepare the column by washing with 3 mL of degassed FACS buffer.
3. Apply the cell suspension (1–10 mL) onto the column while passing them through a 70- μ m cell strainer.
4. Wash the column three times with 3 mL of degassed FACS buffer.
5. Remove the column from the separator, apply 5 mL of degassed FACS buffer and using the plunger firmly flush out the cells into a collection tube.
6. Pellet the cells by centrifuging for 3 min at 500g and resuspend the cells in FACS buffer supplemented with a suitable fluorochrome-coupled secondary antibody (we use an AlexaFluor488-coupled antibody against mouse IgG at a final concentration of 1.3 μ g/mL; use 1 mL/ 10^7 cells; see **Note 14**) and incubate the cells for 45 min at 4°C with end-over-end rotation.
7. Wash the cells by diluting the sample with 10–20 times the volume of FACS buffer and centrifuging 3 min at 500g.
8. Resuspend the cells in FACS buffer (take 1 mL/ 10^6 cells).
9. Set the sorting gate of the flow cytometer using the noninfected sample as a reference, and sort the sample with deposition of the positive cells in separate wells of a multiwell plate containing medium supplemented with penicillin (final concentration 100 U/mL) and streptomycin (final concentration 100 μ g/mL).

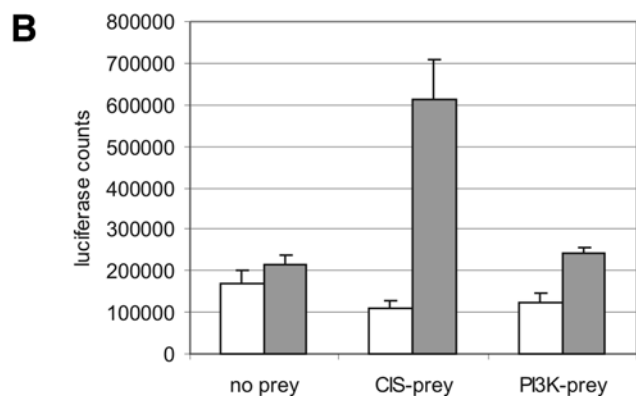
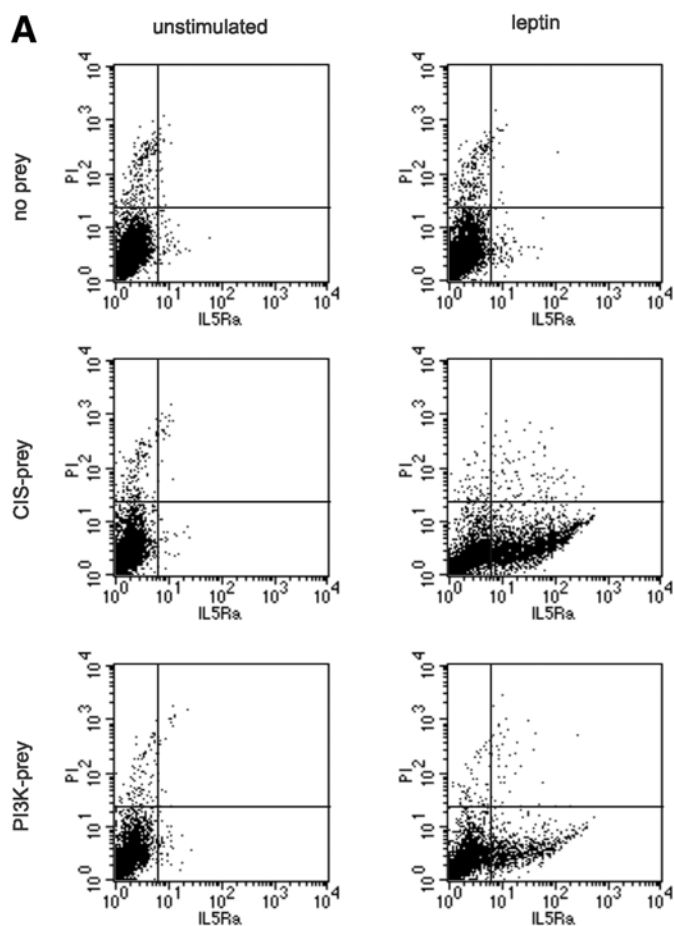
3.4. Downstream Processing of the Isolated Cells

3.4.1. Functional Assay for Interacting Proteins

Since chimeric bait and prey proteins are both stably expressed in the selected clones, transfection of these clones with a rPAP1-luciferase reporter construct can be used to confirm the bait–prey interaction (**Fig. 6**). Together with this reporter, variant receptor–bait constructs can be transfected to further sort out any false positives (**5**). When for example a screen is carried out with a receptor–bait chimera that is fused to the extracellular domain of the EpoR, a variant containing the extracellular part of the LR can be used to double-check the interaction in an Epo-independent fashion. By cotransfection with the same construct lacking the bait, the bait dependence of the interaction is tested.

3.4.2. Prey Identification

Prey-specific sequences are amplified using common methods, either starting from genomic DNA or from RNA by one- or two-step reverse transcriptase-PCR (RT-PCR). PCR is performed using primers specific for the flanking gp130 and retroviral 3'LTR sequences. When using the forward gp130-specific



primer 5'-GGCATGGAGGCTGCGACTG-3' and the reverse 3'LTR-specific primer 5'-TCGTGCACTGTGCTGGC-3', efficient amplification is obtained with an annealing temperature of 70°C. During the steps that precede PCR amplification, care needs to be taken to prevent contamination that could lead to the generation of false positive bands. All manipulations should therefore be carried out in a laminar flow cabinet, and all disposables and reagents should be free from template contamination. After agarose gel separation, DNA from purified candidate bands are sequenced using a gp130-specific primer (5'-GAGGCTGCGACTGATGAAG-3'; see **Note 15**).

4. Notes

1. It is important to note that the rPAP1 promoter is also responsive to activated STAT5. As the endogenous levels of STAT5 are very low in HEK 293-type cells, this does not present a problem in the protocol described here. Caution should be taken, however, when another cell type is used for generating a host cell line for screening.
2. Generally, a stronger signal is obtained when using the extracellular part of the LR, which can be explained by the fact that after binding of its ligand the LR undergoes higher order clustering (8), while the EpoR forms homodimers. The "classical" MAPPIT procedure where selection is based on cell survival in puromycin precluded the use of receptor-bait chimeras containing the extracellular part of the LR because this resulted in a higher background and thus increased levels of false positives. Because in this FACS-based alternative the selection threshold can be adjusted for each screen individually by setting the sorting gate of the flow cytometer, an enhanced background expression is no longer a problem, as long as it does not dramatically increase retention of negative cells on the MACS presort column (see **Note 6**).
3. The cells should not be kept at too high density when starting hygromycin selection because this selection is critically dependent on cell growth, and the onset of

Fig. 6. (see opposite page) Evaluation of protein-protein interactions by FACS-based MAPPIT. (A) T-Rex44 cells stably expressing a receptor chimera containing the extracellular domain of the LR fused to a region of the human EpoR containing the Tyr430-Tyr432 motif were infected with retroviral particles harboring pBG1 prey expression constructs or left uninfected as a control. As model protein-protein interactions, CIS (a member of the SOCS family of inhibitors of cytokine signaling) and the N-terminal SH2 domain of phosphatidylinositol 3-kinase (PI3K) were used as preys. Dot-plots are shown of propidium iodide staining vs hIL-5R α -linked fluorescence of unstimulated cells and cells stimulated for 24 h with 100 ng/mL of leptin. (B) Similarly infected cells were transfected with a rPAP1-luciferase reporter construct and luciferase activity was measured of cells left unstimulated (*white bars*) and cells stimulated for 24 h with 100 ng/mL leptin (*gray bars*). Error bars indicate the standard deviation of measurements performed in triplicate.

selection after addition of hygromycin may take several days. After pooling the colonies that remain after hygromycin selection, an aliquot of the cells should be stored in liquid nitrogen immediately in order to maintain a low passage number.

4. Propidium iodide is used to discriminate dead from living cells.
5. The intensity of the signal obtained may vary among baits; Western blot analysis can be used as an alternative.
6. For stimulation, depending on the nature of the receptor–bait chimera, Epo or leptin are used with or without the addition of forskolin. The latter is an activator of adenylyl cyclase which has been found to strongly enhance rPAP1 promoter induction (9). Thus, the modular buildup of the receptor–bait chimeras (containing the extracellular part of either the LR or the EpoR) together with the alternative stimulation conditions (ligand with or without forskolin) adds flexibility to the screening setup. For screening, a maximal shift in hIL-5R α expression-linked fluorescence in FACS is desired, without, however, drastically increasing the number of cells that is retained on the MACS column as this would result in reduced FACS resolution and increased sorting times.
7. We typically test saturating amounts of the ligand (20 ng/mL of Epo or 100 ng/mL of leptin) with or without the addition of forskolin at a final concentration of 10 μ M.
8. We use stimulation by LIF at a final concentration of 1 ng/mL as a positive control.
9. We use an LS column that has the capacity to retain up to 10^8 positive cells from up to 2×10^9 total cells, which is sufficient for our purpose.
10. For estimating the amount of cells in each of the two fractions, assume that only rarely more than 10% of the cells are retained on the column.
11. Depending on the bait we typically obtained between 0.1% and 1.5% retained cells for the unstimulated control sample, whereas after stimulation with Epo or leptin alone or in combination with forskolin this can increase up to approx 10%. The amount of background that can be tolerated depends on how many cells are being screened and on the sorting speed. We reasoned that when screening 5×10^8 cells, a background resulting in retention of up to 2% of the cells on the MACS column results in sorting 10^7 cells by FACS. When the sorting speed is set at around 3000 events/s, this means a total sorting time of 1 h, which is still quite acceptable.
12. The number of cells to be screened depends on the complexity of the cDNA library used for screening, the desired screening redundancy level and the estimated efficiency of retroviral infection. We typically obtain cDNA libraries with a complexity of 2×10^6 , which we screen 10-fold. We assume that the efficiency of infection varies approx 20%, which means that 10^8 cells have to be infected. When we further assume that the cells double twice in the 48 h between infection and selection, we end up with a total number of about 5×10^8 cells to be sorted.
13. We use a virus dilution that ideally produces an average integration of one prey cDNA per cell.
14. The amount of cells in the eluate can be estimated based on the results of the background evaluation test.
15. When multiple prey cDNA integrants are found in a single colony, these preys should be subcloned into a plasmid expression vector and individually tested by

transient transfection into the isogenic cell pool containing the chimeric-bait expression construct.

Acknowledgments

This work was supported by the Generisch Basisonderzoek aan de Universiteiten (GBOU) program of the Instituut voor de Bevordering van het Wetenschappelijk-Technologisch Onderzoek in de Industrie (IWT 010090), by the GOA 12051401 of Ghent University, and by the Fonds voor Wetenschappelijk Onderzoek Vlaanderen (FWO-V G.0149.99N).

References

1. Eyckerman, S. and Tavernier, J. (2002) Methods to map protein interactions in mammalian cells: different tools to address different questions. *Eur. Cytokine Netw.* **13**, 276–284.
2. Eyckerman, S., Verhee, A., Van der Heyden, J., et al. (2001) Design and application of a cytokine-receptor-based interaction trap. *Nat. Cell Biol.* **3**, 1114–1119.
3. Levy, D. E. and Darnell, J. E. (2002) Stats: Transcriptional control and biological impact. *Nat. Rev. Mol. Cell Biol.* **3**, 651–662.
4. Lemmens, I., Eyckerman, S., Zabeau, L., et al. (2003) Heteromeric MAPPIT: a novel strategy to study modification-dependent protein–protein interactions in mammalian cells. *Nucleic Acids Res.* **31**, e75.
5. Eyckerman, S., Lemmens, I., Lievens, S., et al. (2002) Design and use of a mammalian protein-protein interaction trap (MAPPIT). *Science's STKE*, <http://www.stke.org/cgi/content/full/sigtrans;2002/162/p118>.
6. Tavernier, J., Van der Heyden, J., Verhee, A., et al. (2000) Interleukin 5 regulates the isoform expression of its own receptor α -subunit. *Blood* **95**, 1600–1607.
7. Morita, S., Kojima, T., and Kitamura, T. (2000) Plat-E: An efficient and stable system for transient packaging of retroviruses. *Gene Ther.* **7**, 1063–1066.
8. Zabeau, L., Defeau, D., Van der Heyden, J., Iserentant, H., Vandekerckhove, J., and Tavernier, J. (2004) Functional analysis of leptin receptor activation using a JAK/STAT complementation assay. *Mol. Endocrinol.* **18**, 150–161.
9. Broekaert, D., Eyckerman, S., Lavens, D., et al. (2002) Comparison of leptin- and interleukin-6-regulated expression of the rPAP gene family: evidence for differential co-regulatory signals. *Eur. Cytokine Netw.* **13**, 78–85.

17

Flow Cytometric Screening of Yeast Surface Display Libraries

Michael Feldhaus and Robert Siegel

Summary

A method to screen and isolate antigen specific clones from a library of single-chain antibodies expressed on the surface of yeast cells is presented. Two rounds of magnetic bead enrichment before flow cytometric sorting enables one to screen libraries of far greater diversity than can be screened by just flow cytometry. The strength of flow cytometric sorting is the ability to follow the selection in real time and to isolate easily the highest affinity antigen-specific clones. A major strength of yeast display as a discovery platform is the ability to characterize the binding properties, the affinity of a clone without the need for subcloning, expression, and purification of the scFv. The methodology for directed evolution of single-chain antibodies to increase the affinity of a clone is also described.

Key Words

Affinity, antibodies, “directed evolution,” scFv, scFv libraries, selections, yeast display.

1. Introduction

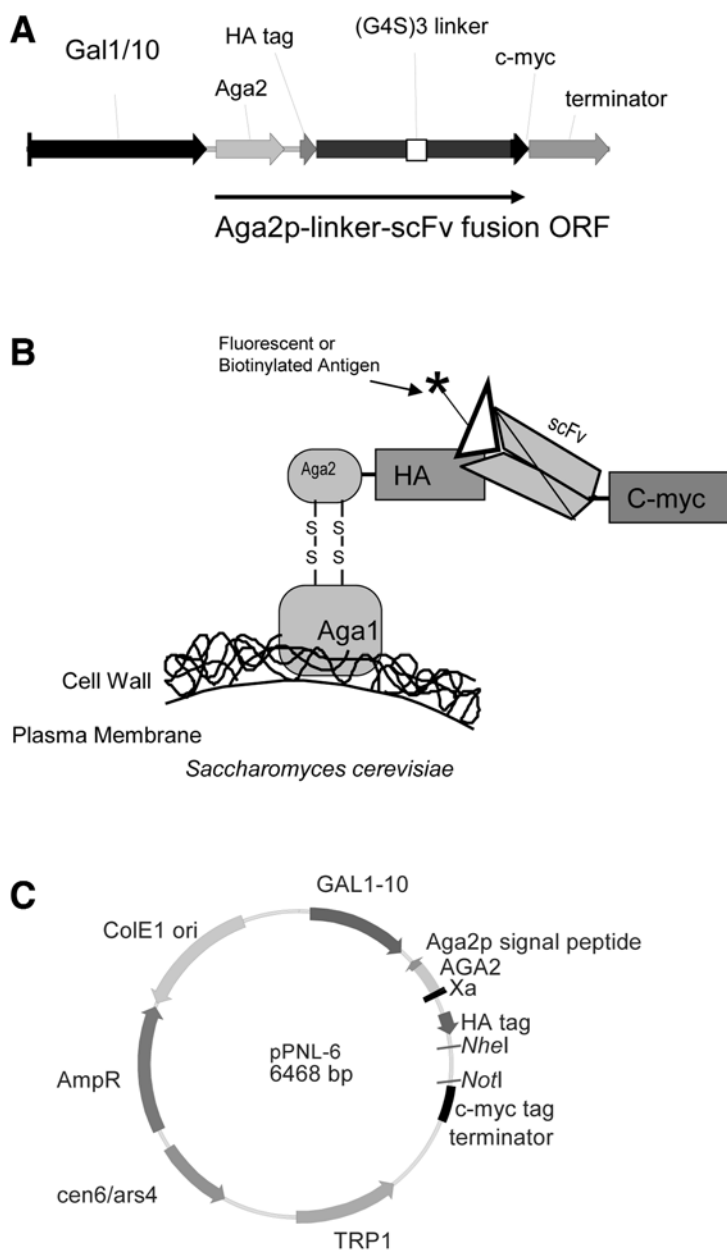
Creating affinity reagents to important biomolecules is one of the most critical, yet one of the most challenging tasks facing biologists. This chapter describes the implementation of a yeast surface display library of scFv (single-chain *Fragment variable*) antibodies as a method to solve part of this problem. The methodology was originally described by Feldhaus et al. (1). The scFv library is specifically designed to display full-length scFv antibodies whose expression on the yeast cell surface can be monitored with either N-terminal HA and C-terminal c-myc epitope tags. These epitope tags allow monitoring of clones or libraries of scFv clones for surface expression of full-length scFv by flow cytometry. The extra cellular surface display of scFv by *Saccharomyces*

From: *Methods in Molecular Biology: Flow Cytometry Protocols*, 2nd ed.
Edited by: T. S. Hawley and R. G. Hawley © Humana Press Inc., Totowa, NJ

cerevisiae also allows the detection of appropriately labeled antigen–antibody interactions by flow cytometry. As a eukaryote, *S. cerevisiae* offers the advantage of posttranslational modifications and processing of mammalian proteins and, therefore is well suited for expression of human derived antibody fragments. In addition, the short doubling time of *S. cerevisiae* allows the rapid analysis and isolation of antigen-specific scFv antibodies.

Yeast display, based on the platform created by Dane Wittrup at Massachusetts Institute of Technology, uses the α -agglutinin yeast adhesion receptor to display recombinant proteins on the surface of *S. cerevisiae* (2,3). In *S. cerevisiae*, the α -agglutinin receptor acts as an adhesion molecule to stabilize cell–cell interactions and facilitate fusion between mating “a” and α haploid yeast cells. The receptor consists of two proteins, Aga1 and Aga2. Aga1 is secreted from the cell and becomes covalently attached to β -glucan in the extra cellular matrix of the yeast cell wall. Aga2 binds to Aga1 through two disulfide bonds, presumably in the Golgi, and after secretion remains attached to the cell via Aga1. The yeast display system takes advantage of the association of Aga1 and Aga2 proteins to display a recombinant scFv on the yeast cell surface. The gene of interest is cloned into the pYD1 vector (Invitrogen, Carlsbad, CA), or a derivative of it, in frame with the AGA2 gene. The resulting construct is transformed into the EBY100 *S. cerevisiae* strain containing a chromosomal integrant of the AGA1 gene. Expression of both the Aga2 fusion protein from pYD1 and the Aga1 protein in the EBY100 host strain is regulated by the GAL1 promoter, a tightly regulated promoter that does not allow any detectable scFv expression in absence of galactose. On induction with galactose, the Aga1 protein and the Aga2 fusion protein associate within the secretory pathway, and the epitope-tagged scFv antibody is displayed on the cell surface (Fig. 1A,B). **Figure 2**

Fig. 1. (see facing page) Features of the pPNL6 vector, the *E. coli*/yeast shuttle vector for the selection and induced expression of an scFv Aga2 fusion protein. (Note: pYD1 is very similar but has modified epitope tags and restriction sites.) The pPNL6 vector (or pYD1) containing a nonimmune scFv library offers several key features that make it easy to display proteins of interest on *S. cerevisiae*. These include: (1) GAL1/10 promoter for strong inducible expression following the addition of galactose. The tight regulation of this promoter during growth on glucose allows for large expansion of the library without worry of clone biased growth. (2) N-terminal HA and C-terminal c-myc (only in pPNL6) epitopes for detection of the displayed scFv antibody with an anti-c-myc (9E10) or anti-HA (12CA5) antibody. (3) TRP1 auxotrophic marker for yeast selection and ampicillin for *E. coli* selection. (4) CEN/ARS origin for selection and maintenance in *S. cerevisiae*. (A) The GAL1/10-regulated scFv surface expression construct. (B) The scFv Aga2 fusion protein surface expression. (C) Plasmid map of pPNL6.



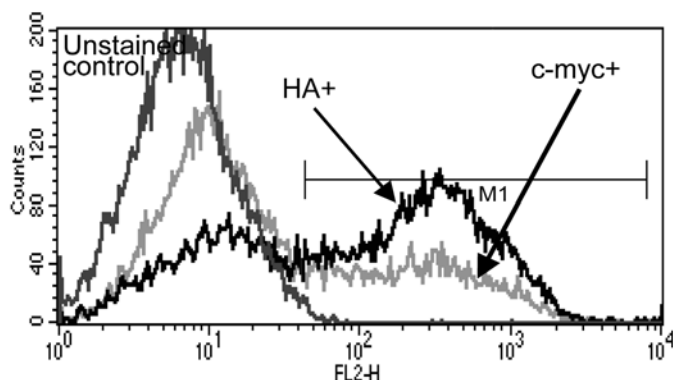


Fig. 2. Flow cytometric analysis of a nonimmune scFv library surface expression on yeast. Typically, 60–70% of the yeast in the scFv library will be HA epitope tag positive and 35–40% c-myc positive.

shows the HA and c-myc epitope staining patterns for an scFv antibody library. Molecular interactions with the scFv antibody can be easily assayed by incubating the cells with a ligand of interest (**Fig. 1C**). **Figure 3** graphically depicts a generalized scheme for enriching and identifying antigen-specific binders within a nonimmune scFv library. A combination of two rounds of selection using magnetic particles followed by two rounds of flow cytometric sorting will generally allow recovery of clones of interest (*see Table 1*).

Yeast surface display of scFv antibodies has also been successfully utilized to isolate higher affinity clones from small ($\sim 1 \times 10^6$) mutagenic libraries generated from a unique antigen binding scFv clone (**4**). Mutagenic libraries are constructed by amplifying the parental scFv gene one wants to obtain higher affinity variants of using error-prone PCR to incorporate three to seven point mutations/scFv (**5,6**). The material is cloned into the surface expression vector using the endogenous homologous recombination system present in yeast, known as “gap repair” (**7**). Gap repair that allows gene insertion in chromosomes or plasmids at exact sites by utilizing as little as 30 basepair regions of homology between your gene of interest and its target site. This allows mutated libraries of $1\text{--}10 \times 10^6$ clones to be rapidly generated and screened, in about 2 wk, by selecting the brightest antigen binding fraction of the population using decreasing amounts of antigen relative to the K_D of the starting parental clone. The screening involves three to four rounds of flow cytometry sorting, however. The flow cytometric sorting protocol is slightly different for a library based on a mutagenized clone than for a nonimmune library, and each is described separately in **Subheadings 3.6.** and **3.4.**, respectively.

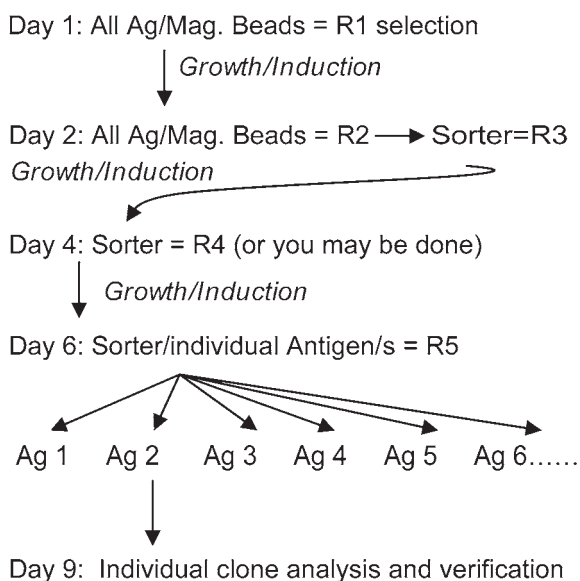


Fig. 3. Isolation of scFv through sequential enrichment of a nonimmune scFv library. Schematic of generalized scFv library screen.

One of the real strengths of the yeast display system is the speed of characterizing the binding affinity of the clones (8). A brief and greatly simplified version is described in **Subheading 3.6**. Additional useful resources to complement the protocols in this chapter include some yeast-specific protocols. For yeast transformation, see <http://www.umanitoba.ca/faculties/medicine/biochem/gietz/Trafo.html>. Also see refs. 9 and 10.

2. Materials

2.1. Media and Agar Plates

In making the media we add the following components in the following order, which appears to help with solubility of some components. Add amino acids to water, then the sugars, then add a 10X solution of buffer. The pH should be approx 6.25. We filter-sterilize all selective media (see **Note 1**).

1. Rich nonselective media (YEPD or YPD [yeast extract peptone dextrose]): 10 g/L of yeast extract, 20 g/L of peptone, and 20 g/L of dextrose. Filter sterilize or autoclave.
2. Selective growth media (SD + CAA): 5 g/L of casamino acids (-ade, -ura, -trp), 20 g/L of dextrose, 1.7 g/L of YNB (yeast nitrogen base) without ammonium sulfate and amino acids (Difco brand, cat. no. 233520, Becton Dickinson, Franklin

Table 1
Enrichment Factor and Recovery of Antigen-Specific Clones Using a Combination of Magnetic Bead Enrichment and Flow Cytometric Cell Sorting

Selection round and type	Complexity	Clone frequency = Ag-specific complexity	Library coverage screened	Ag-specific cells/total cells	Recovery of Ag-specific cells based on 50% recovery per round of selection	Selection output	Enrichment = original complexity × output complexity
R1 magnetic beads	10 ⁹	1/10 ⁹	10X	10/10 ¹⁰	5	1 × 10 ⁷	1/10 ⁹ × 5/10 ⁷ = 500X
R2 magnetic beads	1 × 10 ⁷	5/10 ⁷	1000X	1000/10 ¹⁰	500	1 × 10 ⁷	5/10 ⁷ × 5/10 ⁵ = 500X
R3 cell sorter	1 × 10 ⁷	5/10 ⁵	0	500/1 × 10 ⁷	250	1 × 10 ⁴	5/10 ⁵ × 2.5/10 ² = 2000X
R4 cell sorter	250 × 10 ⁴	2.5/100	1000X	25,000/10 ⁶	12,500	1000	2.5/10 ² × 1000/1000 to 1000/2000 about 50X
R4 output sorter-analysis	5 × 10 ⁴	5–9/10					

It is important to use at least 10-fold coverage of the starting complexity library to screen the library fully. After two rounds of enriching using magnetic beads the 500 Ag-specific cells would theoretically be present in a total of 1 × 10⁷ nonspecific cells. Using the Miltenyi MACS system, we find that from 10¹⁰ cells loaded onto the column, the background is consistently approx 0.5–2 × 10⁷ cells (based on OD₆₀₀), regardless of scFv expression or number of antigen-binding cells. The cell sorter greatly reduces the complexity from 10⁷ to 10⁴–10⁵ total cells depending on the stringency of sort gates and total number of cells sorted. By the second round of flow cytometric sorting, it is usually apparent if an antigen-specific clone is present at a frequency greater than 1/1000. It is always important to have a sample prepared that has been stained with all secondary reagents, but without antigen (i.e., anti-c-myc/GaM–488 and streptavidin–PE).

Lakes, NJ), 5.3 g/L of ammonium sulfate, 10.19 g/L of $\text{Na}_2\text{HPO}_4 \cdot 7\text{H}_2\text{O}$, and 8.56 g/L of $\text{NaH}_2\text{PO}_4 \cdot \text{H}_2\text{O}$ (see **Note 2**).

3. Selective scFv induction media (SG/R + CAA): Same as selective growth media except substitute 20 g/L of galactose, 20 g/L of raffinose, and 1 g/L of dextrose for dextrose.
4. Agar plates: Add 20 g/L of agar to YEPD; SDA-HUT (synthetic defined agar, -histidine, -uracil, -tryptophan). Buy or make them yourself (our supplier is Teknova, Half Moon Bay, CA).

2.2. Strains and Plasmids

1. EBY100 (Invitrogen): (Leu^- , Trp^-) BJ5465 is MATa. It has the auxotrophic: *ura3-52* (a Ty element insertion with no detectable background reversion frequency), *trp1* (an amber point mutation), *leu2 δ 200*, *his3 δ 200*, *pep4:HIS3*, *prbd1.6R*, *can1*, GAL. EBY100 has genomic insertion of AGA1 regulated by GAL promoter with a URA3 selectable marker. The scFv library is displayed in this strain.
2. Plasmids: pYD1 (Invitrogen) is the plasmid that our scFv library is cloned into as a fusion protein to AGA2. Selects for ability to grow in the absence of tryptophan in yeast and on ampicillin in *E. coli*. pPNL6 is based on this plasmid with minor differences such as a C-terminal c-myc epitope tag instead of a V5 epitope tag.

2.3. Antigens

Biotinylated antigens can be generated in a variety of ways. We find the NHS Biotinylation kit and the 2-hydroxyazobenzen-4'-carboxylic acid (HABA) system to quantify the number of biotin/molecule of protein to be robust and easy (both from Pierce Biotechnology, Rockford, IL). We strive to obtain two or three biotin per protein molecule. More biotin/protein is not desirable because of concerns about blocking the epitope/antibody interaction site.

2.4. Flow Cytometry and Magnetic Bead Enrichment

1. Miltenyi magnetic-activated cell sorting (MACS) LS columns and streptavidin magnetic beads (and antibiotin magnetic beads) with manual magnetic separator (Miltenyi Biotech, Auburn, CA).
2. Anti-HA (12CA5) antibody.
3. Anti-c-myc antibody (clone 9E10) (Amersham Biosciences, Piscataway, NJ; or Covance, Babco, Cumberland, VA), 200 $\mu\text{g}/\text{mL}$ for pPNL6-derived libraries; or anti-V5 mAb for pYD1 libraries.
4. Goat antimouse (GaM) Alexa 488-conjugated (Molecular Probes, Eugene, OR).
5. Goat antimouse (GaM) Alexa 633-conjugated (Molecular Probes).
6. Goat antimouse (GaM) PE-conjugated (Molecular Probes).
7. Streptavidin-R-phycoerythrin (SA-PE) (Molecular Probes).
8. Streptavidin-Alexa 633 (SA-633) (Molecular Probes).
9. Streptavidin-Alexa 647 (SA-647) (Molecular Probes).
10. Neutravidin-fluorescein isothiocyanate (FITC) (NA-FITC) (Molecular Probes).

11. Neutravidin-PE (NA-PE) (Molecular Probes).
12. Biotinylated purified antigens, 2 $\mu\text{g}/\text{kDa}$ of antigen (*see Subheading 2.3.* for preparation).
13. Penicillin/streptomycin, 100X tissue culture grade (Gibco™ Invitrogen Corporation).
14. Wash buffer/buffer: Phosphate-buffered saline (PBS), 0.5% bovine serum albumin (BSA), and 2 mM EDTA.

3. Methods

The methods below are divided into six categories: (1) growth and induction for scFv expression of libraries or clones, (2) magnetic bead enrichment of biotinylated antigen binding yeast, (3) fluorescent staining for both antigen binding and scFv expression of the library, (4) flow cytometric sorting of library, (5) clone validation and subsequent affinity determination, and (6) sorting of mutagenic scFv library for isolation of higher affinity clones. Library construction is not covered in this chapter. Only selections of scFv clones of interest are described.

Many of the techniques, growth and induction conditions, and staining protocols are very similar between nonimmune libraries, immune libraries, or mutagenized scFv clone libraries. The major differences between the various library types are both the diversity of the libraries (number of different antibody clones present) and the frequency of antigen-binding clones within that diversity.

3.1. Growth and Induction of Surface Expression of scFv (*see Note 3*)

3.1.1. Libraries of scFv

1. Start a SD + CAA culture that contains a minimum of a 10X representation of the diversity of your library. For a 10^9 diverse library, 10^{10} yeast are needed to start the culture. The culture would be 1 L of 0.5 $\text{OD}_{600}/\text{mL}$. Plating a dilution plate is highly recommended to verify colony-forming units and lack of bacterial contamination.
2. Grow at 30°C with shaking overnight (*see Note 4*). Take a 10X representation of library diversity from the culture and pellet. If you diversity is 10^9 clones, then a 10X representation would be 10^{10} yeast. That means at 2×10^7 yeast/ OD_{600} unit you need 500 OD_{600} . For example, if your OD is 5.0 $\text{OD}_{600}/\text{mL}$ then you need 100 mL of the culture to obtain 10^{10} yeast. Generally, the culture should be freshly saturated or be $<4 \text{ OD}_{600}/\text{mL}$.
3. Resuspend the cell pellet in SG/R + CAA at 0.5 $\text{OD}_{600}/\text{mL}$ and incubate at 20°C with shaking for one to two doublings as determined by OD_{600} . This will generally take 12–16 h.
4. Wash the yeast once in wash buffer. The yeast are now ready to be labeled with biotinylated antigen and enriched on a magnetic column. You can also store the cells by placing the flask at 4°C for up to a week with minimal degradation of

c-myc expression level or positive cells as determined by flow cytometry. However, the yeast do become sticky and tend to clump more, which may affect selections, and viability is often reduced by 50%.

3.1.2. Individual scFv Clones

1. Start a 1- to 5-mL SD + CAA culture from a single isolated yeast colony.
2. Grow at 30°C with shaking overnight.
3. Pellet enough cells to start a 1- to 5-mL culture at 0.5 OD₆₀₀/mL in induction media, SG/R + CAA.
4. Resuspend cell pellet in SG/R + CAA at 0.5 OD₆₀₀/mL and incubate at 20°C with shaking for one to two doublings as determined by OD₆₀₀. This will generally take 12–16 h.
5. Wash cells once in wash buffer before staining for flow cytometry, or store the cells by placing the flask at 4°C for up to a week. *See Subheading 3.1.1., step 4* for notes about 4°C storage of induced cultures.

3.2. Magnetic Bead Enrichment Using Miltenyi MACS LS Columns for Two Rounds of Magnetic Bead Enrichment

Process for enrichment of antigen-specific clones from a nonimmune library of 10⁹ diversity:

1. Resuspend 1×10^{10} yeast (from induced culture) in 10 mL of wash buffer.
2. Add one or more biotinylated antigens at 100 nM final concentration. Incubate at 25°C (room temperature) for 30 min followed by 5–10 min on ice. **All subsequent steps should be done with ice-cold buffer or at 4°C.**
3. Pellet cells (3000g for 3 min) and wash three times with 50 mL of wash buffer.
4. Resuspend the cell pellet in 5 mL of wash buffer with 200 µL of magnetic-activated cell sorting (MACS, Miltenyi) streptavidin magnetic microbeads (or antibiotin magnetic microbeads). Alternating between these beads during subsequent rounds of selection decreases the chance of obtaining secondary reagent-specific clones.
5. Incubate on ice for 10 min with gentle mixing by inversion every 2 min.
6. Pretreat Miltenyi LS column, loaded into magnet, by flowing 3 mL of ice-cold wash buffer through it using gravity.
7. Add 40 mL of wash buffer, pellet cells and resuspend in 50 mL of wash buffer. Make sure it is a single-cell suspension by vortex-mixing and passing cells through a cell strainer cap tube (Falcon brand, cat. no. 352235, BD Biosciences, San Jose, CA) immediately prior to loading onto Miltenyi LS column.
8. Add the 7-mL cell suspension that was just put through the cell strainer cap to the column. After each 7 mL of cells have entered the column and the flow has stopped, remove the column from magnet and immediately put back into magnet. This rearranges the iron beads in the column and allows the cells that are physically trapped between the beads to pass through. With the column back in the magnet, add 1 mL of wash buffer and let flow through, then another 7 mL of

cells onto column. Repeat the column removal procedure between each loading of cells. It will take about 30 min to load all 50 mL of cells.

9. Once all of the cells have been loaded on the column, wash the column with 3 mL of wash buffer. Make sure the upper loading chamber is washed of all residual cells. This wash removes the cells in the void volume of the column. Remove column from magnet and immediately replace as before. Repeat this wash two additional times.
10. Once the column has stopped dripping, remove the column from magnet and then add 7 mL of wash buffer and use the plunger to push all remaining cells out into a 15-mL conical tube. We generally elute approx $1-3 \times 10^7$ cells. Pellet cells and resuspend as follows:
 - a. If round 1 selection: Resuspend yeast in 200 mL of selection media (SD + CAA with pen/strep) for overnight growth to saturation (10^{10} yeast). Plate a dilution to obtain an accurate number of yeast isolated. This is the R1output diversity. Induce as described previously in SG/R + CAA. This allows maximal expansion of library and of your clone of interest for subsequent repeat of magnetic bead enrichment. Use antibiotin magnetic beads as above for second round of selection. This is the R2output.
 - b. If round 2 selection (second enrichment on magnetic column): Resuspend cells in 500 μ L of buffer for subsequent staining for sorting by flow cytometry.

3.3. Fluorescent Staining of Cells From the MACS Column Before Flow Cytometric Cell Sorting (see Note 5)

It is important to note that at the start of each round of selection you should stain your library for anti-HA (12CA5), anti-c-myc (9E10), and secondary only controls. This establishes several important baselines. (1) Were my yeast properly induced? (2) What percent are expressing c-myc (i.e., full length scFv)? (3) Do my secondary reagents bind nonspecifically? (4) Am I enriching for secondary reagent binders? Therefore, if you are going to use SA-PE to label antigen bound cells, you should add just SA-PE to your induced cells to see if it binds. The control for GaM reagents should be stained and analyzed (no anti-c-myc antibody should be added). We generally see very little labeling of the aliquot, $<0.1\%$. If you see labeling try other secondary reagents (i.e., neutravidin, streptavidin or antibiotin monoclonal antibody [MAb]) to minimize enriching for secondary reagent binders.

1. Add 5 μ L of 9E10 anti-c-myc antibody (200 μ g/mL) to the 500 μ L containing $1-10 \times 10^7$ yeast eluted from the magnetic column. You can also add 100 nM biotinylated antigen at this point. However, this is unnecessary if cells were selected on magnetic column as they should already have antigen bound.
2. Incubate for 30 min on ice. Pellet in microfuge on high for 10 s. Wash two times with 500 μ L of buffer.

3. Add a 1:200 dilution of secondary reagents (GaM-Alexa 488 for c-myc and SA-PE for the biotinylated antigen) (*see* **Note 6** and **Fig. 4**).
4. Incubate for 30 min on ice, pellet the cells, and wash two times with 500 μ L of ice-cold wash buffer.
5. Resuspend the cells in 1 mL of buffer and keep on ice in the dark until sorting.

3.4. Flow Cytometry Sorting of Antigen-Specific scFv Clones From Nonimmune Library

3.4.1. Sort Gate Decision

Sorting from a nonimmune library that has gone through two rounds of enrichment on magnetic beads should allow you to see antigen binding yeast at a frequency of 1/1000 to 1/5000 cells. The sort gate is set in one of the following two manners:

1. The first method is based on sorting the top 0.1% of the brightest antigen binders that are also c-myc positive. These may or may not be an obvious or distinct population. Generally for the first sort (round 3 of selection), most or all of the cells coming off the magnetic column should be sorted. In **Fig. 5**, top panel, the population is obvious; however, this is not always the case (depending on enrichment ratios) and sometimes antigen binding cells must be sorted on “faith.”
2. The second method relies on staining the same sublibrary in the presence and absence of antigen. It is often very clear where to set the sort gate at this point. An example of sorting is presented in **Fig. 5**, bottom panels.

The sort criteria are usually less stringent for the first flow cytometric sort. Sort more slowly (less coincidence aborts) and on an enrich mode. The rate of “more slowly” is dependent on the sorter you are using. A skilled operator should be able to provide guidance.

3.4.2. First Sort, Round 3 Selection

1. Sort yeast into Eppendorf tubes containing 100 μ L of YPD media. The YPD helps the yeast recover. We let them sit in the YPD media for about an hour before growth on selectable media.
2. After sorting, plate the cells on SD + CAA pen/strep and an appropriate dilution plate (*see* **Note 7**).
3. Incubate plates at 30°C for 24–48 h.
4. Scrape colonies together and then grow for several hours in SD + CAA media.
5. Subculture at least a 10X representation of sublibrary diversity (determined from the dilution plate of sorted cells) into SG/R + CAA induction media.
6. Make glycerol stock of at least 10X representation of the sublibrary diversity from the SD + CAA culture for storage in case subsequent steps need to be repeated.

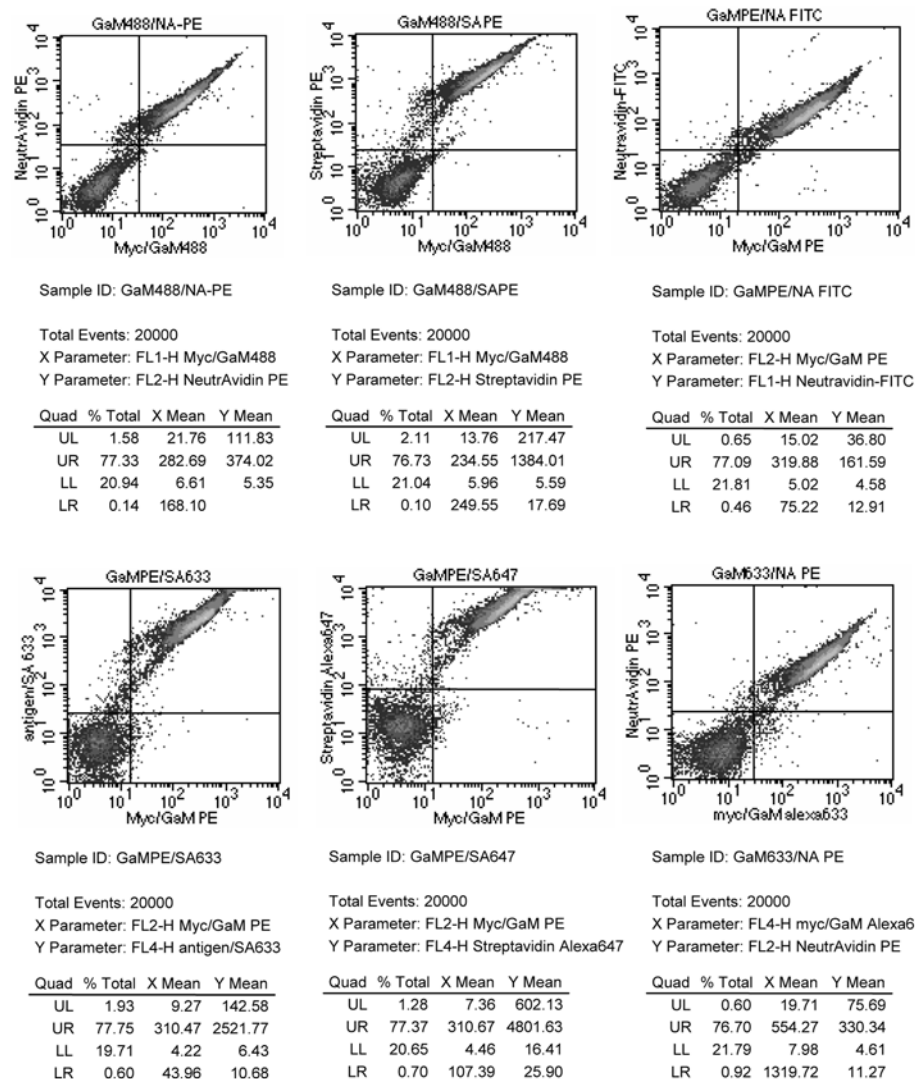


Fig. 4. Different fluorescent reagents that can be employed to detect c-myc expression and biotinylated antigen binding.

The glycerol stock is the yeast in a 15% glycerol solution and can be stored at -80°C . The cell concentration can be from 1 OD₆₀₀/mL up to 100 OD₆₀₀/mL.

3.4.3 Second Sort, Round 4 Selection

At this point your diversity is generally under 100,000. Therefore, staining 2×10^7 yeast gives you a 200-fold coverage of your diversity. You also expect

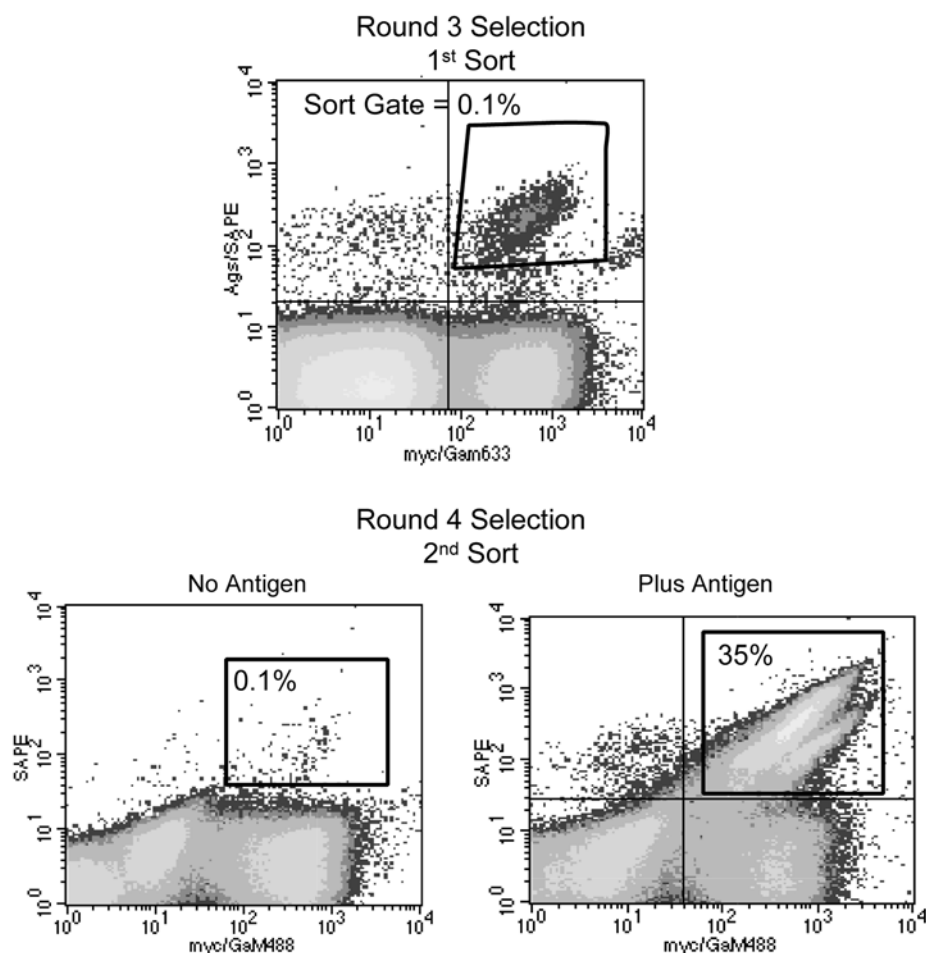


Fig. 5. Sorting of R2 output from second magnetic bead enrichment column to create R3 output and then R4 output. The “no-antigen” control shows that when antigen is present there are many more dual positive yeast and provides confidence that what you are sorting is actually binding your antigen and not the detection reagent.

to see clones that bind your antigen at a frequency of 1–10%. Cells are stained as before, with all controls:

- Control 1 = Unstained
- Control 2 = GaM–Alexa 488 only
- Control 3 = SA–PE only
- Control 4 = anti-myc + GaM–Alexa 488
- Control 5 = anti-myc + GaM–Alexa 488 + SA–PE
- Sample = anti-myc/GaM–Alexa 488 + antigen/SA–PE

A number of controls (listed above) should be done with the induced R3 sublibrary output prior to the fourth round of selection. Control 5 will help distinguish antigen detection reagents specific binders from true antigen binders. Analyze at least 100,000 events to allow patterns to emerge in the bivariate plot. SA-PE-positive clones that do not have the c-myc tag can be easily removed during the subsequent sort by setting the selection gate to isolate only c-myc-positive/antigen binding cells.

If the SA-PE-positive clones from control 5 are also c-myc positive, then careful examination of control 5 to the antigen containing sample may allow a different subpopulation to be visualized in the dual-positive quadrant of the bivariate plot. The population that is present in the antigen containing sample and not in the no-antigen control can be specifically isolated. However, you may also see the percentage dual-positive population change from 2% in the no-antigen control to 4% or more in the antigen-containing sample. These antigen binders are able to be identified in one of two manners. First, after sorting with SA-PE, individual clones can be subsequently screened for antigen binding specificity. The number of clones to analyze will be dictated on the relative differences in the percentage positive between control 5 and the antigen-containing sample. Second, the secondary reagent used to detect antigen-positive cells can be changed to antibiotin MAb or neutravidin, both labeled with an appropriate fluorescent dye. This prevents those clones in the library that specifically bind streptavidin from contaminating the selection process altogether. However, make sure to repeat control 5 with whatever secondary reagent you intend to use to detect antigen binding.

1. Sort on "purity mode" if an antigen specific population is obvious. Sorting a few hundred to a thousand yeast cells at this point will generally suffice to give an antigen positive clone.
2. Sort yeast into Eppendorf tubes containing 100 μ L of YPD media.
3. After sorting, plate the cells on SD + CAA pen/strep. No dilution plate is required when <1000 yeast are plated. We generally see a 50–80% plating efficiency.
4. Incubate plates at 30°C for 24–48 h.
5. Pick individual colonies into SD + CAA media. We will generally pick 10 different clones. These may all be the same or ten unique clones. The number of unique clones will be determined either by sequencing or BstN1 fingerprinting of polymerase chain reaction (PCR)-amplified scFv genes (**11**).
6. Subculture 100 μ L into 1 mL of SG/R + CAA. Grow at 20°C for 16 h to induce expression of scFv.

3.5. Clone Validation and Affinity Determination

This verifies the individual clones from the previous sort are true antigen binders and that they express full-length scFv as determined by c-myc expression. Each sample needs to be stained with antigen and without antigen:

No Ag = anti-c-myc + GaM-Alexa 488 + SA-PE

Plus antigen = anti-c-myc/GaM-Alexa 488 + antigen/SA-PE

3.5.1. Flow Cytometric Staining of Individual Clones

1. Prepare $1-2 \times 10^6$ yeast by washing the induced yeast one time with 1 mL of buffer.
2. Resuspend yeast in 100 μ L containing 1 μ L of anti-c-myc MAb and for plus antigen stain biotinylated antigen (generally 100 nM).
3. Incubate for 30 min at room temperature followed by 5 min on ice. Pellet in microfuge on high for 10 s. Wash two times with 500 μ L of ice-cold buffer.
4. Resuspend pellet in 100 μ L of a 1:200 dilution of secondary reagents (GaM-Alexa 488 and SA-PE). **Figure 4** shows several combinations of fluorescent reagents that can be used.
5. Incubate for 30 min on ice, pellet the cells, and wash two times in cold buffer.
6. Resuspend cells in 1 mL of buffer and keep on ice in the dark until analysis by flow cytometry.

3.5.2. Affinity Determination Using Equilibrium Binding Titration Curves to Determine Equilibrium Dissociation Constants K_D

Because the initial selections are performed at 100 nM, the vast majority of clones identified from a nonimmune library will be in the 1–100 nM affinity range. The lower the concentration of antigen in the initial selection, the lower the affinity range will be and fewer unique clones are generally isolated. Once antigen binding has been verified, we determine clone uniqueness by utilizing a DNA fingerprint of the PCR-amplified scFv restriction digested with *Bst*NI (11,12). This limits the number of clones we need to determine the K_D for, as many clones may be identical as demonstrated by identical *Bst*NI fingerprints obtained as described previously. This range of affinities can be determined on the yeast surface by measuring the amount of antigen bound at different concentration at equilibrium. The technique relies on measuring the mean fluorescence intensity (MFI) of the bound antigen, at a variety of concentrations of antigen, on the c-myc positive yeast. K_D is measured by determining at what concentration of antigen is half of the scFv on the surface of the yeast cell bound to antigen. Therefore measuring the MFI of the yeast when no antigen is bound and determining the concentration of antigen that gives the maximal MFI is needed. This is easily accomplished by setting up a series of antigen concentrations in which to label the yeast with and then measuring the MFI of the antigen binding population by flow cytometry. The MFI, obtained using flow cytometry with each of the antigen concentrations tested, is then plotted against the antigen concentration; using a nonlinear least-squares curve to fit the data, the K_D is determined (see **Figs. 6 and 7**).

Staining 10^5 yeast/antigen concentration represents approx 10^9 – 10^{10} antigen binding sites (scFv) in the sample. We assume 10^5 scFv/yeast and 50% express

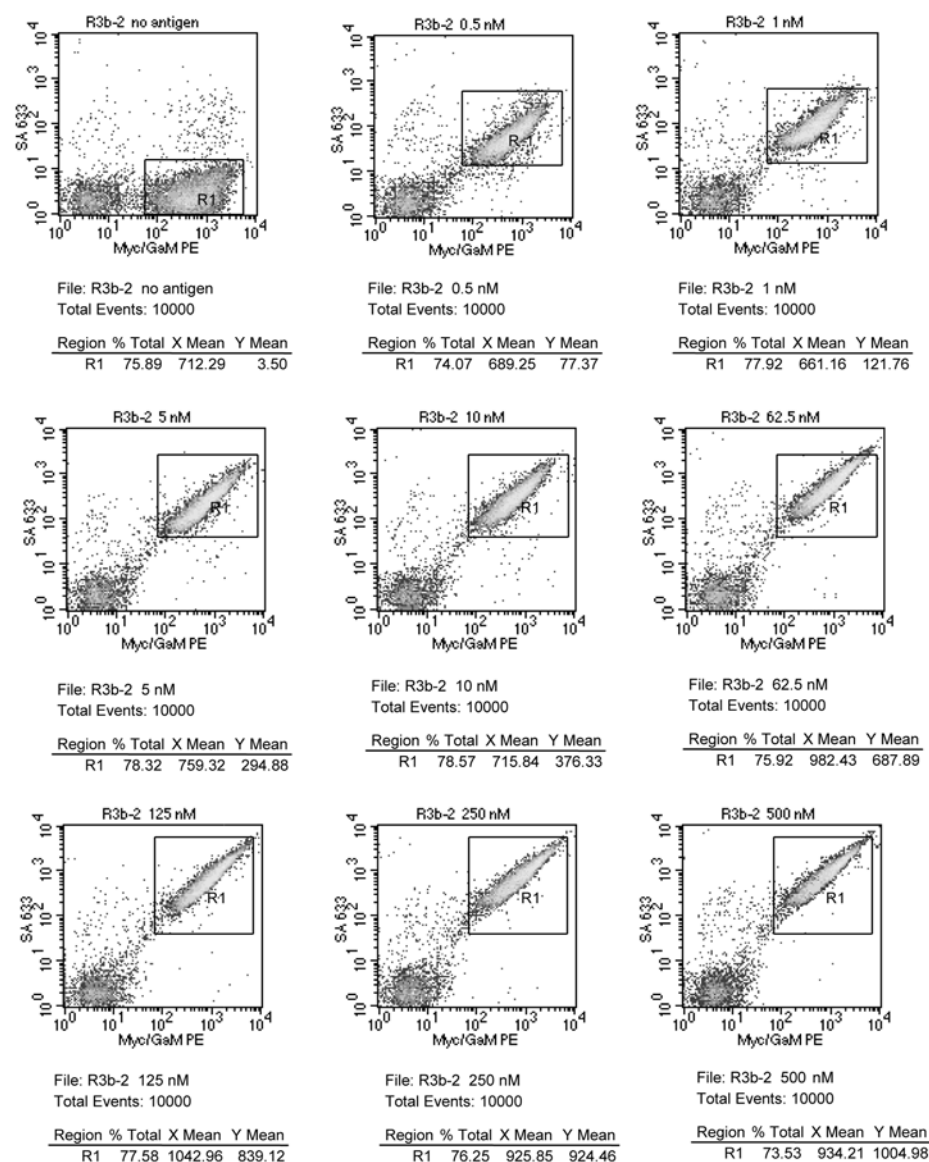


Fig. 6. K_D determination using analysis of MFI from bivariate plots obtained on a flow cytometer looking at c-myc expression (x-axis) and antigen binding (y-axis).

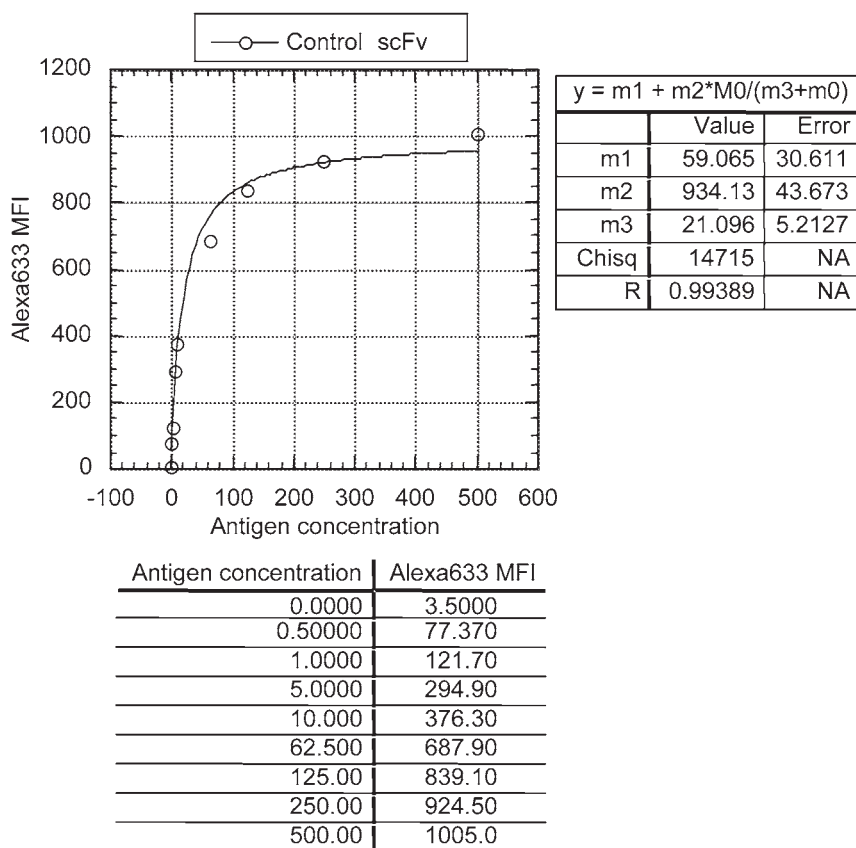


Fig. 7. K_D determination using flow cytometry and nonlinear least-squares fit.

scFv. You want to maintain at least 10X excess of number of molecules of antigen over the number of scFv molecules. This is nondepleting ligand conditions.

We routinely prepare 12 clones using a 96-well microtiter plate format choosing eight concentrations of antigen, which include a “no-antigen” control for background.

1. Label 10^6 induced yeast with 100 μ L of a 1:100 dilution on the c-myc MAb (200 μ g/mL) for 30 min on ice.
2. Add 10 μ L (10^5 yeast) directly into the antigen concentrations (*see step 3* below). This uses very little c-myc antibody, 1 μ L/100 μ L of 10^6 cells.
3. The following concentrations and volumes will allow for an accurate K_D to be measured for affinities between 1 and 100 nM. 10^5 yeast/sample = 5×10^9 scFv. If you have an idea of what your affinity is you can omit the first or last two antigen concentrations. For example, for a 100 nM affinity you do not need the 1 nM or 0.5 nM antigen concentrations. For a 5 nM affinity you do not need the 500 nM

or 100 nM concentrations. You are striving to do a series of two- to fivefold dilutions at 5–10X over K_D to 5–10X below K_D .

Concentration of antigen	Volume of antigen solution	No. of molecules of antigen
500 nM	100 μ L	3×10^{13}
100 nM	100 μ L	6×10^{12}
50 nM	100 μ L	3×10^{12}
25 nM	100 μ L	1.5×10^{12}
10 nM	100 μ L	6×10^{11}
5 nM	100 μ L	3×10^{11}
1 nM	500 μ L	3×10^{11}
0.5 nM	500 μ L	$1.5 \times 10^{11} = 30X \text{ excess}$
0.1 nM	1 mL	$6 \times 10^{10} = 10X \text{ excess}$

4. Incubate the samples at room temperature for 1 h. This allows ample time for the binding reaction to reach 90% equilibrium for antibody clones with off-rates in the 10^{-3} . An off-rate of 10^{-3} is what is generally seen for clones with 10 nM K_D , an affinity representing the majority of clones in the library. For clones with slower off-rates, 10^{-4} or 10^{-5} , 10- to 24-h incubations with antigen would be required to reach 90% equilibrium. These represent nanomolar and subnanomolar affinity antibodies.
5. Place samples on ice for 5 min. The decrease in temperature greatly decreases the off-rate. For a 25°C decrease in temperature, a 50- to 100-fold decrease in the off-rate is seen (13).
6. Wash the sample two times with 500 μ L of ice-cold buffer.
7. Resuspend the sample in 100 μ L of a 1:200 dilution of secondary reagents, GaM-Alexa488 and SA-PE.
8. Incubate on ice for 30 min. Pellet cells and wash one time with 500 μ L of ice-cold buffer.
9. Resuspend in 500 μ L of buffer and store on ice in dark until analyzed by flow cytometry.
10. Gather 10,000 events for a bivariate plot using the fluorescence channels that detect Alexa 488 (emission ~525 nm, usually FL1 on Becton Dickinson and Coulter brand flow cytometers) and phycoerythrin (emission 575 nm, usually FL2 on Becton Dickinson and Coulter brand flow cytometers).
11. Collect the statistical information from the dual c-myc+/antigen+ population.
12. Plot the MFI against the concentration of antigen and use a nonlinear least-squares to fit the curve (such as found in Kaleidgraph or GraphPad) and determine the K_D using the following equation:

$$y = m1 + m2 * m0 / (m3 + m0)$$

where $m1$ = MFI of no antigen control, $m2$ = MFI at saturation, and $m3 = K_D$. If “R” values are generated, values of 0.998 and greater will give K_D values accurate within 30%.

3.6. Sorting of Mutagenic scFv Library for Isolation of Higher Affinity Clones

Boder et al. developed a methodology for generation and isolating higher affinity mutants of a specific scFv. This was demonstrated by the maturation from nanomolar to femtomolar binding K_D for an scFv (4). The construction of a mutagenized library can be done several ways and is not covered here (6,14,15). However, there are several guidelines one should follow. The number of mutations per clone will affect the number of mutants that can display functional full length scFv. The number of mutations per clone will also affect the likelihood of finding a clone of increased affinity (5). A library of 10^6 – 10^7 different mutants can easily be screened using the methodology below.

1. Grow and induce library with a minimum of 10X coverage.
2. Stain no more than 10^8 cells (it takes ~3 h to sort at 10,000 events/s).
3. Label yeast with anti-c-myc to identify full-length scFv antibody clones. The mutagenesis will induce a larger number of stops and truncated proteins. At the same time, add antigen at the K_D of the parental clone. Incubate for 30 min at room temperature followed by 5 min on ice before pelleting and washing cells twice. Proceed to **step 4**.

An alternative approach that is more productive for affinity maturation of clones that are already subnanomolar affinities is to select clones by a combination of fast on-rate and slow off-rate by the following steps:

- a. Label with biotinylated antigen for 1 h at 25°C. Do *not* label with anti-c-myc.
 - b. After washing away unbound antigen, resuspend cells in 100 mL of 25°C wash buffer. Incubate sample at 25°C for 1–24 h (depending on off-rate of the parental antibody from which the library was made). Change buffer twice during incubation.
 - c. Pellet cells and stain for c-myc, 30 min, 25°C. Wash three times.
 - d. Resuspend cells in secondary reagents, GaM–Alexa 488 and SA–PE, 30 min, 4°C.
 - e. Proceed to **step 5**.
4. Resuspend the cell pellet in secondary reagents. Incubate on ice in the dark for 30 min. Wash once and resuspend.
 5. Run the sample on the sorter. Sort the entire sample for the brightest 1.0% of c-myc-positive antigen-binding population. Expect 5–20% of the cells to express c-myc-positive scFv, and of these 10–20% will bind antigen.
 6. Cells will either be plated on selective plates that contain antibiotics or grown in selective liquid media (about 5 mL of SD + CAA). The antibiotics can be any or all of the following: pen/strep (10 mg/mL) used at 100 µg/mL or ampicillin or kanamycin (10 mg/mL) used at 10–20 µg/mL.
 7. Plates are incubated at 30°C for 1–2 d. Colonies are pooled and then induced. Liquid media grown cells are pelleted and induced. An aliquot is generally frozen as well.

8. Therefore, from 10^7 cells you might sort out a total of 10^3 – 10^4 cells. Typically, 50% of the cells will form colonies or will be viable. For subsequent sorts, 70% of the cells will be c-myc-positive, with the vast majority being binding antigen.
9. After regrowth and induction of the yeast from the round 1 selection, 10^8 are labeled with antigen at a concentration of 0.5–0.1X the concentration at K_D . The addition of anti c-myc and the staining with secondary reagents is as described in **Subheading 3.5.1**.
10. Sort on the brightest 0.1% of antigen-binding c-myc positive clones. *Note:* The sublibraries overall K_D can be determined using an approach similar to that used for determining the K_D of an individual clone as outlined in **Subheading 3.5.2**. We will generally do our first sort with antigen concentration at K_D and then drop the concentration by 2- to 10-fold each subsequent sort.
11. Repeat **steps 6–10** for two additional rounds.
12. Individual clones can be assayed for K_D and sequencing of the insert can determine number of unique clones and where particular changes from the parental clone occur. Generally, by the fourth round of selection 80% of the clones in the sublibrary will be improved mutants (*see Note 8*).

3.7. Frequently Asked Questions (FAQS)

1. Some proteins we use seem to stick to all the yeast. Why?
Answer: Before starting any selection we routinely check the protein of interest for binding to a single scFv clone that is not induced, the library not induced and the library in the induced state. You should see no labeling in any case. If there is labeling it could be binding to the yeast surface or the scFv in a nonspecific fashion. We have the most reproducible results and experience with peptides and secreted proteins. However, we have also obtained antigen specific scFv to a variety of cytoplasmic proteins. We recommend trying different selection buffers to decrease or eliminate the nonspecific binding. For example, 0.1% Tween–PBS, no EDTA, and so forth.
2. I have gone through five rounds of selection and all I got were secondary reagents binders or nothing. What's wrong?
Answer: It could be a large number of possibilities. The most common are enumerated below.
 - a. Did you check that the sorter was set up properly? Did the flow cytometer operator show you what was sorted by rerunning that sample or doing a test sort of labeled beads? Did you set up a dilution plate from the sorted cells? Was the number what you expected? We generally see about a 40–70% plating efficiency from the number of cells sorted.
 - b. Do you know your antigen is biotinylated? How? We use the Pierce HABA methodology to determine moles of biotin per mole of antigen and strive for a 1–2 mol of biotin/mol of antigen.
 - c. Try increasing the concentration of antigen up to 1 μ M.
 - d. There is also the possibility there are no binders to your protein (*see Note 9*).

3. Can I just use flow cytometric sorting or just use magnetic beads to get my antigen specific clones?

Answer: Yes; however, we believe combining the two is the most powerful way to screen the complete diversity of the library (*I*). In our paper, HEL was isolated using the MACS system only.

4. Notes

1. YPED cultures saturate between 8 and 10 OD₆₀₀/mL, while SD + CAA cultures saturate between 3 and 5 OD₆₀₀/mL.
2. For 2X SD + CAA we add 10 g of casamino acids, 3.4 g of yeast nitrogen base, and 10.6 g of ammonium sulfate. This formulation can give greater cell numbers for growing the library up and freezing it down, generally yielding cell densities between 6 and 8 OD₆₀₀/mL.
3. Cell numbers are generally determined by OD₆₀₀ reading on a spectrophotometer. We find about 2×10^7 cells/mL per OD₆₀₀ unit. This should be determined by plating yeast on agar plates or using a hemacytometer to calibrate your spectrophotometer.
4. Fisher Scientific (Pittsburg, PA) supplies Pyrex brand "DeLong culture flask" with three baffles on flask bottom. It works best to increase aeration and growth. However, it is not essential.
5. This protocol is for staining up to 5×10^7 cells in 500 μ L of wash buffer. To stain less yeast, decrease the volume proportionally, yet keep the reagent concentration the same. Most secondary reagents should be titered in your laboratory for the most appropriate dilutions. **Figure 4** show several combinations of secondary reagents that work well to label biotinylated antigens and anti-c-myc MAb.
6. It is important to use different secondary antigen-labeling reagents (streptavidin–Alexa 633 or neutravidin–PE) between flow cytometric sorts to eliminate or reduce secondary reagent-specific scFv. **Figure 4** shows several combinations of fluorescent reagents that can be used if secondary reagent binders are obvious.
7. Yeast do not grow very well in liquid culture when grown at low cell densities ($<10^4$ /mL). Therefore, when we sort out $<10,000$ yeast, we generally will plate them.
8. It is often useful to run the original clone side by side with your new mutants to verify even slight differences in K_D , threefold differences in K_D are easily seen.
9. Note, we have never *not* obtained a streptavidin binder if we go through five rounds of selection.

References

1. Feldhaus, M. J., Siegel, R. W., Opresko, L. K., et al. (2003) Flow-cytometric isolation of human antibodies from a nonimmune *Saccharomyces cerevisiae* surface display library. *Nat. Biotechnol.* **21**, 163–170.
2. Boder, E. T. and Wittrup, K. D. (1998) Optimal screening of surface-displayed polypeptide libraries. *Biotechnol. Prog.* **14**, 55–62.

3. Boder, E. T. and Wittrup, K. D. (1997) Yeast surface display for screening combinatorial polypeptide libraries. *Nat. Biotechnol.* **15**, 553–557.
4. Boder, E. T., Midelfort, K. S., and Wittrup, K. D. (2000) Directed evolution of antibody fragments with monovalent femtomolar antigen-binding affinity. *Proc. Natl. Acad. Sci. USA* **97**, 10,701–10,705.
5. Daugherty, P. S., Chen, G., Iverson, B. L., and Georgiou, G. (2000) Quantitative analysis of the effect of the mutation frequency on the affinity maturation of single chain Fv antibodies. *Proc. Natl. Acad. Sci. USA* **97**, 2029–2034.
6. Stemmer, W. P. (1994) Rapid evolution of a protein in vitro by DNA shuffling. *Nature* **370**, 389–391.
7. Orr-Weaver, T. L. and Szostak, J. W. (1983) Yeast recombination: the association between double-strand gap repair and crossing-over. *Proc. Natl. Acad. Sci. USA* **80**, 4417–4421.
8. VanAntwerp, J. J. and Wittrup, K. D. (2000) Fine affinity discrimination by yeast surface display and flow cytometry. *Biotechnol. Prog.* **16**, 31–37.
9. (1993) *Saccharomyces cerevisiae*, in *Current Protocols in Molecular Biology* (Ausubel, F. M., Brent, R., Kingston, R. E., Moore, D. D., Seidman, J. G., and Struhl, K., eds.), John Wiley & Sons, Inc., New York.
10. (2002) Guide to Yeast Genetics and Molecular Cell Biology, in *Methods in Enzymology*, Vol. 350 (Guthrie, C. and Fink, G. R., eds.), Academic Press, San Diego.
11. Marks, J. D., Hoogenboom, H. R., Bonnert, T. P., McCafferty, J., Griffiths, A. D., and Winter, G. (1991) By-passing immunization. Human antibodies from V-gene libraries displayed on phage. *J. Mol. Biol.* **222**, 581–597.
12. Griffiths, A. D., Malmqvist, M., Marks, J. D., et al. (1993) Human anti-self antibodies with high specificity from phage display libraries. *EMBO J.* **12**, 725–735.
13. Mummert, M. E. and Voss, E. W. Jr. (1996) Transition-state theory and secondary forces in antigen-antibody complexes. *Biochemistry* **35**, 8187–8192.
14. Lorimer, I. A. and Pastan, I. (1995) Random recombination of antibody single chain Fv sequences after fragmentation with DNaseI in the presence of Mn²⁺. *Nucleic Acids Res.* **23**, 3067–3068.
15. Zhao, H. and Arnold, F. H. (1997) Optimization of DNA shuffling for high fidelity recombination. *Nucleic Acids Res.* **25**, 1307–1308.

Fluorescence Resonance Energy Transfer-Based HIV-1 Virion Fusion Assay

Marielle Cavois, Jason Neidleman, Martin Bigos,
and Warner C. Greene

Summary

The fluorescence resonance energy transfer (FRET)-based HIV-1 virion fusion assay exploits the incorporation of β -lactamase-Vpr chimeric proteins into HIV-1 virions and their subsequent delivery into the cytoplasm of target cells as a marker of fusion. This transfer can be monitored by the enzymatic cleavage of the CCF2-AM dye, a fluorescent substrate of β -lactamase (BlaM), loaded into the target cells. BlaM cleavage of the β -lactam ring in CCF2-AM prevents the FRET between the coumarin and fluorescein moieties of the dye. This cleavage changes the fluorescence emission spectrum of CCF2-AM from green (520 nm) to blue (447 nm), and thus permits detection of fusion by fluorescence microscopy, flow cytometry, or UV photometry. This assay is simple and rapid to perform, and exhibits high sensitivity and specificity. Importantly, it can be applied to study HIV-1 virion fusion in primary cells and can be combined with immunostaining for subset discrimination in heterogeneous target cell populations. Finally, the assay can also be adapted to study fusion mediated by the envelope proteins from other viruses through the construction of HIV-1 pseudotypes.

Key Words

CCF2-AM, entry, flow cytometry, fluorescence resonance energy transfer, fusion, HIV-1, HIV-1-pseudotyped virions, β -lactamase, peripheral blood mononuclear cells, Vpr.

1. Introduction

The fluorescence resonance energy transfer (FRET)-based HIV-1 virion fusion assay is based on the incorporation of β -lactamase-Vpr chimeric proteins into HIV-1 virions and their subsequent delivery into the cytoplasm of target cells as a marker of fusion (**1**). This transfer can be monitored by the enzymatic cleavage of the CCF2-AM dye, a fluorescent substrate of β -lactamase

(BlaM), loaded into the target cells. BlaM cleavage of the β -lactam ring in CCF2-AM prevents the FRET between the coumarin and fluorescein moieties of the dye. This cleavage changes the fluorescence emission spectrum of CCF2-AM from green (520 nm) to blue (447 nm) and thus permits detection of fusion by fluorescence microscopy, flow cytometry, or UV photometry.

Heterologous proteins can be incorporated into the viral particle as chimera with Vpr (2–5). To incorporate BlaM into the HIV-1 virion, we constructed a chimera of BlaM linked to the N-terminus of Vpr. Because Vpr binds to the p6 component of the Gag polyprotein, BlaM-Vpr is specifically incorporated into the virions (*see Note 1*). Because fewer than 100 molecules of BlaM can be readily detected within a cell (6), the incorporation of several hundred BlaM-Vpr molecules into a virion is theoretically sufficient to allow the detection of the fusion of a single virion to the target cell.

An overview of the FRET-based HIV-1 virion fusion assay is shown **Fig. 1**. HIV-1 virions containing BlaM-Vpr are produced by cotransfection of proviral DNA and BlaM-Vpr expression vectors. These viral preparations are then used to infect target cells. The transfer of BlaM-Vpr during the fusion is revealed by monitoring the degradation of CCF2-AM dye loaded into the target cells. Because fusion is analyzed by flow cytometry, the assay can be combined with immunostaining for subset discrimination in heterogeneous target cell populations.

The fusion of the NL4-3 strain of HIV-1 to CD4⁺ T cells from peripheral blood lymphocytes (PBLs) will be used to illustrate the methods for production of virions containing BlaM-Vpr, the FRET-based HIV-1 virion fusion assay, and the analysis by flow cytometry (*see Note 2*).

2. Materials

2.1. Viral Production

1. pAdVantage (Promega, Madison, WI).
2. pCMV4-BlaM-Vpr (available on request from Dr. Greene, Gladstone Institute of Virology and Immunology, UCSF, San Francisco, CA).
3. pNL4-3 proviral DNA (AIDS Reagent Program, NIH, Bethesda, MD).
4. 293T cells (American Type Culture Collection, Manassas, VA).
5. 2X HEPES-buffered saline (HBS): 280 mM NaCl, 10 mM KCl, 1.5 mM Na₂HPO₄, 12 mM dextrose, 50 mM *N*-(2-hydroxyethyl)piperazine)-*N'*-(2-ethanesulfonic acid) (HEPES), pH 7.05. Store at –20°C.
6. 2 M CaCl₂.
7. Dulbecco's modified Eagle medium (DMEM) culture media: DMEM, 10% fetal bovine serum, 100 U/mL of penicillin, and 100 µg/mL of streptomycin.
8. Ultra-Clear polyallomer centrifuge tubes (25 × 89 mm) (Beckman Instruments, Palo Alto, CA).

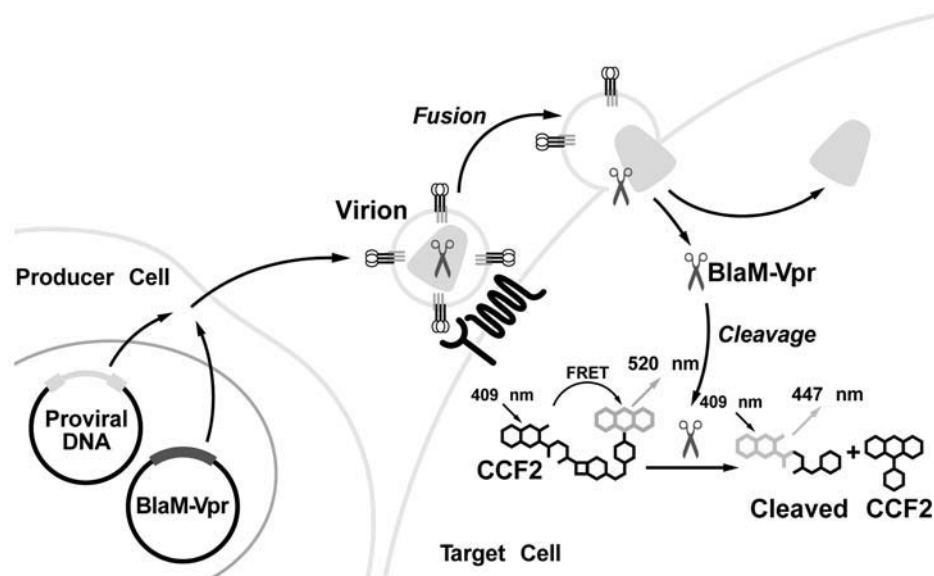


Fig. 1. Overview of the FRET-based HIV-1 virion fusion assay. Expression plasmids encoding an HIV provirus and a BlaM-Vpr chimera are coexpressed in 293T cells. Because Vpr binds to the p6 component of the Gag polypeptide, BlaM-Vpr is specifically incorporated into the virion. Target cells are infected with BlaM-Vpr virions and then loaded with CCF2-AM dye, which diffuses passively across the cell membrane. Inside the cell, CCF2-AM is de-esterified and trapped because of its polyanionic properties. CCF2-AM contains a cephalosporin ring linking a 7-hydroxycoumarin to fluorescein. Excitation of the coumarin at 409 nm causes FRET to the fluorescein, producing a green emission (520 nm). However, if the β -lactam ring in the cephalosporin moiety is cleaved by BlaM, FRET is blocked, and excitation of the coumarin yields a blue emission (447 nm) (6). Thus, the changes in CCF2-AM fluorescence reflect the presence of BlaM, introduced by virion fusion, within the target cells.

9. Ultracentrifugation equipment.
10. Alliance HIV-I p24 ELISA Kit (PerkinElmer Life Sciences, Boston, MA).

2.2. FRET-Based HIV-1 Fusion Assay

1. Peripheral blood lymphocytes.
2. RPMI culture media: RPMI, 10% fetal bovine serum, 100 U/mL of penicillin, and 100 μ g/mL of streptomycin.
3. 96-Well V-bottom plate (Corning Incorporated, Corning, NY).
4. CCF2-AM substrate and β -lactamase loading solutions (PanVera, Madison, WI).
5. CO₂-independent media (Gibco™-Invitrogen Corporation, Carlsbad, CA).
6. Probenecid (Sigma, St. Louis, MO).

7. Fluorescence-activated cell sorting (FACS) staining buffer: 1X phosphate-buffered saline (PBS) and 2% fetal bovine serum. Store at 4°C.
8. Mouse antihuman CD3 conjugated to APC, mouse antihuman CD4 conjugated to PE-Cy7, and mouse antihuman CD8 conjugated to APC-Cy7 (BD Biosciences, San Jose, CA).
9. 16% Paraformaldehyde (Electron Microscopy Sciences, Ft. Washington, PA).

2.3. Analysis by Flow Cytometry

1. Flow cytometer: The FRET-based HIV-1 virion fusion assay alone requires a flow cytometer that incorporates violet laser excitation (violet-enhanced krypton or violet diode) and two measurement parameters on signals excited by that laser (*see Note 3*). Measurement of immunophenotypes requires an additional red laser capable of exciting allophycocyanin (APC) and/or APC-Cy7 and the associated detection system. For this assay, we used a FACSVantage SE with three-laser option (BD Biosciences) including: Innova I-70 argon laser (run at 200 mW, 488 nm), an Innova Spectrum krypton laser (200 mW, 647 nm), and Innova I-302 violet-enhanced krypton laser (200 mW, 407 nm) (all from Coherent, Santa Clara, CA). The detection system employed the following bandpass filters: CCF2-AM blue = HQ445/50, CCF2-AM green = HQ545/90, PE-Cy7 = 740 LP, APC = HQ695/65, and APC-Cy7 = 740 LP (all from Chroma Technology, Rockingham, VT).
2. Software for data analysis: FlowJo 4.3 software (Tree Star, San Carlos, CA).

3. Methods

The methods described in the following subheadings outline: (1) the production of HIV-1 virions containing BlaM-Vpr, (2) the FRET-based HIV-1 virion fusion assay, and (3) the analysis by flow cytometry.

3.1. Production of NL4-3 Virions Containing BlaM-Vpr

This section outlines the optimal procedure for producing NL4-3 virions containing BlaM-Vpr.

3.1.1. Transfection of 293T Cells With Proviral DNA, pCMV4-BlaM-Vpr, and pAdVantage

The transfections are performed using calcium phosphate for precipitation of DNA.

1. Plate 1.5×10^7 293T cells in 40 mL of DMEM culture media in a T175-cm² tissue culture flask and culture overnight at 37°C in a 5% CO₂ humidified incubator.
2. Generate the DNA precipitate.
 - a. Prepare 1.75 mL of H₂O containing 60 µg of pNL4-3 proviral DNA, 20 µg of pCMV-BlaM-Vpr, and 10 µg of pAdVantage vectors (*see Note 4*).
 - b. Slowly add 2 mL of 2X HBS and mix gently by pipetting up and down.
 - c. Add 250 µL of 2 M CaCl₂ drop by drop.
 - d. Incubate 30 min at room temperature to precipitate the DNA.

3. Replace the 293T cell culture media with 40 mL of fresh DMEM culture media prewarmed to 37°C.
4. Slowly add 4 mL of DNA precipitate and incubate for 16 h at 37°C.
5. Replace the media with 40 mL of fresh DMEM culture media prewarmed to 37°C.
6. Incubate for 24 h at 37°C.

3.1.2. Harvest Viral Supernatant and Concentrate the Viral Preparation by Ultracentrifugation

To allow more flexibility in the use of the FRET-based HIV-1 virion fusion assay, viral preparations are concentrated by ultracentrifugation (*see Note 5*).

1. Harvest the supernatant of the transfected 293T cells into a 50-mL Falcon tube.
2. Centrifuge the supernatant at 800g at room temperature for 10 min to remove the cellular debris.
3. Transfer 36 mL of virion-containing supernatant to Ultra-Clear centrifuge tubes.
4. Place the tube in the bucket of the SW28 rotor and balance the tube with DMEM culture media if necessary.
5. Ultracentrifuge (72,000g, 90 min) at 4°C without using brakes.
6. Remove the supernatant, resuspend the viral pellet in 1 mL of DMEM, divide into 100-μL aliquots, and store at -80°C (*see Note 6*).

3.1.3. Quantify p24^{Gag} Content of the Viral Preparation by Enzyme-Linked Immunosorbent Assay

The p24^{Gag} content of the viral preparations is quantified using the Alliance HIV-I p24 ELISA Kit according to the manufacturer's instructions. Viral production after ultracentrifugation ranges from 20–50 μg of p24^{Gag}/mL.

3.2. FRET-Based HIV-1 Virion Fusion Assay

The virion-based fusion assay is performed in three steps: (1) incubation of target cells with NL4-3 virions containing BlaM-Vpr, (2) loading of target cells with the CCF2-AM substrate and development of the BlaM reaction, and (3) immunostaining and fixation.

3.2.1. Incubation of Target Cells With NL4-3 Virions Containing BlaM-Vpr

1. Wash the PBLs with RPMI culture media.
2. Count PBLs and make a suspension 2×10^7 cells/mL in RPMI culture media.
3. Divide the cell suspension in aliquots of 100 μL (2×10^6 cells) per condition to be tested in a V-bottom 96-well plate. Include four additional wells for compensation when the FRET-based HIV-1 virion fusion assay is performed in conjunction with immunostaining (*see Subheading 3.2.3.*).
4. Add a quantity of NL4-3 virions containing BlaM-Vpr equivalent to 400 ng of p24^{Gag} and incubate for 2 h at 37°C.

3.2.2. Loading of Target Cells With the CCF2-AM Substrate and Development of the BlaM Reaction

1. Prepare 1 mL of loading solution according to the PanVera protocol summarized below.
 - a. Resuspend CCF2-AM in dimethylsulfoxide to generate a stock solution (1 mM CCF2-AM). Divide into aliquots and store in the dark at -80°C .
 - b. Mix by vortex-mixing 1 μL of 1 mM CCF2-AM with 9 μL of a solution containing 100 mg/mL of Pluronic-F127 and 0.1% acetic acid (solution B provided by Panvera with the CCF2-AM).
 - c. Add 1 mL of CO_2 -independent media and vortex again.
2. Prepare 1 mL of development media (2.5 mM probenecid, 10% fetal bovine serum in CO_2 -independent media).
 - a. Prepare a stock solution of probenecid (250 mM) in 250 mM NaOH. Divide into aliquots and store at -20°C .
 - b. Dilute 10 μL of the stock solution of probenecid in 1 mL of CO_2 -independent media.
 - c. Add 100 μL of fetal bovine serum.
 - d. Vortex-mix.
3. Collect the cells by centrifugation at 800g for 5 min at room temperature.
4. Wash the cells once with 200 μL of CO_2 -independent media and centrifuge at 800g for 5 min at room temperature.
5. Resuspend the pellet in 100 μL of CCF2-AM loading solution and incubate for 1 h at room temperature in the dark.
6. Collect the cells by centrifugation at 800g for 5 min at room temperature.
7. Wash the cells with 200 μL of development media and centrifuge at 800g for 5 min at room temperature.
8. Resuspend the pellet in 200 μL of development media and incubate the cells at room temperature for 16 h in the dark.

3.2.3. Immunostaining and Fixation

The FRET-based HIV-1 virion fusion assay can be combined with immunostaining to further characterize cellular populations in which HIV-1 fusion has occurred (*see Note 7*). This immunostaining step can be skipped when HIV-1 fusion is analyzed in cell lines or in purified cellular populations. As an example, the FRET-based HIV-1 fusion assay will be followed by immunostaining with antihuman CD3 conjugated to APC, antihuman CD4 conjugated to PE-Cy7, and antihuman CD8 conjugated to APC-Cy7. The compensations are set on uninfected samples, which are loaded with CCF2-AM and singly stained with each antibody.

1. Collect the cells by centrifugation at 800g for 5 min at 4°C .
2. Wash the cells once by addition of 200 μL of FACS staining buffer.

3. Collect the cells by centrifugation at 800g for 5 min at 4°C and resuspend the pellet in 50 μ L of immunostaining solution (in FACS staining buffer) containing a 1:100 dilution of anti-CD3-APC, a 1:50 dilution of anti-CD4-PE-Cy7, and a 1:50 dilution of anti-CD8-APC-Cy7. For the four compensation controls, use FACS staining buffer alone, or with a 1:100 dilution of anti-CD3-APC, a 1:50 dilution of anti-CD4-PE-Cy7, or a 1:50 dilution of anti-CD8-APC-Cy7 (see **Note 8**).
4. Incubate for 30 min at 4°C.
5. Collect the cells by centrifugation at 800g for 5 min at 4°C.
6. Wash the cells twice with 200 μ L of FACS staining buffer.
7. Fix the cells in 1.2% paraformaldehyde for 2 h at 4°C (see **Note 9**).

3.3. Data Collection by Flow Cytometry and Analysis With FlowJo Software

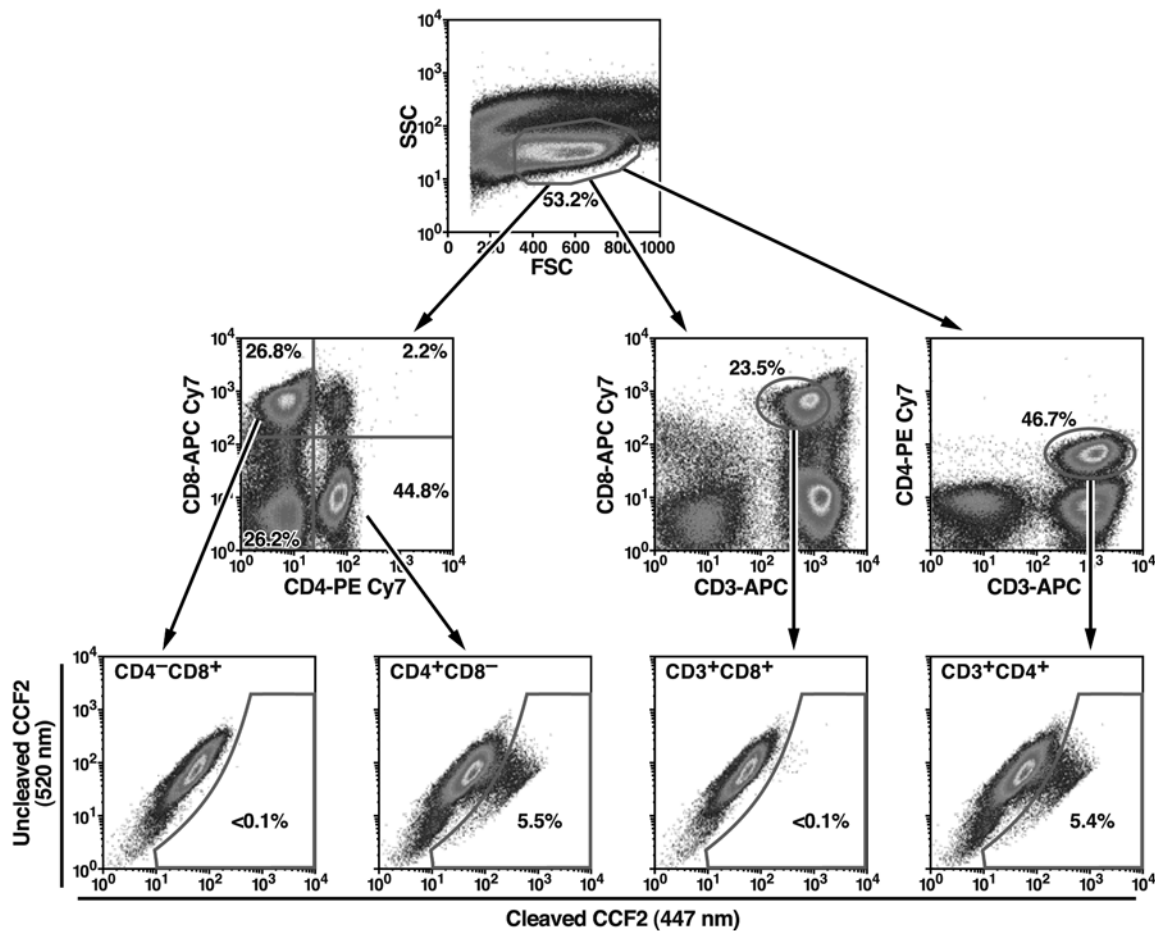
The FACSVantage SE was configured as follows. The FL1 and FL2 electronic measurement channels were connected to the third laser (violet krypton) detectors to record CCF2-AM blue and green signals. The FL6 electronic measurement channel was connected to the first laser (488-nm argon) detector to measure PE-Cy7. FL4 and FL5 were used in the standard second laser (647-nm krypton) position to measure APC and APC-Cy7. All fluorescence detection uses log amplification. Forward scatter from the first laser is used to trigger the instrument, and the combination of forward scatter and side scatter from the first laser is used to delineate the cells of interest.

3.3.1. Data Collection by Flow Cytometry

1. Adjust forward and side scatter to place the cells of interest on scale.
2. Adjust the PMT voltages of the green and blue (third laser) detectors so that these cells are roughly mid-scale. This is done using the uninfected samples loaded with CCF2-AM only. The population is organized on a diagonal reflecting the constant ratio of blue to green fluorescence. When immunophenotyping is done as well, the autofluorescence of the cells in the PE-Cy7, APC, and APC-Cy7 measurement channels is set to encompass the first decade of the log scale. Then, the CCF2-AM loaded samples and immunostained anti-CD3-APC, anti-CD8-APC-Cy7, or anti-CD4-PE-Cy7 alone are run to set the compensation between FL4 and FL5, and to provide controls for software compensation between PE-Cy7 and APC-Cy7.
3. Finally, analyze the infected samples. Upon infection, the ratio of blue to green increases and part of the population shifts toward a higher ratio of blue to green fluorescence.

3.3.2. Analysis With FlowJo Software

The data can be analyzed with FlowJo software. If required, the software allows compensation between APC-Cy7 and PE-Cy7. **Figure 2** shows the typ-



ical data obtained with NL4-3 containing BlaM-Vpr used to infect PBLs, and suggests a gating strategy for analysis of this data.

4. Notes

1. BlaM-Vpr is efficiently incorporated into virions even when the HIV proviral clone retains the Vpr gene. This finding extends the use of the FRET-based HIV-1 fusion assay to many different wild-type HIV proviruses.
2. Multiple cell lines and various primary cell types, including macrophages and HUVEC, have been successfully used in the assay. However, certain cell lines, for example MAGI cells, exhibit endogenous BlaM activity and thus are not suitable for analysis. One of the vectors used to express a transgene in this cell line likely encodes an enzyme that degrades the CCF2-AM substrate. In such case, a portion of the cells is already shifted to high ratio of blue to green of fluorescence in absence of viral infection. Therefore, to rule out endogenous BlaM activity, new cell types should be tested by loading the cells with CCF2-AM and following the protocol described in **Subheading 3.2.2.**
3. The original papers describing CCF2-AM (6,7) used UV excitation for CCF2-AM fluorescence readout. However, there was a limitation of this approach due to excitation mismatch between the laser line (355 nm) and CCF2-AM, and the high autofluorescence of cells generated by the UV light. Using a krypton 406.7-nm line provides optimal excitation and a lower autofluorescence signal from cells. However, this laser is quite expensive and not commonly available. Subsequent tests have demonstrated that excitation with a relatively inexpensive 20-mW solid-state violet diode laser in a cuvet flow system that is now commercially available yields equivalent results.
4. The assay can also be conveniently adapted to study fusion mediated by the envelope proteins from other viruses through the construction of HIV-1 pseudotypes. The pseudotyped HIV-1 virions containing BlaM-Vpr are produced as described in **Subheadings 3.1.1.–3.1.3.** with minor modifications. The DNA precipitate is prepared with 40 μ g of Δ env pNL4-3 proviral DNA, 20 μ g of an envelope encoding construct (VSV-G, A-MLV or other), 20 μ g of pCMV-BlaM-Vpr, and 10 μ g of pAdVantage vectors. Fusion of these pseudotyped virions will occur according to the pathway dictated by the envelope and will be sensitive to the inhibitor of fusion corresponding to this envelope.

Fig. 2. (*see opposite page*) Analysis of HIV-1 fusion to PBLs by the FRET-based HIV-1 virion fusion assay. PBLs (2×10^6 cells) were infected for 2 h with NL4-3 virions containing BlaM-Vpr (400 ng of p24^{Gag}). After CCF2-AM dye loading and incubation for 16 h at room temperature to allow the BlaM cleavage of the substrate, the cells were immunostained with anti-CD3 antibodies conjugated to APC, anti-CD8 antibodies conjugated to APC-Cy7 and anti-CD4 conjugated to PE-Cy7. Fusion events were analyzed in the CD4⁺CD8⁺, CD4⁺CD8⁻, CD3⁺CD4⁺, and CD3⁺CD8⁺ subpopulations of lymphocytes. Percentages represent cells displaying increased blue fluorescence.

5. Viral supernatant from transfected 293T cells can be used directly to infect the target cells. However, because the FRET-based HIV-1 virion fusion assay is a single-round infection assay, fusion will occur in fewer target cells. The infection rates could be further improved by using the “spinoculation” protocol (8).
6. Frozen viral preparations are stable for at least 2 yr at -80°C . They can be thawed and frozen three times without significant loss of infectivity. However, to compare the fusion proprieties of different viral preparations, we recommend using virions that were produced in parallel and subjected to equivalent cycles of thawing/freezing.
7. As pointed out, CCF2-AM is a tandem conjugate of coumarin and fluorescein. The fluorescein component of the substrate excites quite well with the standard 488-nm argon line used in most flow cytometers. Because of the amount of substrate typically loaded in a cell, the resulting fluorescence from fluorescein is bright in the PE, PE-TR, and PE-Cy5 measurement channels. Fluorochromes excited by a red laser (APC, APC-Cy5.5, APC-Cy7, and red-emitting Alexa dyes) are not affected by this problem.
8. When fusion is analyzed in T-cell lines, the shift toward a high ratio of blue fluorescence is more pronounced when the cells have been maintained in 1.2% paraformaldehyde for 6 h. Further incubation in paraformaldehyde had no additional effect. The shift remains the same for at least 24 h.
9. The specified antibody dilutions were optimal for our conditions. However, reagents from different lots and different manufacturers may vary. The optimal dilution should be determined beforehand by performing a titration experiment for each reagent (9).

References

1. Cavrois, M., De Noronha, C., and Greene, W. C. (2002) A sensitive and specific enzyme-based assay detecting HIV-1 virion fusion in primary T lymphocytes. *Nat. Biotechnol.* **20**, 1151–1154.
2. Liu, H., Wu, X., Xiao, H., and Kappes, J. C. (1999) Targeting human immunodeficiency virus (HIV) type 2 integrase protein into HIV type 1. *J. Virol.* **73**, 8831–8836.
3. Muthumani, K., Montaner, L. J., Ayyavoo, V., and Weiner, D. B. (2000) Vpr-GFP virion particle identifies HIV-infected targets and preserves HIV-1Vpr function in macrophages and T-cells. *DNA Cell Biol.* **19**, 179–188.
4. Schaeffer, E., Geleziunas, R., and Greene, W. C. (2001) Human immunodeficiency virus type 1 Nef functions at the level of virus entry by enhancing cytoplasmic delivery of virions. *J. Virol.* **75**, 2993–3000.
5. McDonald, D., Vodicka, M. A., Lucero, G., et al. (2002) Visualization of the intracellular behavior of HIV in living cells. *J. Cell Biol.* **159**, 441–452.
6. Zlokarnik, G., Negulescu, P. A., Knapp, T. E., et al. (1998) Quantitation of transcription and clonal selection of single living cells with beta-lactamase as reporter. *Science* **279**, 84–88.

7. Tsien, R. Y. and Miyawaki, A. (1998) Seeing the machinery of live cells. *Science* **280**, 1954–1955.
8. O'Doherty, U., Swiggard, W. J., and Malim, M. H. (2000) Human immunodeficiency virus type 1 spinoculation enhances infection through virus binding. *J. Virol.* **74**, 10,074–10,080.
9. Owens, M. A. and Loken, M. R. (1995) *Flow Cytometry Principles for Clinical Laboratory Practice*, Wiley-Liss, New York, pp. 65–67.

19

Cell-Cycle Analysis of Asynchronous Populations

Michael G. Ormerod

Summary

Cells are incubated continuously in bromodeoxyuridine (BrdUrd), which is incorporated into cells synthesizing DNA. At intervals, cells are harvested and nuclei are prepared and stained with a *bis*-benzimidazole, Hoechst 33258, and propidium iodide. In the flow cytometer, the dyes are excited by UV and blue and red fluorescences recorded. BrdUrd quenches the blue fluorescence of the Hoechst dye. The degree of quenching records the progress of the cell through S phase(s); the red (PI) fluorescence yields the cell cycle phases. By this means, the progress of cells around the cell cycle can be followed and the effects of cytotoxic drugs, radiation, and other treatments observed.

Key Words

Bromodeoxyuridine, flow cytometry, Hoechst 33258, proliferation.

1. Introduction

Measurement of a DNA histogram can be achieved by fixing or permeabilizing cells and staining them with a DNA-binding dye, such as propidium iodide (PI). The histogram will yield the percentage of cells in the G_1 , S, and G_2/M phases of the cell cycle (*1*). Although some inferences about the movement of cells through the cycle may be drawn, the information gained is essentially static. For example, it is not known whether a cell with S-phase DNA content is actually synthesizing DNA; also, the presence of subpopulations with different cycle times cannot be detected.

Dynamic information about cell cycle progression can be obtained by labeling cells with 5'-bromodeoxyuridine (BrdUrd) which is incorporated into DNA

in place of thymidine. Detection of BrdUrd in the DNA allows the fraction of cells in S-phase to be enumerated and, if samples are taken at different time intervals, also gives information about the cell cycle kinetics.

Three methods have been used. After the application of a pulse-label, monoclonal antibodies that react specifically with BrdUrd reveal those cells that are in S-phase. Counterstaining with PI shows the cell cycle. If cells are harvested at times after the application of the pulse-label, the movement of labeled cells through the cell cycle can be followed. This method has been applied *in vitro* (2) and *in vivo* (3,4). The other two methods exploit the observation of Latt that the fluorescence of *bis*-benzimidazoles (Hoechst 33342 and 33258) bound to DNA is quenched by BrdUrd (5). One method, in which the cells are pulse-labeled and then stained with a combination of Hoechst 33258 and mithramycin, requires a dual-laser flow cytometer and a complex analysis in which fluorescence signals are subtracted in real time (6). In the method described in this chapter, cells are continuously labeled with BrdUrd, permeabilized, and stained with Hoechst 33258 and PI. The quenching of Hoechst/DNA fluorescence reveals whether the cells have incorporated BrdUrd; the PI/DNA fluorescence (unaffected by BrdUrd) gives the cell cycle phase. This method was originally applied to quiescent cells that had been stimulated into the cell cycle (7). It can also be applied to asynchronous populations of cells (8). Although the data analysis is more complex, a wealth of information can be derived. In particular, cell cycle specific effects of toxic treatments can be observed without resorting to artificial cell synchronization (8–16).

It should be noted that, in all three methods, the cells have to be fixed or permeabilized to allow access of reagents to the DNA. Analysis of viable cells is not possible. In addition, for the antibody method, the DNA of the cells has to be partially denatured to allow access of the antibody to the BrdUrd incorporated into the DNA.

In the method described here, BrdUrd is added and cells are harvested at fixed time intervals, typically, every 4 h for 36 h. Samples may be collected and the cells frozen prior to analysis. For analysis, cells are suspended in a buffer containing Hoechst 33258 and a detergent, which releases the nuclei, and PI is then added. Hoechst 33258 is excited in the UV and the analysis requires a flow cytometer equipped with a source of UV light.

2. Materials

1. 5'-Bromo-2'-deoxyuridine (BrdUrd) (Sigma [St. Louis, MO], cat. no. B5002): Make up a stock solution of 10 mM. Store frozen.
2. Hoechst 33258 (Sigma, cat. no. B2883 or Molecular Probes [Eugene, OR], cat. no. H-1398).

3. Propidium iodide (Sigma, cat. no. P4170 or Molecular Probes, cat. no. P-1304): Make up a stock solution of 100 $\mu\text{g/mL}$ in distilled water. Store in the dark at 4°C. Stable for at least 6 mo.
4. Staining solution: 100 mM Tris-HCl, pH 7.4, 154 mM NaCl, 1 mM CaCl_2 , 0.5 mM MgCl_2 , 0.1% (v/v) Nonidet-P40, 0.2% (w/v) bovine serum albumin (BSA), and 1.2 $\mu\text{g/mL}$ of Hoechst 33258. Make up at 10X final strength and store in the dark at 4°C. The solution is stable for at least 6 mo. Batches of staining buffer can be prepared weekly from the 10X concentrated stock solution in distilled water.

3. Methods

3.1. Analysis of Cells

1. If desired, treat the cells (radiation, drug, heat, and so on).
2. Immediately after the treatment, add a suitable concentration of BrdUrd to the cell culture (see **Notes 1–3**).
3. At fixed time intervals (3–8 h, depending on the cell cycle time), harvest an aliquot of cells (see **Notes 4–6**).
4. Centrifuge the cells and resuspend in 500 μL of ice-cold staining buffer. Briefly vortex mix. Stand on ice for 15 min.
5. Add 10 μL of PI solution. Briefly vortex mix. Store on ice (see **Notes 7 and 8**).
6. Analyze on the flow cytometer recording red (PI/DNA) and blue (Hoechst/DNA) fluorescences. Adjust the flow rate to about 500 particles/s. If possible, perform a pulse shape analysis on the red fluorescence signal and gate to exclude any clumped nuclei (**1**) (see **Fig. 1**). Display a cytogram of red vs blue fluorescence (see **Notes 9–12**).

3.2. Data Analysis

Figure 2 shows cytograms obtained from an untreated human embryonic fibroblast cell line (MRC5/34). At time 0, G_1 , S, and G_2/M phases of the cell cycle could be identified from both the red (PI) and blue (Hoechst) fluorescence. When the cells were incubated in 40 μM of BrdUrd, as the cells progressed through S-phase, their red fluorescence increased but their blue fluorescence (which was partially quenched by BrdUrd) did not change. After 4 h in BrdUrd, there had been a small progression giving the S-phase a slight bow shape on a plot of red vs blue fluorescence. At 8 h, the bow shape was more pronounced; also many of the cells originally in G_2/M had divided and moved into G_1 (unlabeled). At 16 h, all the cells in S-phase at time 0 h had reached G_2 (labeled G_2^*) and a few had divided (G_1^*). Some of the cells which had been in G_1 at time 0 h were now in S-phase (Sf); some had progressed as far as G_2/M (G_2f). By 28 h, some cells that began the experiment in G_2 had completed a cell cycle and returned to G_1 again (labeled G_1').

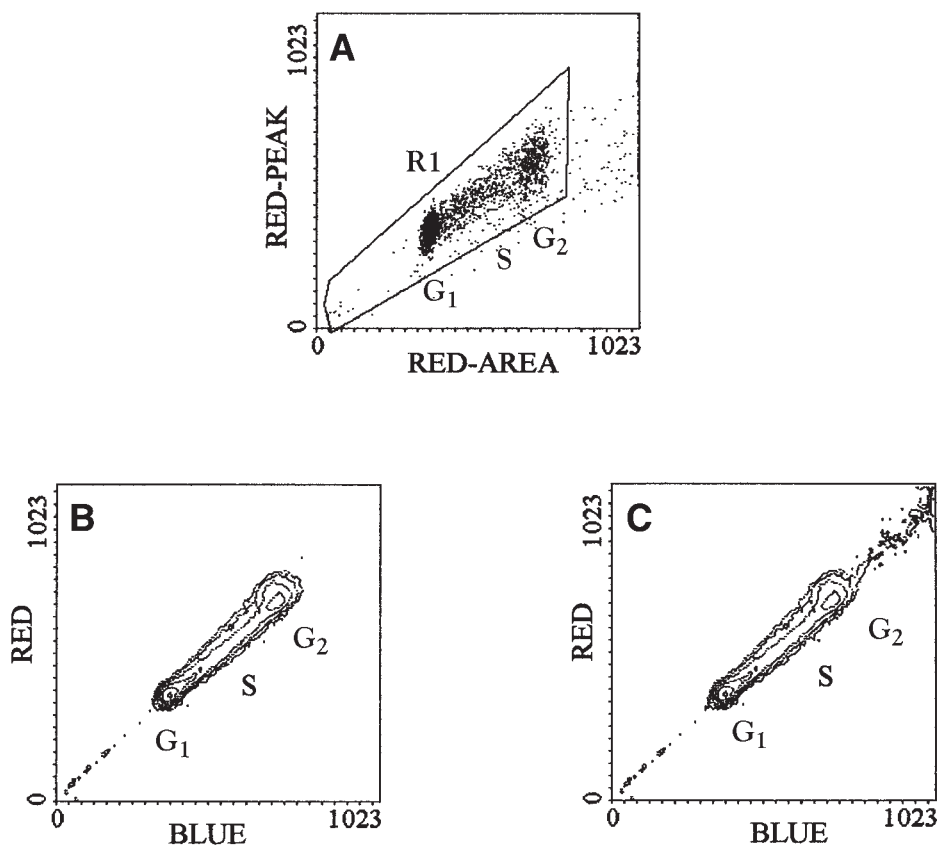


Fig. 1. Hoechst 33258-PI analysis of nuclei from a human embryonic fibroblast cell (MRC5/34) without incubation in BrdUrd. (A) PI/DNA fluorescence (red) showing a cytogram of the peak of the red fluorescence signal vs the integrated area. A gate has been set to include single nuclei and to exclude clumps. The cytogram is displayed as a "dot-plot." (B,C) Hoechst/DNA (blue) vs PI/DNA (red) fluorescence. (cytograms displayed as contour plots). The cytogram in (C) shows ungated data; that in (B) shows the effect of gating on region, R1, in cytogram (A). Cells prepared by Dr. David Gilligan and data recorded by Mrs. Jenny Titley on a Coulter Elite ESP using a Spectra-Physics argon-ion laser tuned to produce 100 mW in the UV. Red (>630 nm) and blue (460 nm) fluorescence were measured. Data were acquired on an IBM-PC compatible computer and the figure was prepared using the WINMDI program supplied by Dr. Joe Trotter (Salk Institute, and BD Biosciences, USA).

Figures 3–5 illustrate typical effects of cell cycle perturbation. **Figure 3** shows MRC5/34 cells that had been given 5 Gy γ -radiation immediately prior to addition of the BrdUrd. The cells suffered a G_2 block. Cells that were irradiated

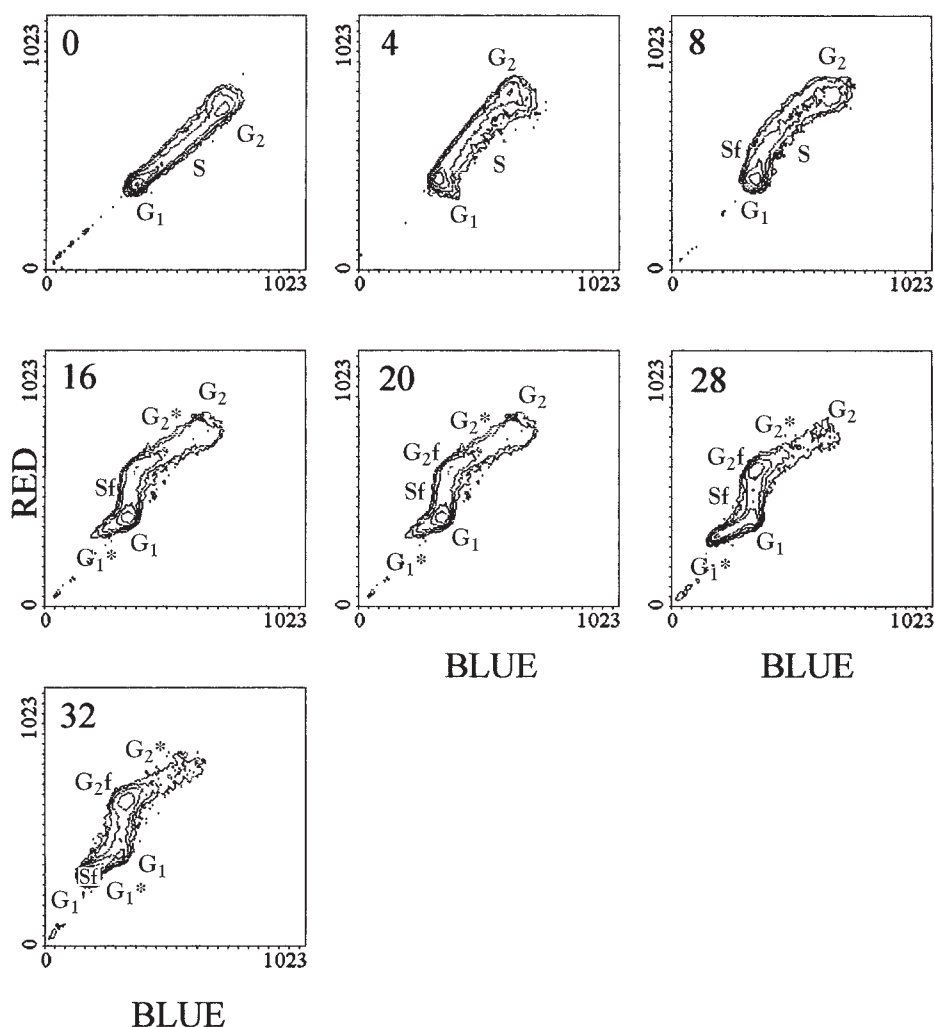


Fig. 2. Cytograms of PI-DNA (red) vs Hoechst 33258-DNA fluorescence of nuclei from MRC5/34 cells incubated in 40 μ M BrdUrd and 40 μ M deoxycytidine BrdUrd for the times shown on the panels. Other details as in **Fig. 1**. For a description of the data, see the main text.

in all phases of the cell cycle had become arrested in G₂. (Compare **Fig. 3** to **Fig. 2**, 32 h time point). **Figure 4** shows W1L2 cells (human lymphoblastoid cell line) that had been incubated with cisplatin for 2 h before adding BrdUrd. Only cells treated with drug in G₁ and early S-phase were arrested in G₂. The other cells had divided. **Figure 5** shows a human medulloblastoma cell line

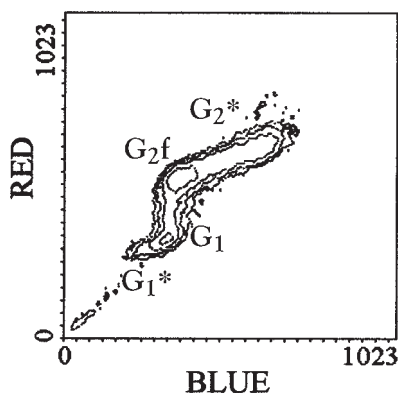


Fig. 3. A cytogram of PI-DNA (red) vs Hoechst 33258-DNA fluorescence of nuclei from MRC5/34 cells given 5 gy γ -radiation and then incubated in 40 μ M BrdUrd and 40 μ M deoxycytidine BrdUrd for 32 h. Other details as in **Fig. 1**. For a description of the data, see the main text.

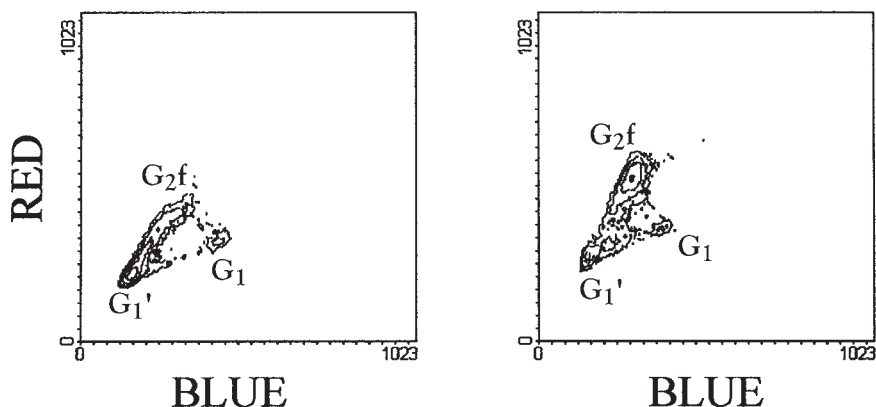


Fig. 4. Cytograms of PI-DNA (red) vs Hoechst 33258-DNA fluorescence of nuclei from WIL2 (human lymphoblastoid cell line) cells either untreated (**left**) or incubated for 2 h with 20 μ M cisplatin (**right**) and then incubated in 40 μ M BrdUrd for 24 h. Experiment run by the author. Other details as in **Fig. 1**.

(D283) that underwent a G_1 block after γ -radiation. Only a proportion of the cells in G_1 became blocked in G_1 , some of the G_1 cells progressed through the cycle and divided (in compartment G_1'). Presumably these were cells irradiated in the late G_1 phase.

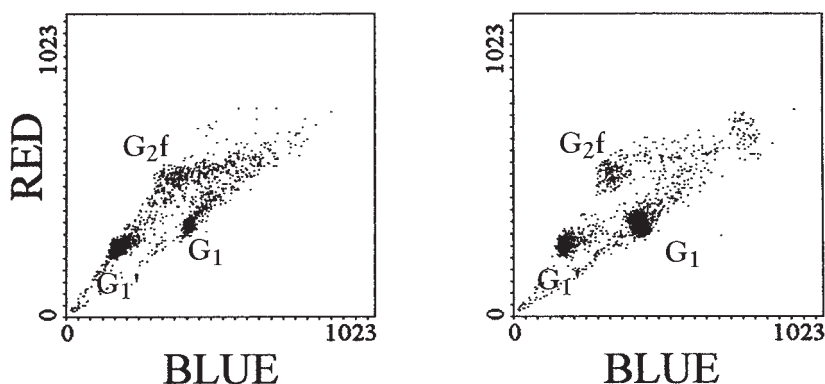


Fig. 5. Cytograms of PI-DNA (red) vs Hoechst 33258-DNA fluorescence of nuclei from a medulloblastoma cell line (D283) either untreated (**left**) or given 8 Gy γ -radiation (**right**) and then incubated in 40 μ M BrdUrd and 40 μ M deoxycytidine BrdUrd for 32 h. Cells prepared by Mrs. Cyd Bush. Other details as in Fig. 1.

4. Notes

1. The correct concentration of BrdUrd must be determined by a preliminary experiment. The concentration should be such that cells in G_1 after one round of replication have about half the blue fluorescence of unlabeled cells in G_1 .
2. Concentrations of BrdUrd vary from 10 to 100 μ M. If the concentration of BrdUrd is $>20 \mu$ M, the BrdUrd may become exhausted by 24 h. The remedy is to either work at a lower cell density or to replenish the BrdUrd every 12 h.
3. A trial experiment should be performed to check that the incorporation of BrdUrd into the DNA is not inhibiting the progression of the cells through the cycle. After different times of incubation with BrdUrd, fix cells in 70% ethanol, centrifuge and resuspend in phosphate-buffered saline containing 20 μ g/mL of PI and 0.1 mg/mL of RNase. Incubate at 37°C for 1 h and record the DNA histogram. Addition of deoxycytidine (equimolar with the BrdUrd) can reduce any deleterious effect of BrdUrd.
4. For suspension cultures, shake to resuspend cells and remove 3 mL. For adherent cell cultures, use a separate flask for each time point. Harvest the cells by a short incubation with trypsin.
5. After harvesting, cells can be frozen and stored for later analysis.
6. The detergent in the staining buffer releases nuclei. At this stage, the samples are stable for several hours on ice.
7. The cell concentration is important and should be between 5×10^5 and 2×10^6 . If the concentration is too high, the nuclei will be understained and may give distorted cytograms.

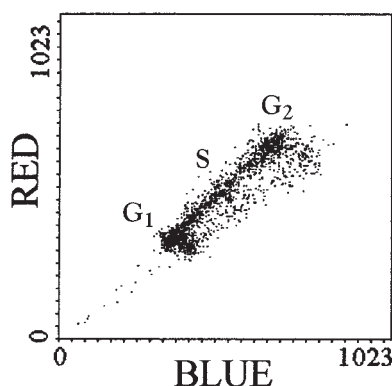


Fig. 6. A cytogram of PI-DNA (red) vs Hoechst 33258-DNA fluorescence of nuclei from MRC5/34 cells. The cells had not lysed completely. The nuclei and the partially lysed cells stained slightly differently, creating a “shadow” in the cytogram. Experimental details as in **Fig. 1**.

8. Either PI, ethidium bromide (EB), or 7-aminoactinomycin D (7-AAD) may be used as a counterstain for DNA. 7-AAD has to be excited at 488 nm using a second argon-ion laser tuned to this wavelength.
9. When setting a gate on a plot of DNA-peak signal vs DNA-area, be careful to include material of DNA content less than that of cells in G_1 .
10. If it is not possible to perform a pulse shape analysis, clumps may usually be differentiated on a cytogram of forward light scatter vs red fluorescence.
11. A PI/DNA complex is excited by UV. It also absorbs blue light and will be excited by energy transfer from the Hoechst dye. When the Hoechst fluorescence is quenched, there will be a consequent reduction in PI fluorescence. If a helium-cadmium (He-Cd) laser is used as a source of UV (325 nm) (rather than an argon-ion laser, 360–390 nm), direct absorption will predominate and the secondary quenching will be reduced. For this reason, it is preferable to use a He-Cd laser (17). Alternatively, if a dual laser instrument is being used, 7-AAD can be used as the DNA stain (16).
12. If the pattern produced from the sample at 0 h has a “shadow” (see **Fig. 6**), the cells have not lysed properly. Incubate the samples at 37°C for 5 min and re-run.

Acknowledgments

I thank Mrs. Jenny Titley, Dr. David Gilligan, and Mrs. Cyd Bush, Institute of Cancer Research, Sutton, England, for supplying the data used to illustrate this chapter. Their work was supported by the Cancer Research Campaign.

References

1. Ormerod, M. G. (2000) Analysis of DNA—general methods, in *Flow Cytometry. A Practical Approach*, 3rd edit. (Ormerod, M. G., ed.), IRL Press at Oxford University Press, Oxford, UK, pp. 83–97.
2. Dolbeare, F. A. Gratzner, H. G., Pallavicini, M. G., and Gray, J. W. (1983) Flow cytometric measurement of total DNA content and incorporated bromodeoxyuridine. *Proc. Natl. Acad. Sci. USA* **80**, 5573–5577.
3. Begg, A. C., McNally, N. J., Shrieve, D. C., and Karcher, H. (1985) A method to measure the duration of DNA synthesis and potential doubling time from a single sample. *Cytometry* **6**, 620–626.
4. Wilson, G. D. (2000) Analysis of DNA—measurement of cell kinetics by the bromodeoxyuridine/anti-bromodeoxyuridine method, in *Flow Cytometry. A Practical Approach*, 3rd edit. (Ormerod, M. G., ed.), IRL Press at Oxford University Press, Oxford, UK, pp. 159–177.
5. Latt, S. A. (1973) Microfluorometric detection of deoxyribonucleic acid replication in human metaphase chromosomes. *Proc. Natl. Acad. Sci. USA* **70**, 3395–3399.
6. Crissman, H. A. and Steinkamp, J. A. (1987) A new method for rapid and sensitive detection of bromodeoxyuridine in DNA replicating cells. *Exp. Cell Res.* **173**, 256–261.
7. Rabinovitch, P. S., Kubbies, M., Chen, Y. C., Schindler, D., and Hoehn, H. (1988) BrdU-Hoechst flow cytometry. A unique tool for quantitative cell cycle analysis. *Exp. Cell Res.* **74**, 309–318.
8. Ormerod, M. G. and Kubbies, M. (1992) Cell cycle analysis of asynchronous cells by flow cytometry using bromodeoxyuridine label and Hoechst-propidium iodide stain. *Cytometry* **13**, 678–685.
9. Ormerod, M. G., Imrie, P. R., Loverock, P., and Ter Haar, G. (1991) A flow cytometric study of the effect of heat on kinetics of cell proliferation of Chinese hamster V79 cells. *Cell Prolif.* **25**, 41–51.
10. Ormerod, M. G., Orr, R. M., and Peacock, J. H. (1994) The role of apoptosis in cell killing by cisplatin, a flow cytometric study. *Br. J. Cancer* **69**, 93–100.
11. Poot, M. and Ormerod, M. G. (2000) Analysis of proliferation using the bromodeoxyuridine-Hoechst/ethidium bromide method, in *Flow Cytometry. A Practical Approach*, 3rd ed. (Ormerod, M. G., ed.), IRL Press at Oxford University Press, Oxford, UK, pp. 179–188.
12. Gilligan, D., Mort, C., McMillan, T. J., Peacock, J. H., Titley, J., and Ormerod, M. G. (1996) Application of a bromodeoxyuridine-Hoechst/ethidium bromide technique for the analysis of radiation-induced cell cycle delays in asynchronous populations. *Int. J. Rad. Biol.* **69**, 251–257.
13. Ormerod, M. G., Orr, R. M., O'Neill, C. F., et al. (1996) The cytotoxic action of four ammine/amine platinum(IV) dicarboxylates: a flow cytometric study. *Br. J. Cancer* **74**, 1935–1943.

14. Skelton, L. A., Ormerod, M. G., Titley, J. C., and Jackson, A. L. (1998) Cell cycle effects of CB30865, a lipophilic quinazoline-based analogue of the antifolate thymidylate synthase inhibitor ICIn 198583 with an undefined mechanism of action. *Cytometry* **33**, 55–66.
15. Poot, M., Silber, J. R., and Rabinovitch, P. S. (2002) A novel flow cytometric technique for drug cytotoxicity gives results comparable to colony-forming assays. *Cytometry* **48**, 1–5.
16. Endl, E., Steinbach, P., Knuchel, R., and Hofstadter, F. (1997) Analysis of cell cycle-related Ki-67 and p120 expression by flow cytometric BrdUrd-Hoechst/7AAD and immunolabeling technique. *Cytometry* **29**, 233–241.
17. Kubbies, M., Goller, B., and Van Bockstaele, D. R. (1992) Improved BrdUrd-Hoechst bivariate cell kinetic analysis by helium-cadmium single laser excitation. *Cytometry* **13**, 782–789.

Solid Tumor DNA Content Analysis

Adel K. El-Naggar and Philippe Vielh

Summary

Flow cytometric DNA content analysis provides a rapid and reliable analysis of DNA ploidy and the proliferative fraction of tumor specimens. Both archival and fresh specimens are suitable for this technique. This information can be used in conjunction with traditional prognostic factors in the biological assessment of certain carcinomas. Among these tumors are early stages of breast, colon, lung, and bladder carcinomas.

Key Words

DNA content S-phase, DNA ploidy, flow cytometry, solid tumors.

1. Introduction

Flow cytometry is a versatile, fast, and accurate technique for analysis of DNA content in solid human tumors (1–24). Recent improvements in software programs and the development of simpler and user-friendly instrumentations have further improved the reliability and consistency of the analysis. DNA content can be performed on a variety of samples including fresh solid tumors, body fluids, fine-needle samples, and archival specimens (25–28). Critical to the reliability and clinically useful application of this technique are the integrity and the quality of target cells for analysis. This is largely attributable to the primary requirement of single-cell preparations and proper fluorochromes for optimal binding to cellular nucleic acids for accurate analysis. These basic steps can be accomplished by paying careful attention to cell disaggregation, incorporating cytologic preparations and light microscopic evaluation of stained slides, and adhering to staining protocol for selected dye. Taken together with guidelines for inclusion and exclusion of specimens outlined in the laboratory manual ensures reliable and consistent results. Fresh preparations are the ideal

From: *Methods in Molecular Biology: Flow Cytometry Protocols*, 2nd ed.
Edited by: T. S. Hawley and R. G. Hawley © Humana Press Inc., Totowa, NJ

media for flow cytometric analysis and generally yield high-quality histograms. On the other hand, archival and fixed specimens are subject to cell loss and yield less than optimal results.

Information on the DNA ploidy status and the proliferative fraction represent objective submicroscopic features that can be used in the biological assessment of human neoplasms. Although objective, reliable, and accurate with appropriate quality control steps, its application to define outcome and predict response of patients with cancer remains controversial. This is attributable largely to the general perception that the value of the DNA content analysis disappears in multivariate analysis with traditional clinicopathologic factors. Most of the studies on which such a conclusion is based are retrospective, heterogeneous, and limited in scope and size. Despite that, DNA content in most studies analyzed fall short of fulfilling the accepted guidelines for the clinical application of tumor markers; its versatility to adapt to simultaneous multiparameter analysis is a powerful advantage in clinical applications.

For universal acceptance and application of this technique, interlaboratory standardization must be improved; especially in specimen processing, software features and applications. Equally important is the development and adherence to a firm quality control procedure for specimen preparation, staining procedure, software application, and the nature and type of controls to be used.

2. Materials

2.1. Solutions for a Fresh Preparation

1. 0.5 mg/mL of propidium iodide (PI): PI is a potential carcinogen and should be handled carefully. Measure 50 mg of PI (Sigma, St. Louis, MO) into a clean glass beaker. Add 100 mL of distilled H₂O and stir until dissolved (~2 h). Filter through no. 1 Whatman filter paper. Store protected from light at 4°C. Stable for 1 yr.
2. 1 mg/mL of ribonuclease-A (RNase): Thaw a 100-mg vial of RNase-A (Worthington Biochemical, Lakewood, NJ). Bring to a final volume of 100 mL by adding approx 94.63 mL of phosphate-buffered saline (PBS). Mix well. Aliquot 5-mL portions into 20 tubes and freeze at -20°C until needed. Aliquots are stable for 6 mo at -20°C. Thawed aliquots may be kept at 4°C for up to 2 wk. Concentrates may be stored at -20°C for 3 yr.
3. PBS: Dilute 10X PBS without calcium and magnesium salts (Irvine Scientific, Santa Ana, CA) to a 1X solution. Adjust the pH to 7.2–7.4. Bulk preparations may be stored at room temperature up to 3 mo. Store working aliquots at 4°C.
4. 0.25% Trypsin: Dilute 1 mL of stock (2.5%) trypsin (Sigma) in 9.0 mL of distilled H₂O. Store at 4°C for 1 wk.

2.2. Solutions for Archival Materials

These solutions should be prepared in addition to the solutions listed in **Subheading 2.1.** (with the exception of trypsin).

1. 0.5% Pepsin: Add 0.5 g of pepsin (Sigma) to 95 mL of distilled H₂O. Adjust the pH to 1.5 using 1 N HCl. Prepare fresh for each batch of specimens.
2. 0.05 mg/mL of pepstatin A: Empty a 5-mg vial of pepstatin A (97% pure) (Sigma) into a 150-mL beaker. Rinse the vial with 5 mL of 100% ethanol and add to the pepstatin A. Place several pieces of gauze on top of a heated stir plate and place the beaker (with stir bar) on top. Cover the beaker with aluminum foil to prevent evaporation. Adjust the mixer speed to a moderate setting and turn the heat to the lowest setting. Stir until completely dissolved and add 95 mL of distilled H₂O. Stable at 4°C for up to 1 mo.
3. Histo-Solv X or xylene substitute (Curtin Matheson Scientific, Houston, TX). Store as directed.

3. Methods

3.1. Fresh Fixed Cells for PI Staining

1. Place tissue into a 60 × 15 mm Petri dish. Add 2 mL of fresh cell culture media or PBS.
2. Mince the tissue into fine sections using a no. 21 surgical blade. Sieve tissue and solution through a 500-μm stainless steel mesh (*see Note 1*).
3. Transfer cell suspension to a fresh tube by filtering solution through a 35-μm nylon mesh (Small Parts, Miami Lakes, FL).
4. Add 3 mL of PBS and pipet to mix.
5. Spin cells in a tabletop centrifuge at 500g for 5 min. Decant the supernatant.
6. Resuspend cells with 3 mL of PBS and mix well. Repeat **step 5**.
7. Resuspend cells in 1 mL of PBS and filter through a 35-μm nylon mesh (*see Note 2*).
8. Perform a cell count. Use 3×10^5 cells to prepare a cytospin.
9. Centrifuge the remainder of the cell suspension for 5 min at 500g. Decant the supernatant.
10. Resuspend the cells gently with 1 mL of 0.9% saline.
11. Add 2.5 mL of *cold* 95% ethanol while vortex-mixing at slow speed. Place samples at 4°C for at least 1 h or until ready to perform flow cytometric analysis.
12. Prepare two tubes for each specimen as follows:
 - tube 1 = Patient cells
 - tube 2 = 1 : 1 mixture of patient cells and normal lymphocytes (*see Notes 3 and 4*).
13. Aliquot a total of 1×10^6 70% ethanol-fixed cells into appropriate tube.
14. Add 3 mL of PBS and centrifuge at 500g for 5 min. Decant the supernatant. Repeat once.

15. Resuspend the cells in 800 μL of PBS.
16. Add 70 μL of RNase and 50 μL of PI and incubate in a 37°C water bath for 20 min.
17. Filter samples through 35- μm nylon mesh and place on ice.

3.2. Archival Sample Preparation: Paraffin-Embedded Tissue

3.2.1. Initial Preparation

1. Prepare a 16 \times 100 mm borosilicate culture tube and two 12 \times 75 mm plastic culture tubes per specimen. Tape an identification label to the upper circumference of tubes.
2. Section one to three 50- μm sections from each paraffin block depending on the content of tissue. Blocks should be at room temperature (*see Note 5*).
3. Place sections into a 16 \times 100 mm tube. Handle sections carefully to avoid shattering.
4. Tubes may be sealed and stored at 22°C until processing.

3.2.2. Day 1

Fill tubes with the following solutions to cover tissue sections and incubate as directed (*see Notes 6 and 7*). At the end of each incubation period, aspirate as much solution as possible without interrupting, leaving tissue sections at the bottom of the tubes.

1. Histo-Solv X or xylene substitute, three times for 15 min each.
2. Absolute ethyl alcohol, two times for 10 min each.
3. 95% EtOH, two times for 10 min each.
4. 80% EtOH, one time for 10 min.
5. 70% EtOH, one time for 10 min.
6. Add 50% EtOH, cover tubes and leave overnight.

3.2.3. Day 2

1. Prepare pepsin (*see Note 8*). Place in a 37°C water bath for 30 min prior to use.
2. Aspirate EtOH from the tube.
3. Resuspend tissue sections in PBS for 10 min for rehydration. Centrifuge at 500g for 5 min. Repeat once.
4. Remove PBS and add 2.5–3 mL of prewarmed pepsin.
5. Place the tubes in a 37°C water bath for 20–45 min (*see Note 9*).
6. Aspirate the tissue sections and pepsin using 18-gage needles and 3-cc syringes, and dispel forcefully one or two times (*see Note 10*).
7. Add 175 μL of pepstatin A to the tube and agitate to mix. Place tubes on ice.
8. Centrifuge at 500g for 5 min.
9. Resuspend in 2–3 mL of PBS and centrifuge. Remove the supernatant and repeat this step.
10. Filter the solution through a 35- μm nylon mesh into a clean 12 \times 75 mm plastic tube.

11. Perform a cell count and adjust the cell concentration to 1×10^6 cells/mL.
12. Transfer 900 μ L of the cell suspension to a second 12×75 mm plastic tube, and add 100 μ L of prewarmed RNase. Incubate for 30 min in a 37°C water bath. The remaining cell suspension may be placed at -20°C for storage (see **Note 11**).
13. Add 50 μ L of PI and place the tube for 30 min in a refrigerator or on ice.

3.3. Analysis

3.3.1. Instrumentation and Acquisition

Adjust the cytometer with blue light for excitation and red filter for detection. PI is excited at 488 nm and its emission can be detected with a >610 -nm long-pass filter. Instrument performance should be monitored according to manufacturer guidelines, with emphasis on obtaining consistent resolution and mean peak channels for calibration particles on a daily basis. Linearity of photomultiplier tubes (PMTs) should be tested monthly. Test protocols should be structured to acquire forward scatter, DNA peak, integral, and pulse width fluorescence signals to discriminate G_2/M cells from cell doublets. **Figure 1** illustrates a typical acquisition protocol (see **Notes 4** and **12**).

3.3.2. Controls

For fresh solid tumor analysis, normal peripheral blood lymphocytes (NPBLs) are used as a biological control to assess the quality of PI staining and the consistency of the diploid G_0/G_1 mean channels. Tests should also be performed after mixing equal parts of tumor cell suspension and normal control; ploidy can be assessed for tumor specimens (**Fig. 2**; see **Note 3**). If lymphocytes are used as controls, they should be harvested after gradient separation and prepared as outlined in **Subheading 3.1., steps 4–11**.

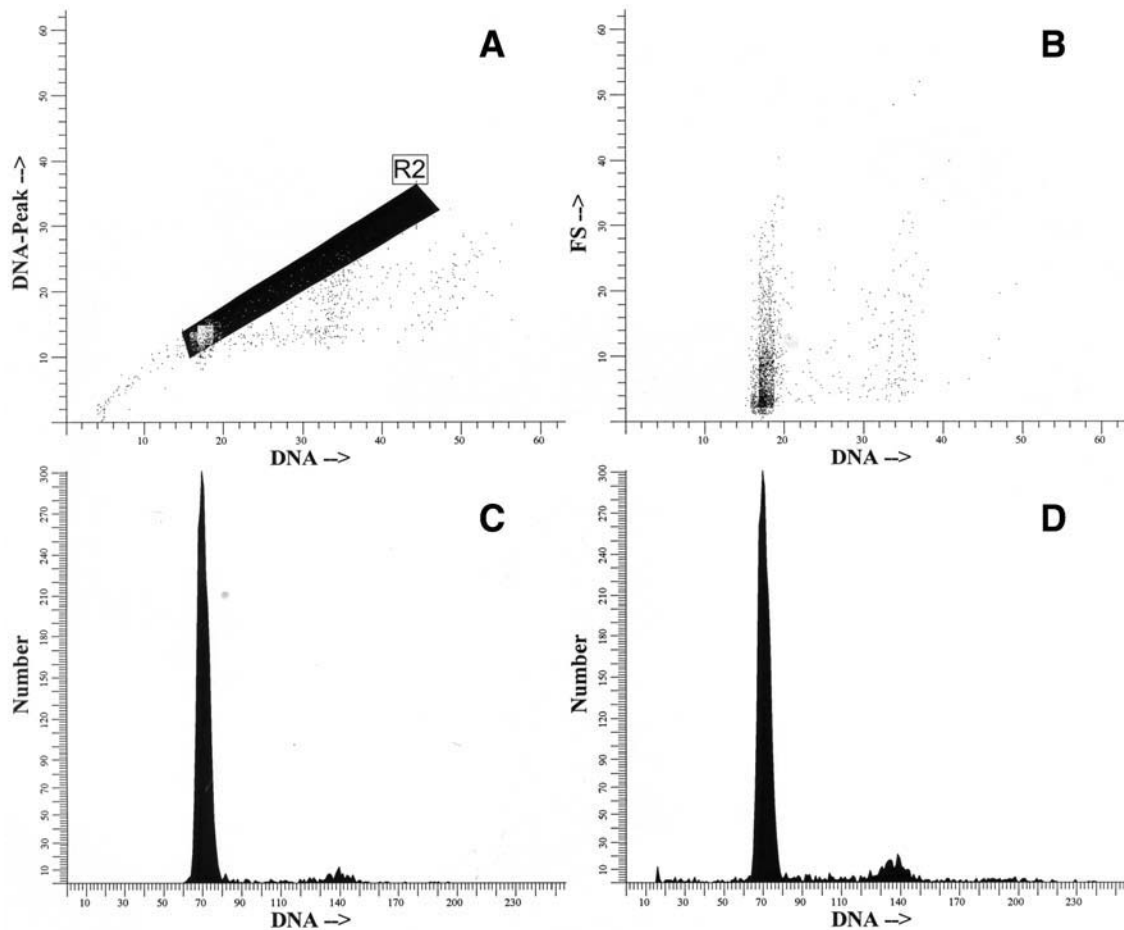
3.3.3. Measurements

DNA indices and cell cycle data can be obtained using commercial software programs or manually. For manual analysis, cursors may be placed around G_0/G_1 peaks and $S+G_2/M$ areas. DNA indices are calculated by dividing the mean channel value (x -axis) for the G_0/G_1 aneuploidy peak by the mean channel value for the intrinsic diploid G_0/G_1 peak. By definition, the diploid DNA index (DI) is equal to 1.00 (3). Cell cycle analysis of S-phase or $S+G_2/M$ is typically calculated using the number of cells (area) for the respective cell cycle compartment divided by the total number of cells analyzed.

3.3.4. Interpretation

3.3.4.1. DNA PLOIDY

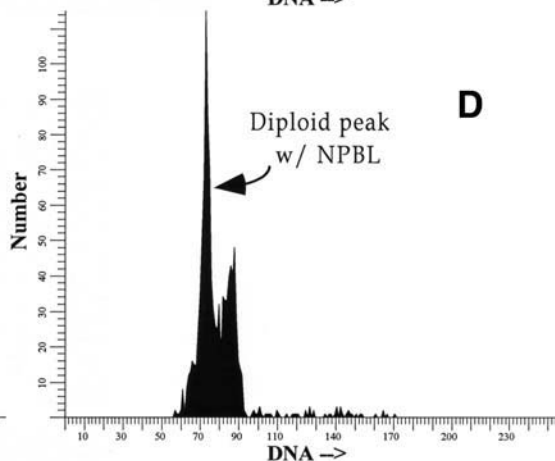
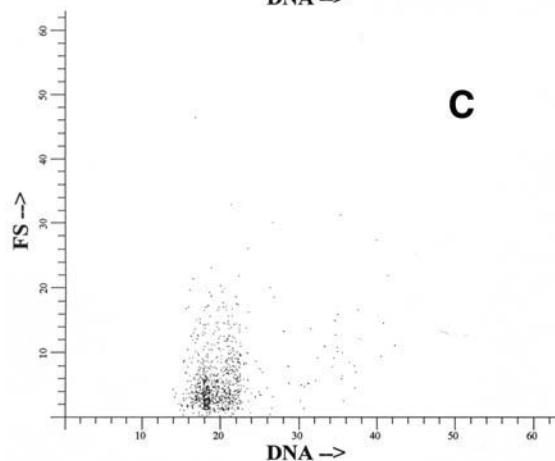
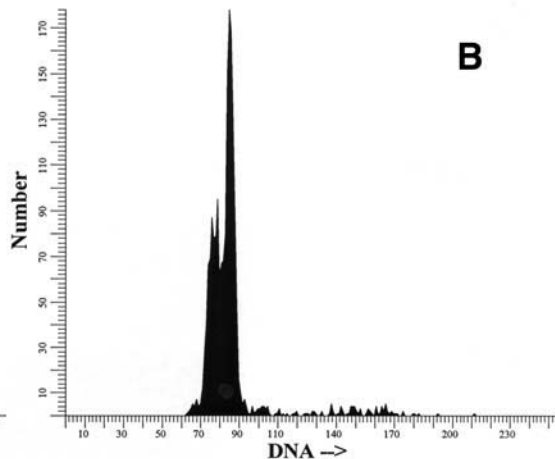
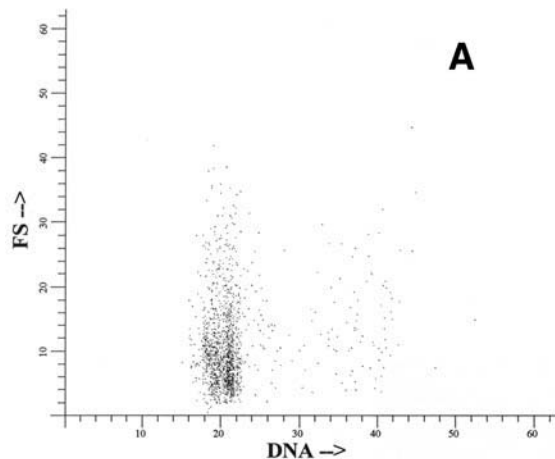
1. Analysis of nucleic acids is one of the most common applications of flow cytometry in clinical practice. This is aided further by progress in instrumentation and



software that have led to marked improvement in DNA measurement to allow for the detection of small near-diploid clones (*see Note 13*). Current flow cytometer can resolve a >5% DNA content difference between tumor cell populations. Therefore, minor numerical chromosomal changes may not be detected (**Fig. 3**) (25–27). Assuming proper instrument performance and a stable biological control (normal lymphocytes or normal tissue from the same individual) are obtained, histogram interpretation can be reproducibly achieved.

2. Generally, DNA ploidy is defined as DNA diploid, a single G_0/G_1 peak corresponding to the same channel of the biological control, and DNA aneuploid, a separate distinct G_0/G_1 peak from the diploid G_0/G_1 . DNA aneuploidy may be characterized further as hypodiploid ($DI < 1.00$) and hyperdiploid ($DI > 1.00$). The tetraploid ($DI = 2.00$) category should be strictly defined. A narrow, well-defined peak of >10% of cells analyzed can be defined as a tetraploid peak. On the other hand, a peak with a more Gaussian distribution, with up to 20% of the total population, should be considered as G_2/M (**Figs. 4–6**).
3. Classifying near-diploid aneuploidy into hypodiploid or hyperdiploid categories can be difficult. Generally, this is possible in the analysis of fresh tissues, where a mixture of normal lymphocytes and the sample can allow for the definitive determination of DNA indices in the majority of cases (*see Note 14*). A perfect superimposition of the normal biologic control channel number and that of the sample is necessary for such analysis. This, however, is difficult to accomplish using paraffin-embedded tissues.
4. A definable limit of acceptable coefficient variations (CVs) may be restrictive and must be flexible to allow for the interpretation of rare and special specimens. Strict application of a cutoff may lead to the exclusion of otherwise reasonable histograms that may reflect the innate properties of different cell populations in certain solid tumors, such as pleomorphic epithelial and mesenchymal tumors. Accordingly, interpretation should be based on the features of each individual histogram and the knowledge of the cellular composition after reviewing cytopspins of the disaggregated sample (*see Notes 15–17*). Histograms with extensive debris, wide CV, and skewed ascending and descending limbs of the G_0/G_1 peaks should be considered unfit for analysis.
5. DNA ploidy analysis may be used along with other clinicopathologic characteristics to aid in the interpretation of borderline lesions and reactive vs neoplastic tissues (29). However, DNA aneuploidy should not be used as the sole criteria for malignancy, especially on fine-needle aspiration materials of thyroid and other clinically benign neuroendocrine tumors (*see Notes 18–21*). Ploidy analysis of histologically malignant tumors may provide prognostic information as a guide in stratification of patients for management protocols in early stages of melanoma and breast, colon, bladder, prostate, ovarian, and lung cancer (30–47).

Fig. 1. (*see opposite page*) A typical acquisition protocol with doublet discrimination (A), DNA vs forward light scatter (B), and gated and ungated DNA histograms (C,D, respectively).



3.3.4.2. S-PHASE (PROLIFERATIVE FRACTION)

1. Measurement of the proliferative fraction is assumed to reflect tumor growth rate and potential progression. Accurate and consistent analysis of the S-phase, however, has been a vexing issue because the definition of S-phase or S+G₂/M is often arbitrary and subjective. For diploid neoplasms, the contamination with host cells may cause problems (**Fig. 1**). This, however, can be resolved by using cytokeratin for gating tumor cells.
2. The assessment of this parameter depends on the quality and the simplicity of the histogram analyzed. Diploid DNA and single-peak aneuploid DNA histograms with minimal debris contamination and good CVs are suitable for S-phase analysis (**Fig. 2A,B**).
3. Multiploid, uneven G₀/G₁ (skewed) peaks with large amounts of debris in background may not be suitable for S-phase analysis (**Fig. 3**). It must be realized that cells within the S-phase boundaries may not represent cycling cells, but possibly include apoptotic, noncycling, or DNA aneuploid cells.

4. Notes

1. To improve yield of intact cells, tumor fragments can be minced with or without passing them through the stainless steel sieve. This should depend on the nature of the specimens.
2. If tumor cells remain clumped after mechanical disaggregation, centrifuge cell suspension, decant, and add 1 mL of diluted trypsin (0.25%) at room temperature for 15 min. Gently resuspend the cells with a Pasteur pipet for better cell separation. Wash with PBS, perform a cell count, and adjust to 1×10^6 cells/mL. Proceed with cell fixation as described in **Subheading 3.1., steps 9–11**.
3. Cell density is critical to fluorochrome binding, especially when conducting lymphocyte and tumor mixtures. An equal number of cells from each is important for reliable staining and determination of near-diploid populations.
4. PMT voltages may be adjusted during acquisition according to the nature of the specimen. Mixtures of specimen and normal peripheral blood lymphocytes (NPBL) may be acquired at higher PMT voltages to separate near-diploid G₀/G₁ peaks. For acquisition of tumor cells with DNA hyperdiploid peaks, the PMT voltages should be lowered to include all cycling cells.
5. For paraffin-embedded small core biopsies and tissue measuring <1 cm, additional sections may be necessary for adequate analysis. Blocks should be sectioned at room temperature to minimize tissue fragmentation and breakage (**28**).
6. Overexposure to absolute alcohol will increase the likelihood of fragmentation. Strict adherence to incubation times is recommended.

Fig. 2. (see opposite page) (A,B) DNA distribution of a tumor with a near-diploid aneuploid peak. (C,D) DNA histograms of the tumor specimen mixed with an equal portion of NPBLs. Note the increase in cell number for the diploid G₀/G₁ peak in (D).

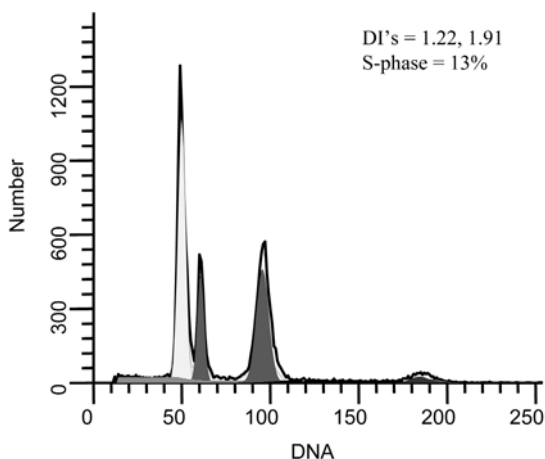


Fig. 3. Near-diploid and hyperdiploid cell population with DIs of 1.2 and 1.9.

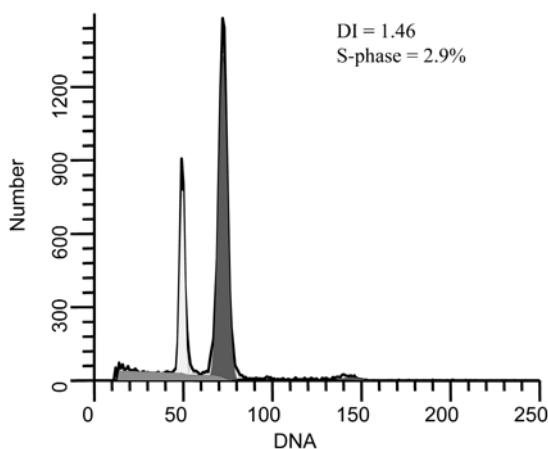


Fig. 4. DNA histogram displaying hyperdiploid stemline with low S-phase.

7. Vortex-mix specimens during solvent and hydration steps to aid in unrolling tissue sections. Do not fill culture tubes fully to allow for proper agitation of sections.
8. Prepare a sufficient amount of pepsin to treat the number of specimens being processed (2.5–3 mL/specimen).
9. Monitor pepsin incubation carefully to avoid overdigestion. Tubes may be agitated by thumping with a forefinger to aid in cell dispersal. The suspension will begin to cloud as cells are released. Tubes should be removed from the water bath at this point, syringed, and treated with pepstatin A to halt enzymatic action.

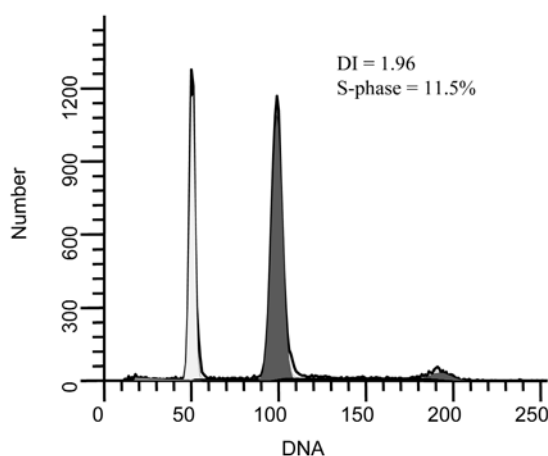


Fig. 5. Near-tetraploid stemline with DI of 1.96 and S-phase of 11.5%.

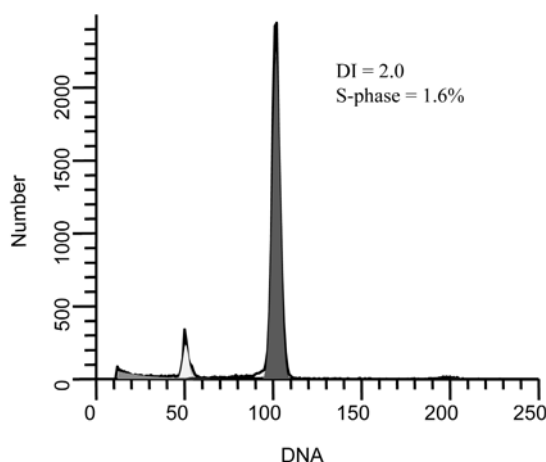


Fig. 6. Histogram of a tetraploid stemline with DI of 2.0 and low S-phase.

10. Ejecting liquid forcefully from the syringe is usually sufficient to dissociate cells. Limit the number of times sections are aspirated and dispelled. Observe the cloudiness of the solution to monitor release of cells.
11. If cell yield permits, do a cytospin on each sample from diluted, filtered cells not exposed to RNase.
12. Observe the mean channel location of the diploid G_0/G_1 peak during the initial phases of specimen acquisition. Restart the acquisition frequently until a stable mean channel is achieved.

13. Occasionally, benign tumors and reactive conditions manifest aneuploidy by flow cytometry and *in situ* hybridization. DNA aneuploidy in these situations should not be interpreted as diagnostic of malignancy. Correlation with histologic evaluation is necessary.
14. Chromatin condensation is a factor especially in interpreting mixtures of tumor and NPBLs. Epithelial-derived tumor cells may allow more accessibility to the dye; therefore, they may fluoresce brighter than NPBLs, and may lead to a false classification of the histogram as aneuploidy (3). Histograms should be classified as aneuploidy only when two separate distinct peaks are discernible (without control lymphocytes added). This is especially the case in specimens with lymphocytes or in specimens with a high lymphoid content.
15. Mechanical disaggregation of solid tumors to obtain dispersed cells may lead to selective loss of neoplastic elements. To assess the integrity of the specimen, prepare cytopsin preparations on all disaggregated solid tumors and paraffin-embedded tissues to assess cellular integrity and normal contamination. Cytopsin may be stained with Wright/Giemsa.
16. Host cell contamination may markedly affect tumor cell representation. Specimens with more than 30% normal cells should be deemed uninterpretable if a diploid histogram is obtained (48,49). This may be circumvented by acquiring DNA fluorescence of a tumor-enriched population, through cytokeratin gating or lymphocyte depletion (LCA staining) (50–54).
17. Cellular debris or red blood cell contamination may interfere with the detection of aneuploidy and/or cause inaccurate S-phase determination. In addition, cell clumping may result in an artificial elevation of S- and G₂/M-phase values. Commercial software programs for debris subtraction and aggregate modeling should alleviate this problem.
18. A biological control must be used to ensure linearity, doublet discrimination, and S-phase measurement. Typically, lymphocytes harvested and processed the same day are an ideal control, providing a tight CV. The control should run first and then the specimens. If diploid or near-aneuploidy is in question, an equal mixture of sample and control should be performed.
19. Histological evaluation of cytopsin preparation of specimens is one of the most valuable quality control steps. It provides important information on the number of tumor to host cells (4:1) and the quality of the cellular composition.
20. The application of software should be based on the knowledge and familiarity of the biological specimens being analyzed. This includes number of cells, cellular composition, extent of debris, doublet formation, and the ploidy status. Because each software program available differs in the manner of CV, ploidy, and S-phase analysis, the software features must be suitable for the biological nature of the specimens.
21. The concentration of both fluorochrome and cells (1:18) should be kept constant to prevent shifting of the cell population on histograms resulting from staining variabilities. This is attributable to staining differences between cells, cellular to nuclear composition, and compactness of chromatin. Ideally optimum staining

time should be guided by using known cell populations and known concentrations of the dye measured over time. This will determine the optimum staining time if no shifting occurs.

References

1. Barlogie, B., Göhde, W., Johnston, D. A., et al. (1978) Determination of ploidy and proliferative characteristics of human solid tumors by pulse cytophotometry. *Cancer Res.* **38**, 3333–3339.
2. Barlogie, B., Drewinko, B., Schumann, J., et al. (1980) Cellular DNA content as a marker of neoplasia in man. *Am. J. Medicine* **69**, 195–203.
3. Hiddemann, W., Schumann, J., Andreeff, M., et al. (1984) Convention on nomenclature for DNA cytometry. *Cytometry* **5**, 445–446.
4. Merkel, D. E., Dressler, L. G., and McGuire, W. L. (1987) Flow cytometry, cellular DNA content, and prognosis in human malignancy. *J. Clin. Oncol.* **5**, 1690–1703.
5. Koss, L. G., Czerniak, B., Herz, F., and Wersto, R. P. (1989) Flow cytometric measurements of DNA and other cell components in human tumors: a critical appraisal. *Hum. Pathol.* **20**, 528–548.
6. Seckinger, D., Sugarbaker, E., and Frankfurt, O. (1989) DNA content in human cancer. *Arch. Pathol. Lab. Med.* **113**, 619–626.
7. Shapiro, H. M. (1989) Flow cytometry of DNA content and other indicators of proliferative activity. *Arch. Pathol. Lab. Med.* **113**, 591–597.
8. Vohn, M. (1989) Prognostic implications of DNA aneuploidy and proliferative activity in solid human tumors. *Tumor Diagn. Ther.* **10**, 229–232.
9. Raber, M. N. and Barlogie, B. (1990) DNA flow cytometry of human solid tumors, in *Flow Cytometry and Cell Sorting*, 2nd edit. (Melamed, M. R., Lindmo, T., and Mendelsohn, M. L., eds.), Wiley-Liss, New York, pp. 745–754.
10. Williams, N. N. and Daly, J. M. (1990) Flow cytometry and prognostic implications in patients with solid tumors. *Surgery* **171**, 257–266.
11. Wersto, R. P., Liblit, R. L., and Koss, L. G. (1991) Flow cytometric DNA analysis of human solid tumors: a review of the interpretation of DNA histograms. *Hum. Pathol.* **22**, 1085–1098.
12. Camplejohn, R. S. (1992) Critical summaries, flow cytometry. *J. Pathol.* **166**, 323–326.
13. El-Naggar, A. K. (1992) Clinical relevance of the flow cytometric analysis in cancer. *Cancer J.* **5**, 321–327.
14. Sasaki, K. and Murakami, T. (1992) Clinical application of flow cytometry for DNA analysis of solid tumors. *Acta Pathol. Jpn.* **42**, 1–14.
15. Barlogie, B., McLaughlin, P., and Alexanian, R. (1987) Characterization of hematologic malignancies by flow cytometric. *Anal. Quant. Cytol. Histol.* **9**, 147–155.
16. Andreeff, M. (1990) Flow cytometry of leukemia, in *Flow Cytometry and Cell Sorting*, 2nd edit. (Melamed, M. R., Lindmo, T., and Mendelsohn, M. L., eds.), Wiley-Liss, New York, pp. 697–724.

17. Andreeff, M. (1990) Flow cytometry of lymphoma, in *Flow Cytometry and Cell Sorting*, 2nd edit. (Melamed, M. R., Lindmo, T., and Mendelsohn, M. L., eds.), Wiley-Liss, New York, pp. 725–743.
18. Hedley, D. W., Shankey T. V., and Wheelless, L. L. (1993) DNA cytometry consensus conference. *Cytometry* **14**, 471.
19. Shankey, T. V., Rabinovitch, P. S., Bagwell, B., et al. (1993) Guidelines for the implementation of clinical DNA cytometry. *Cytometry* **14**, 472–477.
20. Wheelless, L. L., Badalament, R. A., de Vere White, R. W., Fradet, Y., and Tribukait, B. (1993) Consensus review of the clinical utility of DNA cytometry in bladder cancer. *Cytometry* **14**, 482–485.
21. Hedley, D. W., Cark, G. M., Cornelisse, C. J., Killander, D., Kute, T., and Merkel, D. (1993) Consensus review of the clinical utility of DNA cytometry in carcinoma of the breast. *Cytometry* **14**, 482–485.
22. Bauer, K. D., Bagwell, C. B., Giaretti, W., et al. (1993) Consensus review of the clinical utility of DNA flow cytometry in colorectal cancer. *Cytometry* **14**, 486–491.
23. Duque, R. E., Andreeff, M., Braylan, R. C., Diamond, L. W., and Peiper, S. C. (1993) Consensus review of the clinical utility of DNA flow cytometry in neoplastic hematopathology. *Cytometry* **14**, 492–496.
24. Shankey, T. V., Kallioniemi, O.-P., Koslowski, J. M., et al. (1993) Consensus review of the clinical utility of DNA content cytometry in prostate cancer. *Cytometry* **14**, 497–500.
25. Kute, T. E., Gregory, B., Galleshaw, J., Hopkins, M., Buss, D., and Case, D. (1988) How reproducible are flow cytometry data from paraffin-embedded blocks? *Cytometry* **9**, 494–498.
26. Hedley, D. W. (1989) Flow cytometry using paraffin-embedded tissue: five years on. *Cytometry* **10**, 229–241.
27. Joensuu, H. and Kallioniemi, O.-P. (1989) Different opinions on classification of DNA histograms produced from paraffin-embedded tissue. *Cytometry* **10**, 711–717.
28. McLemore, D. D., El-Naggar, A., Stephens, L. C., and Jardine, J. H. (1990) Modified methodology to improve flow cytometric DNA histograms from paraffin-embedded material. *Stain. Technol.* **65**, 279–291.
29. Arber, D. A. and Speights, V. O. (1991) Aneuploidy in benign seminal vesicle epithelium: an example of the paradox of ploidy studies. *Mod. Pathol.* **4**, 687–689.
30. Alderision, M., Cenci, M., Valli, C., et al. (1998) Nm23-H1 protein, DNA-ploidy and S-phase fraction in relation to overall survival and disease free survival in transitional cell carcinoma of the bladder. *Anticancer Res.* **18**, 4225–4230.
31. Gregoire, M., Fradet, Y., Meyer, F., et al. (1997) Diagnostic accuracy of urinary cytology, and deoxyribonucleic acid flow cytometry and cytology on bladder washings during follow-up for bladder tumors. *J. Urol.* **157**, 660–664.
32. Granfors, T., Duchek, M., Tomic, R., Roos, G., and Ljungberg, B. (1996) Predictive value of DNA ploidy in bladder cancer treated with preoperative radiation therapy and cystectomy. *Scand. J. Urol. Nephrol.* **30**, 281–285.

33. Ross, J. S., Sheehan, C. E., Ambros, R. A., et al. (1999) Needle biopsy DNA ploidy status predicts grade shifting in prostate cancer. *Am. J. Surg. Pathol.* **161**, 296–301.
34. Amling, C. L., Lerner, S. E., Martin, S. K., Slezak, J. M., Blute, M. L., and Zincke, H. (1999) Deoxyribonucleic acid ploidy and serum prostate specific antigen predict outcome following salvage prostatectomy for radiation refractory prostate cancer. *J. Urol.* **161**, 857–862.
35. Astrom, L., Weimarck, A., Aldenborg, F., et al. (1998) S-phase fraction related to prognosis in localized prostate cancer. No specific significance of chromosome 7 gain or deletion of 7q31.1. *Int. J. Cancer* **79**, 553–559.
36. Witzig, T. E., Ingle, N. K., Schaid, D. J., et al. (1993) DNA ploidy and percent S-phase as prognostic factors in node-positive breast cancer: results from patients enrolled in two prospective randomized trials. *J. Clin. Oncol.* **11**, 351–359.
37. Romero, H., Schneider, J., Burgos, J., Bilbao, J., and Rodriguez-Escudero, F. J. (1996) S-phase fraction identifies high-risk subgroups among DNA-diploid breast cancers. *Breast Cancer Res. Treat.* **38**, 265–275.
38. Clinical practice guidelines for the use of tumor markers in breast and colorectal cancer. Adopted on may 17, 1996 by the American Society of Clinical Oncology [see comments]. (1996) *J. Clin. Oncol.* **14**, 2843–2877.
39. Wenger, C. R. and Clark, G. M. (1998) S-phase fraction and breast cancer—a decade of experience. *Breast Cancer Res. Treat.* **51**, 255–265.
40. Giella, J. G., Ring, K., Olsson, C. A., Karp, F. S., and Benson, M. C. (1992) The predictive value of flow cytometry and urinary cytology in the follow-up of patients with transitional cell carcinoma of the bladder. *J. Urol.* **148**, 293–296.
41. Wheelless, L. L., Badalament, R. A., de Vere White, R. W., Fradet, Y., and Tribukait, B. (1993) Consensus review of the clinical utility of DNA cytometry in bladder cancer. Report of the DNA Cytometry Consensus Conference. *Cytometry* **14**, 478–481.
42. Reles, A. E., Gee, G., Schellschmidt, I., et al. (1998) Prognostic significance of DNA content and S-phase fraction in epithelial ovarian carcinomas analyzed by image cytometry [see also comments]. *Gynecol. Oncol.* **71**, 3–13.
43. Zanetta, G., Keeney, G. L., Cha, S. S., Wieand, H. S., Katzmann, J. A., and Podratz, K. C. (1996) DNA index by flow cytometric analysis: an additional prognostic factor in advanced ovarian carcinoma without residual disease after primary operation. *Gynecol. Oncol.* **74**, 208–212.
44. Muguerza, J. M., Diez, M., Torres, A. J., et al. Prognostic value of flow cytometric DNA analysis in non-small-cell lung cancer: rationale of sequential processing of frozen and paraffin-embedded tissue. *World J. Surg.* **21**, 323–329.
45. Roberts, H. L., Komaki, R., Allen, P., and El-Naggar, A. K. (1998) Prognostic significance of DNA content in stage I adenocarcinoma of the lung. *Int. J. Rad. Oncol. Biol. Phys.* **41**, 573–578.
46. Karlsson, M., Boeryd, B., Carstensen, J., et al. (1996) Correlations of Ki-67 and PCNA to DNA ploidy, S-phase fraction and survival in uveal melanoma. *Eur. J. Cancer* **32A**, 357–362.

47. Lanza, G., Gafa, R., Santini, A., et al. (1998) Prognostic significance of DNA ploidy in patients with stage II and stage III colon carcinoma: a prospective flow cytometric study. *Cancer* **82**, 49–59.
48. Nervi, C., Badaracco, G., Maisto, A., Mauro, F., Tirindelli-Danesi, D., and Starace, G. (1982) Cytometric evidence of cytogenetic and proliferative heterogeneity in human solid tumors. *Cytometry* **2**, 303–308.
49. Kallioniemi, O.-P. (1988) Comparison of fresh and paraffin-embedded tissue as starting material for DNA flow cytometry and evaluation of intratumor heterogeneity. *Cytometry* **9**, 164–169.
50. van der Linden, J. C., Herman, C. J., Boenders, J. G., van de Sandt, M. M., and Lindeman, J. (1992) Flow cytometric DNA content of fresh tumor specimens using keratin-antibody as second stain for two parameter analysis. *Cytometry* **13**, 163–168.
51. Frei, J. V. and Martinez, V. J. (1993) DNA flow cytometry of fresh and paraffin-embedded tissue using cytokeratin staining. *Mod. Pathol.* **6**, 599–605.
52. Park, C. H. and Kimler, B. F. (1994) Tumor cell-selective flow cytometric analysis for DNA content and cytokeratin expression of clinical tumor specimens by “cross-gating.” *Anticancer Res.* **14**, 29–36.
53. Kenyon, N. S., Schmitting, R. J., Siiman, O., Burshteyn, A., and Bolton, W. E. (1994) Enhanced assessment of DNA/proliferative index by depletion of tumor infiltrating leukocytes prior to monoclonal antibody gated analysis of tumor cell DNA. *Cytometry* **16**, 175–183.
54. Zarbo, R. J., Brown, R. D., Linden, M. D., Torres, F. X., Nakhleh, R. E., and Schultz, D. S. (1994) Rapid (one-shot) staining method for two-color multiparametric DNA flow cytometric analysis of carcinoma using staining for cytokeratin and leukocyte common antigen. *Am. J. Clin. Pathol.* **101**, 638–642.

21

Concurrent Flow Cytometric Analysis of DNA and RNA

Adel K. El-Naggar

Summary

Concurrent analysis of DNA and RNA by flow cytometry provides information on the DNA content and the transcriptional status of cells. This can be accomplished using metachromatic fluorochromes that bind to DNA by intercalation and to single-stranded RNA electrostatically. Because cell viability is a prerequisite for the analysis, freshly prepared cells must be used. Simultaneous DNA/RNA analysis can be used primarily in the classifications and biological assessment of hematoreticular malignancies including multiple myeloma.

Key Words

Flow cytometry, nucleic acids analysis, RNA content, RNA and DNA analysis.

1. Introduction

Simultaneous analysis of DNA and RNA can be accomplished by using the metachromatic acridine orange fluorochrome (AO), one of the most known of the acridine fluorescent family members (*1-10*). AO is a unique and versatile dye that can be used in the detection of a wide variety of cellular components. By combining RNA and DNA quantitation using AO, it is possible to discriminate between cell populations with the same DNA content and to assess their translational activity, cell proliferation, and differentiation status (*11*).

AO is a 3,6-(dimethylamino) acridine that binds to double-stranded nucleic acids irrespective of base composition or ligand type. Cells to be stained must be permeabilized with non-ionic detergent (e.g., Triton X-100) at low pH with serum proteins. This is an important step that allows for the dissociation of histones from DNA for better accessibility of AO (*12*). The dye intercalates the double-stranded conformation of nucleic acids and stacks electrostatically

From: *Methods in Molecular Biology: Flow Cytometry Protocols*, 2nd ed.
Edited by: T. S. Hawley and R. G. Hawley © Humana Press Inc., Totowa, NJ

on the RNA in the presence of EDTA. On excitation, DNA fluoresces approximately 530 nm (green) and RNA fluoresces with maximum emission above 630 nm (red). AO can also bind to cellular dsRNA leading to spurious elevation of DNA content measurement.

Since cellular rRNA and tRNA have double strand conformation, these have to be selectively denatured in the processing using EDTA (13).

2. Materials

2.1. General Guidelines

1. Prepare stock solutions prior to specimen preparation, with the exception of the AO working solution. The latter should be prepared only at the time of sample staining.
2. All glassware to be used for reagent preparation must be RNase free.
3. Rigorous adherence to molarity and pH conditions must be followed.
4. Peripheral blood lymphocytes and bone marrow aspirates are harvested after Ficoll-Hypaque gradient centrifugation. Solid tumor and bone marrow biopsies should be carefully minced and agitated to release individual cells.
5. Fluids and fine-needle aspirates are either washed directly in buffer or separated by gradient centrifugation depending on the extent of red blood cell contamination.
6. Specimens should be washed in phosphate-buffered saline (PBS) with MgCl_2 and cell concentrations adjusted to 1×10^6 cells/mL. If surface membrane markers are to be performed, the PBS with MgCl_2 step (*see Subheading 3.1., step 1*) should be eliminated.

2.2. Stock Solutions

1. 1 mg/mL of AO: (**Caution:** AO is a mutagen. Chemical, physical, and toxicological properties are not fully established for this material. Handle with care). Measure 50 mg of AO powder (Polysciences, Warrington, PA; *see Note 1*) into a clean glass beaker. Add 50 mL of distilled H_2O , cover with aluminum foil and stir until dissolved, protected from light. Filter solution through a no. 1 Whatman filter paper. Store solution protected from light at 4°C , wrap in aluminum foil. Stable for 1 yr (*see Note 2*).
2. 0.2 M Citric acid: Add 19.21 g of citric acid (Sigma, St. Louis, MO) to 500 mL of distilled H_2O . Stir until dissolved and store at 4°C . Stable for 2 mo.
3. 10 mM Ethylenediaminetetraacetic acid (EDTA): Add 2.17 g of EDTA (Gibco™ Invitrogen Corporation, Carlsbad, CA) to 500 mL of distilled H_2O , stir until dissolved and store at 4°C . Stable for 2 mo.
4. PBS with 2 mM MgCl_2 : Dilute 10X PBS without calcium and magnesium salts (Irvine Scientific, Santa Ana, CA) to a 1X solution. Add 0.408 mL of 4.9 M MgCl_2 for each liter of PBS. Adjust the pH to 7.2–7.4. Bulk preparations may be stored at room temperature up to 3 mo. Store working aliquots at 4°C .
5. 1 M Sodium chloride (NaCl): Add 29.0 g of NaCl (Fisher, Houston, TX) to 500 mL of distilled H_2O and stir until dissolved. Store at 4°C . Stable for 3 mo.

6. 0.4 M Sodium phosphate dibasic (Na_2HPO_4): Add 28.39 g of Na_2HPO_4 (Fisher) to 500 mL of distilled H_2O and stir until dissolved. Store at room temperature, 22°C. Stable for 2 mo.
7. Triton 10X: Add 10 mL of Triton X-100 (CMS, Houston, TX) to 90 mL of distilled water. Store at 4°C. Stable for 3 mo.

2.3. Working Solutions

Working solutions are prepared from the stock solution described above.

1. Solution A: Add 1 mL of Triton X-100, 8 mL of 1 N HCl, 15 mL of 1 M NaCl to 76 mL of distilled H_2O . Adjust to pH 1.2 with 1 N HCl. Store at 4°C. Stable for 2 wk.
2. Solution B: Add 50 mL of 10 mM EDTA, 75 mL of 1 M NaCl, 157.5 mL of 0.4 M Na_2HPO_4 , 92.5 mL of 0.2 M citric acid to 120 mL of distilled water. Adjust to pH 6.0 with 1 N NaOH or 1 N HCl. Store at 4°C. Stable for 1 mo.
3. AO working solution: Add 0.1 mL of AO stock solution to 9.9 mL of solution B. Prepare daily and keep on ice. EDTA enhances AO interaction with RNA to form condensed samples.

3. Method

3.1. Staining

The following steps should be performed at 0–4°C in disposable glass tubes.

1. Adjust cell suspension at a concentration of 1.0×10^6 cells/mL in PBS with 2 mM MgCl_2 . Cells can either be fixed in ethanol or permeabilized with Triton X-100.
2. Place solution A and AO working solution on ice.
3. Aliquot 0.2 mL of freshly prepared cell suspension into a 12 × 75 mm glass disposable test tube.
4. Add 0.4 mL of solution A (see **Note 3**). Incubate for 45 s at 0–4°C.
5. Add 1.2 mL of AO working solution and analyze immediately.
6. Repeat **steps 3–5** for each specimen.
7. Wash the cytometer with bleach and rinse thoroughly with distilled H_2O (see **Note 4**).

3.2. Analysis

3.2.1. Instrumentation and Acquisition

Excitation of AO is achieved between 455 and 490 nm. Because the emission spectra of AO DNA binding overlaps with the red fluorescence from RNA, filter combinations should be chosen to minimize this occurrence. We recommend a 550-longpass (LP) dichroic with a 525-bandpass (BP) for DNA fluorescence and a 630-LP for RNA fluorescence. Further compensation may be needed to reduce overlapping emissions (see **Note 5**).

Instrument performance should be monitored to ensure consistent resolution and mean peak channels for calibration particles. Protocols should be designed to acquire light scatter signals, dual-parameter DNA/RNA histograms, along with single-parameter fluorescence distributions of each fluorescent signal. Doublet discrimination should be performed if required. An example of acquisition protocol is depicted in **Fig. 1**.

3.2.2. RNA Content Standards

RNA and DNA cellular contents can be quantitatively measured by comparison to the same contents in biological standard (lymphocyte, cell line, and so on). Freshly harvested lymphocytes is a popular and stable control for such purpose. RNase treated and untreated standard should be run and measured concurrently. RNA and DNA contents of the test cells must be measured under conditions similar to those used for the control. The RNA index should be expressed by dividing the test level by the level of the control. Lymphocytes can also be used for DNA content calibrations to determine the DNA index.

3.2.3. Standards

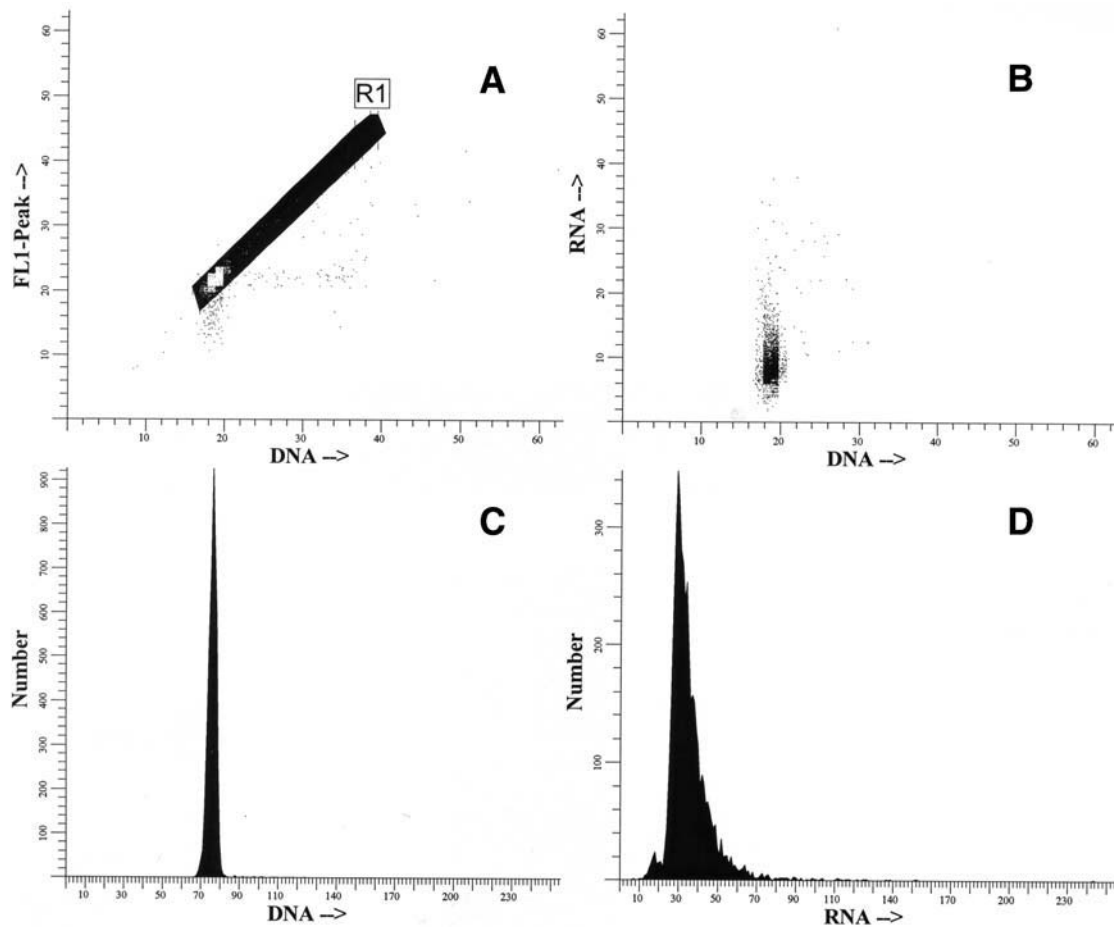
Normal peripheral blood lymphocytes (NPBLs) are used as a biological control to assess the quality of AO staining and the stability of the diploid G_0/G_1 mean channels (**Fig. 2**). Lymphocytes harvested after Ficoll-Hypaque gradient separation and cell count adjusted to 1×10^6 cells/mL can be used to establish an acceptable range of RNA mean channel values (*see Note 6*). The lymphocyte cell suspension should be simultaneously stained and concurrently run with each set of specimens to be analyzed.

NPBLs can also be used to determine DNA ploidy, especially in tumors with near-diploid peaks (*see Notes 7 and 8*). Equal parts (i.e., 100 μ L each) of NPBL and tumor cell suspension are mixed together and stained with acridine orange (**Fig. 3**).

3.2.4. Histogram Analysis

DNA indices and cell cycle data can either be generated using commercial software programs or manually. For manual analysis, cursors may be placed around G_0/G_1 peaks and S+ G_2/M areas. DNA indices are calculated by dividing the mean channel value (x -axis) for the G_0/G_1 aneuploidy peak by the mean channel value for the intrinsic diploid G_0/G_1 peak. By definition, diploid DNA

Fig. 1. (*see facing page*) A typical acquisition protocol displaying a doublet discrimination histogram (peak vs integral fluorescence) (**A**), a two-parameter DNA/RNA display (**B**), and one-parameter DNA and RNA histograms (**C,D**, respectively).



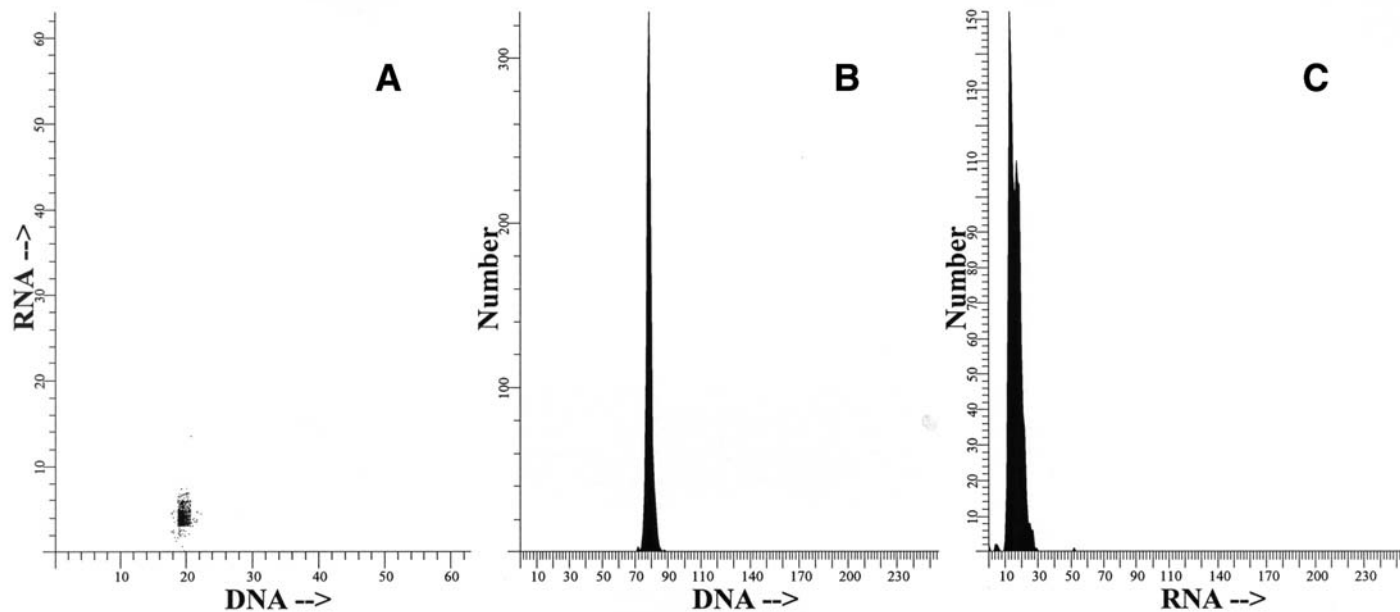


Fig. 2. Two-parameter DNA/RNA (A) and one-parameter DNA and RNA histograms (B,C, respectively) of NPBLs stained with AO.

index is equal to 1.00 (**14**). Cell cycle percentages may be calculated using the actual number of cells included within the cursor boundaries (area). RNA indices are calculated by dividing the mean G_0/G_1 RNA fluorescence of the test sample by the mean G_0/G_1 RNA fluorescence for NPBL.

3.2.5. Principles of RNA Content Analysis

RNA measurement is largely a rough estimation of the ribosomal RNA content which comprises more than 80% of the cellular RNA content. This in turn is an indirect reflection of the translational potential of cells analyzed.

RNA analysis can be used in:

1. The identification of different cell populations (i.e., lymphocytes, host cells and tumor cells) in a given sample.
2. Assessment of cell cycle status. Progression of the cell cycle is associated with increased RNA content which occurs during the G_0/G_1 . Cellular RNA can, therefore, be used in the DNA histogram to determine the number of cycling cells.

3.3. Applications of Concurrent DNA/RNA Analysis

Various applications of this technique have been investigated including the assessment of cellular differentiation of cellular phenotypes, determination of cell cycle phases, and biological assessment of hematologic malignancies and solid tumors. Reproducible measurements of DNA/RNA contents depend on the quality of specimen preparation and staining conditions (*see Note 9*).

3.3.1. Lymphoreticular Malignancies

Cells from leukemias and the leukemia phase of lymphoma are typically uniform, do not require processing, and are ideal for such analysis. Analysis of bone marrow specimens, however, varies depending on the extent of neoplastic involvement and residual normal marrow elements. RNA values and the histogram profile of normal bone marrow aspirates should be used to guide interpretation of data generated from these specimen types. RNA/DNA values can be used in the diagnosis and biological assessment of multiple myeloma, acute and chronic leukemias, and chronic myeloid leukemias (**15–31**). Examples of AO staining in different hematologic malignancies are displayed in **Figs. 4** and **5**.

3.3.2. Solid Tumors

AO analysis of solid neoplasms are more complicated because of tumor cell heterogeneity, cell membrane disruption, and contamination by host normal cells. Evaluation of Wright–Giemsa stained cytospin preparations is of vital importance in specimen qualification and interpreting these results (*see Note 10*). If sufficient intact tumor cells are present, histogram interpretation can be reliably analyzed. In general, at least 70% of the cells in a given specimen should contain

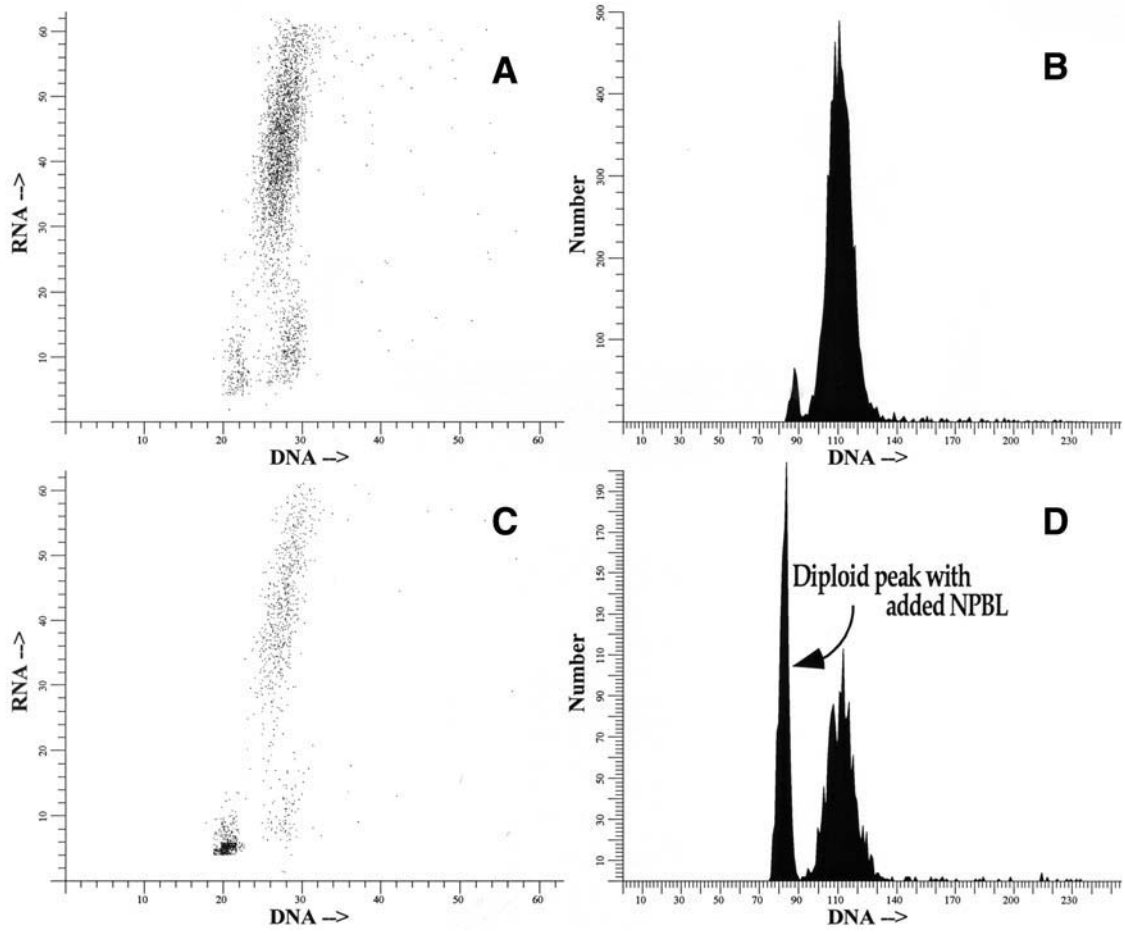


Fig. 3.

neoplastic elements and, of these, 60% should be intact. RNA indices should be reported for the diploid stemline in DNA diploid histograms and the aneuploid stemline for DNA aneuploid histograms.

4. Notes

1. The purity of AO is critical to the successful application of this technique. We recommend AO from Polysciences (Warrington, PA).
2. AO concentration may be adjusted to achieve optimum stainability for different instruments in a given setting (*I*). We recommend trials of various concentrations to achieve the optimal working solution conditions.
3. Maintain intact cells during permeabilization by suspending cells in the presence of serum or albumin. Solution A is used to permeabilize cells and remove histones and acid-soluble proteins. Incubate cell suspensions in this solution at 0–4°C (**Subheading 3.1., step 4**). Vortex-mix gently, as vigorous agitation of cell suspension in solution A may disrupt cell membranes.
4. Cleaning flow cytometers is essential after using AO. This is further stressed if other applications are to follow. Regular cleansing with bleach followed by water should alleviate any AO carryover. If problems persist after cleaning, tubing can be changed between protocols.
5. Paired samples treated with and without RNase and DNase should be stained with AO (*I*). The purpose is twofold; to assess the specificity of staining and determine the amount of spectral overlap. Acquire DNase-treated preparations to ensure AO specificity for RNA (red fluorescence). Likewise, RNase-treated preparations should be acquired to collect DNA (green) fluorescence. Acquire consecutive, independent samples and lymphocyte preparations with and without RNase. These data are important in determining the extent of spectral overlap to adjust compensation accordingly.
6. A series of lymphocyte preparations should be used to determine an acceptable range of RNA values only after spectral overlap has been accounted for

Fig. 3. (*see opposite page*) Two parameter (A) DNA/RNA and one-parameter (B) DNA histograms of a tumor specimen before mixing with NPBLs. (C,D) AO analysis after mixing equal portions of the tumor cell suspension with NPBLs. Note the increase in cell number for the diploid G0/G1 peak in (D).

Fig. 4. (*see page 380*) (A–C) Typical acute lymphocytic leukemia patterns. (*left*: DNA/RNA; *middle*: one-parameter DNA histogram; *right*: one-parameter RNA distribution). The specimen in (A) shows a high proliferative fraction and low RNA content. (B) shows an increasing RNA content with lower proliferative activity. (C) illustrates a classic DNA aneuploid ALL pattern.

Fig. 5. (*see page 381*) (A,B) Two multiple myeloma distributions with high RNA levels and different DNA indices. (C) Typical AML pattern, with high-trailing RNA and high proliferation (*left*: DNA/RNA; *middle*: one-parameter DNA histogram; *right*: one-parameter RNA distribution).

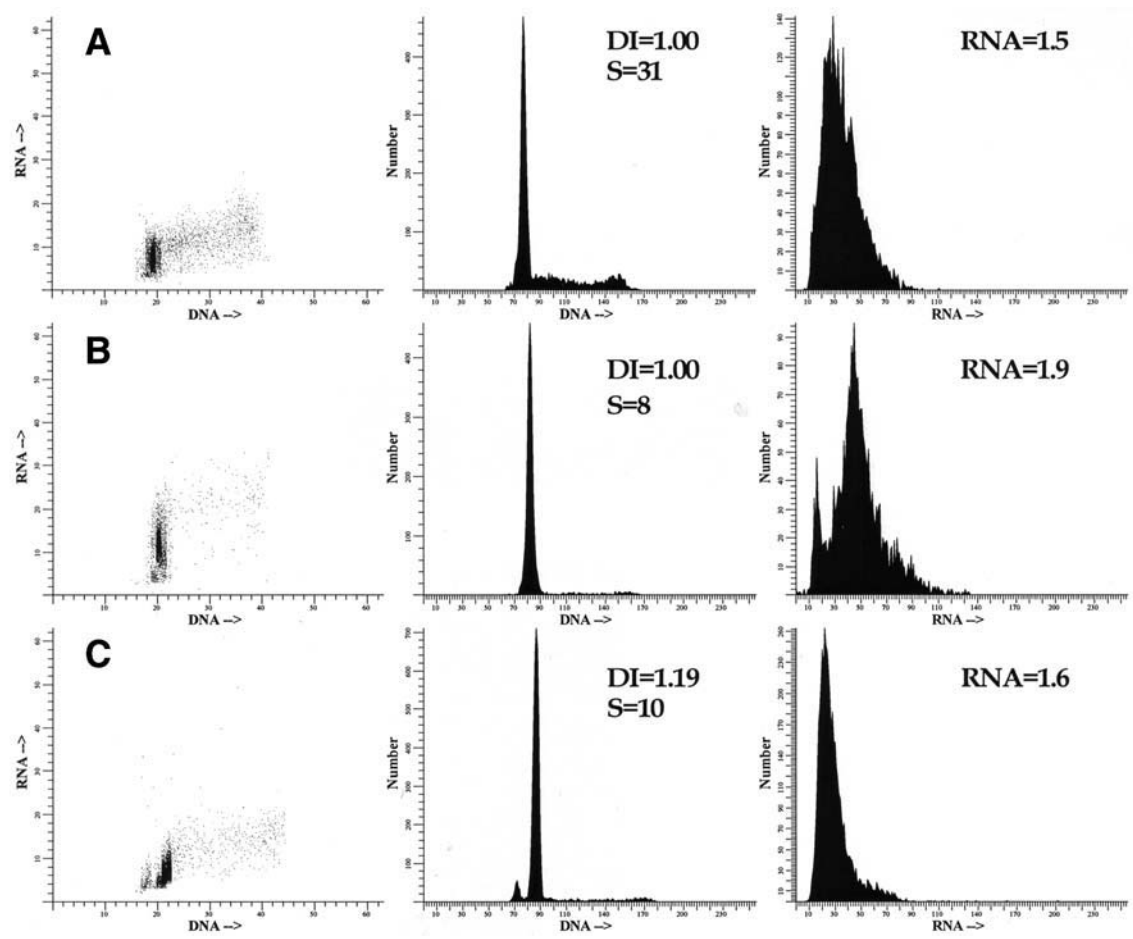


Fig. 4 (see legend on p. 379).

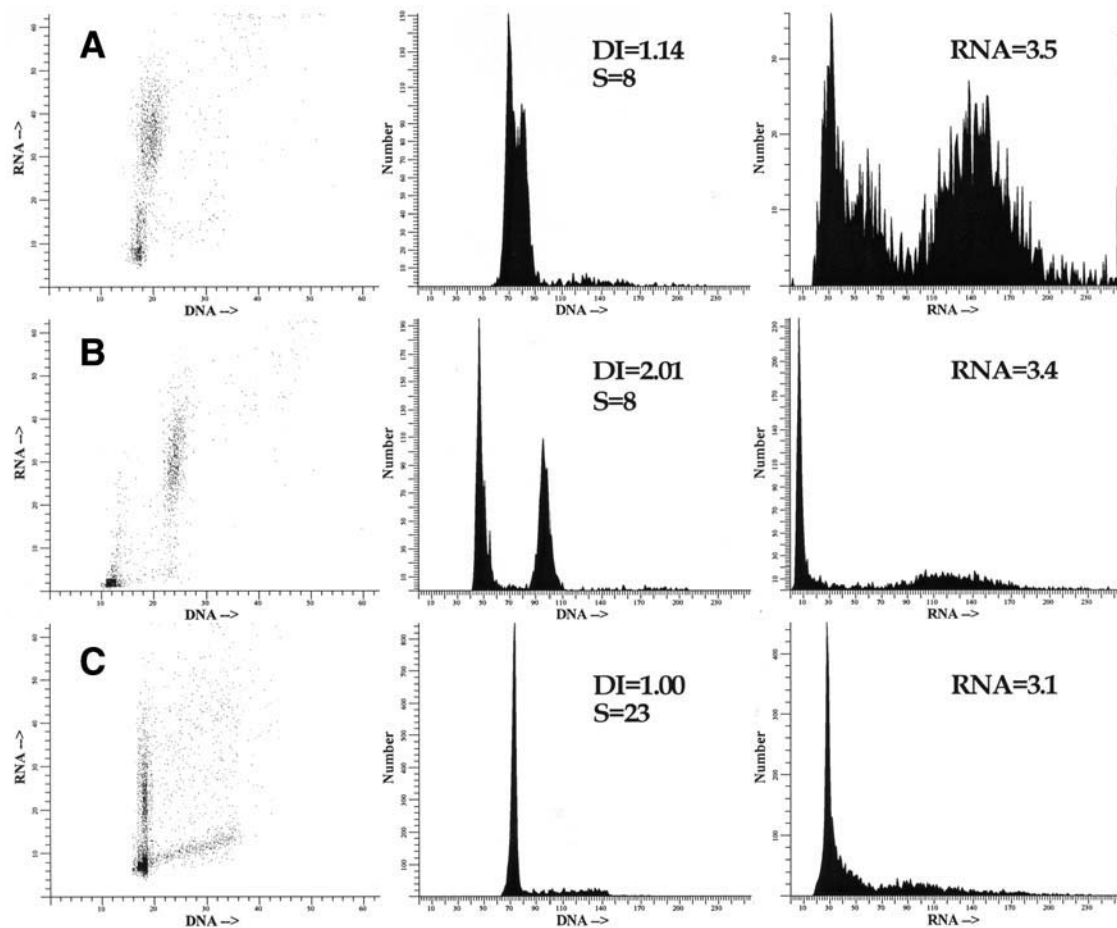


Fig. 5 (see legend on p. 379).

(Note 5). Acquire NPBL with each group of specimens and record the mean RNA fluorescence.

7. Cell concentration is critical, particularly for lymphocyte and tumor mixtures. Equal portions of each are necessary to classify near-diploid populations accurately as hypodiploid (DNA index <1.00) or hyperdiploid (DNA index >1.00).
8. Chromatin condensation differences in solid tumor cells and NPBLs may lead to incorrect histogram classification. Epithelial-derived tumor cells may allow more accessibility to the dye, therefore fluorescing brighter than NPBLs.
9. Debris or red blood cell contamination appear on the left of the diploid population on histograms and may interfere with the detection of a hypodiploid peak and/or cause inaccurate S-phase values, but the use of commercial programs with debris subtraction and aggregate modeling may overcome these problems.
10. Specimens with more than 30% non-neoplastic elements should be eliminated. If lymphocytes are predominant, gate on light scatter and reacquire DNA/RNA fluorescence. Should more than 40% bare nuclei be present, the specimen should be deemed inappropriate for RNA evaluation. Specimens should be used only for DNA ploidy and cell-cycle analysis.

References

1. Darzynkiewicz, Z. (1990) Differential staining of DNA and RNA in intact cells and isolated cell nuclei with acridine orange, in *Methods in Cell Biology*, Vol. 33 (Darzynkiewicz, Z. and Crissman, H.A., eds.), Academic, San Diego, CA, pp. 285–298.
2. Myc, A., Traganos, F., Lara, J., Melamed, M. R., and Darzynkiewicz, Z. (1992) DNA stainability in aneuploidy breast tumors: comparison of four DNA fluorochromes differing in binding properties. *Cytometry* **13**, 389–394.
3. Traganos, F. and Darzynkiewicz, Z. (1994) Lysosomal proton pump activity: supravital cell staining with acridine orange differentiates leukocyte subpopulations, in *Methods in Cell Biology*, Vol. 41 (Darzynkiewicz, Z., Robinson, J. R., and Crissman H. A, eds.), Academic, San Diego, CA, pp. 185–194.
4. Darzynkiewicz, Z. (1994) Simultaneous analysis of cellular DNA and RNA content, in *Methods in Cell Biology*, Vol. 41 (Darzynkiewicz, Z., Robinson, J. P, and Crissman, H. A., eds.), Academic Press, San Diego, CA, pp.185–194.
5. Larson, A. M., Dougherty, M. J., Nowowielski, D. J., et al. (1994) Detection of *Bartonella (Rochalimaea) quintana* by routine acridine orange staining of broth blood cultures. *J. Clin. Microbiol.* **32**, 1492–1496.
6. Preisler, H. D., Raza, A., Gopal, V., Banavali, S. D., Bokhari, J., and Lampkin, B. (1994) The study of acute leukemia cells by mean of acridine orange staining and flow cytometry. *Leukemia Lymphoma* **13**, 61–73.
7. Frey, T. (1995) Nucleic acid dyes for detection of apoptosis in live cells. *Cytometry* **21**, 265–274.
8. Smithwick, R. W., Bigbie, M. R., Ferguson, R. B., Kartix, M. A., and Wallis, C. K. (1995) Phenolic acridine orange fluorescent stain for mycobacteria. *J. Clin. Microbiol.* **33**, 2763–2764.

9. Lopez-Roman, A. and Armengol, J. A. (1995) A fast and easy fluorescent counterstaining method for neuroanatomical studies by using acridine orange. *J. Neurosci. Methods* **60**, 39–42.
10. Gonzalez, K., McVey, S., Cunnick, J., Udovichenko, I. P., and Takemoto, D. J. (1995) Acridine orange differential staining of total DNA and RNA in normal and galactosemic lens epithelial cells in culture using flow cytometry. *Curr. Eye Res.* **14**, 269–273.
11. Grunwald, D. (1993) Flow cytometry and RNA studies. *Biol. Cell* **78**, 27–30.
12. Darzynkiewicz, Z. and Kapuscinski, J. (1990) Acridine orange: a versatile probe of nucleic acids and other cell constituents, in *Flow Cytometry and Sorting*, 2nd ed. (Melamed, M. R., Lindmo, T., and Mendelsohn, M. L., eds.), Wiley-Liss, New York, pp. 291–314.
13. Traganos, F., Darzynkiewicz, Z., Sharpless, T., and Melamed, M. R. (1977) Simultaneous staining of ribonucleic and deoxyribonucleic acids in unfixed cells using acridine orange in a flow cytofluorometric system. *J. Histochem. Cytochem.* **25**, 46–56.
14. Hiddemann, W., Schumann, J., Andreeff, M., et al. (1984) Convention on nomenclature for DNA cytometry. *Cytometry* **5**, 445–446.
15. Andreeff, M., Darzynkiewicz, Z., Sharpless, T. K., Clarkson, B. D., and Melamed, M. R. (1980) Discrimination of human leukemic subtypes by flow cytometric analysis of cellular DNA and RNA. *Blood* **55**, 282–293.
16. Barlogie, B., Maddox, A. M., Johnston, D. A., et al. (1983) Quantitative cytology in leukemia research. *Blood Cells* **9**, 35–55.
17. Barlogie, B., McLaughlin, P., and Alexanian, R. (1987) Characterization of hematologic malignancies by flow cytometry. *Ann. Quant. Cytol. Histol.* **9**, 147–155.
18. Andreeff, M. (1990) Flow cytometry of leukemia, in *Flow Cytometry and Sorting*, 2nd edit. (Melamed, M. R., Lindmo, T., and Mendelsohn, M. L., eds.), Wiley-Liss, New York, pp. 697–724.
19. Andreeff, M. (1990) Flow cytometry of lymphoma, in *Flow Cytometry and Sorting*, 2nd edit. (Melamed, M. R., Lindmo, T., and Mendelsohn, M. L., eds.), Wiley-Liss, New York, pp. 725–743.
20. Darzynkiewicz, Z., Sharpless, T., Stalano-Coico, L., and Melamed, M. R. (1980) Subcompartments of the G1 phase of the cell-cycle detected by flow cytometry. *Proc. Natl. Acad. Sci. USA* **77**, 6696–6700.
21. Darzynkiewicz, Z., Traganos, F., and Melamed, M. R. (1980) New cell cycle compartments identified by multiparameter flow cytometry. *Cytometry* **1**, 98–108.
22. Tyrer, H. W., Golden, J. F., Vansickel, M. H., et al. (1979) Automatic cell identification and enrichment in lung cancer. II. Acridine orange for cell sorting of sputum. *J. Histochem. Cytochem.* **27**, 552–556.
23. Collste, L. G., Darzynkiewicz, Z., Traganos, F., et al. (1980) Flow cytometry in cancer detection and evaluation using acridine orange metachromatic nucleic acid staining of irrigation cytology specimens. *J. Urol.* **123**, 478–485.

24. Barlogie, B., Alexanian, R., Gehan, E. A., Smallwood, L., Smith, T., and Drewinko, B. (1983) Marrow cytometry and prognosis in myeloma. *J. Clin. Invest.* **72**, 853–861.
25. Barlogie, B., Alexanian, R., Dixon, D., Smith, L., Smallwood, L., and Delasalle, K. (1985) Prognostic implications of tumor cell DNA and RNA content in multiple myeloma. *Blood* **66**, 338–341.
26. Srigley, J., Barlogie, B., Butler, J. J., et al. (1985) Heterogeneity of non-Hodgkin's lymphoma probed by nucleic acid cytometry. *Blood* **65**, 1090–1096.
27. Andreef, M., Hansen, H., Cirrincione, C., Filippa, D., and Thaler, H. (1986) Prognostic value of DNA/RNA flow cytometry on B-cell non-Hodgkin's lymphoma: development of laboratory model and correlation with four taxonomic systems. *Ann. NY Acad. Sci.* **486**, 368–386.
28. El-Naggar, A. K., Batsakis, J. G., Teague K., Giacco, G., Guinee, V. F., and Swanson, D. (1990) Acridine orange flow cytometric analysis of renal cell carcinoma. *Am. J. Pathol.* **137**, 275–280.
29. Enker, W. E., Kimmel, M., Cibas, E. S., Cranor M. L., and Melamed, M. R. (1991) DNA/RNA content and proliferative fractions of colorectal carcinomas: a five year prospective study relating flow cytometry to survival. *J. Natl. Cancer Inst.* **83**, 701–707.
30. El-Naggar, A. K., Barlogie, B., McCabe, K., Teague, K., Ensign, L. G., and Pollock, R. E. (1994) Acridine orange DNA/RNA content analysis of soft-tissue tumors: correlation with clinicopathologic factors and biological behavior. *C.M.B.* **1**, 237–247.
31. El-Naggar, A. K., Kemp, B. L., Sneige, N., et al. (1996) Bivariate RNA and DNA content analysis in breast carcinoma: biological significance of RNA content. *Clin. Cancer Res.* **12**, 419–426.

Telomere Length Measurement by Fluorescence *In Situ* Hybridization and Flow Cytometry

Veena Kapoor and William G. Telford

Summary

Telomere length is an important measure of cellular differentiation and progression to senescence. Flow cytometric assays for measuring telomere length have become an important adjunct to more laborious Southern blotting methods; telomere length can be estimated with considerable accuracy in small numbers of individual cells by flow cytometry, and can be measured in cell population subsets with simultaneous fluorescent immunophenotyping. In this chapter, we describe the standard flow cytometric assay for measuring telomere length, including the incorporation of fluorochrome-conjugated antibody immunolabeling for measurement in cell subsets.

Key Words

Peptide nucleic acid probe, quantitative flow cytometry, senescence, telomerase, telomere.

1. Introduction

Telomere length has been actively investigated in the latest decade for its relationship to the telomerase activity and its involvement in several major diseases and in the aging process (1,2). Telomerase, the enzyme responsible for maintaining telomere length, is essential and strictly regulated for the synthesis of telomeres in normal cells during development (2). Telomeres are GT-rich sequences present in DNA as chromosomal end-caps that interact with telomeric binding proteins, providing various genetic and cellular functions such as genomic integrity and stability (1,3). For normal human somatic cells presenting minimal or no telomerase activity, the telomere length decreases at each step of the cell division (4,5). It has been concluded that telomere length acts as a possible internal cellular clock or feedback checkpoint, providing a marker

From: *Methods in Molecular Biology: Flow Cytometry Protocols*, 2nd ed.
Edited by: T. S. Hawley and R. G. Hawley © Humana Press Inc., Totowa, NJ

for the number of accumulated cell divisions and controlling the onset of cellular senescence (5,6).

Telomerase activity appears to be highly correlated to the onset of various diseases. An increase in telomerase activity leads to telomere synthesis, resulting in higher stability of the genome with greater telomere length (1). On the other hand, an accelerated reduction of the telomere length reaching critical limits provides a senescent signal to stop cell division. Such excessive conditions can alter the homeostasis of normal cellular aging, and can result in a number of age-related diseases (7–9).

Indeed, the number of cell replication for normal cells cannot exceed the Hayflick limit, the number of cell divisions that can occur prior to the onset of senescence. Above this number, the critical telomere length will trigger the senescent signal to stop growth (10). For other cells, by selective inactivation of cell cycle checkpoints and by massive selective death, cellular immortalization is observed by maintaining or stabilizing the telomere length above the critical limit with the presence of telomerase activity such as in tumor or cancer cells (11,12). Controlling the telomerase activity to stabilize or to push the telomere length toward defined ranges has been a goal for various therapeutic purposes (13–15). Before being able to modify the telomerase activity, it is essential to have an accurate assessment of its biomarker, the telomere length.

It is therefore necessary to develop a reliable, rapid, and sensitive biomedical technology for the determination of telomere length as an important physiological marker for diseases and treatments. Traditional methods for determining telomere length have generally required whole genomic DNA extraction and Southern blotting for the telomere repeat, a labor-intensive procedure that does not allow estimation of telomere length in individual cells. A fluorescence-based *in situ* telomere-length assay would have significant advantages over the traditional approach, including the integration of fluorescent immunophenotyping for identification of telomere length in specific cell subsets. Flow-fluorescence *in situ* hybridization (flow-FISH), an *in situ* flow cytometric assay utilizing fluorochrome-tagged telomere-complementary oligo probes to estimate telomere length, has become widely used for this purpose (16–23).

This chapter focuses on the general principles for the determination of telomere length by flow cytometry. It describes techniques to standardize the assay, calibrate the flow cytometer, and quantify telomere length. An additional protocol for combining phenotyping and telomere length quantification is also discussed.

2. Materials

2.1. General Supplies

1. Phosphate-buffered saline (PBS) without Ca^{2+} and Mg^{2+} .
2. Bovine serum albumin (BSA).

3. Equipment: Water bath or heating block for 40°C and 82°C, centrifuge, vortex mixer.
4. Tubes: 1.5-mL Eppendorf tubes, disposable 12 × 75 mm polystyrene tubes.
5. Cell counter or hemacytometer.
6. Flow cytometer.

2.2. Reagents

2.2.1. Calibration of Flow Cytometer

Quantum™²⁴ premixed fluorescein isothiocyanate molecules of equivalent soluble fluorochrome (FITC MESF) beads (Bangs Laboratories, Fishers, IN; formerly Flow Cytometry Standards Corporation, San Juan, PR).

2.2.2. FISH

1. Peptide nucleic acid (PNA) fluorescence probe for the telomere repeat sequence: Fluorescein-conjugated PNA probes can either be specifically synthesized (PerSeptive Biosystems, Framingham, MA (17); Boston probes, Bedford, MA [22]), or purchased as a kit, Telomere PNA Kit/FITC (DAKO, Carpinteria, CA). *See Note 1.*
2. Hybridization buffer: 70% Formamide, 20 mM Tris-HCl, pH 7.0, 1% BSA, with or without 0.3 µg/mL of PNA probe.
3. Wash buffer: 70% Formamide, 10 mM Tris-HCl, 0.1% BSA, and 0.1% Tween-20.
4. Resuspension buffer with DNA stain: PBS, 0.1% BSA, either propidium iodide (PI) at 0.06 µg/mL with DNase-free RNase-A at 10 µg/mL, or 7-aminoactinomycin D (7-AAD) at 0.01 µg/mL without RNase-A. *See Note 2.*

3. Methods

3.1. Standardization and Calibration

The FISH technique presently used for labeling telomeres relies on the introduction of specific synthetic peptides that mimic the DNA sequences complementary to the telomere sequence. These synthetic peptides are labeled with low molecular weight fluorochromes, allowing a quantitative measurement by flow cytometry of the number of probes noncovalently bound to the telomeric sites. The PNA probe specific for the telomere repeat sequence ([CCCTAA]₃-PNA) has proven to be very reliable for FISH analysis for telomere length measurements (16–25). PNA probes have significant advantages over traditional cDNA oligo probes, including reduced nonspecific binding to DNA, resistance to nuclease activity, and strong binding stability to the telomere sequence. The mathematical association between PNA probe binding and fluorescence and the approximate number of telomere repeats has been previously determined empirically by comparison to Southern blotting data and can be applied to a variety of cell types (16); however, the quantification of the number of noncovalently

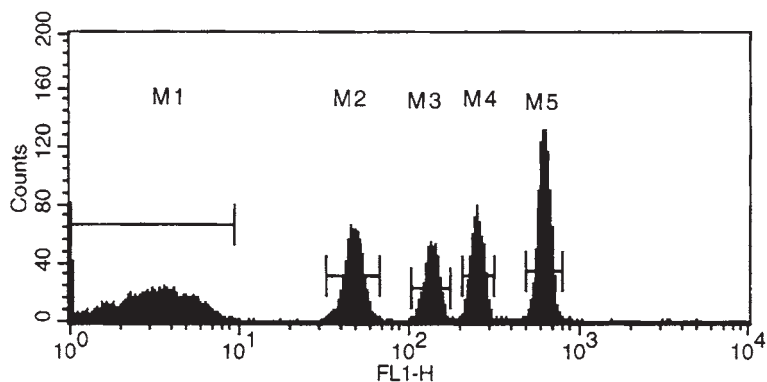


Fig. 1. FL-1 Histograms of MESF beads mixtures (QuantumTM 24 premixed FITC MESF beads). Region M1 corresponds to the blank beads; regions M2 to M5 correspond to the labeled fluorochrome beads with varying MESF values.

bound PNA probes per telomere repeat needs to be calibrated and standardized for each flow cytometer and directly linked to some internal fluorescence value. These arbitrary units are then converted to the telomere length in kbs.

3.1.1. Assay Standardization and MESF Calibration

To compensate the differences existing between flow cytometers and their daily characteristics (laser intensity responses, change in alignment, etc.), a standardization/calibration procedure is necessary to quantify telomere length accurately (16,18). QuantumTM 24 premixed fluorescent MESF beads are used to both calibrate the individual instrument and to establish a fluorochrome-based standard curve for the assay. These beads have known numbers of fluorochrome molecules on their surfaces, allowing for the calibration and linearity determination of the flow cytometer. Thus, a particular fluorescence intensity value on a flow cytometer can be correlated with an actual number of fluorochrome molecules; if the number of fluorochrome molecules attached to a PNA probe is known, a standard fluorescence curve can be established that will correlate relative fluorescence signal with the number of PNA probes bound (and the number of telomere repeats) per cell. An example of this is shown in **Figs. 1** and **2**. A “cocktail” of unlabeled and labeled MESF beads with progressively larger numbers of bound fluorochrome molecules (such as FITC or phycoerythrin [PE]) is analyzed by flow cytometry.

1. Adjust the population of unlabeled beads between channel numbers 1–10 (the first log decade of a four-log scale).
2. Analyze the mixture of beads with different MESF values at the same instrument setting (**Fig. 1**). Ideally, the resulting profile should give a linear relationship

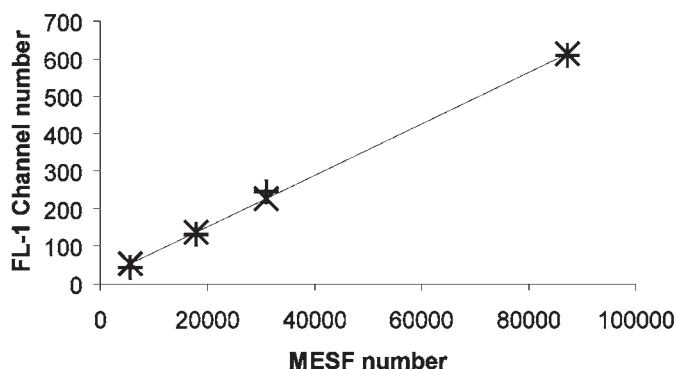


Fig. 2. Typical calibration of the FL1 channel of flow cytometer using MESF. The MESF numbers are lot specific and are determined by the bead manufacturer. (+) ticks correspond to the recorded FL-1 channel number and (-x-) ticks to the adjusted value of the detector channel number using a linear regression method.

between different MESF beads, assuming the flow cytometer detector gives a linear response over its entire dynamic range (**Fig. 2**).

3. Calculate the linear relationship between the MESF beads number (MESF #) and the fluorescence channel number (FLchannel#) using linear regression:

$$\text{FLchannel\#} - \text{FLchannel\#(blank)} = \text{Slope} \times \text{MESF \#} \quad (1)$$

Detector linearity for the fluorochrome in question (such as PE) can thereby be evaluated for individual flow cytometers, a necessary requirement for telomere length measurement (*see Note 3*). The slope of the regression line as shown in **Fig. 2** will also be subsequently used for the determination of the telomere length of the samples. Ideally, an MESF bead calibration should be incorporated into every flow-FISH assay to account for day-to-day instrument variations.

3.1.2. Flow Cytometer Calibration for Telomere Length Using a Conversion Line

1. Rufer et al. (**16**) has previously calculated the correlation between telomere fluorescence measured by flow-FISH using a FITC-conjugated PNA probe, and the telomere length determine by Southern blots for different subpopulations of lymphocytes. This correlation can be generally applied for many cell types. In this system, FITC fluorescence was arbitrarily quantified in terms of a flow cytometer channel number by the equation (**16**):

$$\text{TelomereLength(kb)} = 0.019 \times (\text{FLchannel\#} - \text{FLchannel\#[blank]}) \quad (2)$$

2. A later study from Rufer et al. (**16**) used a more quantitative system using FITC-conjugated MESF beads to calibrate the FITC channel values as described in the preceding. Taking the MESF value as a standard unit instead of the arbitrary chan-

nel number for FITC, the telomere length from Southern blot is therefore expressed in MESF units using the following equation (16):

$$\text{FLchannel\#} - \text{FLchannel\#(blank)} = \text{MESF} \times 0.02604 \quad (3)$$

3. Eliminating the arbitrary units from **Eqs. 2** and **3** provides the final expression of the telomere length in standard MESF units (16,18):

$$\text{TelomereLength(kb)} = \text{MESF} \times 0.019 \times 0.02604 \quad (4)$$

This equation is independent of the flow cytometer used for the assay if it is calibrated with the same standardized MESF beads.

4. Eliminating MESF units from **Eqs. 1** and **4** provide a direct calibration of the flow cytometer FITC channel for the determination of the telomere length by flow-FISH using the following equation:

$$\text{Telomere length(kb)} = (\text{FLchannel\#} - \text{FLchannel\#[blank]}) \times 0.019 \times 0.02604 / \text{Slope} \quad (5)$$

3.2. Experimental Protocol for Quantifying Telomere Length

Cells should be reduced to single-cell suspensions prior to labeling. Each cell sample should be divided, one fraction for incubation with the PNA probe, and one without as a background control. Duplicate or triplicate samples are highly recommended if cell numbers permit (*see Note 4*). It is of critical importance to run control cells with each assay to check the hybridization process. Ideally, cell controls for both short- and long-telomere lengths should be run simultaneously with actual samples. Hultdin et al. (17) have used 1301 cell line with in each sample as internal control. These immortalized cells have very long telomeres and are easily distinguishable from the other cells. Other cell lines are also available for control. Our laboratory has used CCRF-CEM cells as long telomere length controls and Jurkat cells as short telomere length controls. These controls are run with each experiment as separate samples to allow comparisons between multiple experiments run on different days. Once control cell lines were identified, cells with the same passage numbers were aliquoted in large numbers and frozen before being used, giving a reliable source of internal controls (*see Note 4*).

3.2.1. Sample Preparation

1. Wash cells in PBS containing 0.1% BSA.
2. Count cells and add 0.5×10^6 cells to 1.5-mL Eppendorf tubes. Centrifuge cells at 500g to pellet, and decant supernatant.
3. Resuspend the pellet in 300 μL of hybridization buffer with PNA probe at 0.3 $\mu\text{g/mL}$ (90 ng/sample final concentration). A corresponding tube without PNA probe should be included with each sample as a negative control. Some

titration of PNA concentration may be necessary for different probe preparations and cell types.

4. Incubate the tubes in an 82°C heat block or water bath for 10 min. *See Note 5.*
5. Mix the samples by vortexing and incubate them for 2 h (**16,24**) or overnight (**17**) at room temperature in the dark for hybridization.
6. Resuspend the cells in 1 mL of wash buffer, mix, and incubate in a 40°C water bath or heating block for 10 min.
7. Centrifuge the cells at 500g for 7 min. Decant the supernatant and repeat the **step 6**.
8. Resuspend the cells in 500 μ L of resuspension buffer with DNA stain. Transfer the cells to standard 12 \times 75 mm polystyrene tubes and incubate at room temperature for 2–4 h.
9. Analyze the cells on the flow cytometer.

3.2.2. Flow Cytometry

The calibration and linearity of the flow cytometer should be checked at the beginning and at the end of the experiment (*see Note 6*).

1. Run the fluorescent MESF beads prior to cell samples to establish the standard fluorescence curve, as described in **Subheading 3.1.1**.
2. Analyze the cell samples, leaving the FITC detector (usually denoted arbitrarily as FL1) at the same voltage setting as that used for the MESF beads. Initially visualize the cells for forward scatter (FSC) vs DNA dye fluorescence, both with linear scaling (**Fig. 3A**). For both PI and 7-AAD, this will usually be done through the instrument's long red detector. The detector voltage settings for FSC and DNA dye fluorescence can be changed from those used for the MESF beads. All fluorescence compensation settings should be set to zero.
3. Draw a gate around the G₀/G₁ cell cycle phase, and display a histogram for FITC fluorescence gated on this population (**17**) (*see Fig. 3B*).
4. Record the data as a listmode file including FSC (linear), DNA dye (linear), and FITC PNA probe fluorescence (log) as saved parameters.

3.2.3. Data Analysis

1. As described in **Subheading 3.1.1**, linear regression between the MESF quantum beads and the FITC channels is calculated for the flow cytometer used for the experiment using **Eq. 1**:

$$\text{FLchannel\#} - \text{FLchannel\#(blank)} = \text{Slope} \times \text{MESF \#} \quad (1)$$

2. Gate the single G₀/G₁ cell population using FSC vs PI or 7-AAD as described in **Subheading 3.2.2., step 3 (Fig. 3A)**, and gate into a FITC histogram displaying the FITC PNA probe fluorescence (**Fig. 3B**).
3. Record the mean fluorescence intensity (MFI) for both PNA probe and control samples.

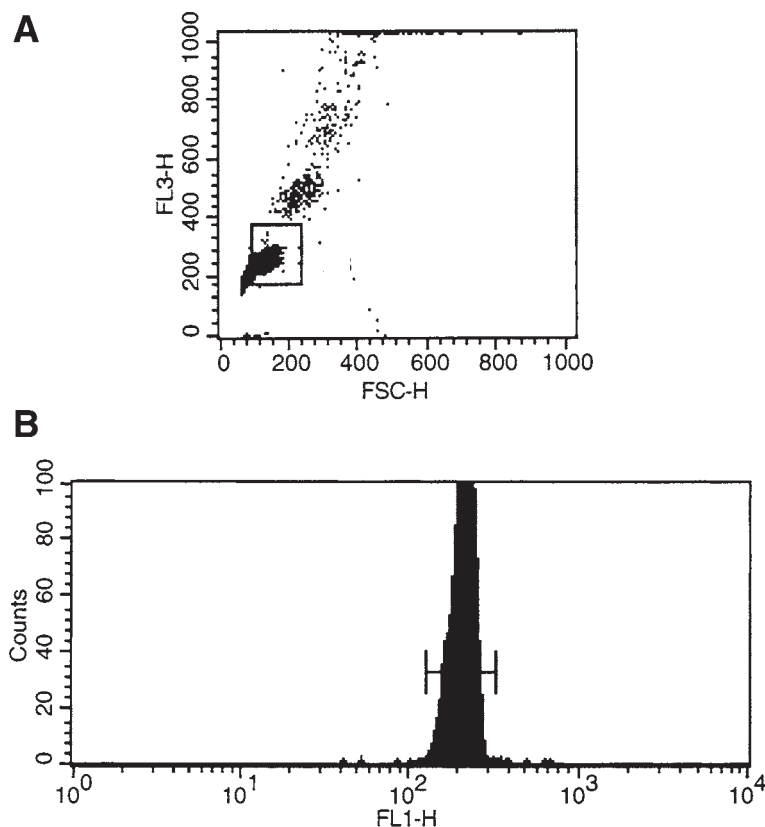


Fig. 3. (A) Dot-plot of forward scatter (FSC) vs PI fluorescence (FL3). *Boxed* or gated cells are in the G₀/G₁ phase cell cycle phase. (B) Histogram of FITC intensity for gated cells from (A).

4. Subtract the MFI value of the control cells from the PNA probe labeled cells.
5. The telomere length can then be calculated from the MSEF standard curve using Eq. 5 (as described in Subheading 3.1.2.):

$$\text{Telomere length(kb)} = (\text{FLchannel\#} - \text{FLchannel\#[blank]}) \times 0.019 \times 0.02604 / \text{Slope} \quad (5)$$

3.2.4. Data Example Using Human CD4 Naïve and Memory T-Cells

A useful test of this assay is to measure the telomere lengths of naïve and memory T cells isolated from normal human peripheral blood mononuclear cells (PBMCs); memory T cells would be expected to have shorter telomere lengths than naïve. The results of this experiment are shown in **Fig. 4**. Jurkat

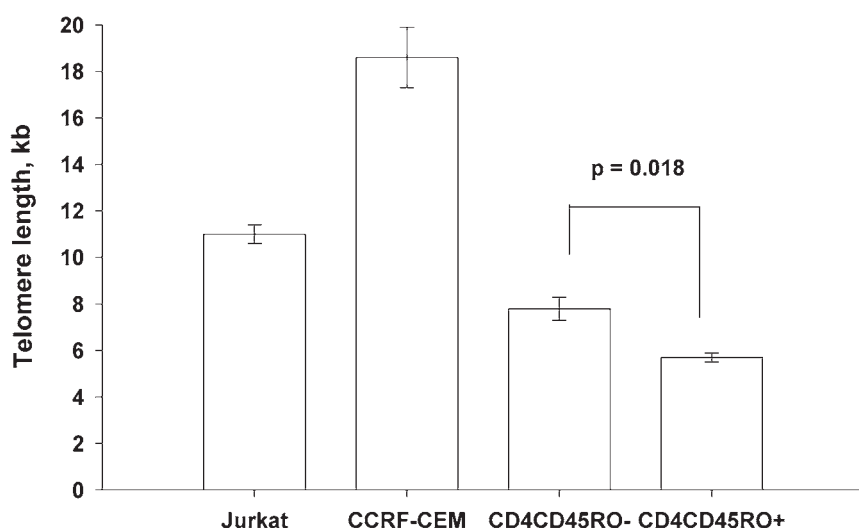


Fig. 4. Telomere length determination using flow-FISH for CD45RO-negative naïve and CD45RO-positive memory CD4⁺ T cells. Jurkat and CCRF-CEM, controls.

and CCRF-CEM cell lines were simultaneously used as short and long telomere controls, respectively. CD4⁺ naïve and memory cells were obtained from the same donors by fluorescence-activated cell sorting, based on their expression of CD4 and presence or absence of the memory marker CD45RO. The results are shown in **Fig. 4** for five independent assays using the same cell populations. Reproducibility between replicates was excellent based on the standard deviation, and sensitivity between naïve and memory telomere length was easily detectable based on the *T*-test analysis, which gave a *p*-value of 0.018 ($n = 5$).

3.3. Experimental Protocol for Phenotyping and Telomere Length Quantification

A key advantage of using flow cytometry to measure telomere length or any cell characteristic is the ability to measure multiple fluorescent parameters simultaneously in the same cell; telomere length measurements can therefore be made in cells simultaneously labeled for cell surface markers, a valuable method for characterizing telomere length in diverse populations of immune cells. To use the above method for complex blood cells or tissues, samples have to be physically sorted prior to telomere length for the different populations (as was done for the naïve and memory T-cell subsets in **Fig. 4**). Incorporation of fluorescent immunophenotyping using fluorochrome-conjugated antibodies would eliminate the need for subset isolation; however, to measure the telomere length,

cells have to be heated to 82°C; many fluorochrome and antibody–antigen complexes cannot withstand these conditions (20). Recently Batliwalla et.al. (24) published a procedure using one color cell surface marker in conjunction with the measurement of telomere length. The low molecular weight monomeric cyanin probe Cy5 fluorochrome (Amersham Biosciences, Piscataway, NJ) was used as a secondary label because it is stable at high temperatures (24). In addition, the antibody–surface antigen complex was stabilized with a covalent crosslinking reagent, protecting it from heat treatment.

3.3.1. Additional Reagents

1. BS3 (*Bis*[sulfosuccinimidyl] suberate) (Pierce, Rockford, IL): This reagent is used for crosslinking phenotyping antibodies to the cells surface prior to heat denaturation. The powdered stock should be stored desiccated at –20°C. Solutions of BS3 should be used promptly and the remainder discarded.
2. Stop buffer: 100 mM Tris-HCl, pH 7.0, and 150 mM NaCl.
3. Cy5-conjugated antibody against the marker of interest (*see Note 7*): Cy5-conjugated secondary antibodies and streptavidin can be obtained from Caltag (Burlingame, CA) or Jackson ImmunoResearch (West Grove, PA). Kits for direct conjugation of Cy5 to most antibodies can be obtained from Amersham Biosciences.
4. Flow cytometer equipped with two lasers, a 488-nm argon-ion and a 633-nm red He–Ne or 635-nm red diode: Cy5 requires a red laser for excitation, usually a He–Ne 633-nm or red diode 635-nm source. Most cell sorters and several commercial bench top flow cytometers offer this option (*see Note 8*).

3.3.2. Cell Surface Labeling

1. Count 1×10^6 cells and label with either the directly conjugated Cy5 antibody, or a biotinylated antibody against the surface marker of interest for 25 min at 4°C.
2. If using directly conjugated antibody, centrifuge and wash the labeled cells with 4 mL of PBS containing 0.1% BSA, and resuspend the cell pellet in 100 μ L of PBS. If using biotinylated antibody, add streptavidin–Cy5 as the second step of labeling.

3.3.3. Crosslinking of Antibody

Prior to the 82°C denaturation step, the Cy5 label complex is stabilized by crosslinking with BS3. BS3 is water soluble and acts by crosslinking primary amines. It covalently bridges the antibody–fluorochrome complex to the cell surface.

1. Prepare BS3 at 2 mM stock concentration in PBS. BS3 should be freshly prepared for each experiment, as it rapidly hydrolyzes in solution. To crosslink cells, add an equal volume of BS3 solution to the resuspended cell pellet (usually approx 100 μ L) and incubate for 30 min at 4°C.

2. Quench the excess BS3 by adding 1 mL of stop buffer for 20 min.
3. Centrifuge the cells and proceed with the protocol described in **Subheading 3.2.1**.

3.3.4. Flow Cytometry and Data Analysis

1. Analyze the sample for FSC and DNA dye fluorescence, and gate on a single G_0/G_1 cell population as described in **Subheading 3.2.2**.
2. Analyze this gated G_0/G_1 cell population for Cy5 fluorescence using a histogram set to the appropriate fluorescence channel, and gate on the Cy5-positive cells.
3. Analyze this gated G_0/G_1 Cy5⁺ cell population in the FITC PNA probe histogram as described in **Subheading 3.2.2**.
4. Proceed with the measurement of telomere length described in **Subheading 3.2.3**.

3.4. Recent Developments

It is theoretically possible to perform immunophenotyping for multiple surface markers in combination with flow-FISH for characterization of multiple subpopulations in a complex sample. However, analysis is limited to fluorochromes that are sufficiently heat stable. The ever-increasing variety of low molecular weight fluorochromes available for flow cytometry (including the Cy dyes from Amersham Biosciences and the Alexa Fluor series of dyes from Molecular Probes) are providing a number of likely candidates. Phycobiliproteins, extremely bright protein fluorochromes commonly used in flow cytometry, are unstable at high temperatures even with covalent crosslinking and are not recommended for flow-FISH. Recently Schmidt et al. (25) have published positive results using Alexa Fluor 488 and Alexa Fluor 546 for simultaneous immunophenotyping with a Cy5-conjugated PNA probe and Hoechst 33342 for DNA analysis; a multiple-laser flow cytometer with red and UV excitation sources was necessary for this combination.

4. Notes

1. Kits: The components of the flow-FISH can be assembled separately, or the system can be purchased in kit form (such as the FITC-PNA flow-FISH system from DAKO). When using a kit, it is recommended to follow the manufacturer's directions. Cy5 immunophenotyping can be easily incorporated into these kits.
2. DNA binding dyes: PI or 7-AAD can both be used for flow-FISH assays. PI can be obtained from many suppliers; it is well excited by 488-nm argon-ion lasers and emits in the 570–620 nm range. 7-AAD can be obtained from Sigma (St. Louis, MO) or Molecular Probes (Eugene, OR). It is also well excited by blue-green lasers and emits farther in the red, with an emission maxima of 650 nm. Both can be analyzed in the far red detector (often designated "FL3") on most commercial flow cytometers. While both dyes work well for flow-FISH, 7-AAD might be preferable in some systems owing to its better spectral separation from FITC.

3. **Instrument linearity:** Flow cytometer photomultiplier tube linearity can depend on a number of factors, including the detector itself and the log amplifier circuits of the cytometer. Generally detector linearity does not extend to all four log decades of most commercial flow cytometers; linearity usually starts to fall off in the first and fourth log decades. Most flow-FISH samples will fall within these boundaries. If a detector appears to be nonlinear throughout its entire dynamic range, both the PMT and the log amp circuits can be replaced to detect this problem. While this problem will affect all flow cytometric analysis, it is particularly acute in quantitative flow techniques such as flow-FISH. The recent advent of fully digital flow cytometers (rather than the hybrid analog-digital systems available earlier) will reduce the errors introduced by electronic log conversion and should improve apparent detector linearity considerably.
4. **Controls:** A common problem in designing flow-FISH assays is the identification of good long-telomere controls. Cell lines derived from fetal tissue or pediatric tumors would be expected to have long telomeres; however, these cell lines are often available only in isolates that have undergone multiple passages, resulting in eventual telomere shortening. The 1301 cell lines has been used previously as a control; however, any cell lines (particularly ones with a long passage history) should be scrutinized carefully prior to use. Cord blood lymphocytes may make a useful long-telomere control if they can be obtained in sufficient quantity.
5. **Denaturation/hybridization temperature:** The denaturation and hybridization temperatures are critical parameters; they cannot vary more than $\pm 2^{\circ}\text{C}$.
6. **Instrumentation:** Most commercial flow cytometers are equipped with a 488-nm argon-ion laser source and are therefore applicable for flow-FISH using a FITC PNA probe and PI or 7-AAD. Instruments from BD Biosciences (San Jose, CA) (including the FACScan, FACSsort, FACSCalibur, FACStar and FACS Vantage) and from Beckman Coulter (Miami, FL) (including the EPICS XL, EPICS ALTRA and Cytomics FC500) are the most common and are all capable of this analysis. Instruments from other manufacturers (such as Partec [Münster, Germany] and DakoCytomation [Fort Collins, CO]) should be equally useful. Benchtop instruments (such as the FACSCalibur and EPICS XL) are particularly useful for flow-FISH, as their fixed alignments and semi-automated quality control allow for good reproducibility in quantitative flow assays. For BD Biosciences and Beckman Coulter instruments, the detector designation for FITC is usually "FL1"; for PI and 7-AAD, the designation is usually "FL3."
7. **Cy5:** The monomeric cyanin dye Cy5 excites with most red laser sources and emits at a peak of 670 nm. It is spectrally well separated from most other fluorochromes (including FITC, PI, and 7-AAD) and is poorly excited by 488-nm laser light, avoiding any crossbeam compensation issues with blue-green excited fluorochromes.
8. **Dual-laser instruments** (equipped with 488-nm and a second red laser) are now quite common. The FACSCalibur is one such instrument, equipped with a second red diode laser emitting at 635 nm. The Cytomics FC500 uses a red HeNe laser emitting at 633 nm. More complex cell sorters (such as the FACS Vantage or

EPICS ALTRA) usually have multiple lasers (including red); however, their adjustable alignments will make them more complex for analyzing flow-FISH, unless a larger number of included fluorochromes mandates their use.

References

1. Saldanha, S. N., Andrews, L. G., and Tollefsbol, T. O. (2003) Assessment of telomere length and factors that contribute to its stability. *Eur. J. Biochem.* **270**, 389–403.
2. Cong, Y. S., Wright, W. E., and Shay, J. S. (2002) Human telomerase and its regulation. *Microbiol. Mol. Biol. Rev.* **66**, 407–425.
3. Dahse, R., Fielder, W., and Ernst, G. (1997) Telomere and telomerase: biological and clinical importance. *Clin. Chem.* **43**, 708–714.
4. Hodes, R. J. (1999) Telomere length, aging and somatic cell turnover. *J. Exp. Med.* **190**, 153–157.
5. Blackburn, E. H. (2000) Telomere states and cell fates. *Nature* **408**, 53–56.
6. Harley, C. B. (1991) Telomere loss: mitotic clock or genetic time bomb? *Mutat. Res.* **256**, 271–282.
7. Oshimura, M. and Barrett, J. C. (1997) Multiple pathways to cellular senescence: role of telomerase repressors. *Eur. J. Cancer* **33**, 710–715.
8. Yang, L., Suwa, T., Wright, W. E., Shay, J. W., and Hornsby, P. J. (2001) Telomere shortening and decline in replicative potential as a function of donor age in human adrenocortical cells. *Mech. Ageing Dev.* **122**, 1685–1694.
9. Goyns, M. H. and Lavery, W. L. (2000) Telomerase and mammalian ageing: a critical appraisal. *Mech. Ageing Dev.* **114**, 69–77.
10. Shay, J. W. and Wright, W. E. (2000) Hayflick, his limit, and cellular ageing. *Nat. Rev. Mol. Cell Biol.* **1**, 72–76.
11. Shay, J. W. and Bacchetti, S. (1997) A survey of telomerase activity in human cancer. *Eur. J. Cancer* **33**, 787–791.
12. Morin G. B. (1997) The implications of telomerase biochemistry for human disease. *Eur. J. Cancer* **33**, 750–760.
13. Mo, Y., Gan, Y., Song, S., Johnston, J., Xiao, X., Wientjes, M. G., and Au, J. L. (2003) Simultaneous targeting of telomeres and telomerase as a cancer therapeutic approach. *Cancer Res.* **63**, 579–585.
14. Hahn, W. C., Stewart, S. A., Brooks, M. W., et al. (1999) Inhibition of telomerase increases the growth of human cancer cells. *Nat. Med.* **5**, 1164–1170.
15. Herbert, B., Pitts, A. E., Baker, S. I., et al. (1999) Inhibition of human telomerase in immortal human cells leads to progressive telomere shortening and cell death. *Proc. Natl. Acad. Sci. USA* **96**, 14,276–14,281.
16. Rufer, N., Dragowska, W., Thornbury, G., Roosnek, E., and Lansdorp, P. M. (1998) Telomere length dynamics in human lymphocyte subpopulations measured by flow cytometry. *Nat. Biotechnol.* **16**, 743–747.
17. Hultdin, M., Gronlund, E., Norrback, K., Eriksson-Lindstrom, E., Just, T., and Roos, G. (1998) Telomere analysis by fluorescence in situ hybridization and flow cytometry. *Nucleic Acids Res.* **26**, 3651–3656.

18. Rufer, N., Brummendorf, T. H., Kolvraa, S., et al. (1999) Telomere fluorescence measurements in granulocytes and T-lymphocyte subsets point to a high turnover of hematopoietic stem cell and memory T cells in early childhood. *J. Exp. Med.* **190**, 157–167.
19. Martens, U. M., Brass, V., Engelhardt, M., et al. (2000) Measurement of telomere length in haematopoietic cells using in situ hybridization techniques. *Biochem. Soc. Trans.* **28**, 245–250.
20. Lauzon, W., Sanchez Dardon, J., Cameron, D. W., and Badley, A. D. (2000) Flow cytometric measurement of telomere length. *Cytometry* **42**, 159–164.
21. Law, H. and Y. Lau (2001) Validation and development of quantitative flow cytometry-based fluorescence in situ hybridization for intercenter comparison of telomere length measurement. *Cytometry* **43**, 150–153.
22. Baerlocher, G. M., Mak, J., Tien, T., and Lansdorp, P. M. (2002) Telomere length measurement by fluorescence in situ hybridization and flow cytometry: tips and pitfalls. *Cytometry* **47**, 89–99.
23. Martens, U. M., Brass, V., Sedlacek, L., et al. (2002) Telomere maintenance in human B lymphocytes. *Br. J. Haematol.* **119**, 810–818.
24. Batliwalla, F. M., Damle, R. N., Metz, C., Chiorazzi, N., and Gregersen, P. K. (2001) Simultaneous flow cytometric analysis of cell surface markers and telomere length: analysis of human tonsillar B cells. *J. Immunol. Methods* **247**, 103–109.
25. Schmid, I., Dagarag, M. D., Hausner, M. A., et al. (2002) Simultaneous flow cytometric analysis of two cell surface markers, telomere length, and DNA content. *Cytometry* **49**, 96–105.

23

Small Lasers in Flow Cytometry

William G. Telford

Summary

Laser technology has made tremendous advances in recent years, particularly in the area of diode and diode-pumped solid state sources. Flow cytometry has been a direct beneficiary of these advances, as these small, low-maintenance, inexpensive lasers with reasonable power outputs are integrated into flow cytometers. In this chapter we review the contribution and potential of solid-state lasers to flow cytometry, and show several examples of these novel sources integrated into production flow cytometers. Technical details and critical parameters for successful application of these lasers for biomedical analysis are reviewed.

Key Words:

Diode, diode-pumped solid state lasers, laser.

1. Introduction

Flow cytometers are dependent on lasers as an excitation source for the ever-expanding group of fluorogenic molecules available for biological analysis. The choice of what lasers to use for flow cytometry has been dependent not only on available laser technology, but also on the efficiency of a flow cytometer's light collecting optics and detectors, and on the characteristics of available fluorescent probes (*1*).

Water-cooled gas lasers have been a traditional choice for fluorochrome excitation in flow cytometry for more than 30 yr; they possess extremely low noise levels, stable power levels, and true TEM₀₀ Gaussian beam configurations. The drawbacks of water-cooled gas sources are their size, their high cost, and their intensive utility and maintenance requirements. Nevertheless, they remain in daily use on many high-end flow cytometers, particularly those with jet-in-air sample systems; this is largely attributable to the low light collection efficiency of these systems, which possess numerical apertures in the area of 0.4–0.6.

From: *Methods in Molecular Biology: Flow Cytometry Protocols*, 2nd ed.
Edited by: T. S. Hawley and R. G. Hawley © Humana Press Inc., Totowa, NJ

Their power levels have also given practical emission levels for a larger group of laser emission lines that possess relatively weak emission energies, such as the array of wavelengths available from krypton-ion sources. For some of these wavelengths (such as the UV, near-UV, and violet) they have traditionally represented the only practical option for flow cytometric applications. The plethora of fluorescent probes now available to biomedical investigators for flow cytometry requires the availability of a wide variety of excitation wavelengths.

Advances in laser, optical, and fluorochrome technology have reduced the requirements for laser power, opening up a wide variety of lower-power laser sources for flow cytometry applications. *Air-cooled gas lasers*, although similar in principle to water-cooled sources, have been integrated into smaller benchtop flow cytometers for years; these include argon-ion, helium–neon (He–Ne), and helium–cadmium (He–Cd) lasers as the most prominent examples (2–7). They have lower cooling requirements and generally require lower levels of routine maintenance. Air-cooled argon-ion lasers emitting at 488 nm are standard equipment on most benchtop analyzers, and He–Ne red 633-nm lasers make robust and long-lived sources for red-excited fluorescent probes (5–7). These lasers have lower output levels than their water-cooled predecessors; their current usefulness is also attributable to improvements in flow cytometer cuvet and light collection optics design (with numerical apertures now approaching 1.2), more sensitive photomultiplier tube detectors, and the availability of fluorochromes with greater excitation/emission efficiency.

Nevertheless, air-cooled gas lasers still possess some drawbacks, primarily high levels of heat generation. The number of available wavelengths from these low-power gas sources is also somewhat limited; air-cooled argon-ion lasers generally emit only at 488 and 514.5 nm, and He–Ne sources other than red 633 nm have traditionally been low in power and less than suitable for flow cytometric applications (7). Recent advances in solid-state laser technology have therefore been an exciting development for flow cytometry (8,9).

Diode lasers (in which laser light is generated by pumping electricity into a solid medium rather than a gas plasma tube) have been integrated into a number of flow cytometers. Among the first diode lasers available were the gallium aluminum arsenide (GaAlAs) variety, which emit in the infrared and formed the basis for optical disk scanning and barcode recognition systems; the development of aluminum gallium indium phosphide (AlGaInP) diodes that emit at 635 nm ultimately gave a laser useful for exciting allophycocyanin and the monomeric cyanin dyes, both useful for fluorescent immunophenotyping (10–12). Diode lasers are now dropping in wavelength; blue and violet diodes are now mass produced; violet laser diodes are now available on many benchtop flow cytometers (13–16). Near-UV diodes are at this writing (2003) in the prototyping stage, and should be practical within the year (17). These violet and near-UV lasers are

small, have minimal cooling requirements and are relatively inexpensive; they are also achieving power levels in the 5–30 mW range, quite applicable for cuvette-based flow cytometry (and even jet-in-air systems at the higher power levels).

Diode-pumped solid-state (DPSS) lasers are a related laser development that are also having a significant impact on flow cytometry. DPSS lasers use a diode source to pump another crystalline material (frequently neodymium yttrium aluminum garnet, or ND-YAG). Frequency doubling or tripling of the pumped laser output can produce laser wavelengths of considerable value in flow cytometry. DPSS 532-nm green lasers are being integrated into a number of instruments, including the Guava Technologies analyzer and the Luminex multiplex bead analyzer; this wavelength excites phycoerythrin (PE) with considerable efficiency. Frequency tripled lasers emitting at 355 nm, originally developed for metal fabrication, are now being reduced in power as air-cooled sources of UV laser light. DPSS 488 nm lasers are now available on several benchtop flow cytometers, including the BD LSR II and the Cytomation CyAn; these lasers emit in the 20-mW range (the same as an air-cooled argon-ion laser) but occupy a fraction of the size and cooling requirements. As for diodes, DPSS lasers are becoming available in an increasing number of wavelengths, many of which may be useful for flow cytometry.

Small, low-power gas and solid-state lasers have therefore found considerable application in flow cytometry, frequently replacing unwieldy water-cooled gas sources. Although low power levels and a lack of laser lines were early problems with these sources, improved instrument sensitivity, better fluorochromes, and an increased array of available laser wavelengths have addressed many of these concerns. In this chapter, several of these small laser sources are evaluated for their applicability in flow cytometry, with comparison to traditional laser sources wherever possible. Information for setting up these laser sources on production flow cytometers will also be provided. The following systems are examined:

He-Ne green 543- and yellow 594-nm lasers. Red He-Ne lasers have found extensive use in flow cytometry; they operate at low temperatures, are extremely reliable, and have easily controlled beam geometries (5–7). He-Ne laser have also been available at other wavelengths, notably green (543 nm), yellow (594 nm), and orange (612 nm); however, generation of these lines is generally inefficient, with the result being very low laser power levels (usually 1–3 mW). These low power levels have made these lasers uncommon sources in flow cytometry. Recent advances in light collection optics, as well as better laser designs have renewed interest in these sources; their wavelengths are of considerable interest for a number of fluorescent applications (7). Integration of He-Ne 543- and 594-nm lasers onto a modern benchtop cuvette flow cell analyzer will therefore be described.

Violet diode lasers (VLD). The gallium nitride and indium gallium nitride UV and violet laser diodes recently developed by Nakamura and colleagues have been adapted to several commercial flow cytometers; they provide a valuable wavelength range (395–410 nm) for the excitation of phenotyping fluorochromes such as Cascade and Pacific Blue, and expressible fluorescent proteins such as cyan fluorescent protein (13–17). These laser continue to improve in power level and beam profile; several such sources will be reviewed here, both on cuvette and jet-in-air flow cell systems.

Near-UV diode lasers (NUVLD). Indium gallium nitride laser diodes have been developed that can extend into the near-UV range (370–385 nm). At this writing, these lasers are beginning to achieve useful power levels with adequate laser lifetimes (>5000 h). While these lasers are already proving useful for the determination of cell cycle using UV-excited DNA probes, they may soon be applicable to other UV-based applications such as calcium flux detection with the fluorogenic chelator indo-1 (an application requiring a shorter wavelength than that provided by violet sources). A prototype source has been installed onto a cuvet system and will be reviewed here.

Although these lasers are only a sampling of novel small sources available for flow cytometry, they provide general principles for integrating these devices into flow cytometers. These excitation sources are rapidly becoming the dominant source of laser light for flow cytometry, a technological trend that should continue.

2. Materials

1. Lasers: The lasers and their manufacturers are listed below. Although this list should not be considered exhaustive or exclusive, some products are manufacturer specific, or conform to custom requirements adhered to by particular suppliers. This will be noted where it occurs.
 - a. He–Ne green 543-nm laser: The laser used in this study was manufactured by Research Electro-Optics, Inc. (Boulder, CO) and emitted at 3 mW following warmup. No power stabilization circuitry was incorporated into this system. Beam was circular to within 1.1 mradians, a beam diameter of 1.2 mm at the outermost beam fringe (**Fig. 1**). This laser showed true TEM₀₀ beam mode and an excellent Gaussian beam profile (*see Note 1*). Other manufacturers include Melles Griot (Boulder, CO) and JDS Uniphase (San Jose, CA).

Fig. 1. (*see facing page top*) (A) He–Ne green 543-nm laser. (B) Beam profile of the above laser with no beam expansion, or (C) with beam expansion using a 5X adjustable optic.

Fig. 2. (*see facing page bottom*) (A) He–Ne yellow 594-nm laser. (B) Beam profile of a Melles Griot standard laser (2.7 mW). (C) Beam profile of a Melles Griot bottle-spec'd laser (4.0 mW). (D) Beam profile of a Research Electro-Optics laser (7.0 mW). All profiles taken with no beam expansion.

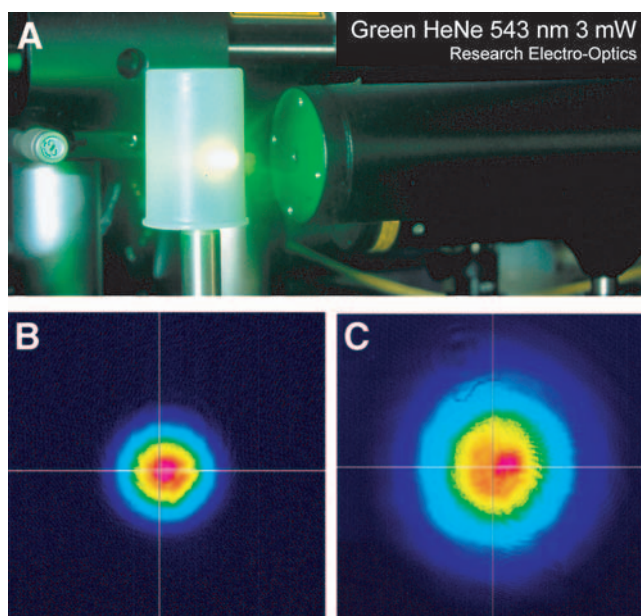


Fig. 1.

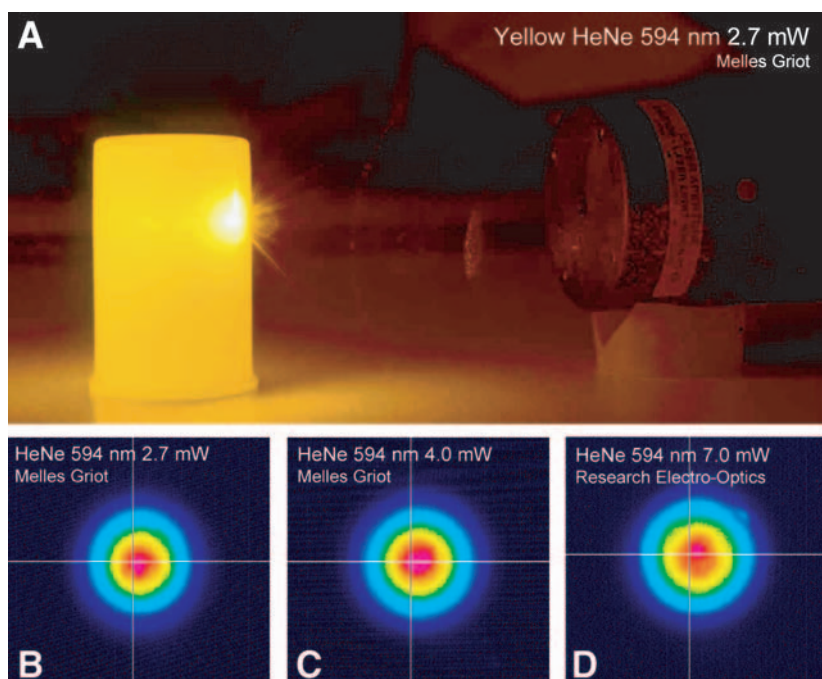
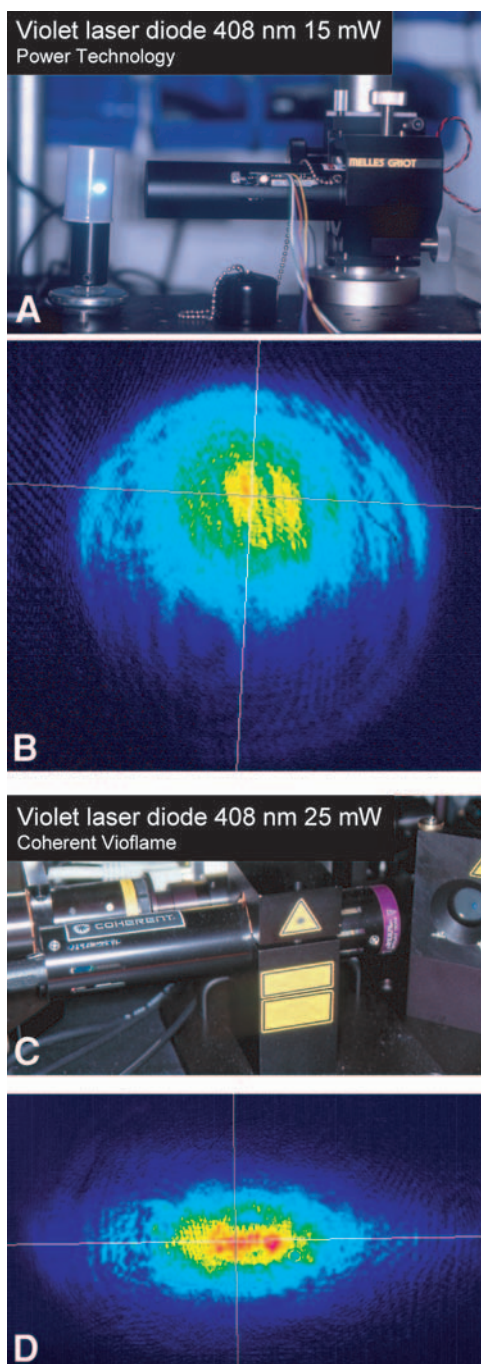


Fig. 2.

- b. He–Ne yellow 594-nm laser: Three yellow He–Ne lasers were evaluated in this study; a stock laser from Melles Griot emitting at 2.7 mW, a custom laser from Melles Griot using the plasma tube with the highest power rating from an entire manufacturing lot, emitting at 4 mW, and a custom laser from Research Electro-Optics with an extended coaxial plasma tube, emitting at 7 mW (**Fig. 2**). These lasers also showed true TEM₀₀ beam modes and excellent Gaussian beam profiles.
 - c. Violet diode 408 nm (Power Technology): This laser was manufactured by Power Technology, Inc. (Alexander, AR) and emitted at 15 mW following warmup. Violet laser diodes are inherently multimodal and require dual prisms to circularize the beam. The beam dimensions following circularization was approx 3 mm × 2.5 mm at the outermost beam fringe, with a somewhat asymmetrical single-mode beam (*see* **Fig. 3B** and **Note 2**).
 - d. Violet diode 408 nm (Coherent): This laser was manufactured by Coherent, Inc. (Santa Clara, CA) under the tradename Vioflame, and emitted at 25 mW following warmup. The beam dimensions following circularization were elliptical and approx 3.5 mm × 1 mm at the outermost beam fringe, with a reasonably symmetrical single-mode beam (**Fig. 3D**).
 - e. Near-UV diode 372 nm: This laser was also manufactured by Power Technology, Inc. and emitted at approx 1.5 mW following warmup. The beam dimensions following circularization were roughly elliptical and approx 4 mm × 1.5 mm at the outermost beam fringe, with a reasonably symmetrical single-mode beam.
 - f. Traditional gas laser sources: Where possible small lasers are compared to traditional gas lasers sources. The green He–Ne and violet diode sources were compared to the green (530 nm) and violet (407 nm) lines of a Coherent I-302C water-cooled krypton-ion laser.
2. Power meter: Laser power was estimated using a NIST-traceable 2W broadband power meter (400 nm–2 mm) with a thermopile graphite detector head from Melles Griot. Comparable power meters are available from many manufacturers, and should be selected based on the power level of the lasers to be tested.
 3. Charge-coupled device (CCD) beam profiling system: CCD chip-based beam profiling systems are useful for determining modality, beam circularity and shape, and Gaussian (or non-Gaussian) beam distributions. This study used the WinCamD system manufactured by DataRay, Inc. (Boulder Creek, CA) and utilizes a 6.3 mm × 4.7 mm Sony CCD chip with neutral density filter blockers. Care should be taken when using CCD chip-based beam profiling optics to attenuate the laser beam and prevent damage to the CCD element (*see* **Note 3**).
 4. Flow cytometers:

Fig. 3. (*see facing page*) **(A)** Power Technology 408-nm violet laser diode at 15 mW. **(B)** Beam profile of this laser. **(C)** Coherent Vioflame 408-nm violet laser diode at 25 mW. **(D)** Beam profile of this laser.



- a. FACS Vantage DiVa Cell Sorter (BD Biosciences, San Jose, CA): This instrument is a typical jet-in-air or stream-in-air cell sorter, where the laser beam directly intercepts the cell stream with no intervening cuvet or flow cell. The instrument uses a set of steering dichroics and prisms to aim the lasers, a flat prism to shape the beams, a standard 50-mm focal length laser focusing lens to focus them onto the sample stream, and a 70- μ m sample/sheath nozzle. Data acquisition and analysis was carried out in digital mode. Long- or shortpass dichroics and narrow band-pass filters are used to separate and isolate fluorescent signals.
 - b. LSR II (BD Biosciences): This instrument utilizes a quartz cuvet or flow cell rather than a jet-in-air system. As with the FACS Vantage DiVa, a set of reflecting dichroics are used to steer the beams to the cuvet, with an intersecting flat prism and a laser focusing lens for beam shaping and focusing. In contrast to the FACS Vantage DiVa, the resulting fluorescent signals are focused onto a set of pinholes coupled to fiber optics, which direct the signals to the appropriate banks of PMT detectors.
5. Alignment standards: Fluorochrome-tagged microspheres are used as quality control and alignment standards for flow cytometers; microspheres with graded levels of incorporated fluorochrome can also be used to gauge the sensitivity and signal-to-noise ratios of detectors. The following bead standards were used for laser evaluation, although many alternatives are available:
- a. He-Ne green 543-nm: Green lasers provide excellent excitation of phycoerythrin (PE) and other yellow- and orange-emitting fluorochromes. The PE-like bead standard is therefore useful for this laser line. The Linear Flow Carmine bead array (Molecular Probes, Eugene, OR) was used for this source; this bead series has an incorporated proprietary fluorochrome at levels of 100%, 10%, 2%, 0.4%, 0.1%, and 0.02%, with the highest level being an arbitrary value. An example of these beads with He-Ne 543-nm excitation is shown in **Fig. 4A**.
 - b. He-Ne yellow 594 nm: Yellow lasers can excite Texas Red and allophycocyanin, which emit in the orange to red range. The InSpeck Deep Red bead array (Molecular Probes) was used for this source; this bead series has an incorporated red-emitting fluorochrome at levels of 100%, 30%, 10%, 3%, 1%, and 0.3% and unlabeled, with the highest level being an arbitrary value. An example of these beads with He-Ne 594 nm excitation is shown in **Fig. 5A**.
 - c. Violet diode 408 nm and near-UV diode 372 nm: Violet lasers excite fluorochrome such as Cascade Blue and Pacific Blue. Although microbead standards specific for violet excitation are not commonly available, UV-excited bead standards are useful for this purpose. The InSpeck Blue bead array (Molecular Probes) was used for this source; this bead series has an incorporated blue-emitting fluorochrome at levels of 100%, 30%, 10%, 3%, 1%, and 0.3% and unlabeled, with the highest level being an arbitrary value. For laser alignment, yellow-green 2- μ m beads from Polysciences (Warrington, PA) were used along with a fluorescein isothiocyanate (FITC) excitation filter; while these beads are mainly used to align instruments with blue-green 488-nm lasers, they are also well-excited by UV and violet sources.
6. Cells and fluorochromes: Cells were labeled with fluorochromes appropriate to

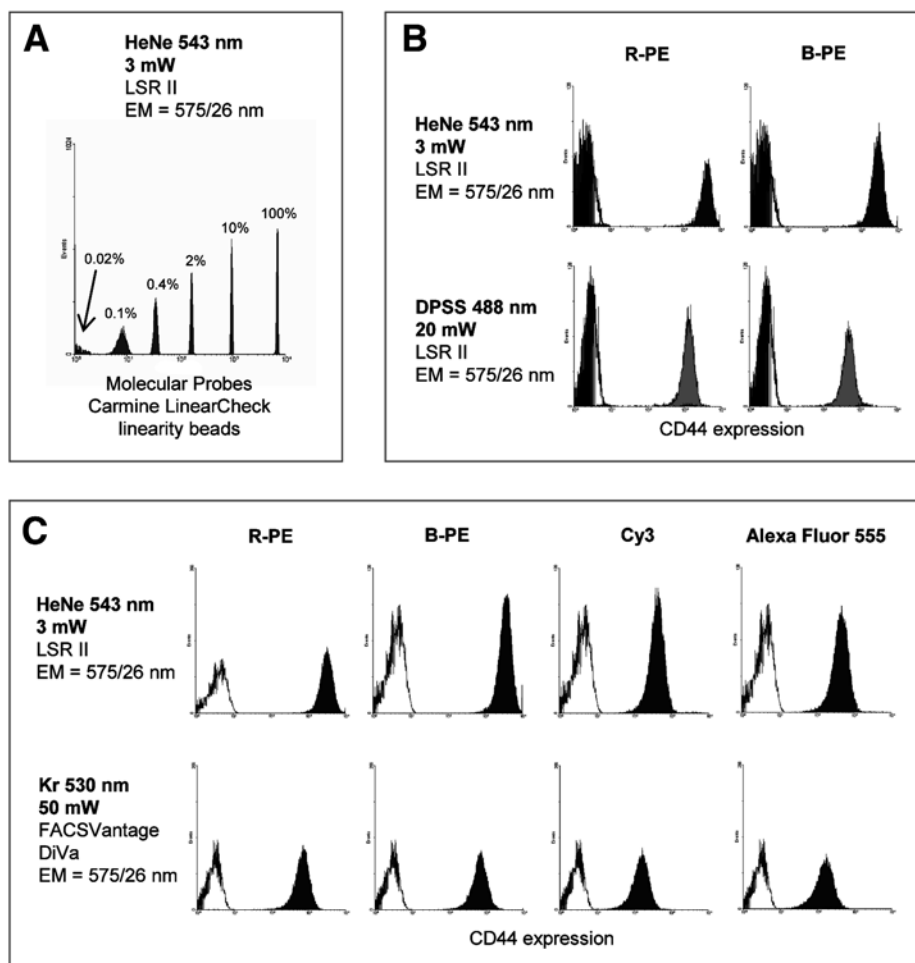
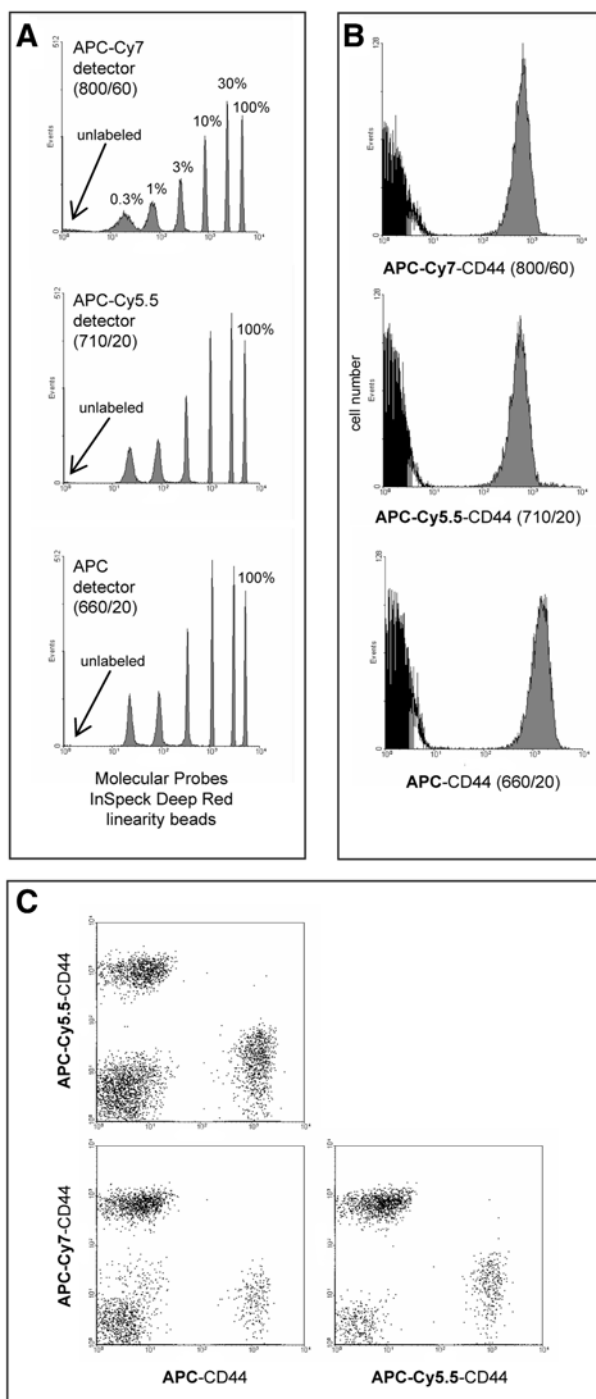


Fig. 4. (A) Analysis of Molecular Probes LinearCheck Carmine microspheres using He-Ne 543 nm excitation on the LSR II. Percentage relative fluorescence of each bead population is shown. (B) Analysis of EL4 thymoma cells labeled with biotin-anti-CD44 followed by streptavidin conjugated to R-PE (left column) or B-PE (right column), using either He-Ne 543 nm (top row) or DPSS 488-nm excitation (bottom row). (C) Analysis of EL4 cells labeled as above for (left to right columns) R-PE, B-PE, Cy3, or Alexa Fluor 555, using either He-Ne 543 nm (top row) or krypton-ion 530 nm (bottom row) excitation. Emission filter used for all sample analyses is indicated (EM = 575/26 nm).

the evaluated lasers. For most evaluations, EL4 mouse thymoma cells (ATCC, Manassas, VA) were labeled with biotin-conjugated anti-CD44 or CD90 followed by a streptavidin conjugate of the fluorochrome of interest. For DNA content analysis using violet or near-UV diode lasers, chicken red blood cells (CRBCs),



trout red blood cells (TRBCs) or calf thymus nuclei (CTNs) were labeled with the UV-excited DNA probe DAPI at 2 $\mu\text{g/mL}$ prior to analysis. These cell standards can be used for evaluating any new laser configuration.

- a. He-Ne green 543 nm: The green He-Ne was used to excite EL4 cells labeled with both the R- and B- form of PE. R-PE is the most commonly used form of this phycobiliprotein; however, B-PE has a somewhat longer wavelength excitation/emission spectrum and can be useful for green excitation sources. The ability of the green He-Ne laser to excite low molecular weight fluorochromes including Cy3 and Alexa Fluor 555 was also assessed. Both R-PE- and B-PE-conjugated streptavidin were obtained from ProZyme, Inc. (San Leandro, CA). Cy3 was obtained from Jackson ImmunoResearch (West Grove, PA), and Alexa Fluor 555 from Molecular Probes.
- b. He-Ne yellow 594 nm: Yellow He-Ne lasers can excite allophycocyanin (APC) and its tandems with efficiency approaching red He-Ne lasers; additionally, they can also excite Texas Red, allowing simultaneous analysis of this useful fluorochrome, APC, and its tandems. EL4 cells, EL4 cells labeled with APC, the APC tandem probes APC-Cy5.5 and APC-Cy7, and Texas Red (and its Molecular Probes equivalent Alexa Fluor 594) were therefore all tested. APC, APC-Cy5.5, and APC-Cy7 conjugated streptavidin were obtained from Caltag (Burlingame, CA). Texas Red and Alexa Fluor 594 conjugated streptavidin were obtained from Molecular Probes.
- c. Violet diode 408 nm: Violet diode lasers can excite the phenotyping fluorochromes Cascade Blue and Pacific Blue, as well as cyan fluorescent protein (CFP). EL4 cells labeled with Cascade Blue and Pacific Blue were therefore used as a cell standard. Cascade Blue and Pacific Blue conjugated streptavidin were obtained from Molecular Probes.
- d. Near-UV diode 372 nm: The relatively low power output of this prototype laser (372 nm) made it unsuitable for exciting UV phenotyping dyes such as 7-aminomethylcoumarin (AMCA) or Alexa Fluor 350. However, the DNA standards (CRBCs, TRBCs, and CTNs) were used to evaluate this source for

Fig. 5. (*see opposite page*) **(A)** Analysis of Molecular Probes InSpeck Deep Red microspheres through detectors equipped with filters for APC-Cy7 (800/60-nm filter), APC-Cy5.5 (710/20 nm), and APC (660/20 nm) using 594-nm He-Ne excitation on the LSR II. A 735-longpass dichroic was used to split the APC-Cy7 signal from APC-Cy5.5 and APC, and a 695-longpass to split the APC-Cy5.5 signal from APC. Percentage relative fluorescence of each bead population is shown. **(B)** Analysis of EL4 thymoma cells labeled with biotin-anti-CD44 followed by streptavidin conjugated to APC-Cy7 (**top**), APC-Cy5.5 (**middle**), or APC (**bottom**) using the above filter/dichroic configuration. **(c)** Simultaneous analysis of the above three fluorochromes using a "cocktail" of APC-Cy7, APC-Cy5.5, and APC conjugated EL4 cells using the above filter/dichroic configuration. Emission filters used for all sample analyses are indicated in parentheses.

DNA content measurement using the DNA probe DAPI.

3. Methods

Laser safety: All of the lasers described below are class IIIa or IIIb laser sources and should be handled with caution (*see Note 4*).

3.1. He-Ne Green 543-nm Laser

1. Laser and instrument configuration: The He-Ne 543-nm laser is shown in **Fig. 1A**. The beam profile shows an excellent Gaussian distribution (**Fig. 1B**). This laser was mounted on the BD LSR II in place of the conventional He-Ne 633-nm laser. The cuvet and pinhole design of the LSR II light collection optics frequently requires some laser beam shaping, expanding the brightest point of the beam somewhat; this is accomplished using a 5X beam expanding optic (Newport Corporation, Irvine, CA), resulting in a wider beam profile and flatter beam top (*see Fig. 1C* and **Note 1**).
2. Alignment and sensitivity: LinearCheck Carmine alignment microspheres were analyzed on the green He-Ne-equipped LSR II both for alignment and assessment of sensitivity. Alignment was carried out by a combination of adjusting the laser dichroic mirrors and the beam expanding optic. **Figure 4A** shows the results from the microsphere analysis—excellent peak CVs are achieved, and the dim 0.1% bead population can be easily distinguished from the lowest 0.02% component.
3. Fluorochrome analysis: EL4 cells labeled with either R-PE or B-PE were analyzed with the He-Ne 543-nm laser and compared to excitation with a DPSS 488-nm 20-mW laser source on the same instrument (**Fig. 4B**). Blue-green 488-nm laser light is most commonly used to excite PE to its ubiquity on most benchtop sorters. However, the He-Ne 543 nm gave much better excitation than the 488-nm line, despite a far lower power level. The ability of the He-Ne 543 nm to excite cells at more than adequate levels is further illustrated in **Fig. 4C**, where green He-Ne excitation of R-PE, B-PE, and the low molecular weight fluorochromes Cy3 and Alexa Fluor 555 was compared to green excitation with a krypton-ion 530-m laser at 50 mW on the FACS Vantage DiVa. The more efficient light collection optics on the cuvet instrument combined with green He-Ne excitation gave better sensitivity than a more powerful gas laser on a jet-in-air instrument.

3.2. He-Ne Yellow 594-nm Laser

1. Laser and instrument configuration: A typical He-Ne 594-nm laser is shown in **Fig. 2A**. Three He-Ne yellow 594-nm lasers were evaluated, with the objective of obtaining a laser with maximum power output (a problem with yellow He-Ne lasers, as the emission of the yellow line is relatively inefficient). Beam profiles for lasers emitting at 2.7, 4, and 7 mW are shown in **Fig. 2B,C,D**. As with the green He-Ne, excellent Gaussian profiles were obtained. Beam expansion to maximize the brightest point of the beam was also useful for these sources (*see Note 1*). The lasers were individually mounted on the LSR II in the default red

He–Ne position as was done for the green.

2. Alignment and sensitivity: The LSR II was equipped to detect three fluorochromes with the yellow He–Ne; therefore, the detectors were configured to detect APC (with a 660/20 nm narrow bandpass filter), APC-Cy5.5 (710/20 nm), and APC-Cy7 (800/60 nm). Analysis of the InSpeck Deep Red bead array gave excellent sensitivity in all detectors, with the dimmest 0.3% microsphere population easily distinguishable from the unlabeled spheres (**Fig. 5A**).
3. Analysis of APC and APC tandem conjugates: EL4 cells labeled with APC, APC-Cy5.5, or APC-Cy7 were all well excited with the yellow laser (**Fig. 5B**). Comparative studies between yellow and red He–Ne lasers show a negligible loss of APC excitation with the yellow sources; these lasers are quite adequate for use with red-excited phycobiliproteins (data not shown). Three-color analysis of a “cocktail” of APC-, APC-Cy5.5-, and APC-Cy7-labeled EL4 cells showed that all three fluorochromes could be simultaneously analyzed with reasonable color compensation values, as is commonly done with red laser sources.
4. Analysis of Texas Red: The most significant advantage of replacing a red He–Ne laser with a yellow is the ability to analyze Texas Red in addition to APC and its tandems. Texas Red and its more recent derivatives (such as Alexa Fluor 594) are very bright fluorochromes; however, they now see little use in flow cytometry, primarily because of the lack of simple yellow excitation sources. Dye head lasers emitting in the 580- to 620-nm range have been typically required to excite Texas Red; these lasers require a powerful water-cooled gas laser as a dye “pump,” and are very maintenance-intensive. Yellow He–Ne lasers can excite Texas Red extremely well, allowing it to be combined with APC and its tandems for up to four-color analysis off one yellow source. Yellow He–Ne excitation of Texas Red and Alexa Fluor 594 (using a 630/22 nm filter) is shown in **Fig. 6A**, and in combination with APC and APC-Cy7 in **Fig. 6B**. Yellow He–Ne excitation therefore allows the addition of an additional fluor to APC and its tandems.

3.3. Violet Laser Diode 408 nm

1. Laser and instrument configuration: Two typical violet laser diodes are shown in **Fig. 3**. A Power Technology VLD is shown in **Fig. 3A**, with its beam profile in **Fig. 3B**. A Coherent Vioflame VLD and its beam profile are shown in **Fig. 3C,D**. Unlike He–Ne lasers, diode lasers often have multimodal and highly asymmetrical beam configurations; commercial lasers usually attempt to correct this with a pair of cylindrical lenses mounted at 90° angles to one another, circularizing the beams to some degree (*see Notes 1 and 2*). The Power Technology beam has been circularized but with an uneven distribution over the entire beam diameter; however, the brightest point of the beam has been roughly centered (**Fig. 3B**). The Coherent beam has a more uniform elliptical shape (**Fig. 3D**). In both cases, the lasers were mounted on either the LSR II or FACSVantage DiVa flow cytometers and rotated until the broadest beam axis was horizontal; this resulted in a more elliptical beam profile on the flow cell or sample stream. This profile is desirable

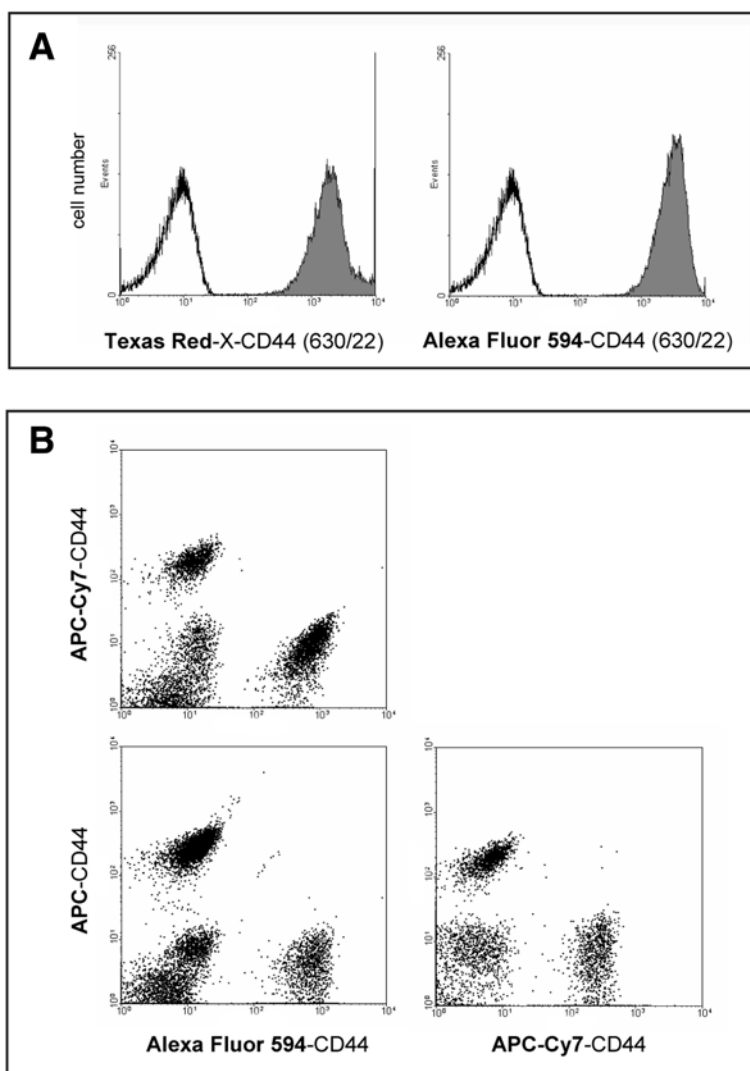


Fig. 6. **(A)** Analysis of EL4 cells labeled with biotin-anti-CD44 followed by streptavidin conjugated to Texas Red (**left**) or Alexa Fluor 594 (**right**) with He-Ne 594-nm excitation on the LSR II. **(B)** Simultaneous analysis of the above fluorochromes using a “cocktail” of APC-Cy7-, APC-, and Alexa Fluor 594-conjugated EL4 cells using the above filter/dichroic configuration. Emission filters used for all sample analyses are indicated in parentheses.

for good cell illumination, since the cell path will be maximally illuminated horizontally but will have a reduced vertical cross-section.

The relatively large power outputs of these lasers make them applicable not only for cuvet instruments such as the LSR II, but also for jet-in-air instruments the FACSVantage DiVa cell sorter. These lasers were therefore mounted on both instruments. The mounting system for the cell sorter is shown in **Fig. 7**. The mounting hardware (identified in **Fig. 7A,B**) was obtained from Newport Instruments (Irvine, CA), although any optical component supplier can provide these standard parts. This mounting system allowed both translational and rotational movement along all the relevant axes. The lasers are shown mounted on the cell sorter in **Fig. 7C,7D**.

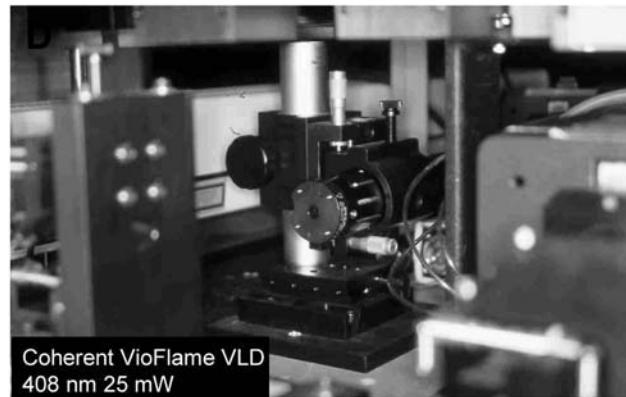
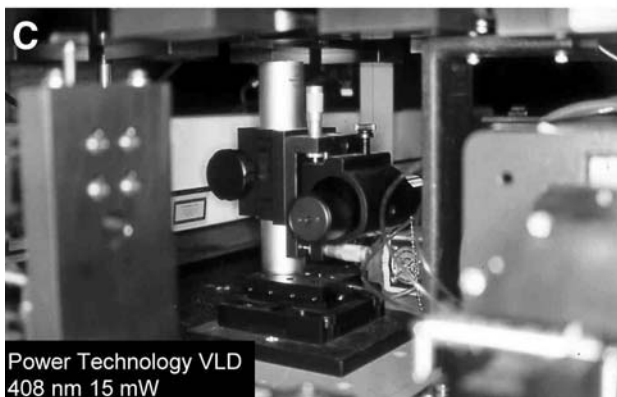
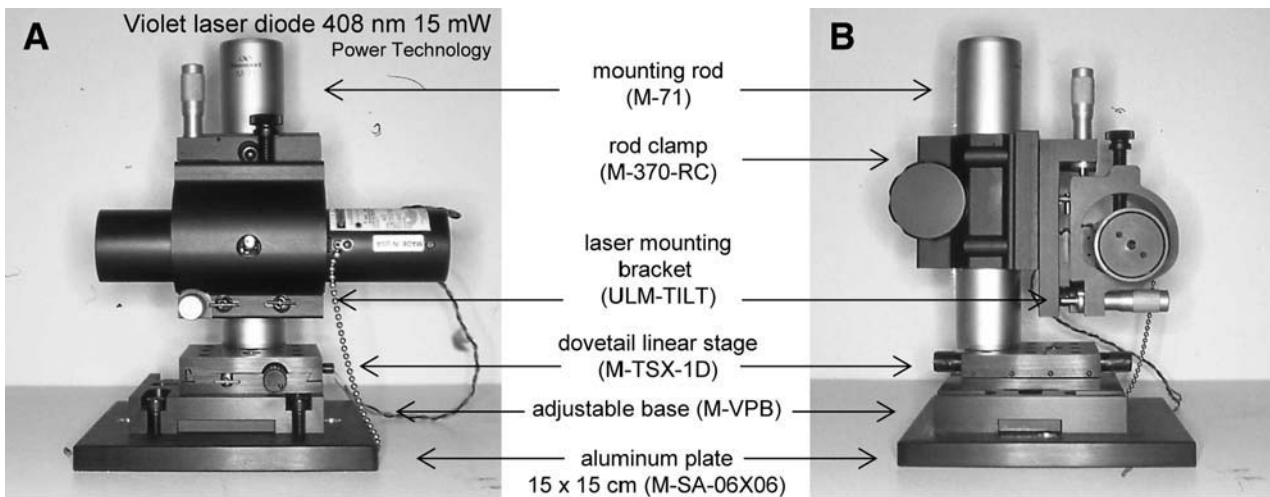
2. Alignment and sensitivity: All alignments were carried out using the InSpeck Blue microspheres.
3. Fluorochrome analysis: Violet laser diodes excite Cascade Blue and Pacific Blue particularly well. This is shown in **Fig. 8A**, where Cascade Blue and Pacific Blue labeled EL4 cells were analyzed on the LSR II. Interestingly, mounting the same lasers on the FACSVantage DiVa jet-in-air sorter give similar signal-to-noise ratios to that seen on the LSR II for both lasers (**Fig. 8B**). Despite their differing beam profiles and power levels, both lasers in this study performed comparably. This suggests that, while these lasers work well on cuvet instruments, their power levels make them applicable to open-stream systems as well despite their reduced light collecting capabilities. In fact, VLDs provide similar excitation efficiency to more powerful gas lasers emitting in the violet; the comparison in **Fig. 8C** shows that the 15-mW VLD excited Cascade and Pacific Blue labeled cells as well as a krypton-ion source emitting 50 mW at 407 nm.

3.4. 372-nm Near-UV Laser Diode

1. Laser and instrument configuration: An engineering prototype 372-nm diode is shown in **Fig. 9A**, and mounted on the LSR II in **Fig. 9B**. Despite its low power, the laser gave excellent results for cell cycle analysis; analysis of CRBC, TRBC, and CTN standards labeled with the DNA binding dye DAPI at 2 $\mu\text{g/mL}$ gave excellent CVs (**Fig. 9C**). Violet laser diodes can also be used to measure DNA content in 4',6'-diamidino-2-phenylindole (DAPI)-labeled cells; however, the UV wavelength gave better resolution despite a lower power level (**Fig. 9C**). When these lasers achieve higher power levels and diode lifetimes, they may prove very useful not only for cell cycle analysis, but dimmer UV-based applications such as indo-1 calcium measurement and Hoechst 33342 "side population" stem cell analysis as well.

3.5. Conclusions

This chapter has shown practical examples of small, low-power laser integration into flow cytometers. Results obtained with these sources can be comparable to those obtained using more traditional lasers sources. Incorporation of



these lasers into commercial instruments is already well under way; it is expected that this technology will become ubiquitous in modern instrument design.

4. Notes

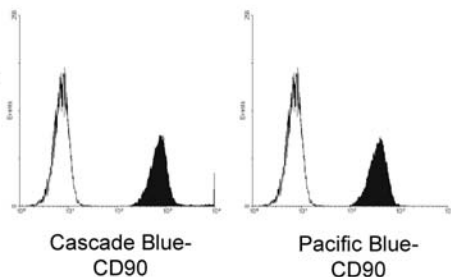
1. Beam profile and mode: Special attention should be paid to beam profile when integrating a new laser into a flow cytometric system. Gas lasers (both large and small) traditionally produce a TEM₀₀ or single-mode profile, appearing as a symmetrical Gaussian distribution. These beams are often subsequently shaped to produce an elliptical spot that will illuminate the entire sample stream in the horizontal axis, with a flatter beam top. Small gas lasers (such as He–Ne) usually produce extremely uniform Gaussian beams. Diode lasers, on the other hand, frequently produce multimodal (or mixed mode) beams with multiple peaks and valleys; these can be shaped with cylindrical optics to produce a roughly circular or elliptical spot. When adapting one of these lasers to a flow cytometer, the beam profile should be measured at the distance the beam will travel to the cell intercept point, to ensure that the shape is appropriate or at least acceptable for stream interrogation. In the case of He–Ne lasers, beam shape can be modified with beam expanding optic. For diode lasers, most commercial models allow some adjustment to the cylindrical lenses, with the help of the manufacturer.
2. Circularization optics: Modifying the beam shape in diode lasers with prisms or cylindrical optics inevitably reduces the power output, sometimes significantly. This decrease can run up to 30% in some cases, and should be taken into account when choosing diode lasers.
3. CCD camera profiling systems: CCD chip beam profiling systems can suffer permanent damage if too powerful a laser beam is directed against their surface. The manufacturers usually provide the necessary equations to calculate the maximum beam power their systems can endure; these should be followed closely. Neutral density filters can usually be inserted in the beam path to attenuate more powerful lasers and still allow their beam profile to be measured.
4. Safety: Although these lasers described below have power outputs well below that typically observed from water-cooled gas sources, eye damage can still result from direct beam exposure. The violet and near-UV sources in particular can cause both eye and skin damage. Proper protective eyewear and beam shielding is highly recommended when working with any class III laser source.

Acknowledgments

Fig. 7. (*see opposite page*) (A,B) VLD mounting system for integration into the FACSvantage DiVa cell sorter (*front and side views*). Part descriptions and numbers correspond to materials available from Newport Corporation. (C) Power Technology VLD mounted on the cell sorter. (D) Coherent Vioflame VLD mounted on the cell sorter.

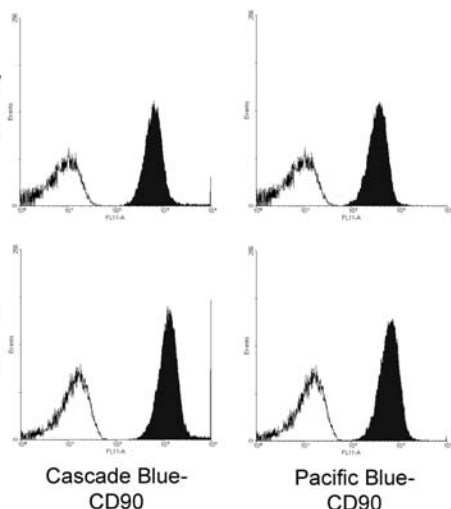
A

Coherent Vioflame
408 nm 25 mW
LSR II
EM = 440/10

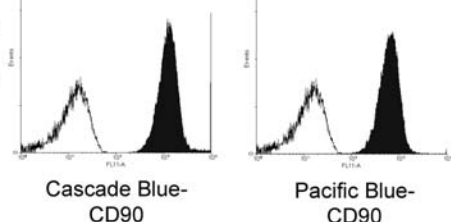


B

Power Technology
408 nm 15 mW
FACSVantage DiVa
EM = 440/10

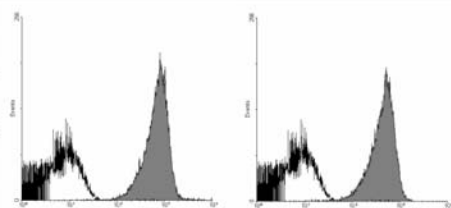


Coherent Vioflame
408 nm 25 mW
FACSVantage DiVa
EM = 440/10

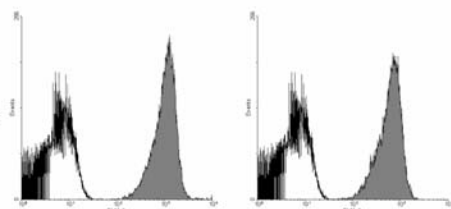


C

Power Technology
408 nm 15 mW
FACSVantage DiVa
EM = 440/10



Kr 407 nm 50 mW
FACSVantage DiVa
EM = 440/10



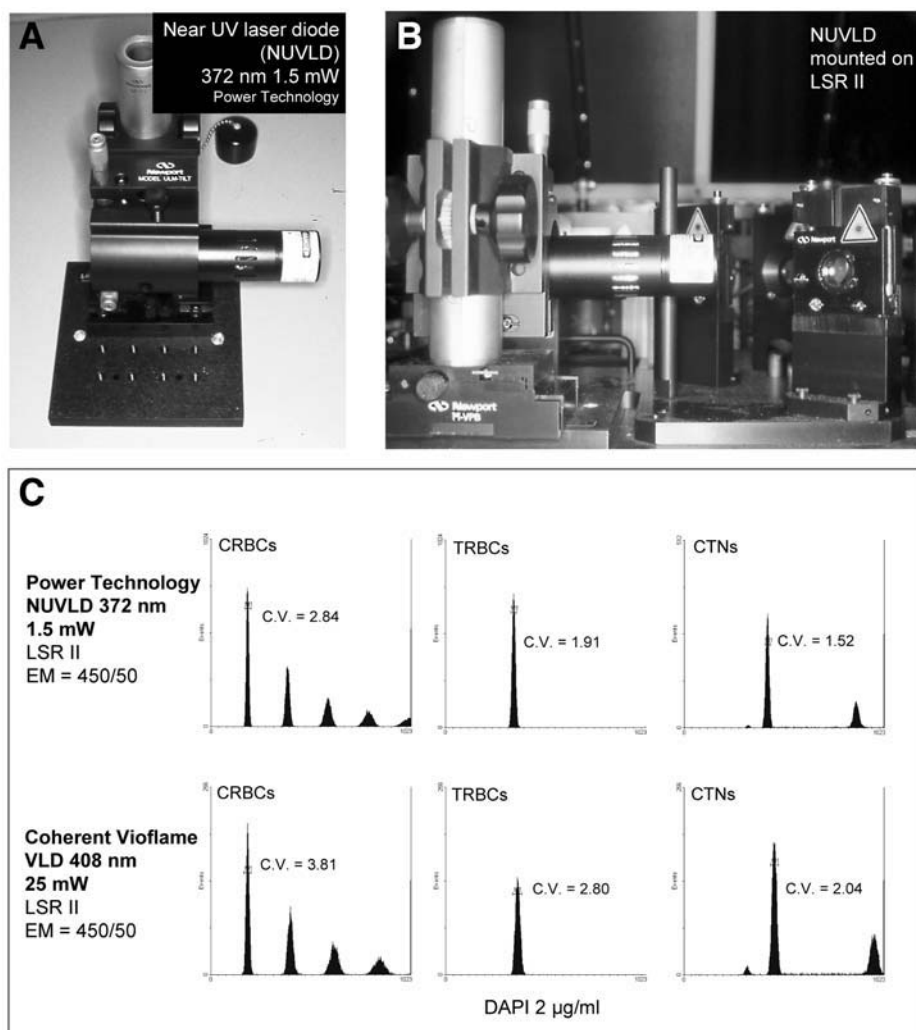


Fig. 9. (A) Power Technology near-UV laser diode 372 nm at 1.5 mW. (B) NUVLD mounted on the LSR II. (C) DNA content analysis of chicken red blood cells (CRBCs, **left column**), trout red blood cells (TRBCs, **middle column**), and calf thymus nuclei (CTNs, **right column**) labeled with DAPI at 2 µg/mL using the NUVLD (**top row**) or VLD (**bottom row**) on the LSR II. Singlet peak CVs are indicated. Emission filters used for all sample analyses are indicated (EM).

Fig. 8. (see opposite page) (A) Analysis of EL4 cells labeled with biotin-anti-CD90 followed by streptavidin conjugated to Cascade Blue (**left**) or Pacific Blue (**right**) using VLD excitation on the LSR II. (B) Analysis of the above cells using either Power Technology or Coherent VLD excitation on the FACS Vantage DiVa cell sorter. (C) Analysis of the above cells using either VLD or krypton-ion 407-nm excitation on the FACS Vantage DiVa cell sorter. Emission filters used for all sample analyses are indicated (EM).

The author wishes to acknowledge James Jackson and his colleagues at Power Technology, Inc. for their generous loan of a prototype near-UV diode laser and for valuable discussion.

References

1. Shapiro, H. (1995) How flow cytometers work, in *Practical Flow Cytometry*, John Wiley & Sons, New York, pp. 111–113.
2. Shapiro, H. M. and Stephens, S. (1986) Flow cytometry of DNA content using oxazine 750 or related laser dyes with 633 nm excitation. *Cytometry* **7**, 107–110.
3. Shapiro, H. M. and Perlmutter, N. G. (1993) Bivariate chromosome flow cytometry using single-laser instruments. *Cytometry (Suppl. 6)*, 71.
4. Frey, T., Stokdijk, W., and Hoffman, R. A. (1993) Bivariate flow karyotyping with air-cooled lasers. *Cytometry (Suppl. 6)*, 71.
5. Snow, C. and Cram, L. S. (1993) The suitability of air-cooled helium cadmium (HeCad) lasers for two color analysis and sorting of human chromosomes. *Cytometry (Suppl. 6)*, 20.
6. Hoffman, R. A., Reinhardt, B. N., and Stevens, F. E. (1987) Two-color immunofluorescence using a red helium neon laser. *Cytometry (Suppl. 1)*, 103.
7. Telford, W. G., Moss, M. M., Morseman, J. P., and Allnutt, F. C. T. (2001) Cryptomonad algal phycobiliproteins as fluorochromes for extracellular and intracellular antigen detection by flow cytometry. *Cytometry* **44**, 16–23.
8. Shapiro, H. M. (1993) Trends and developments in flow cytometry instrumentation, in *Clinical Flow Cytometry*, *Ann. NY Acad. Sci.* **677**, 155–166.
9. Shapiro, H. M. (1986) The little laser that could: applications of low power lasers, in *Clinical Flow Cytometry*, *Ann. NY Acad. Sci.* **468**, 18.
10. Loken, M. R., Keij, J. F., and Kelley, K. A. (1987) Comparison of helium-neon and dye lasers for the excitation of allophycocyanin. *Cytometry* **8**, 96.
11. Doornbos, R. M. P., De Grooth, B. G., Kraan, Y. M., Van Der Poel, C. J., and Greve, J. (1994) Visible diode lasers can be used for flow cytometric immunofluorescence and DNA analysis. *Cytometry* **15**, 267–271.
12. Doornbos, R. M. P., Hennink, E. J., and Putman, C. A. J. (1993) White blood cell differentiation using a solid state flow cytometer. *Cytometry* **14**, 589–594.
13. Nakamura, S. and Fasol, G. (1997) The blue laser diode, in *GaN Based Light Emitters and Lasers*, Springer-Verlag, Berlin, pp. 85–108.
14. Shapiro, H. M. and Perlmutter, N. G. (2001) Violet laser diodes as light sources for cytometry. *Cytometry* **44**, 133–136.
15. Telford, W. G., Hawley, T. S., and Hawley, R. G. (2002) Analysis of violet-excited fluorochromes by flow cytometry using a violet laser diode. *Cytometry (Suppl. 11)*, 123.
16. Telford, W. G., Hawley, T. S., and Hawley, R. G. (2003) Analysis of violet-excited fluorochromes by flow cytometry using a violet laser diode. *Cytometry* **54A**, 48–55.
17. Hoffman, R. A. (2002) Multicolor immunofluorescence flow cytometry using 400 nm laser diode excitation. *Cytometry (Suppl. 11)*, 124.

Viable Infectious Cell Sorting in a BSL-3 Facility

Stephen P. Perfetto, David R. Ambrozak, Mario Roederer,
and Richard A. Koup

Summary

With the increase in demand for high-speed cell sorting of viable infectious and now therapeutic cell samples, safety concerns for the protection of flow cytometer operators have increased. This chapter describes a quick, sensitive, and reproducible procedure to assure sample containment before sorting these samples. This procedure includes aerosol containment, physical barriers, environmental controls, and personal protection. An aerosol management system produces a negative pressure within the sort chamber where aerosols are vacuumed directly into a HEPA filter. Physical barriers include the manufacturer's standard plastic shield and panels. The flow cytometer is contained in a BSL-3 laboratory for maximum environmental control and the operator is protected using a respiratory system. Containment is measured using highly fluorescent Glo-Germ™ particles under the same conditions as the cell sort but with the sorter adjusted to produce large amounts of aerosols. These aerosols are collected by a vacuum air sampling system for 10 min in three locations onto a glass slide and examined microscopically. With this system in place, aerosol containment can be measured quickly and efficiently, therefore reducing the risk to the operator when sorting viable infectious cells.

Key Words

Biohazard, biosafety, flow cytometry, high-speed sorting.

1. Introduction (see Note 1)

With the advent of high-speed sorters and the increased demand for infectious cell sorting, containment of infectious aerosols and an effective means for measuring containment is crucial. We developed a sensitive, reproducible, and efficient method for determining aerosol containment, which can be performed before each infectious sort procedure (*1*). In addition, we provide a complete safety protocol with guidelines to minimize operator risk of exposure.

From: *Methods in Molecular Biology: Flow Cytometry Protocols*, 2nd ed.
Edited by: T. S. Hawley and R. G. Hawley © Humana Press Inc., Totowa, NJ

The measurement of aerosol containment began with T4 bacteriophage sorting into *E. coli*-sensitive plates. Plaques form as a result of natural infection, which could be enumerated. Hence, the greater the plaque counts the poorer the aerosol containment (2,3). Several instrument “failure” modes were tested but this system was found to be both cumbersome and nonreproducible. These tests took several days to perform and therefore were measured every 2–3 mo. In addition, laboratories involved in sorting viable cells for cultures were faced with the possibility of *E. coli* contamination. In light of these drawbacks highly fluorescent particles were used as a substitution for T4 bacteriophage sorting (4,5). These particles, called Glo-germ™ were developed to mimic hospital infection for studying the possible spread of bacteria within a hospital setting. Under a Woods lamp (UV light) these particles are extremely fluorescent and are ideal for this type of application. However, these techniques were not sensitive as needed to measure particle containment because of the inefficiency of aerosol collection. Hence, our laboratory developed the following procedure to measure aerosols using a highly efficient method of aerosol collection. Using this method, aerosols containing Glo-Germ particles produced as a result of poor containment can be detected by the examination of fluorescent particles on a microscope slide. Thus, loss of containment was correlated with increased number of particles per slide. Acceptable tolerance was determined to be the detection of no particles outside of the sorting chamber.

2. Materials

2.1. Equipment

1. AeroTech 6TM viable microbial particle sampler (Aerotech Laboratories, Inc., Phoenix, AZ [www.aerotechlabs.com], cat. no. 6TM).
2. Matheson flow meter: Vacuum Meter (Thomas Scientific, Swedesboro, NJ, cat. no. 5083R60).
3. Aerosol Management System with the Whisper HEPA filter system (AMS) (BD Biosciences, San Jose, CA).
4. Dupuy Bio-Hazard Respiratory System (Chesapeake Surgical, Ltd., Sterling, VA): PV Helmet w/Battery, cat. no. 5430-01-000; Battery, cat. no. 5430-35-000; 4 Station Charger, cat. no. 5430-48-000; Hytrel Universal Toga, 5430-32-000; Knee High Boot Covers, cat. no. 5409-55-000.
5. Flow cytometer with sorting capability (e.g., FACSDiVa, , BD Biosciences).
6. Fluorescent microscope, (e.g., Nikon Microscopes, Image systems, Columbia, MD).
7. Laminar flow hood (e.g., Baker Co., Sanford, ME).

2.2. Reagents and Supplies

1. Glo-Germ™ Particles (GLOGERM Inc., Moab, UT [www.glogerm.com], cat. no. GGP): 5- μ m melamine copolymer resin beads in a 5-mL volume of ethanol. If

Glo-Germ is in powder form, resuspend in 5 mL of 100% ethanol before proceeding.

- a. Wash Glo-germ™ particles 2X in 100% ethanol, at 900g for 10 min. Resuspend in 100 mL of wash media (*see step 2*). Store particles in an opaque glass container at 4°C for up to 1 yr.
- b. Filter particles through a 100-μm filter. Dilute this stock with phosphate-buffered saline (PBS) (~1:20) prior to sorting to achieve a 20,000 particle per second acquisition rate.
2. Wash media: PBS containing 10% fetal calf serum (FCS), 1% Tween-20, and 1 mg/mL of sodium azide.
3. Microscope slides and Petri dishes.

3. Methods

3.1. Aerosol Management System (AMS)

While sorting viable infectious material (infected cells) under high pressure the following guidelines and procedures must be followed for proper aerosol containment. The AMS is designed for two modes of vacuum, high (20 ft³/min) and low (3 ft³/min). Because the sort chamber of the FACSDiVa is 0.49 ft³, the exchange rate for the low vacuum setting is one chamber volume per 10 s. We found this setting to be high enough for the removal of aerosols from the sort chamber, yet low enough to not disrupt the sort streams. Although the sort chamber could be cleared of aerosols faster on the high vacuum setting, this setting cannot be used for cell sorting because of sort stream disruption.

1. The AMS must be on and functioning according to the manufacturer's guidelines.
2. Tolerance range for the vacuum monitor must be between 1.5 and 2.0 inches of water. If this is not between 1.5 and 2.0 inches of water, replace the high-efficiency particulate air (HEPA) filter unit and tubing. Autoclave replaced HEPA filter and tubing.
3. Tolerance for the filter life indicator must be greater than 40%. If this is below 40%, replace HEPA filter unit and tubing. Autoclave replaced HEPA filter and tubing.
4. The Accudrop system on the FACSDiVa is used to determine the droplet delay and must be functioning normally according to the manufacturer's guidelines. In addition, this camera system can be used to monitor the sort stream and alerts the operator to potential increased aerosols. In this situation, the operator should immediately correct the sort stream and reduce aerosol contamination.

3.2. Tolerances and Measurement of Containment

The AMS must be tested under similar sorting conditions as cell sorting, and tolerances must be maintained to assure proper functioning of the AMS before sorting viable infectious material. However, to provide the greatest opportunity to measure containment, the sorter is placed in a "failure mode" of operations described in this section.

1. Add a clean microscope slide to a clean Petri dish and place into the AeroTech 6TM viable microbial particle sampler. Close the top lid and carefully secure clasps on each side. This device is kept under the Laminar flow hood until containment is completed (*see step 9 and Note 2*).
2. Add a clean microscope slide to the inside of the sort chamber on top of the Auto-Clone arm. This slide will be used as the positive control.
3. Adjust the vacuum to the AeroTech 6TM viable microbial particle sampler to 45 L/min (measure by the Matheson flow meter). Record the vacuum setting in **Table 1**.
4. Check all aerosol vacuum connections and turn on the AMS vacuum. Record the vacuum pressure in inches of water in **Table 1**.
5. Adjust Glo-Germ particle rate to 20,000 events per second at 25 pounds per square inch (psi) (*see Note 3*).
6. With door shut and deflection plates on, adjust the flow stream to glance off of the waste catcher to create as large an aerosol as possible. This situation is considered the “failure mode” of operation.
7. Close all containment barriers according to the manufacturer’s guidelines.
8. Place and move the AeroTech 6TM viable microbial particle sampler to three locations for 10 min at each location. The recommended locations are directly in front of sort chamber door, on top of the sort chamber, and 2 ft away from the front of sorter (usually on the operator’s chair).
9. Stop the sort; remove the microscope slide from the AeroTech 6TM viable microbial particle sampler and the positive control slide from inside the sort chamber (*see Note 4*). Do not allow sample tube to back-drip (*see Note 5*). To remove excess particles from the sample tubing, place 70% ethanol on sample station and run through sample tubing for 5 min while under sort containment.
10. Examine the entire slide using a fluorescent microscope scanning with a 10X objective and a fluorescein isothiocyanate (FITC) emission filter (520–640 nm). Examine both slides.
11. Record results in **Table 1**. All tolerances must be achieved before proceeding with the viable infectious sort. Repeat procedure if there are any discrepancies in the results.
12. Tolerance of particles outside the sort chamber: Zero tolerance, no particles on entire slide. Any positive result must be investigated, resolved and retested before proceeding with infectious sort.
13. Tolerance of particles inside the sort chamber (positive control): Greater than 50 per field (10X objective field, result may vary with slide location). *See Note 6* for additional controls.

3.3. Personnel Safety Equipment (Primary Barriers): Dupuy HEPA Filter Suit and Respiratory System

This system is used before any potentially infectious sort where infectious aerosols may be formed during the procedure.

Table 1

Infectious Cell Sorting Aerosol Containment Documentation Table

Operator				
Date				
Measurement	Particles/slide			
Front of shield / sort chamber		Containment vacuum		Inches HoH
Top of instrument		AeroTech vacuum		L/min
Two feet from sort chamber		Particle rate		Particles/sec
Positive control	*			

Critical tolerances for the AMS:

Filter life tolerance = Greater than 40%. Below this tolerance, replace tubing and HEPA filter.

Vacuum tolerance = Range between 1.5 and 2.0 inches of water (HoH). Below this tolerance, replace tubing and HEPA filter.

Particles outside Zero tolerance, no particles on entire slide. Any positive result must be investigated, resolved and retested before proceeding with infectious sort.

**Particles inside (positive control)* = Greater than 50 per field (10× objective field, result may vary with slide location).

This table shows critical values measured and tolerance ranges required at the time of every viable infectious sort. Gray areas represent data information input. This form documents instrument containment and is required by the VRC (Vaccine Research Center, NIH) laboratory before infectious samples are sorted.

1. Connect battery to helmet; turn on to ensure the helmet fan is working correctly, and turn off (*see Note 7*).
2. Place disposable boots over shoes.
3. Remove the Hytrel Universal Toga from the sterile plastic bag and attach the helmet to the face shield using the Velco strips on the front surface of the shield.
4. Check to assure the HEPA filter in the Hytrel Universal Toga is located over the helmet motor fan.
5. Fit the Hytrel Universal Toga with helmet over body and adjust sleeves and helmet. The battery pack should be attached to belt on the inside of suit. If operating correctly air flow will cause the suit to balloon out from the body surface.
6. Double glove and add sleeve guards. The airflow should filter from the top of the helmet through the HEPA filter and exit out of the bottom of the suit. Make any final adjustments prior to entering the BSL-3 laboratory.

4. Notes

1. NIH does not endorse or recommend any commercial products, processes, or services. The views and opinions of authors expressed in this manuscript do not necessarily state or reflect those of the U.S. Government, and they may not be used for advertising or product endorsement purposes. The U.S. Government does not warrant or assume any legal liability or responsibility for the accuracy, completeness, or usefulness of any information, apparatus, product, or process disclosed.
2. Test microscope slides must be clean and care must be taken not to touch surface. Slides can be further cleaned with 70% ethanol prior to use.
3. Glo-Germ particles are smaller relative to the size of lymphocytes; therefore the FSC detector will require a higher voltage setting.
4. After every infectious cell sort, wait 30 s before opening the sort chamber (air exchange from the sort chamber is rated at one exchange per 10 s). While still under sort containment, sample tubing is cleared by disinfecting with 10% povidine iodine for 1 min. If continuing to another sort, culture media are run until no further counts are detected.
5. Never allow the sample line to back-drip without disinfecting with 10% povidine iodine for 1 min under sort containment.
6. As an additional control for the AeroTech 6TM viable microbial particle sampler, collect particles in failure mode with the AMS off and the sort chamber door closed for a 10-min period. This slide should be positive for particles and indicates the collection system is working correctly.
7. Batteries are allowed to recharge after each use and expire after 2 yr.

References

1. Perfetto, S. P., Ambrozak, D. R., Koup, R. A., and Roederer, M. (2003) Measuring containment of viable infectious cell sorting in high-velocity cell sorters. *Cytometry* **52A**, 122–130.
2. Ferbas, J., Chadwick, K. R., Logar, A., Patterson, A. E., Gilpin, R. W., and Margolick, J. B. (1995) Assessment of aerosol containment on the ELITE flow cytometer. *Cytometry* **22**, 45–47.
3. Merrill, J. T. (1981) Evaluation of selected aerosol-control measures on flow sorters. *Cytometry* **1**, 342–345.
4. Sorensen, T. U., Gram, G. J., Nielsen, S. D., and Hansen, J. E. (1999) Safe sorting of GFP-transduced live cells for subsequent culture using a modified FACS vintage. *Cytometry* **37**, 284–290.
5. Oberyshyn, A. S. and Robertson, F. M. (2001) Novel rapid method for visualization of extent and location of aerosol contamination during high-speed sorting of potentially biohazardous samples. *Cytometry* **43**, 217–222.